NUREG/CR-0815
TREE-1229
For U.S. Nuclear Regulatory Commission

EXPERIMENT DATA REPORT FOR SEMISCALE MOD-3 LOWER PLENUM INJECTION TEST S-07-9 (BASELINE TEST SERIES)

DEAN H. MIYASAKI KENNETH E. SACKETT
DAVID R. PACK

JUNE 1979

EG&G Idaho, Inc.

IDAHO NATIONAL ENGINEERING LABORATORY

DEPARTMENT OF ENERGY

IDAHO OPERATIONS OFFICE UNDER CONTRACT DE-AC07-76IDO1570

Available from
National Technical Information Service
Springfield, Virginia 22161
Price: Printed Copy A12; Microfiche $3.00

The price of this document for requesters outside the North American continent can be obtained from the National Technical Information Service.

507 050

NUREG/CR-0815
TREE-1229
R2

EXPERIMENT DATA REPORT FOR SEMISCALE MOD-3 LOWER PLENUM INJECTION TEST S-07-9 (BASELINE TEST SERIES)

Dean H. Miyasaki
Kenneth E. Sackett
David R. Pack

EG&G Idaho, Inc.
Idaho Falls, Idaho 83401

Published June 1979

PREPARED FOR THE
U.S. NUCLEAR REGULATORY COMMISSION
AND THE U.S. DEPARTMENT OF ENERGY
IDAHO OPERATIONS OFFICE
UNDER CONTRACT NO. DE-AC07-76IDO1570
NRC FIN NO. A6038

507 051

ABSTRACT

Recorded test data are presented for Test S-07-9 of the Semiscale Mod-3 baseline test series. This test is one of several Semiscale Mod-3 experiments conducted to investigate the thermal and hydraulic phenomena accompanying a hypothesized loss-of-coolant accident in a pressurized water reactor (PWR) system. Test S-07-9 was conducted from initial conditions of 16.10 MPa and 559 K to investigate the response of the Semiscale Mod-3 system to a blowdown transient following a simulated double-ended offset shear of the broken loop cold leg piping. The specific objective of this test was to provide reference data to evaluate integral blowdown and reflood behavior during a 200% cold leg break with emergency core coolant (ECC) injection into the vessel lower plenum of the Mod-3 system. The purpose of this report is to make available the uninterpreted data from Test S-07-9 for future data analysis. The data, presented in the form of graphics in engineering units, have been analyzed only to the extent necessary to ensure that they are reasonable and consistent.

This test was identical to Test S-07-8, except that the ECC injection from the accumulator was initiated at a higher accumulator pressure (6.92 MPa).

507 052

SUMMARY

Test S-07-9 was performed as part of the Semiscale Mod-3 portion of the Semiscale Program conducted by EG&G Idaho, Inc., for the United States Government. This test was part of the Mod-3 baseline test series (Test Series 7) performed to investigate the response of the Mod-3 system during a blowdown and reflood transient. Hardware configuration and test parameters were selected to yield a system response that simulates the response of a pressurized water reactor to the blowdown and reflood portions of a hypothesized loss-of-coolant accident (LOCA).

The objective of Test S-07-9 was to provide reference data to evaluate integral blowdown and reflood behavior during a 200% cold leg break with emergency core coolant injection into the vessel lower plenum of the Mod-3 system.

The Mod-3 system was equipped with a pressure vessel with simulated reactor internals and an external downcomer assembly; an intact loop with steam generator, pump, and pressurizer; a broken loop with steam generator, pump, and rupture assembly; high and low pressure coolant injection pumps and coolant injection accumulator for the vessel lower plenum; and a pressure suppression system with header, suppression tank, and steam supply system. The electrically heated core consisted of 25 rods of which 23 were powered.

Test S-07-9 was conducted from initial conditions of 16.10 MPa and 559 K with a simulated full size (200%) double-ended offset shear of the broken loop piping at an initial core power level of 2.00 MW. After initiation of blowdown, power to the heated core was reduced to simulate the predicted heat flux response of nuclear fuel rods during a LOCA.

Test S-07-9 was generally conducted as specified. Conditions which did not conform to the specified test configuration were considered acceptable for analysis purposes within the test objectives. The instrumentation used generally functioned as intended. Of 211 measurements taken, 206 produced usable data.

507 053

CONTENTS

FIGURES

507 054

507 055

507 056

507 058

507 060

507 061

507 062

507 063

507 066

507 067

507 068

TABLES

507 069

EXPERIMENT DATA REPORT FOR SEMISCALE MOD-3 LOWER PLENUM INJECTION TEST S-07-9 (BASELINE TEST SERIES)

I. INTRODUCTION

The Semiscale Mod-3 experiment represent the current phase of the Semiscale Program conducted by EG&G Idaho, Inc., for the United States Government. The program, which is sponsored by the Nuclear Regulatory Commission through the Department of Energy, is part of the overall program designed to investigate the response of a pressurized water reactor (PWR) system to a hypothesized loss-of-coolant accident (LOCA). The underlying objectives of the Semiscale Program are to quantify the physical processes controlling system behavior during a LOCA and to provide an experimental data base for assessing reactor safety evaluation models. The Semiscale Mod-3 Program has the further objective of providing support to other experimental programs in the form of instrumentation assessment, optimization of test series, selection of test parameters, and evaluation of test results.

Test S-07-9 was conducted March 21, 1979, in the Semiscale Mod-3 system as part of the baseline test series (Test Series 7). This series was designed to obtain thermal-hydraulic response data from blowdown, refill, and reflood transients in a simulated nuclear reactor having an electrically heated core. The specific objective of Test S-07-9 was to provide reference data to evaluate integral blowdown and reflood behavior during a 200% cold leg break with emergency core coolant (ECC) injection into the vessel lower plenum of the Mod-3 system. Hardware configuration and test parameters were selected to yield a system response that simulates the response of a PWR to a hypothesized LOCA blowdown transient.

The purpose of this report is to present the test data in an uninterpreted but readily usable form for use by the nuclear community in advance of detailed analysis and interpretation. Section II briefly describes the system configuration, procedures, and initial test conditions, and events that are applicable to Test S-07-9; Section III presents the data graphs and provides comments and supporting information necessary for interpretation of the data. A description of the overall Semiscale Program and test series, a more detailed description of the Semiscale Mod-3 system, and a description of the measurement and data processing techniques and uncertainties can be found in References 1 and 2.

507 070

II. SYSTEM, PROCEDURES, CONDITIONS, AND EVENTS FOR TEST S-07-9

The following system configuration, procedures, initial test conditions, and events are specific to Test S-07-9 as indicated.

1. SYSTEM CONFIGURATION AND TEST PROCEDURES

The Semiscale Mod-3 system used for the test consisted of a pressure vessel with simulated reactor internals, including a 25-rod core with 23 electrically heated rods and an external downcomer assembly; an intact loop with steam generator, pump, and pressurizer; a broken loop with steam generator, pump, and rupture assembly; high and low pressure injection pumps and coolant injection accumulator for the vessel lower plenum; and a pressure suppression system with a suppression tank, header, and steam supply system. The Semiscale Mod-3 experimental system configuration is described further in Reference 2. Figures 1 and 2 show the system configuration for the test.

For Test S-07-9, the nine center rods were powered 12.8% higher than the remaining 14 low powered rods, resulting in high and low power rod peak densities of 39.7 kW/m and 35.2 kW/m, respectively. The total core power was 2.00 MW. One rod (Rod E-5) was unpowered and another rod (Rod A-1) was replaced by a liquid level probe.

In preparation for the test, the system was filled with treated demineralized water and vented at strategic points to ensure a liquid-full system. Treated demineralized water in the steam generator feedwater tank was heated to 486 K, and the required levels were established in the steam generator secondary sides. The accumulator for the vessel lower plenum was filled with treated demineralized water, drained to specified initial levels, and pressurized with nitrogen to 6.92 MPa.[a] Prior to warmup, the system was pressurized to check for leakage; system instrumentation was checked; and transducer readings were set to zero. Warmup to initial test conditions was accomplished with the heaters in the vessel core. During warmup, the purification and sampling systems were valved into the primary system to maintain water chemistry requirements and to provide a water sample at system conditions for subsequent analysis. At 50-K temperature intervals during warmup, detector readings were sampled to allow the integrity of the measurement instrumentation and the operability of the data acquisition system to be checked.

Prior to the initial core power level being established, the pressure suppression system was pressurized to 0.24 MPa with saturated steam from the steam supply system. After the core power was increased to 2.00 MW, initial test conditions were held for 607 s to establish equilibrium in the system. At the end of this period all auxiliary systems were isolated to prevent blowdown through those systems.

The system was successfully subjected to a simulated double-ended cold leg break through a rupture assembly and two blowdown nozzels having a total break area of 4.59 cm^2. Pressure to operate the rupture assembly and initiate blowdown was taken from an accumulator system filled with water and pressurized to 15.6 MPa with gaseous nitrogen. Immediately (within 0.02 s) after initiation for blowdown, the lines to the accumulator were again isolated. The effluent was ejected from the primary system into the pressure suppression system which was vented to maintain a constant pressure of 0.243 MPa. At blowdown, power to the primary coolant circulation pump was reduced and the pump was allowed to coast down to a speed of 130 rad/s which was maintained for the duration of the test. During the blowdown transient, power to the electrically heated core was automatically controlled to simulate the thermal response of nuclear heated fuel rods.

---

a. All pressures are presented as absolute values.

507 071

507 073

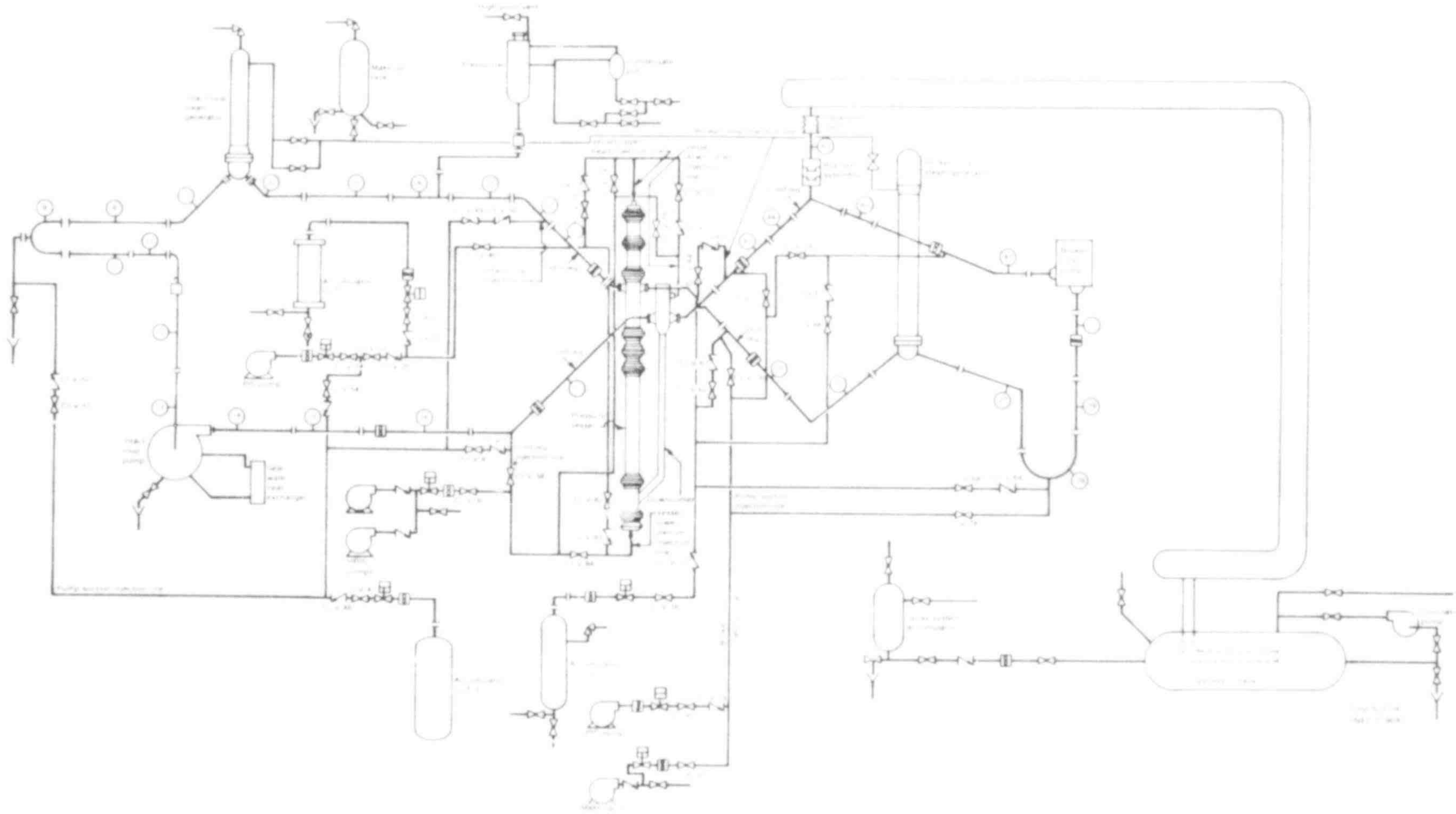

Fig. 2 Semiscale Mod-3 system for cold leg break configuration — schematic

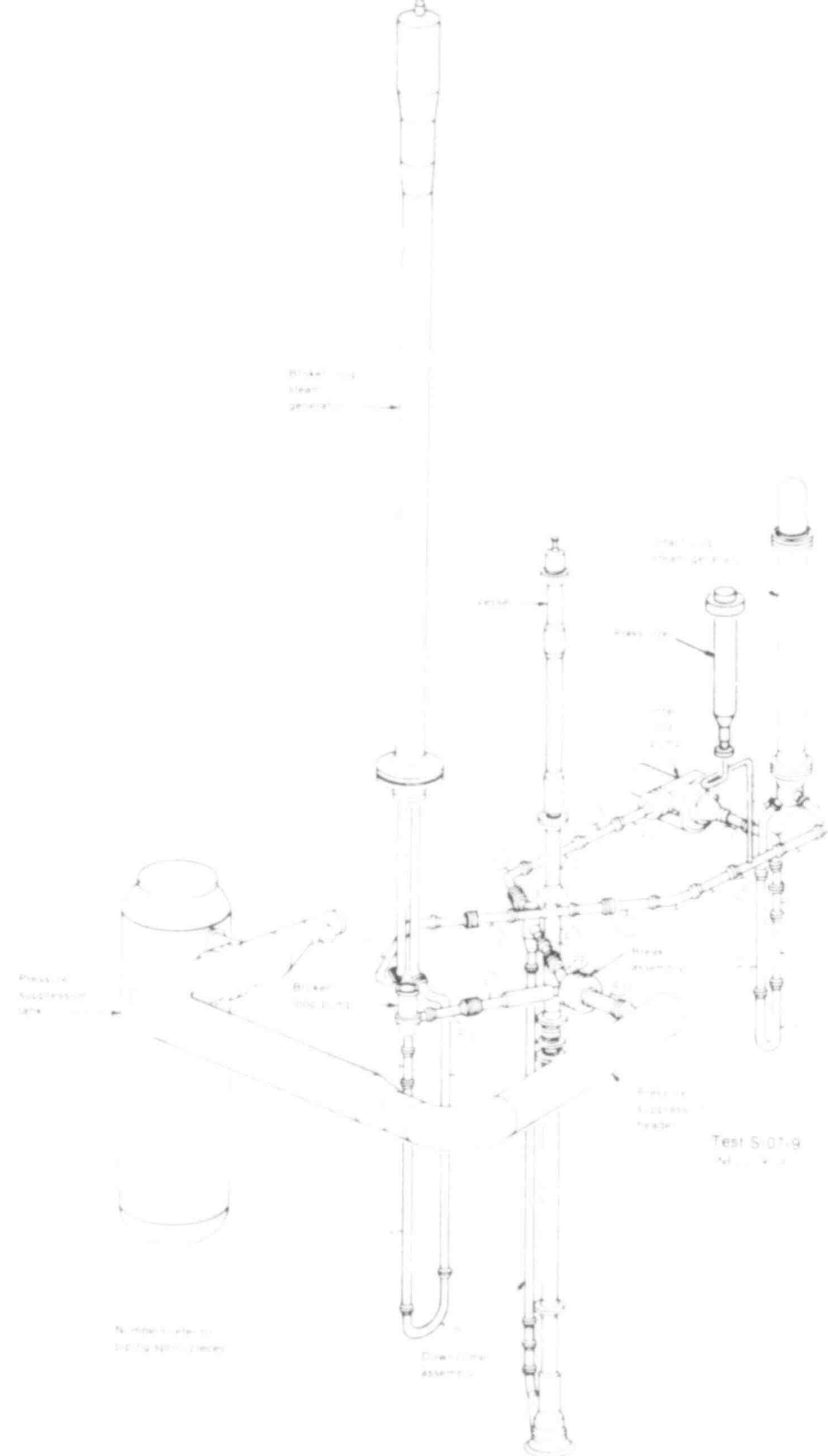

Fig. 1 Semiscale Mod-3 system for cold leg break configuration — isometric.

For Test S-07-9, the coolant injection systems were arranged to discharge into the vessel lower plenum. The high pressure coolant injection pumps were started at initiation of blowdown with coolant injection starting at a pressure of 12.41 MPa, and continued running (as pressure decreased) to the end of the test (350 s). Low pressure coolant injection was initiated 34.5 s after blowdown at a system pressure of 1.10 MPa and was continued until test termination (350 s). Coolant injection from the vessel accumulator (CI-T-1) started 8.5 s after blowdown, and was terminated 46 s after blowdown. Total volume of coolant injected into the vessel from the accumulator was 44.5 l. Nitrogen from the accumulator was not discharged into the vessel lower plenum.

2. INITIAL TEST CONDITIONS AND SEQUENCE OF EVENTS

Conditions in the Semiscale Mod-3 system at initiation of blowdown are given in Tables I and II and the sequence of events relative to rupture is given in Table III.

507 074

TABLE I

CONDITIONS AT BLOWDOWN INITIATION

	Test S-07-9	
	Measured[a]	Specified
Core power (MW)	2.00	2.0 ± 0.05
System pressure (MPa)	16.09	15.51 ± 0.17
Intact loop cold leg fluid temperature (K)	559	557 ± 1
Broken loop cold leg fluid temperature (K)	555	557 ± 1
Intact loop hot leg to cold leg temperature differential (K)	35	37 ± 1
Broken loop hot leg to cold leg temperature differential (K)	39	37 ± 1
Intact loop cold leg flow (1/s)	9.05	b
Broken loop cold leg flow (1/s)	2.60	b
Steam generator feedwater temperature[c] (K)	486	497 ± 6
Intact loop steam generator liquid level (cm) (above top of tube sheet)	287	295 ± 5
Broken loop steam generator liquid level (cm) (above top of tube sheet)	1,047	996 ± 5
Pressure suppression tank pressure (MPa)	0.244	0.241 ± 0.007
Pressure suppression tank temperature (K)	298	297 ± 1

a. Measured initial conditions are taken from digital acquisition system read just prior to blowdown initiation. Those measured conditions which did not meet the specified conditions were considered acceptable.

b. Flow is not specified, since it must be adjusted to achieve the required differential temperature across the core.

c. One source of feedwater for both intact and broken loops.

507 075

TABLE II

PRIMARY COOLANT TEMPERATURE DISTRIBUTION
PRIOR TO RUPTURE[a]

	Test S-07-9	
	Detector	Temperature (K)
Vessel lower plenum (bottom of lower plenum)	TFV-572W	555
Vessel lower plenum (top of lower plenum)	TFV-552A	555
Intact loop hot leg (near vessel)	RFI-2	594
Broken loop hot leg (near vessel)	RFB-20	594
Intact loop cold leg (near pump inlet)	TFI-11	555
Broken loop cold leg (near pump inlet)	TFB-37	559
Intact loop cold leg (near downcomer)	RFI-17	559
Broken loop cold leg (near downcomer)	RFB-45	555
Vessel upper head (middle)	TFV+221Q	555
Downcomer (top)	TFD-18F	558
Downcomer (middle)	TFD-294	559
Downcomer (bottom)	TFD-435	559

a. Average of data taken from -5 s to -0.5 s prior to blowdown initiation.

507 076

TABLE III

SEQUENCE OF EVENTS DURING TEST S-07-9[a]

Event	Time Relative To Rupture (s)
Core power level established	-607
Makeup pump and pressurizer heaters off	-2.5
Intact and broken loop steam generator feedwater and discharge valves closed	-1
Intact and broken loop pump controls initiated	0
High pressure injection system flow started	0
Core power decay transient started	2.5
ECC accumulator vessel lower plenum flow started	8.5
Low pressure injection system flow started[b]	34.5
Broken loop pump power terminated	350
Core power terminated	350

a. A time controlled sequencer was used to control critical events during the test.

b. Injection from high and low pressure injection system pumps and ECC accumulators did not start until system pressure dropped below preset pump or accumulator pressure, respectively.

III. DATA PRESENTATION

The data from Semiscale Mod-3 Test S-07-9 are presented with brief comment. Processing analysis has been performed only to the extent necessary to obtain appropriate engineering units and to ensure that the data are reasonable and consistent. In all cases, in converting transducer output to engineering units, a homogeneous fluid was assumed. Further interpretation and analysis should consider that sudden decompression processes such as those occurring during blowdown may have subjected the measurement devices to nonhomogeneous fluid conditions.

The performance of the system during Test S-07-9 was monitored by 211 detectors. The data obtained were recorded on both digital and analog data acquisition systems. The analog system was used to provide redundant data. The long-term data (-20 to 300 s) presented in this report were recorded at an effective sample rate of 2.875 points per second. Short-term data (-6 to 42 s) were recorded at an effective sample rate of 19.16 points per second.

The data are presented in some instances in the form of composite graphs to facilitate comparison of the values of given variables at several locations. The scales selected for the graphs do not reflect the obtainable resolution of the data. (The data processing techniques are described further in Reference 2 and Appendix A.)

Figures 3 through 10 and Table IV provide supporting information for interpretation of the data graphs shown in Figures 11 through 320 and provide relative locations of all detectors used during Test S-07-9. Table III groups the measurements according to measurement type, identifies the specific measurement location and range of the detector and actual recording range of the data acquisition system, provides brief comments regarding the data, and references the measurements and comments to the corresponding figure. Figures 11 through 320 present all the blowdown data obtained. Time zero on the graphs is the time of rupture initiation. Appendix A provides information explaining the data acquisition system capabilities. Appendix B explains posttest data processing for data conversion into engineering units and data adjustments. Appendix C presents an analysis of selected data which provide a guide to the uncertainty associated with data measurements in the Semiscale Mod-3 system.

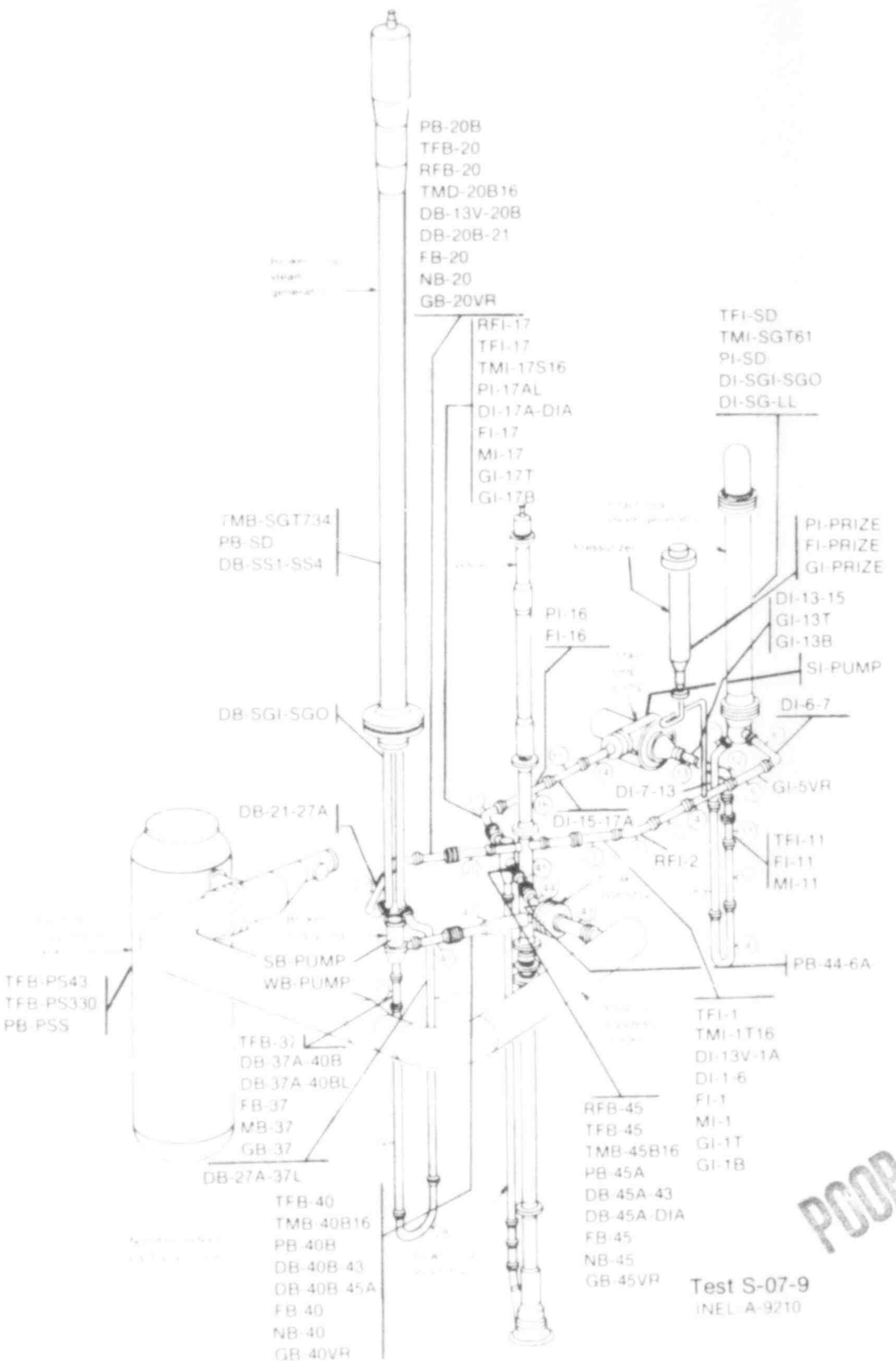

Fig. 3 Semiscale Mod-3 system and instrumentation for cold leg break configuration — isometric.

POOR ORIGINAL

507 079

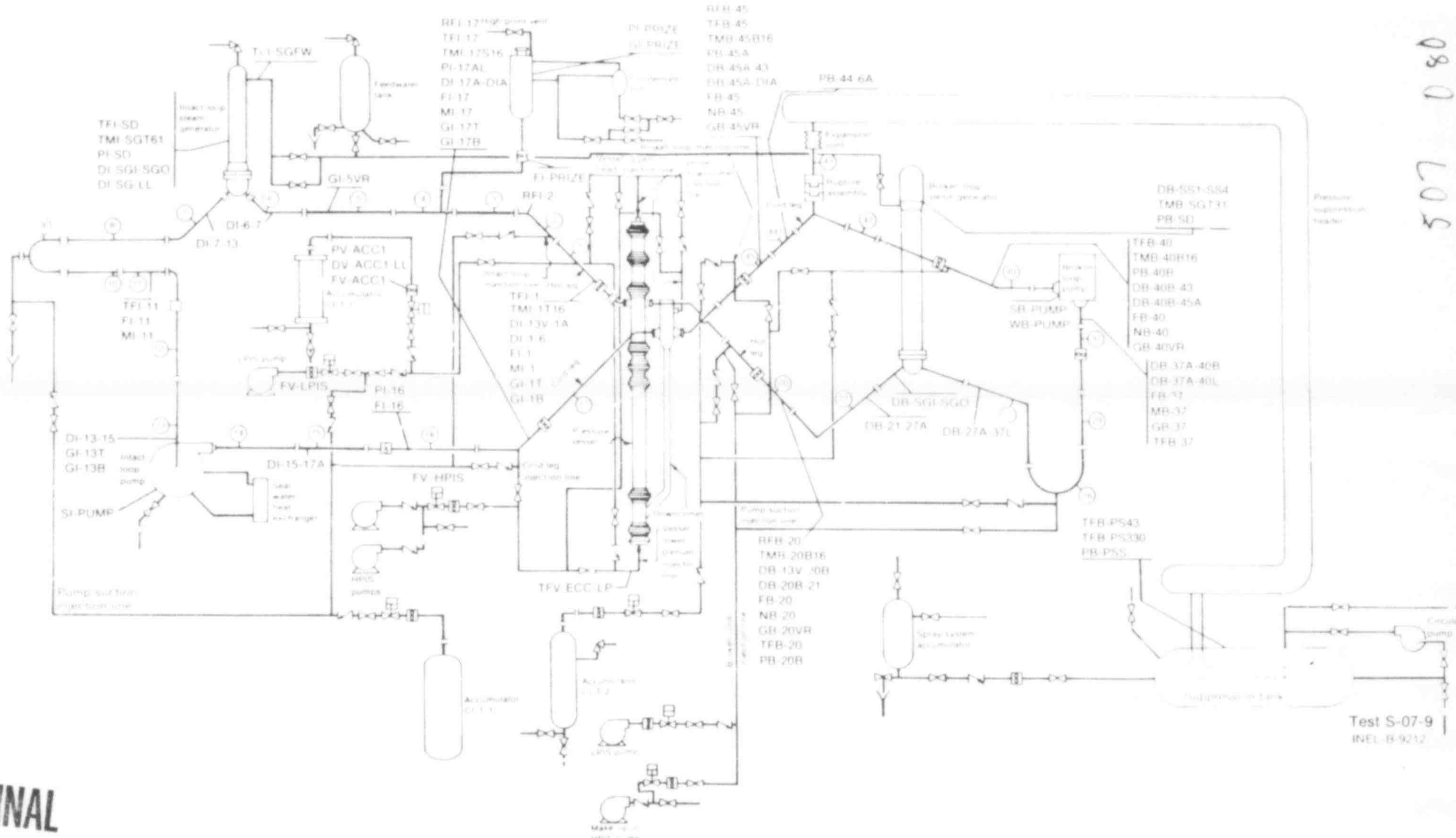

Fig. 4 Semiscale Mod-3 system and instrumentation for cold leg break configuration — schematic.

OR ORIGINAL

507 080

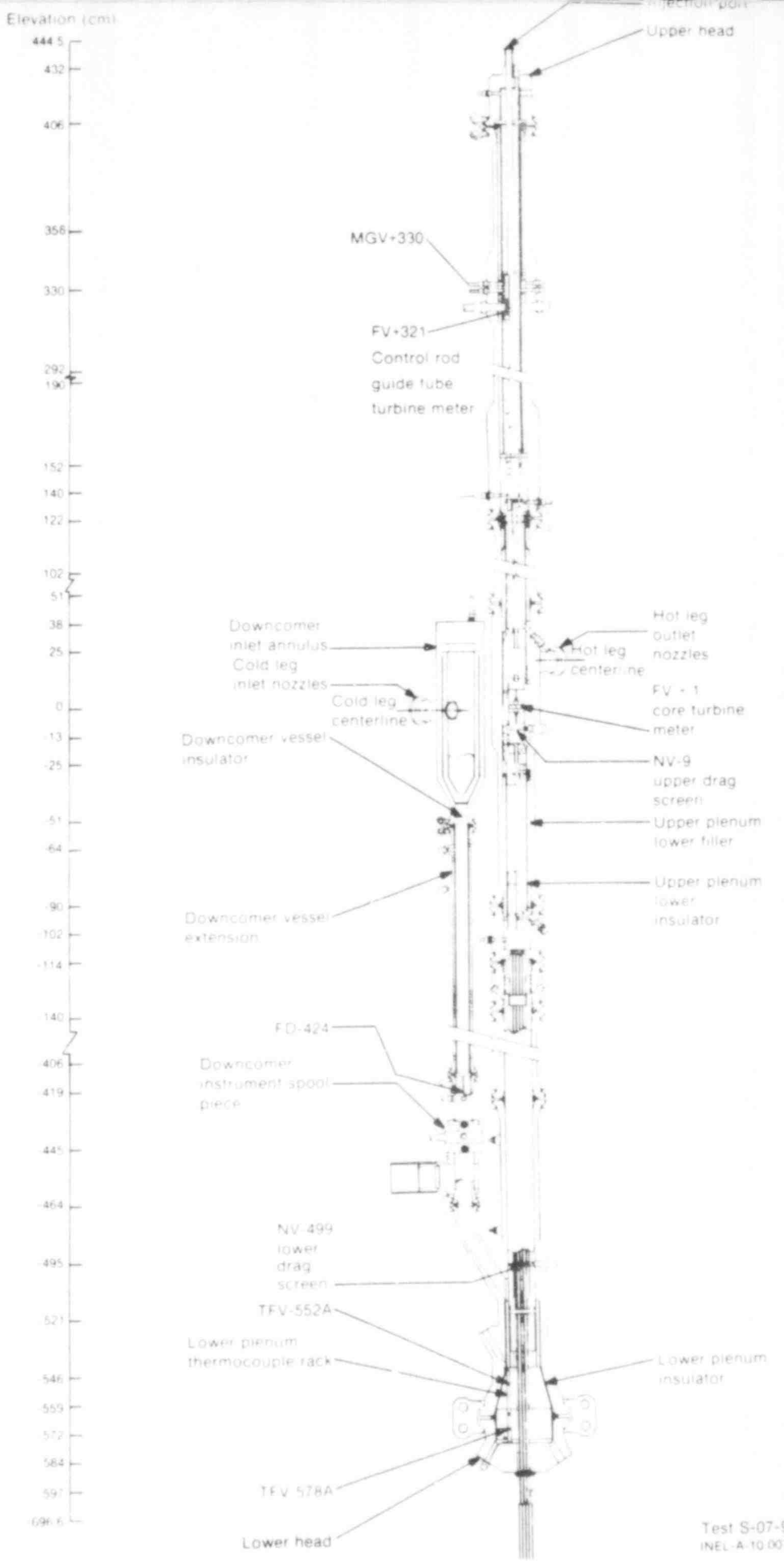

Fig. 5 Semiscale Mod-3 pressure vessel and downcomer — cross section showing instrumentation.

507 081

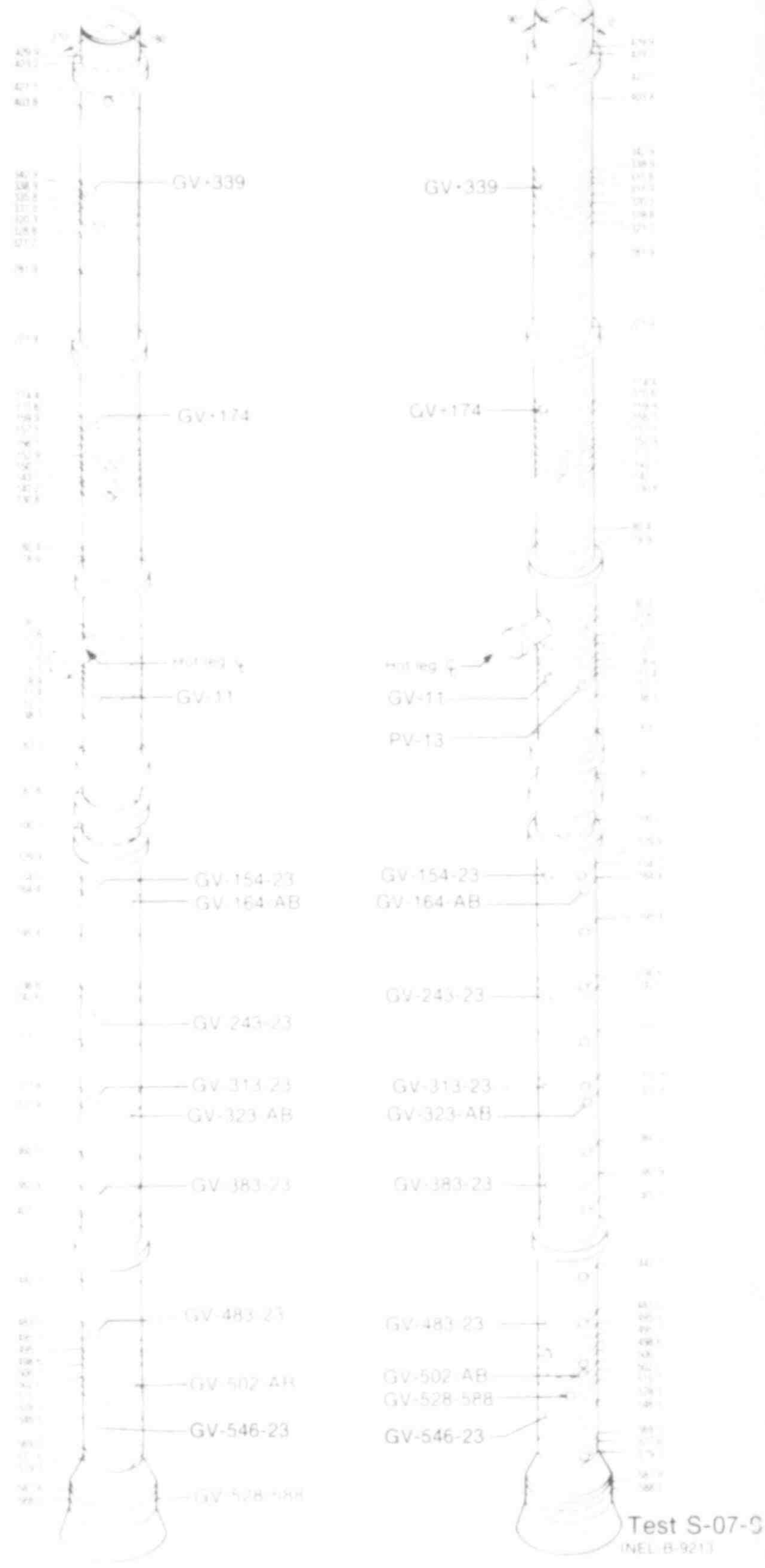

Fig. 6 Semiscale Mod-3 pressure vessel — isometric showing instrumentation.

POOR ORIGINAL

507 082

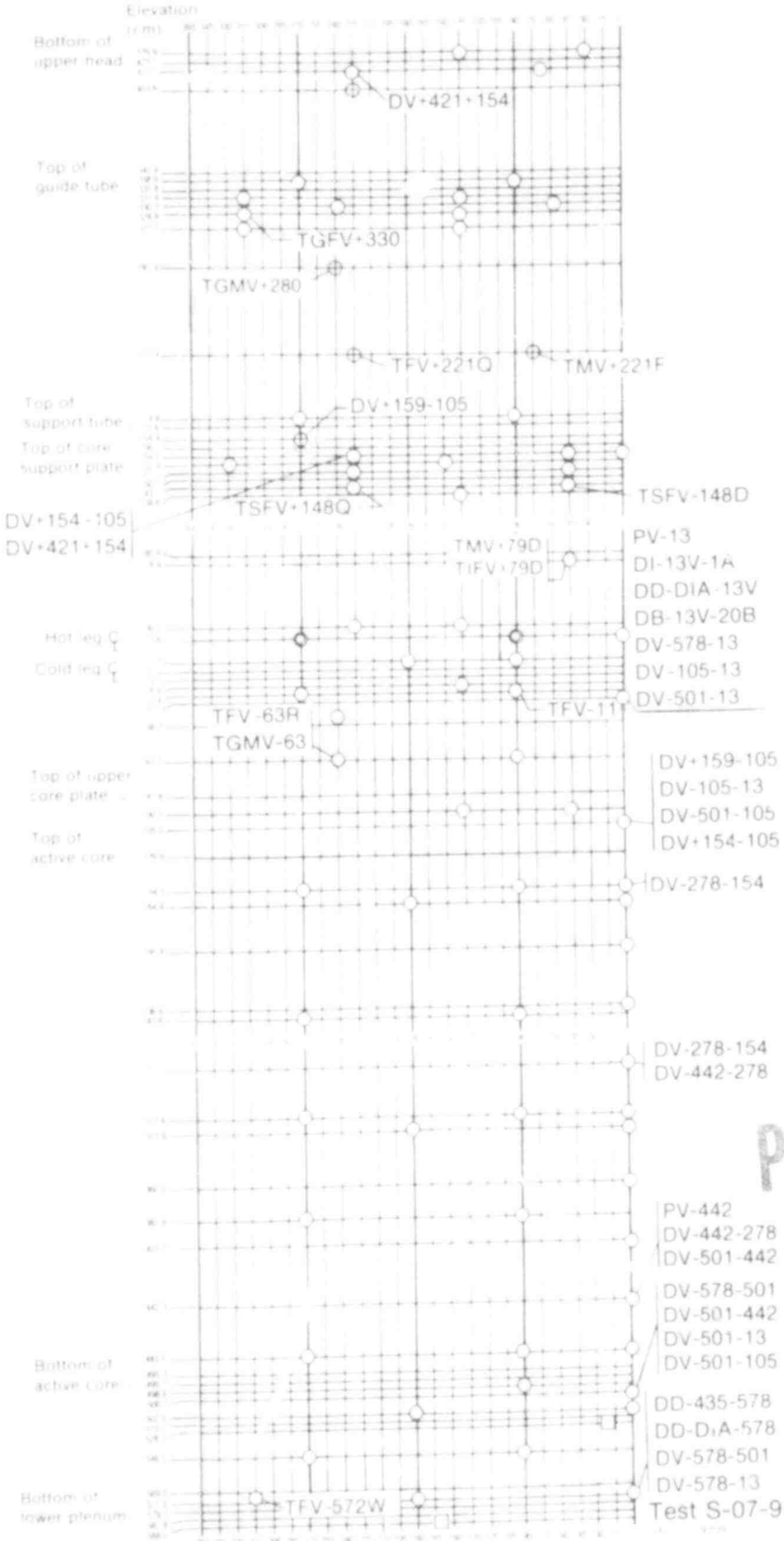

Fig. 7 Semiscale Mod-3 pressure vessel — penetrations and instrumentation.

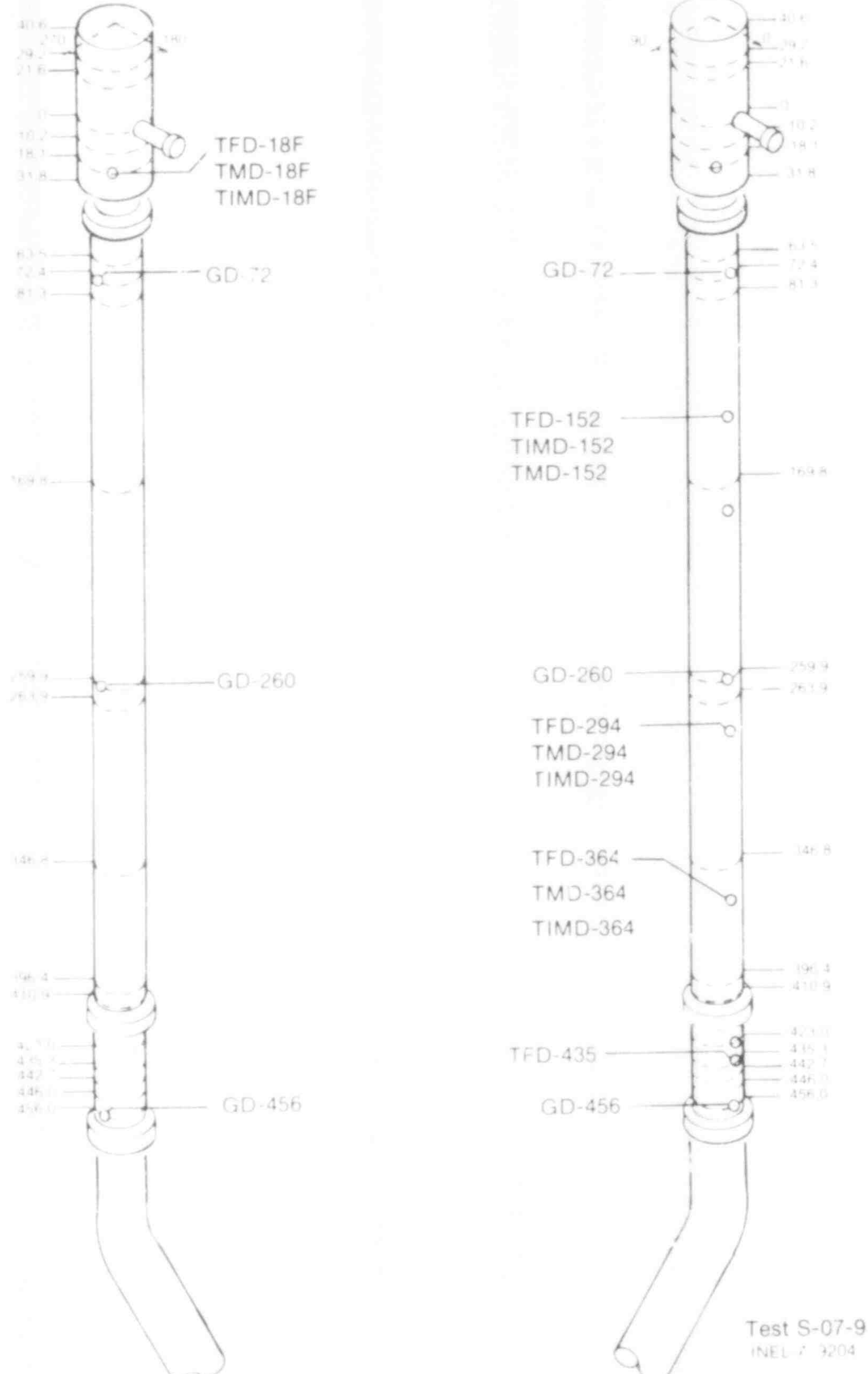

Fig. 8 Semiscale Mod-3 downcomer — isometric showing instrumentation.

507 084

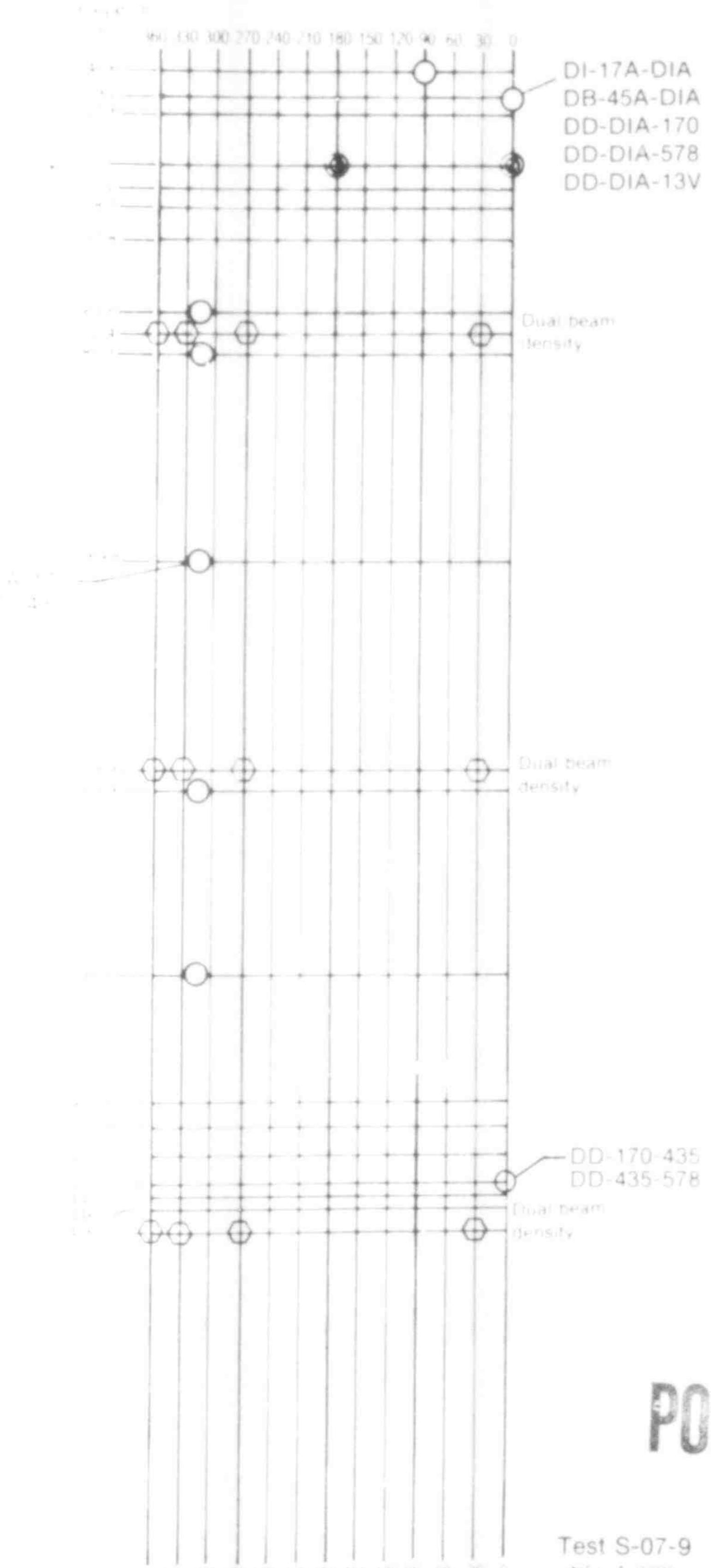

Fig. 9 Semiscale Mod-3 downcomer — penetrations and instrumentation.

POOR ORIGINAL

507 085

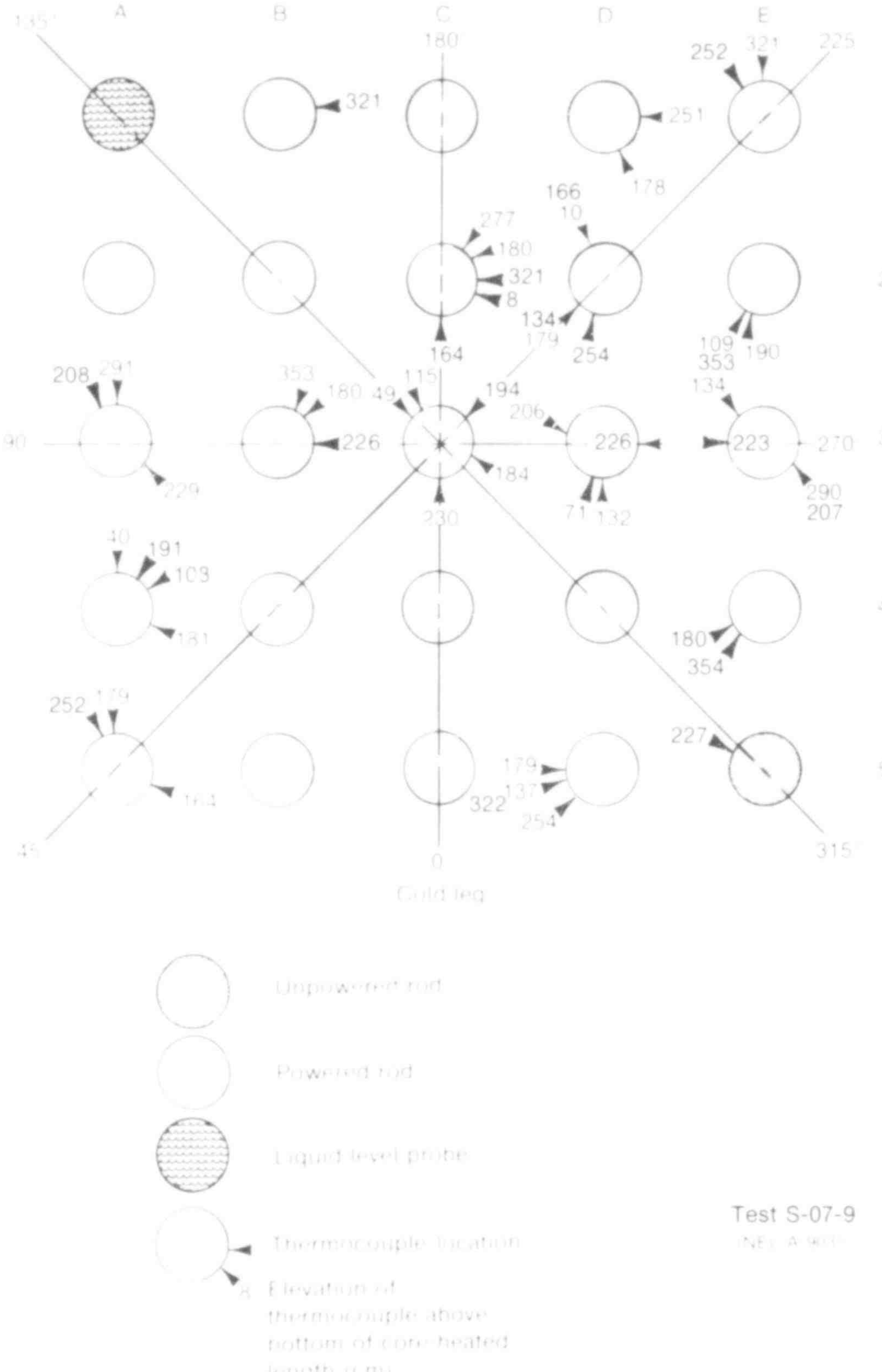

Fig. 10 Semiscale Mod-" heater core — plan view.

TABLE IV

DATA PRESENTATION FOR SEMISCALE MOD-3 TEST S-07-9

Measurement	Location and Comments[a]	Data Acquisition Range[a] Detector	System	Figure[a]	Measurement Comments[b]
FLUID TEMPERATURE	Chrome-Alumel thermocouples unless specified otherwise.				
Intact Loop		0 to 1533 K	0 to 820 K		
TFI-1	Hot leg, Spool 1, 50 cm from vessel center.			11,12	
RFI-2	Hot leg, Spool 2, 99 cm from vessel center, 10 cm upstream of hot leg injection port (platinum resistance bulb).	0 to 811 K	0 to 811 K	11,12	Temperature data applicable only for initial conditions. Transient temperature is to be used for trend only.
TFI-11	Cold leg, Spool 11, 438 cm from downcomer center.			13,14	Data appear normal, but data acquisition system noise caused a stepping of 1.5% of full scale.
RFI-17	Cold leg, Spool 17, 92 cm from downcomer center, 2 cm upstream of cold leg injection port (platinum resistance bulb).	0 to 811 K	0 to 811 K	15,16	Temperature data applicable only for initial conditions. Transient temperature is to be used for trend only.
TFI-17	Cold leg, Spool 17, 60 cm from downcomer center.			15,16	
Broken Loop		0 to 1533 K	0 to 820 K		
RFB-20	Hot leg, Spool 20, 59 cm from vessel center, 14 cm downstream of hot leg injection port (platinum resistance bulb).	0 to 811 K	0 to 811 K	17,18	Temperature data applicable only for initial conditions. Transient temperature is to be used for trend only.
TFB-20	Hot leg, Spool 20, 84 cm from vessel center, 25 cm downstream of hot leg injection port.			17,18	
TFB-37	Cold leg, Spool 37, 348 cm from downcomer center.			19,20	Data appear normal, but data aquisition system noise caused a stepping of 1.5% of full scale.
TFB-40	Cold leg, Spool 40, 220 cm from downcomer center, 16 cm downstream of cold leg injection port.				Detector failed.
RFB-45	Cold leg, Spool 45, 89 cm from downcomer center (platinum resistance bulb).	0 to 811 K	0 to 811 K	21,22	Temperature data applicable only for initial conditions. Transient temperature is to be used for trend only.
TFB-45	Cold leg, Spool 45, 38 cm from downcomer center.			21,22	
Downcomer		0 to 1533 K	0 to 820 K		
TFD-18F	In downcomer inlet annulus, 18 cm below cold leg centerline at 75°.			23,24	
TFD-152	In downcomer extension, 152 cm below cold leg centerline.			23,24	
TFD-294	In downcomer extension, 294 cm below cold leg centerline.			23,24	
TFD-364	In downcomer extension, 364 cm below cold leg centerline.			23,24	
TFD-435	In downcomer instrument spool, 435 cm below cold leg centerline.			23,24	
Vessel		0 to 1533 K	0 to 820 K		
Vessel Upper Plenum					
TFV+221Q	In vessel upper head filler, 221 cm above cold leg centerline at 225°.			25,26	
TFV-11	In vessel, 11 cm below cold leg centerline.			27,28	
TFV-63R	In vessel, 63 cm below cold leg center at 240°.			27,28	
Vessel Lower Plenum		0 to 1533 K	0 to 820 K		
TFV-552A	On thermocouple rack in vessel lower plenum 552 cm below cold leg centerline at 0°.			29,30	
TFV-572W	In vessel lower plenum, 572 cm below cold leg centerline at 315°.			29,30	

POOR ORIGINAL

507 087

TABLE IV (continued)

Measurement	Location and Comments[a]	Data Acquisition Range[a] Detector	System	Figure[a]	Measurement Comments[b]
Vessel Lower Plenum (continued)					
TFV-178A	On thermocouple rack in vessel lower plenum 178 cm below cold leg centerline at 0°.			29,30	
Vessel Filler Insulator Gap		0 to 1533 K	0 to 820 K		
TIFV-79D	In vessel upper filler insulator gap, 79 cm above cold leg centerline at 45°.			31,32	Data appear normal, but data aquisition system noise caused a stepping of 1.5% of full scale.
Vessel Guide Tube		0 to 1533 K	0 to 820 K		
TGV+110	In vessel guide tube, 110 cm above cold leg centerline.			33,34	Data appear normal, but data aquisition system noise caused a stepping of 1.5% of full scale.
Vessel Support Tube					
TSV+148D	In a vessel support tube, 148 cm above cold leg centerline at 45°.				Detector failed.
Core Grid Spacers		0 to 1533 K	0 to 1580 K		
Grid Spacer 1	490 cm below cold leg centerline, 6 cm above bottom of heated length.				
TFC-1AB-12	Thermocouple in space defined by Columns A and B, Rows 1 and 2.			35,36	
Grid Spacer 2	410 cm below cold leg centerline, 86 cm above bottom of heated length.				
TFC-2AB-12	Thermocouple in space defined by Columns A and B, Rows 1 and 2.			37,38	
Grid Spacer 3	330 cm below cold leg centerline, 166 cm above bottom of heated length.				
TFC-3AB-45	Thermocouple in space defined by Columns A and B, Rows 4 and 5.			39,40	
Grid Spacer 4	290 cm below cold leg centerline, 206 cm above bottom of heated length.				
TFC-4BC-34	Thermocouple in space defined by Columns B and C, Rows 3 and 4.				Detector failed.
Grid Spacer 8	210 cm below cold leg centerline, 286 cm above bottom of heated length.				
TFC-8AB-23	Thermocouple in space defined by Columns A and B, Rows 2 and 3.			41,42	
Grid Spacer 10	130 cm below cold leg centerline, 366 cm above bottom of heated length.				
TFC-10AB-45	Thermocouple in space defined by Columns A and B, Rows 4 and 5.			43,44	Data appear normal, but data acquisition system noise caused a stepping of 1.5% of full scale.
ECC System		0 to 1533 K	0 to 820 K		
TFV-ECC+LP	In ECC line leading to vessel lower plenum, 49 cm from vessel center.			45,46	Data appear normal, but data acquisition system noise caused a stepping of 1.5% of full scale.
Steam Generator		0 to 1533 K	0 to 820 K		
Intact Loop					
TFI-SGFW	In feedwater line leading to steam generator.			47,48	Data appear normal, but data acquisition system noise caused a stepping of 1.5% of full scale.
TFI-SD	In steam generator steam dome, 320 cm above bottom of tube sheet.			49,50	Data appear normal, but data acquisition system noise caused a stepping of 1.5% of full scale.
Pressure Suppression System		0 to 1533 K	0 to 820 K		
TFB-PS43	43 cm above bottom of suppression tank.			51,52	
TFB-PS330	330 cm above bottom of suppression tank.			51,52	

POOR ORIGINAL

507 083

TABLE IV (continued)

Measurement	Location and Comments[a]	Data Acquisition Range[a]: Detector	Data Acquisition Range[a]: System	Figure[a]	Measurement Comments[b]
MATERIAL TEMPERATURE	Chromel-Alumel thermocouples unless specified otherwise.				
Intact Loop		0 to 1533 K	0 to 820 K		
TMI-1T16	Hot leg, Spool 1, top, 1.6 mm from pipe inside diameter (ID) 68 cm from vessel center.			53,54	
TMI-17S16	Cold leg, Spool 17, side, 1.6 mm from pipe ID, 68 cm from downcomer center.			53,54	
Broken Loop		0 to 1533 K	0 to 820 K		
TMB-20B16	Hot leg, Spool 20, bottom, 1.6 mm from pipe ID, 91 cm from vessel center.			55,56	
TMB-40B16	Cold leg, Spool 40, bottom, 1.6 mm from pipe ID, 202 cm from downcomer center.			57,58	
TMB-45B16	Cold leg, Spool 45, bottom, 1.6 mm from pipe ID, 98 cm from downcomer center.			57,58	
Downcomer		0 to 1533 K	0 to 820 K		Data appear normal, but data acquisition system noise caused a stepping of 1.5% of full scale.
TMD-18E	On downcomer inlet annulus, 18 cm below cold leg centerline at 35°.			59,60	
TMD-152	On downcomer extension, 152 cm below cold leg centerline.			59,60	
TMD-294	On downcomer extension, 294 cm below cold leg centerline.				Detector failed.
TMD-364	On downcomer extension, 364 cm below cold leg centerline.			59,60	
Downcomer Insulator		0 to 1533 K	0 to 820 K		
TIMD-18E	On downcomer inlet annulus insulator, 18 cm below cold leg centerline at 225°.			61,62	
TIMD-152	On downcomer extension insulator, 152 cm below cold leg centerline.			61,62	
TIMD-294	On downcomer extension insulator, 294 cm below cold leg centerline.			61,62	
TIMD-364	On downcomer extension insulator, 364 cm below cold leg centerline.			61,62	
Vessel		0 to 1533 K	0 to 820 K		
TMV+221E	In vessel on upper head filler, 221 cm above cold leg centerline at 35°.			63,64	
TMV+79D	In vessel on upper plenum upper filler, 79 cm above cold leg centerline at 45°.			63,64	
Guide Tube		0 to 1533 K	0 to 820 K		
TGMV+280	On guide tube, 280 cm above cold leg centerline.			65,66	
TGMV-61	On guide tube, 61 cm below cold leg centerline.			65,66	
Steam Generator		0 to 1533 K	0 to 820 K		
Intact Loop					
TMI-SGT61	On a steam generator tube, 61 cm above bottom of tube sheet on OD of tube.			67,68	Data appear normal, but data acquisition system noise caused a stepping of 1.5% of full scale.
Broken Loop		0 to 1533 K	0 to 820 K		
TMB-SGT734	On steam generator tube, 787 cm above bottom of tube sheet on OD of tube.			69,70	
CORE HEATER CLADDING TEMPERATURE	Chromel-Alumel thermocouples.				
High Power Heaters		0 to 1533 K	0 to 1580 K		
TH-B3-180 TH-B3-226 TH-B3-353	Heater at Column B, Row 3. Thermocouples 180 cm (225°), 226 cm (270°), and 353 cm (210°) above bottom of heated length.			71,72 71,72 71,72	

POOR ORIGINAL

507 089

TABLE IV (continued)

Measurement	Location and Comments[a]	Data Acquisition Range[a]: Detector	Data Acquisition Range[a]: System	Figure[a]	Measurement Comments[b]
High Power Heaters (continued)					
TH-C2-8 TH-C2-164 TH-C2-180 TH-C2-227 TH-C2-321	Heater at Column C, Row 2. Thermocouples 8 cm (285°), 164 cm (0°), 180 cm (225°), 227 cm (210°), and 321 cm (210°) above bottom of heated length.			73,74 73,74 73,74 73,74 73,74	
TH-C3-49 TH-C3-115 TH-C3-184 TH-C3-196 TH-C3-230	Heater at Column C, Row 3. Thermocouples 49 cm (135°), 115 cm (165°), 184 cm (285°), 196 cm (225°), and 230 cm (0°) above bottom of heated length.			75,76 75,76 75,76 75,76 75,76	
TH-D2-10 TH-D2-134 TH-D2-166 TH-D2-179 TH-D2-254	Heater at Column D, Row 2. Thermocouples at 10 cm (150°), 134 cm (45°), 166 cm (150°), 179 cm (45°), and 254 cm (15°) above bottom of heated length.			77,78 77,78 77,78 77,78 77,78	
TH-D3-71 TH-D3-132 TH-D3-206 TH-D3-326	Heater at Column D, Row 3. Thermocouples 71 cm (15°), 132 cm (0°), 206 cm (120°), and 326 cm (120°) above bottom of heated length.			79,80 79,80 79,80 79,80	
Low Power Heaters		0 to 1533 K	0 to 1580 K		
TH-A3-208 TH-A3-229 TH-A3-291	Heater at Column A, Row 3. Thermocouples 208 cm (165°), 229 cm (315°), and 291 cm (180°) above bottom of heated length.			81,82 81,82 81,82	
TH-A4-40 TH-A4-108 TH-A4-181 TH-A4-191	Heater at Column A, Row 4. Thermocouples 40 cm (195°), 108 cm (225°), 181 cm (300°), and 191 (210°) above bottom of heated length.			83,84 83,84 83,84 83,84	
TH-A5-164 TH-A5-179 TH-A5-252	Heater at Column A, Row 5. Thermocouples 164 cm (300°), 179 (180°), and 252 cm (165°), above bottom of heated length.			85,86 85,86 85,86 85,86	
TH-B1-321	Heater at Column B, Row 1. Thermocouple 321 cm (270°) above bottom of heated length.			87,88	
TH-D1-178 TH-D1-251	Heater at Column D, Row 1. Thermocouples 178 cm (110°) and 251 (270°) above bottom of heated length.			89,90 89,90	
TH-D5-137 TH-D5-179 TH-D5-254 TH-D5-322	Heater at Column D, Row 5. Thermocouples 137 cm (35°), 179 cm (90°), 254 cm (45°), and 322 cm (75°) above bottom of heated length.			91,92 91,92 91,92 91,92	
TH-E1-252 TH-E1-321	Heater at Column E, Row 1. Thermocouples 252 cm (120°), and 321 cm (180°) above bottom of heated length.			93,94 93,94	
TH-E2-109 TH-E2-190 TH-E2-353	Heater at Column E, Row 2. Thermocouples 109 cm (30°), 190 cm (15°), and 353 cm (300°) above bottom of heated length.			95,96 95,96 95,96	
TH-E3-134 TH-E3-207 TH-E3-223 TH-E3-290	Heater at Column E, Row 3. Thermocouples 134 cm (135°), 207 cm (300°), 223 (90°), and 290 cm (300°) above bottom of heated length.			97,98 97,98 97,98 97,98	
TH-E4-180 TH-E4-354	Heater at Column E, Row 4. Thermocouples 180 cm (60°) and 354 cm (45°) above bottom of heated length.			99,100 99,100	
TH-E5-227	Heater at Column E, Row 5. Thermocouple 227 cm (120°) above bottom of heated length.			101,102	
PRESSURE					
Intact Loop					
PI-16	Cold leg, Spool 16, 144 cm from downcomer center (tee off DP tap).	0 to 17.237 MPa	0 to 20.79 MPa	103,104	
PI-17AL	Cold leg, Spool 17, 60 cm from downcomer center (low range).	0 to 3.447 MPa	0 to 3.45 MPa	103,104	Data acquisition system saturated to t = 21 s.
Broken Loop		0 to 17.237 MPa			
PB-20B	Hot leg, Spool 20, 84 cm from vessel center.		0 to 21.08 MPa	105,106	
PB-40B	Cold leg, Spool 40, 209 cm from downcomer center.		0 to 21.96 MPa	[illegible]	

TABLE IV (continued)

Measurement	Location and Comments[a]	Data Acquisition Range[a]: Detector	Data Acquisition Range[a]: System	Figure[a]	Measurement Comments[b]
Broken Loop (continued)					
PB-44-6A	Cold leg, Spool 44, downcomer side nozzle throat, 125 cm from downcomer center, 0°.		0 to 20.85 MPa	109,110	
PE-45A	Cold leg, Spool 45, 90 cm from downcomer center, 0°.		0 to 20.77 MPa	111,112	
Vessel		0 to 17.237 MPa			
PV-13	In vessel hot leg extension, 13 cm below cold leg centerline (tee off DP tap).		0 to 21.00 MPa	113,114	
PV-442	In vessel, 442 cm below cold leg centerline.		0 to 20.67 MPa	113,114	
ECC System					
PV-ACC1	In accumulator for vessel.	0 to 6.895 MPa	0 to 8.53 MPa	115,116	
Steam Generator		0 to 17.237 MPa			
Intact Loop					
PI-SD	Intact loop steam generator, secondary side steam dome.		0 to 21.02 MPa	117,118	
Broken Loop					
PB-SD	Broken loop steam generator, secondary side steam dome.		0 to 21.34 MPa	117,118	
Pressurizer		0 to 17.237 MPa			
PI-PRIZE	Pressurizer steam dome.		0 to 22.83 MPa	119,120	
Pressure Suppression System		0 to 0.689 MPa			
PB-PSS	Suppression tank top.		0 [illegible] 5 MPa	121,122	
DIFFERENTIAL PRESSURE	Elevation difference between transducer taps is zero unless specified otherwise.				
Intact Loop					
DI-13V-1A	From vessel lower section of upper plenum, 13 cm below cold leg centerline to hot leg, Spool 1, 60 cm from vessel center. Lower upper plenum tap is 35 cm below Spool 1 tap.	±127 cm water	±16.78 kPa	123, 124	
DI-1A-6	Hot leg, Spool 1, 60 cm from vessel center to hot leg, Spool 6, 271 cm from vessel center.	±256 cm water	±33.76 kPa	125,126	
DI-6-7	Hot leg, Spool 6, 27_ cm from vessel center to cold leg, Spool 7, 927 cm from downcomer center. Spool 6 tap is 47 cm above Spool 7 tap.	±345 kPa	±345 kPa	127,128	
DI-SGI-SGO	Intact loop steam generator, inlet plenum to outlet plenum, across primary side tubes.	±254 cm water	±33.49 kPa	129,130	
DI-7-13	Cold leg, Spool 7, 927 cm from downcomer center to primary pump suction, Spool 13, 332 cm from downcomer center.	±254 cm water	±33.42 kPa	131,132	
DI-13-15	Cold leg, Spool 13, 332 cm from downcomer center, across primary pump to cold leg, Spool 15, 175 cm from downcomer center. Spool 13 tap is 25 cm below Spool 15 tap.	±690 kPa	±690 kPa	133,134	
DI-15-17A	Cold leg, Spool 15, 175 cm from downcomer center, across cold leg injection port to cold leg, Spool 17, 60 cm from downcomer center.	±254 cm water	±34.0 kPa	135,136	
DI-17A-DIA	Cold leg, Spool 17, 60 cm from downcomer to downcomer inlet annulus, 30 cm above cold leg centerline. Spool 17 tap is 30 cm below DIA tap.	±254 cm water	±33.6 kPa	137,138	
Broken Loop					
DB-13V-20B	In vessel from lower section of upper plenum, 13 cm below cold leg centerline to hot leg, Spool 20, 22 cm above cold leg centerline, 84 cm from vessel center. 13V tap is 35 cm below Spool 20 tap.	±762 cm water	±105 kPa	139,140	

POOR ORIGINAL

507 091

TABLE IV (continued)

Measurement	Location and Comments[a]	Data Acquisition Range[a] Detector	System	Figure[a]	Measurement Comments[b]
Broken Loop (continued)					
DB-20B-21	Hot leg, Spool 20, 84 cm from vessel center to hot leg, Spool 21, 220 cm from vessel center.	±762 cm water	±100 kPa	141,142	
DB-21-27A	Hot leg, Spool 21, 220 cm from vessel center to cold leg, Spool 27, 897 cm is 4 cm above Spool 27A tap.	±345 kPa	±344 kPa	143,144	Data acquisition system saturated from t = 0 to t = 2.2 s, from t = 5.0 to 8.2 s, and from 8.5 to 14.8 s
DB-SGI-SGO	Broken loop steam generator inlet leg, 382 cm from vessel center across primary side tubes to steam generator outlet leg, 951 cm from downcomer center. SGI tap is 72 cm above SGO tap.	±1380 kPa	±1381 kPa	145,146	
DB-27A-37A	Cold leg, Spool 27, 897 cm from downcomer center across broken loop pump suction to Spool 37, 348 cm from downcomer center. Spool 27 tap is 81 cm above Spool 37 tap.	±1270 cm water	±170 kPa	147,148	
DB-37A-40B	Cold leg, Spool 37, broken loop pump inlet, 348 cm from downcomer center to cold leg, Spool 40 pump discharge, 209 cm from downcomer center. Spool 37 tap is 68 cm below Spool 40 tap.	±6895 kPa	±9223 kPa	149,150	
DB-37A-40C	Cold leg, Spool 37, broken loop pump inlet, 348 cm from downcomer center to cold leg, Spool 40 pump discharge 209 cm from downcomer center. Spool 37 tap is 68 cm below Spool 40 tap (low range).	±690 kPa	±710 kPa	151,152	Data acquisition system saturated from t = 0 to t = 34 s.
DB-40B-43A	Cold leg, Spool 40 pump discharge, 209 cm from downcomer center across noncommunicative break nozzle and rupture assembly to cold leg, Spool 43, 180 cm from downcomer center.	±10 342 kPa	±13 799 kPa	153,154	Data acquisition system saturated from -20 to to t = 0 s.
DB-40B-45A	Cold leg, Spool 40 pump discharge, 209 cm from downcomer center across noncommunicative break nozzle to cold leg, Spool 45, 89 cm from downcomer center.	±234 cm water	±33.75 kPa	155,156	Data acquisition system saturated to t = 0 s.
DB-45A-43	Cold leg, Spool 45, 89 cm from downcomer across noncommunicative break nozzle to cold leg, Spool 43, 180 cm from downcomer center.	±10 342 kPa	±13 782 kPa	157,158	Data acquisition system saturated to t = 0 s.
DB-45A-DIA	Cold leg, Spool 45, 89 cm from downcomer center to downcomer inlet annulus, 30 cm above cold leg centerline. Spool 45 tap is 30 cm below DIA tap.	±690 kPa	±690 kPa	159,160	
Downcomer					
DD-DIA-13A	Downcomer inlet annulus, 30 cm above cold leg centerline to vessel lower upper plenum, 13 cm below cold leg centerline. Elevation difference between taps is 43 cm.	±345 kPa	±342 kPa	161,162	
DD-DIA-170	Downcomer inlet annulus, 30 cm above cold leg centerline to downcomer extension, 170 cm below cold leg centerline. Elevation difference between taps is 200 cm.	±762 cm water	±102 kPa	163,164	
DD-DIA-578	Downcomer inlet annulus, 30 cm above cold leg centerline to vessel lower head, 578 cm below cold leg centerline. Elevation difference between taps is 608 cm.	±1270 cm water	±174 kPa	165,166	
DD-170-435	Downcomer extension, 170 cm below cold leg centerline to downcomer instrumented spool piece, 435 cm below cold leg centerline. Elevation difference between taps is 265 cm.	±762 cm water	±104 kPa	167,168	
DD-435-578	Downcomer instrumented spool piece, 435 cm below cold leg centerline to vessel lower head, 578 cm below cold leg centerline. Elevation difference between taps is 143 cm.	±254 cm water	±33.54 kPa	169,170	

TABLE IV (continued)

Measurement	Location and Comments[a]	Data Acquisition Range[a]: Detector	Data Acquisition Range[a]: System	Figure[a]	Measurement Comments[b]
Downcomer (continued)					
DV-578-501	Vessel lower head, 578 cm below cold leg centerline to lower core region, 501 cm below cold leg centerline. Elevation difference between taps is 77 cm.	±127 cm water	±31.8 kPa	171,172	
DV-578-13	Vessel lower head, 578 cm below cold leg centerline to lower section of upper plenum, 13 cm below cold leg centerline. Elevation difference between taps is 565 cm.	±690 kPa	±687 kPa	173,174	
DV-501-442	Vessel lower core region, 501 cm below cold leg centerline to lower core region, 442 cm below cold leg centerline. Elevation difference between taps is 59 cm.	±254 cm water	±34.2 kPa	175,176	
DV-501-105	Vessel lower core region, 501 cm below cold leg centerline to heater rod ground hub, 105 cm below cold leg centerline. Elevation difference between taps is 396 cm.	±762 cm water	±107 kPa	177,178	
DV-501-13A	Vessel lower plenum extension, 501 cm below cold leg centerline to lower upper plenum, 13 cm below cold leg centerline. Elevation difference between taps is 488 cm.	+345 kPa	±345 kPa	179,180	
DV-442-278	Vessel lower core region, 442 cm below cold leg centerline, to mid-core region, 278 cm below cold leg centerline. Elevation difference between taps is 164 cm.	±1270 cm water	±168.8 kPa	181,182	
DV-278-154	Vessel mid-core region, 278 cm below cold leg centerline [illegible] upper core region 154 cm below [illegible] leg centerline. Elevation dif[illegible]ence between taps is 124 cm.	±1270 cm water	±172 kPa	183,184	
DV-105-13	Heater rod ground hub, 105 cm below cold leg centerline to lower section of upper plenum, 13 cm below cold leg centerline elevation difference between taps is 92 cm.	±762 cm water	±101 kPa	185,186	
DV+421+154	Vessel top head, 421 cm above cold leg centerline to core support tube, 154 cm above cold leg centerline. Elevation difference between taps is 267 cm.	±762 cm water	± 99.89 kPa	187,188	
DV+159-105	Lower section of vessel upper head extension, 159 cm above cold leg centerline to heater ground rod hub, 105 cm below cold leg centerline. Elevation difference between taps is 264 cm.	±2032 cm water	±266.7 kPa	189,190	Data acquisition system saturated from 13.8 to 14.8 s.
DV+154-105	Core support tube, 154 cm above cold leg centerline to heater ground rod hub, 105 cm below cold leg centerline. Elevation difference between taps is 259 cm.	±762 cm water	±102.8 kPa	191,192	Data acquisition system near or saturated from 13 to 16 s.
ECC System					
DV-ACC1-LL	Top to bottom of vessel accumulator. Elevation difference between taps is 284 cm.	±762 cm water	±104 kPa	193,194	
Steam Generator					
DI-SG-LL	Liquid level for intact loop steam generator. Elevator difference between taps is 206 cm.	±1270 cm water	±166 kPa	195,196	
DB-651-884	Liquid level for broken loop steam generator. Elevation difference between taps is 1067 cm.	±1270 cm water	±168.6 kPa	197,198	
VOLUMETRIC FLOW RATE	Turbine flowmeter, bidirectional.				Data acquisition system range may exceed rated detection range; however, turbine response is linear to flow rates well beyond the rated range.

POOR ORIGINAL

507 093

TABLE IV (continued)

Measurement	Location and Comments[a]	Data Acquisition Range[a] Detector	System	Figure[a]	Measurement Comments[b]
Intact Loop	3-in. Schedule 160 pipe.				
FI-1	Hot leg, Spool 1, 38 cm from vessel center.	±2.52 to ±25.2 l/s	±80 l/s	199,200	
FI-11	Cold leg, Spool 11, 429 cm from downcomer center.	±2.52 to ±25.2 l/s	±100 l/s	199,200	
FI-16	Cold leg, Spool 16, 145 cm from downcomer center.	±5.05 to ±50.5 l/s	±100 l/s	201,202	
FI-17	Cold leg, Spool 17, 38 cm from downcomer center.	±2.52 to ±25.2 l/s	±100 l/s	201,202	
Broken Loop					
FB-20	Cold leg, Spool 20, 100 cm from vessel center.	±2.52 to ±25.2 l/s	±60 l/s	203,204	
FB-37	Cold leg, Spool 37, 316 cm from downcomer center.	±2.52 to ±25.2 l/s	±60 l/s	203,204	
FB-40	Cold leg, Spool 40, 193 cm from downcomer center.	±2.52 to ±25.2 l/s	±80 l/s	205,206	
FB-45	Hot leg, Spool 45, 110 cm from downcomer center.	±2.52 to ±25.2 l/s	±80 l/s	205,206	
Downcomer					
FD-424	In downcomer, upstream of instrumented spool piece, 424 cm below cold leg centerline.	±2.52 to ±25.2 l/s	±40 l/s	207,208	
Vessel					
FV*	Core exit, 1 cm above cold leg centerline.	±2.52 to ±25.2 l/s	±80 l/s	209,210	
ECC System					
FV-HPIS	In line immediately after HPIS pump for vessel, 1/2-in. line.	±0.0316 to ±0.315 l/s	±0.10 l/s	211,212	
FV-LPIS	In line leading from LPIS pump for vessel, 1/2-in. line.	±0.042 to ±0.421 l/s	±0.20 l/s	213,214	
FV-ACC1	In line leading from vessel accumulator.	±0.315 to ±3.15 l/s	±5.0 l/s	215,216	
Pressurizer					
FI-PRIZE	In pressurizer surge line.	±0.920 to ±8.20 l/s	±9.0 l/s	217,218	
MOMENTUM FLUX	Drag-screen, bidirectional.				
Broken Loop					
NB-20	Hot leg, Spool 20, 29 cm from vessel center.	±0.05 to ±10.7 N	±16.07 N	219,220	
NB-40	Cold leg, Spool 40, 215 cm from downcomer center.	±0.09 to ±17.8 N	±24.08 N	221,222	
NB-45	Cold leg, Spool 45, 84 cm from downcomer center.	±0.22 to ±44.5 N	±61.71 N	223,224	
Vessel					
NV-9	In vessel lower upper plenum region, 9 cm below cold leg centerline. Drag screen target flow area 34% of flow area.	±0.11 to ±22.2 N	±30.55 N	225,226	
NV-499	In vessel at entrance to heated core, 499 cm below cold leg centerline. Drag screen target area 34% of flow area.	±0.08 to ±15.1 N	±23.54 N	227,228	
DENSITY					
Intact Loop		1.6 to 1600 kg/m^3	0 to 1600 kg/m^3		
GI-1T GI-1B GI-1C	Hot leg, Spool 1, 77 cm from vessel center. T (tangential) ranges 270° to 360°. B (body) ranges 30° to 330°. C is a mathematical composite of T and B.			229,230 229,230 231,232	
GI-5VR	Hot leg, Spool 5, 228 cm from vessel center, vertical.			233,234	

TABLE IV (continued)

Measurement	Location and Comments[a]	Data Acquisition Range[a]: Detector	Data Acquisition Range[a]: System	Figure[a]	Measurement Comments[b]
Intact Loop (continued)					
GI-13T GI-13B GI-13C	Cold leg, Spool 13, 342 cm from downcomer center. T (tangential) ranges 270° to 360°. B (body) ranges 30° to 330°. C is a mathematical composite of T and B.			235,236 235,236 237,238	
GI-17T GI-17B GI-17C	Cold leg, Spool 17, 73 cm from downcomer center. T (tangential) ranges 270° to 360°. B (body) ranges 30° to 330°. C is a mathematical composite of T and B.			239,240 239,240 241,242	
Broken Loop		1.6 to 1600 kg/m³	0 to 1600 kg/m³		
GB-20VR	Hot leg, Spool 20, 64 cm from vessel center, vertical.			243,244	
GB-37	Cold leg, Spool 37, 360 cm from downcomer center.			245,246	
GB-40VR	Cold leg, Spool 40, 230 cm from downcomer vertical.			247,248	
GB-45VR	Cold leg, Spool 45, 66 cm from downcomer vertical.			249,250	
Downcomer		1.6 to 1600 kg/m³	0 to 1600 kg/m³		
GD-72B	Downcomer, 72 cm below cold leg centerline. B (body) ranges 30° to 330°.			251,252	
GD-260B	Downcomer, 260 cm below cold leg centerline. B (body) ranges 30° to 330°.			253,254	
GD-456B	Downcomer, 456 cm below cold leg centerline. B (body) ranges 30° to 330°.			255,256	
Vessel		1.6 to 1600 kg/m³	0 to 1600 kg/m³		
GV+339	Vessel at top of control rod guide tube, 339 cm above cold leg centerline.			257,258	
GV+174	Vessel at top of core support tube, 174 cm above cold leg centerline.			259,260	Questionable data. Analysis of beam path indicated possible obstruction by thermocouple or heater rod. Effect is unknown. To be used for trend only.
GV-11	Vessel at base of core flow instrument housing, 11 cm below cold leg centerline.			261,262	
GV-154-23	Near top of core heated length, 154 cm below cold leg centerline between heater rod Rows 2 and 3.			263,264	Questionable data. Analysis of beam path indicated possible obstruction by thermocouple or heater rod. Effect is unknown. To be used for trend only.
GV-164-AB	Near top of core heated length, 164 cm below cold leg centerline between heater rod Columns A and B.			263,264	Questionable data. Analysis of beam path indicated possible obstruction by thermocouple or heater rod. Effect is unknown. To be used for trend only.
GV-243-23	Upper part of core heated length, 243 cm below cold leg centerline between heater rod Rows 2 and 3.			265,266	
GV-313-23	Near center of core heated length, 313 cm below cold leg centerline between heater rod Rows 2 and 3.			267,268	Questionable data. Analysis of beam path indicated possible obstruction by thermocouple or heater rod. Effect is unknown. To be used for trend only.
GV-323-AB	Near center of core heated length, 323 cm below cold leg centerline between heater rod Columns A and B.			267,268	
GV-383-23	Lower part of core heated length, 383 cm below cold leg centerline between heater rod Rows 2 and 3.			269,270	Questionable data. Analysis of beam path indicated possible obstruction by thermocouple or heater rod. Effect is unknown. To be used for trend only.
GV-483-23	At bottom of core heated length, 483 cm below cold leg centerline between heater rod Rows 2 and 3.			271,272	

TABLE IV (continued)

Measurement	Location and Comments[a]	Data Acquisition Range[a] Detector	System	Figure[a]	Measurement Comments[b]
Vessel (continued)					
GV-502-AB	At bottom of core heated length, 502 cm below cold leg centerline between heater rod Columns A and B.				Detector failed.
GV-528-588	Vessel lower head, 528 cm below cold leg centerline, at 15° t 588 cm below cold leg centerline at 165°.			273,274	
GV-546-23	In upper part of vessel lower plenum 546 cm below cold leg centerline between heater rod Rows 2 and 3.			275,276	
Pressurizer					
GI-PRIZE	Pressurizer surge line.	1.6 to 1600 kg/m^3	0 to 1600 kg/m^3	277,278	
MASS OW RATE	Mass flow rate obtained by combining density (gamma attenuation technique) with volumetric flow rate (turbine flowmeter) or momentum flux (drag disc).	Range for mass flow is determined from ranges of individual detectors used in calculation.			
Intact Loop					
FI-1, GI-1C	Hot leg, Spool 1.			279,280	
FI-16, GI-17C	Cold leg, Spool 16.			281,282	
FI-17, GI-17C	Cold leg, Spool 17.			283,284	
Broken Loop					
FB-20, GB-20VR NB-20, GB-20VR	Hot Spool 20.			285,286 287,288	
FB-37, GB-37	Cold leg, Spool 37.			289,290	
FB-40, GB-40VR NB-40, GB-40VR	Cold leg, Spool 40.			291,292 293,294	
FB-45, GB-45VR NB-45, GB-45VR	Cold leg, Spool 45.			295,296 297,298	
Downcomer					
FD-424, GD-456B	Instrumented spool piece.			299,300	
Vessel					
FV+1, GV-11	Core outlet.			301,302	
NV-9, GV-11	Core inlet.			303,304	
NV-499, GV-483-23	Core inlet.			305,306	
CORE CHARACTERISTICS					Loose heater rod ground connections, resulted in uncertainties in core power levels of up to 2% of actual power, with a probability of effects being .2% of actual power or less.
High Power Bus					
AH-HI	Core amperage.	0 to 10 000 A	0 to 10 030 A	307,308	
VH-HI	Core voltage.	0 to 400 V	0 to 402 V	309,310	
Low Power Bus					
AH-LO	Core amperage.	0 to 10 000 A	0 to 9330 A	311,312	
VH-LO	Core voltage.	0 to 400 V	0 to 402 V	313,314	
PUMP CHARACTERISTICS					
Intact Loop					
SI-PUMP	Pump speed.	377 rad/s	372 rad/s	315,316	

507 096

POOR ORIGINAL

TABLE IV (continued)

Measurement	Location and Comments[a]	Data Acquisition Range[a] Detector	System	Figure[a]	Measurement Comments[b]
Broken Loop					
[illegible]-PUMP	Pump speed.	3770 rad/s	3770 rad/s	317,318	
[illegible]	Pump power.		20 KW	319,320	

a. Statements at the beginning of a measurement category regarding location and comments, range, and figure apply to all subsequent measurements within the given category unless specified otherwise.

b. Detectors which were subjected to overrange conditions during portions of the test were capable of withstanding these conditions without change in operating or measuring characteristics when the physical conditions were again within the detector range.

POOR ORIGINAL

507 097

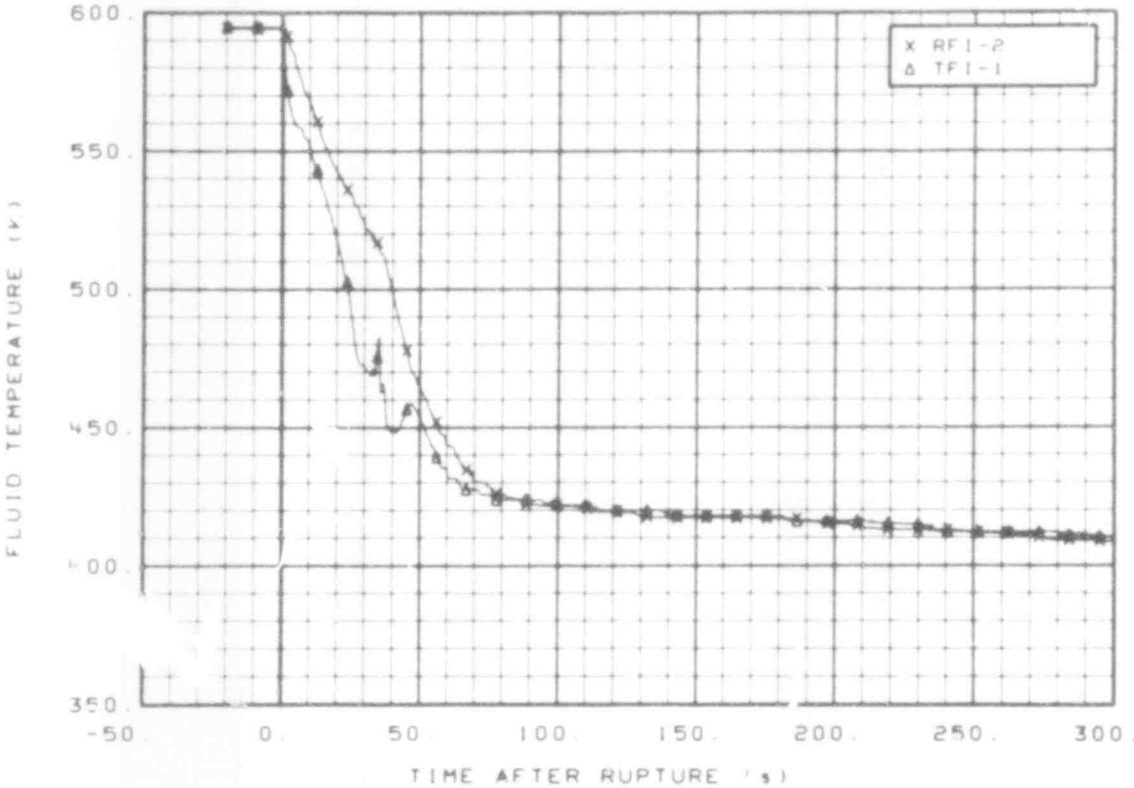

Fig. 11 Fluid temperature in intact loop hot leg (RFI-2 and TFI-1), from -20 to 300 s.

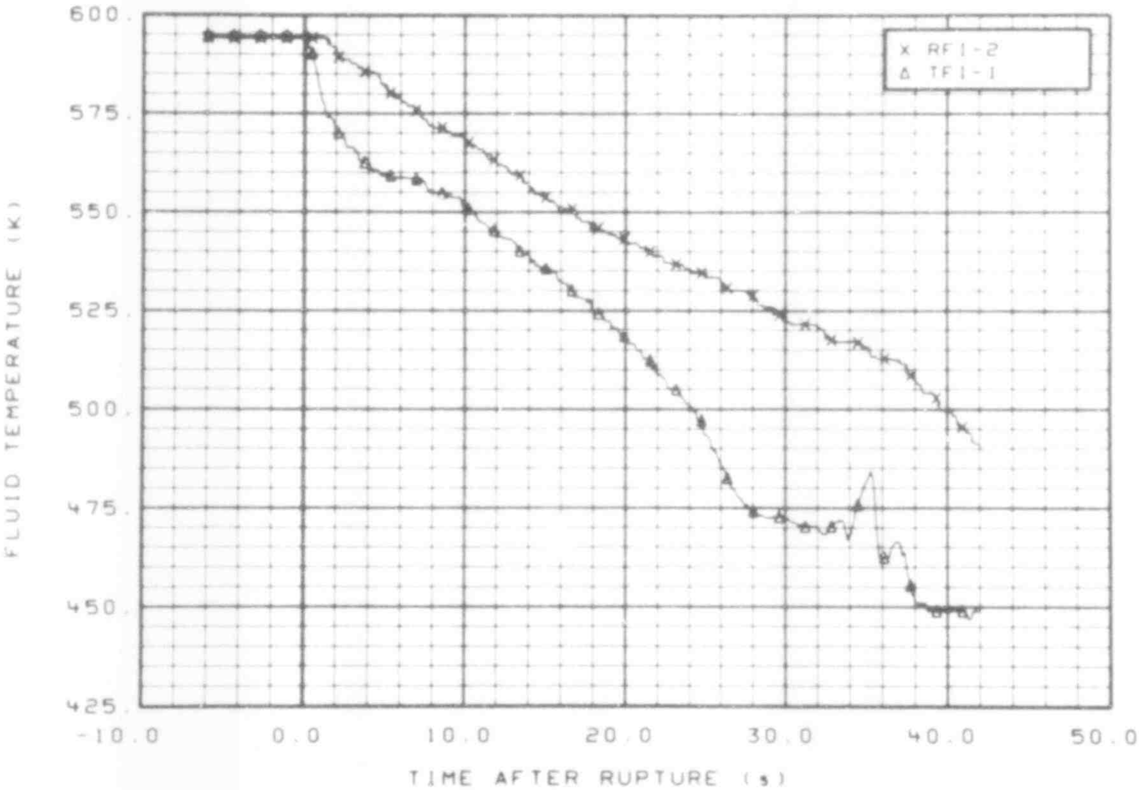

Fig. 12 Fluid temperature in intact loop hot leg (RFI-2 and TFI-1), from -6 to 42 s.

507 098

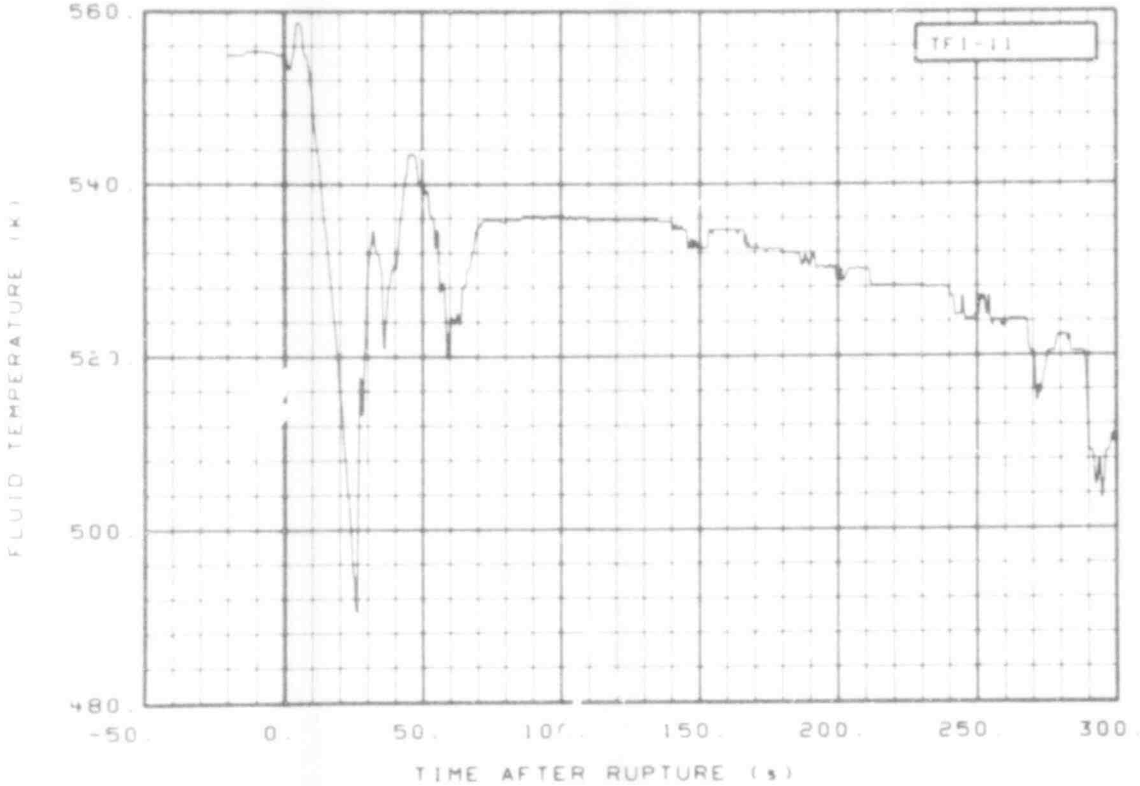

Fig. 13 Fluid temperature in intact loop cold leg (TFI-11), from -20 to 300 s.

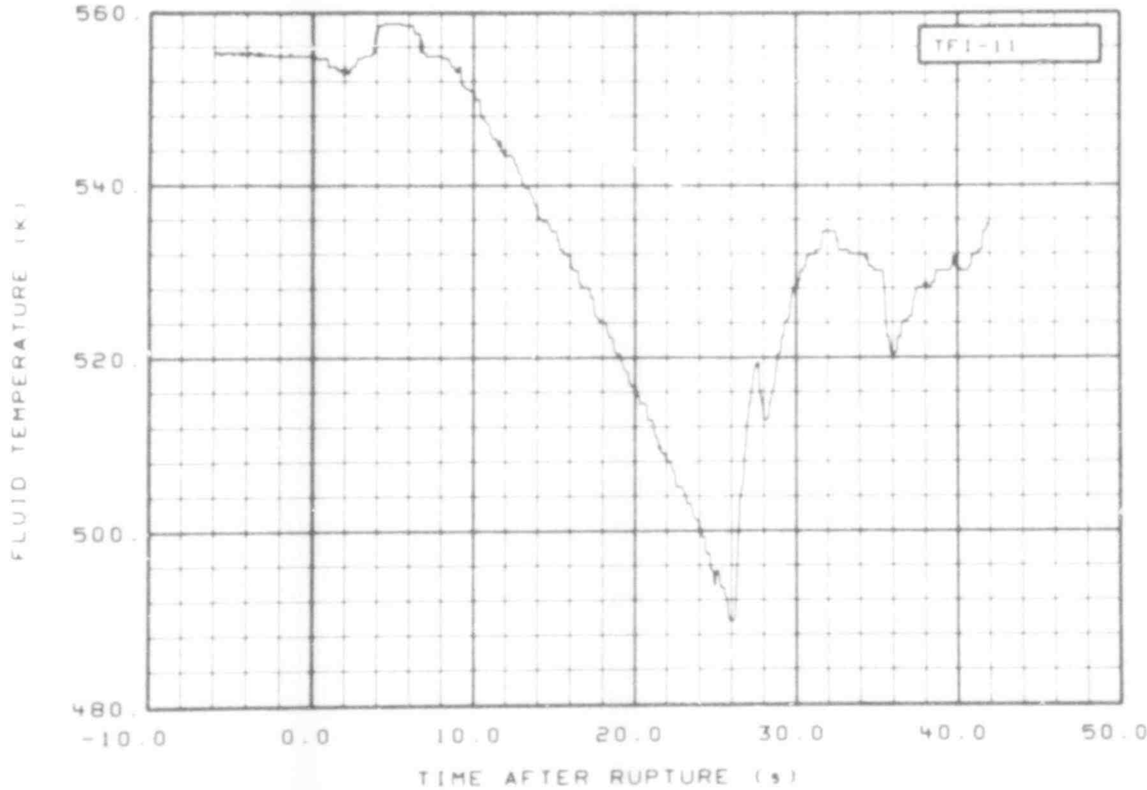

Fig. 14 Fluid temperature in intact loop cold leg (TFI-11), from -6 to 42 s.

507 099

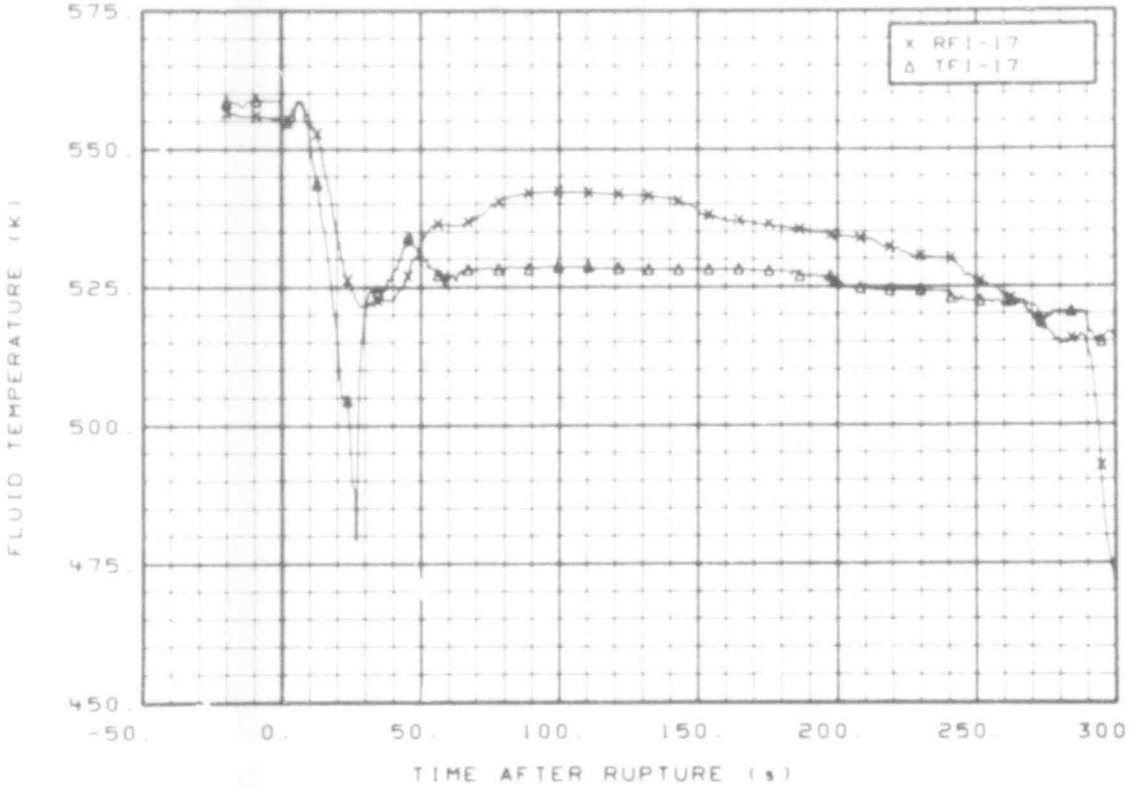

Fig. 15 Fluid temperature in intact loop cold leg (RFI-17 and TFI-17), from -20 to 300 s.

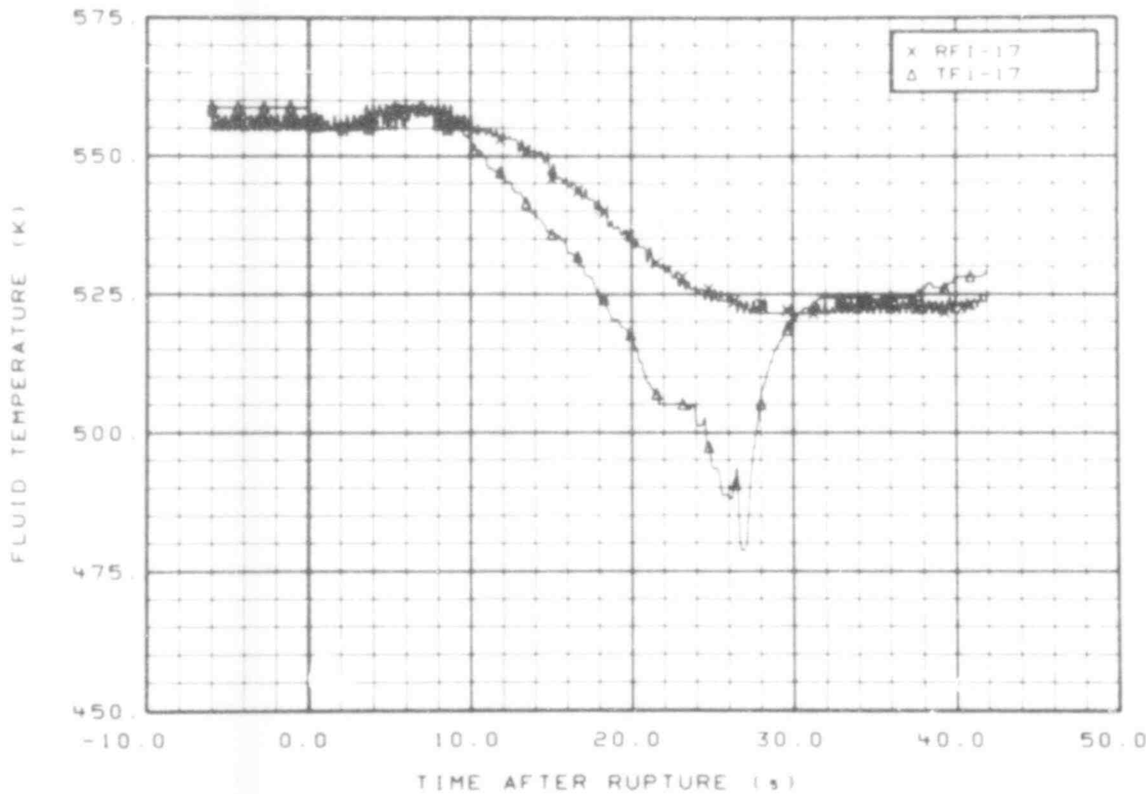

Fig. 16 Fluid temperature in intact loop cold leg (RFI-17 and TFI-17), from -6 to 42 s.

507 100

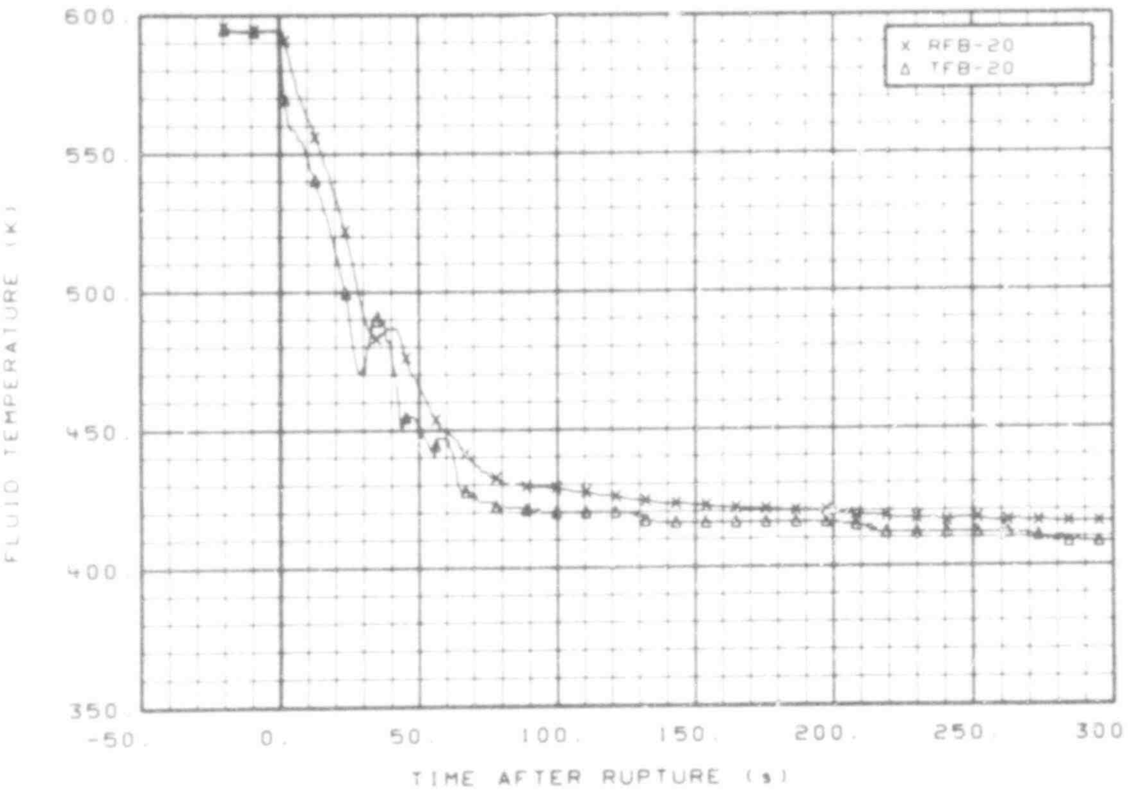

Fig. 17 Fluid temperature in broken loop hot leg (RFB-20 and TFB-20), from -20 to 300 s.

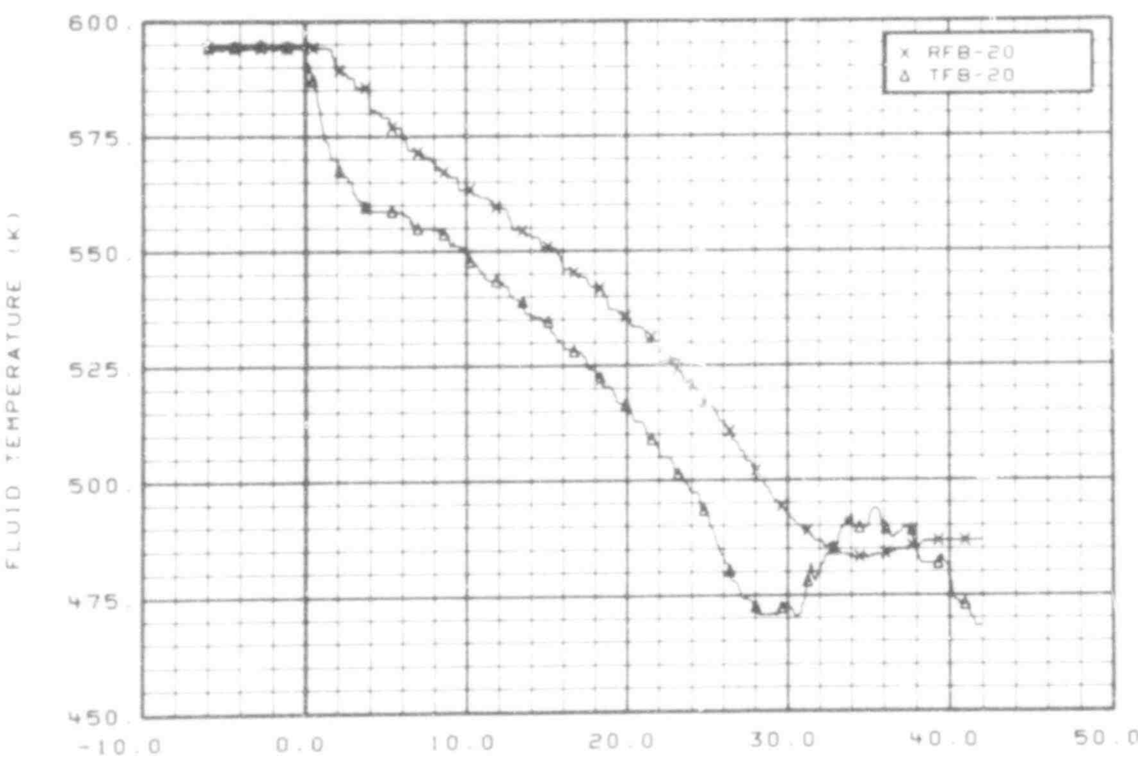

Fig. 18 Fluid temperature in broken loop hot leg (RFB-20 and TFB-20), from -6 to 42 s.

507 101

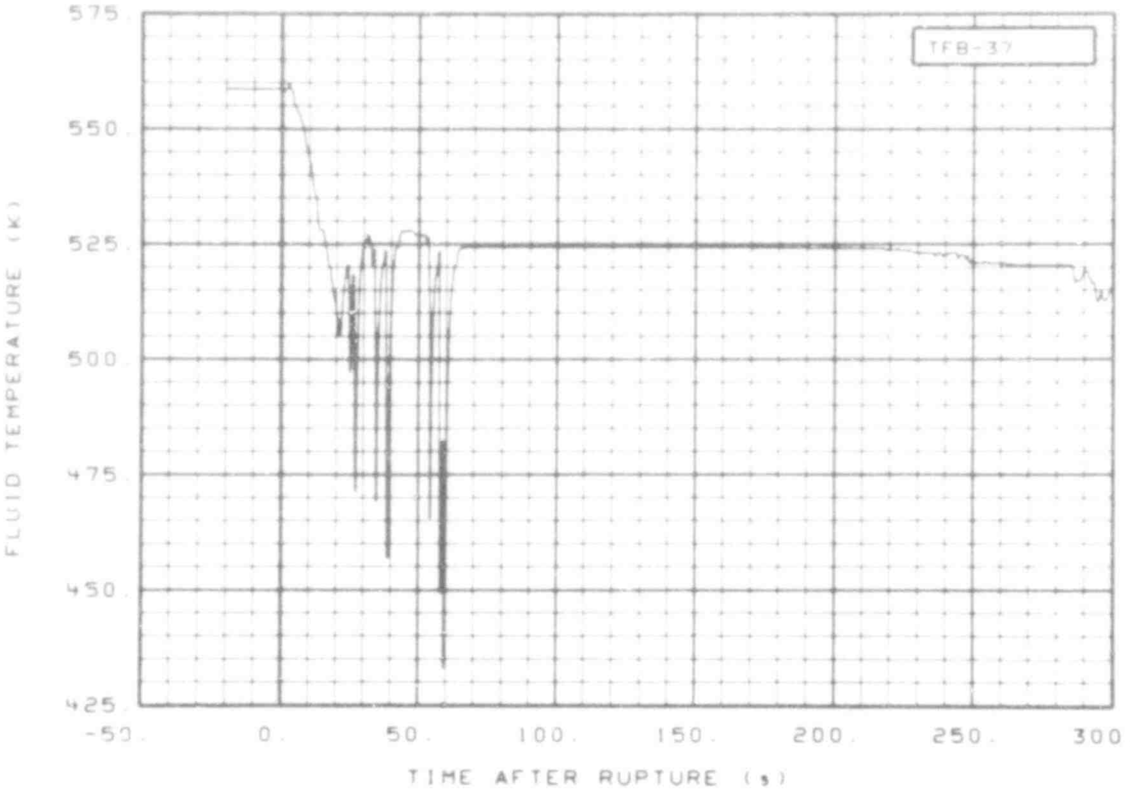

Fig. 19 Fluid temperature in broken loop cold leg (TFB-37), from -20 to 300 s.

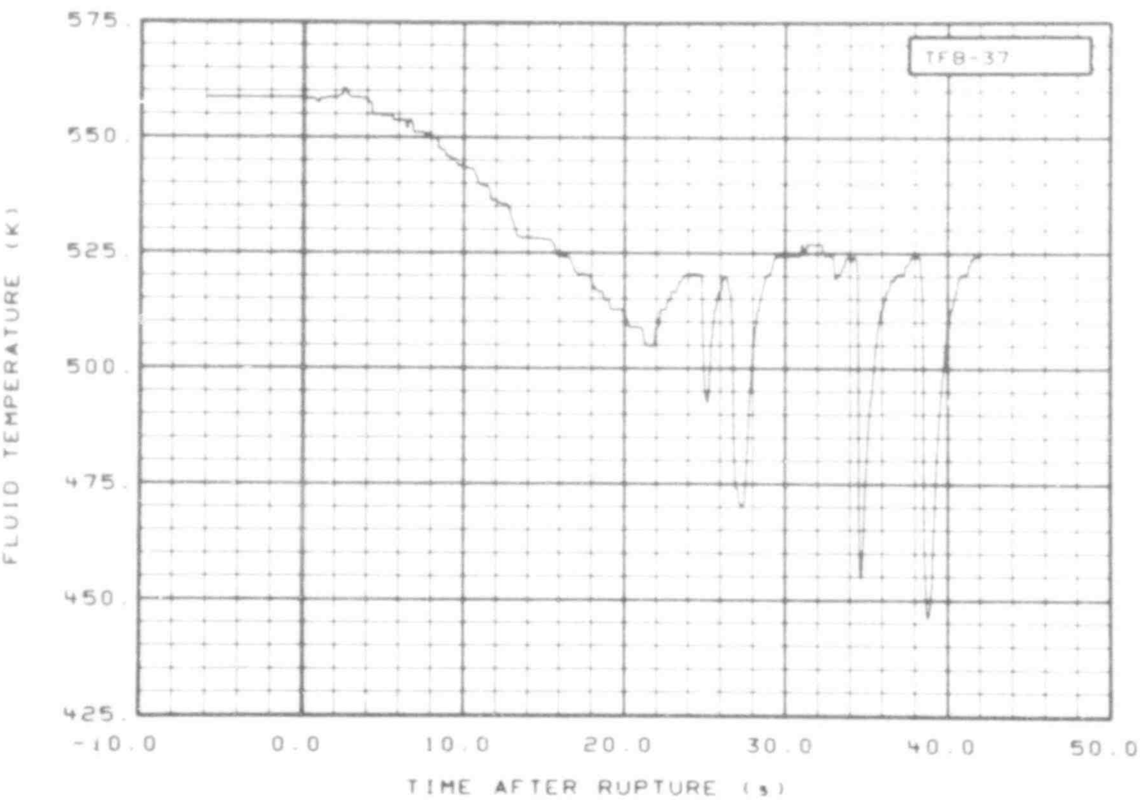

Fig. 20 Fluid temperature in broken loop cold leg (TFB-37), from -6 to 42 s.

507 102

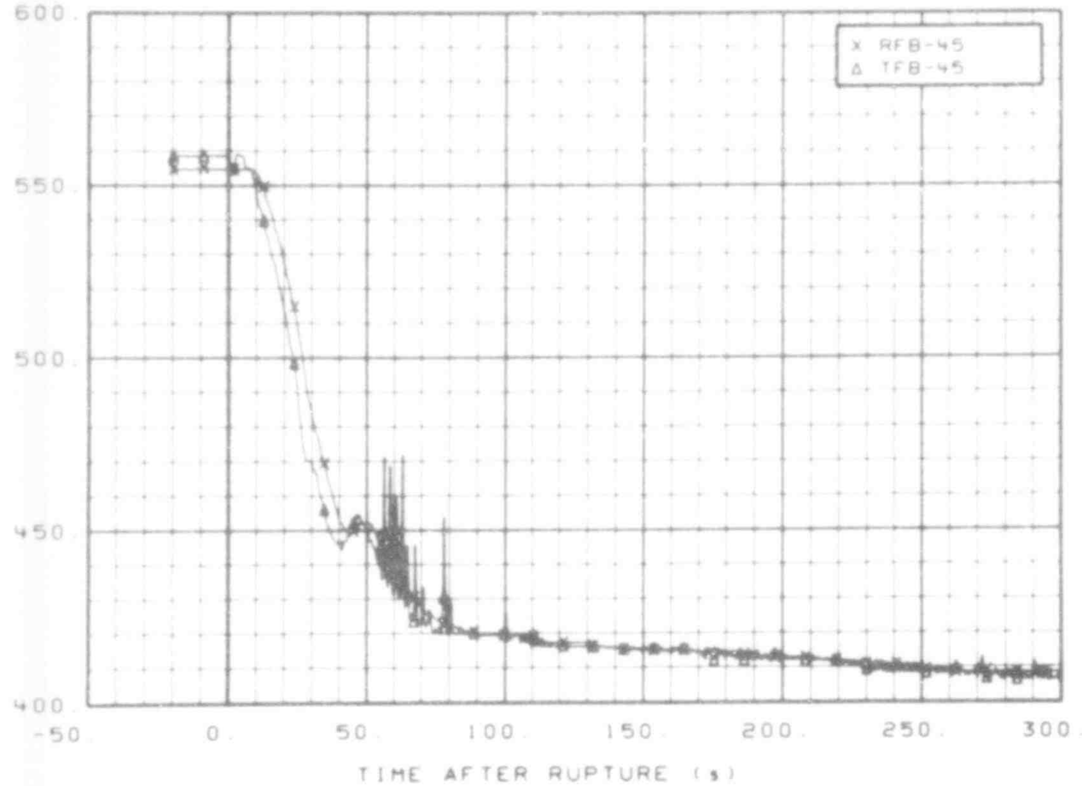

Fig. 21 Fluid temperature in broken loop cold leg (RFB-45 and TFB-45), from -20 to 300 s.

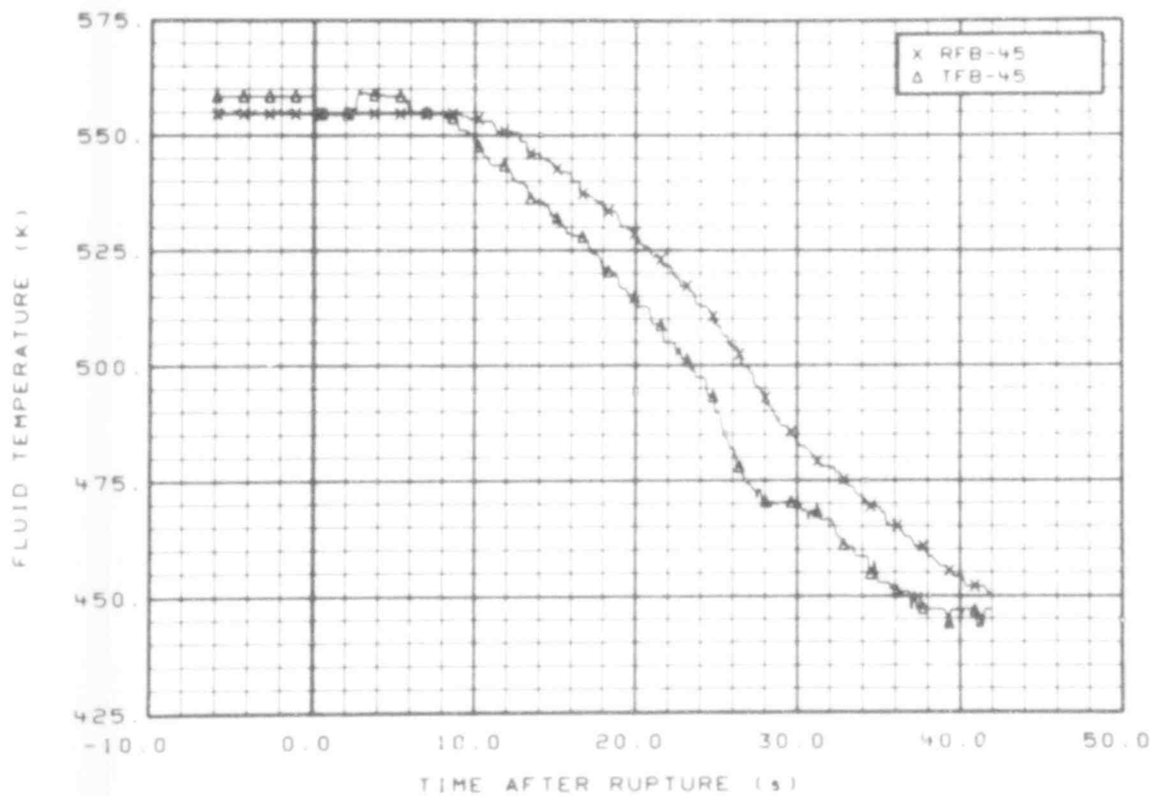

Fig. 22 Fluid temperature in broken loop cold leg (RFB-45 and TFB-45), from -6 to 42 s.

507 103

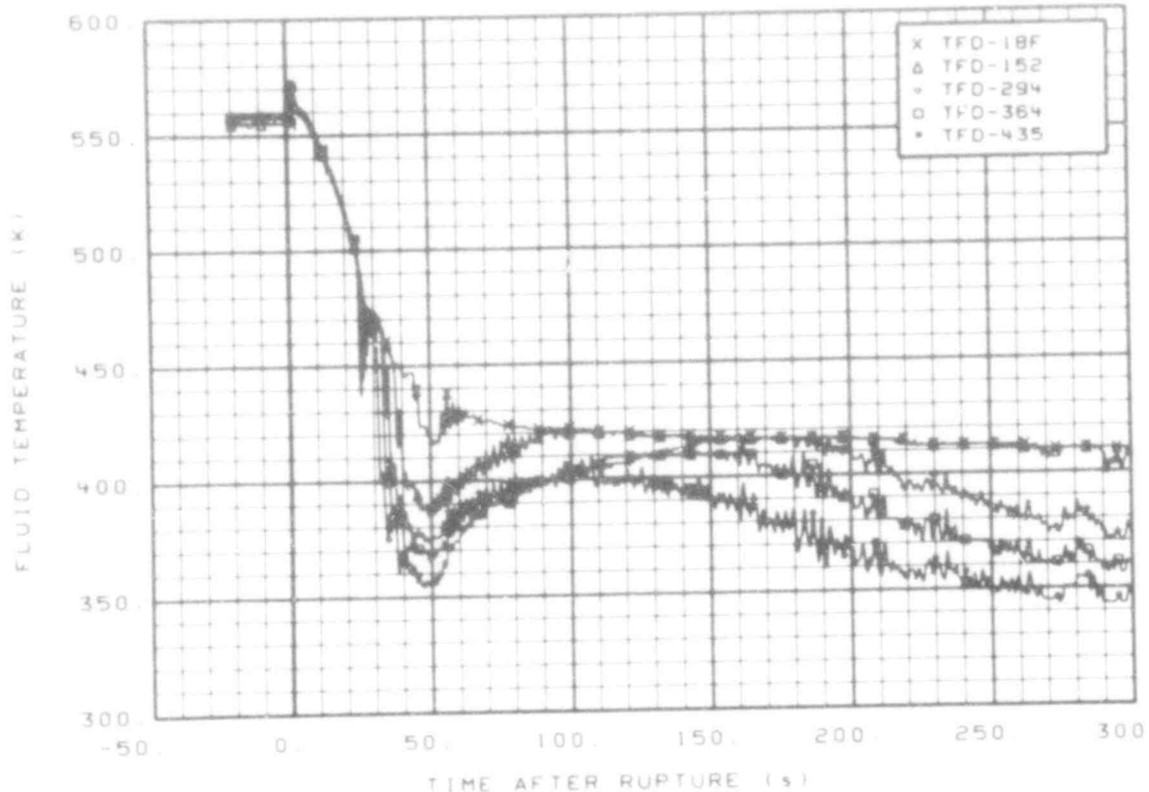

Fig. 23 Fluid temperature in downcomer (TFD-18F, TFD-152, TFD-294, TFD-364, and TFD-435), from -20 to 300 s.

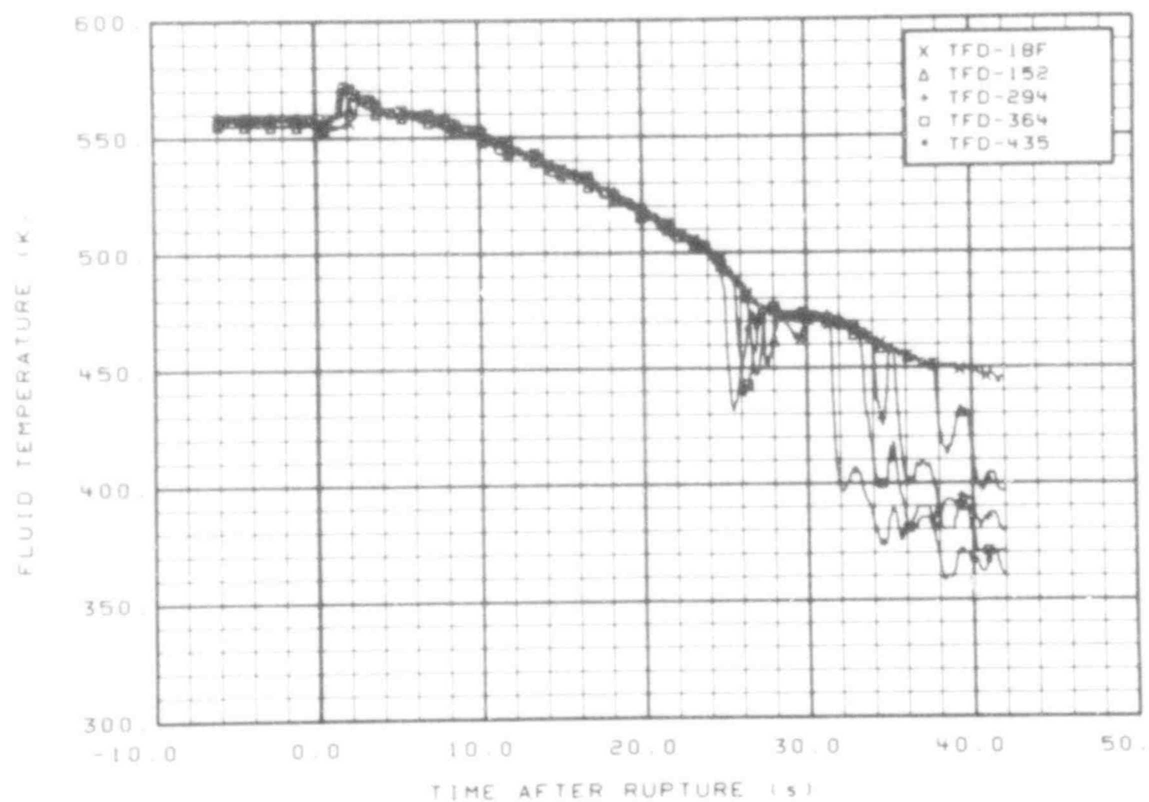

Fig. 24 Fluid temperature in downcomer (TFD-18F, TFD-152, TFD-294, TFD-364, and TFD-435), from -6 to 42 s.

507 104

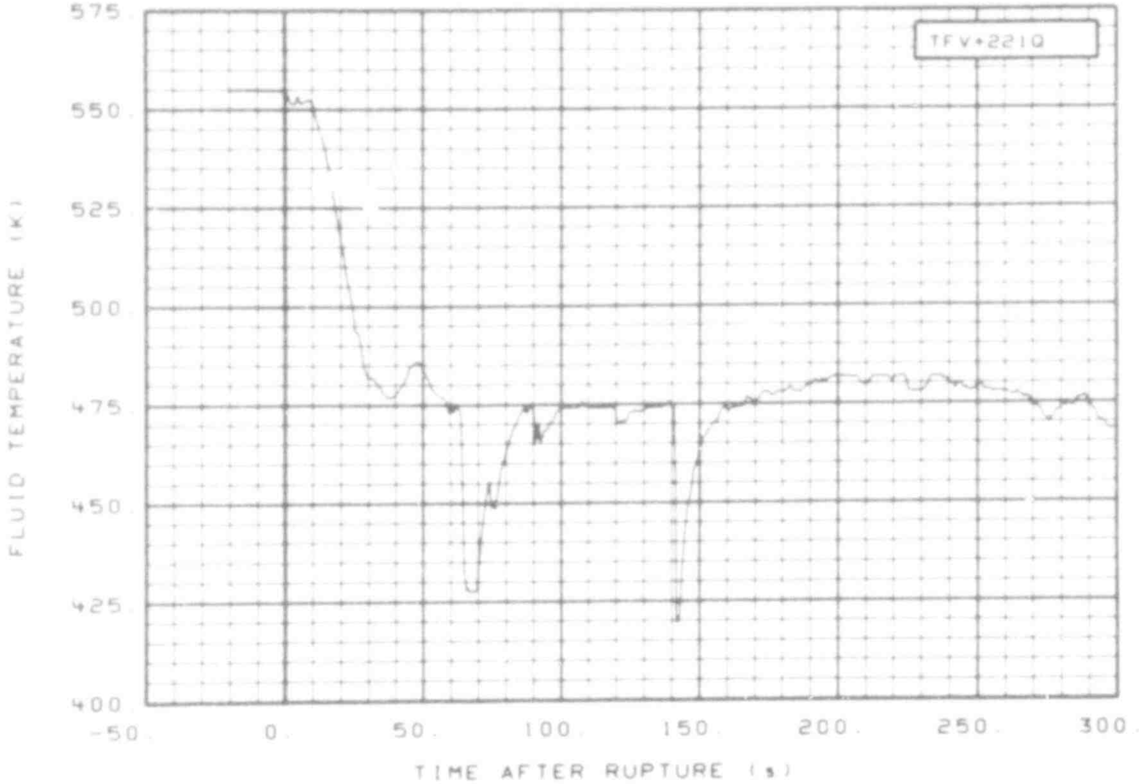

Fig. 25 Fluid temperature in vessel (TFV + 221Q), from -20 to 300 s.

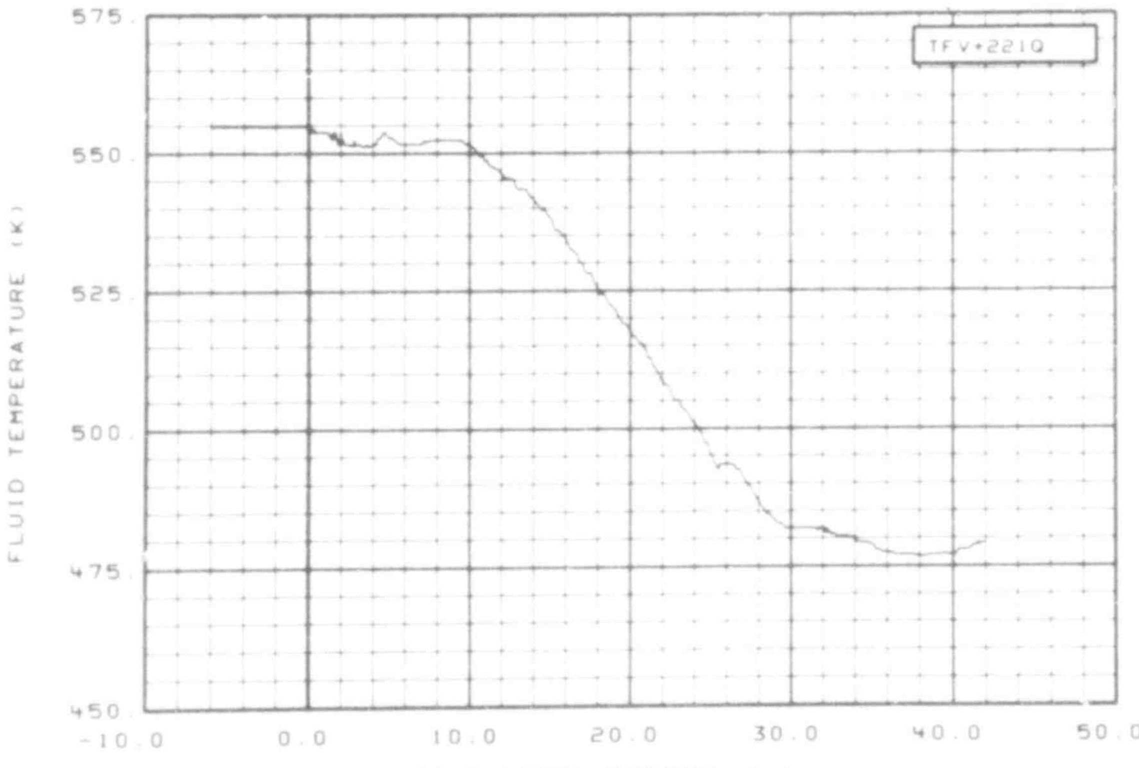

Fig. 26 Fluid temperature in vessel (TFV + 221Q), from -6 to 42 s.

507 105

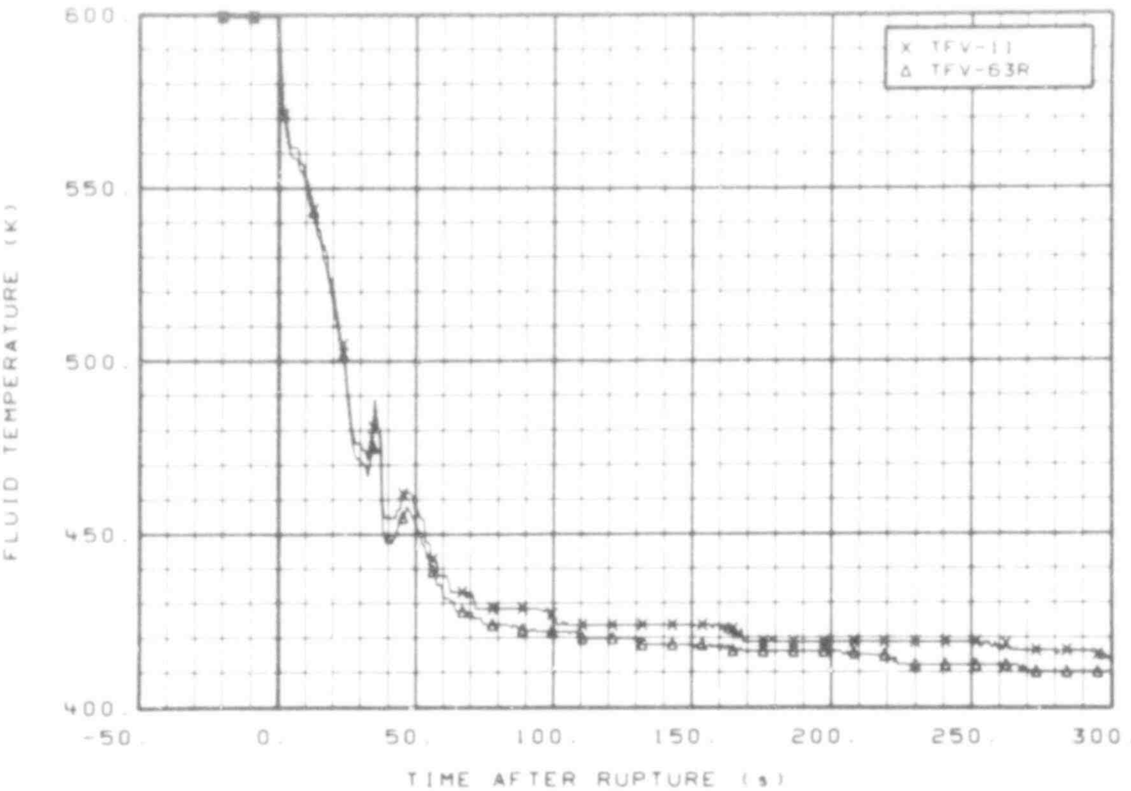

Fig. 27 Fluid temperature in vessel (TFV-11 and TFV-63R), from -20 to 300 s.

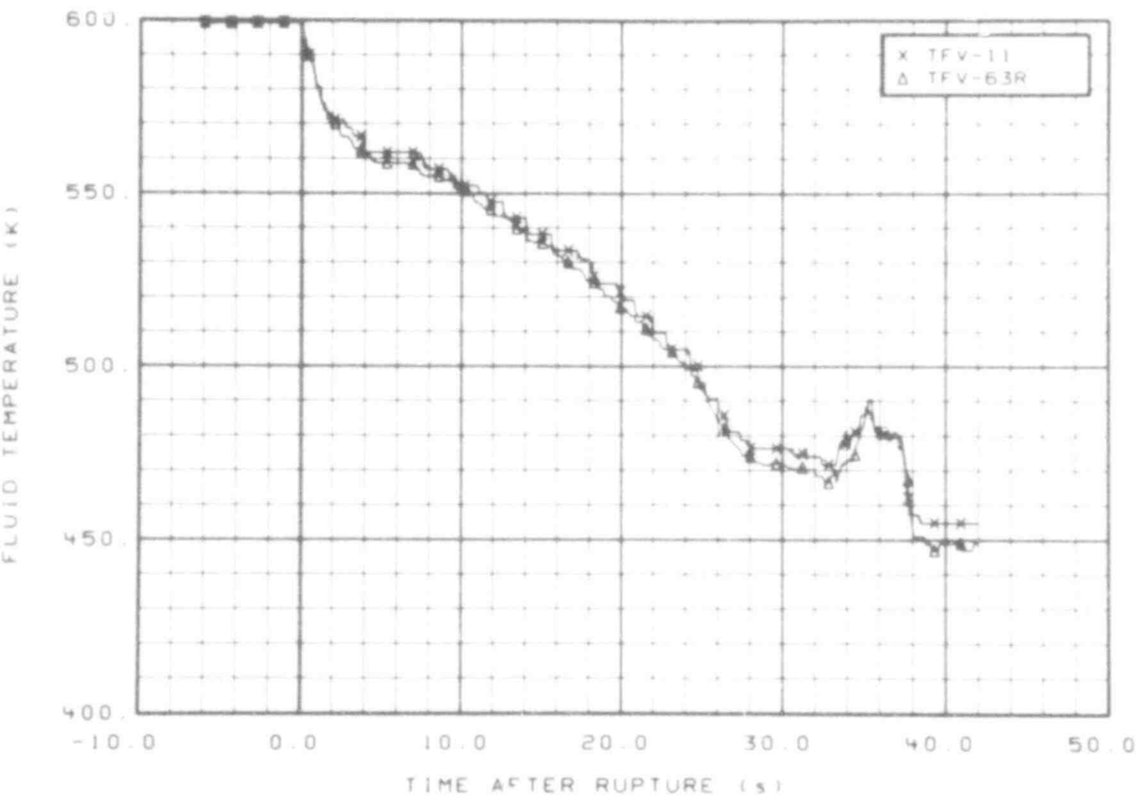

Fig. 28 Fluid temperature in vessel (TVF-11 and TFV-63R), from -6 to 42 s.

507 106

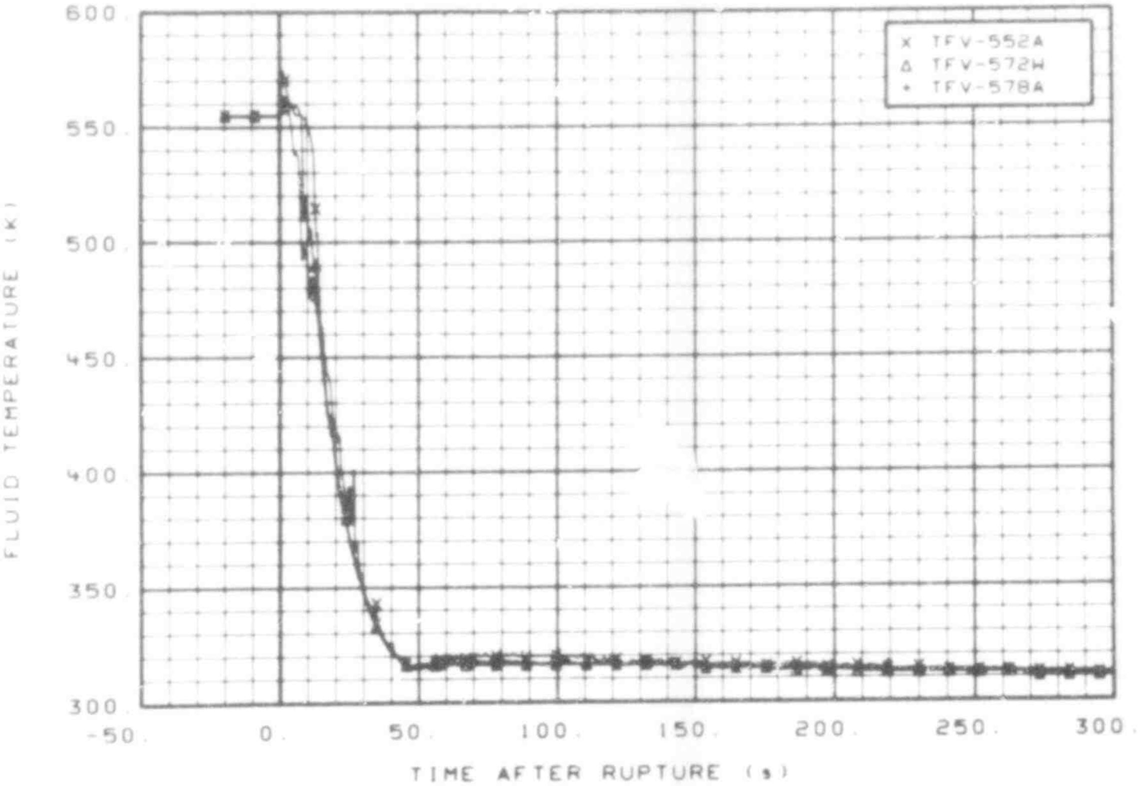

Fig. 29 Fluid temperature in vessel (TFV-552A, TFV-572W, and TFV-578A), from -20 to 300 s.

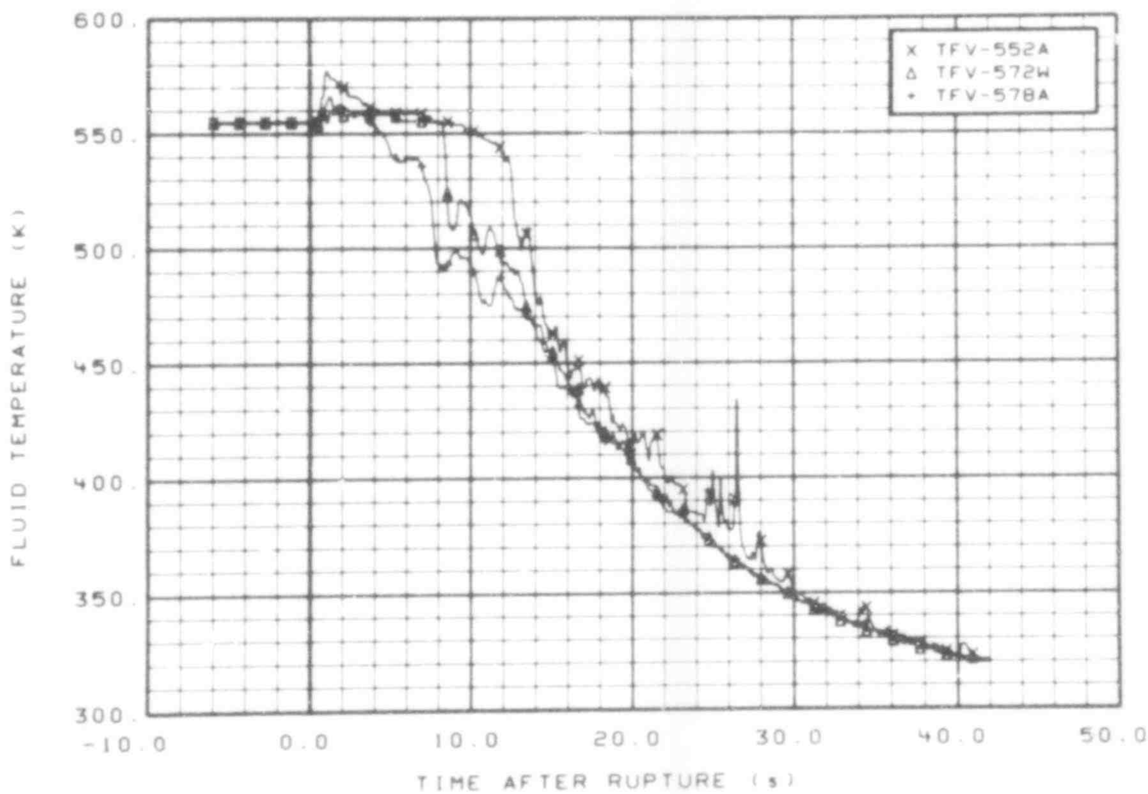

Fig. 30 Fluid temperature in vessel (TFV-552A, TFV-572W, and TFV-578A), from -6 to 42 s.

507 107

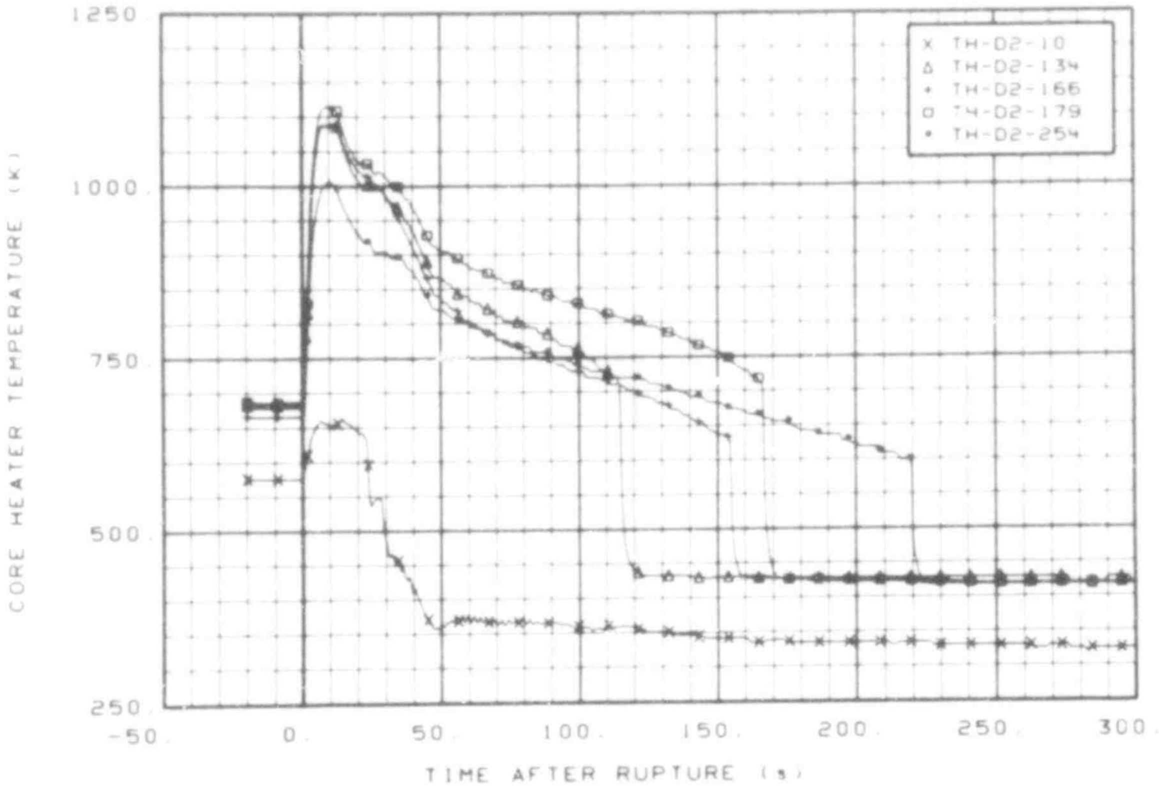

Fig. 77 Core heater temperature, Rod D-2 (TH-D2-10, TH-D2-134, TH-D2-166, TH-D2-179, and TH-D2-254), from -20 to 300 s.

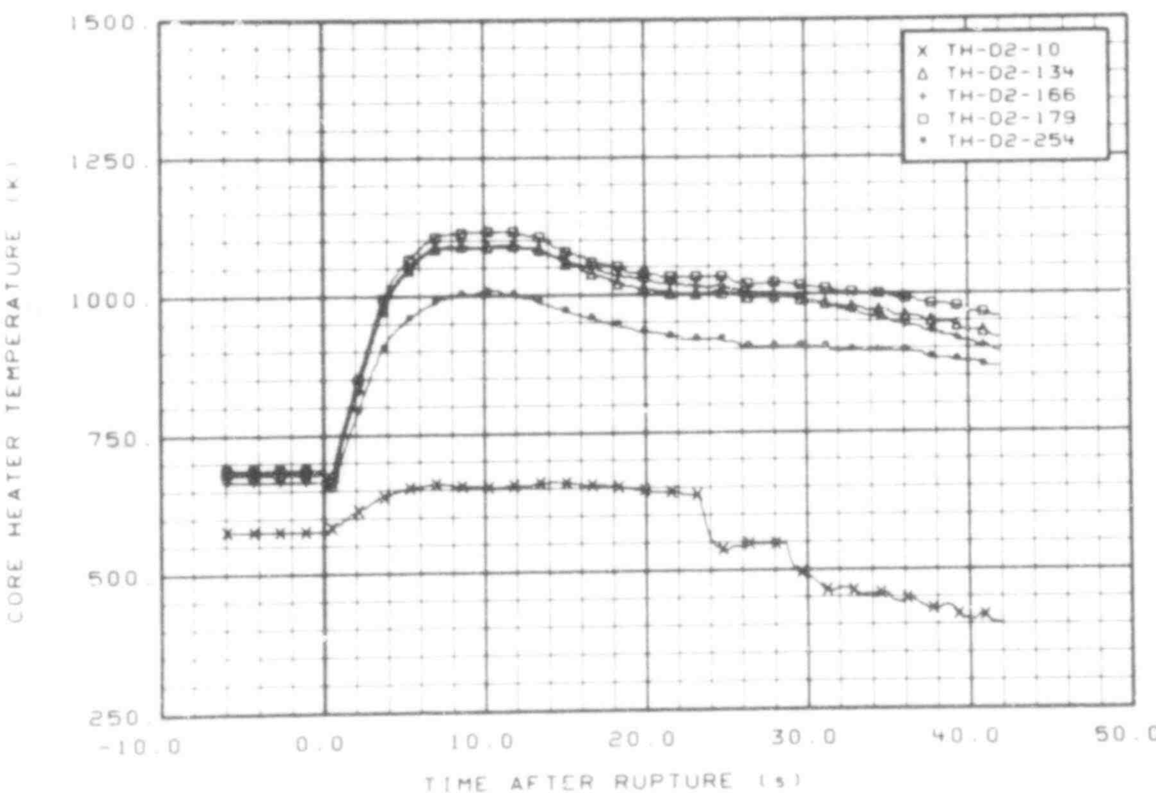

Fig. 78 Core heater temperature, Rod D-2 (TH-D2-10, TH-D2-134, TH-D2-166, TH-D2-179, and TH-D2-254), from -6 to 42 s.

507 107

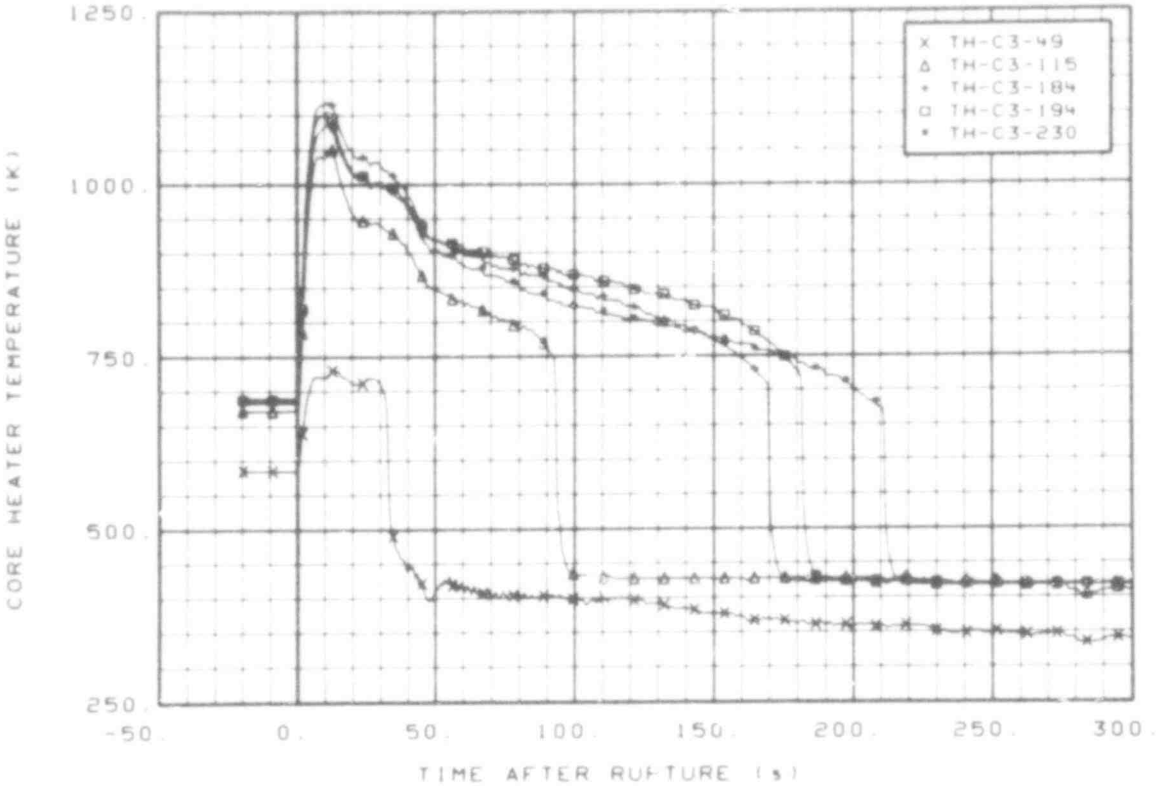

Fig. 75 Core heater temperature, Rod C-3 (TH-C3-49, TH-C3-115, TH-C3-184, TH-C3-194, and TH-C3-230), from -20 to 300 s.

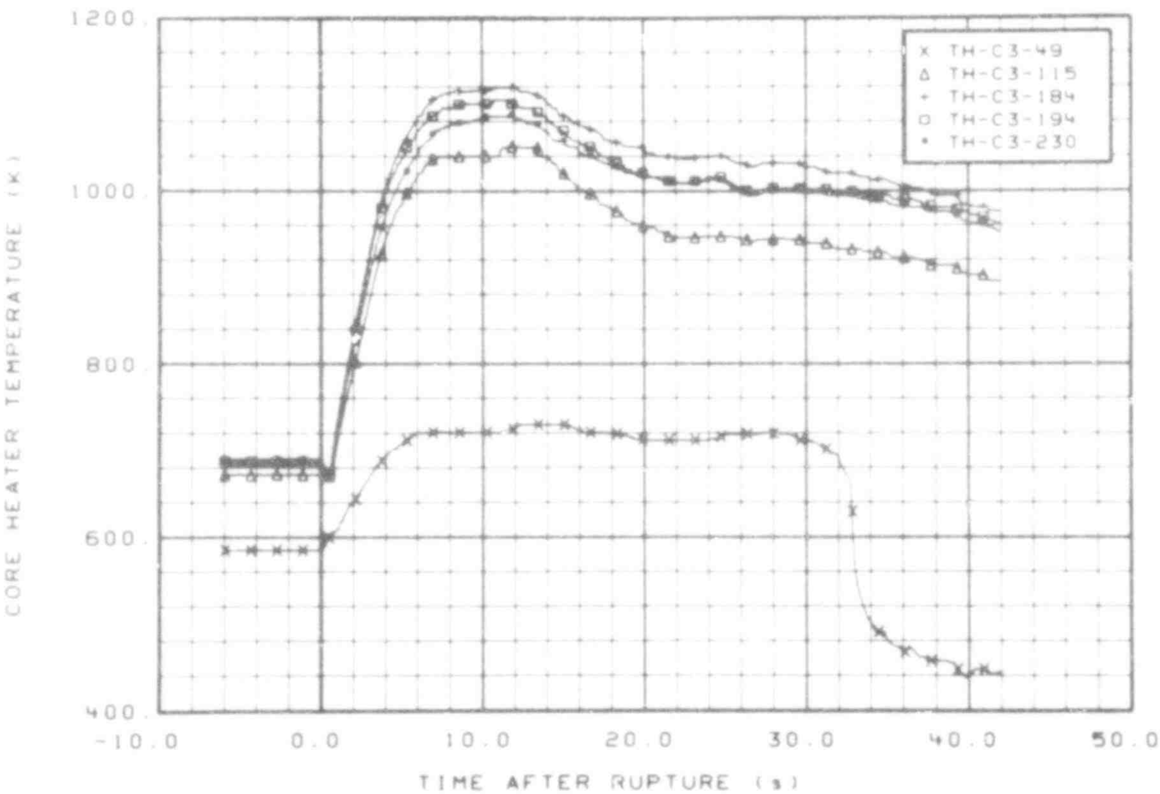

Fig. 76 Core heater temperature, Rod C-3 (TH-C3-49, TH-C3-115, TH-C3-184, TH-C3-194, and TH-C3-230), from -6 to 42 s.

011 709

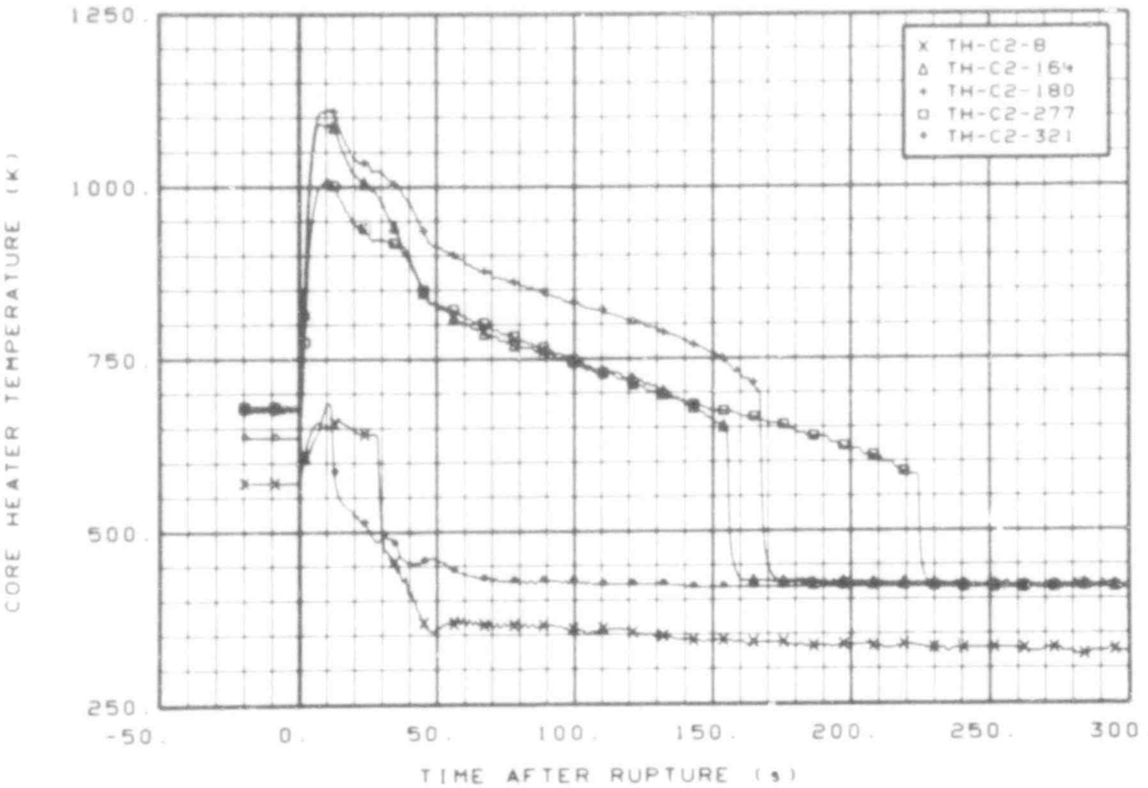

Fig. 73 Core heater temperature, Rod C-2 (TH-C2-8, TH-C2-164, TH-C2-180, TH-C2-277, and TH-C2-321), from -20 to 300 s.

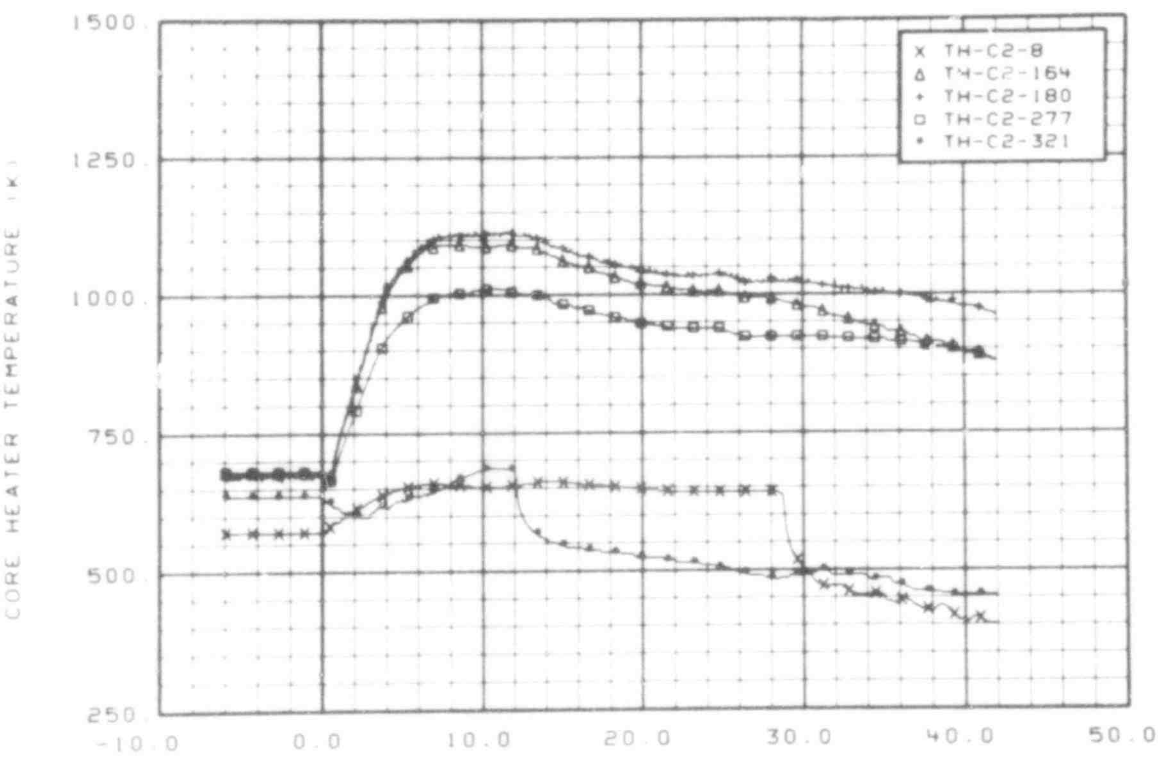

Fig. 74 Core heater temperature, Rod C-2 (TH-C2-8, TH-C2-164, TH-C2-180, TH-C2-277, and TH-C2-321), from -6 to 42 s.

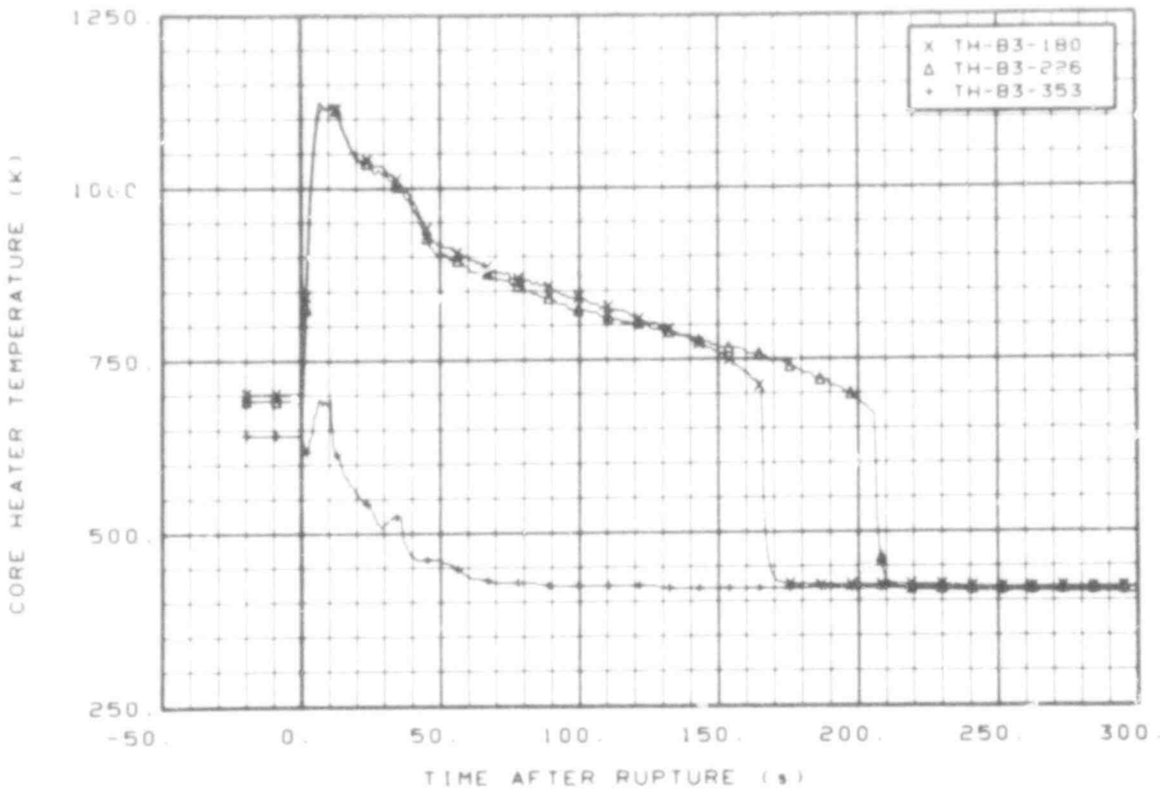

Fig. 71 Core heater temperature, Rod B-3 (TH-B3-180, TH-B3-226, and TH-B3-353), from -20 to 300 s.

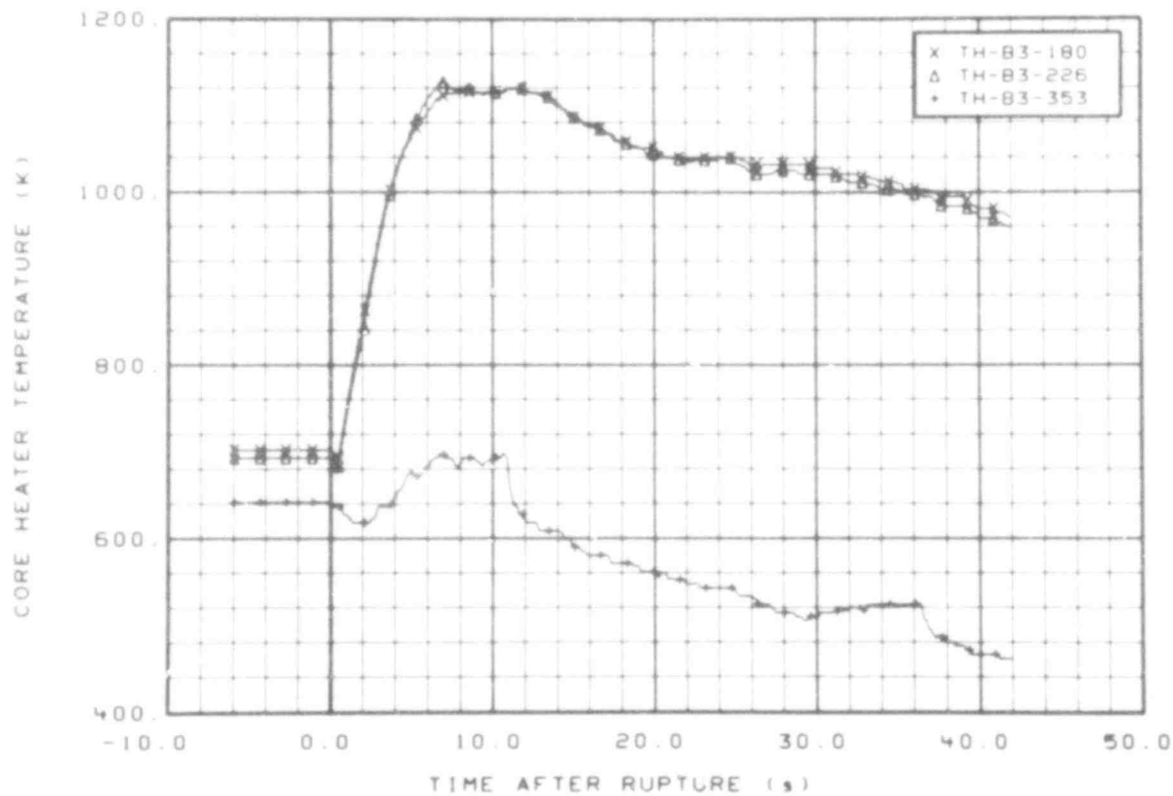

Fig. 72 Core heater temperature, Rod B-3 (TH-B3-180, TH-B3-226, and TH-B3-353), from -6 to 42 s.

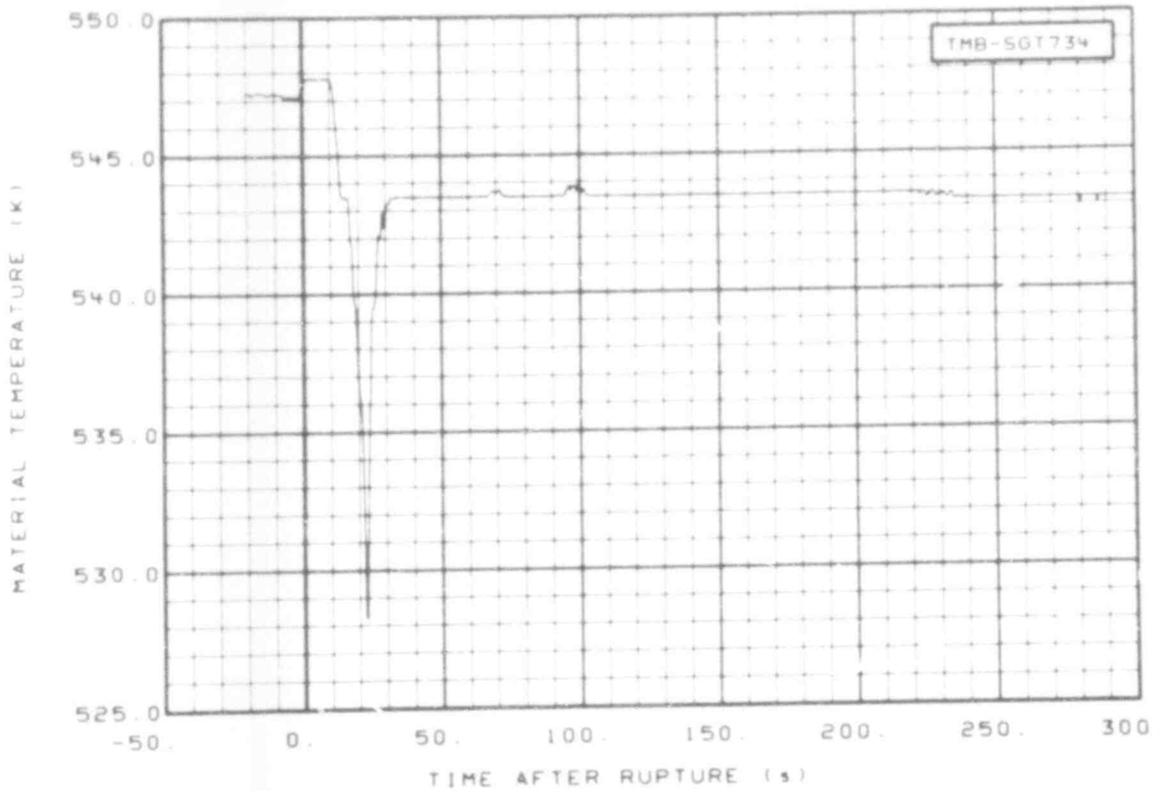

Fig. 69 Material temperature in broken loop, steam generator tube (TMB-SGT734), from -20 to 300 s.

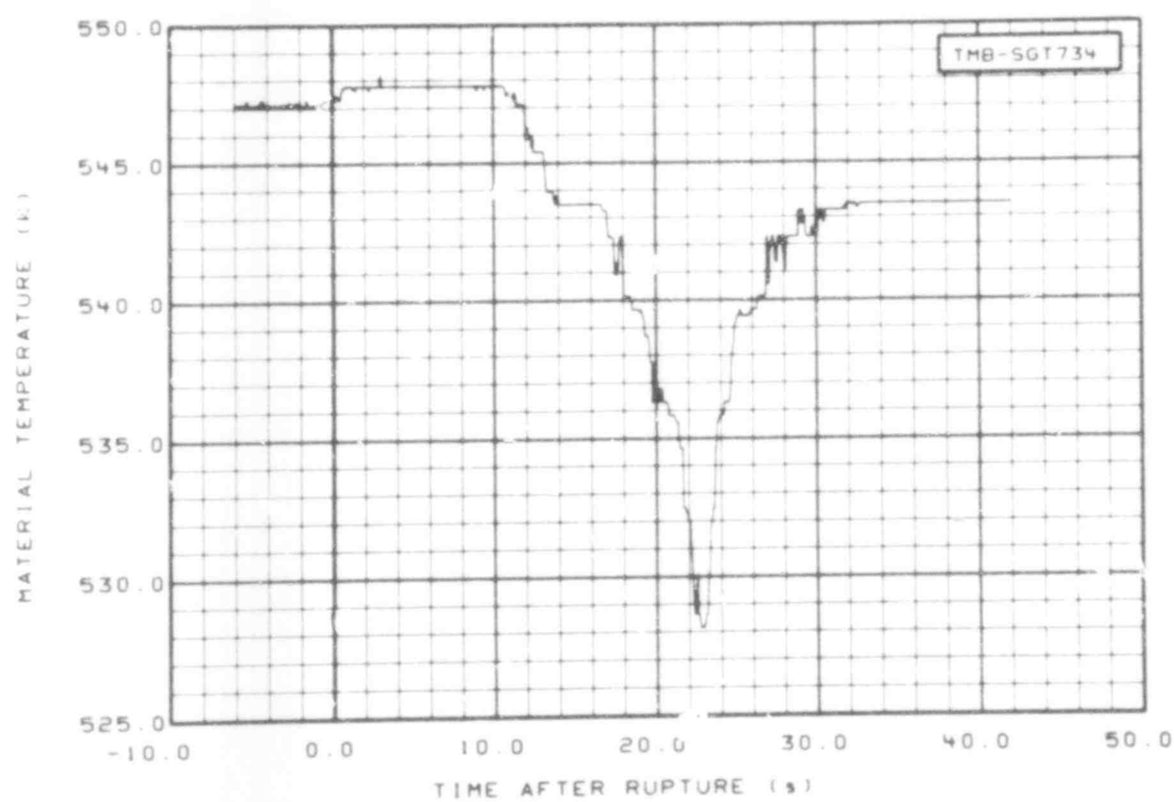

Fig. 70 Material temperature in broken loop, steam generator tube (TMB-SGT734), from -6 to 42 s.

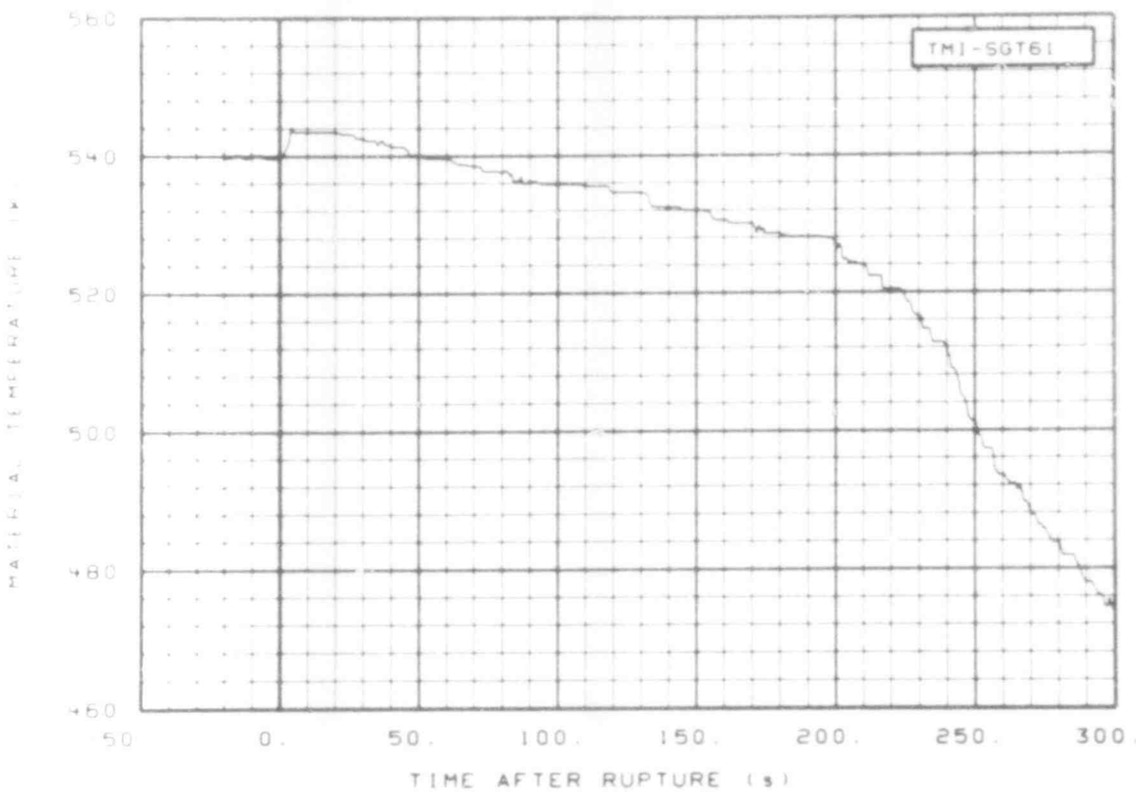

Fig. 67 Material temperature in intact loop, steam generator tube (TMI-SGT61), from -20 to 300 s.

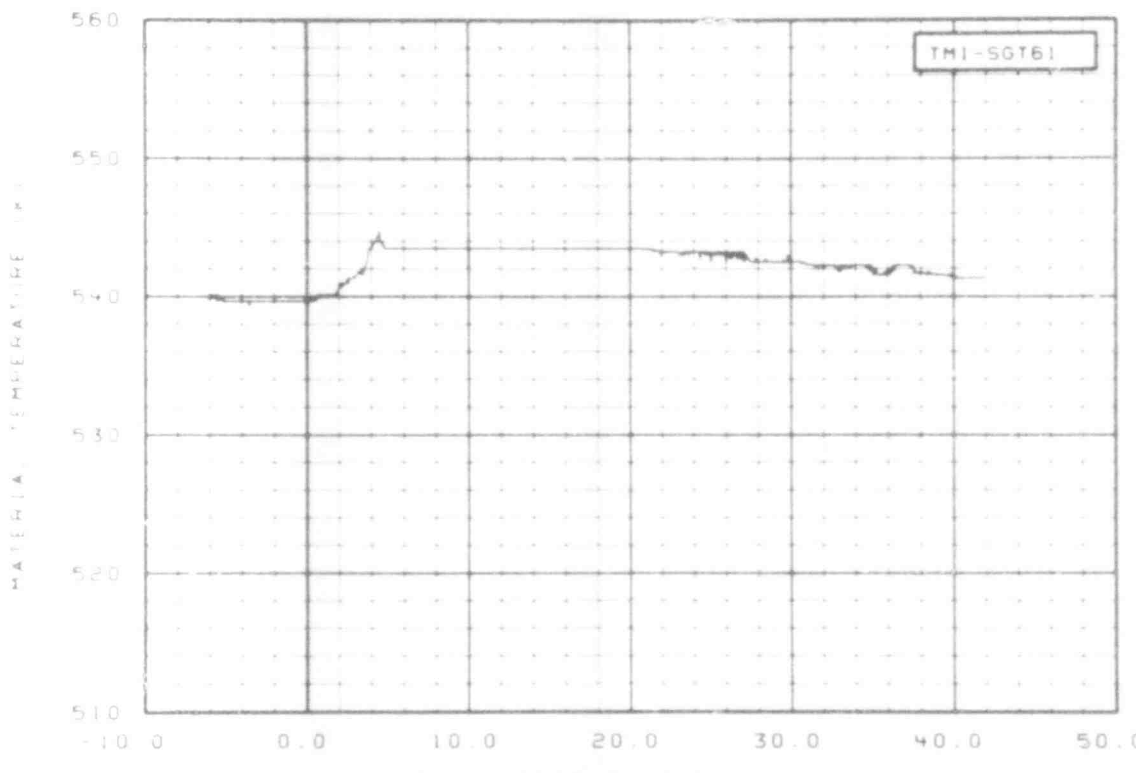

Fig. 68 Material temperature in intact loop, steam generator tube (TMI-SGT61), from -6 to 42 s.

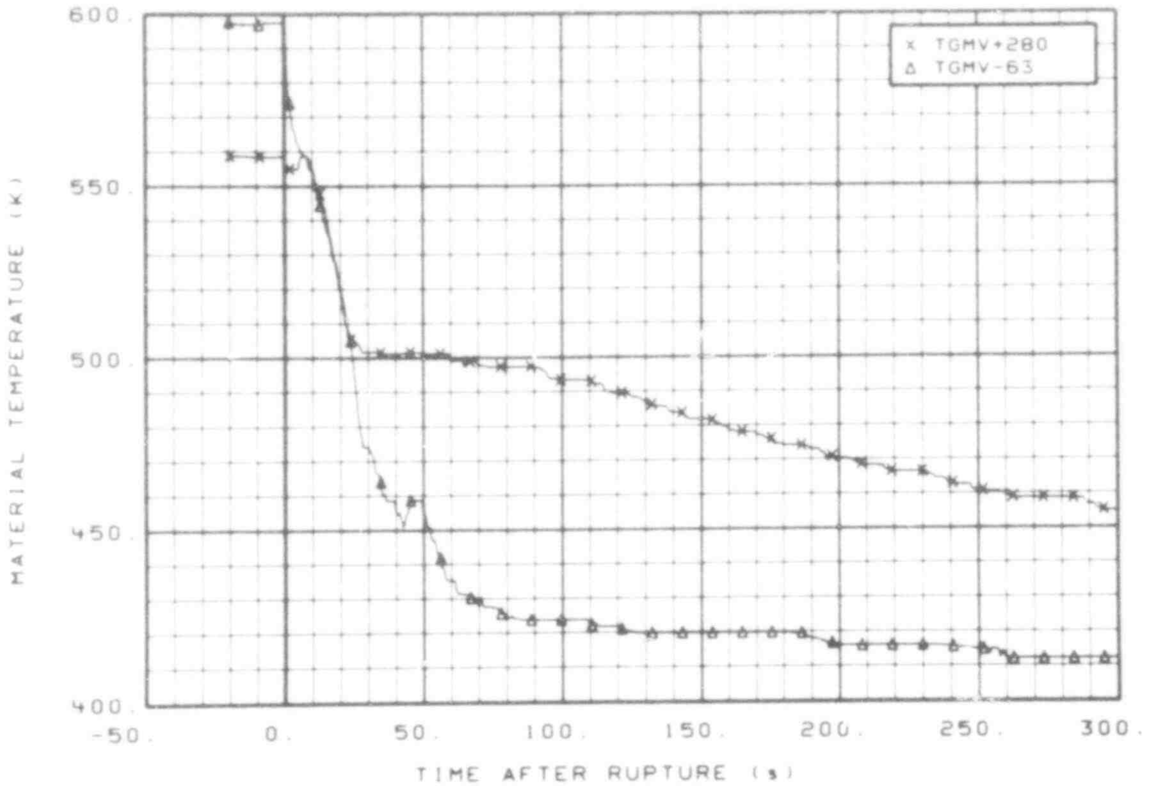

Fig. 65 Material temperature in vessel, core guide tube (TGMV + 280 and TGMV-63), from -20 to 300 s.

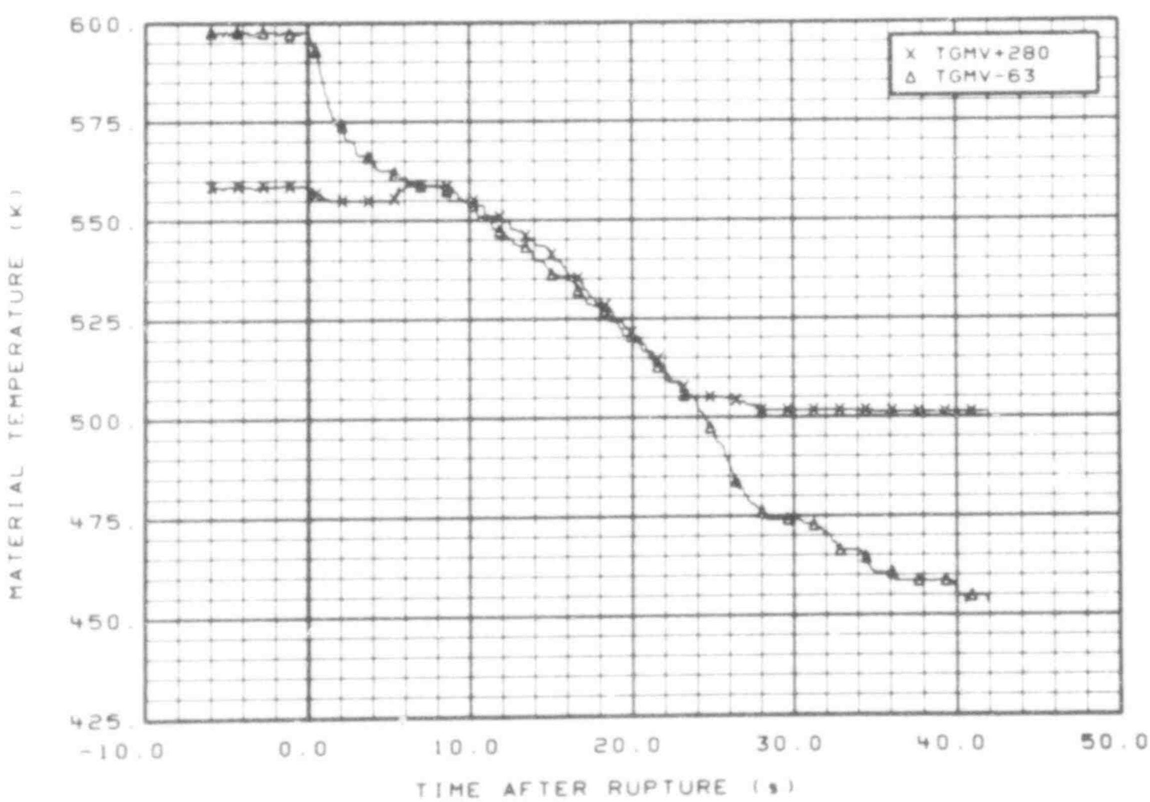

Fig. 66 Material temperature in vessel, core guide tube (TGMV + 280 and TGMV-63), from -6 to 42 s.

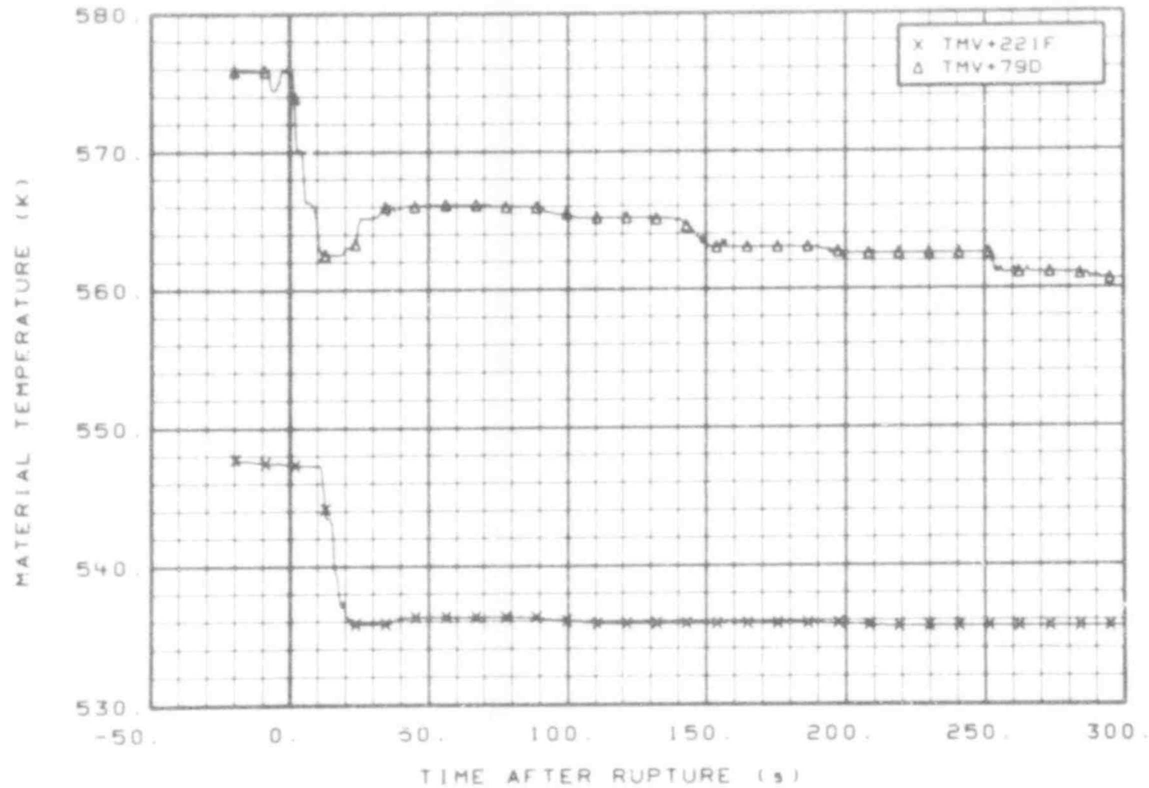

Fig. 63 Material temperature in upper vessel (TMV + 221F and TMV + 79D), from -20 to 300 s.

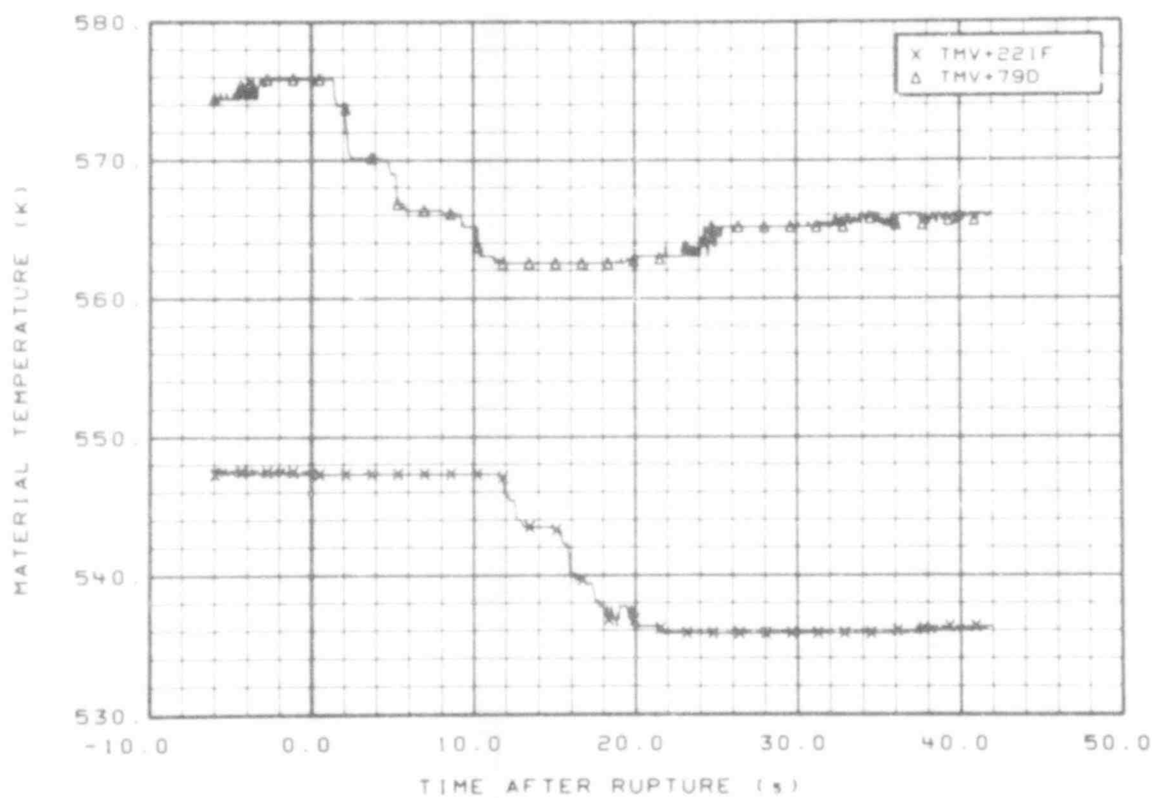

Fig. 64 Material temperature in upper vessel (TMV + 221F and TMV + 79D), from -6 to 42 s.

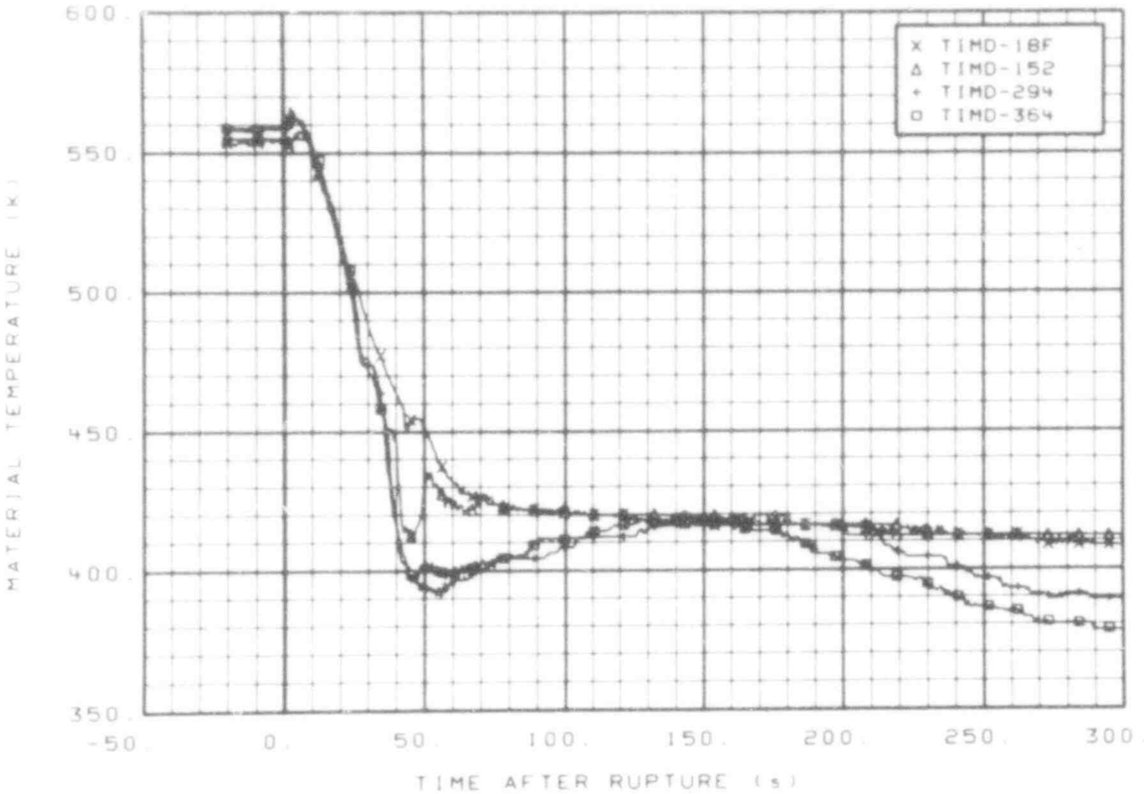

Fig. 61 Material temperature in downcomer insulator (TIMD-18F, TIMD-152, TIMD-294, and TIMD-364), from -20 to 300 s.

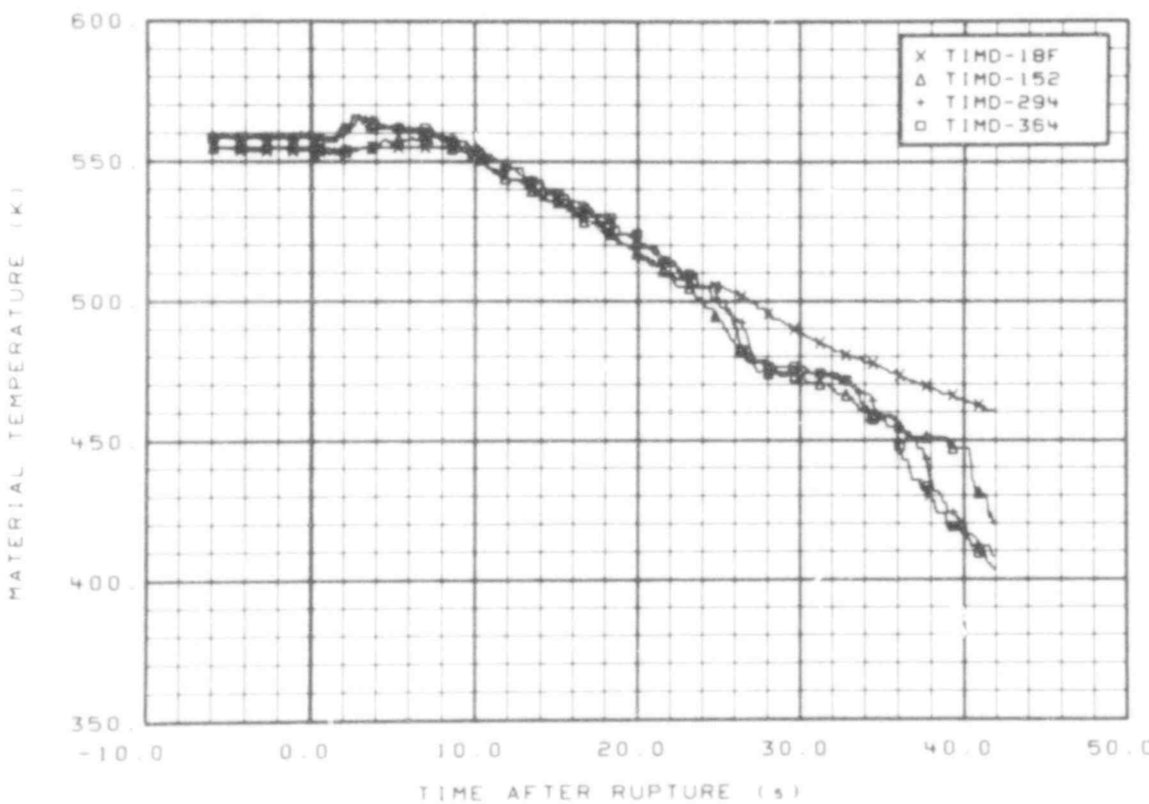

Fig. 62 Material temperature in downcomer insulator (TIMD-18F, TIMD-152, TIMD-294, and TIMD-364), from -6 to 42 s.

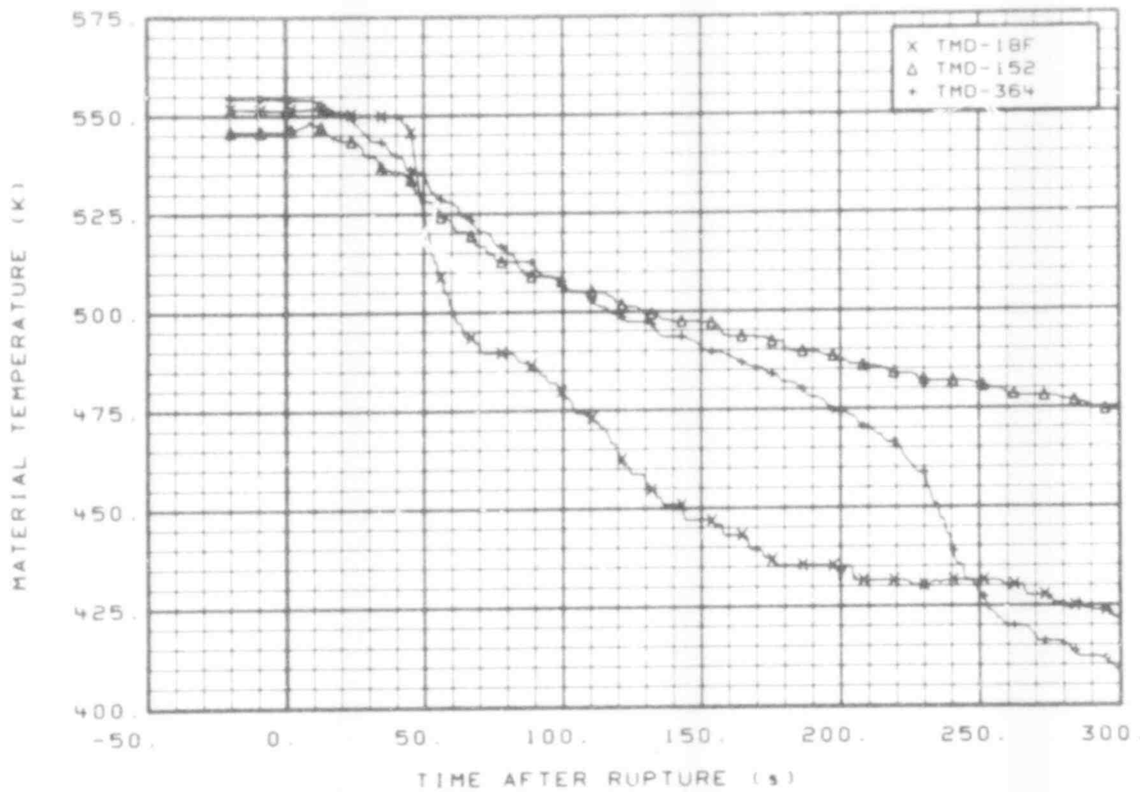

Fig. 59 Material temperature in downcomer (TMD-18F, TMD-152, and TMD-364), from -20 to 300 s.

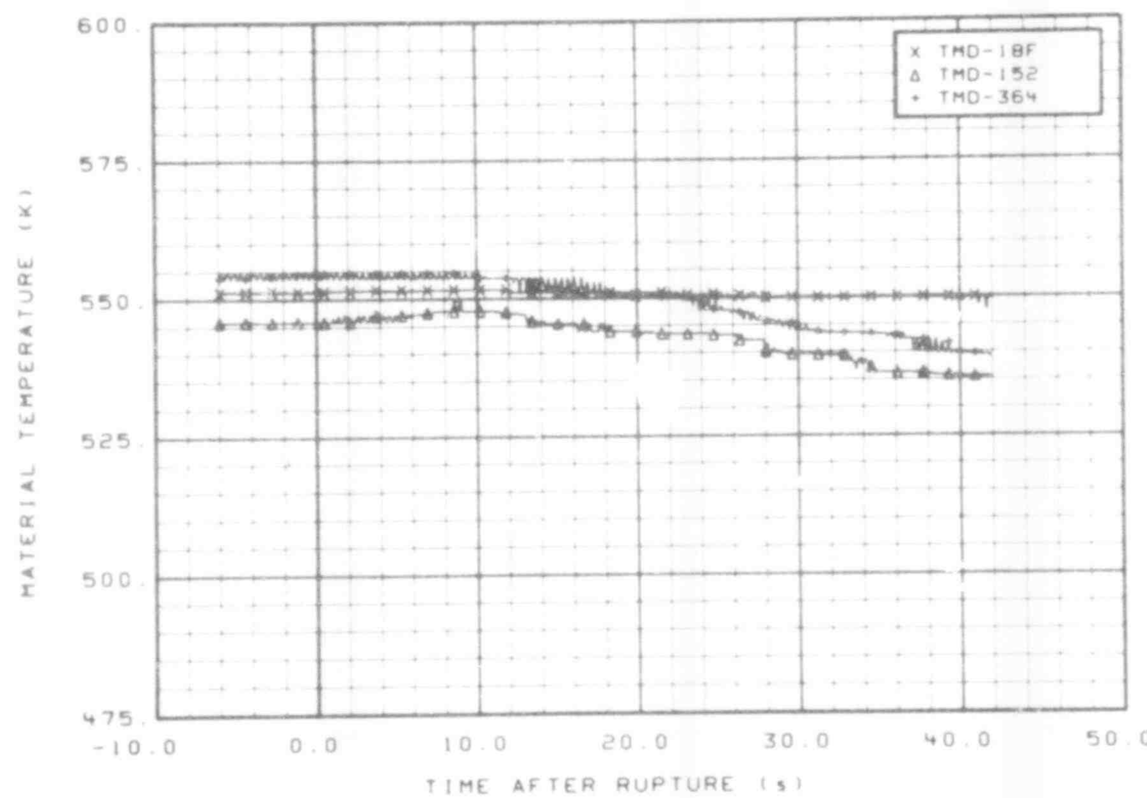

Fig 60 Material temperature in downcomer (TMD-18F, TMD-152, and TMD-364), from -6 to 42 s.

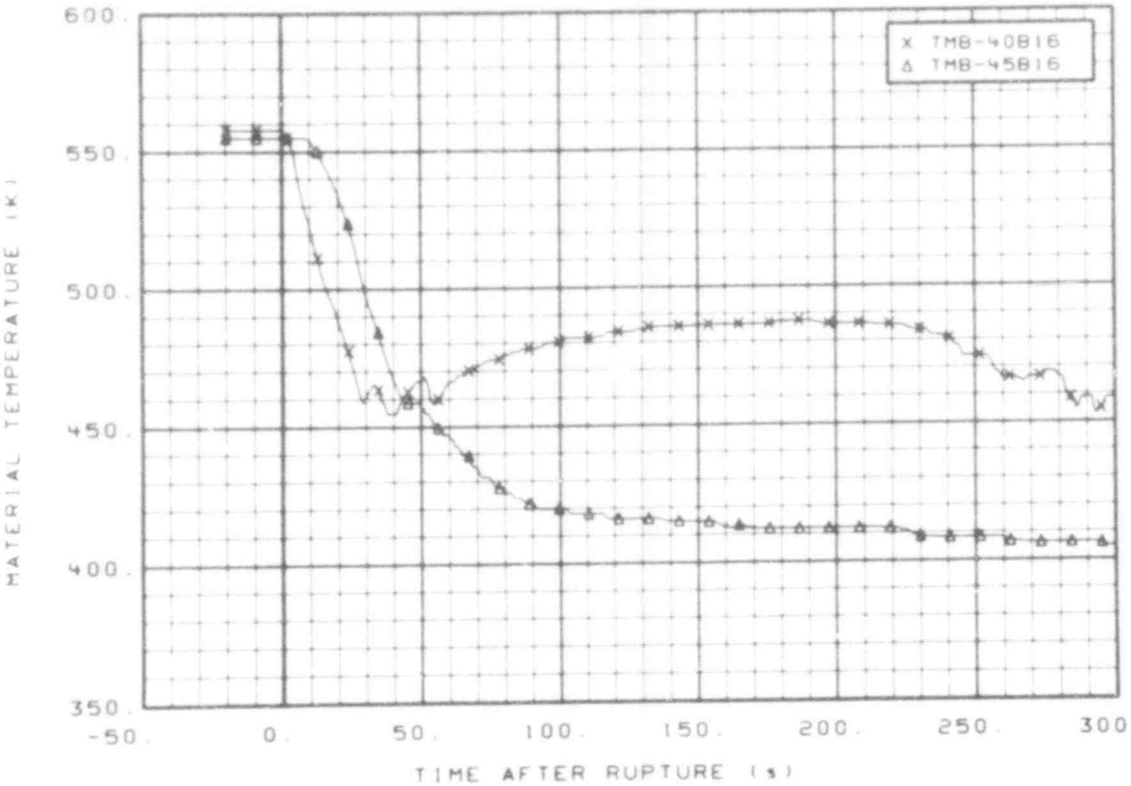

Fig. 57 Material temperature in broken loop (TMB-40B16 and TMB-45B16), from -20 to 300 s.

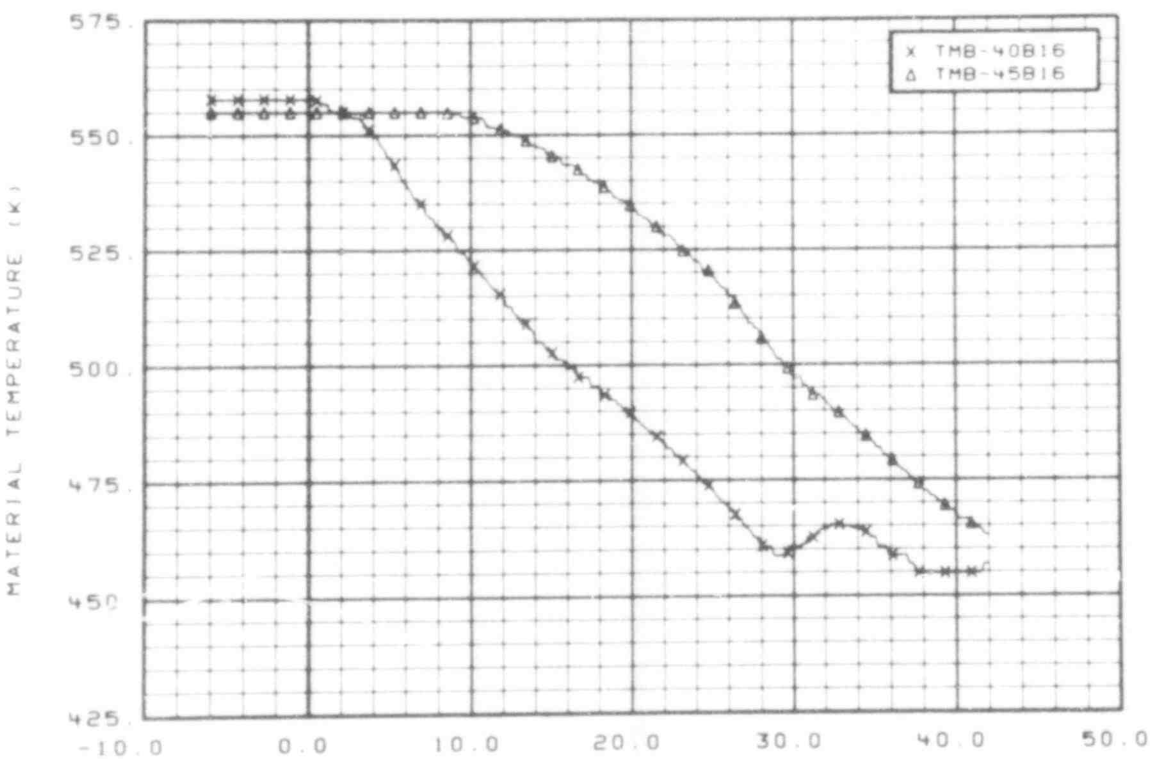

Fig. 58 Material temperature in broken loop (TMB-40B16 and TMB-45B16), from -6 to 42 s.

507 119

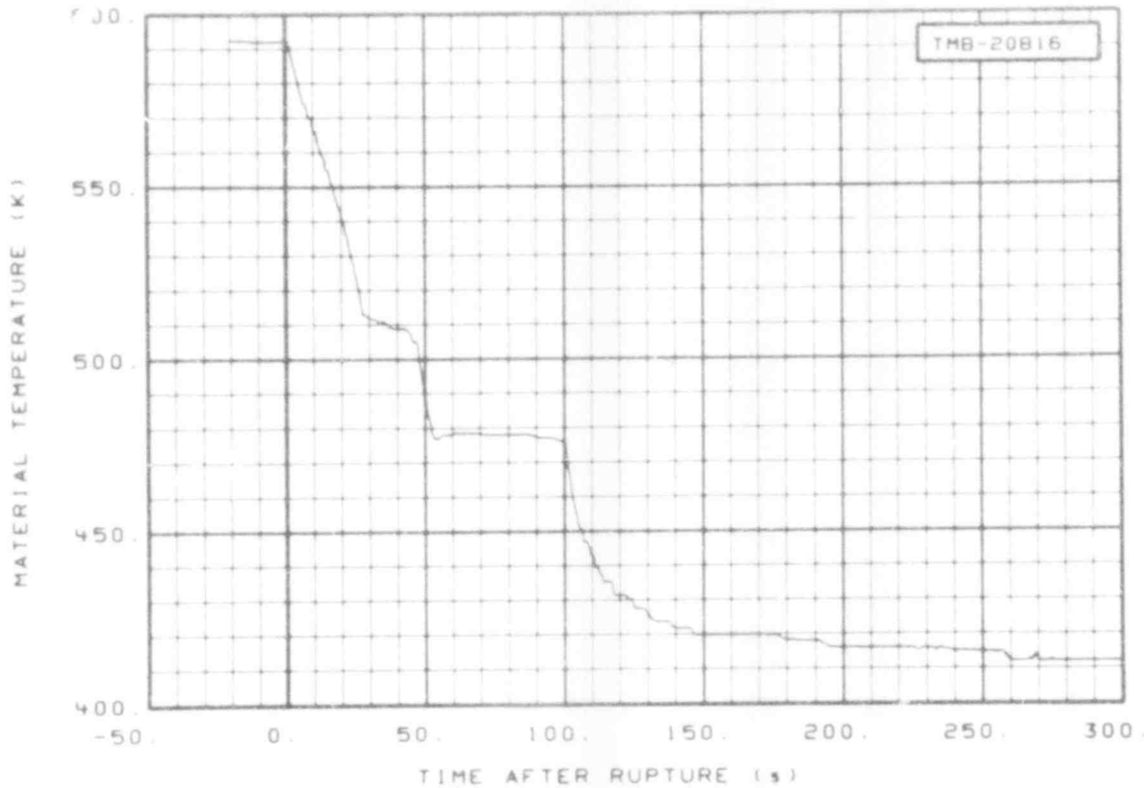

Fig. 55 Material temperature in broken loop (TMB-20B16), from -20 to 300 s.

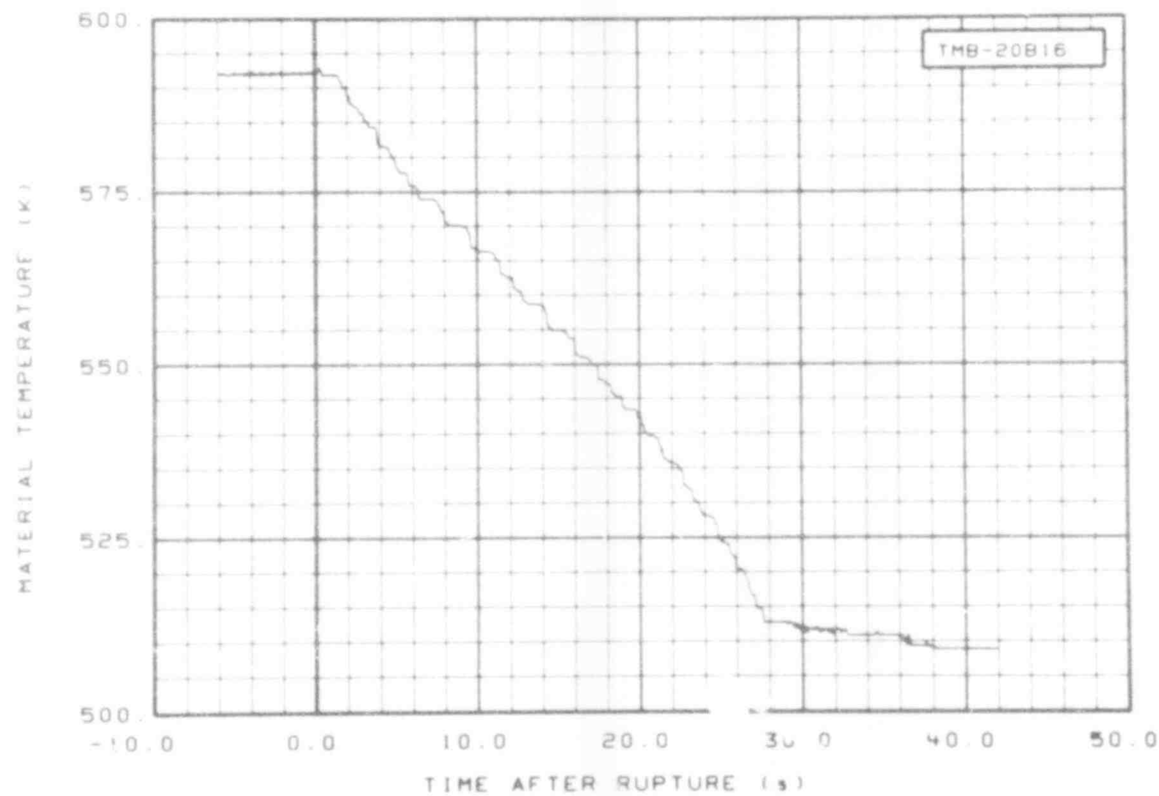

Fig. 56 Material temperature in broken loop (TMB-20B16), from -6 to 42 s.

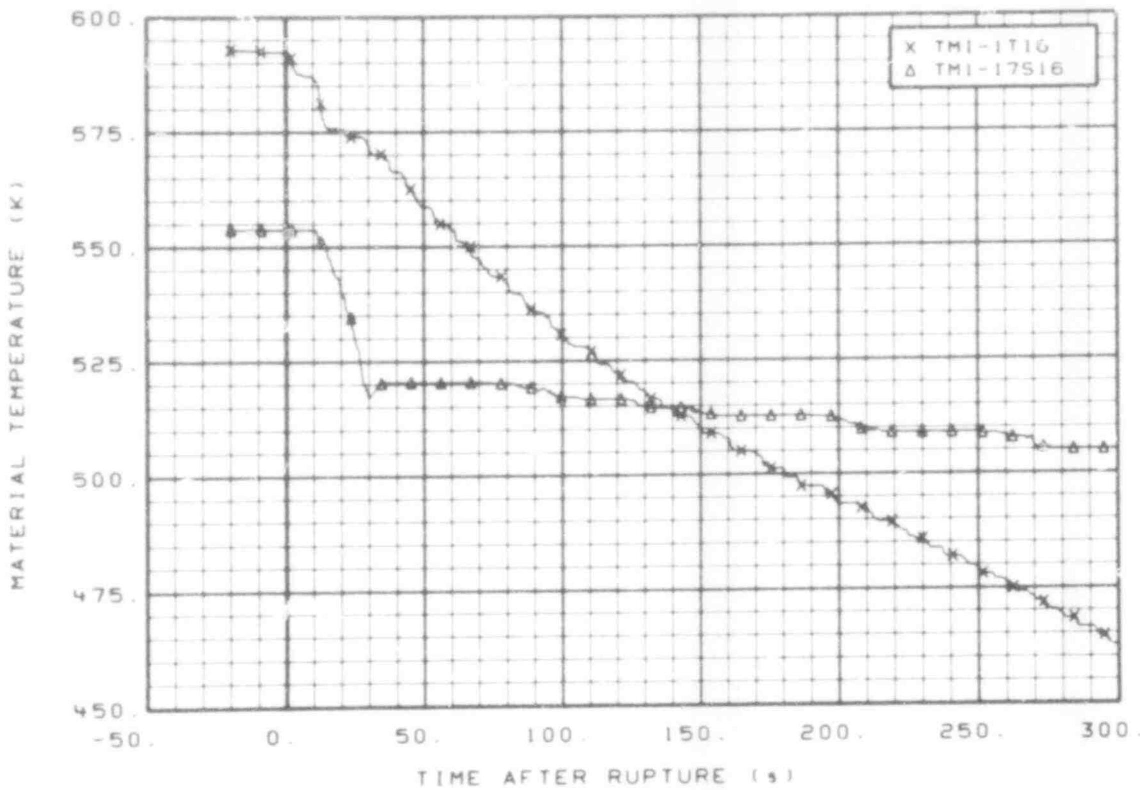

Fig. 53 Material temperature in intact loop (TMI-1T16 and TMI-17S16), from -20 to 300 s.

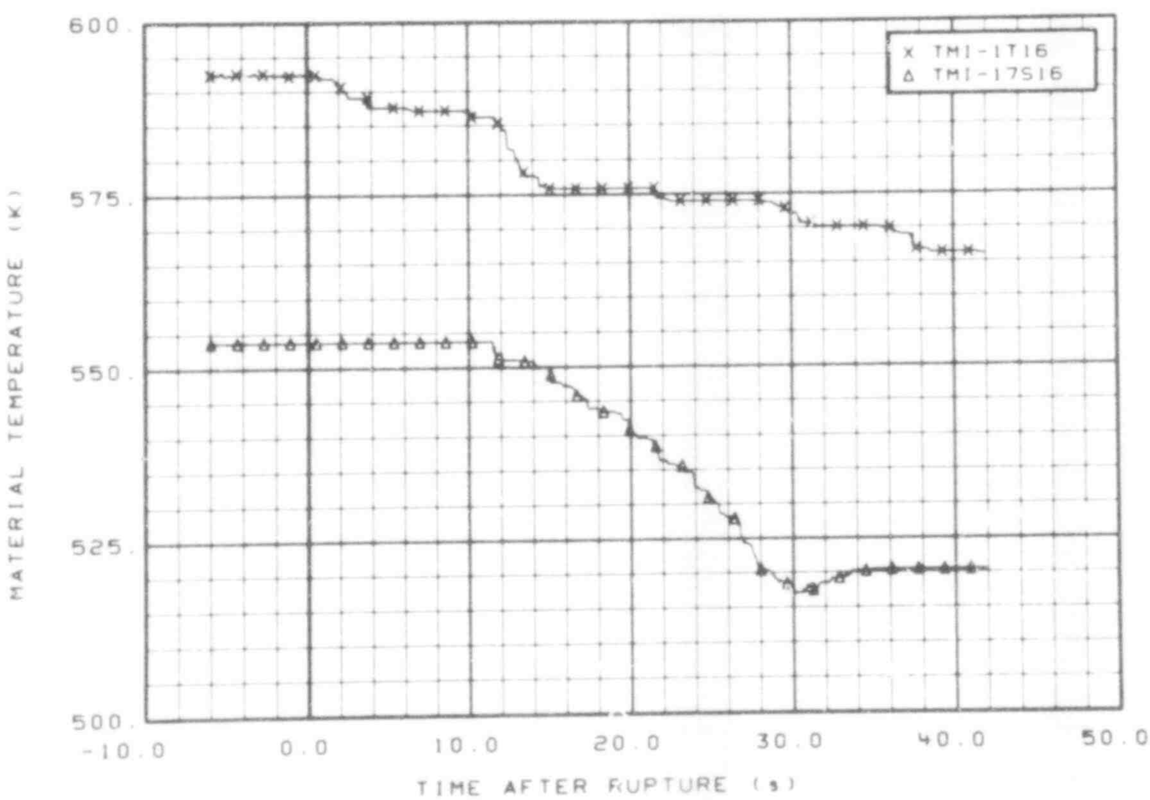

Fig. 54 Material temperature in intact loop (TMI-1T16 and TMI-17S16), from -6 to 42 s.

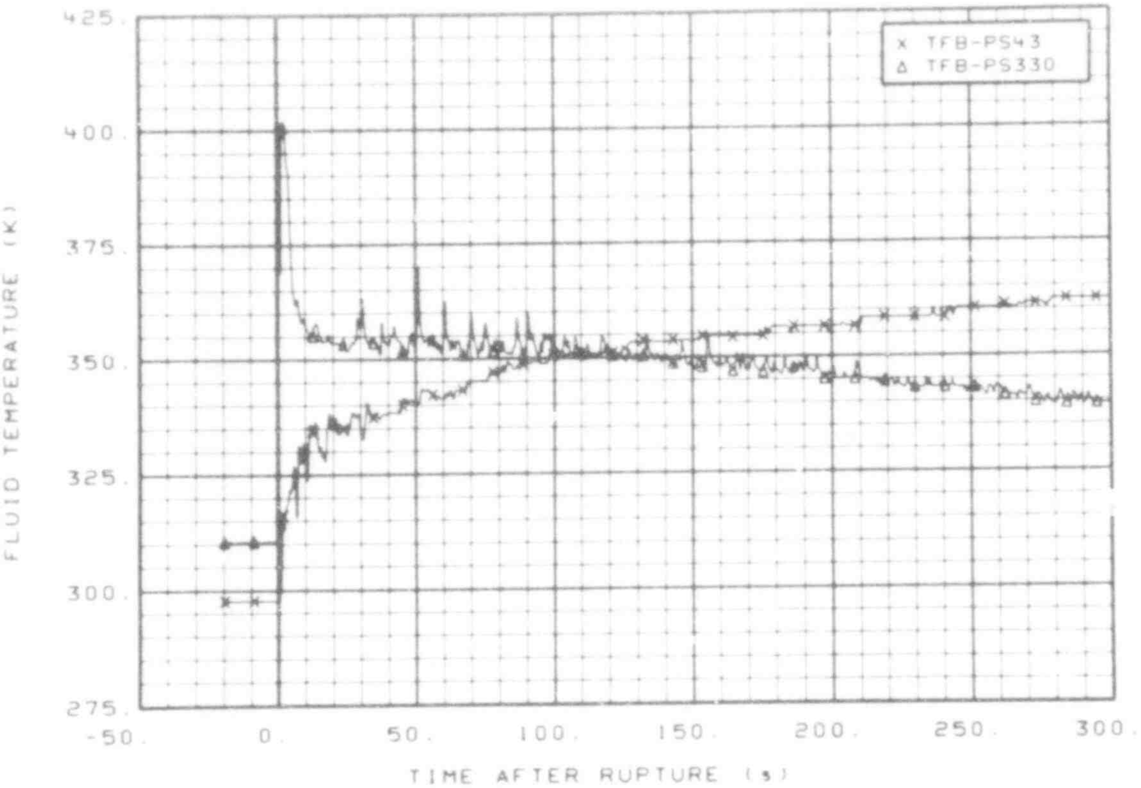

Fig. 51 Fluid temperature in broken loop, pressure suppression system tank (TFB-PS43 and TFB-PS330), from -20 to 300 s.

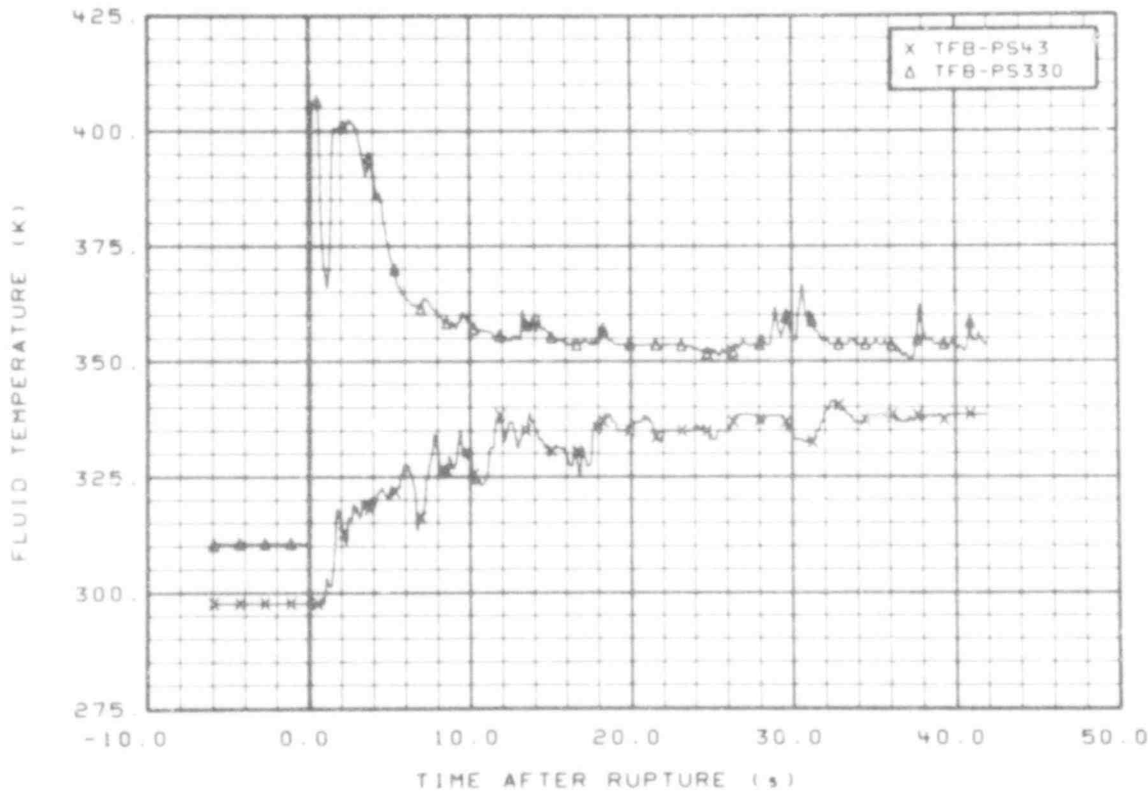

Fig. 52 Fluid temperature in broken loop, pressure suppression system tank (TFB-PS43 and TFB-PS330), from -6 to 42 s.

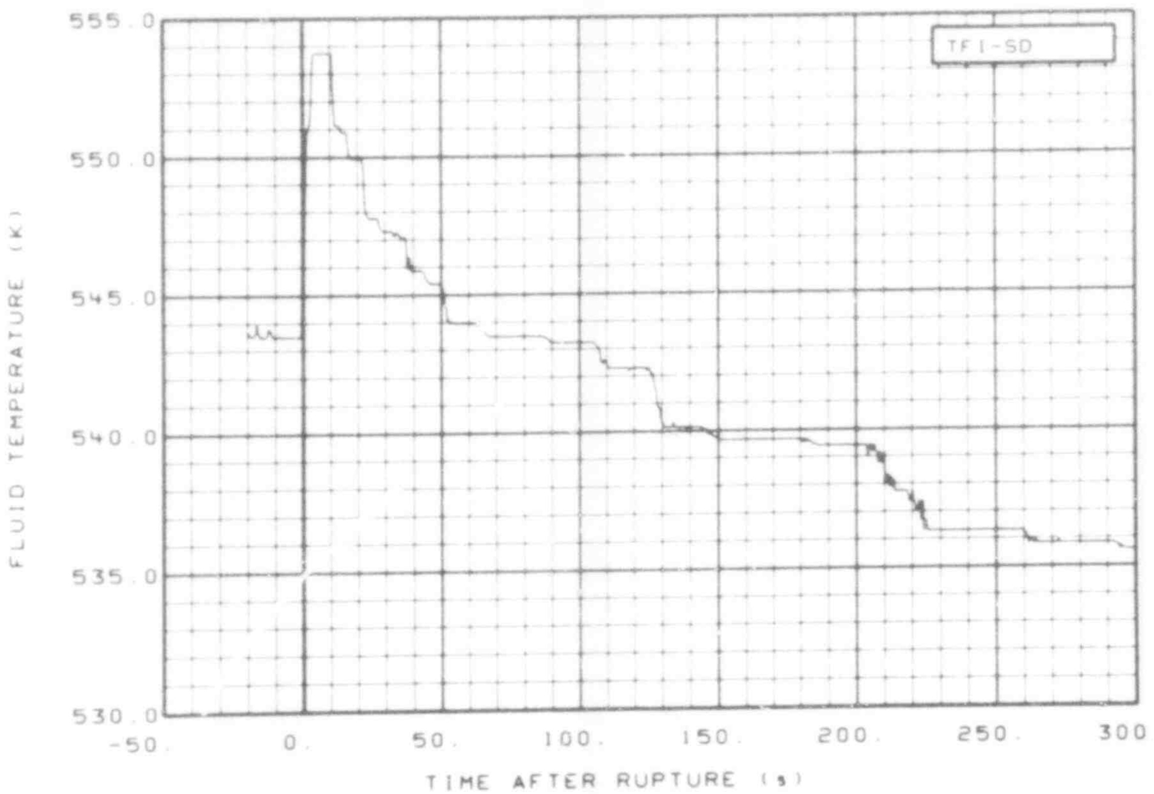

Fig. 49 Fluid temperature in intact loop steam generator, secondary side steam dome (TFI-SD), from -20 to 300 s.

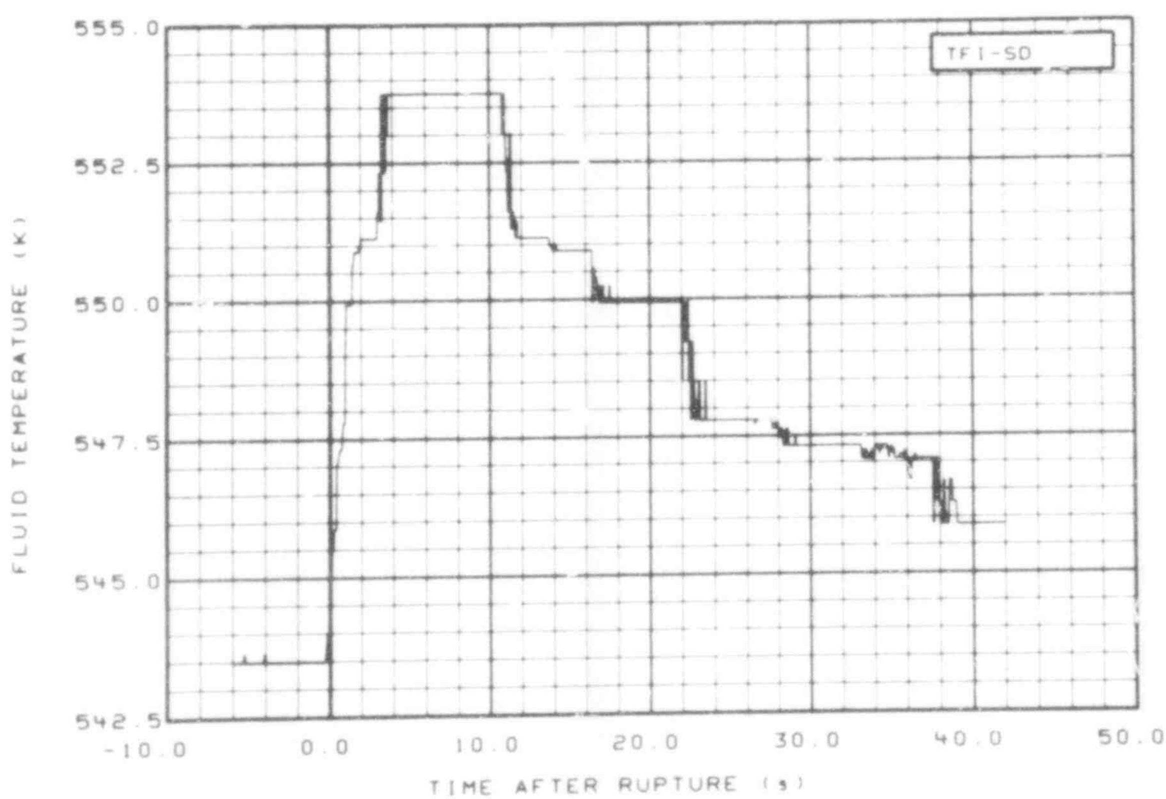

Fig. 50 Fluid temperature in intact loop steam generator, secondary side steam dome (TFI-SD), from -6 to 42 s.

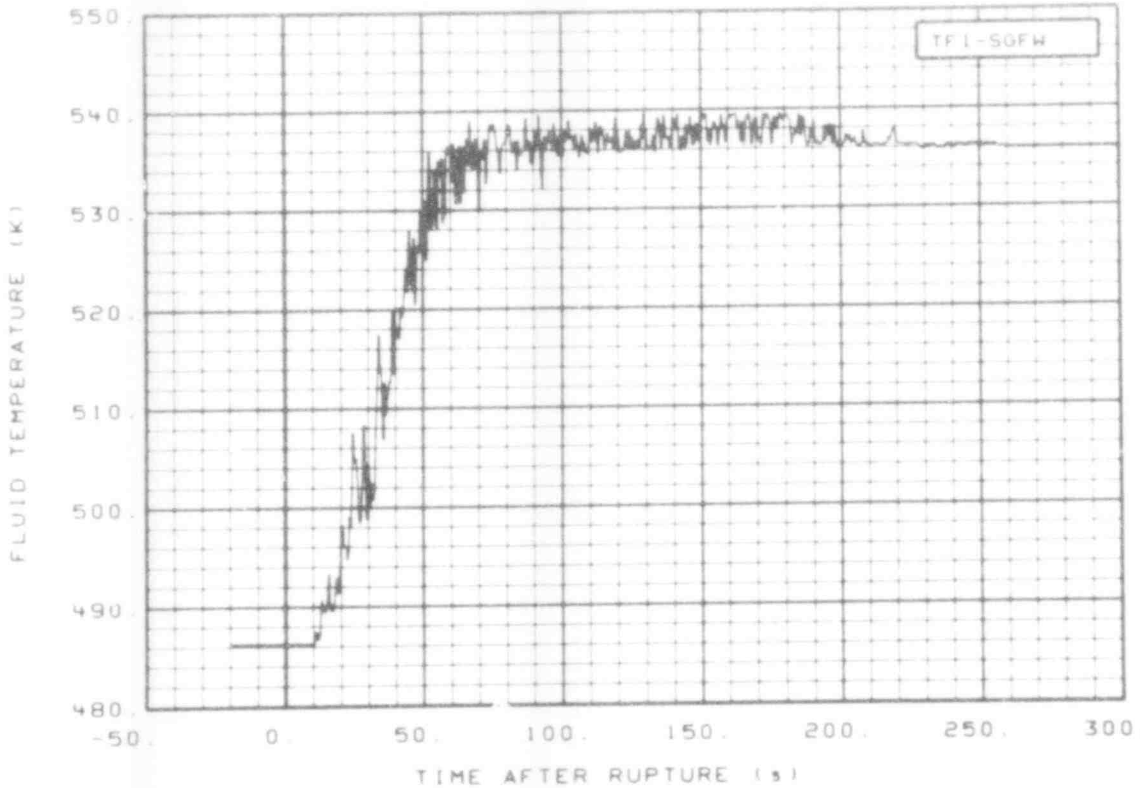

Fig. 47 Fluid temperature in intact loop steam generator, secondary feedwater line (TFI-SGFW), from -20 to 300 s.

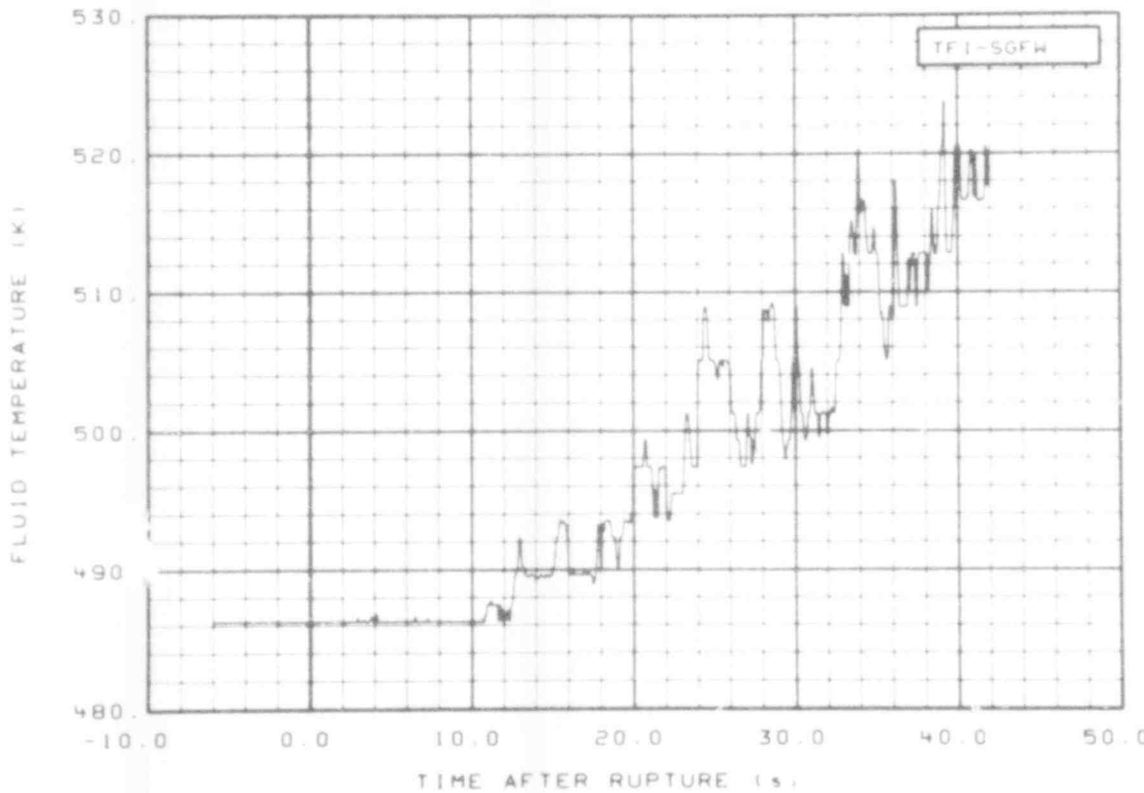

Fig. 48 Fluid temperature in intact loop steam generator, secondary feedwater line (TFI-SGFW), from -6 to 42 s.

507 124

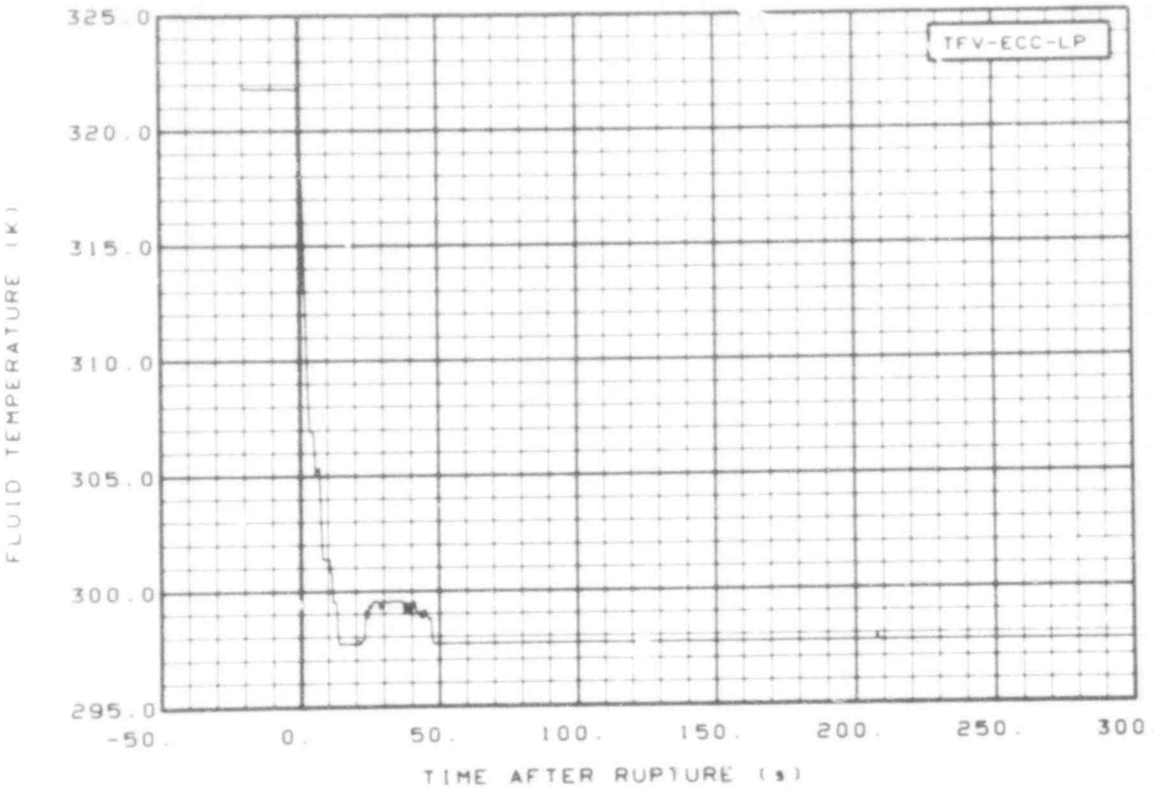

Fig. 45 Fluid temperature in vessel accumulator, coolant injection line (TFV-ECC-LP), from -20 to 300 s.

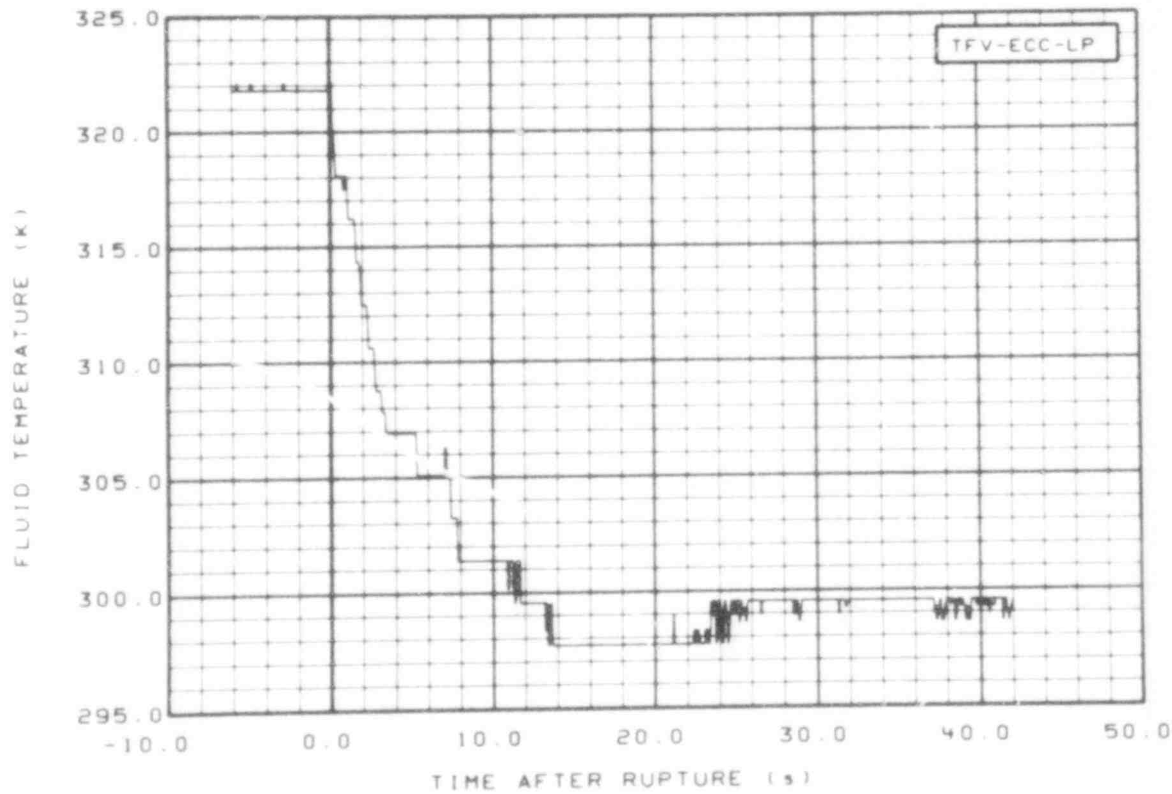

Fig. 46 Fluid temperature in vessel accumulator, coolant injection line (TFV-ECC-LP), from -6 to 42 s.

507 125

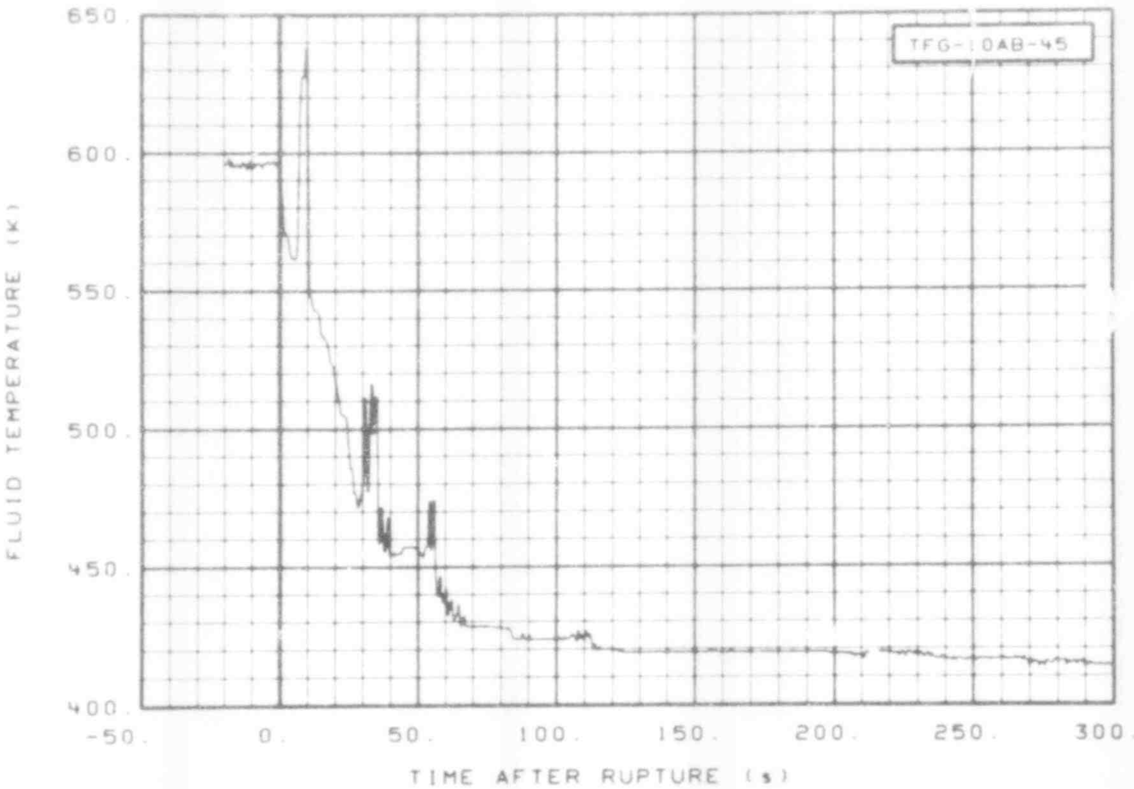

Fig. 43 Fluid temperature in core, Grid Spacer 10 (TFG-10AB-45), from -20 to 300 s.

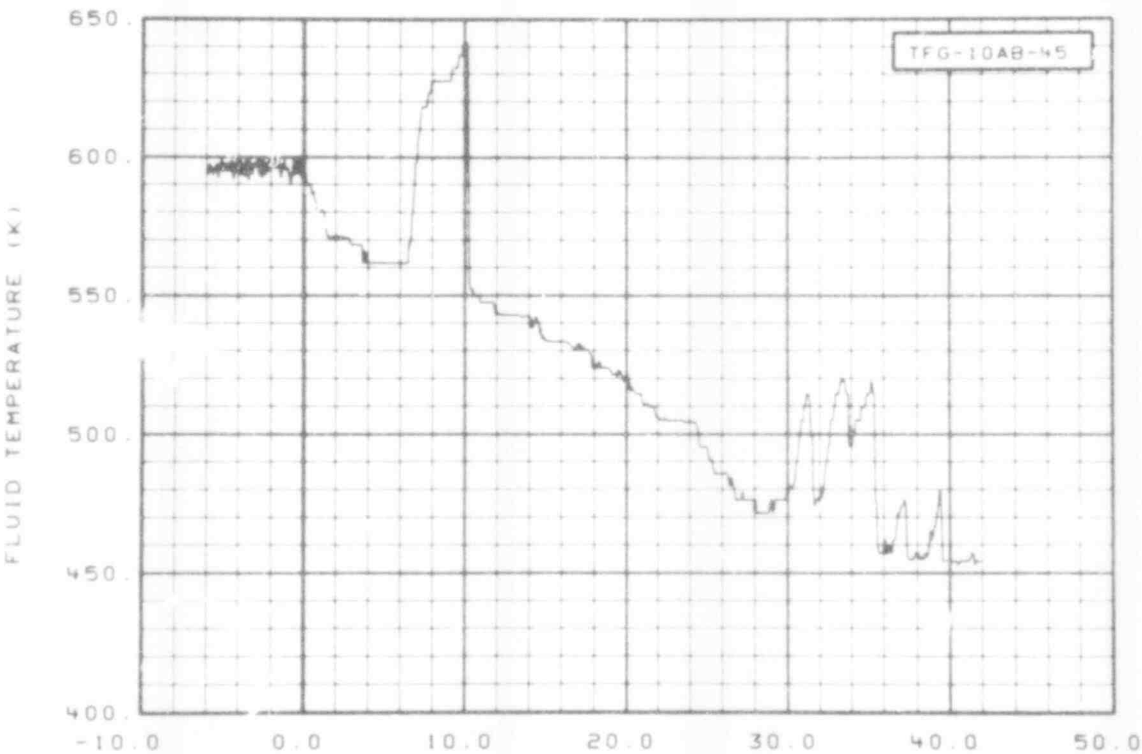

Fig. 44 Fluid temperature in core, Grid Spacer 10 (TFG-10AB-45), from -6 to 42 s.

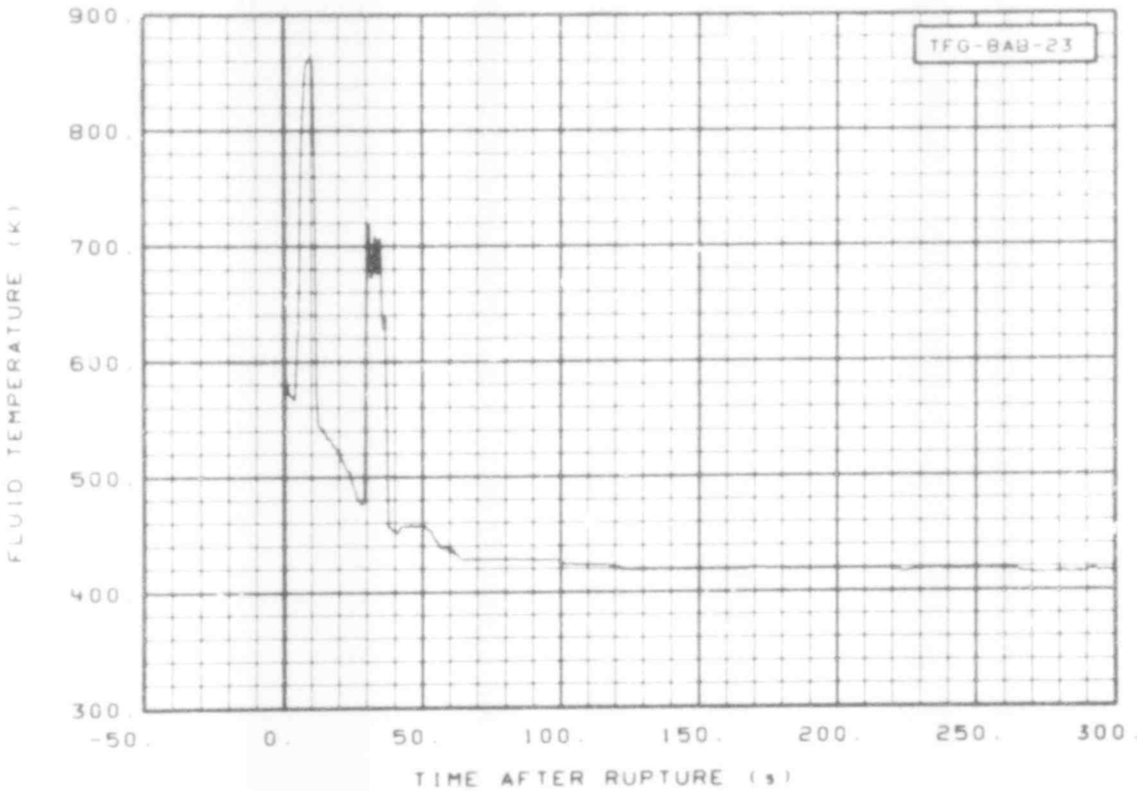

Fig. 41 Fluid temperature in core, Grid Spacer 8 (TFG-8AB-23), from -20 to 300 s.

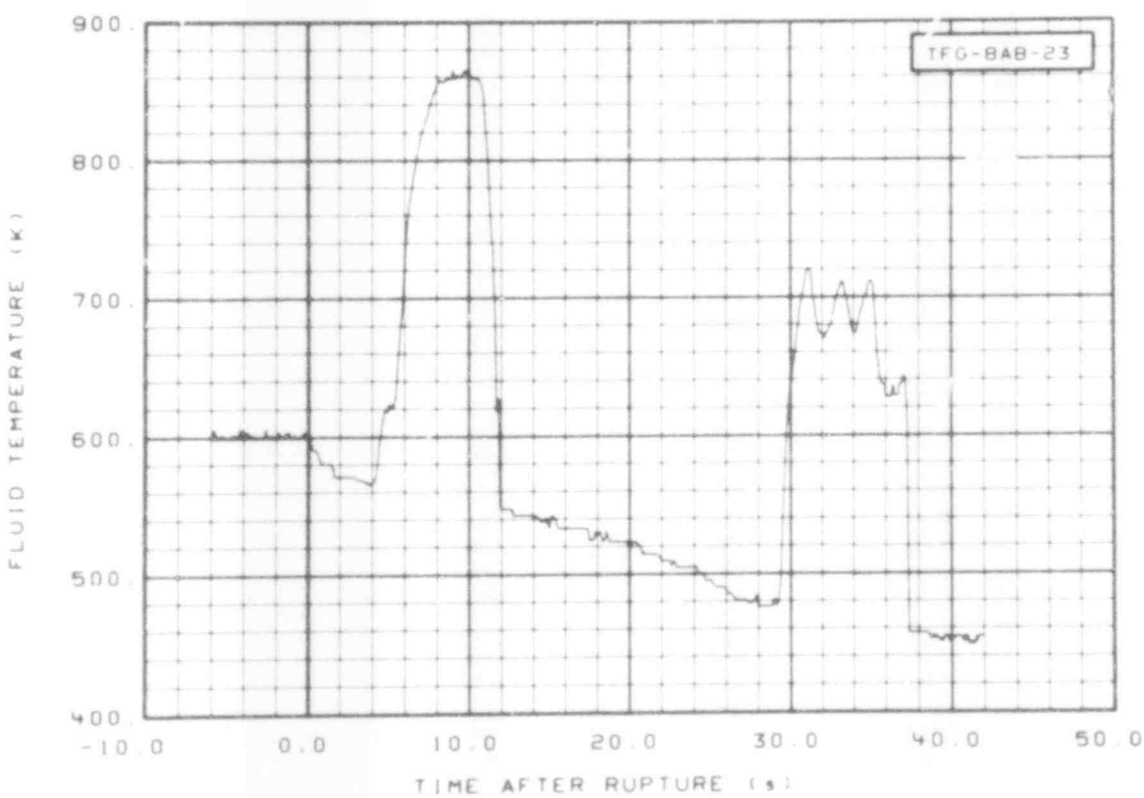

Fig. 42 Fluid temperature in core, Grid Spacer 8 (TFG-8AB-23), from -6 to 42 s.

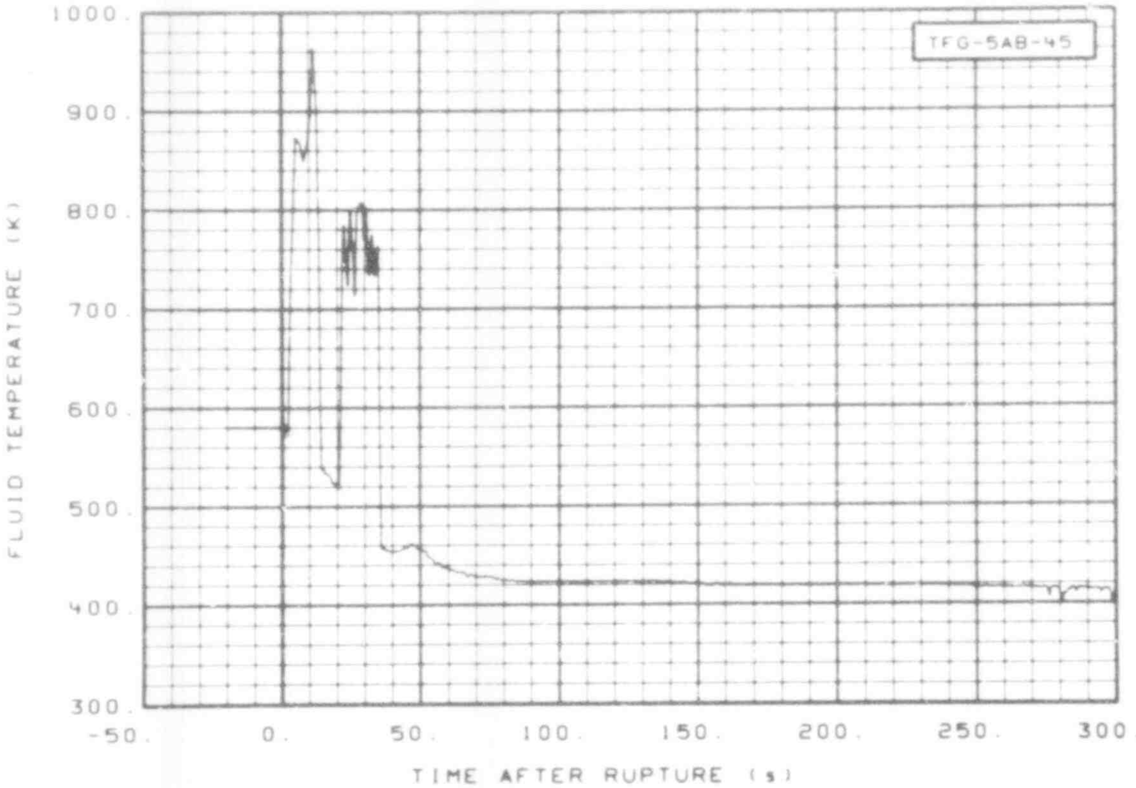

Fig. 39 Fluid temperature in core, Grid Spacer 5 (TFG-5AB-45), from -20 to 300 s.

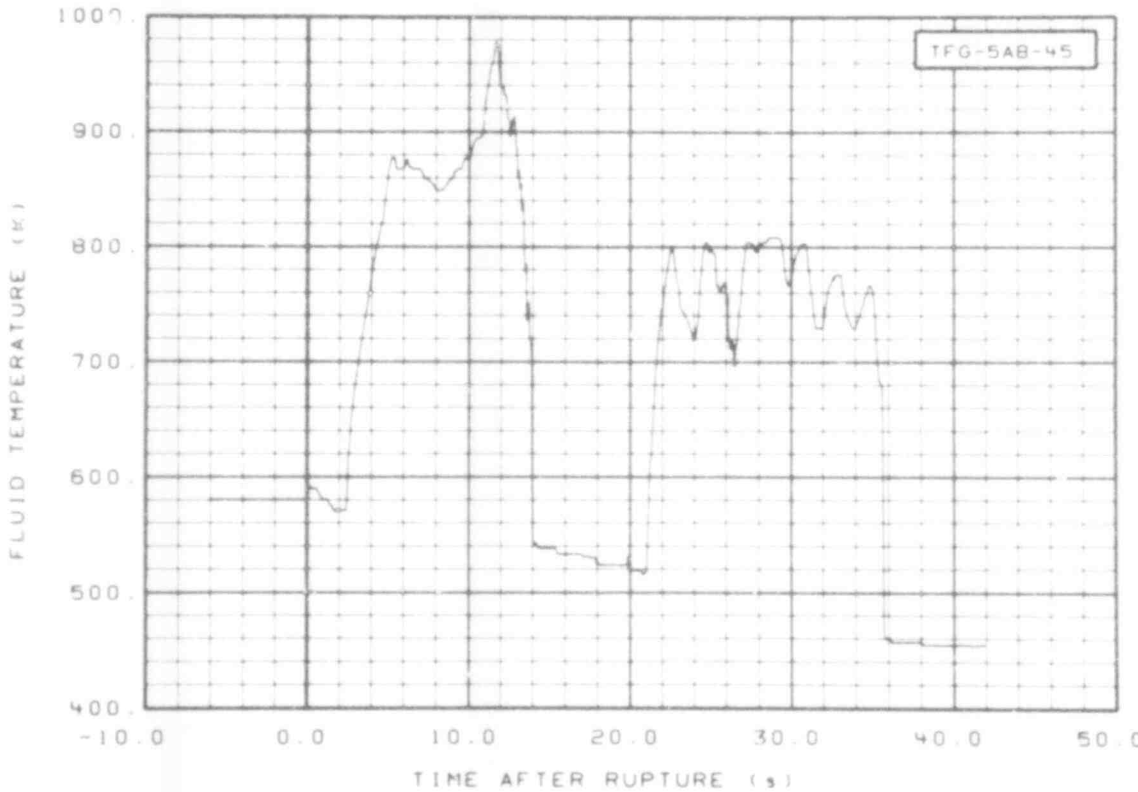

Fig. 40 Fluid temperature in core, Grid Spacer 5 (TFG-5AB-45), from -6 to 42 s.

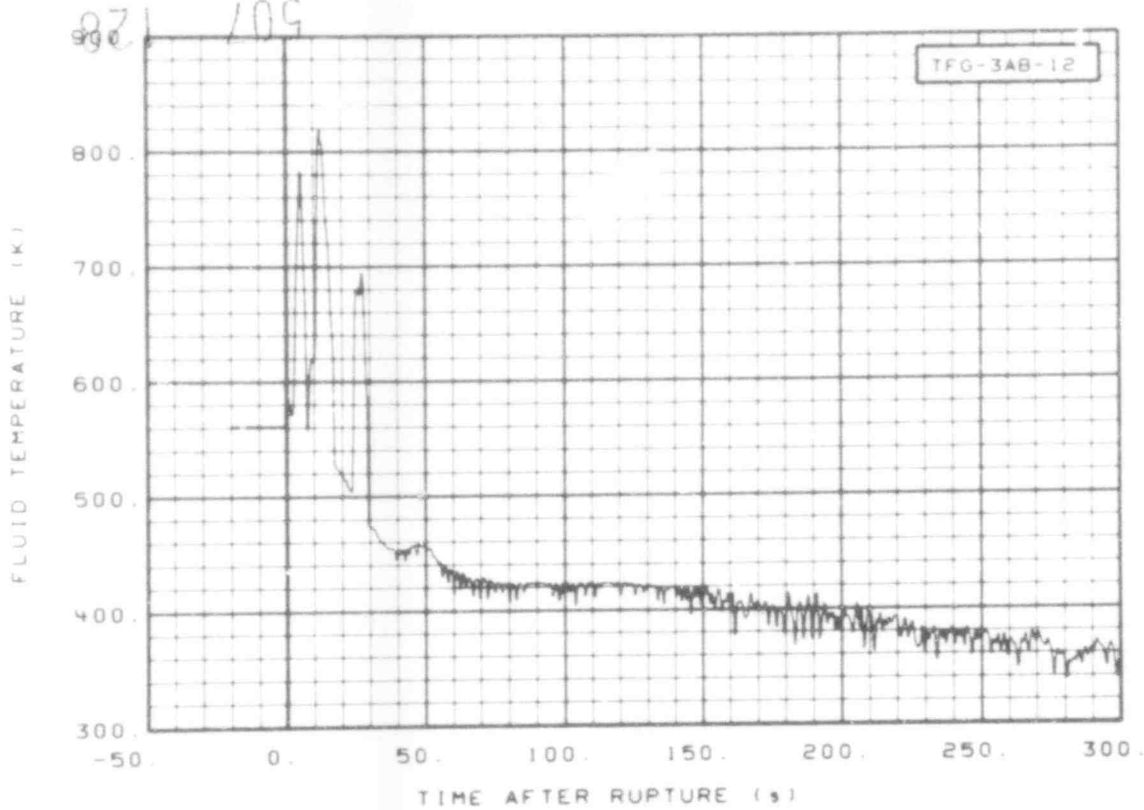

Fig. 37 Fluid temperature in core, Grid Spacer 3 (TFG-3AB-12), from -20 to 300 s.

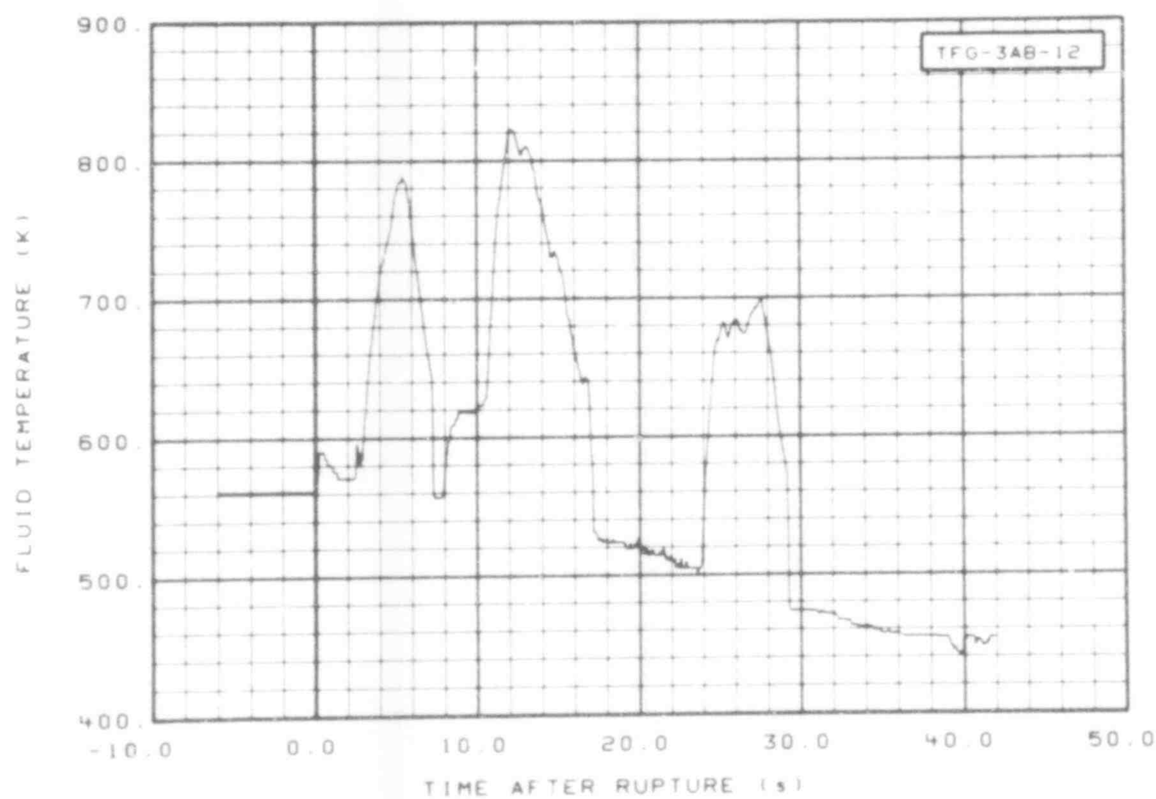

Fig. 38 Fluid temperature in core, Grid Spacer 3 (TFG-3AB-12), from -6 to 42 s.

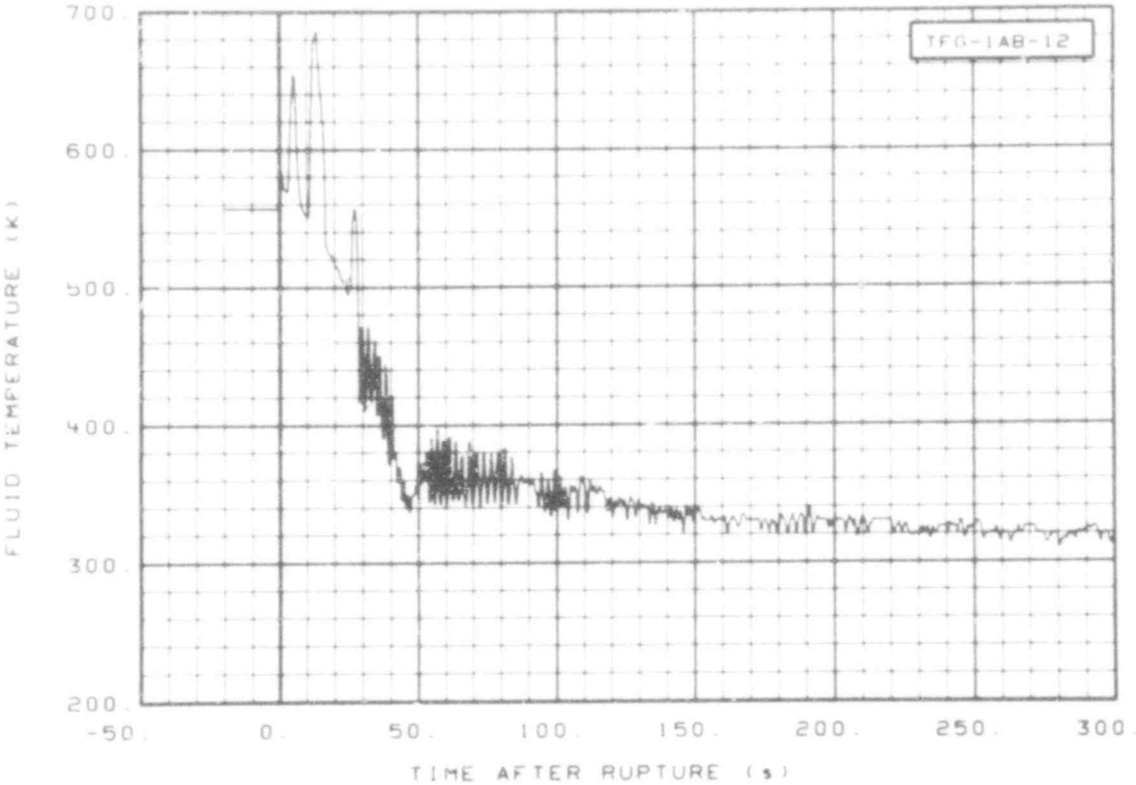

Fig. 35 Fluid temperature in core, Grid Spacer 1 (TFG-1AB-12), from -20 to 300 s.

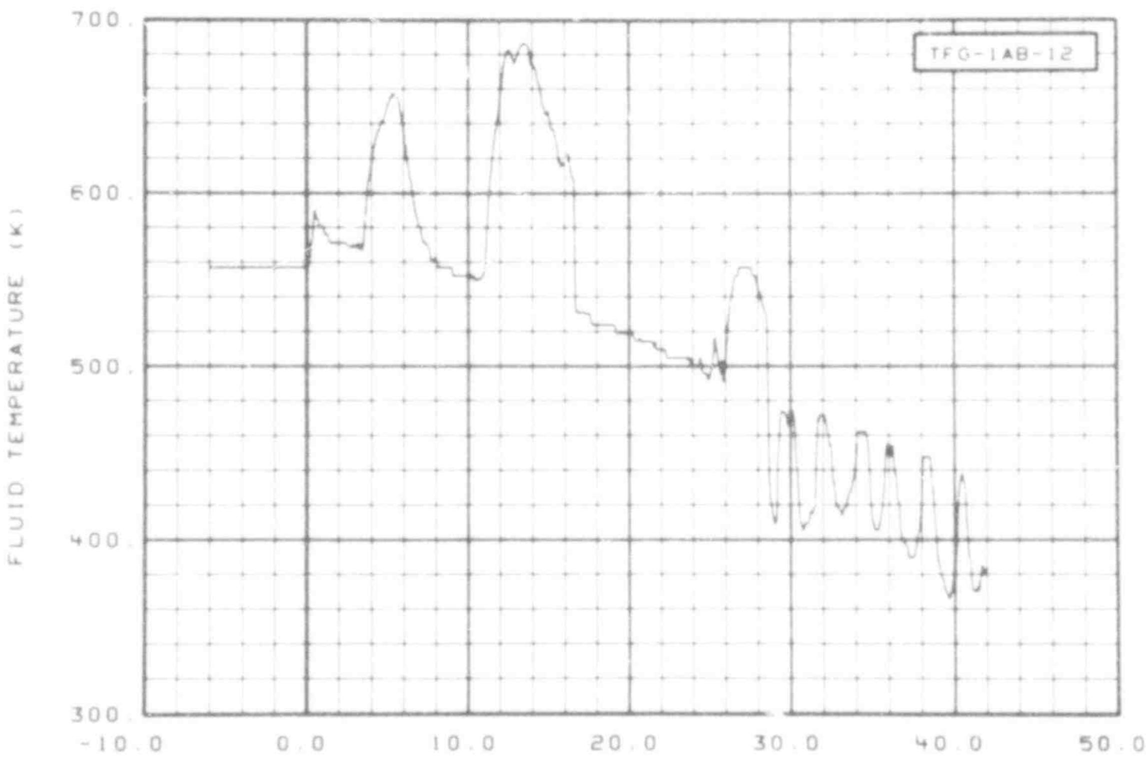

Fig. 36 Fluid temperature in core, Grid Spacer 1 (TFG-1AB-12), from -6 to 42 s.

507 130

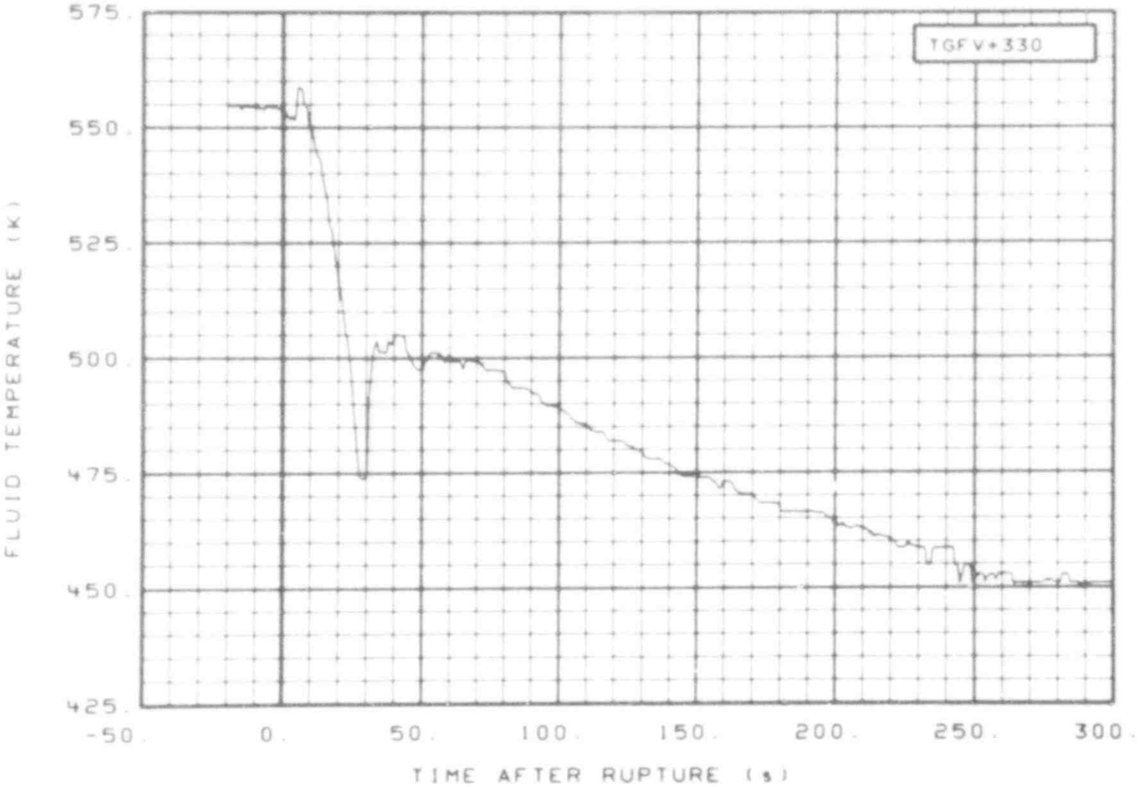

Fig. 33 Fluid temperature in vessel, core guide tube (TGFV + 330), from -20 to 300 s.

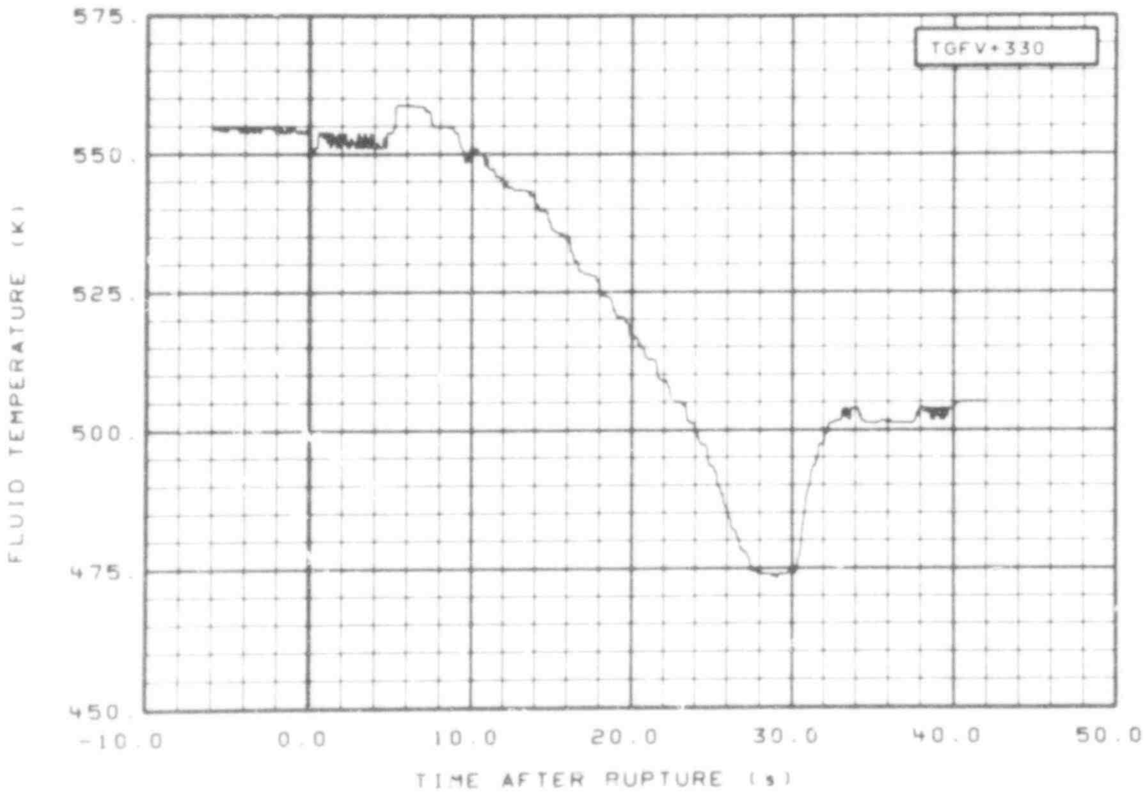

Fig. 34 Fluid temperature in vessel, core guide tube (TGFV + 330), from -6 to 42 s.

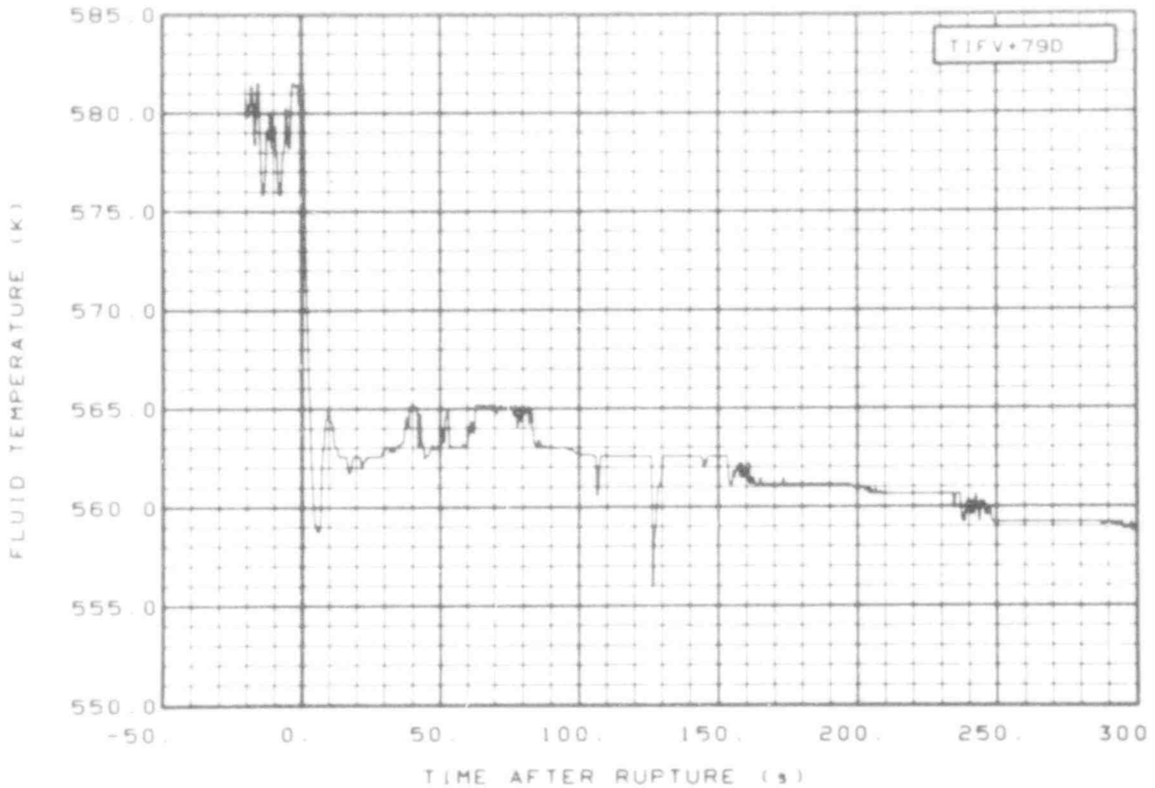

Fig. 31 Fluid temperature in vessel filler insulator gap (TIFV + 79D), from -20 to 300 s.

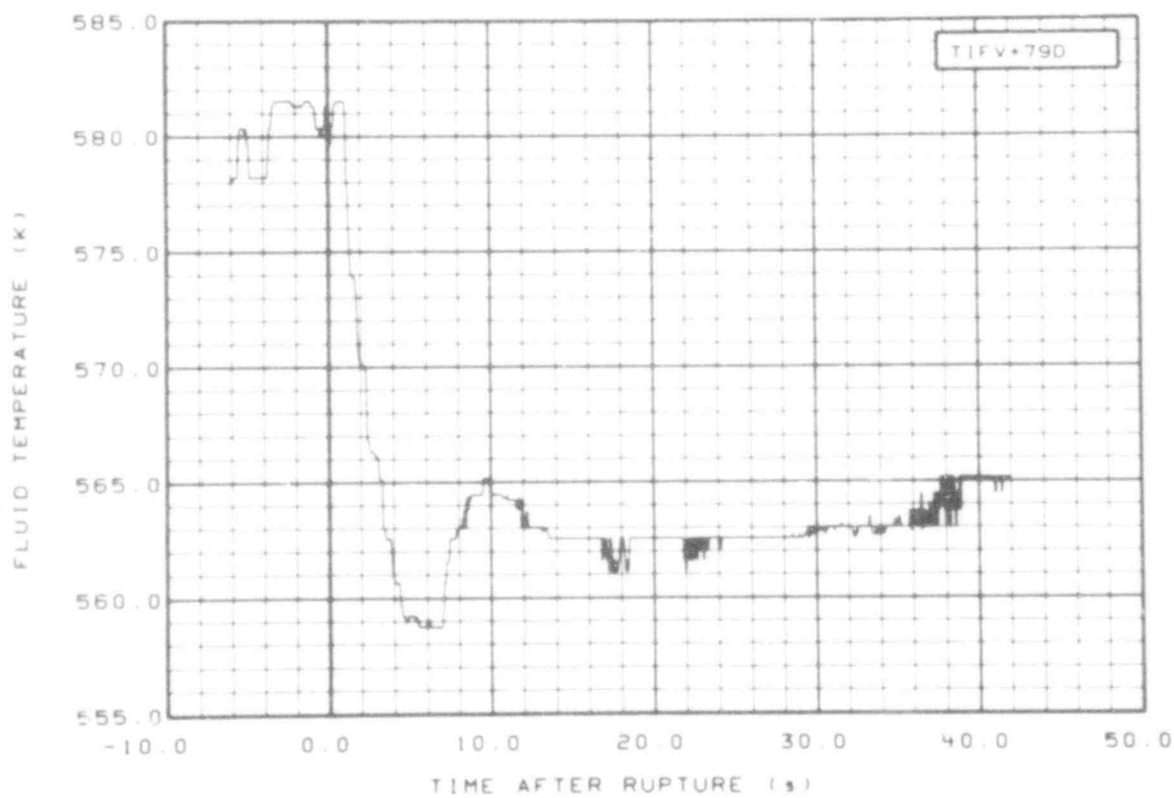

Fig. 32 Fluid temperature in vessel filler insulator gap (TIFV + 79D), from -6 to 42 s.

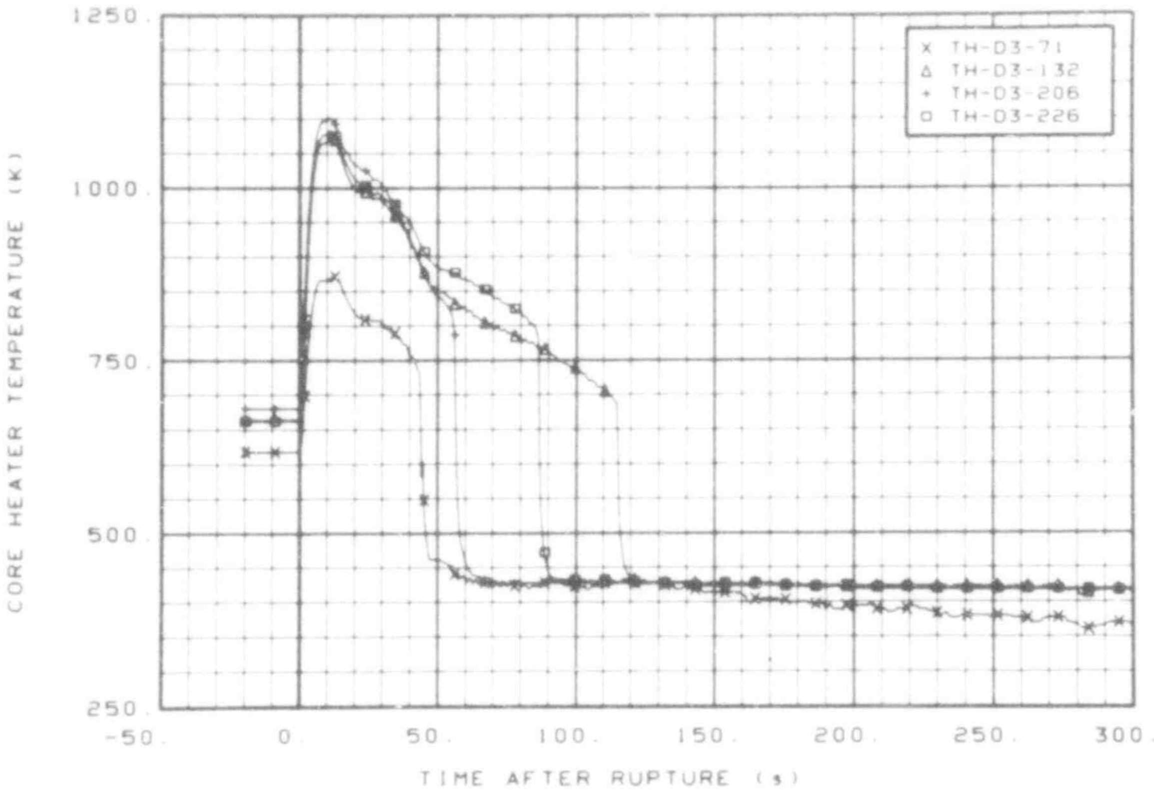

Fig. 79 Core heater temperature, Rod D-3 (TH-D3-71, TH-D3-132, TH-D3-206, and TH-D3-226), from -20 to 300 s.

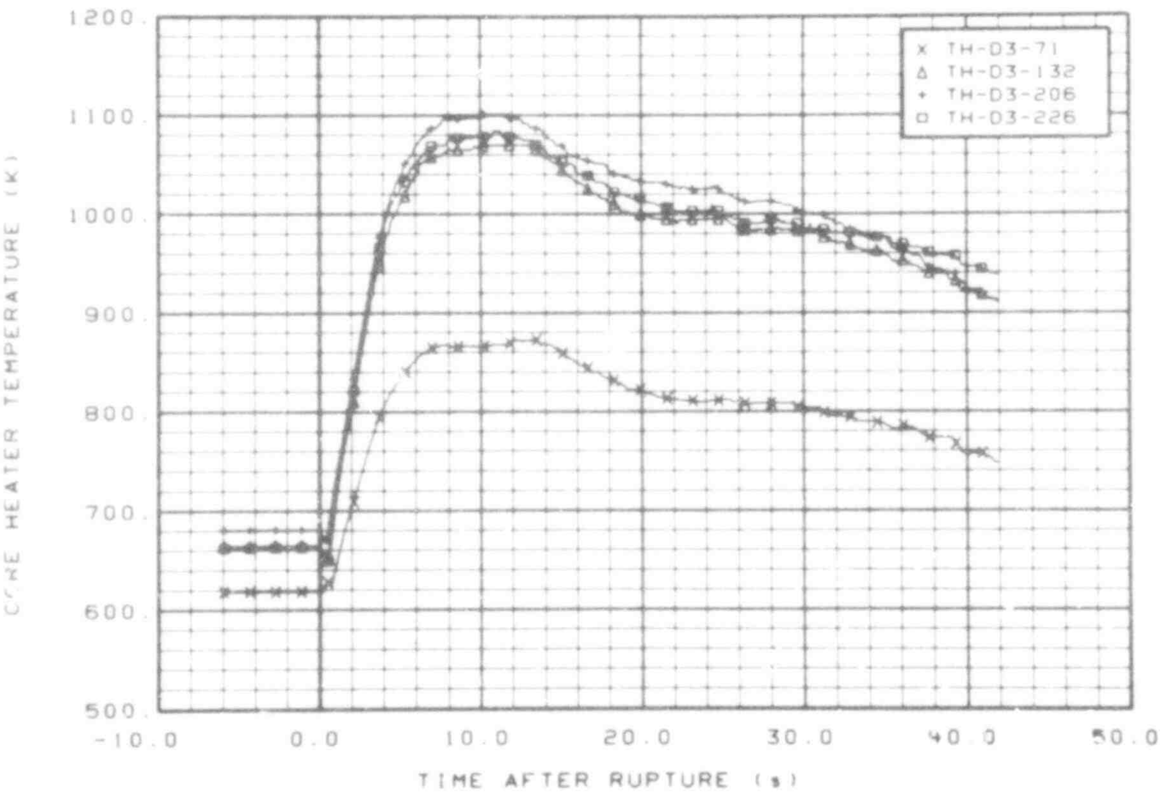

Fig. 80 Core heater temperature, Rod D-3 (TH-D3-71, TH-D3-132, TH-D3-206, and TH-D3-226), from -6 to 42 s.

507 132

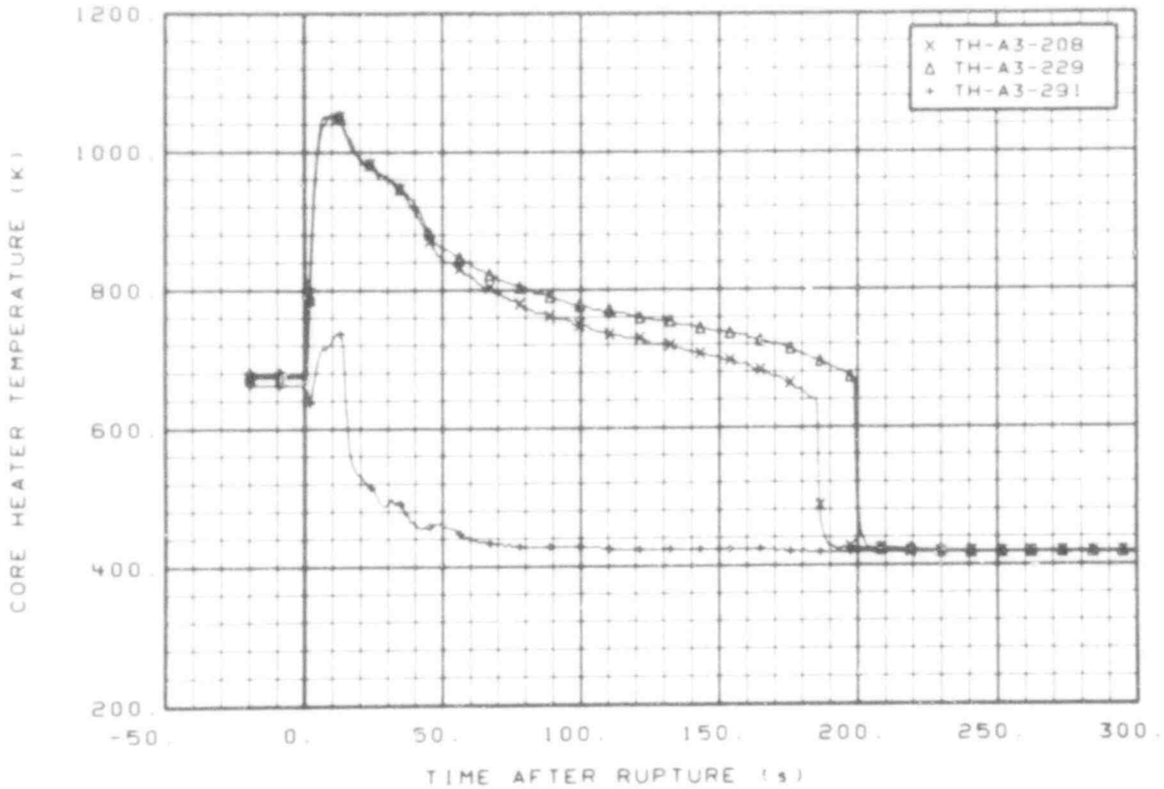

Fig. 81 Core heater temperature, Rod A-3 (TH-A3-208, TH-A3-229, and TH-A3-291), from -20 to 300 s.

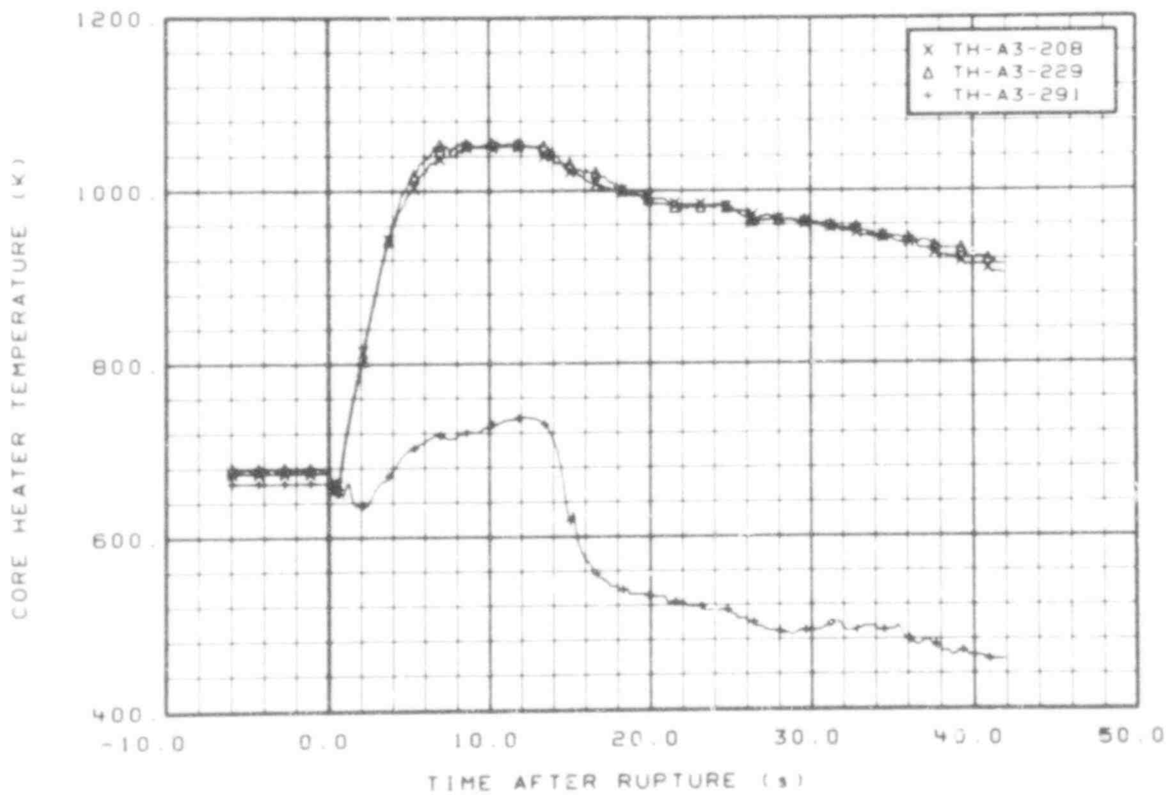

Fig. 82 Core heater temperature, Rod A-3 (TH-A3-208, TH-A3-229, and TH-A3-291), from -6 to 42 s.

507 133

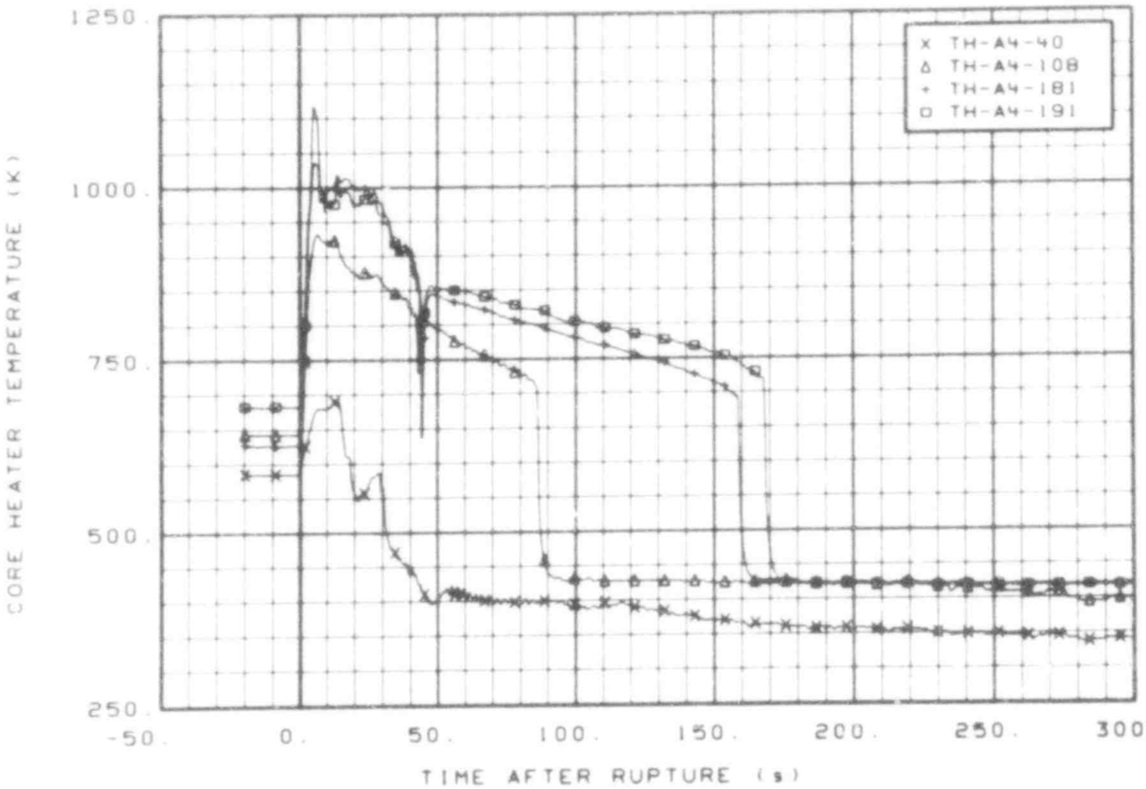

Fig. 83 Core heater temperature, Rod A-4 (TH-A4-40, TH-A4-108, TH-A4-181, and TH-A4-191), from -20 to 300 s.

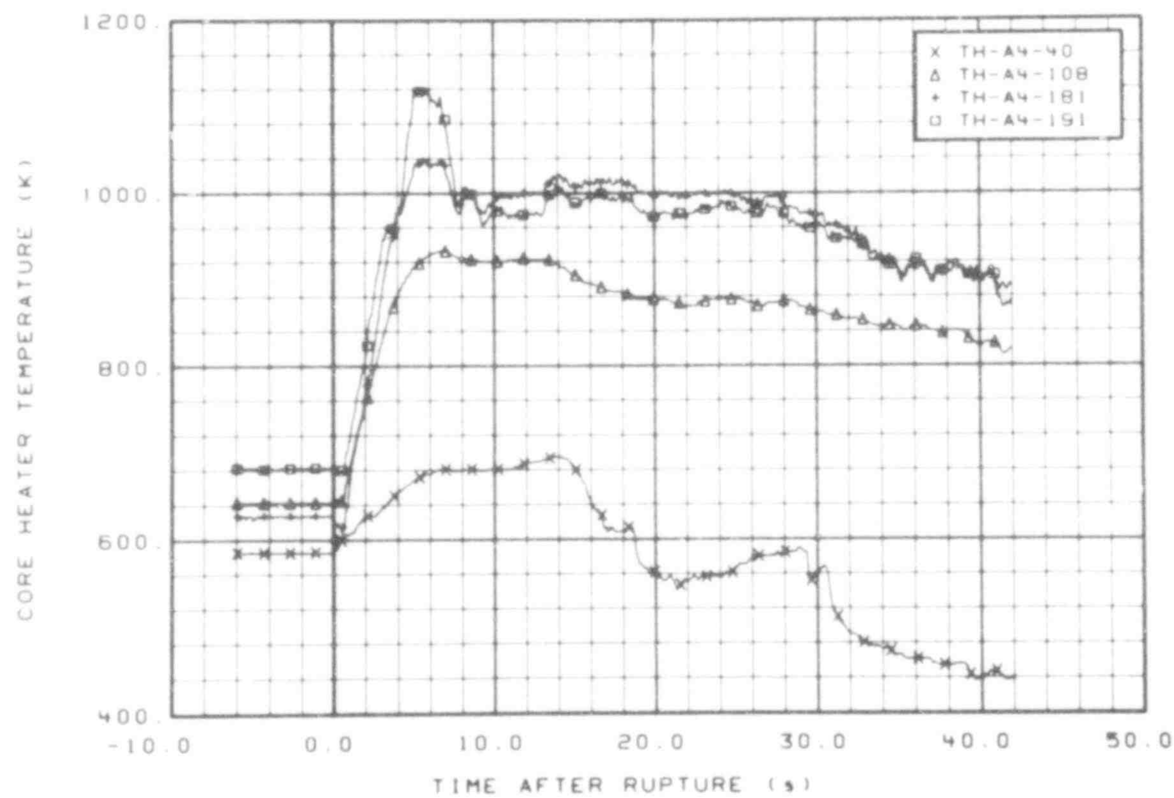

Fig. 84 Core heater temperature, Rod A-4 (TH-A4-40, TH-A4-108, TH-A4-181, and TH-A4-191), from -6 to 42 s.

507 134

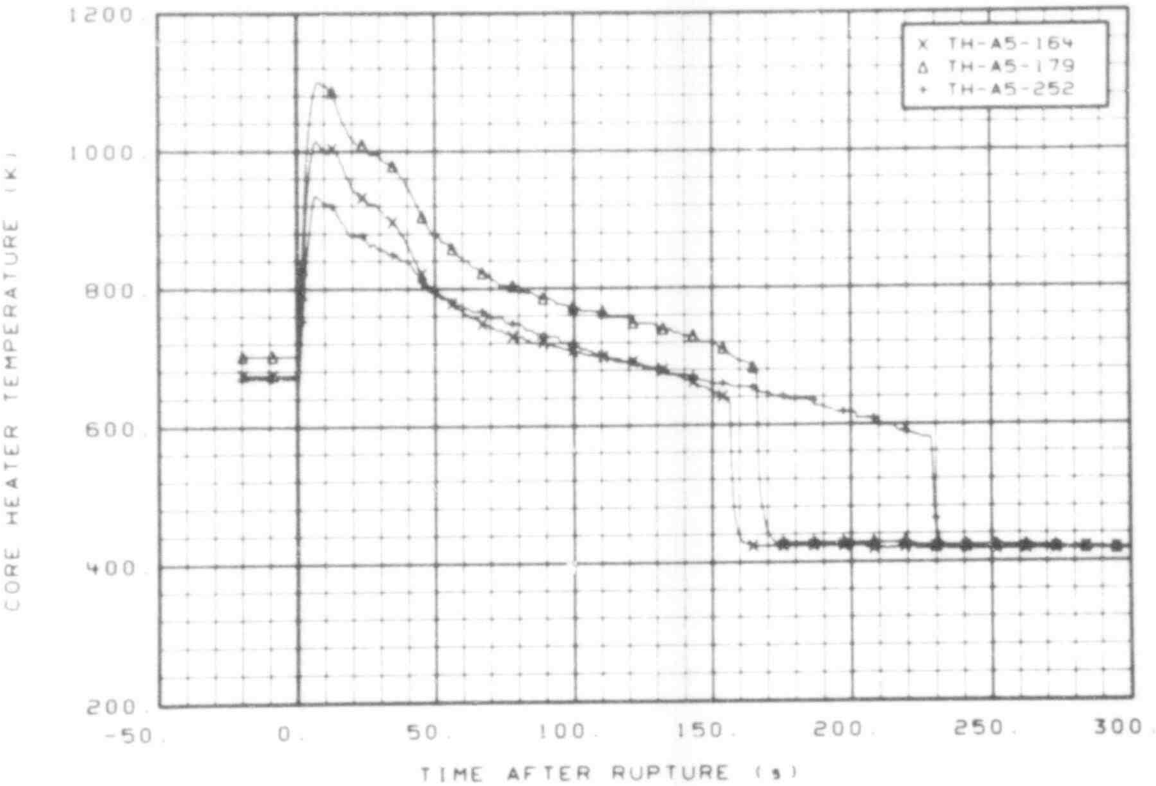

Fig. 85 Core heater temperature, Rod A-5 (TH-A5-164, TH-A5-179, and TH-A5-252), from -20 to 300 s.

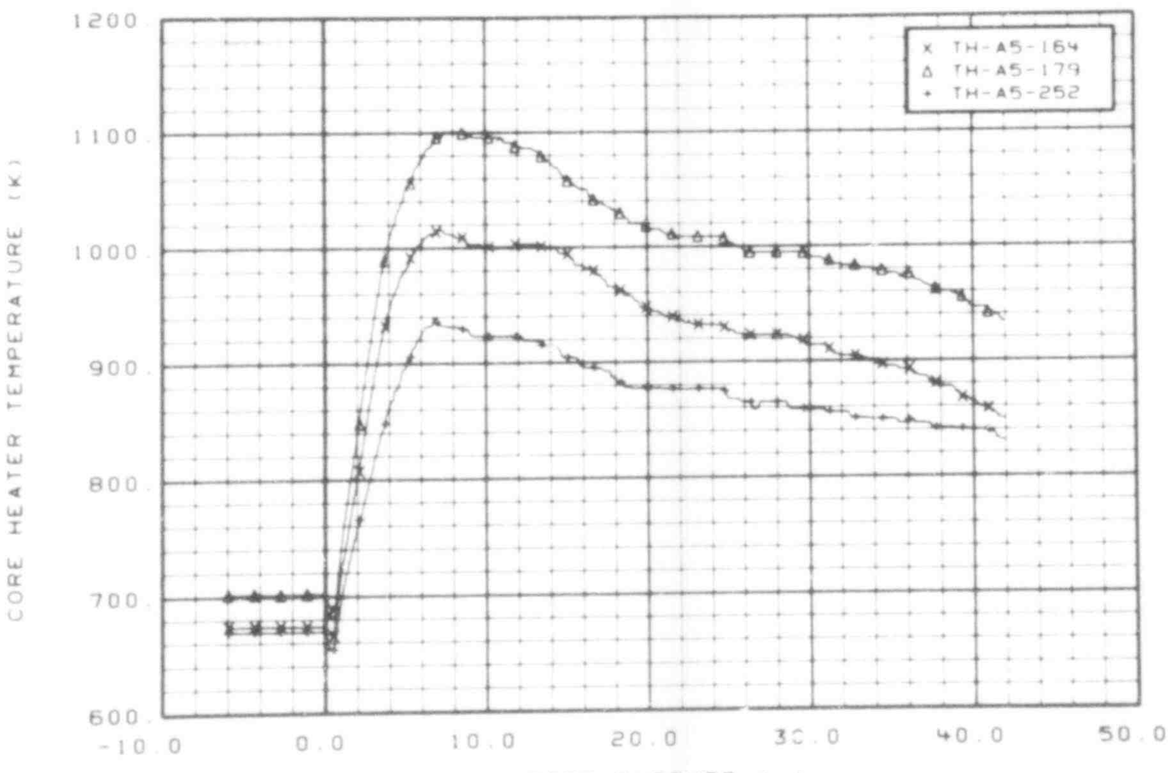

Fig. 86 Core heater temperature, Rod A-5 (TH-A5-164, TH-A5-179, and TH-A5-252), from -6 to 42 s.

507 135

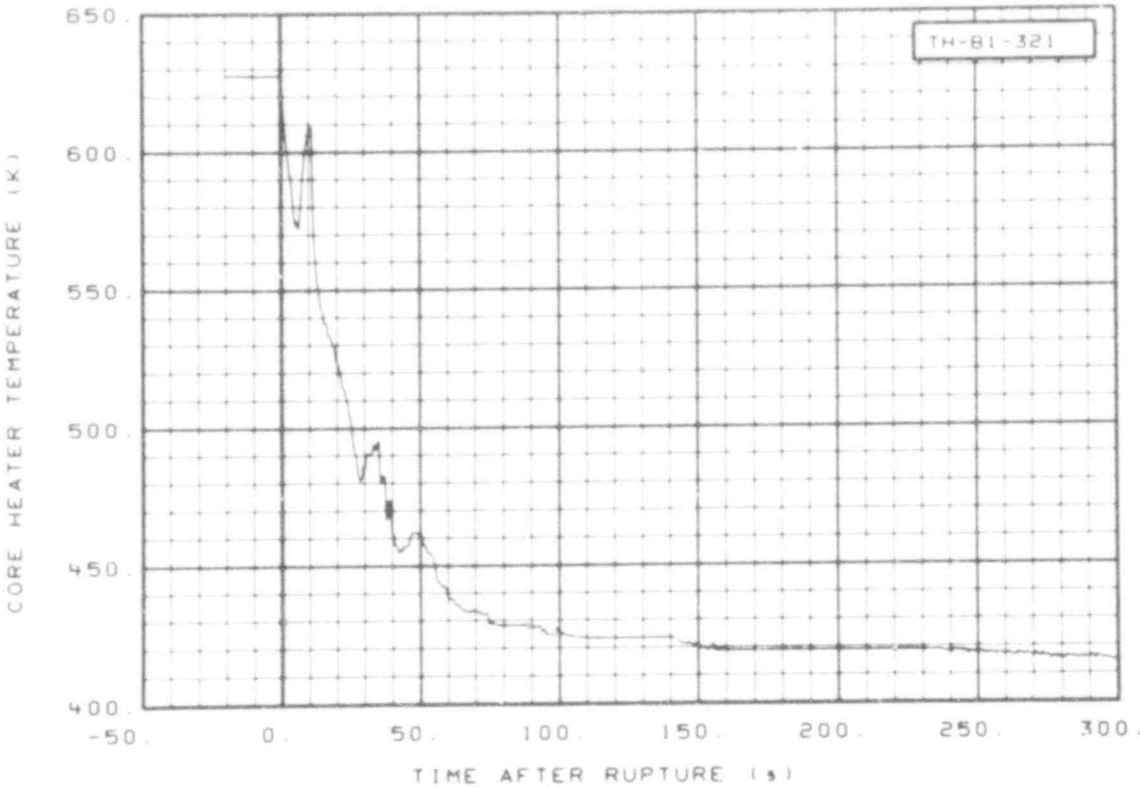

Fig. 87 Core heater temperature, Rod B-1 (TH-B1-321), from -20 to 300 s.

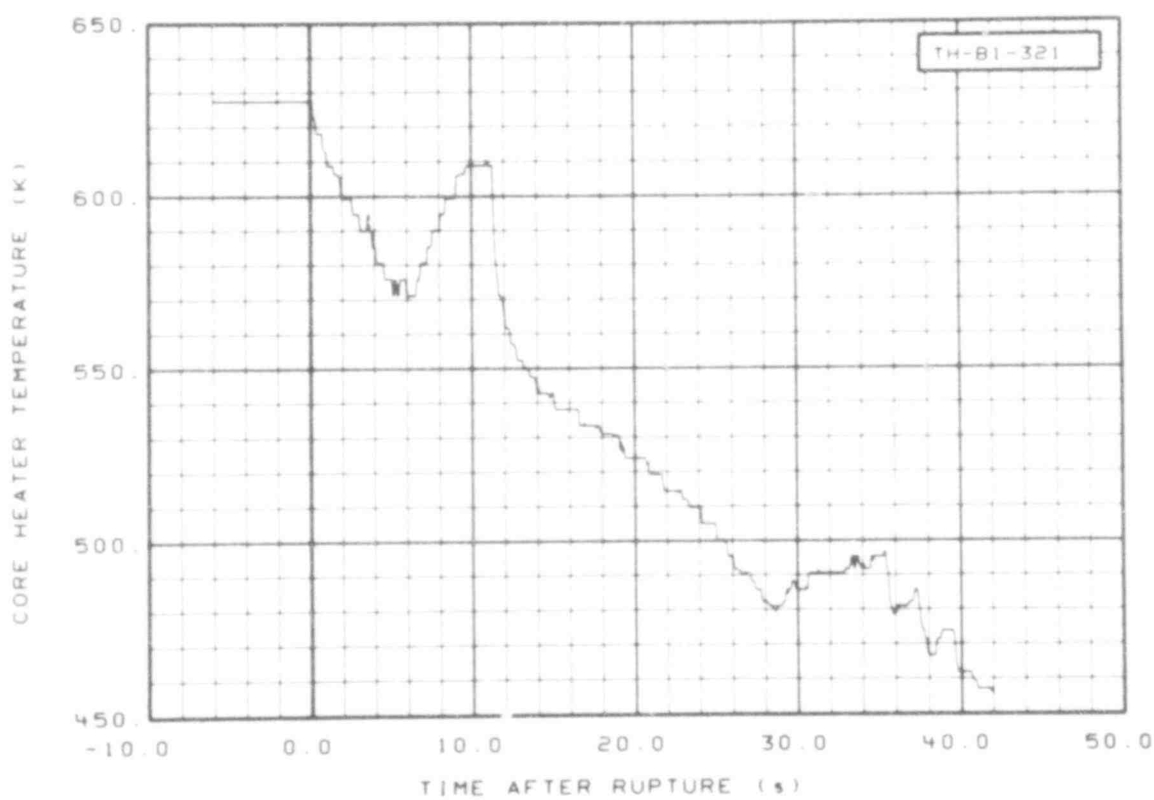

Fig. 88 Core heater temperature, Rod B-1 (TH-B1-321), from -6 to 42 s.

507 136

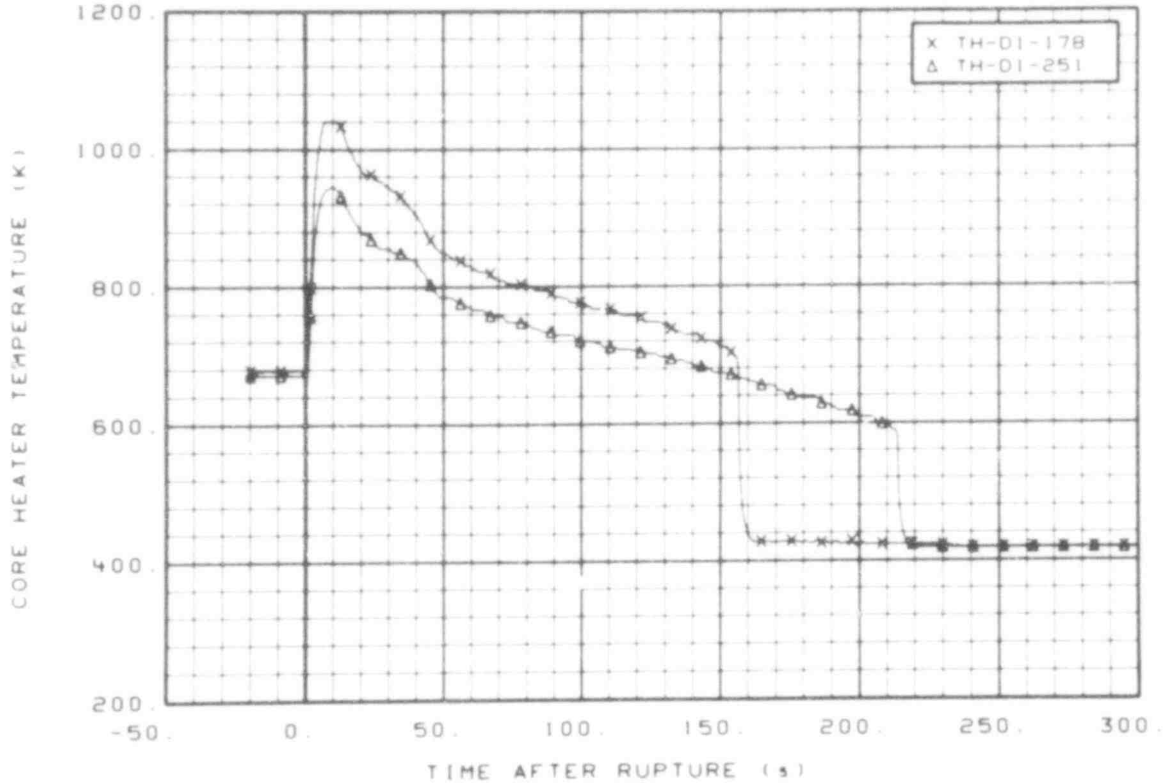

Fig. 89 Core heater temperature, Rod D-1 (TH-D1-178 and TH-D1-251), from -20 to 300 s.

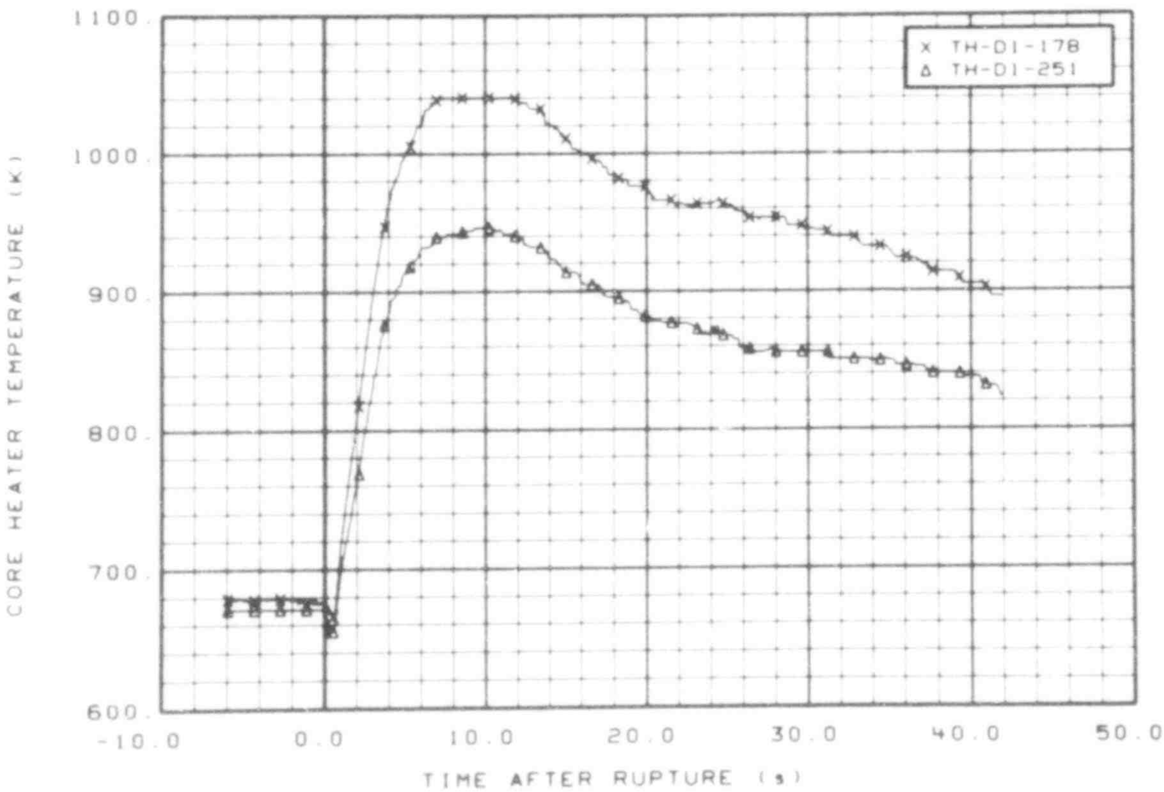

Fig. 90 Core heater temperature, Rod D-1 (TH-D1-178 and TH-D1-251), from -6 to 42 s.

507 137

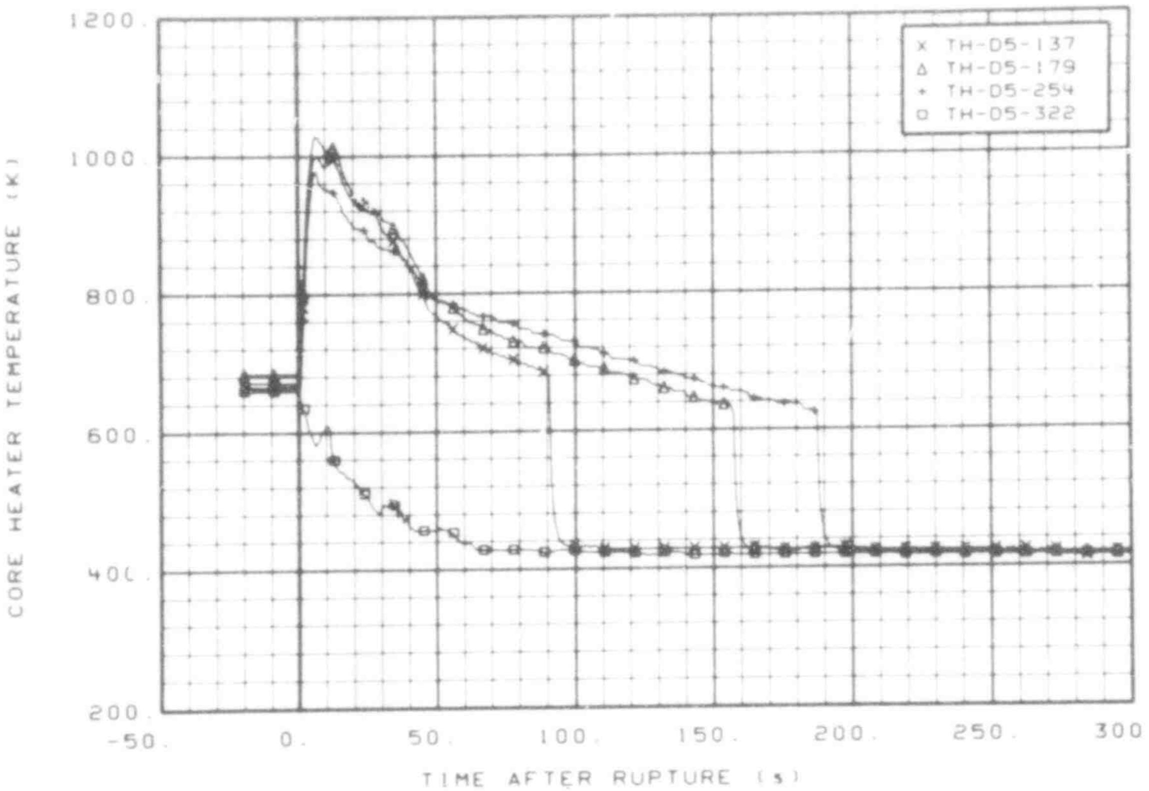

Fig. 91 Core heater temperature, Rod D-5 (TH-D5-137, TH-D5-179, TH-D5-254, and TH-D5-322), from -20 to 300 s.

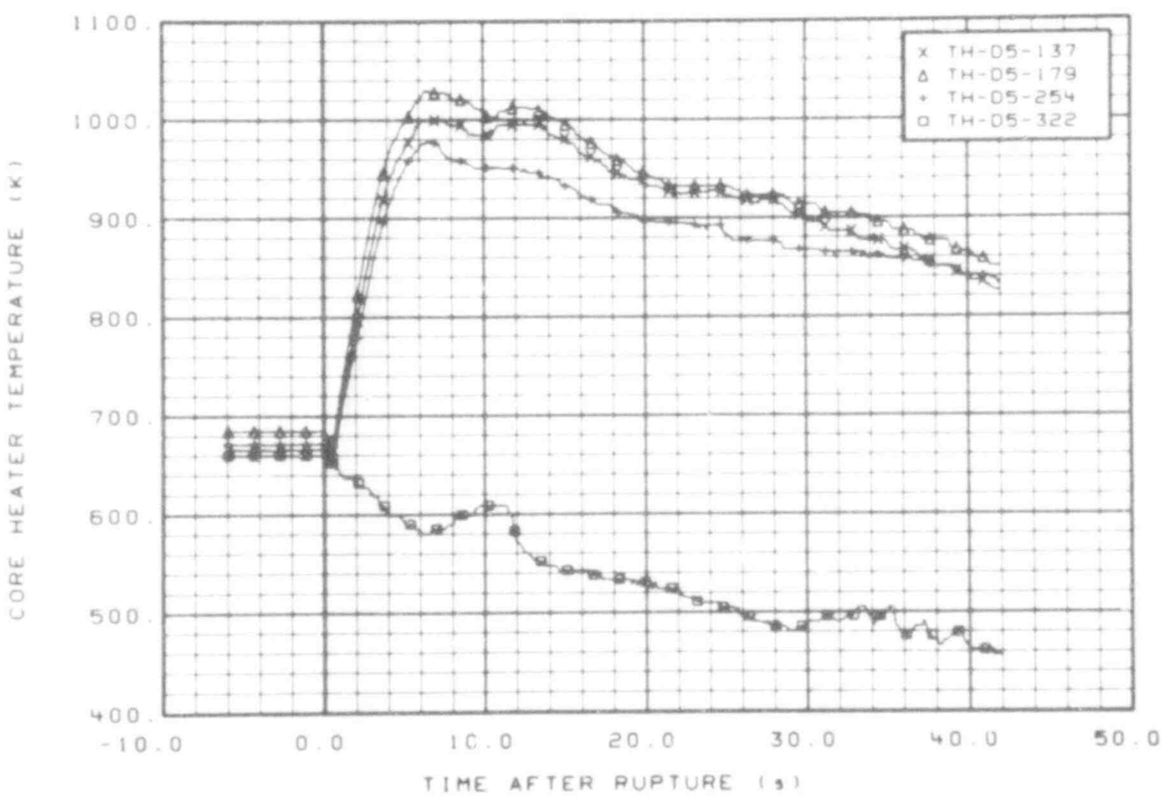

Fig. 92 Core heater temperature, Rod D-5 (TH-D5-137, TH-D5-179, TH-D5-254, and TH-D5-322), from -6 to 42 s.

507 138

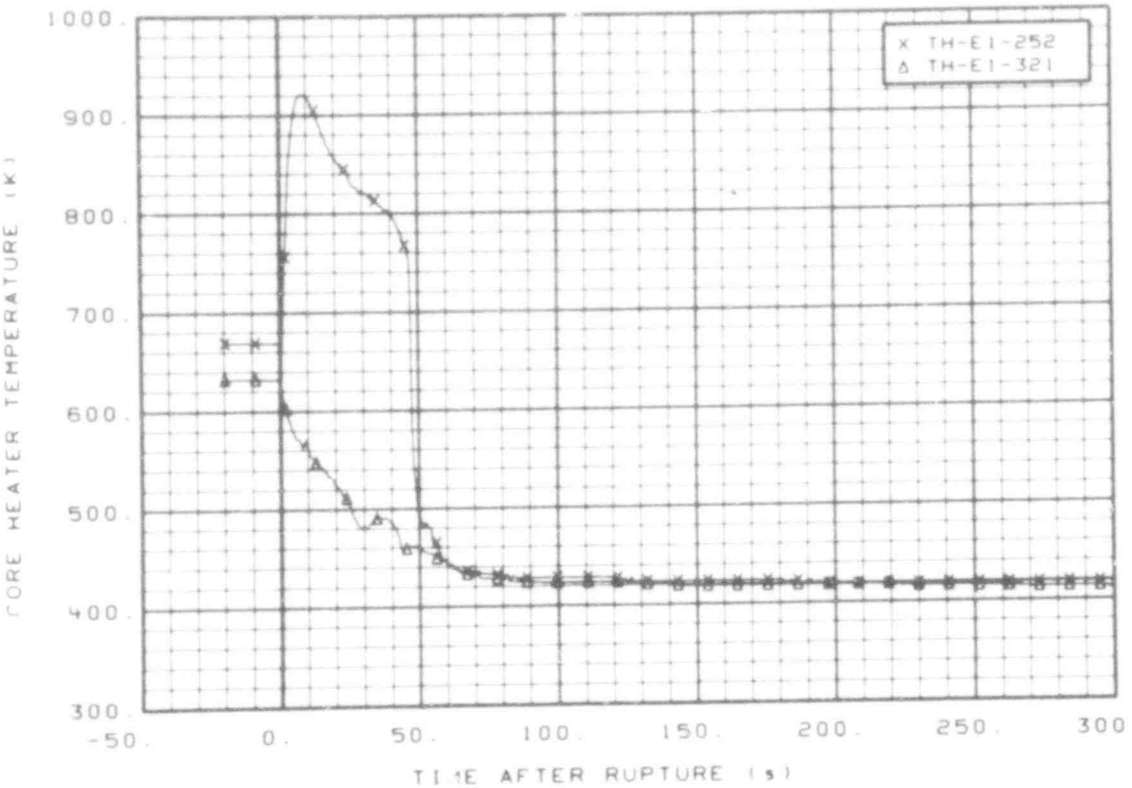

Fig. 93 Core heater temperature, Rod E-1 (TH-E1-252 and TH-E1-321), from -20 to 300 s.

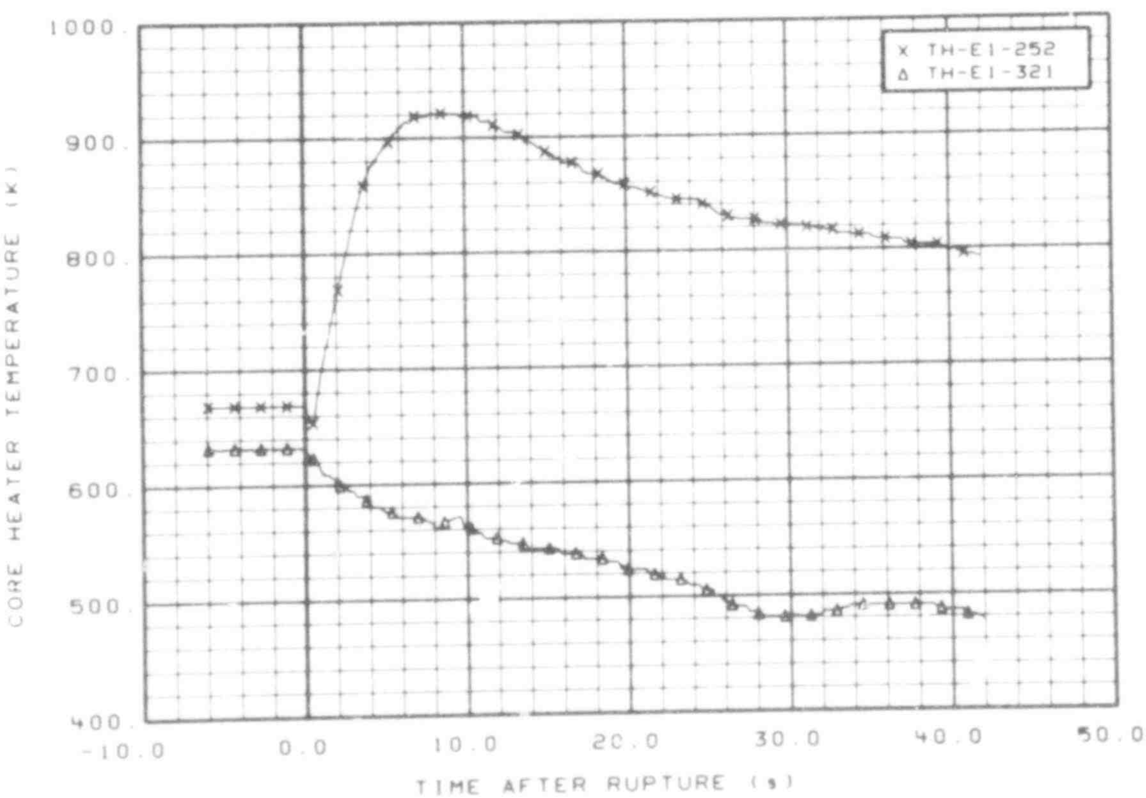

Fig. 94 Core heater temperature, Rod E-1 (TH-E1-252 and TH-E1-321), from -6 to 42 s.

507 139

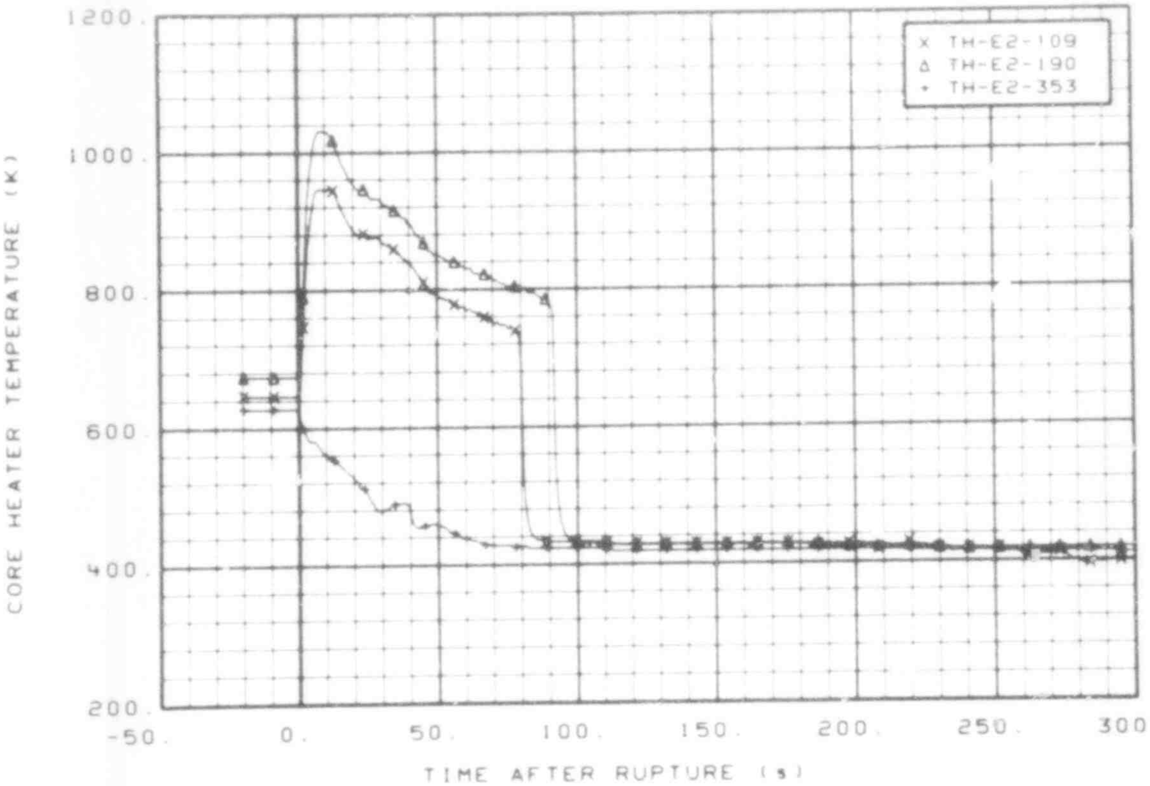

Fig. 95 Core heater temperature, Rod E-2 (TH-E2-109, TH-E2-190, and TH-E2-353), from -20 to 300 s.

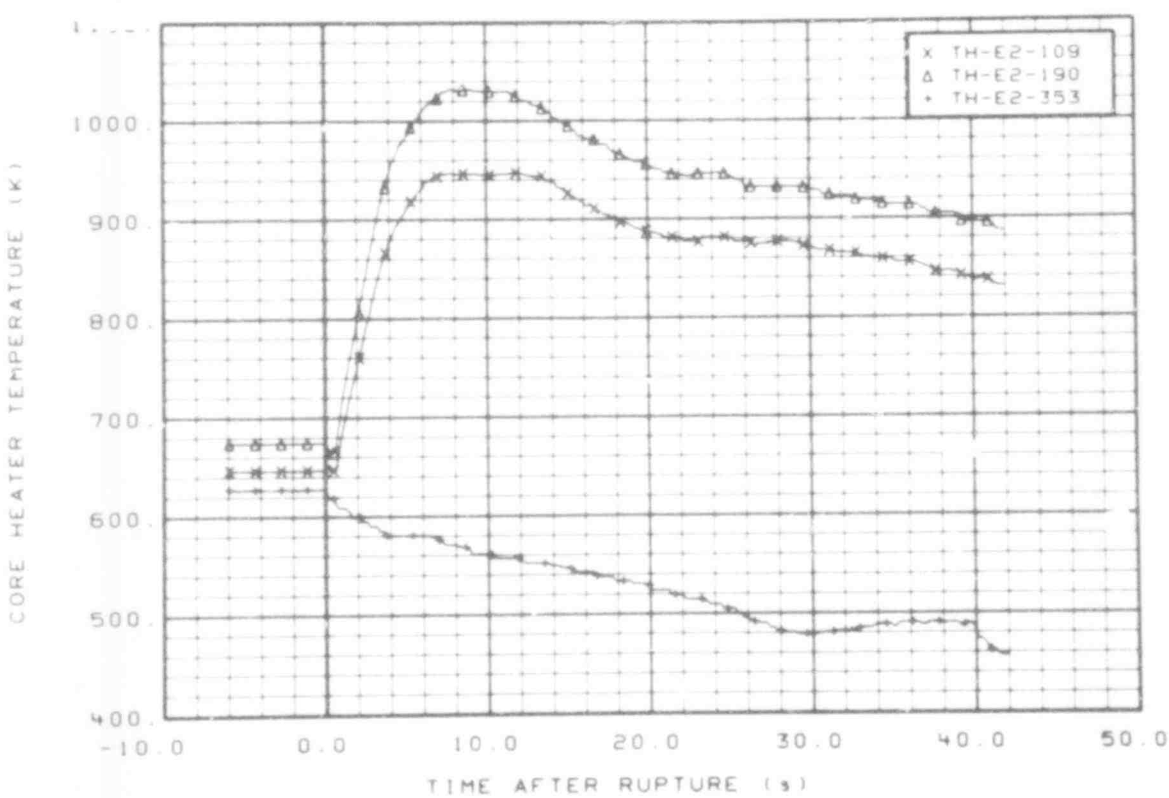

Fig. 96 Core heater temperature, Rod E-2 (TH-E2-109, TH-E2-190, and TH-E2-353), from -6 to 42 s.

507 140

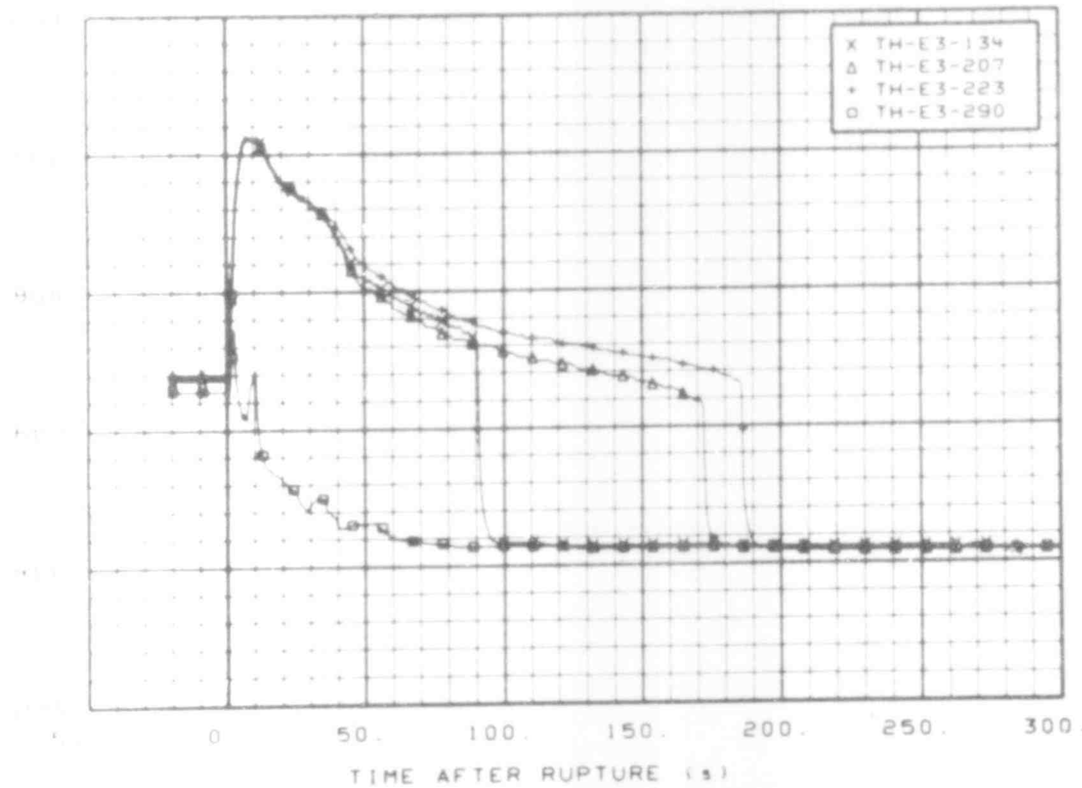

Core heater temperature, Rod E-3 (TH-E3-134, TH-E3-207, TH-E3-223, and TH-E3-290), from -20 to 300 s.

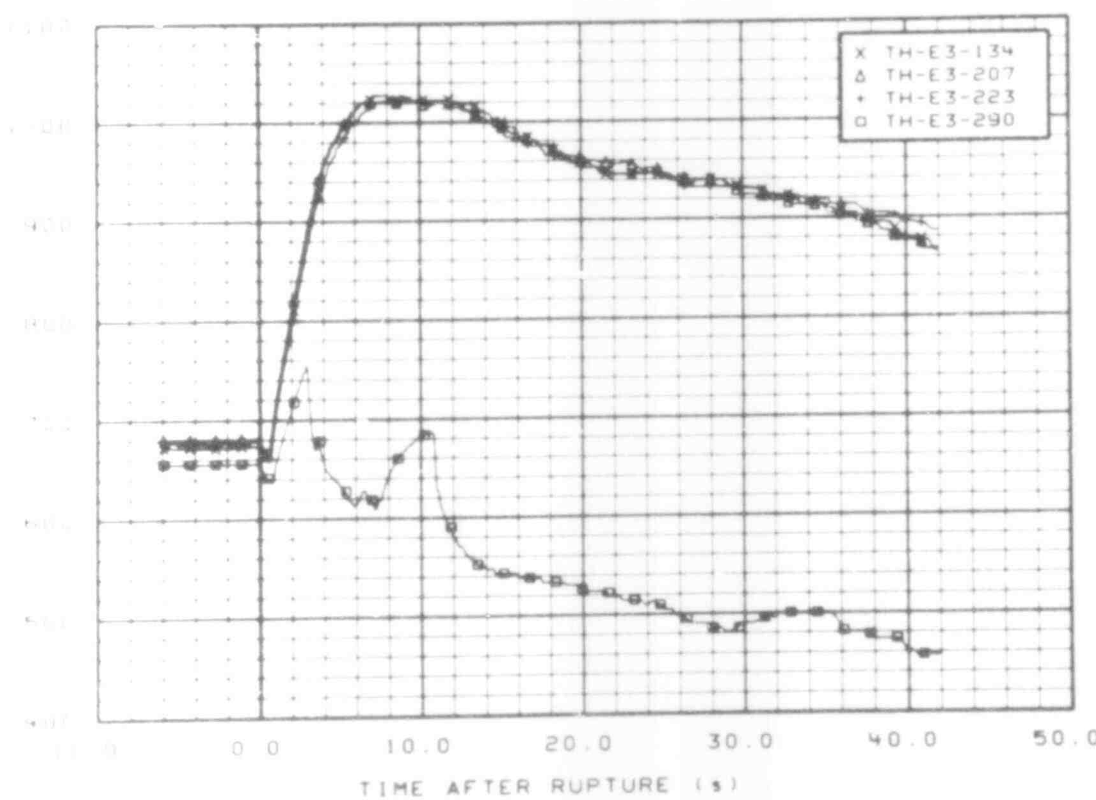

Core heater temperature, Rod E-3 (TH-E3-134, TH-E3-207, TH-E3-223, and TH-E3-290), from -6 to 42 s.

507 141

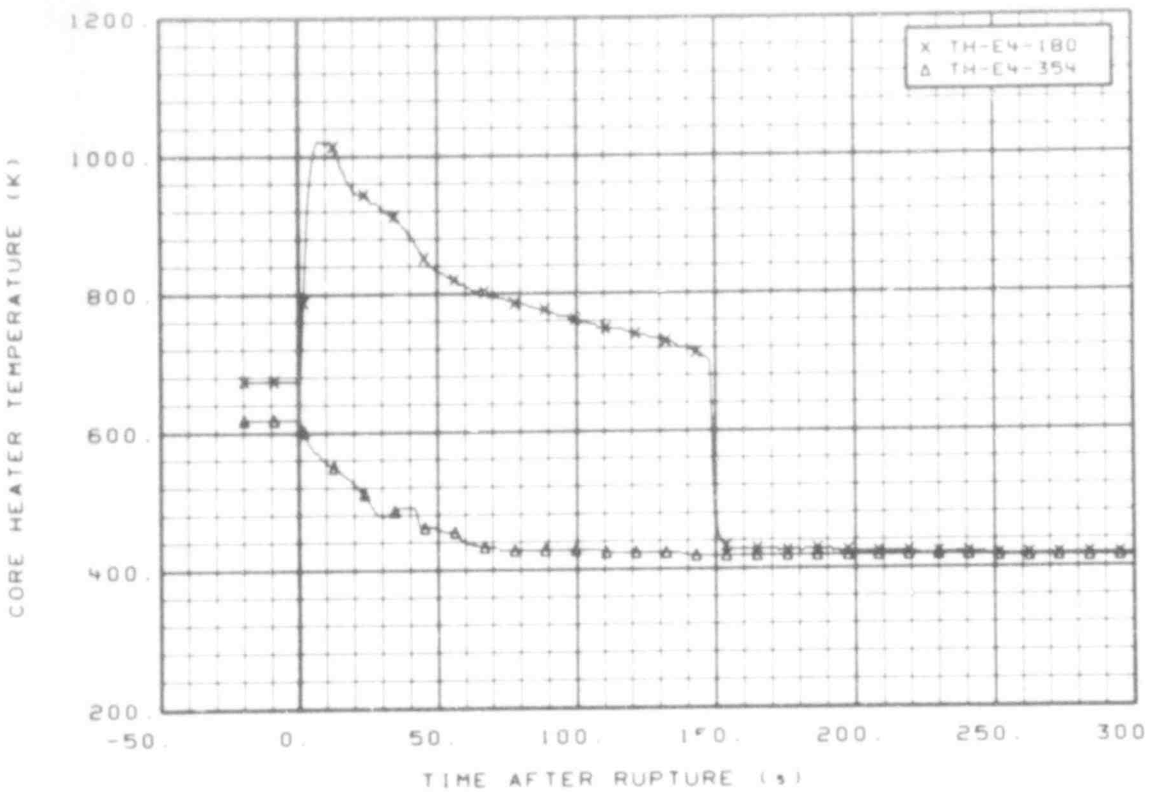

Fig. 99 Core heater temperature, Rod E-4 (TH-E4-180 and TH-E4-354), from -20 to 300 s.

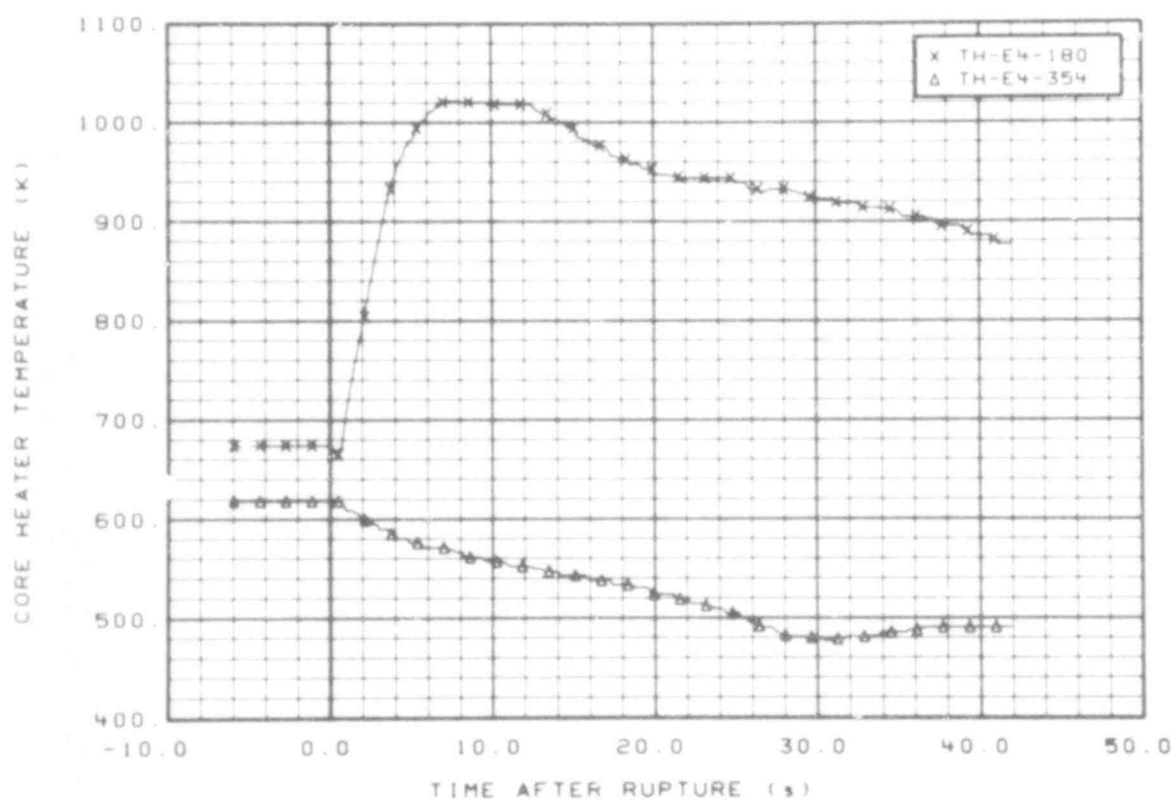

Fig. 100 Core heater temperature, Rod E-4 (TH-E4-180 and TH-E4-354), from -6 to 42 s.

507 142

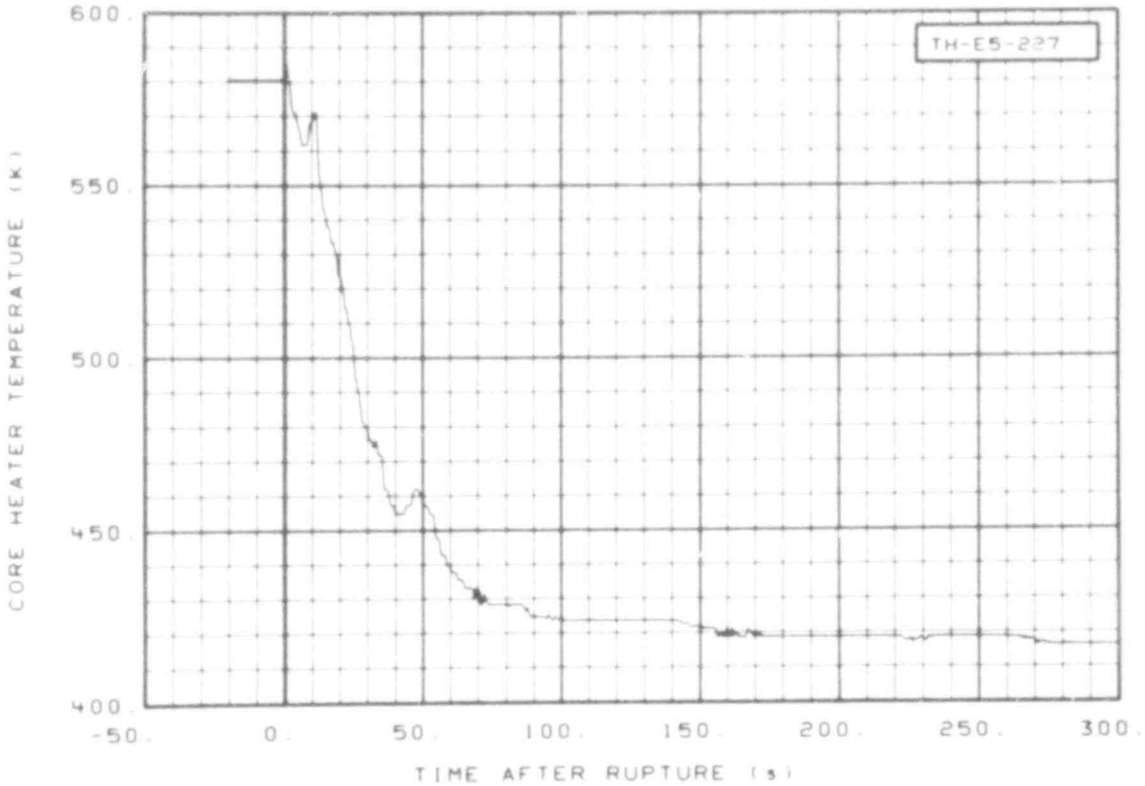

Fig. 101 Core heater temperature, Rod E-5 (TH-E5-227), from -20 to 300 s.

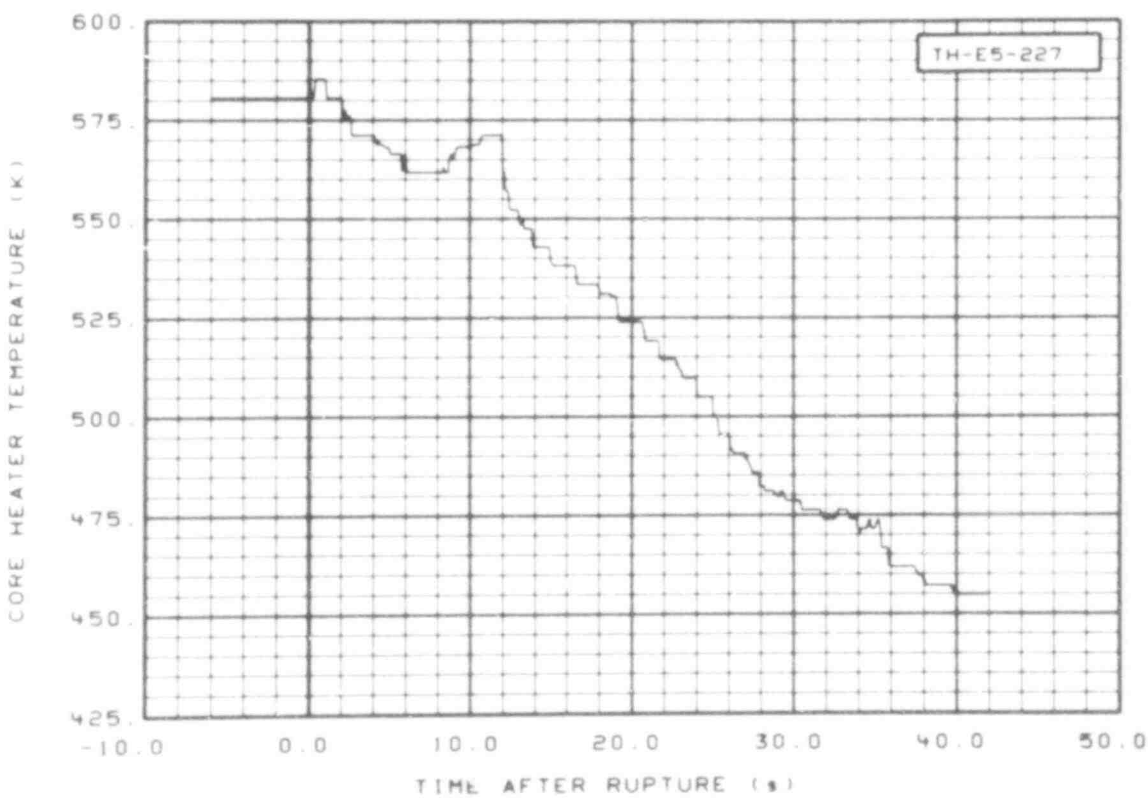

Fig. 102 Core heater temperature, Rod E-5 (TH-E5-227), from -6 to 42 s.

507 143

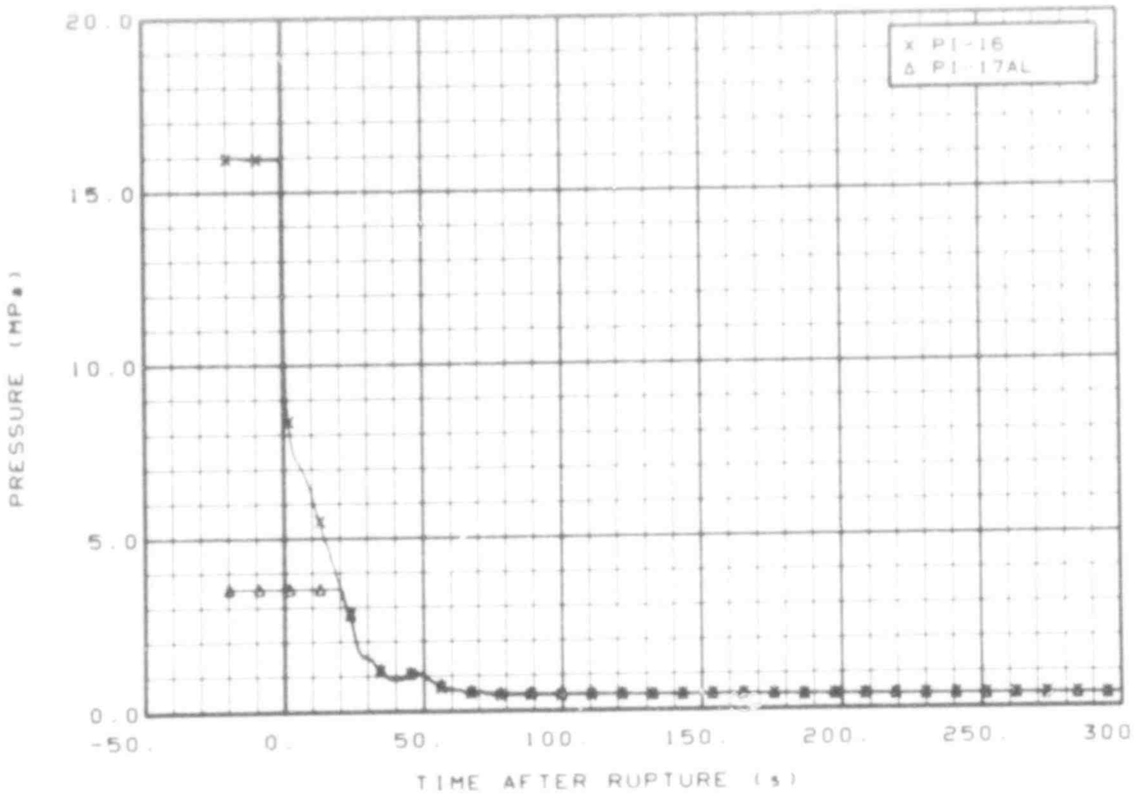

Fig. 103 Pressure in intact loop cold leg (PI-16 and PI-17AL), from -20 to 300 s.

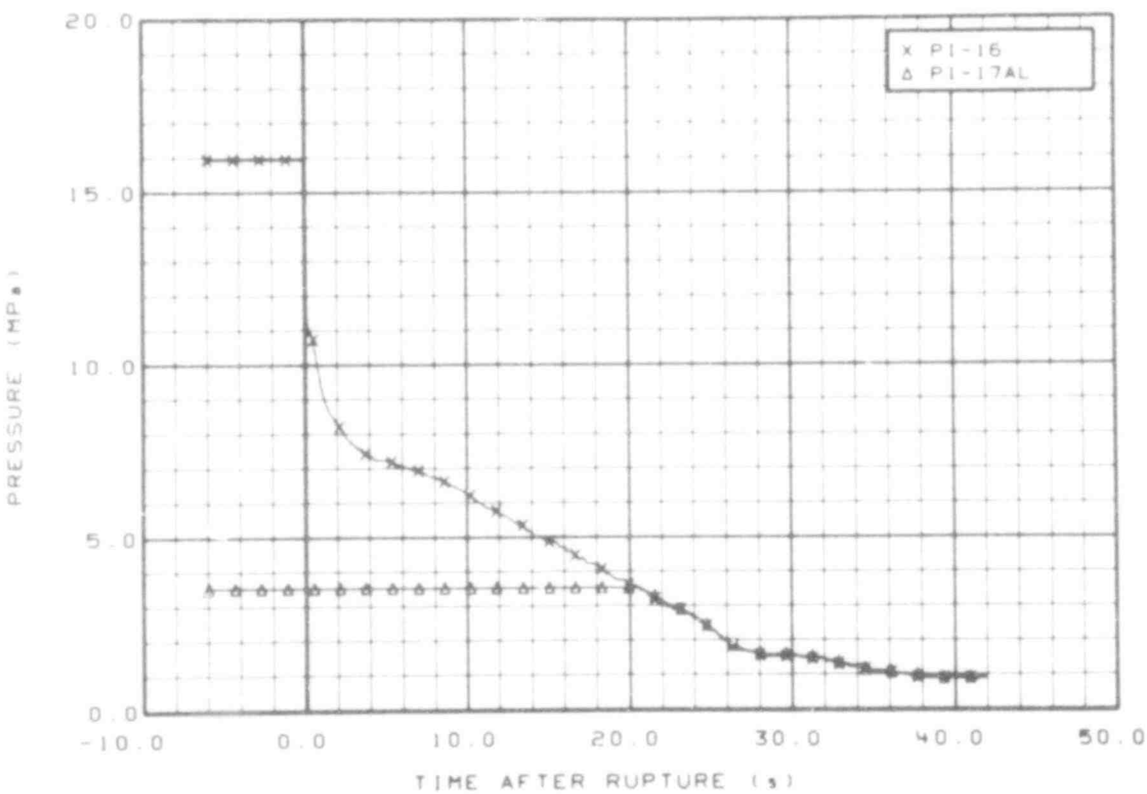

Fig. 104 Pressure in intact loop cold leg (PI-16 and PI-17AL), from -6 to 42 s.

507 144

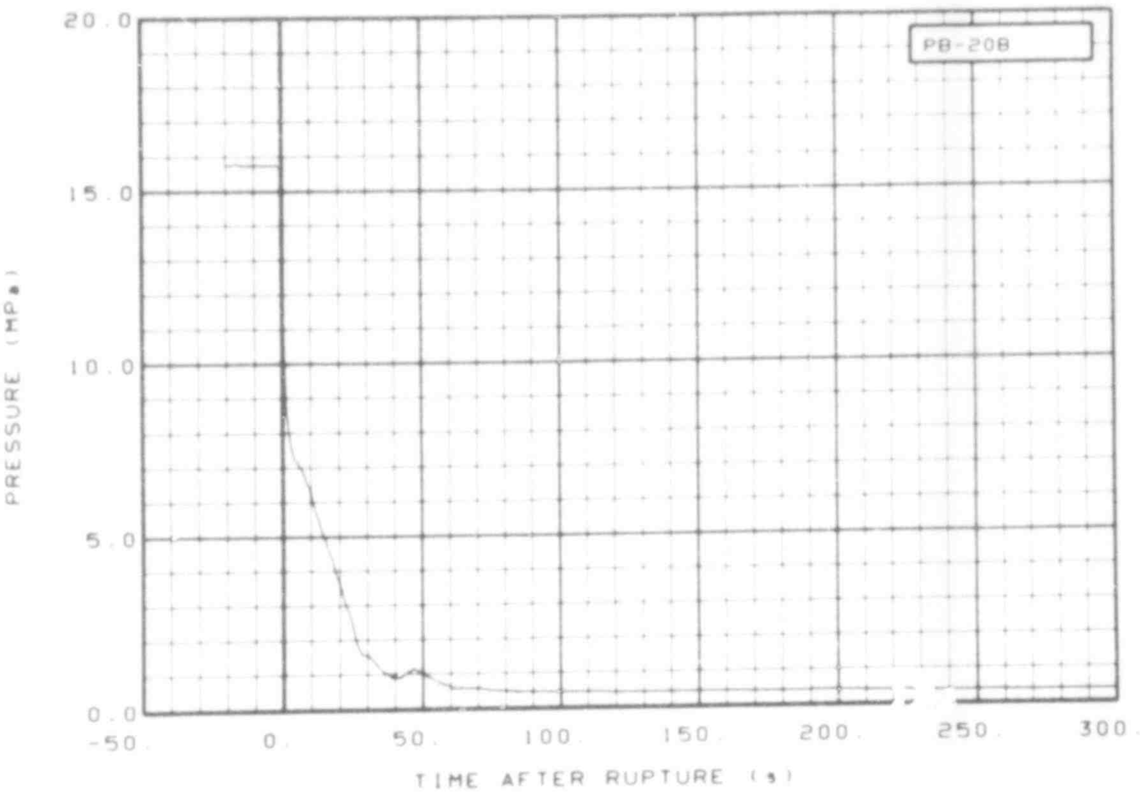

Fig. 105 Pressure in broken loop hot leg (PB-20B), from -20 to 300 s.

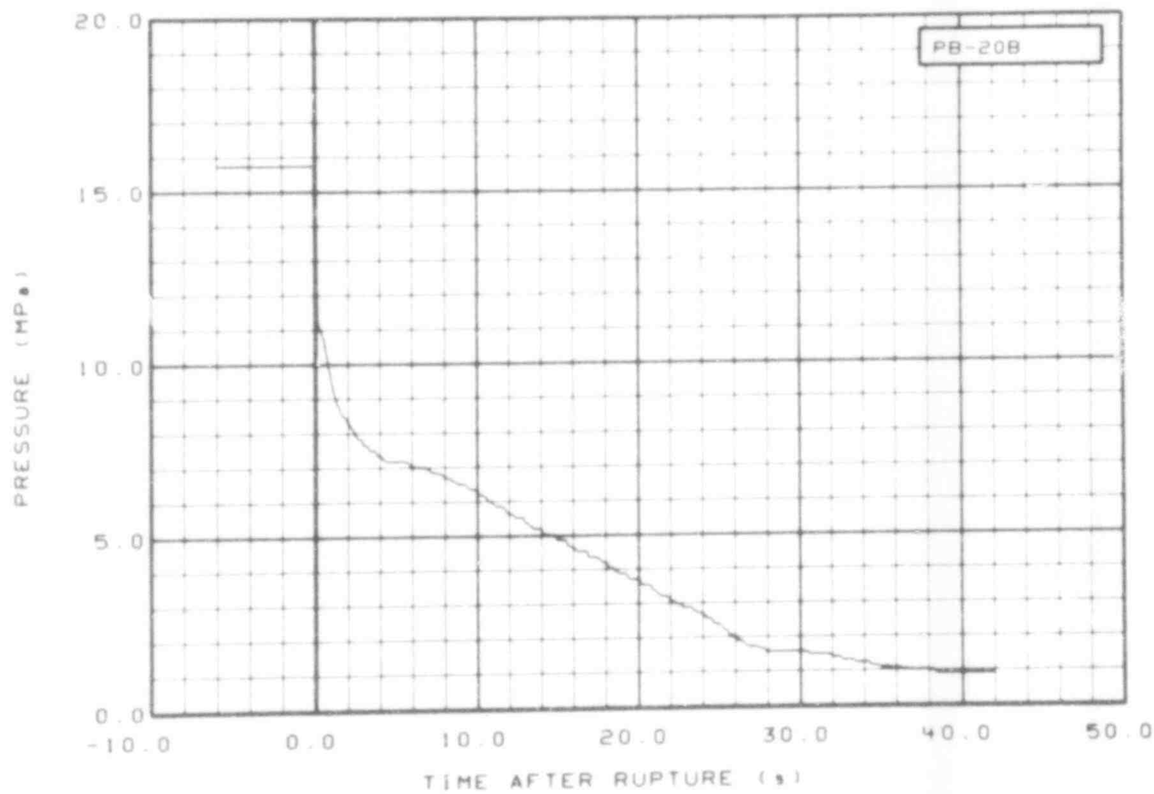

Fig. 106 Pressure in broken loop hot leg (PB-20B), from -6 to 42 s.

507 145

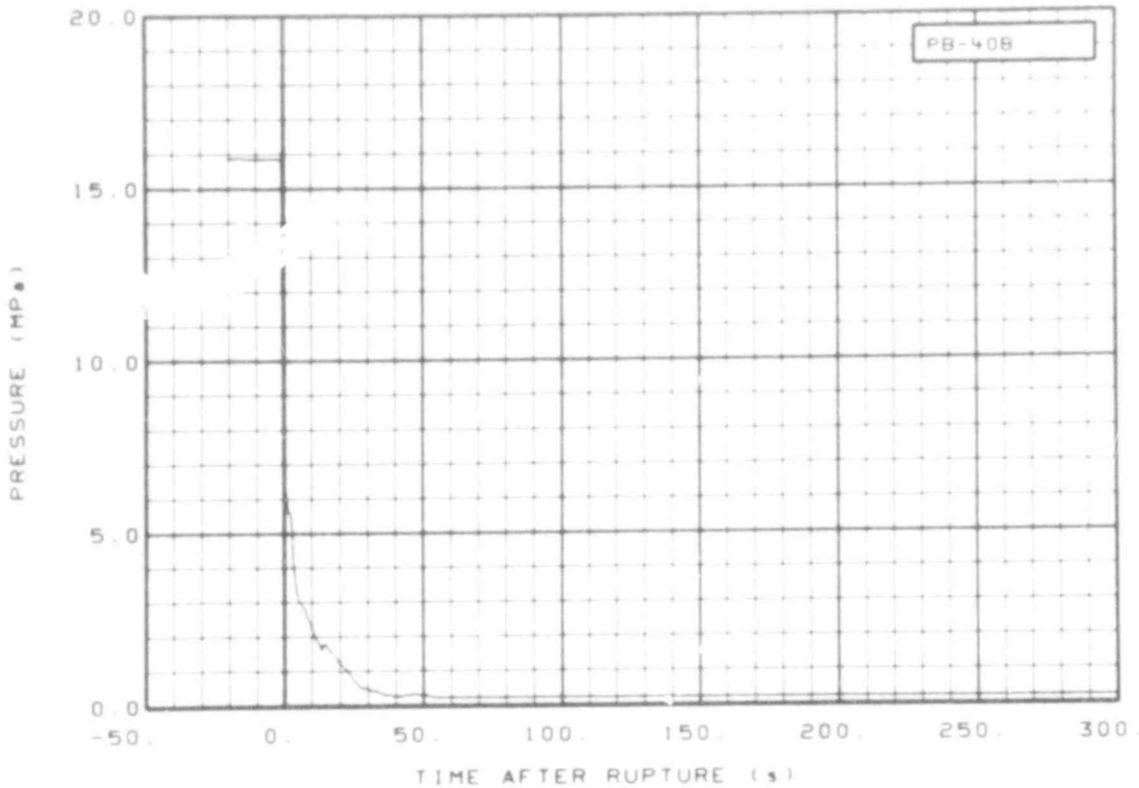

Fig. 107 Pressure in broken loop cold leg, pump side (PB-40B), from -20 to 300 s.

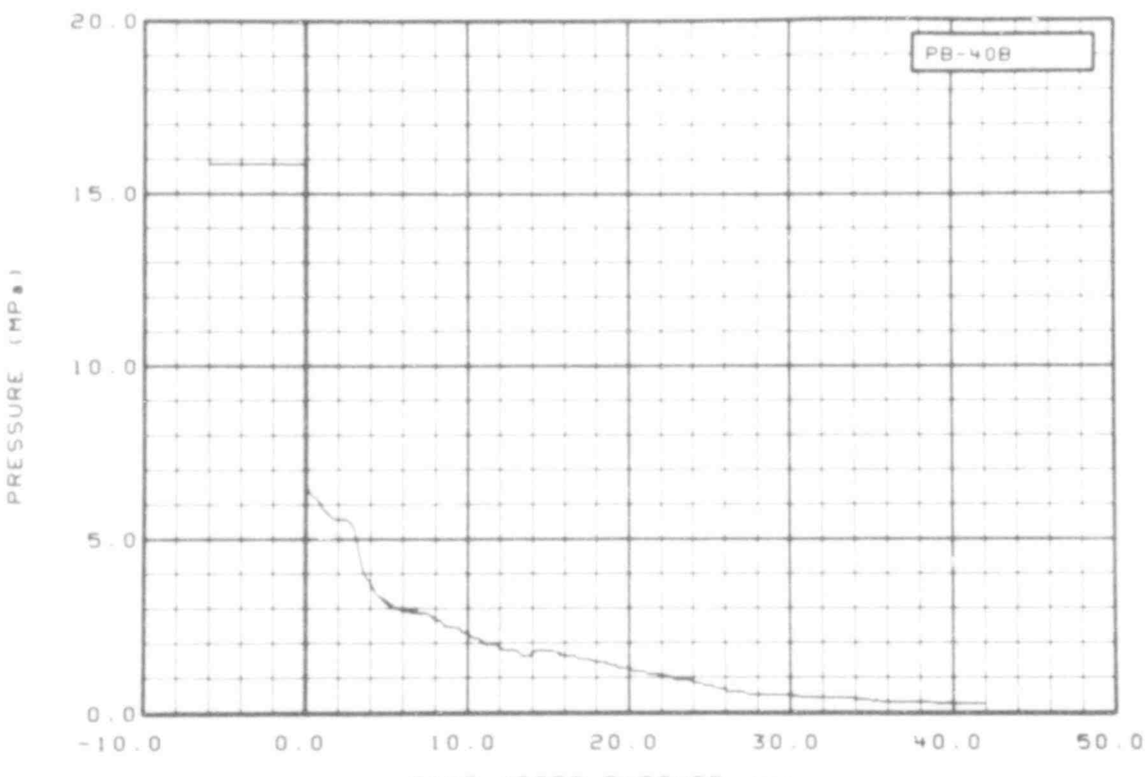

Fig. 108 Pressure in broken loop cold leg, pump side (PB-40B), from -6 to 42 s.

507 146

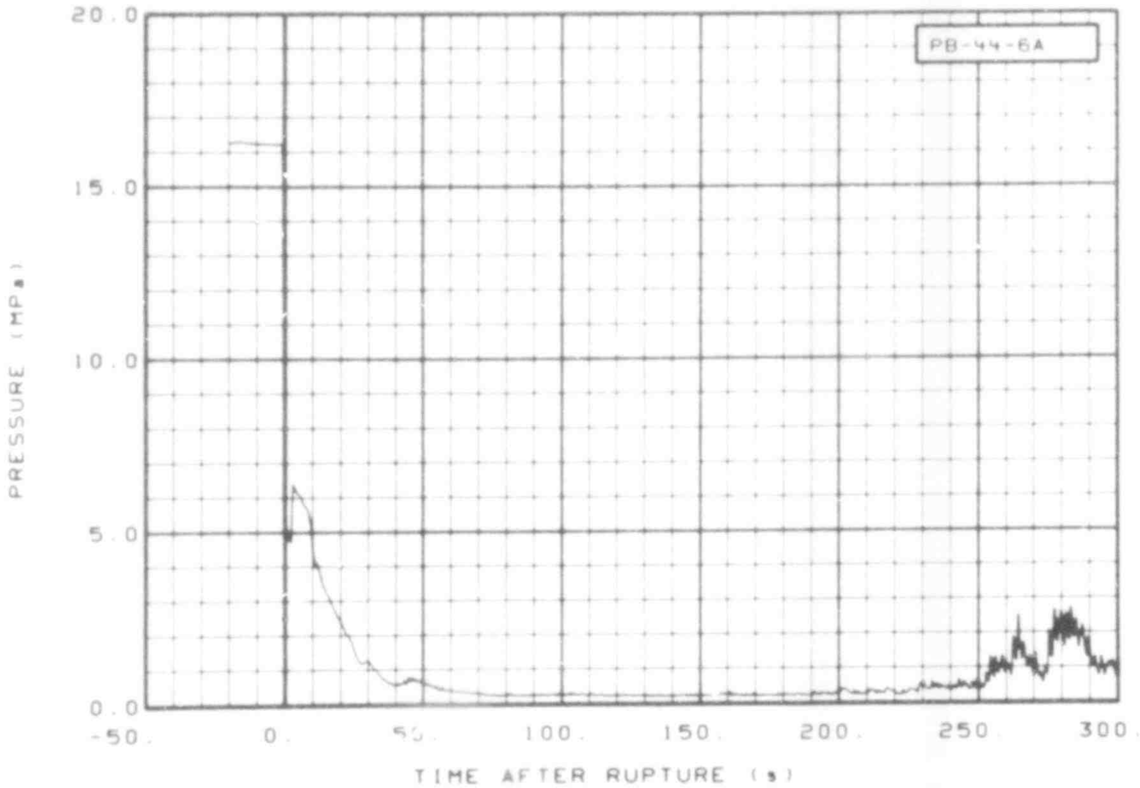

Fig. 109 Pressure in broken loop blowdown nozzle (PB-44-6A), from -20 to 300 s.

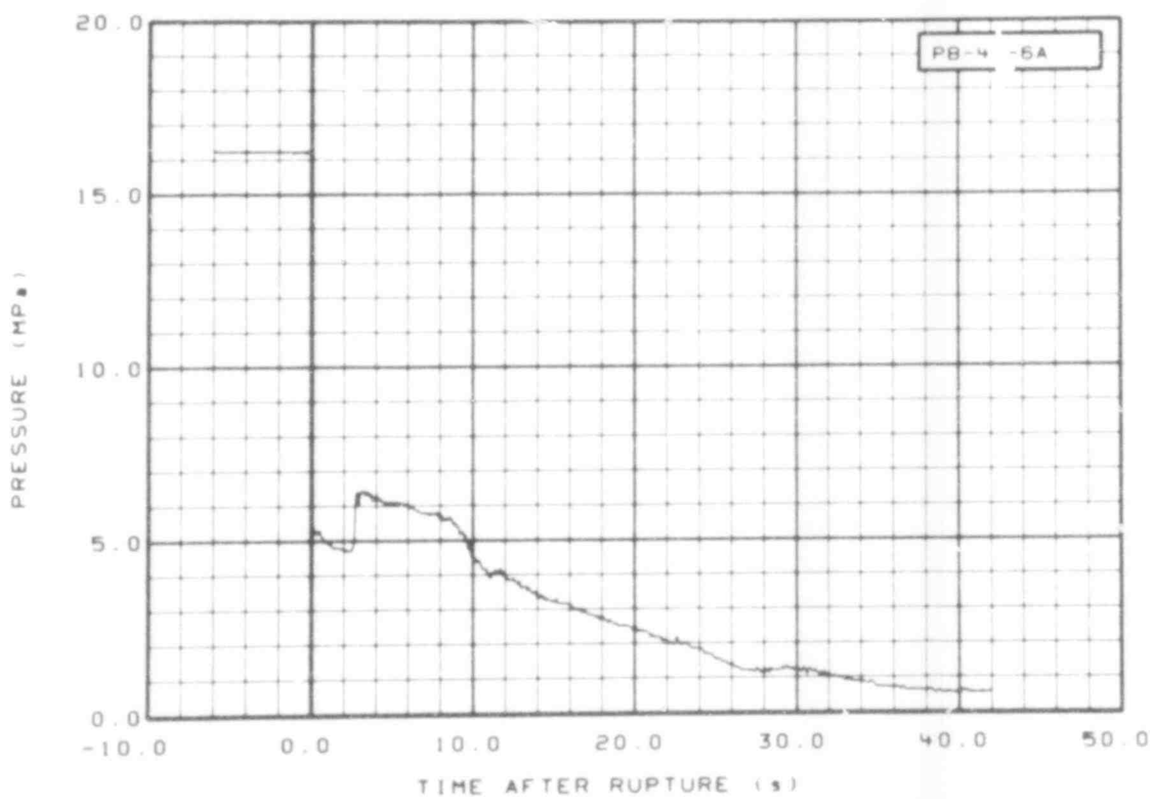

Fig. 110 Pressure in broken loop blowdown nozzle (PB-44-6A), from -6 to 42 s.

507 147

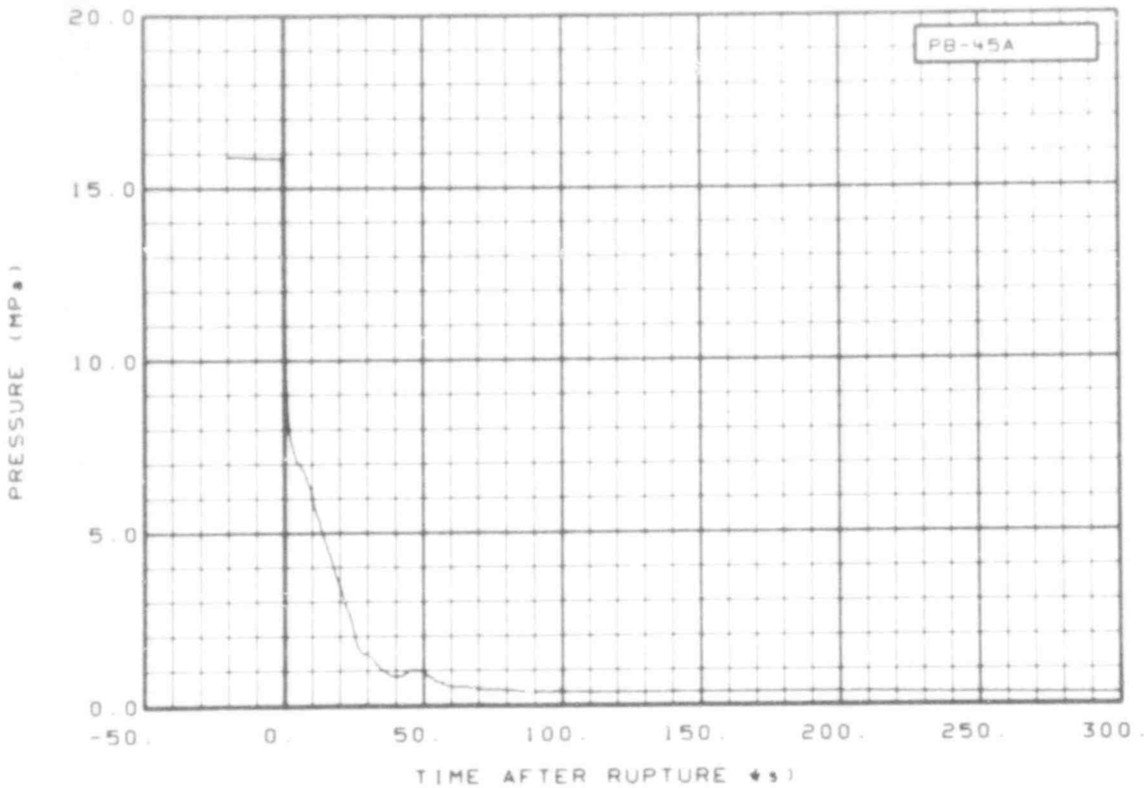

Fig. 111 Pressure in broken loop cold leg, vessel side (PB-45A), from -20 to 300 s.

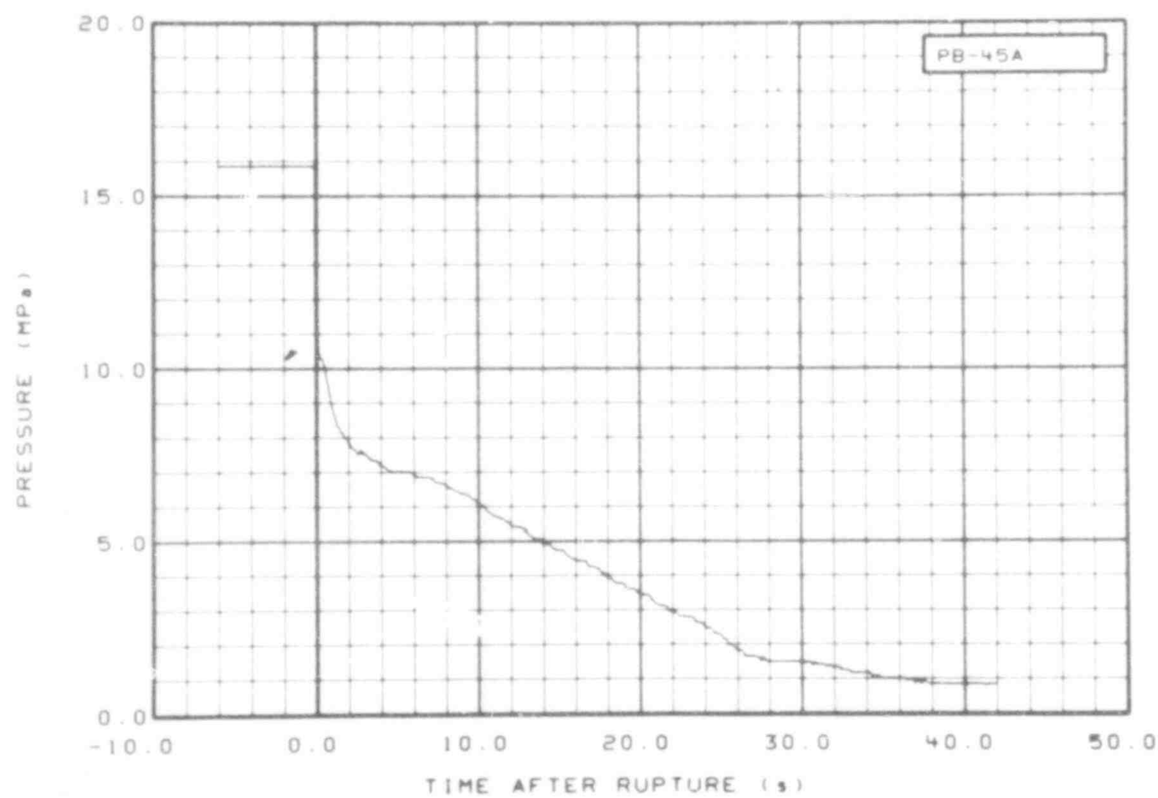

Fig. 112 Pressure in broken loop cold leg, vessel side (PB-45A), from -6 to 42 s.

507 148

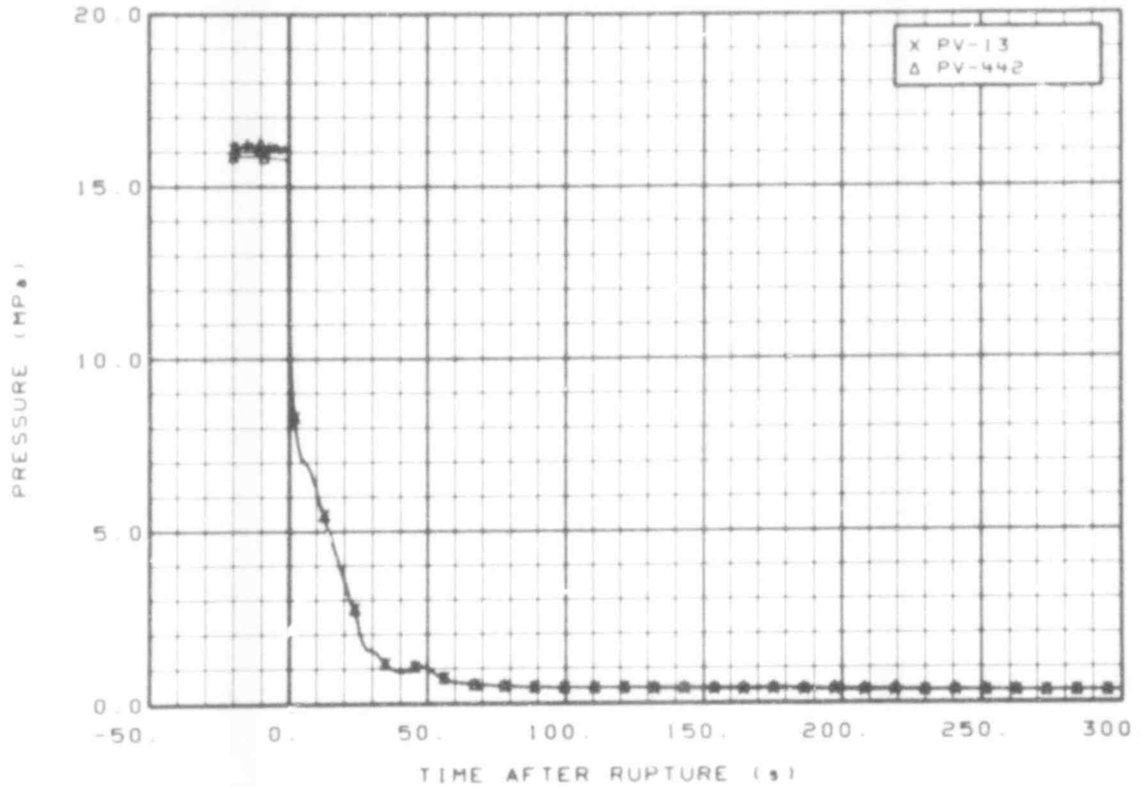

Fig. 113 Pressure in vessel upper and lower plenum (PV-13 and PV-442), from -20 to 300 s.

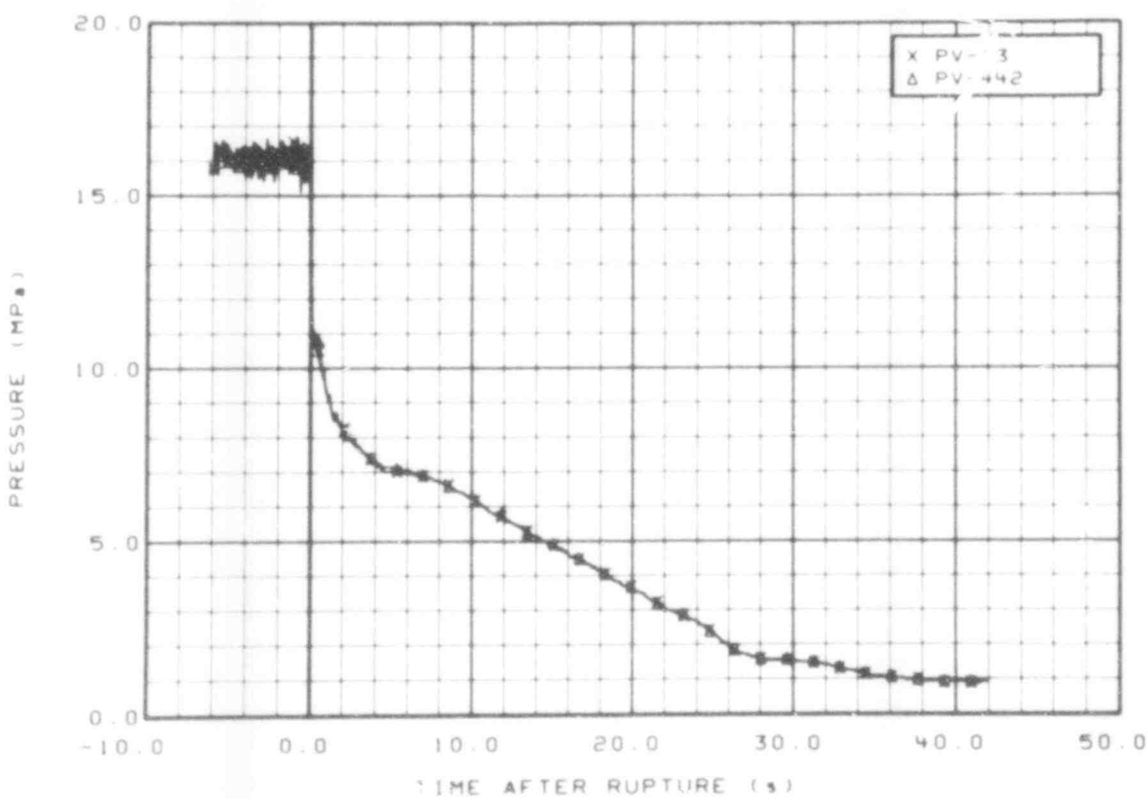

Fig. 114 Pressure in vessel upper and lower plenum (PV-13 and PV-442), from -6 to 42 s.

507 149

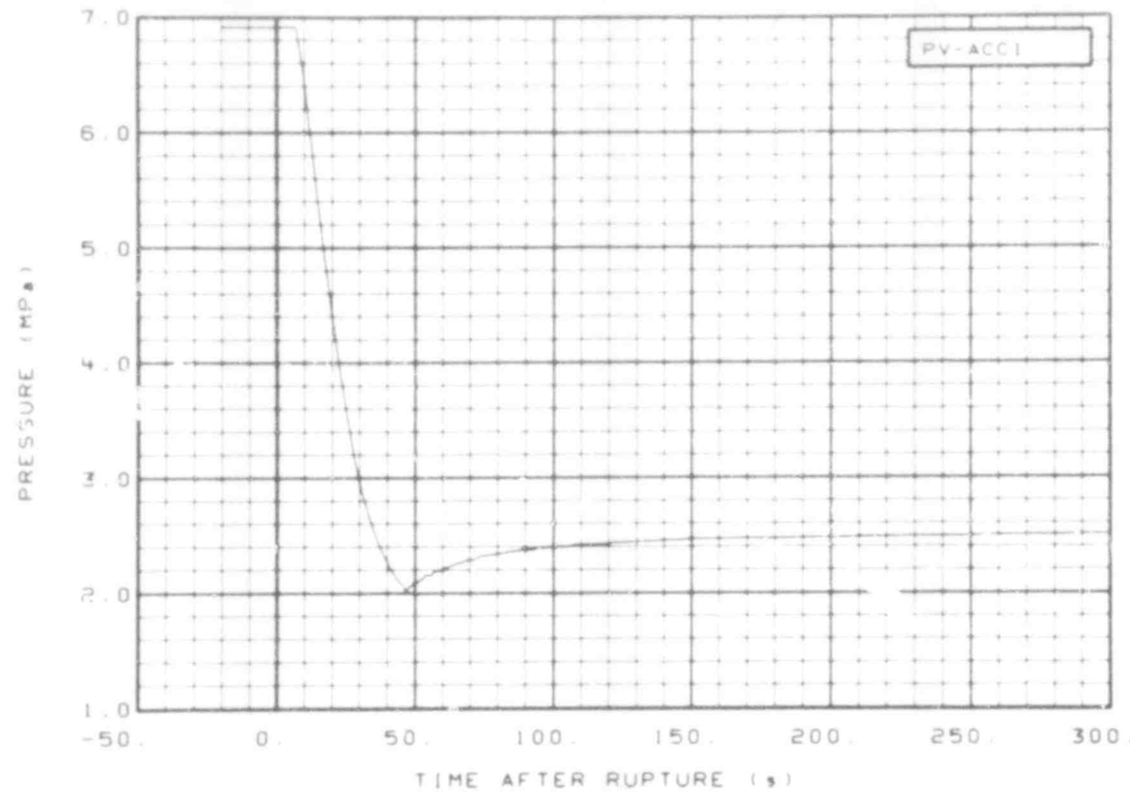

Fig. 115 Pressure in vessel ECC injection accumulator (PV-ACC1), from -20 to 300 s.

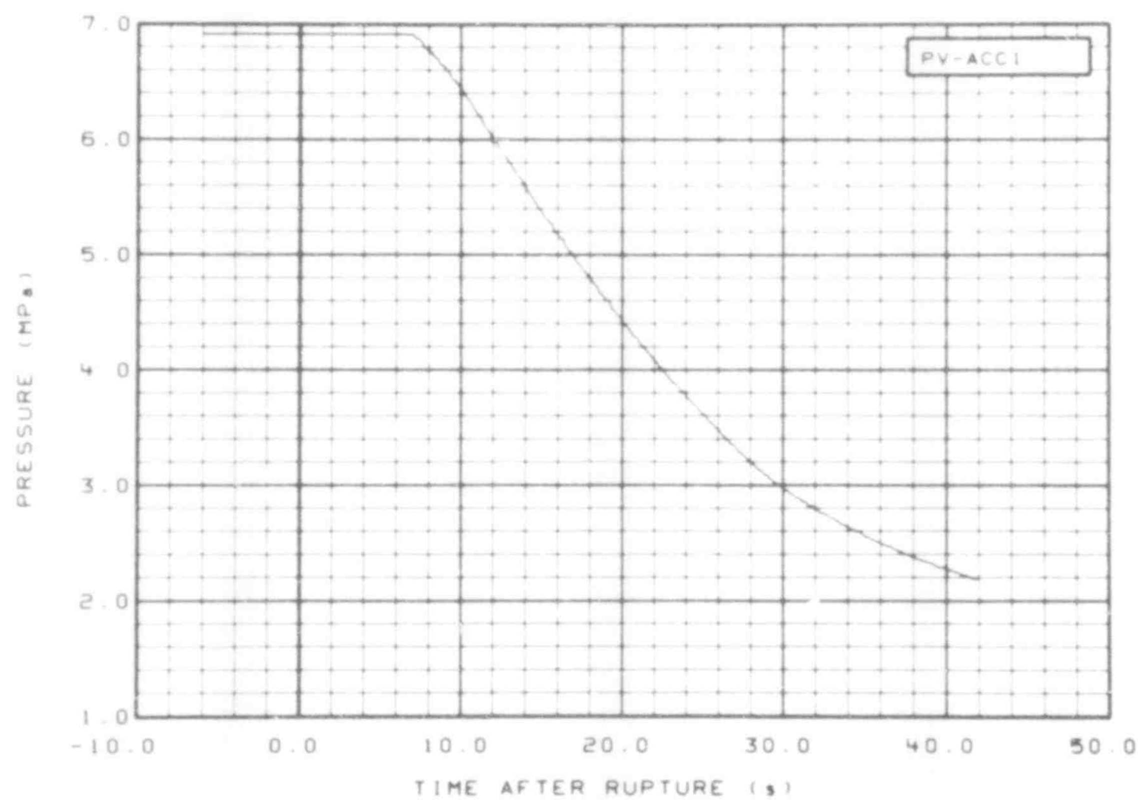

Fig. 116 Pressure in vessel ECC injection accumulator (PV-ACC1), from -6 to 42 s.

507 150

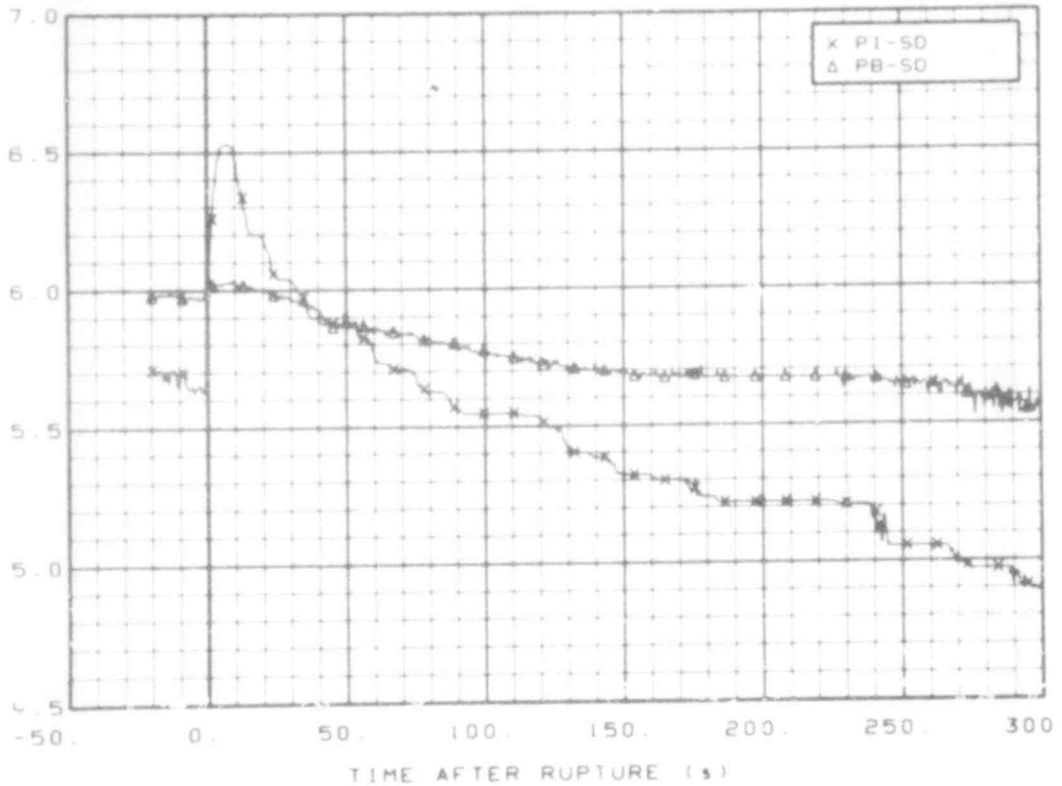

Fig. 117 Pressure in system steam generators, secondary side steam dome (PI-SD and PB-SD), from -20 to 300 s.

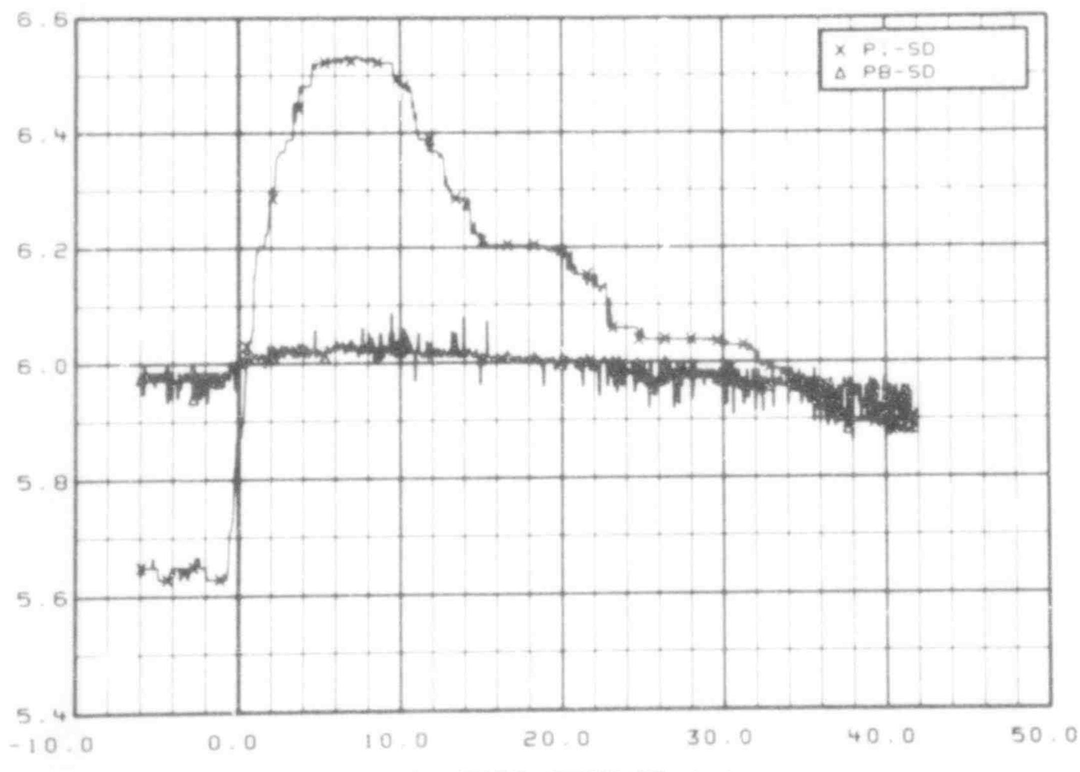

Fig. 118 Pressure in system steam generators, secondary side steam dome (PI-SD and PB-SD), from -6 to 42 s.

507 151

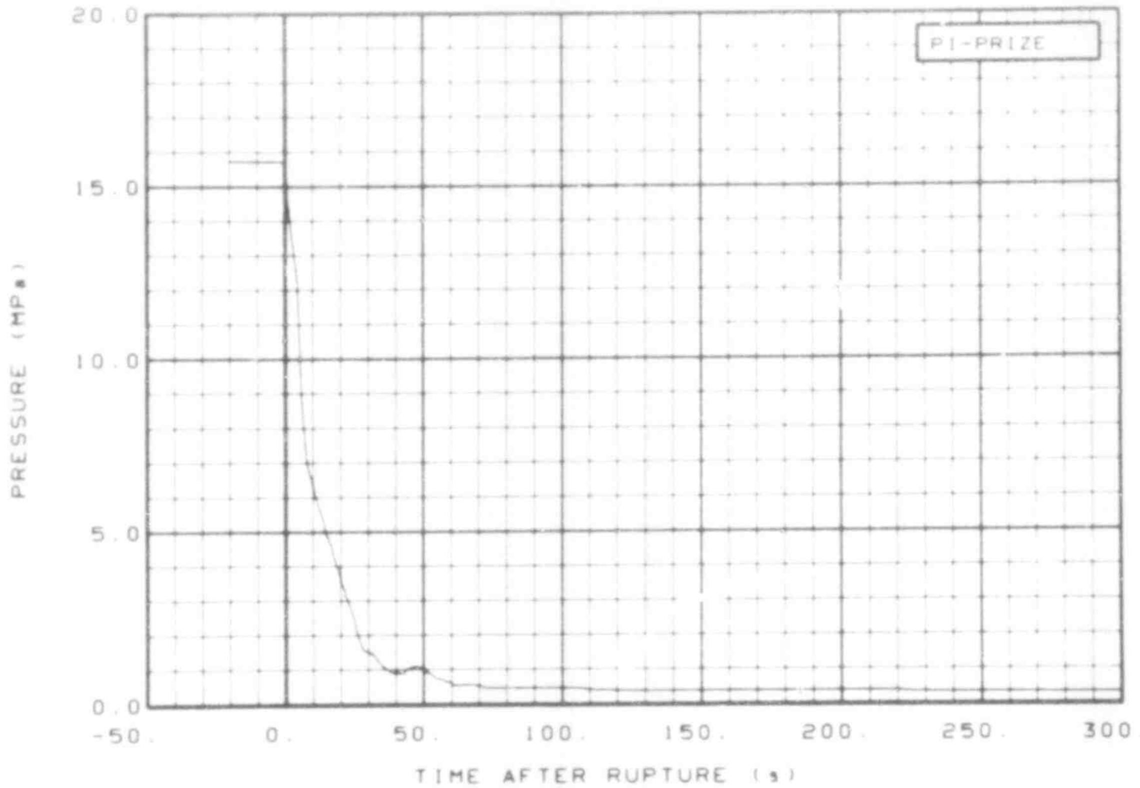

Fig. 119 Pressure in pressurizer (PI-PRIZE), from -20 to 300 s.

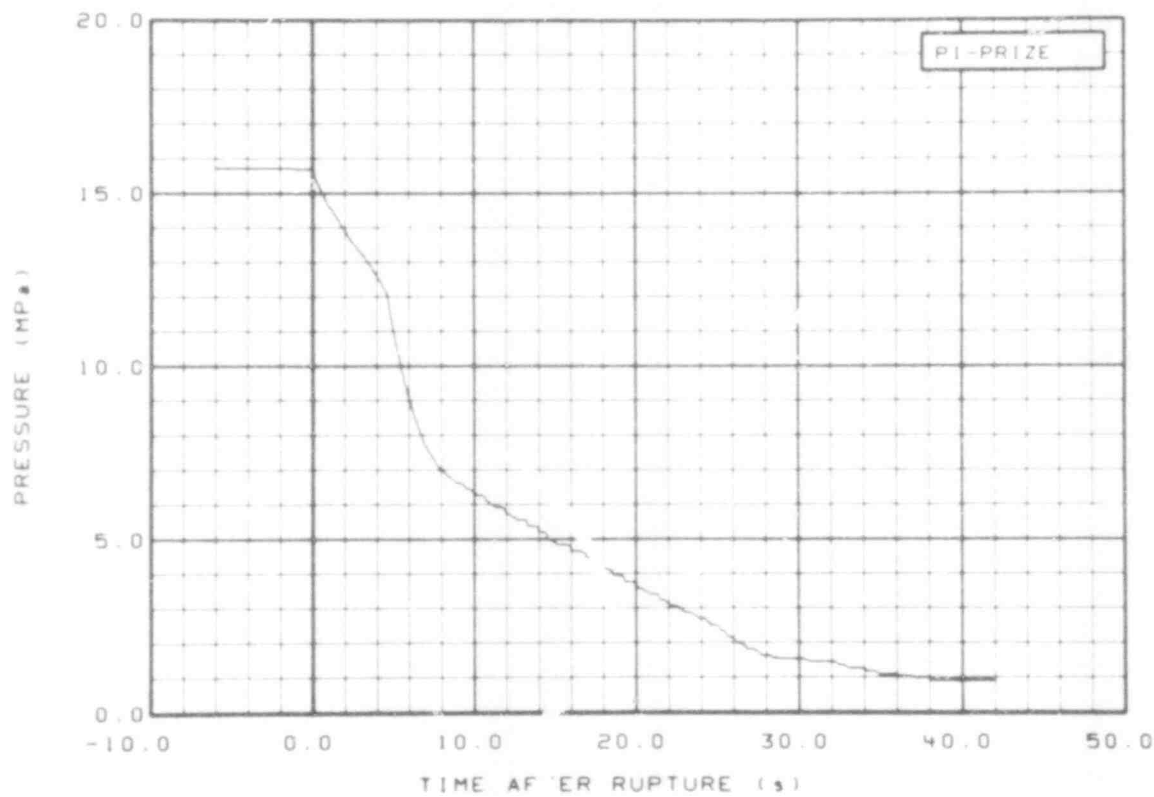

Fig. 120 Pressure in pre surizer (PI-PRIZE), from -6 to 42 s.

507 152

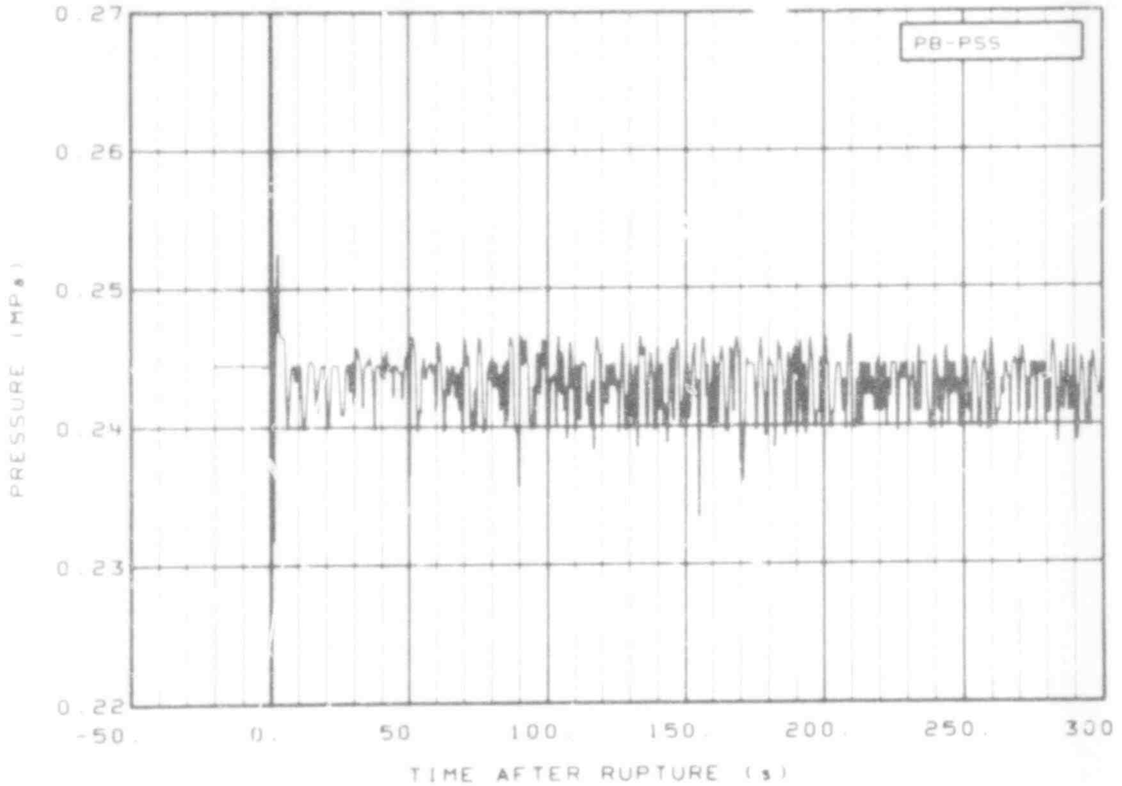

Fig. 121 Pressure in broken loop pressure suppression tank (PB-PSS), from -20 to 300 s.

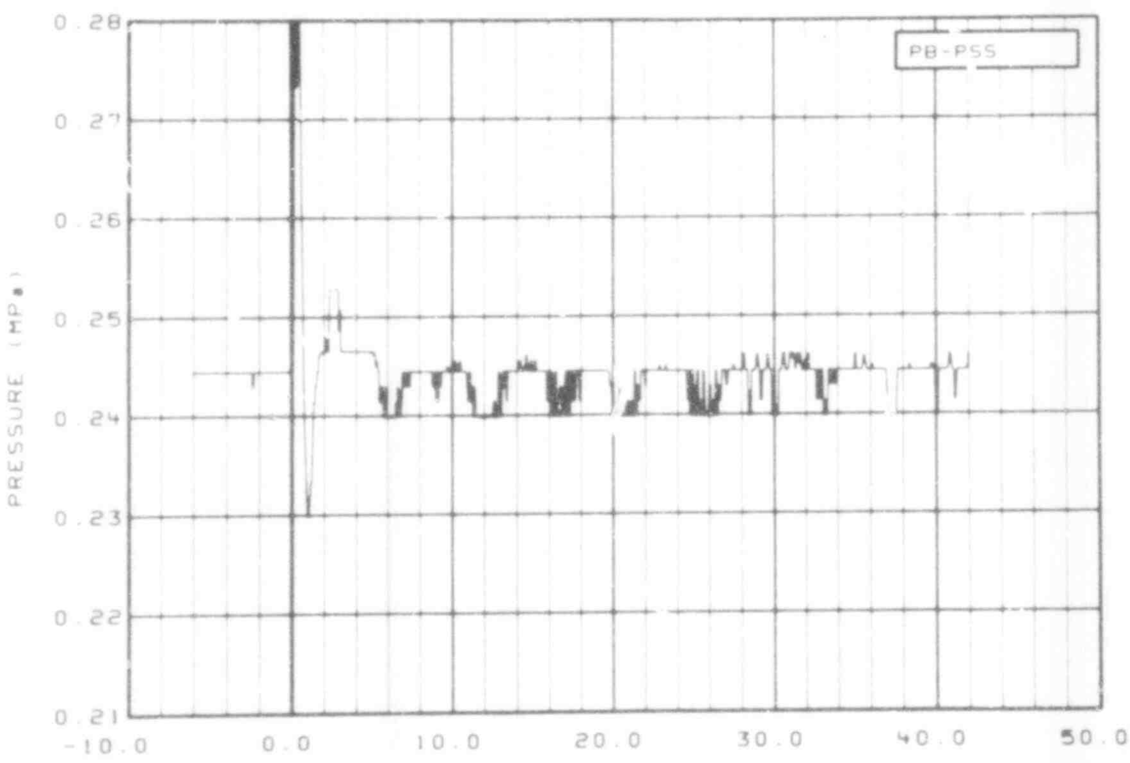

Fig. 122 Pressure in broken loop pressure suppression tank (PB-PSS), from -6 to 42 s.

507 153

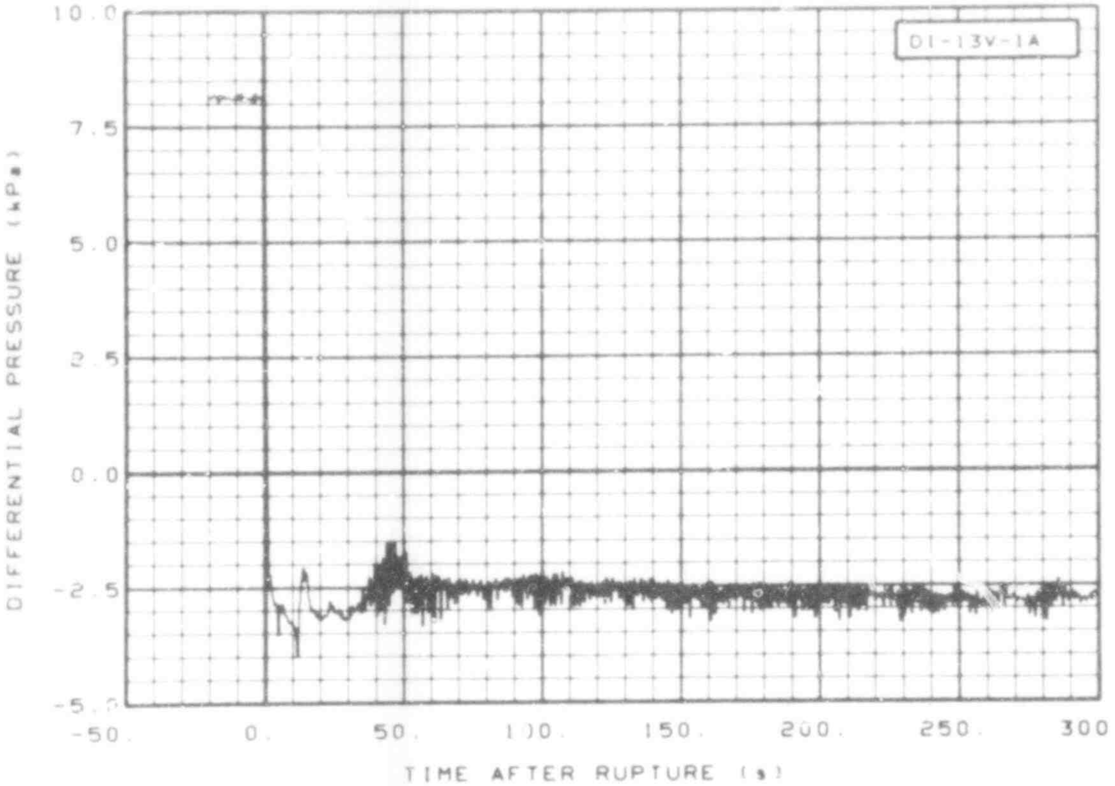

Fig. 123 Differential pressure in intact loop (DI-13V-1A), from -20 to 300 s.

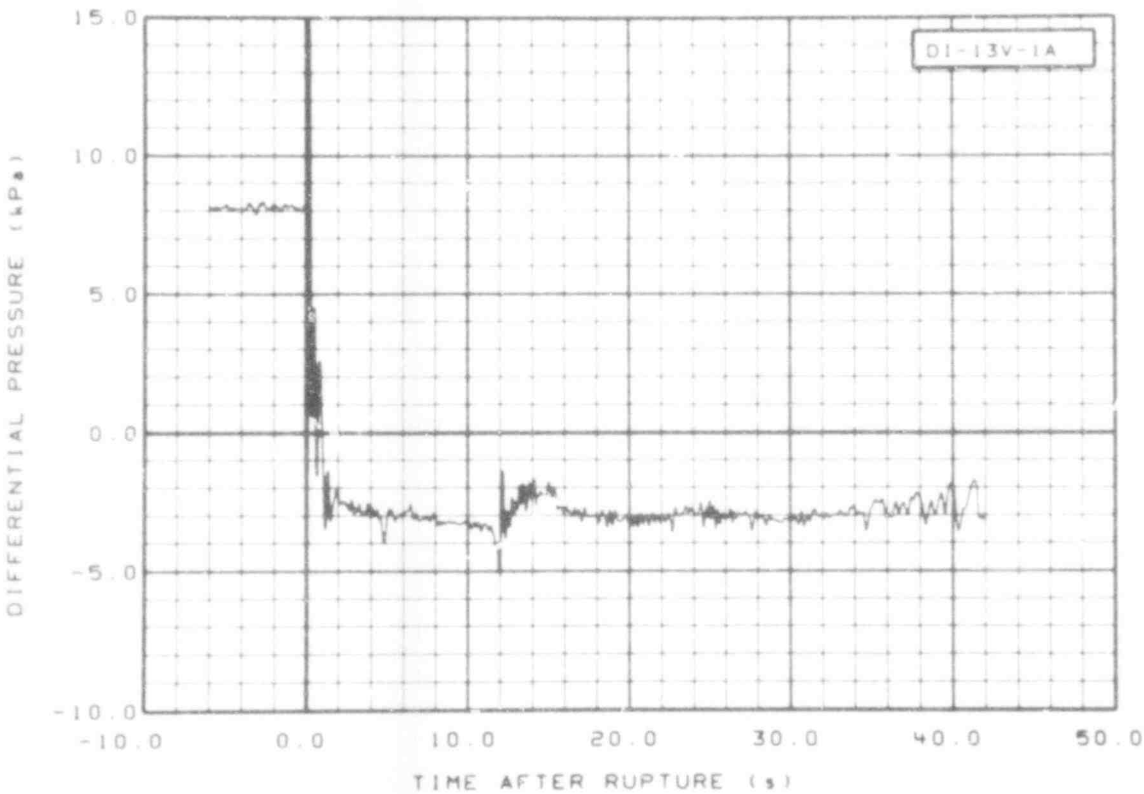

Fig. 124 Differential pressure in intact loop (DI-13V-1A), from -6 to 42 s.

507 154

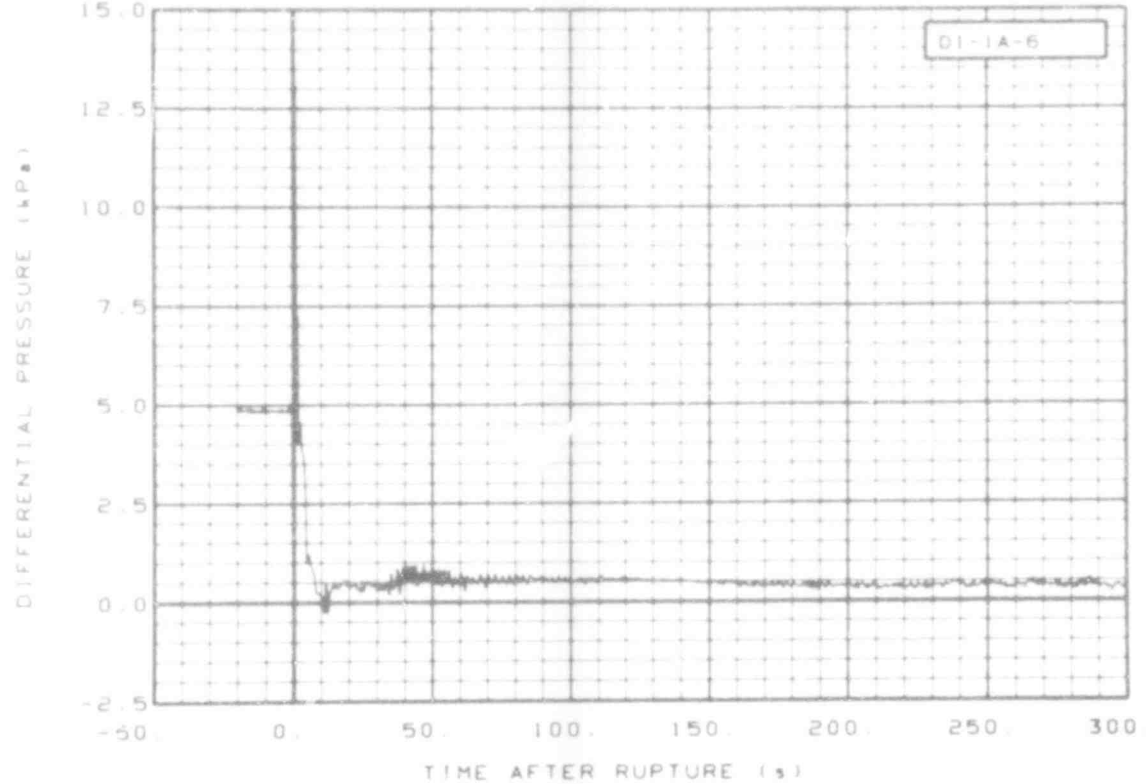

Fig. 125 Differential pressure in intact loop (DI-1A-6), from -20 to 300 s.

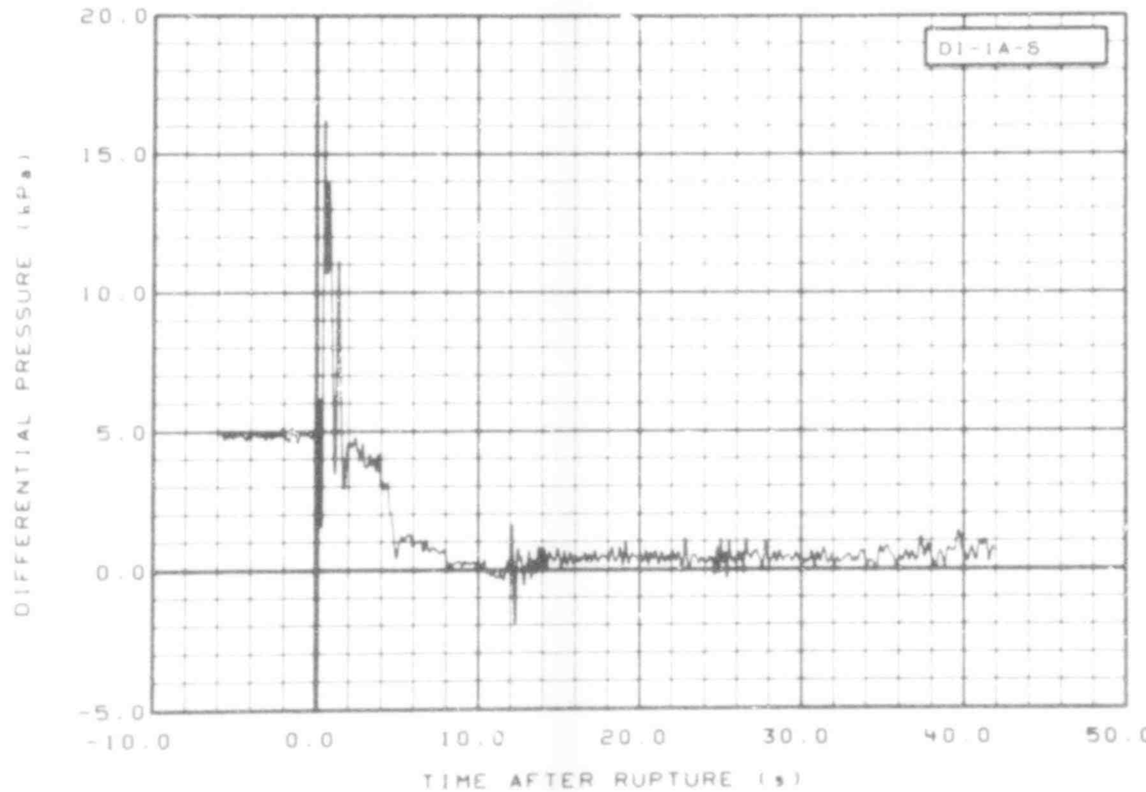

Fig. 126 Differential pressure in intact loop (DI-1A-6), from -6 to 42 s.

507 155

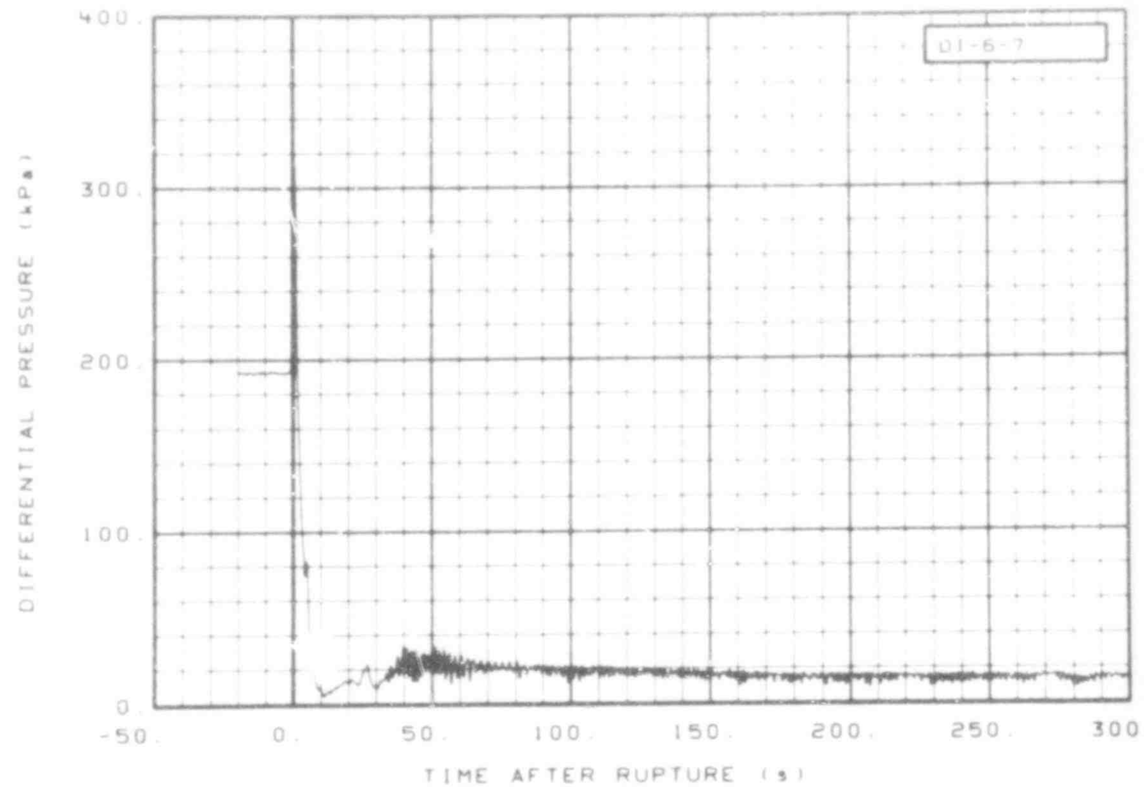

Fig. 127 Differential pressure in intact loop (DI-6-7), from -20 to 300 s.

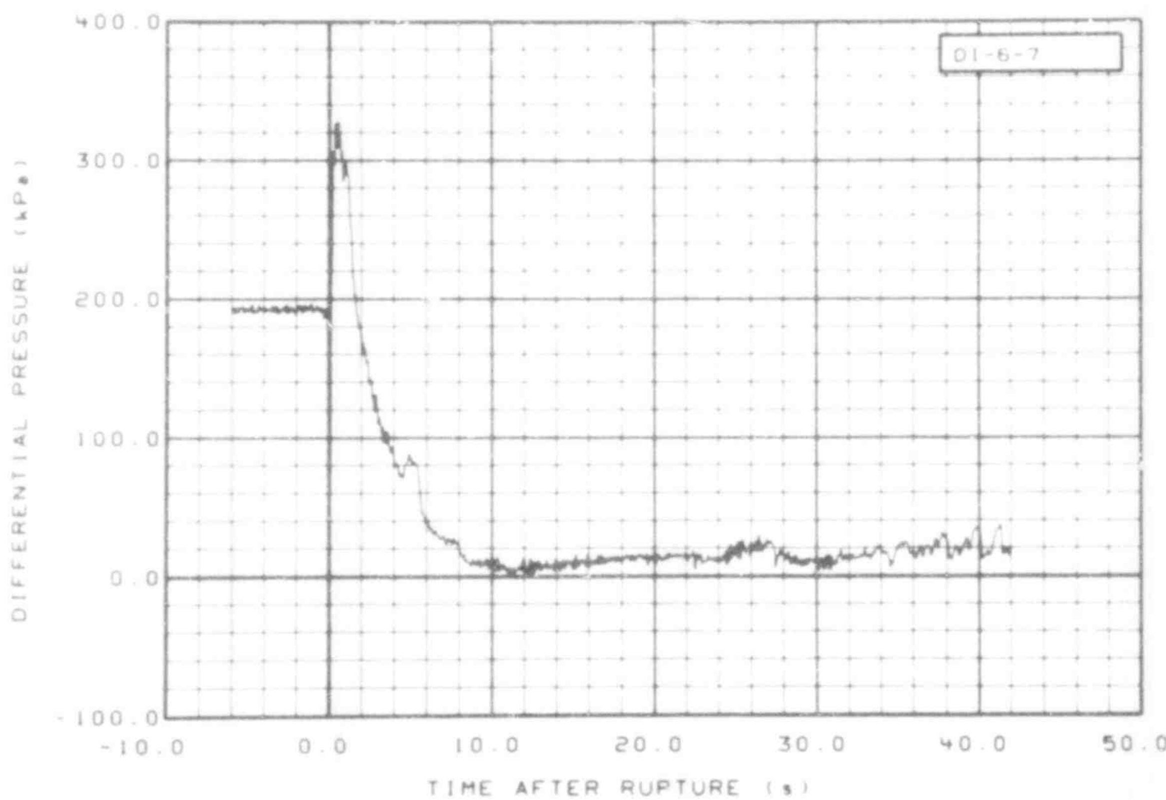

Fig. 128 Differential pressure in intact loop (DI-6-7), from -6 to 42 s.

507 156

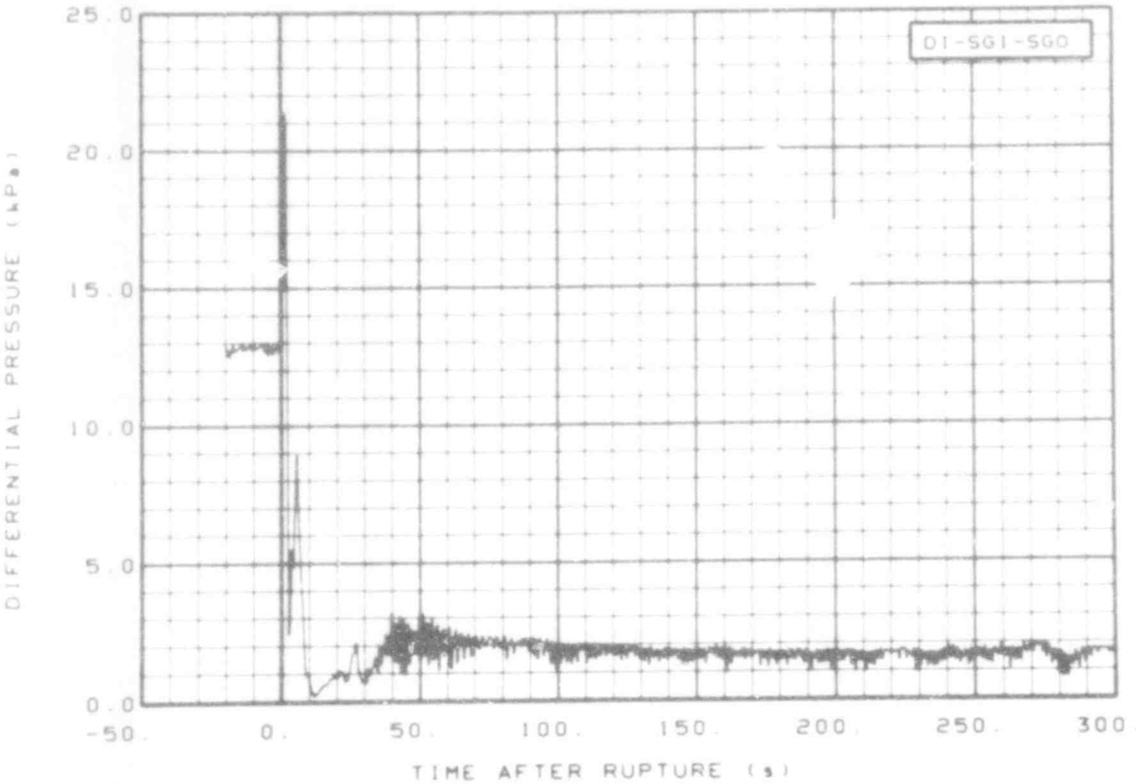

Fig. 129 Differential pressure in intact loop steam generator, inlet plenum to outlet plenum (DI-SGI-SGO), from -20 to 300 s.

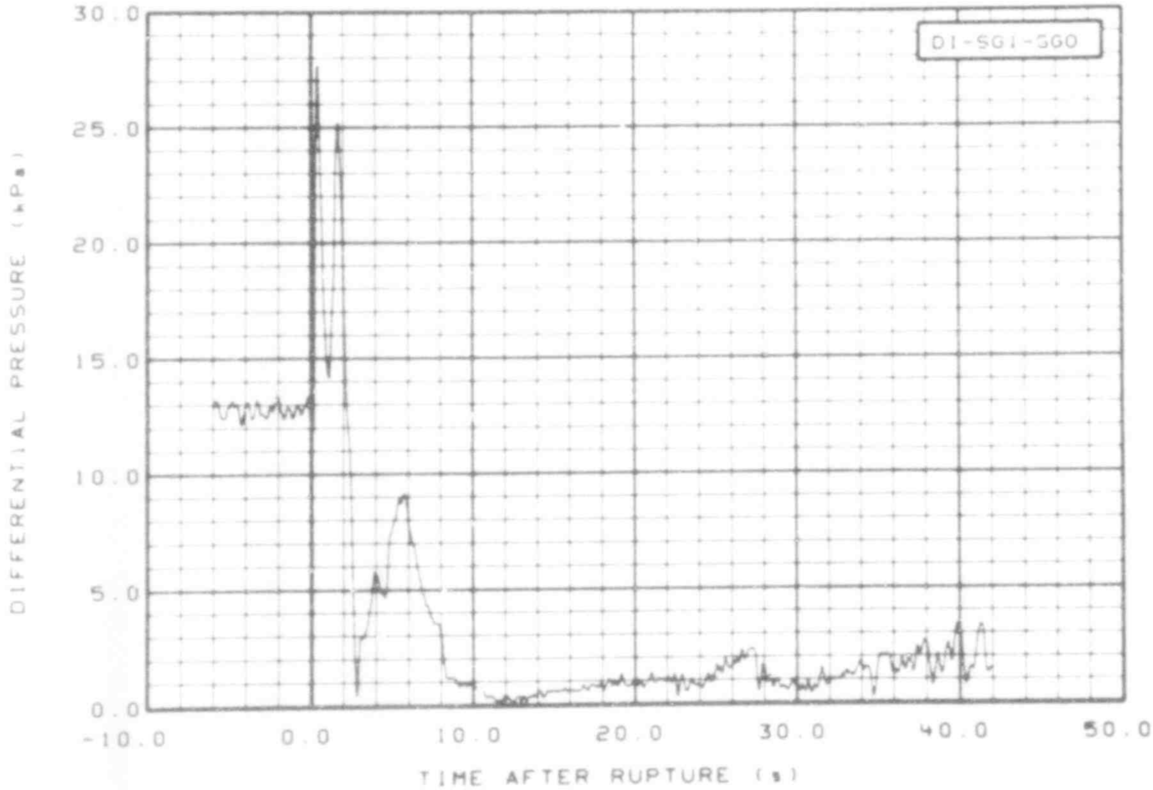

Fig. 130 Differential pressure in intact loop steam generator, inlet plenum to outlet plenum (DI-SGI-SGO), from -6 to 42 s.

507 157

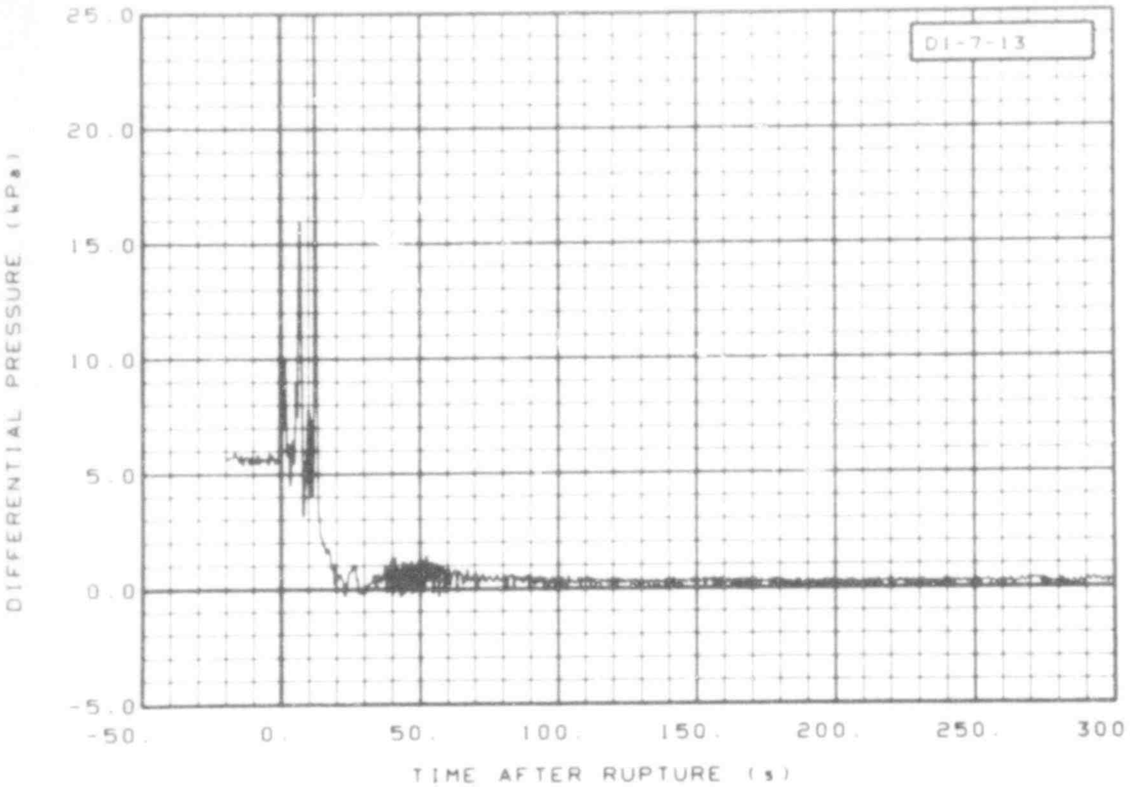

Fig. 131 Differential pressure in intact loop (DI-7-13), from -20 to 300 s.

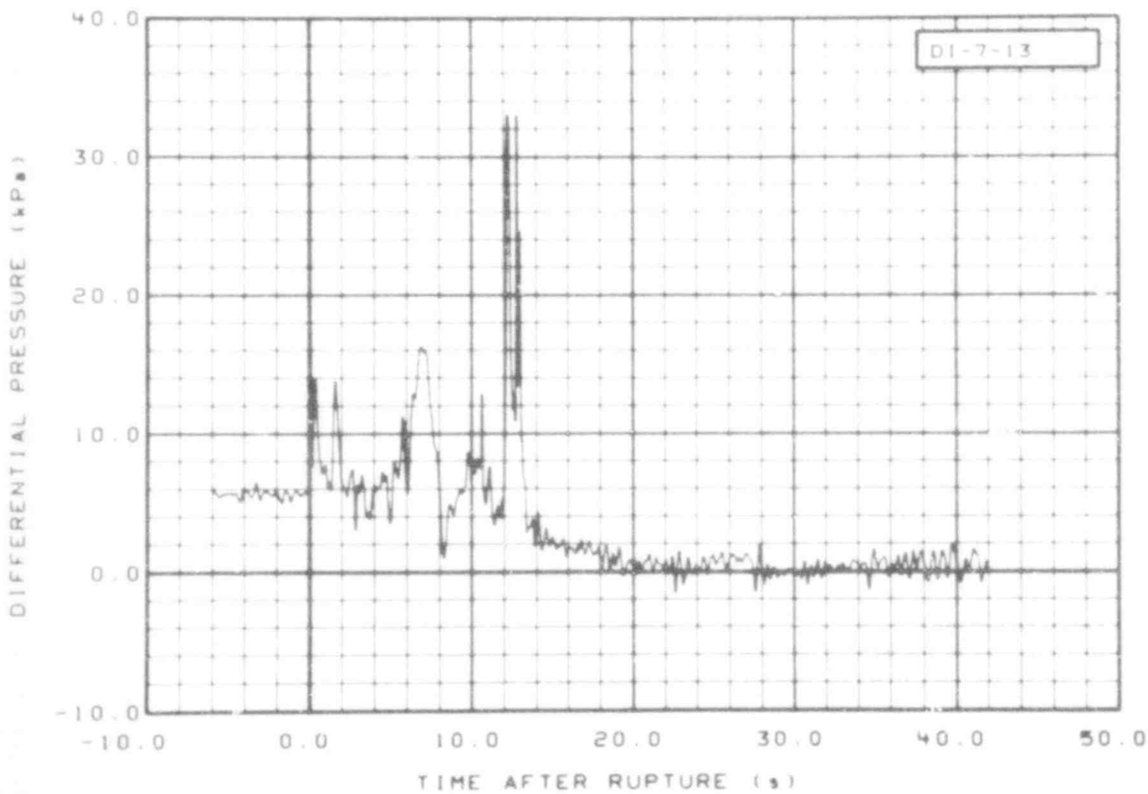

Fig. 132 Differential pressure in intact loop (DI-7-13), from -6 to 42 s.

507 158

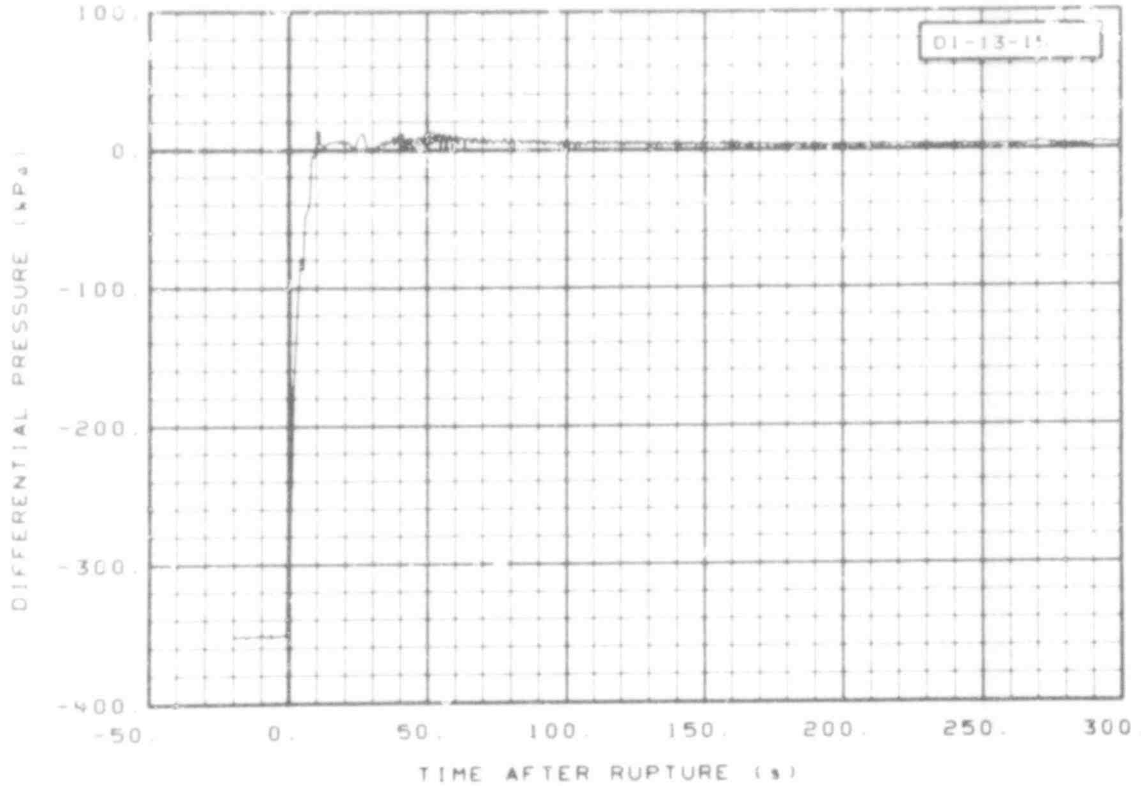

Fig. 133 Differential pressure in intact loop (DI-13-15), from -20 to 300 s.

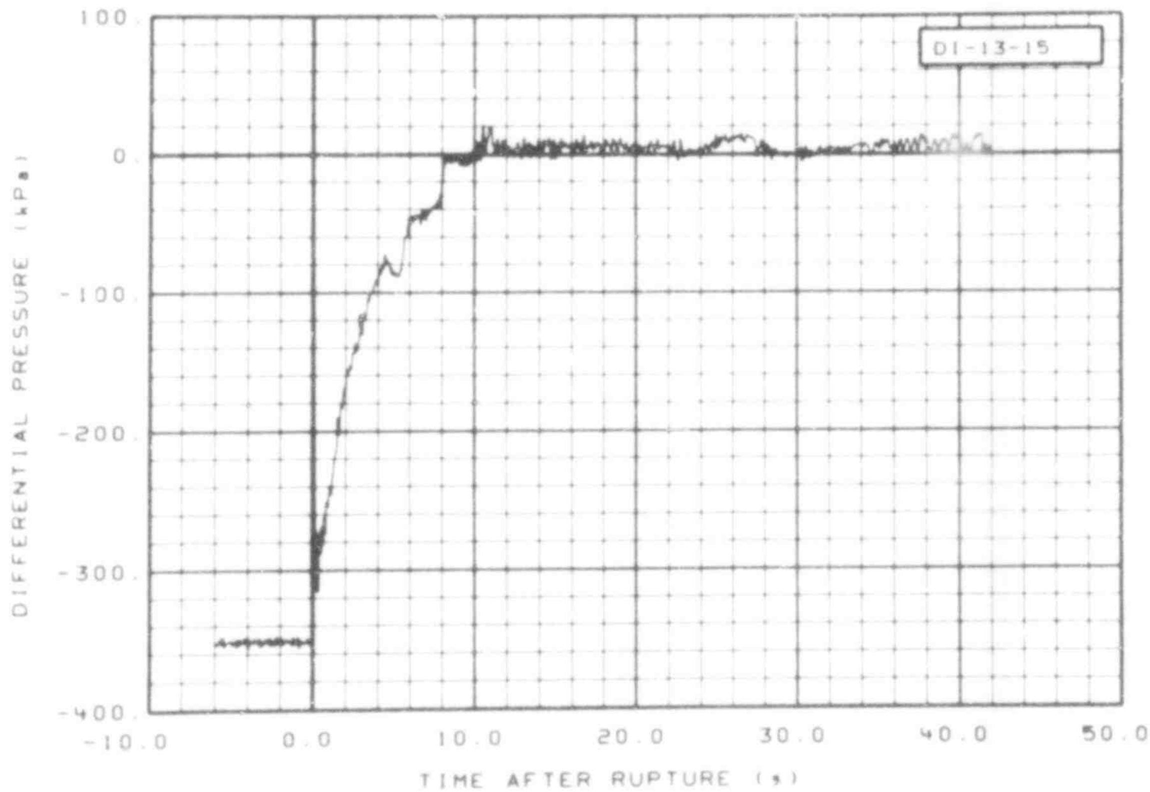

Fig. 134 Differential pressure in intact loop (DI-13-15), from -6 to 42 s.

507 159

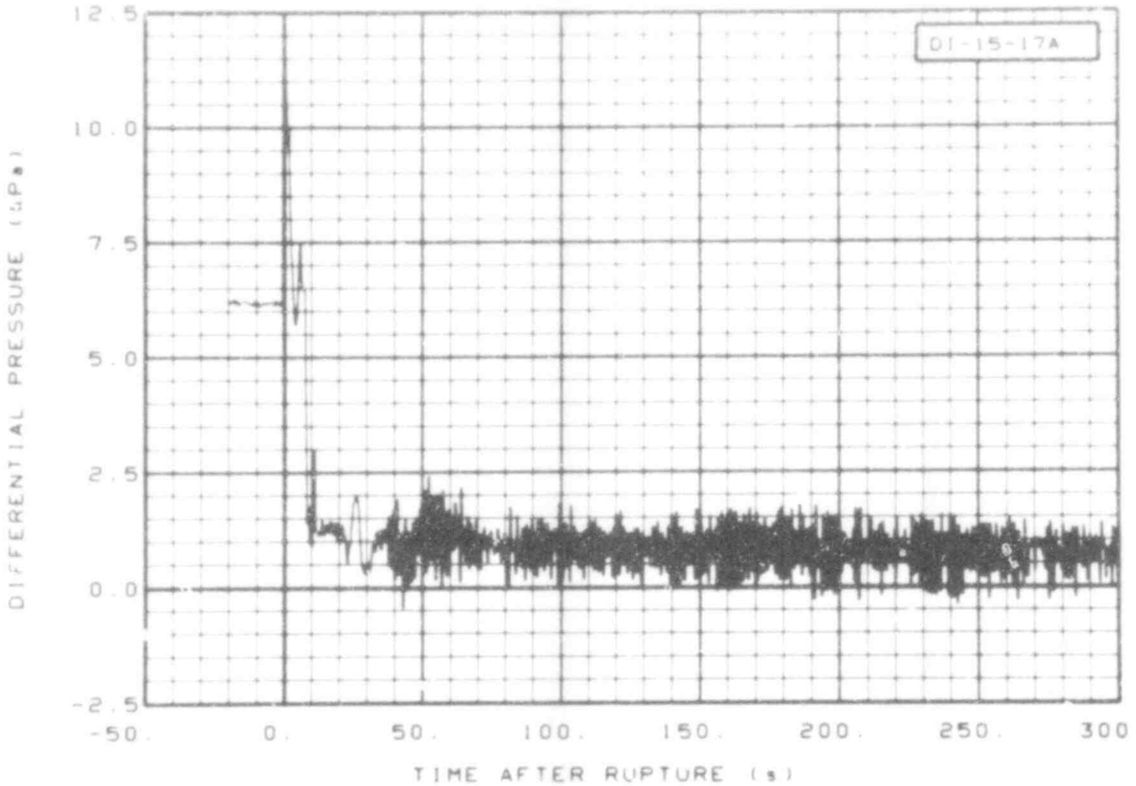

Fig. 135 Differential pressure in intact loop (DI-15-17A), from -20 to 300 s.

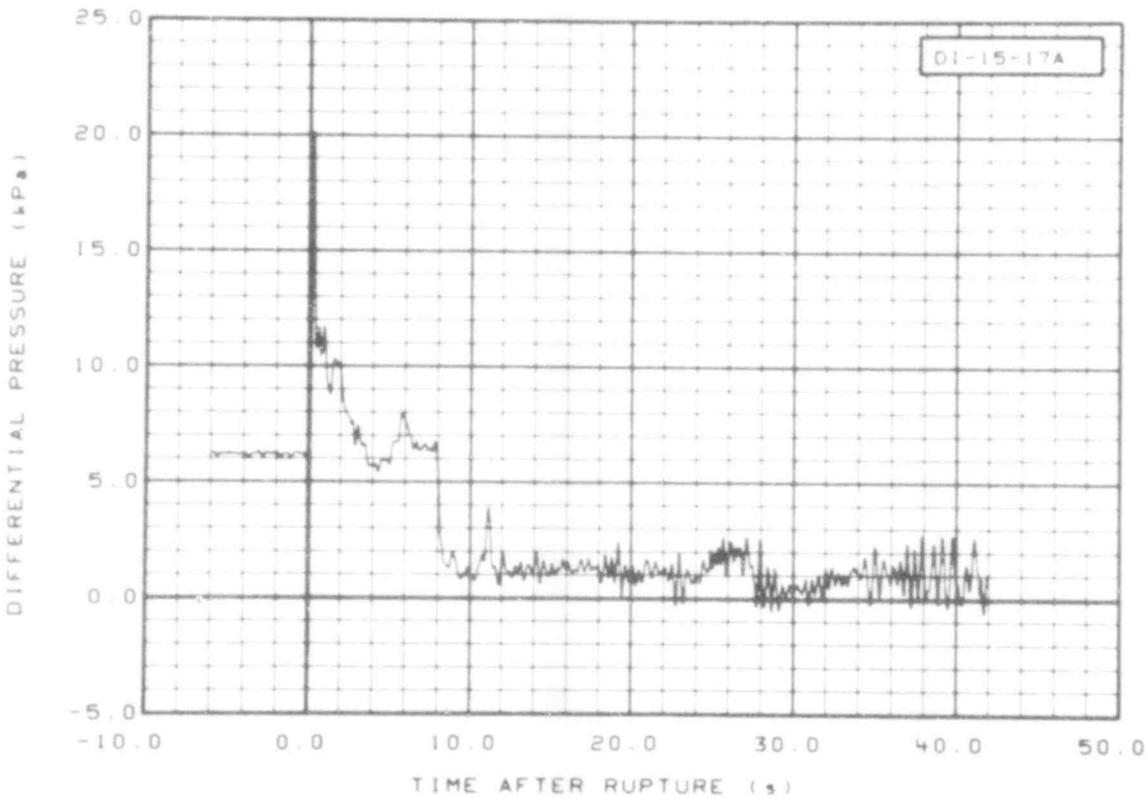

Fig. 136 Differential pressure in intact loop (DI-15-17A), from -6 to 42 s.

507 160

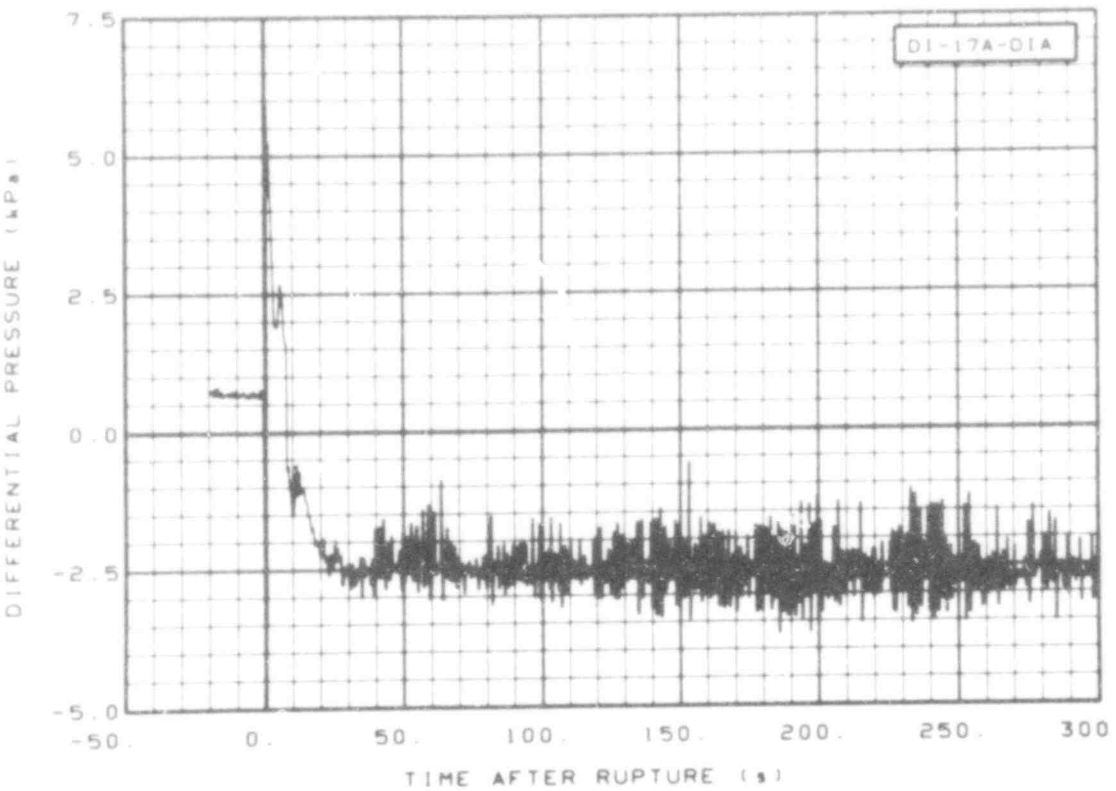

Fig. 137 Differential pressure in intact loop (DI-17A-DIA), from -20 to 300 s.

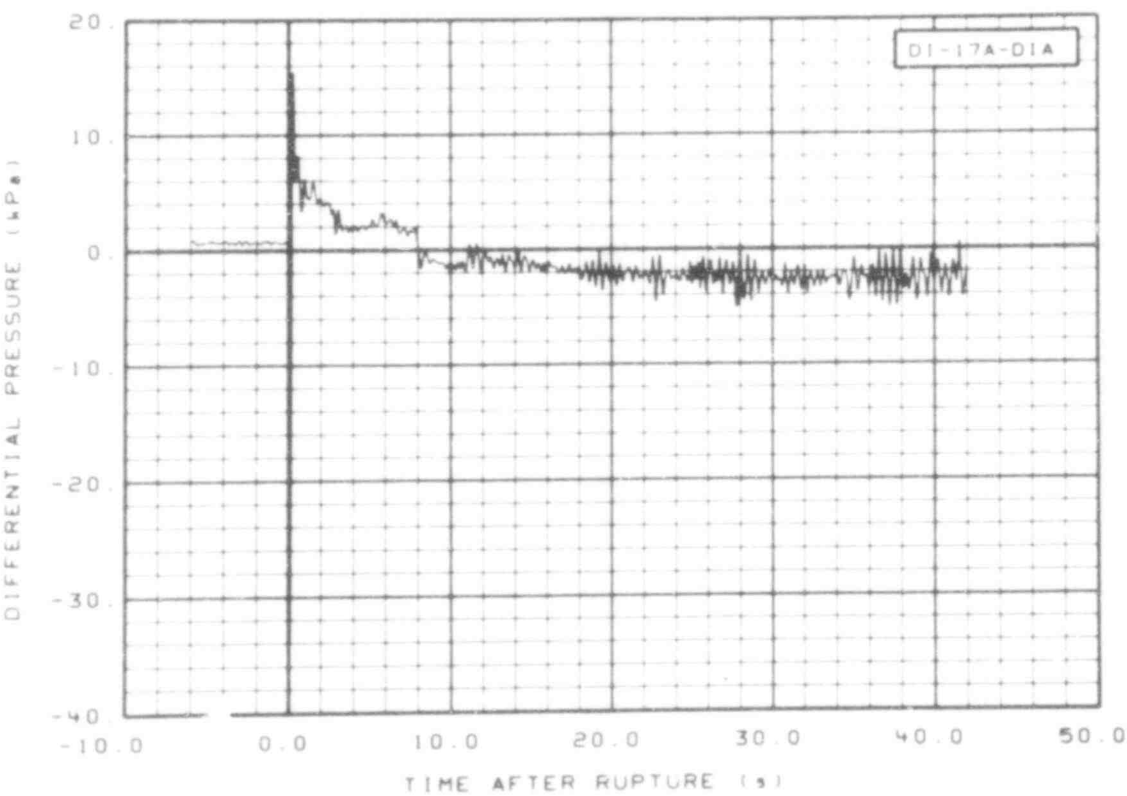

Fig. 138 Differential pressure in intact loop (DI-17A-DIA), from -6 to 42 s.

507 161

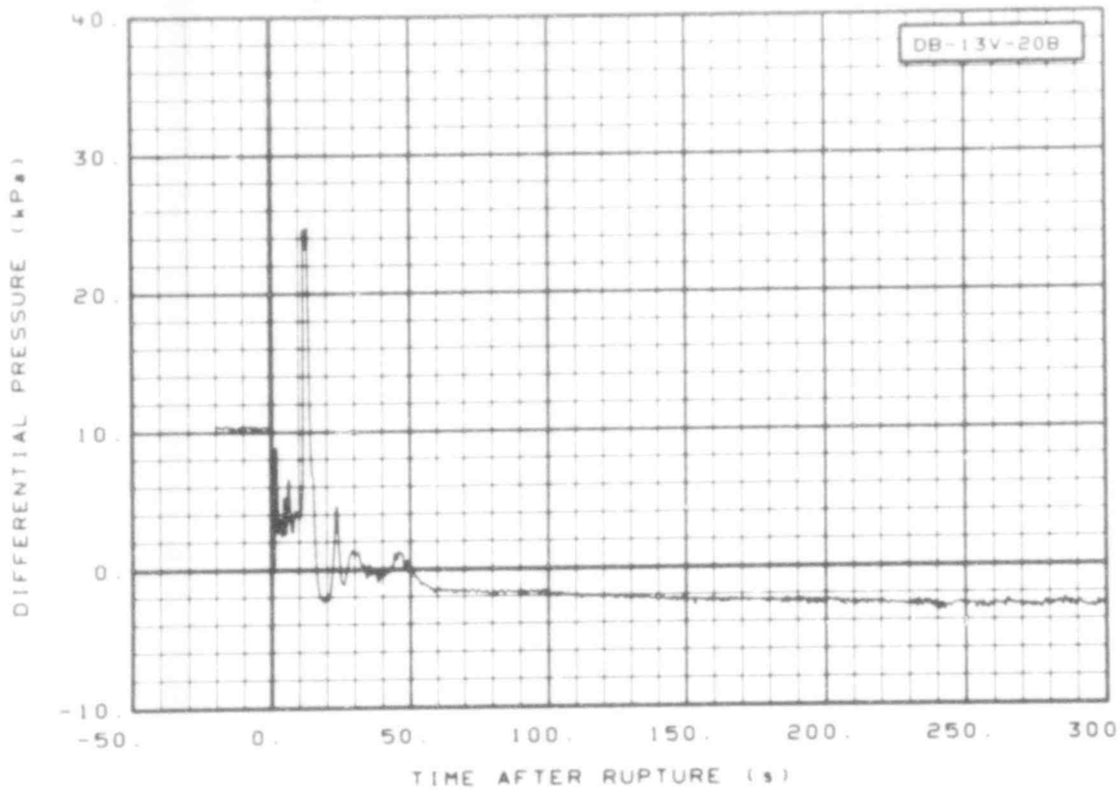

Fig. 139 Differential pressure in broken loop (DB-13V-20B), from -20 to 300 s.

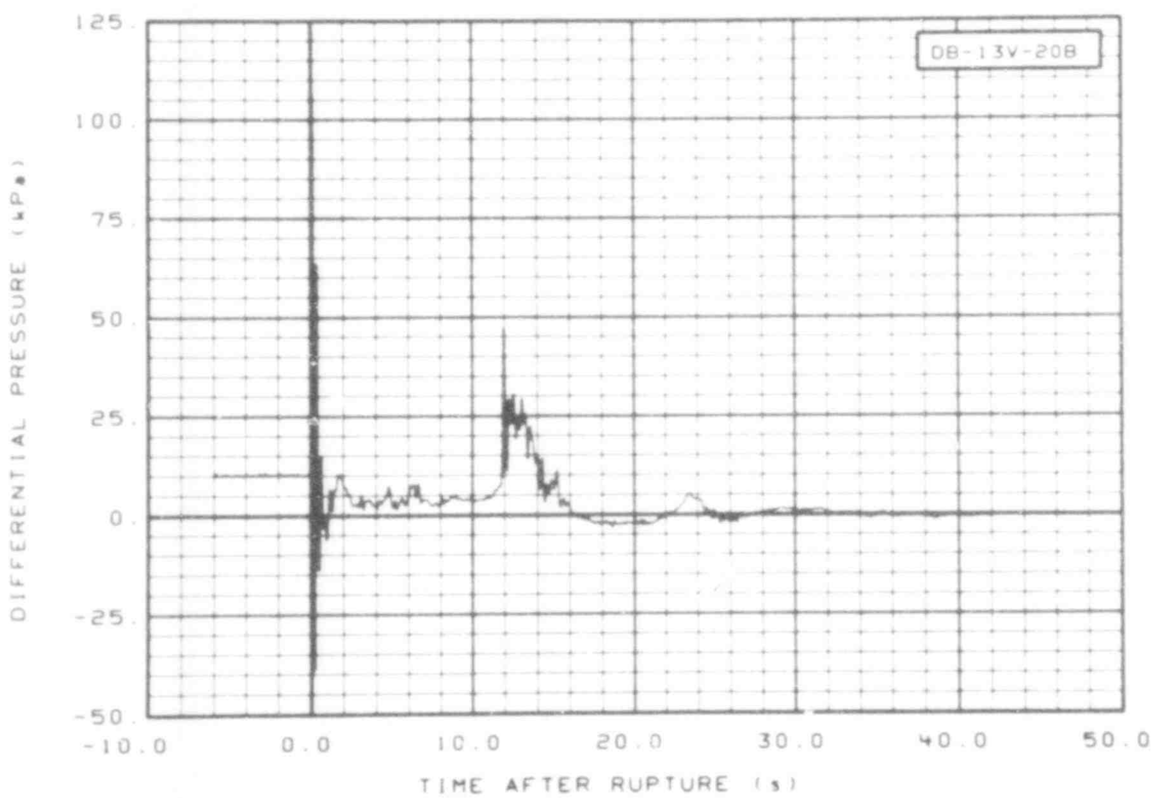

Fig. 140 Differential pressure in broken loop (DB-13V-20B), from -6 to 42 s.

507 162

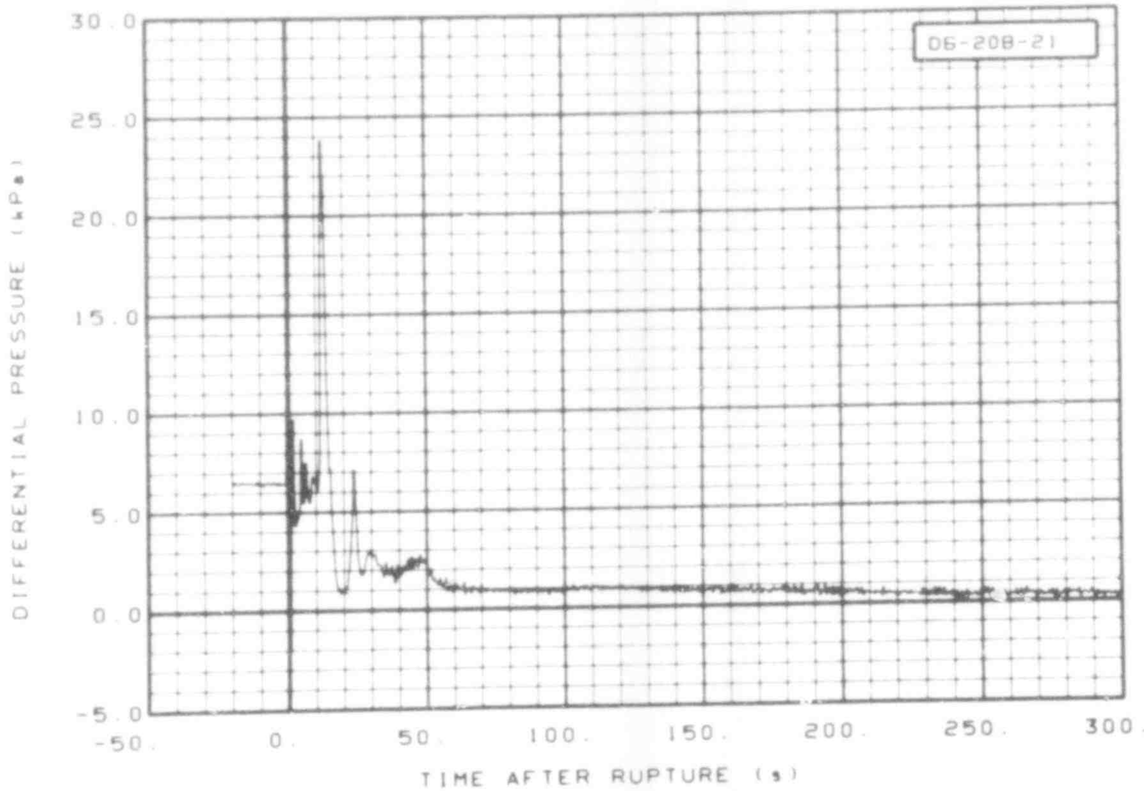

Fig. 141 Differential pressure in broken loop (DB-20B-21), from -20 to 300 s.

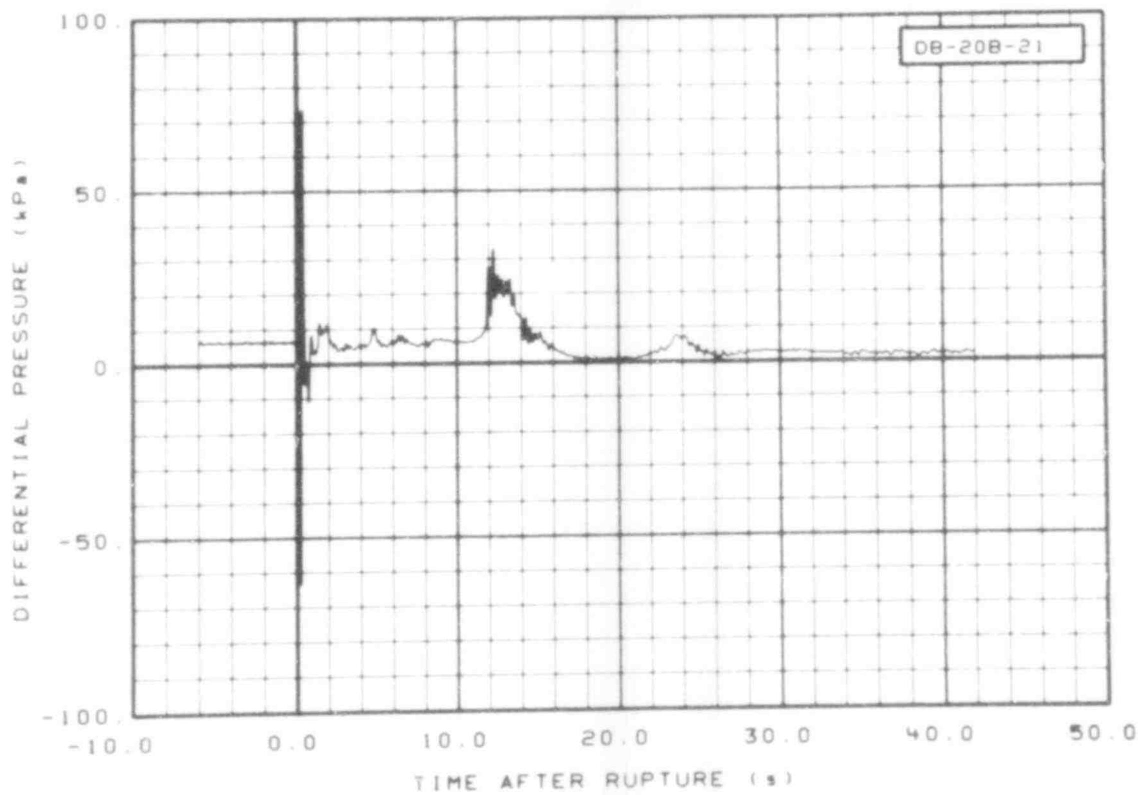

Fig. 142 Differential pressure in broken loop (DB-20B-21), from -6 to 42 s.

507 163

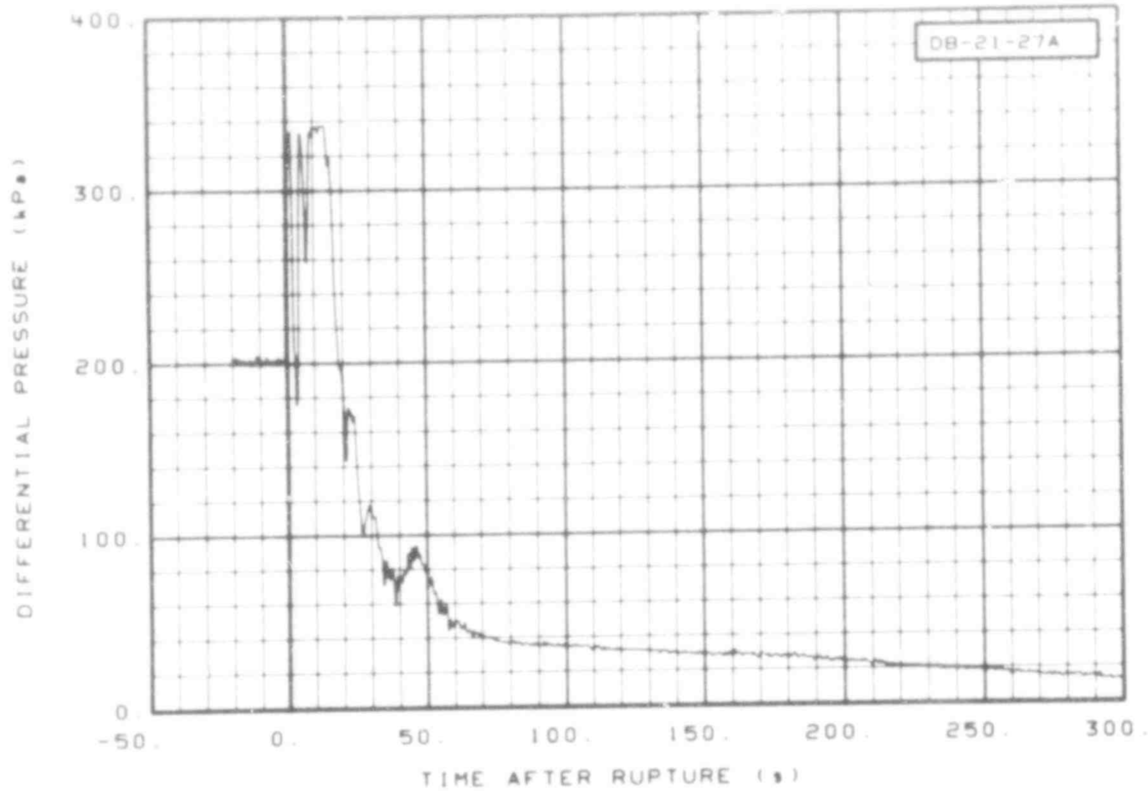

Fig. 143 Differential pressure in broken loop (DB-21-27A), from -20 to 300 s.

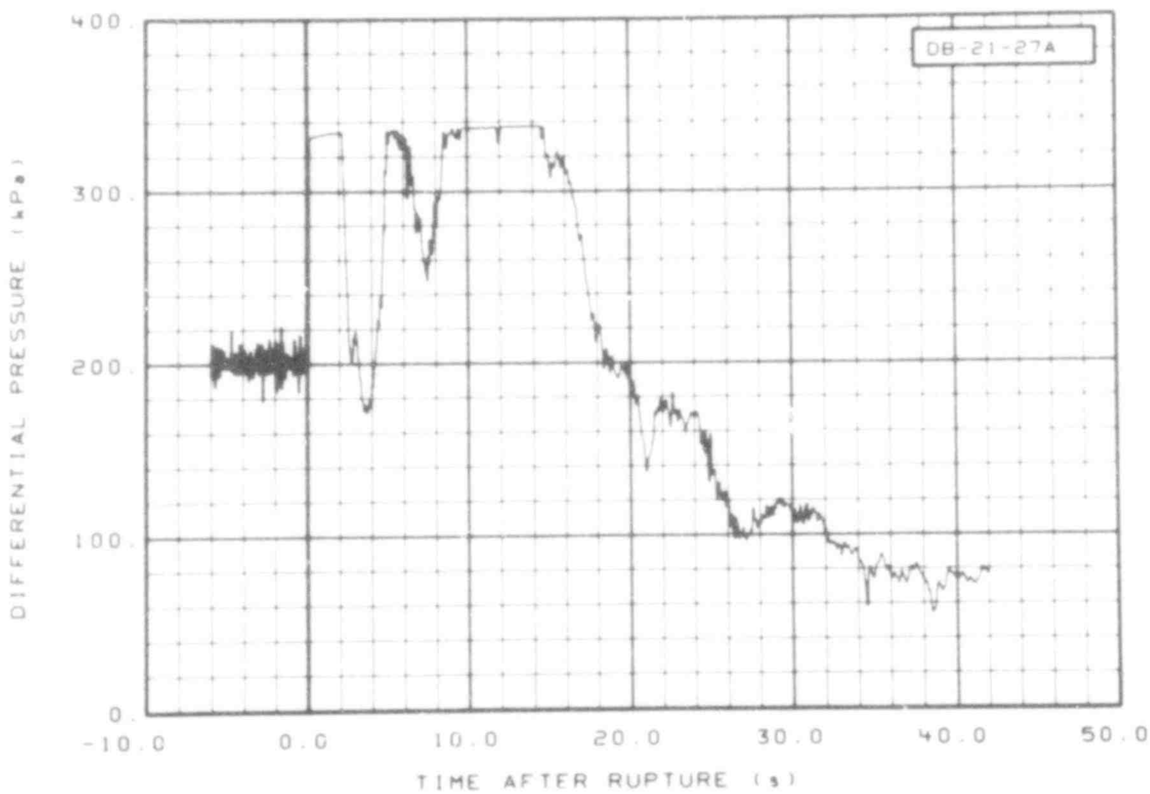

Fig. 144 Differential pressure in broken loop (DB-21-27A), from -6 to 42 s.

507 164

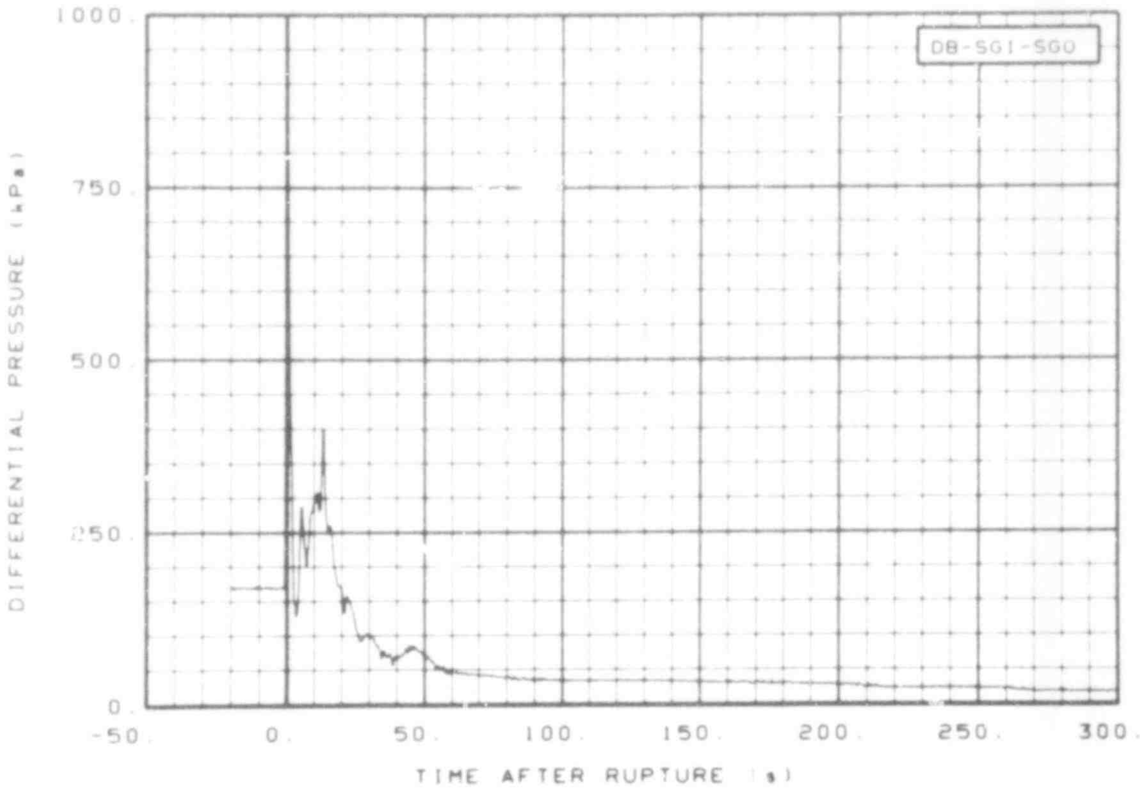

Fig. 145 Differential pressure in broken loop steam generator (DB-SGI-SGO), from -20 to 300 s.

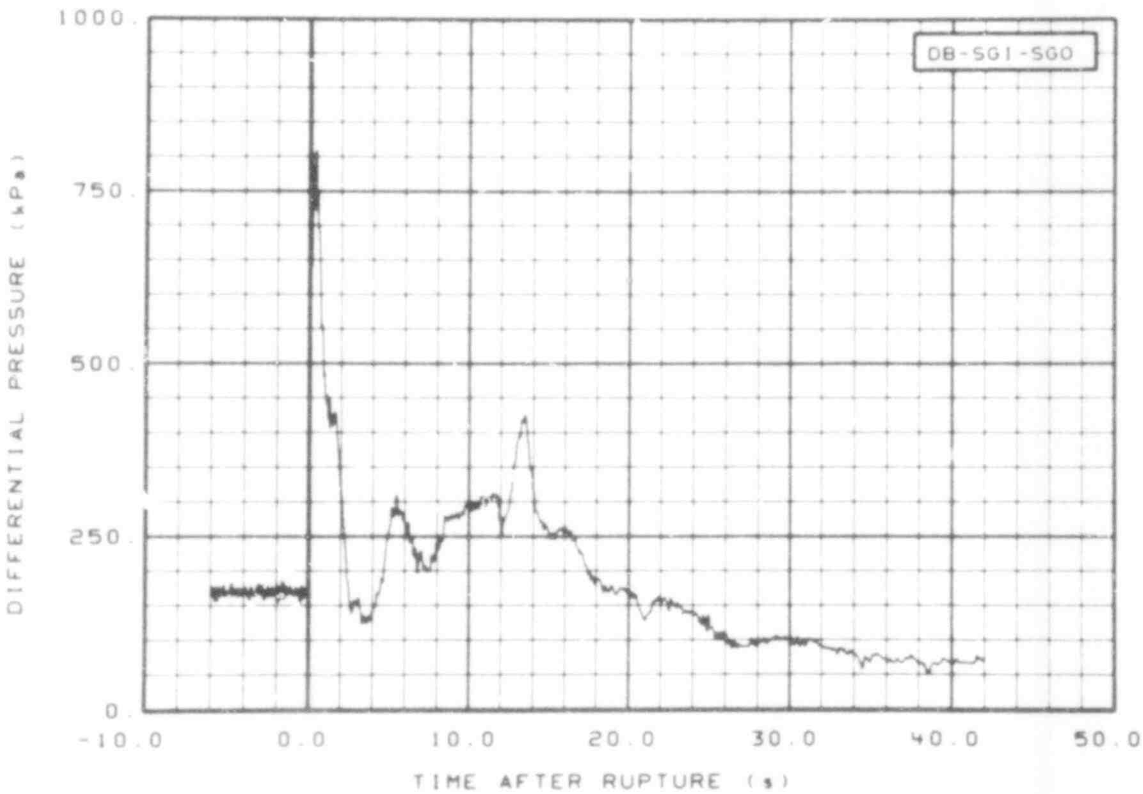

Fig. 146 Differential pressure in broken loop steam generator (DB-SGI-SGO), from -6 to 42 s.

507 165

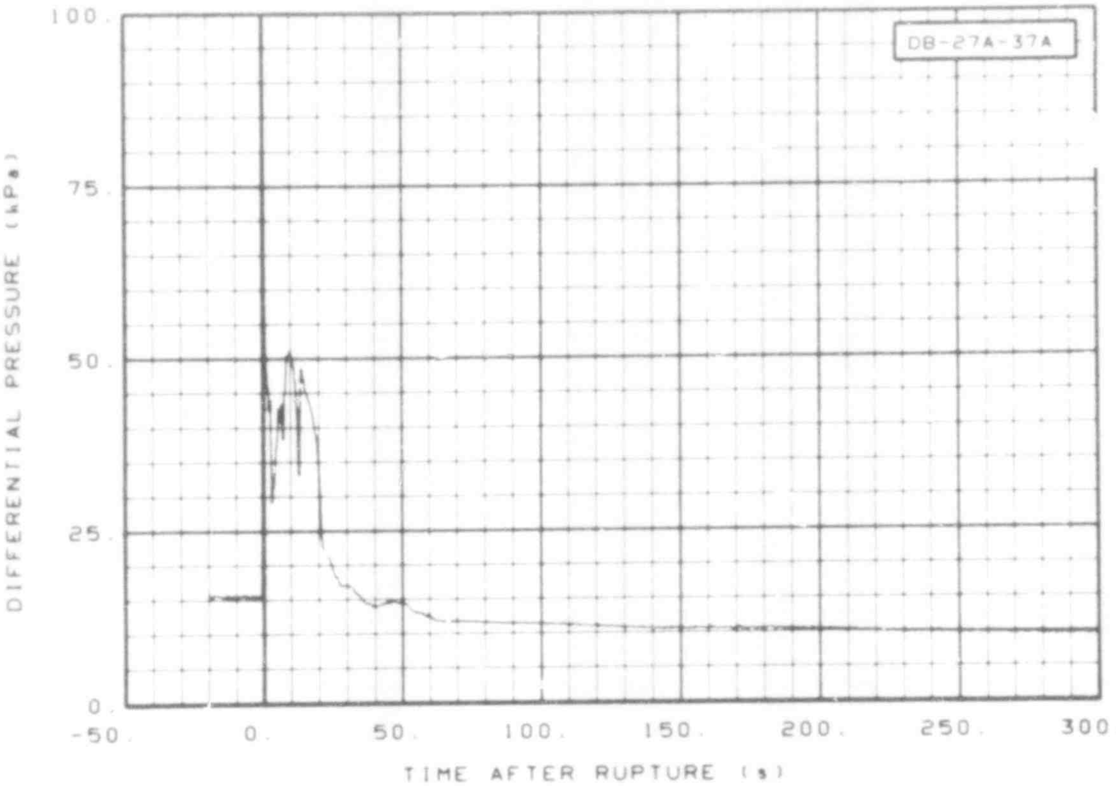

Fig. 147 Differential pressure in broken loop (DB-27A-37A), from -20 to 300 s.

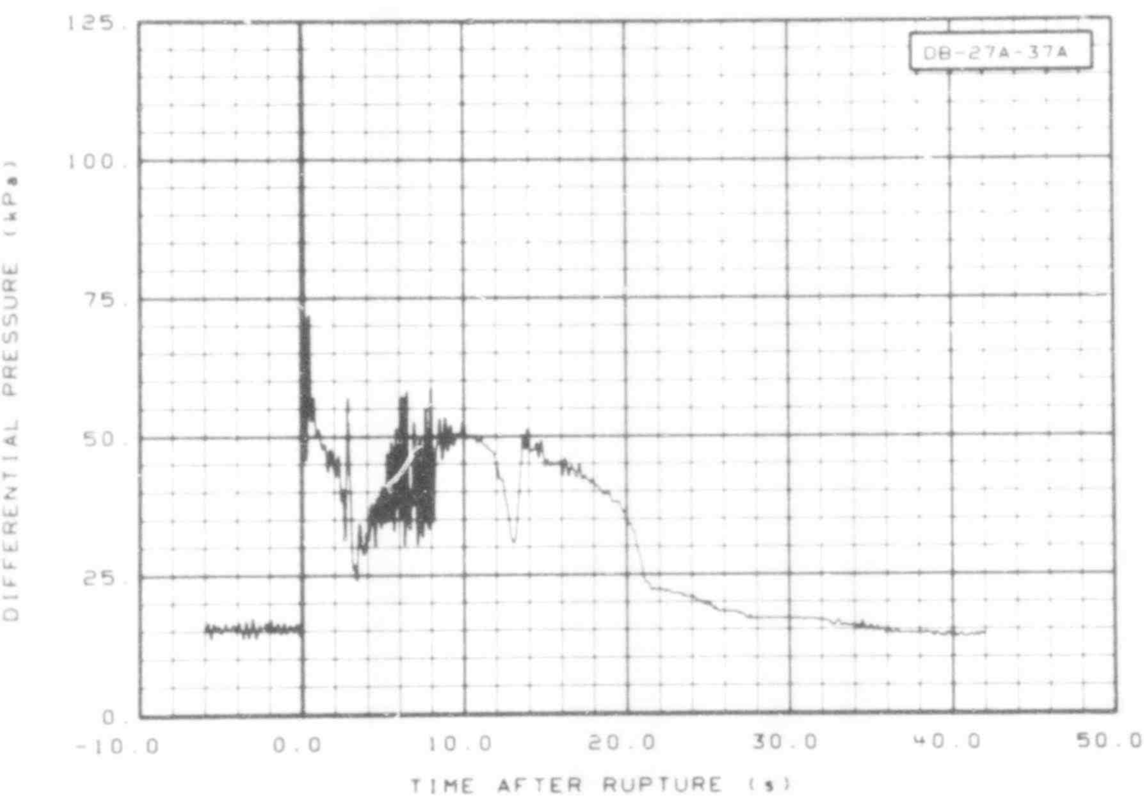

Fig. 148 Differential pressure in broken loop (DB-27A-37A), from -6 to 42 s.

507 166

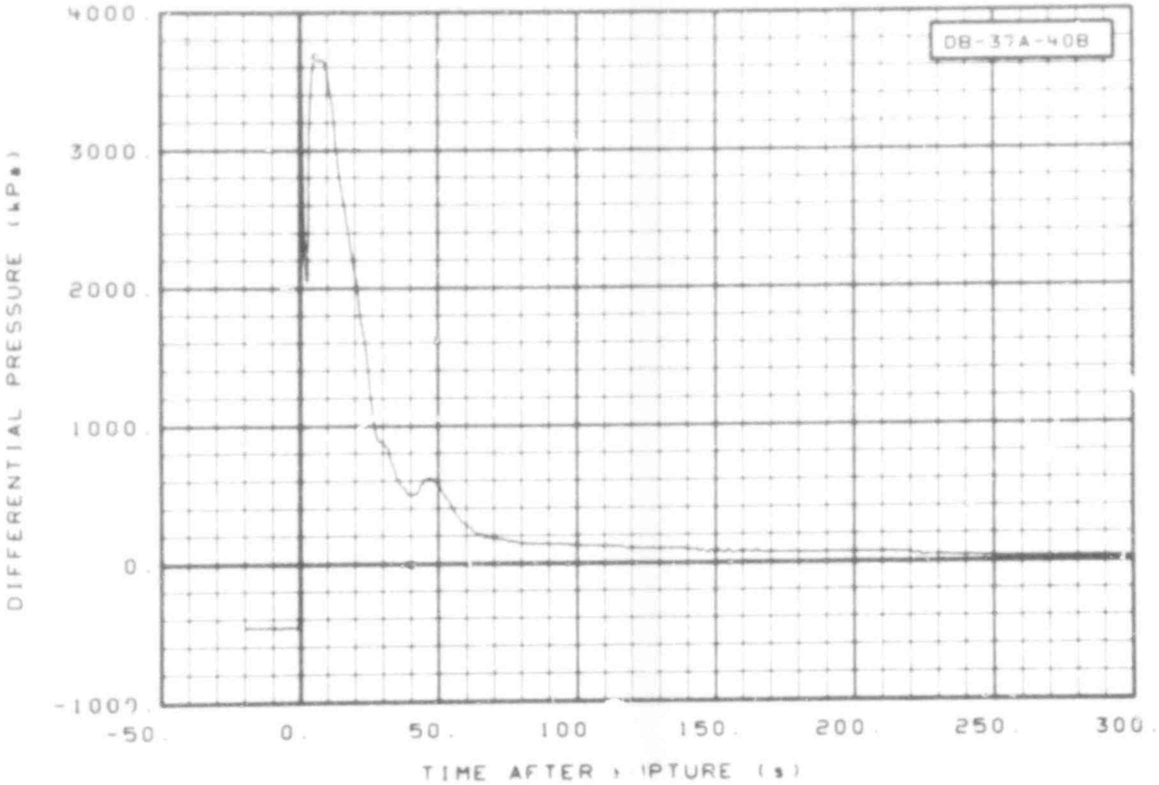

Fig. 149 Differential pressure in broken loop (DB-37A-40B), from -20 to 300 s.

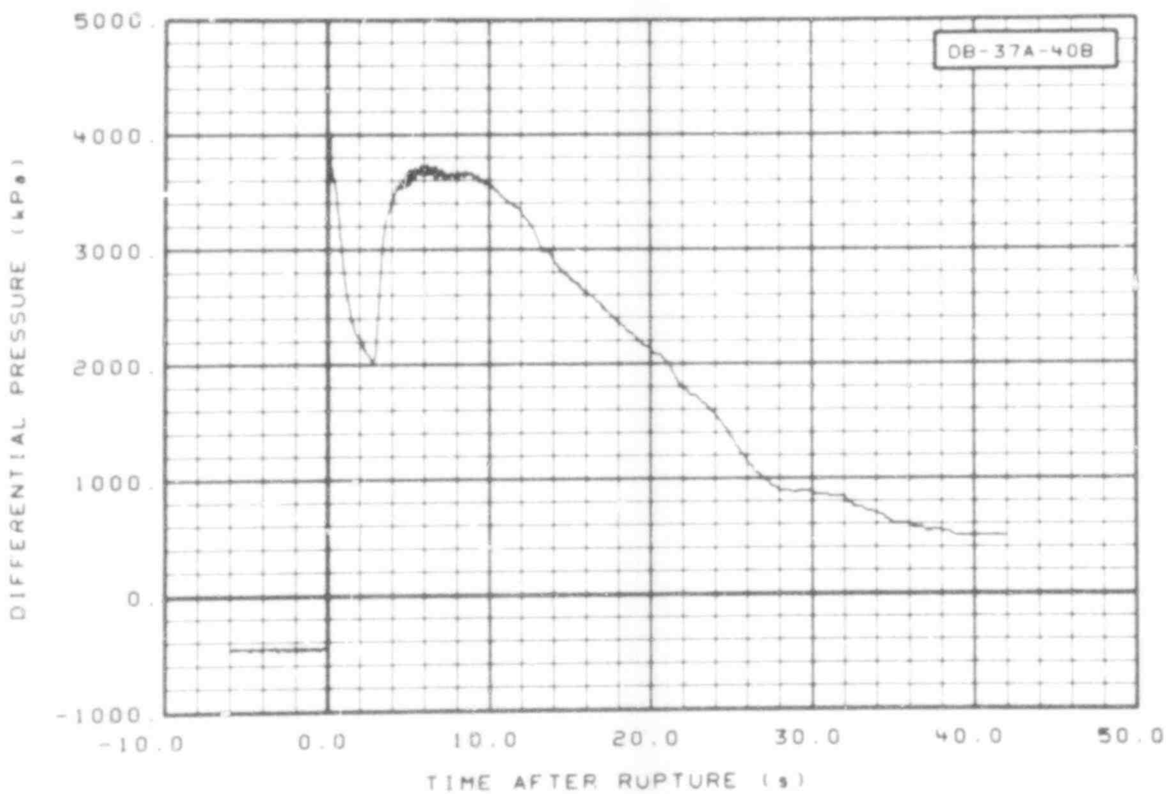

Fig. 150 Differential pressure in broken loop (DB-37A-40B), from -6 to 42 s.

507 167

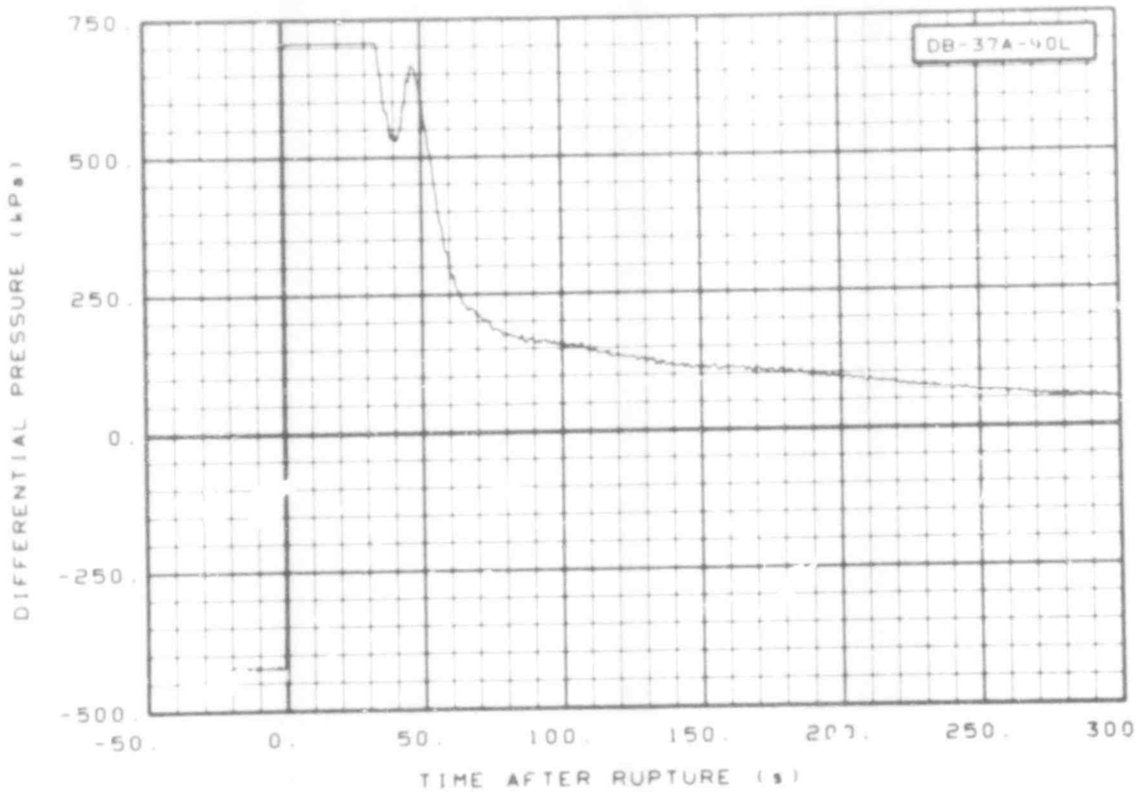

Fig. 151 Differential pressure in broken loop (DB-37A-40L), from -20 to 300 s.

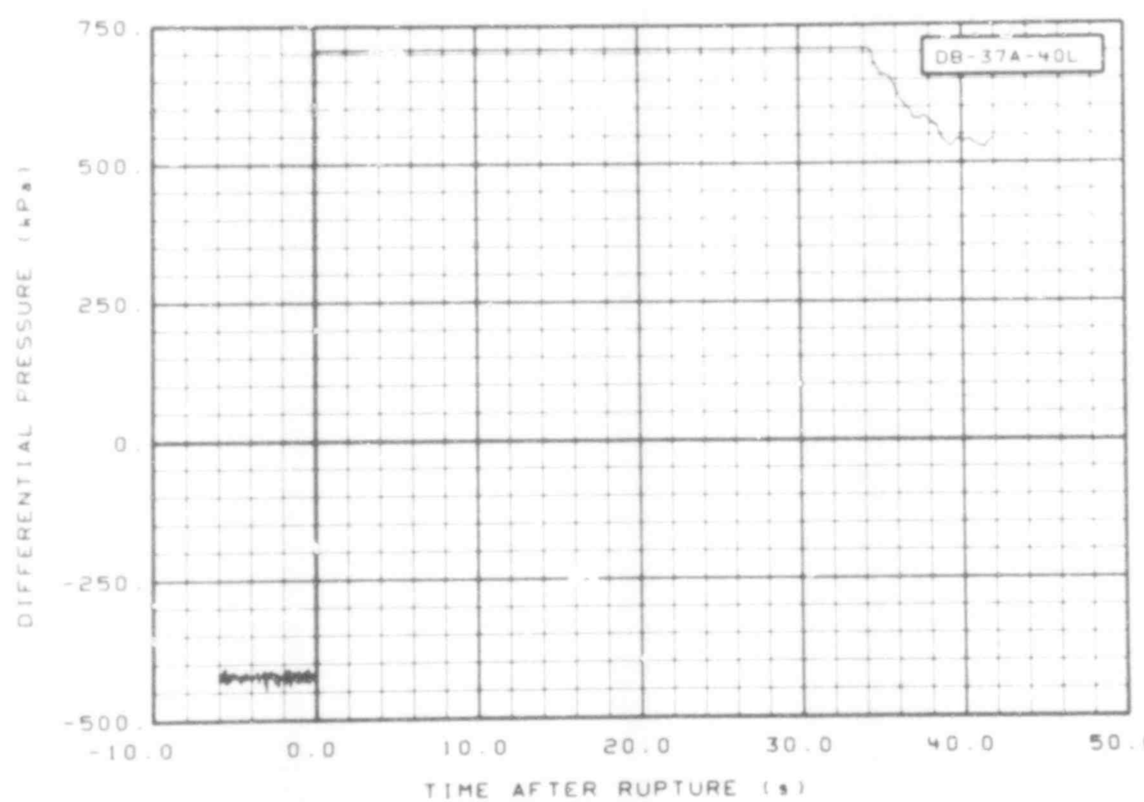

Fig. 152 Differe[illegible]ial pressure in broken loop (DB-37A-40L), from -6 to 42 s.

507 168

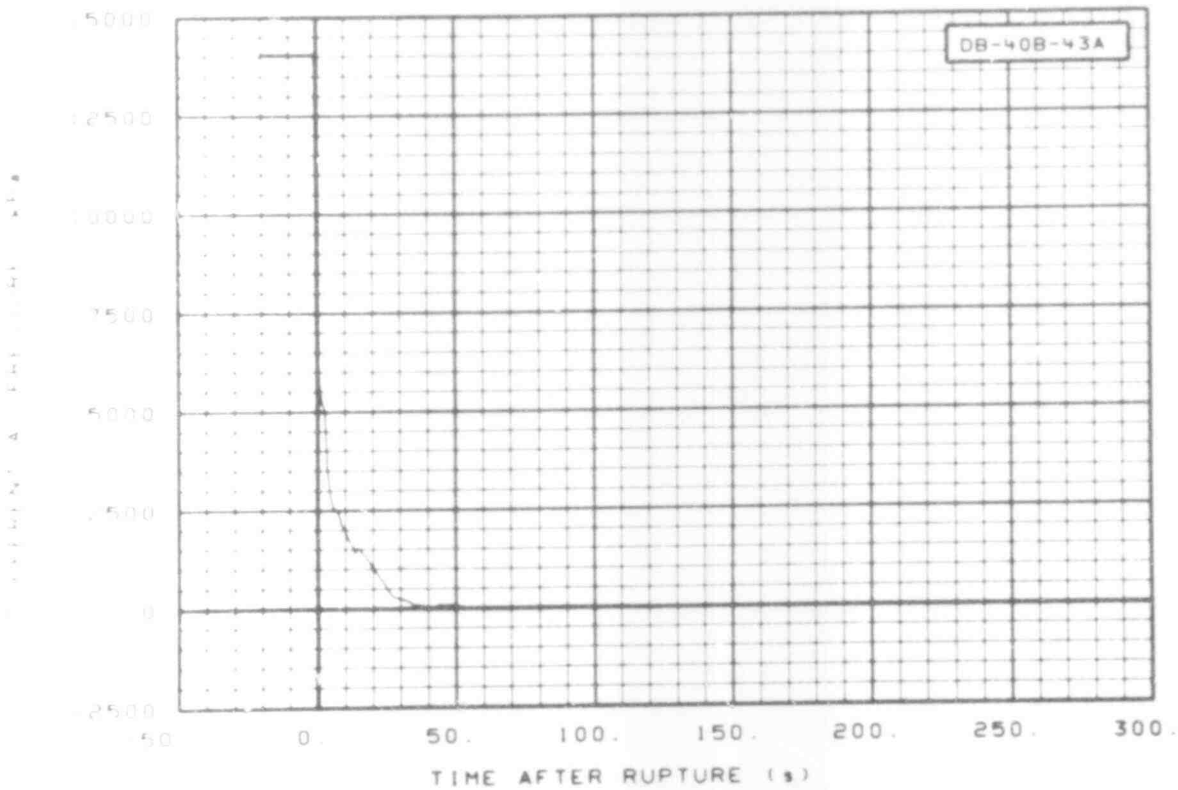

Fig. 153 Differential pressure in broken loop (DB-40B-43A), from -20 to 300 s.

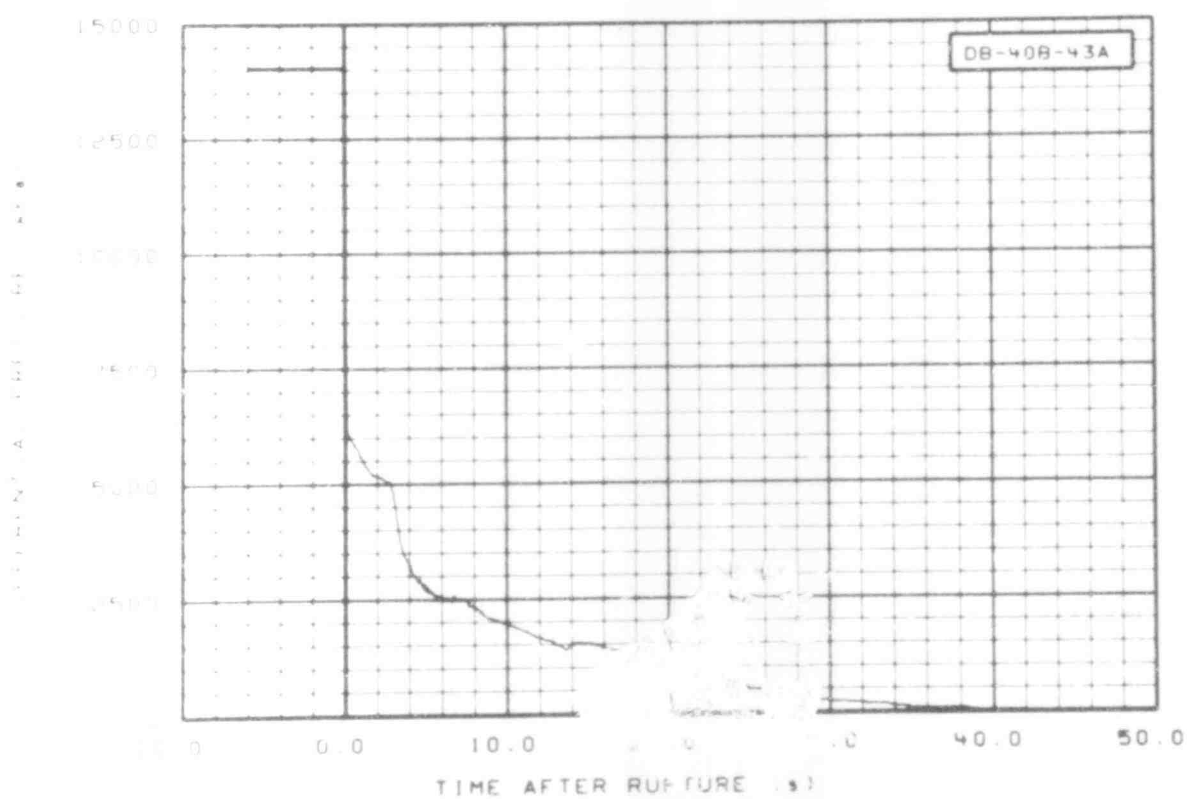

Fig. 154 Differential pressure in broken loop (DB-40B-43A), from -6 to 42 s.

507 169

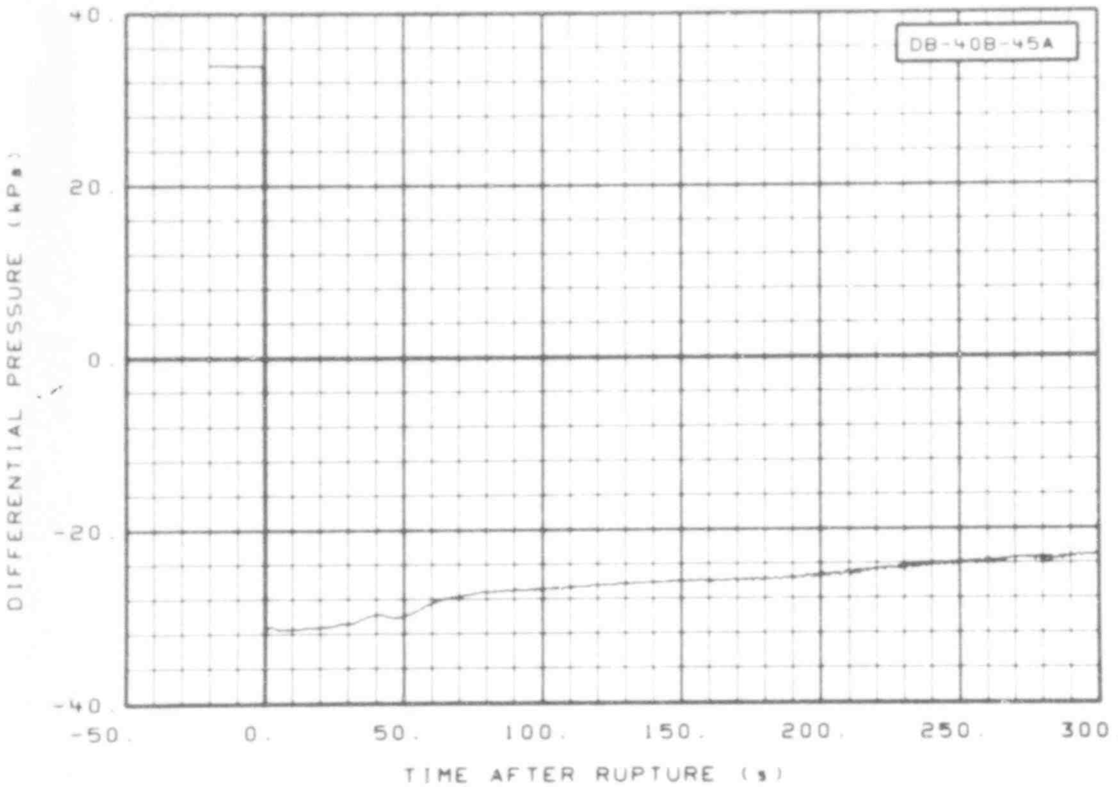

Fig. 155 Differential pressure in broken loop (DB-40B-45A), from -20 to 300 s.

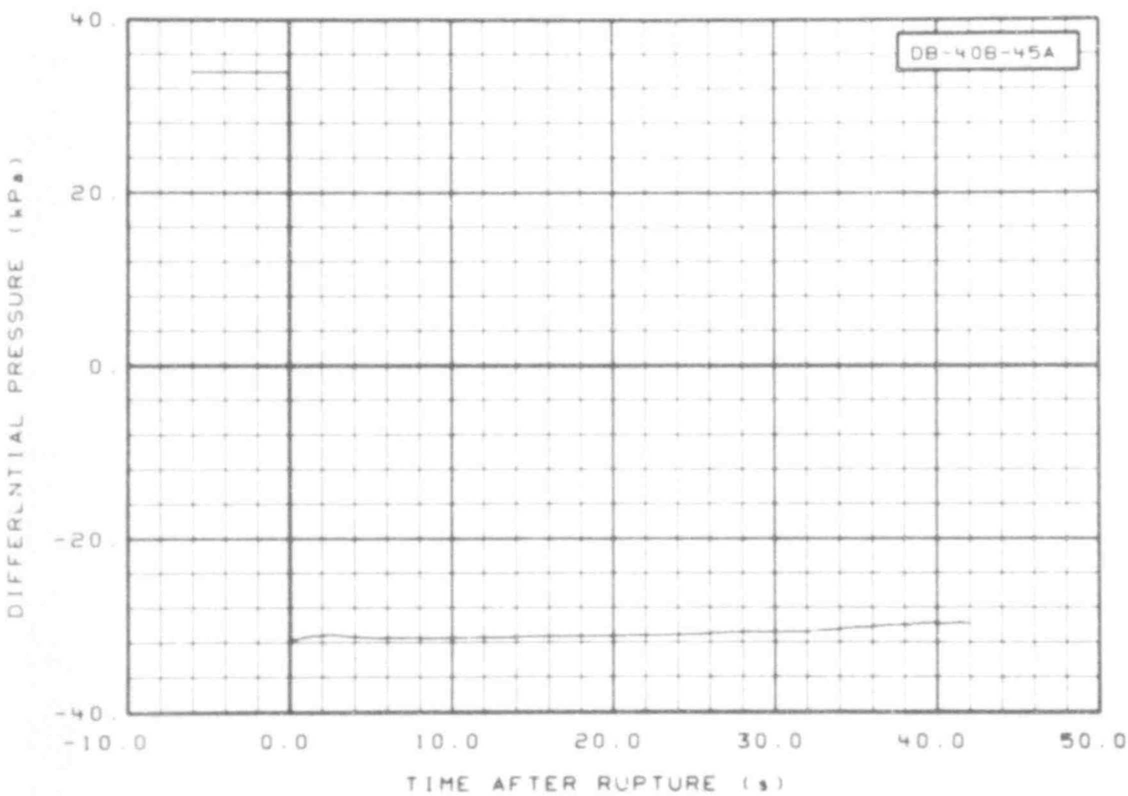

Fig. 156 Differential pressure in broken loop (DB-40B-45A), from -6 to 42 s.

507 170

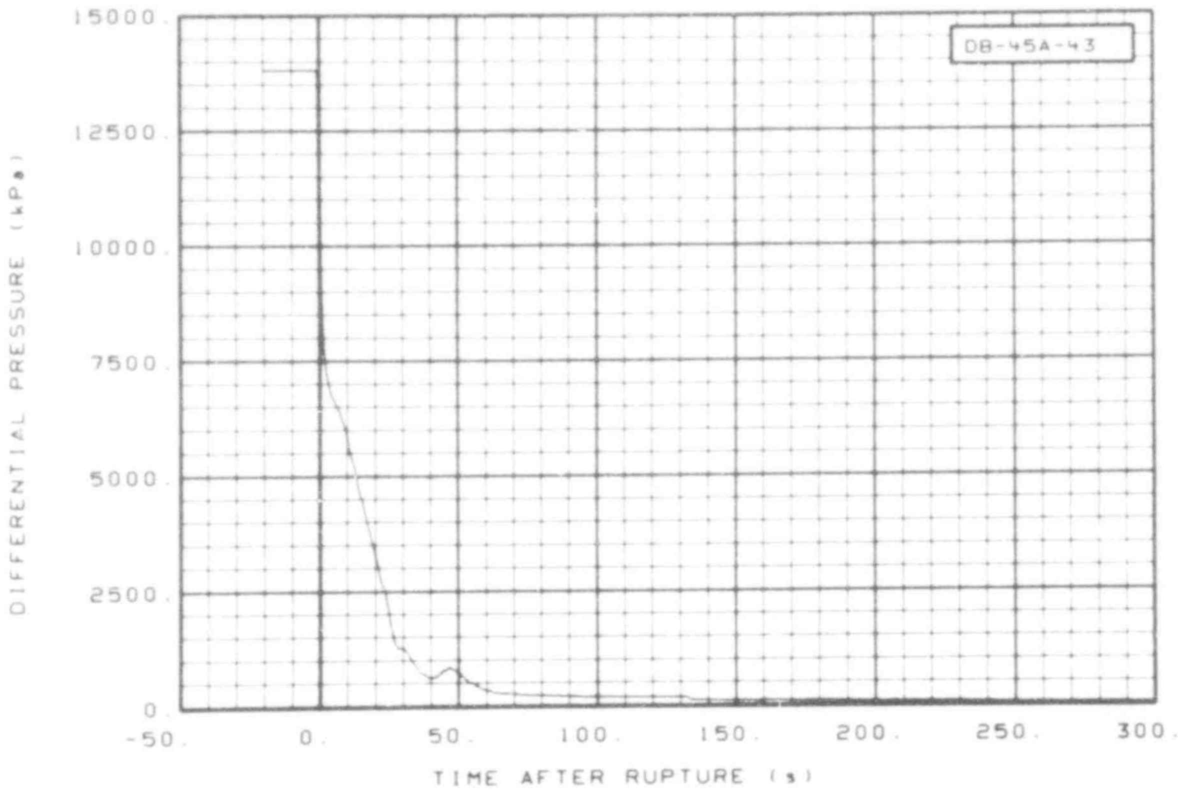

Fig. 157 Differential pressure in broken loop (DB-45A-43), from -20 to 300 s.

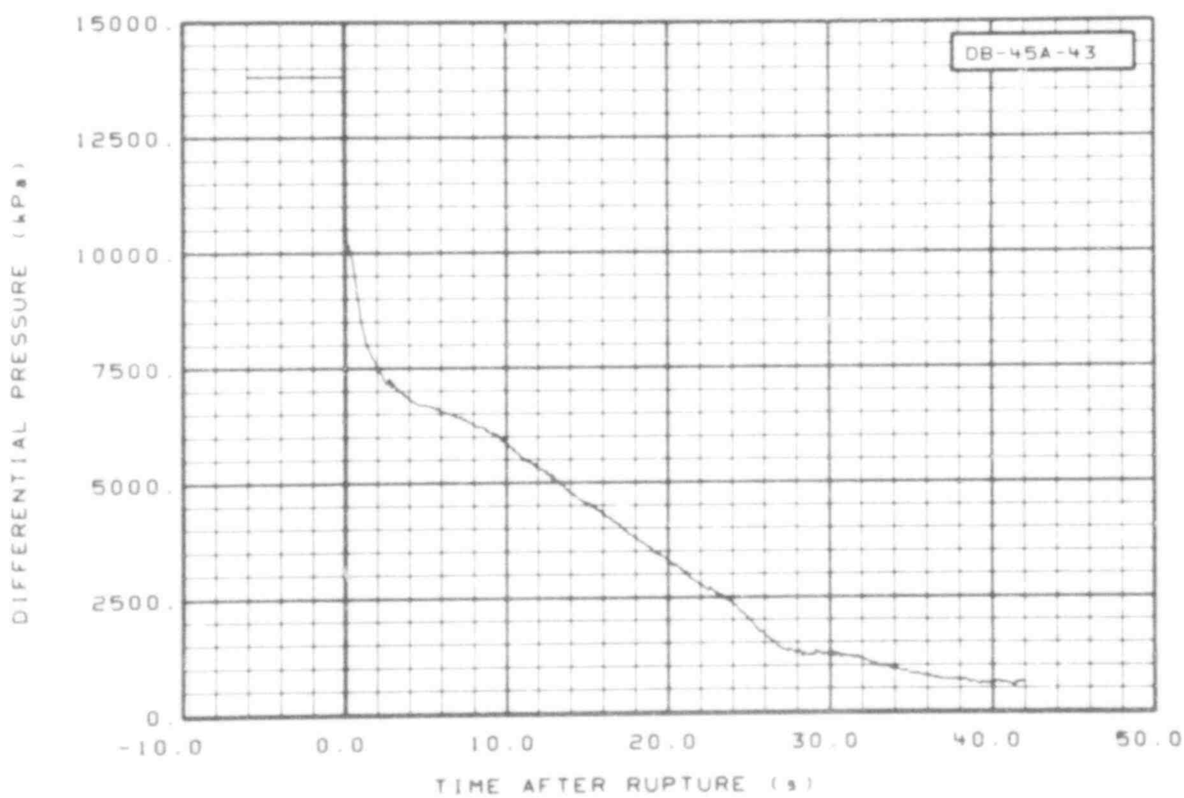

Fig. 158 Differential pressure in broken loop (DB-45A-43), from -6 to 42 s.

507 171

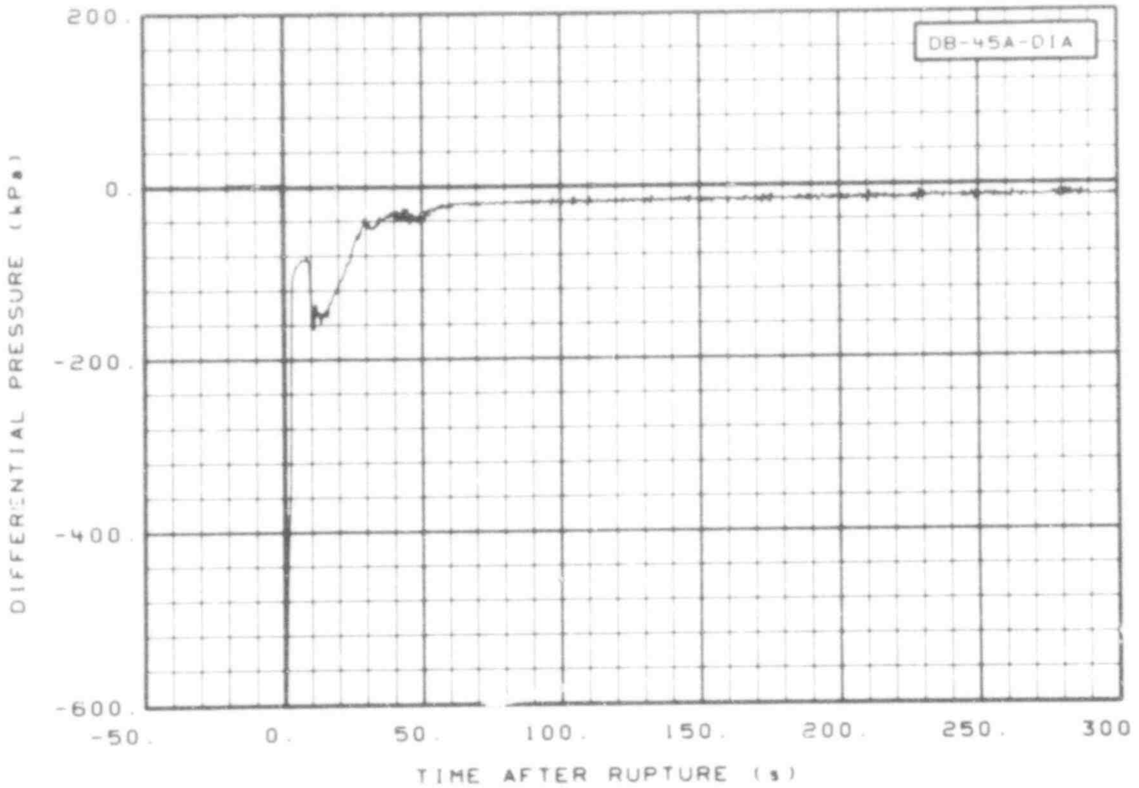

Fig. 159 Differential pressure in broken loop (DB-45A-DIA), from -20 to 300 s.

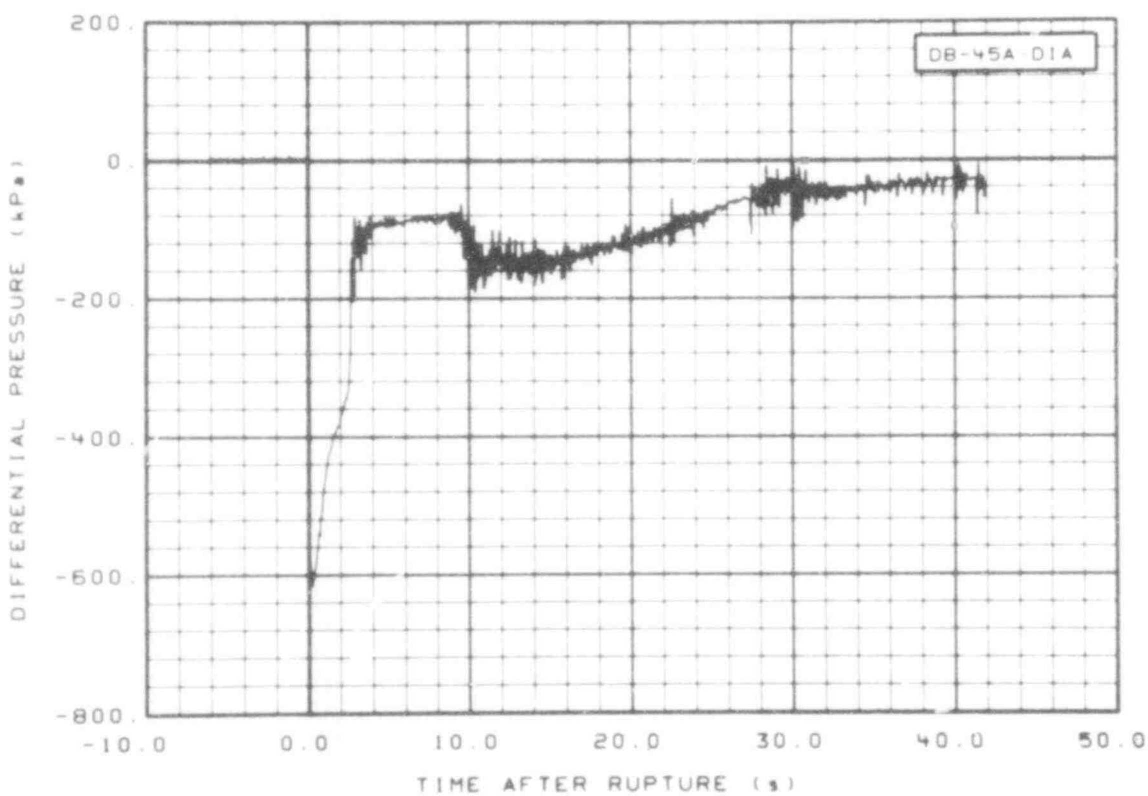

Fig. 160 Differential pressure in broken loop (DB-45A-DIA), from -6 to 42 s.

507 172

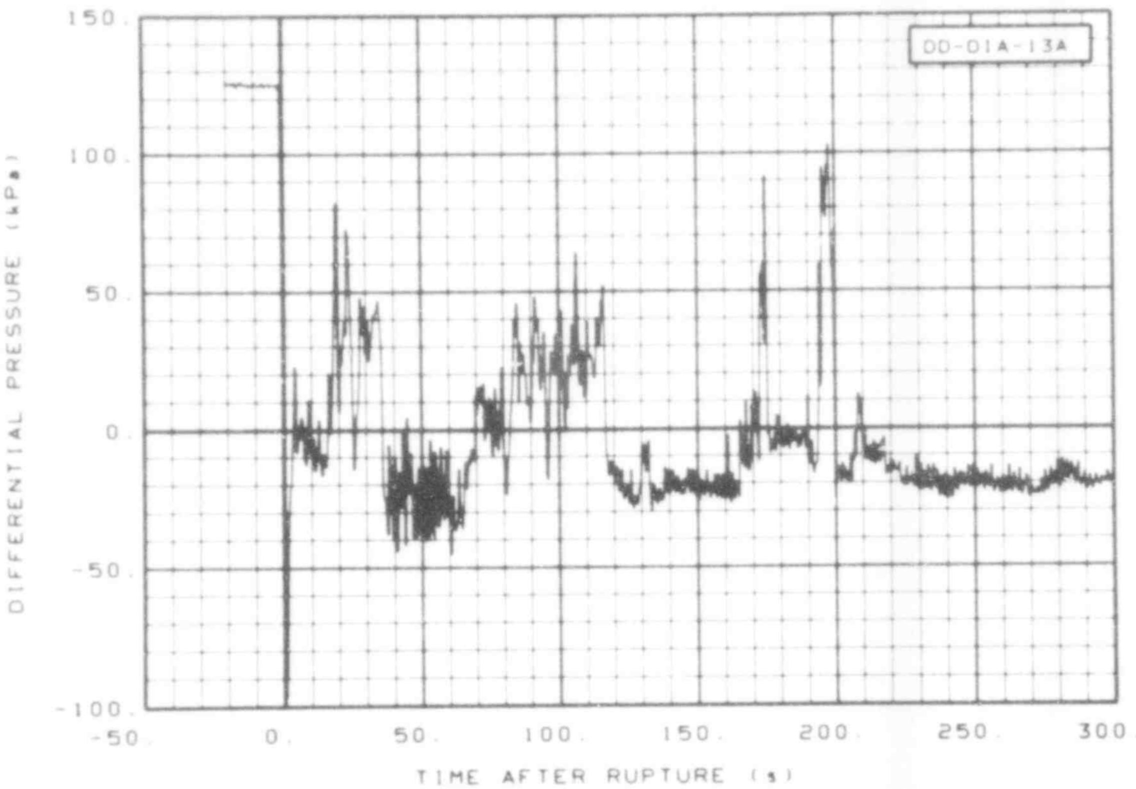

Fig. 161 Differential pressure in downcomer (DD-DIA-13A), from -20 to 300 s.

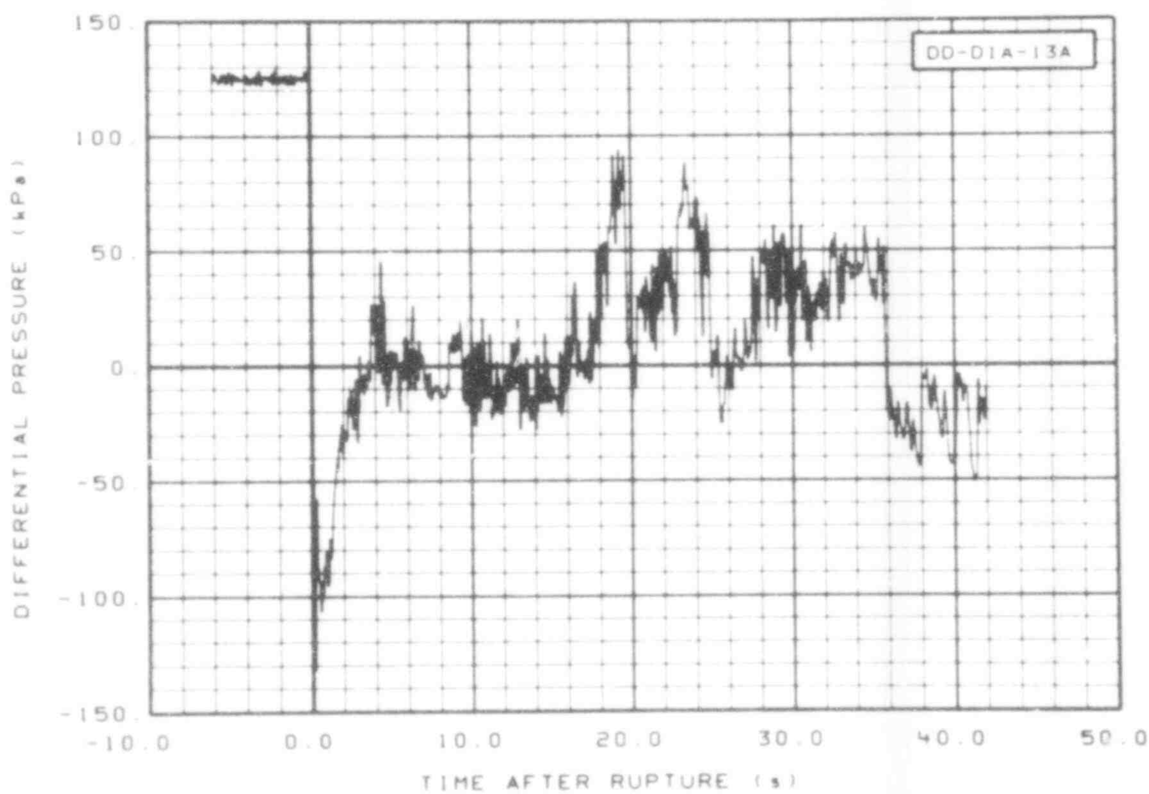

Fig. 162 Differential pressure in downcomer (DD-DIA-13A), from -6 to 42 s.

507 173

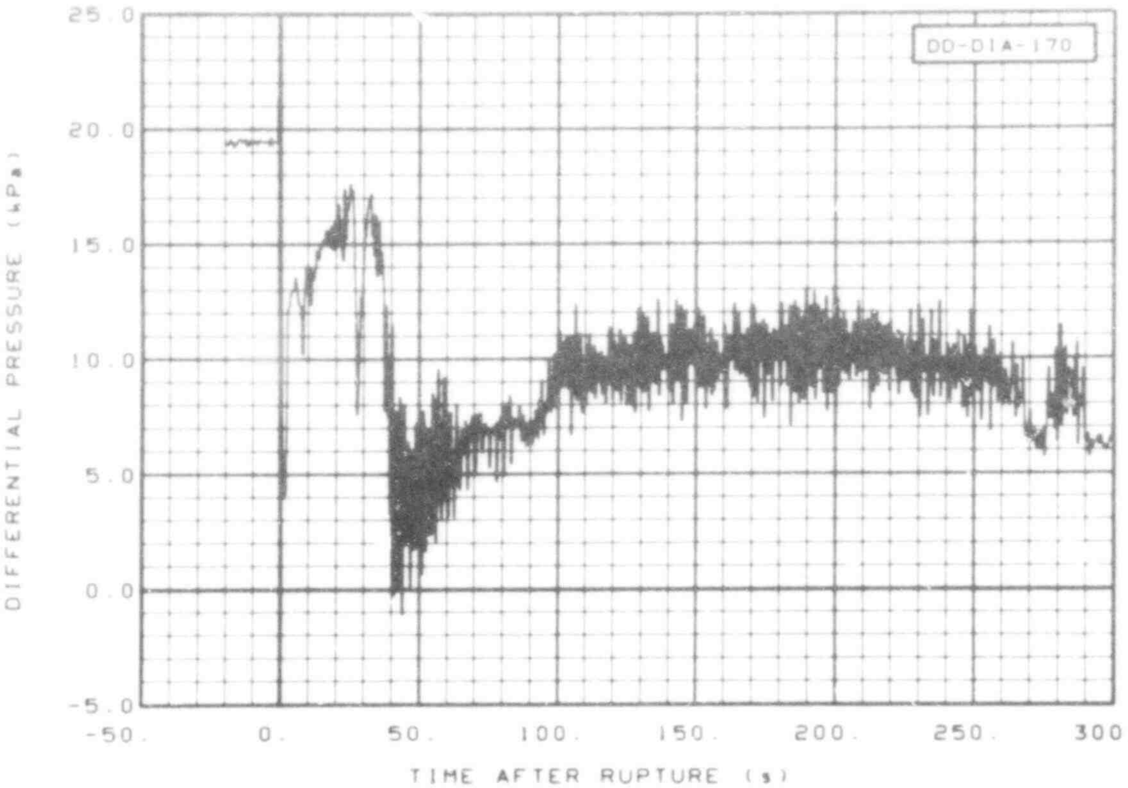

Fig. 163 Differential pressure in downcomer (DD-DIA-170), from -20 to 300 s.

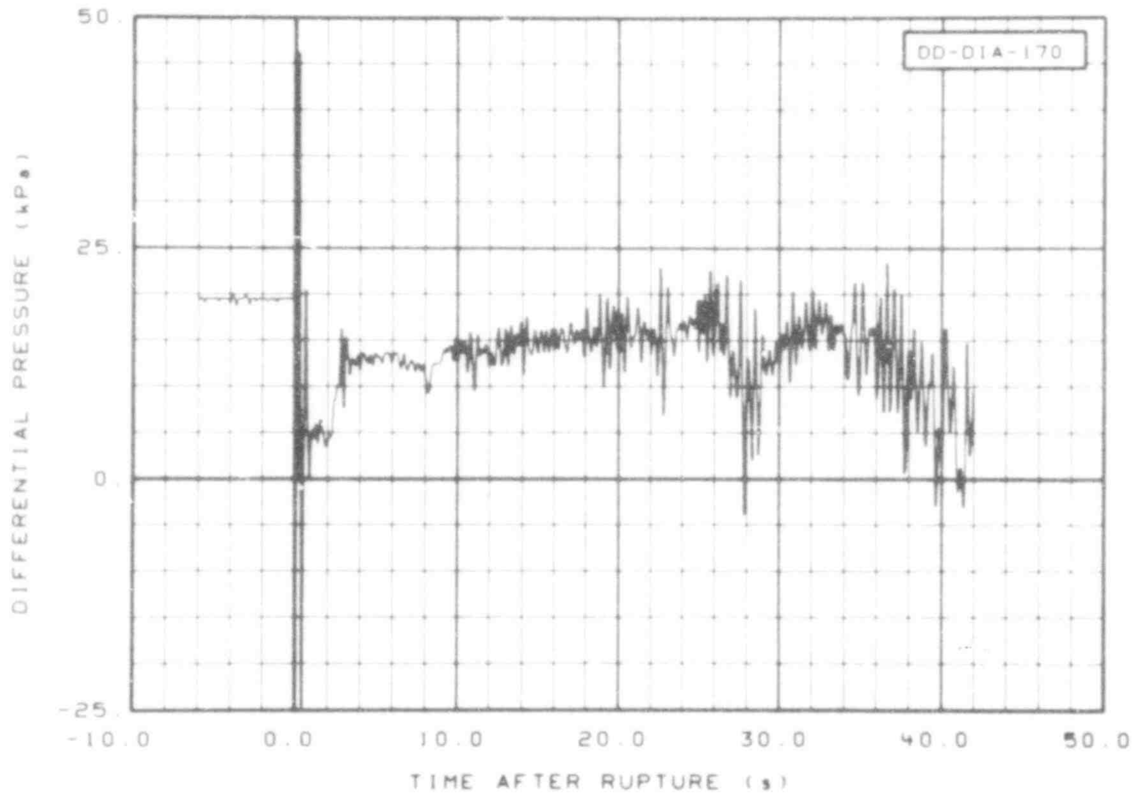

Fig. 164 Differential pressure in downcomer (DD-DIA-170), from -6 to 42 s.

507 174

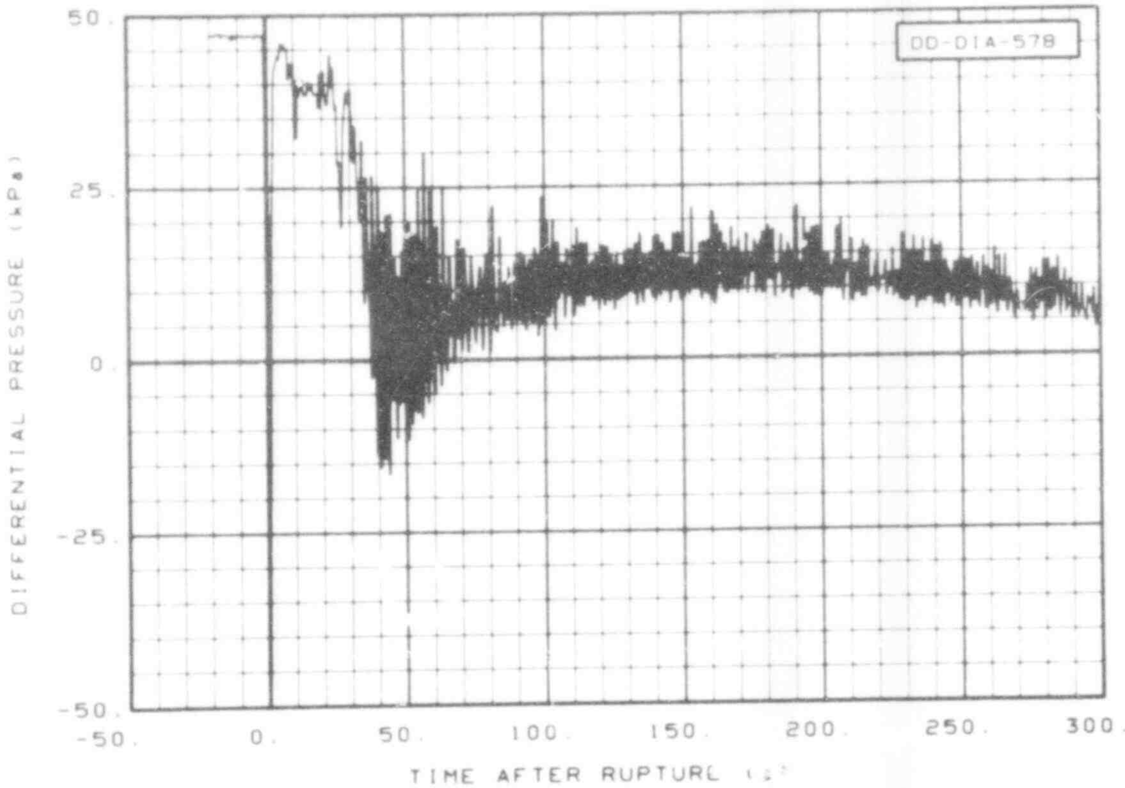

Fig. 165 Differential pressure in downcomer (DD-DIA-578), from -20 to 300 s.

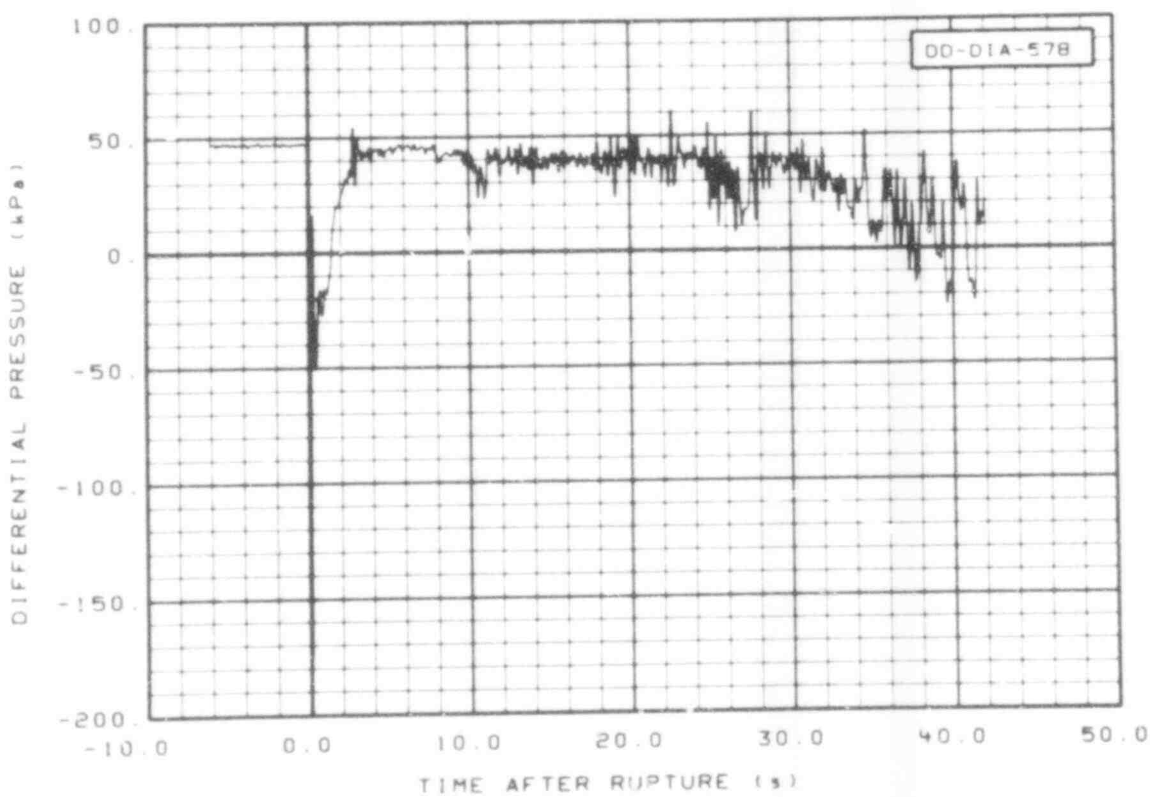

Fig. 166 Differential pressure in downcomer (DD-DIA 578), from -6 to 42 s.

507 175

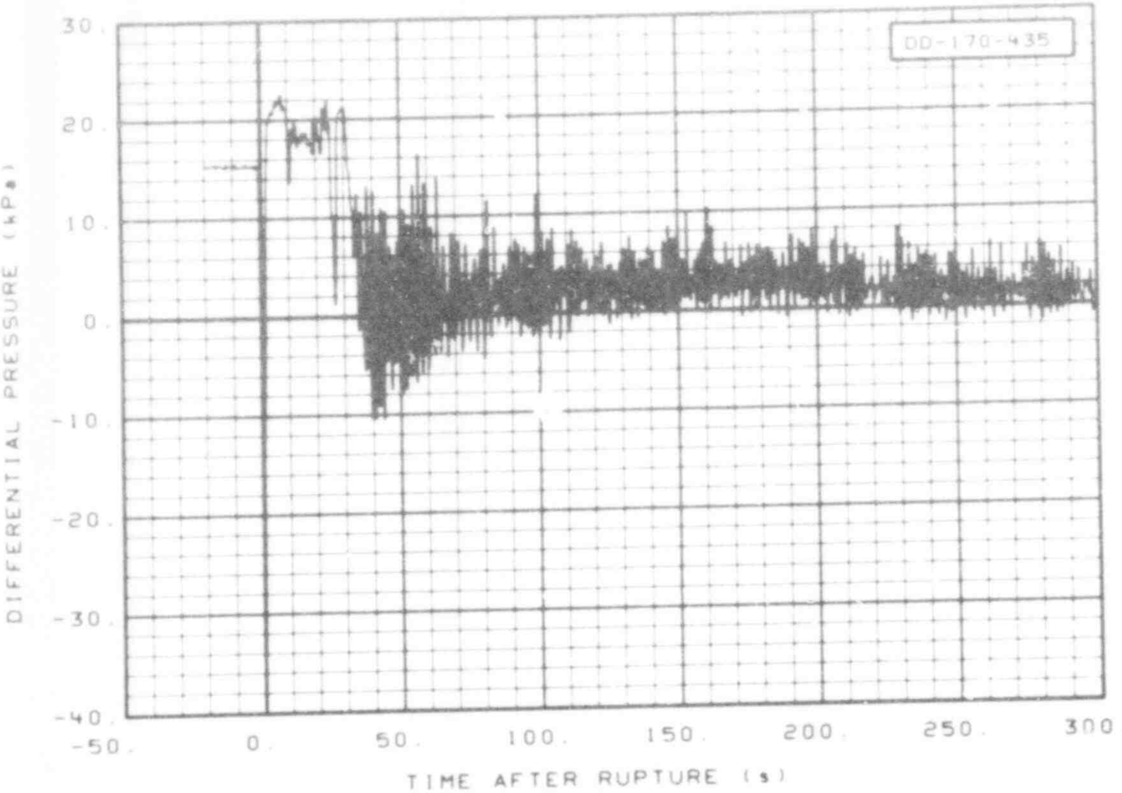

Fig. 167 Differential pressure in downcomer (DD-170-435), from -20 to 300 s.

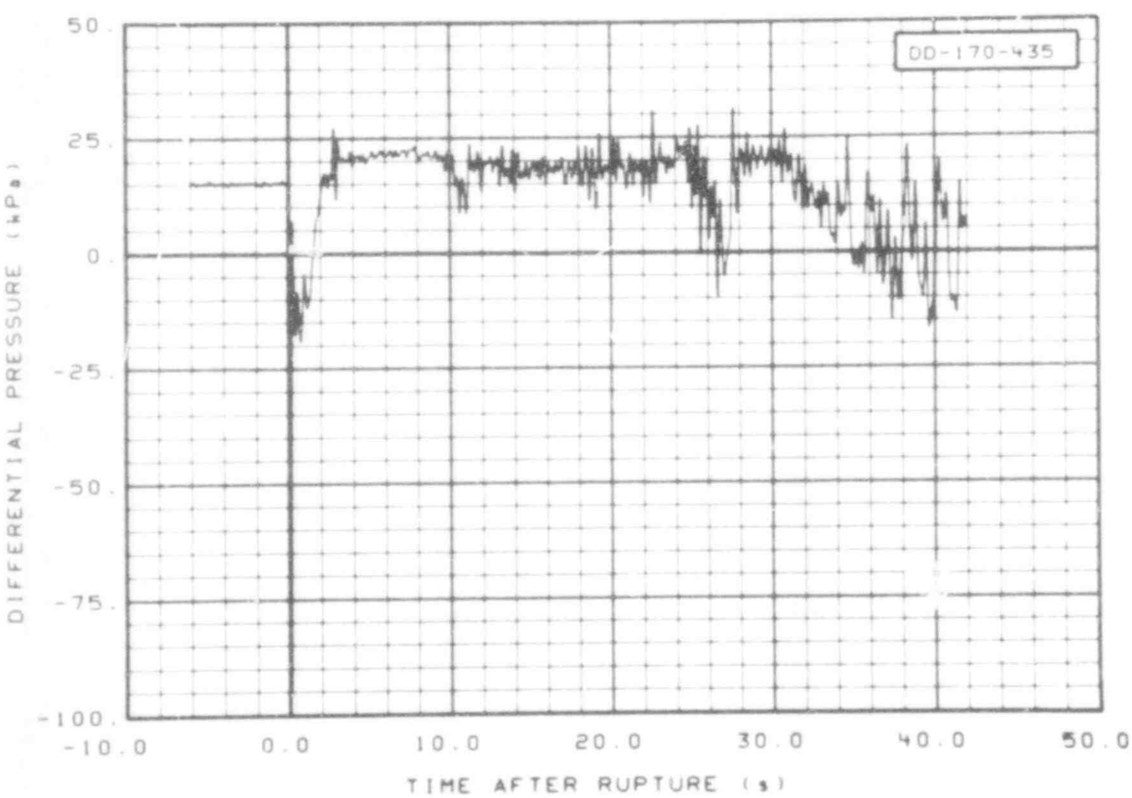

Fig. 168 Differential pressure in downcomer (DD-170-435), from -6 to 42 s.

507 176

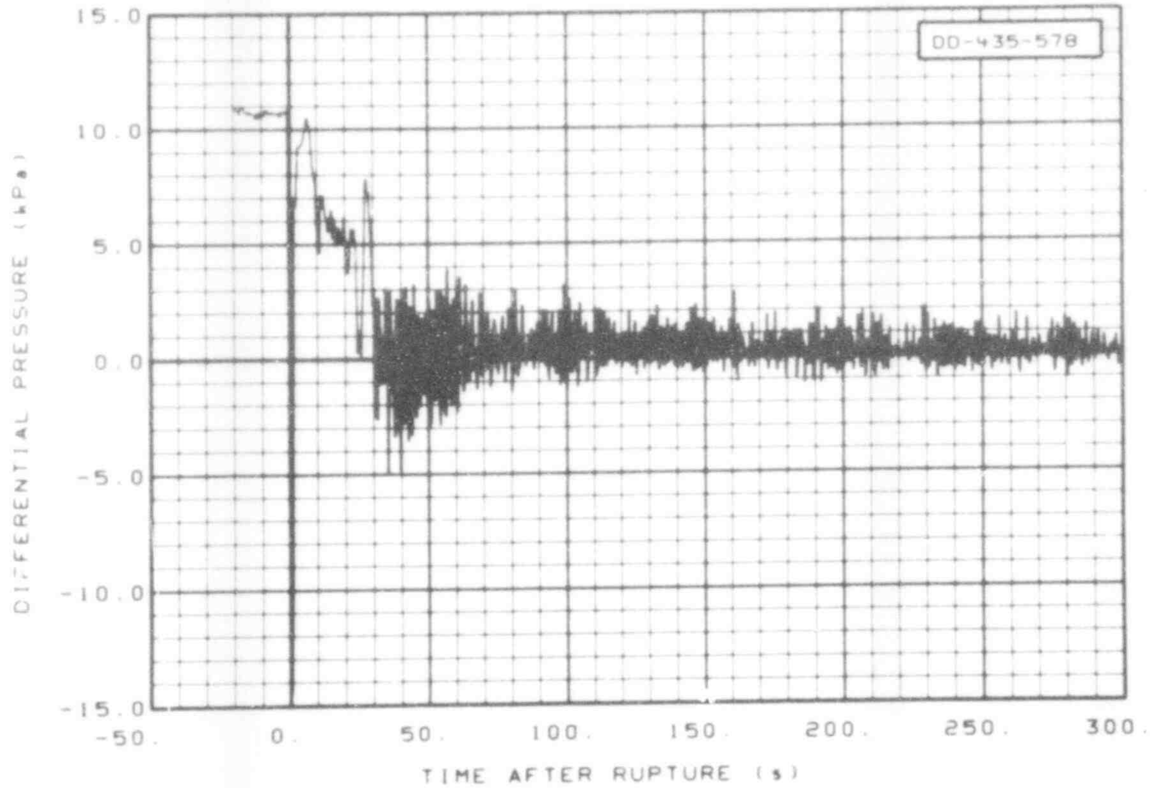

Fig. 169 Differential pressure in downcomer (DD-435-578), from -20 to 300 s.

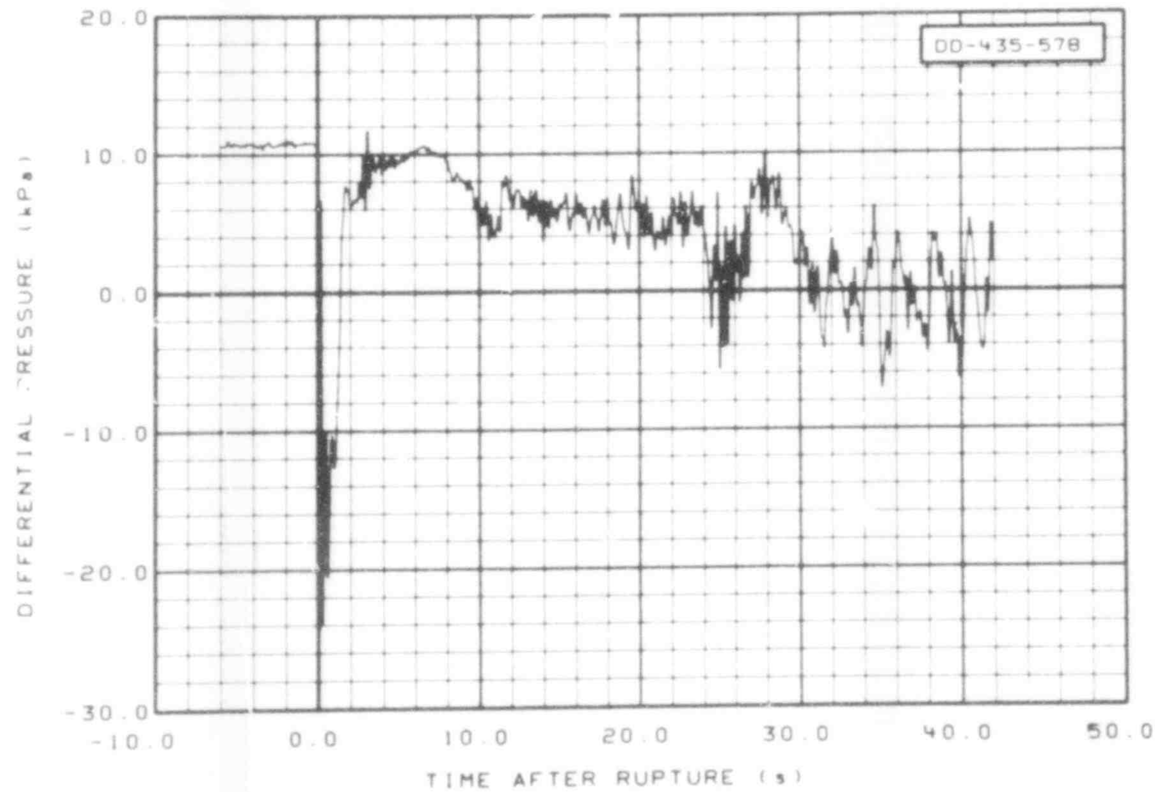

Fig. 170 Differential pressure in downcomer (DD-435-578), from -6 to 42 s.

507 177

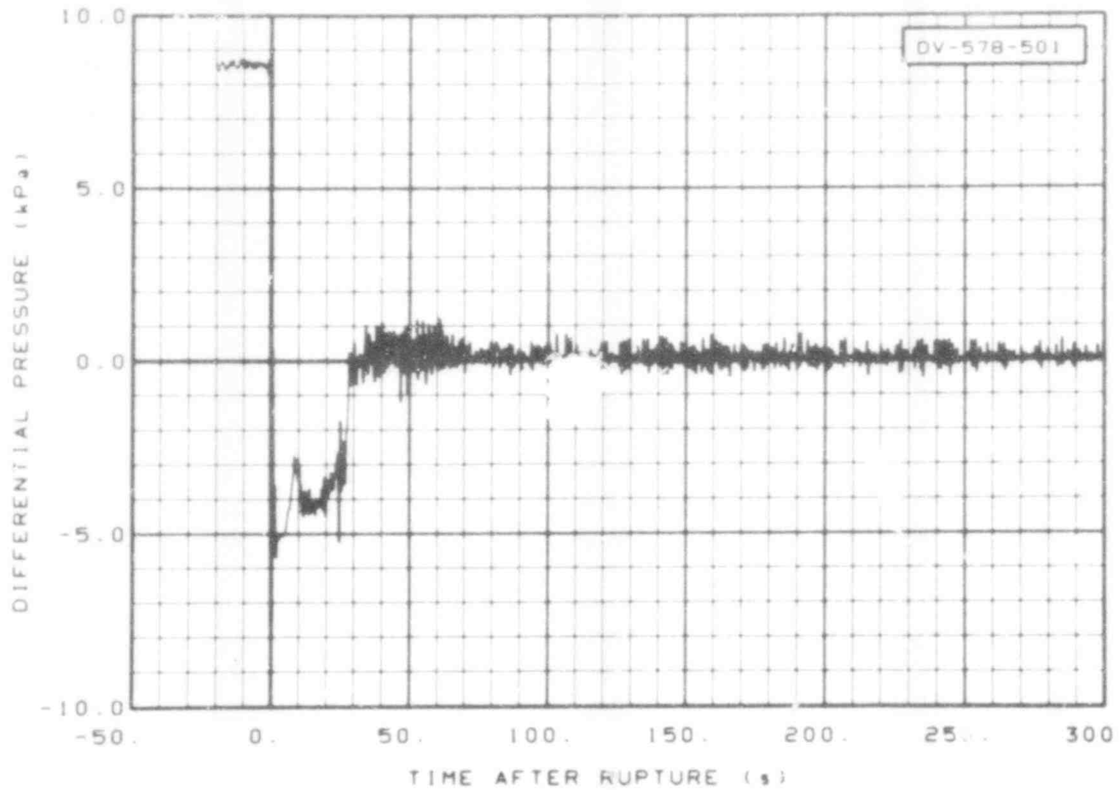

Fig. 171 Differential pressure in vessel (DV-578-501), from -20 to 300 s.

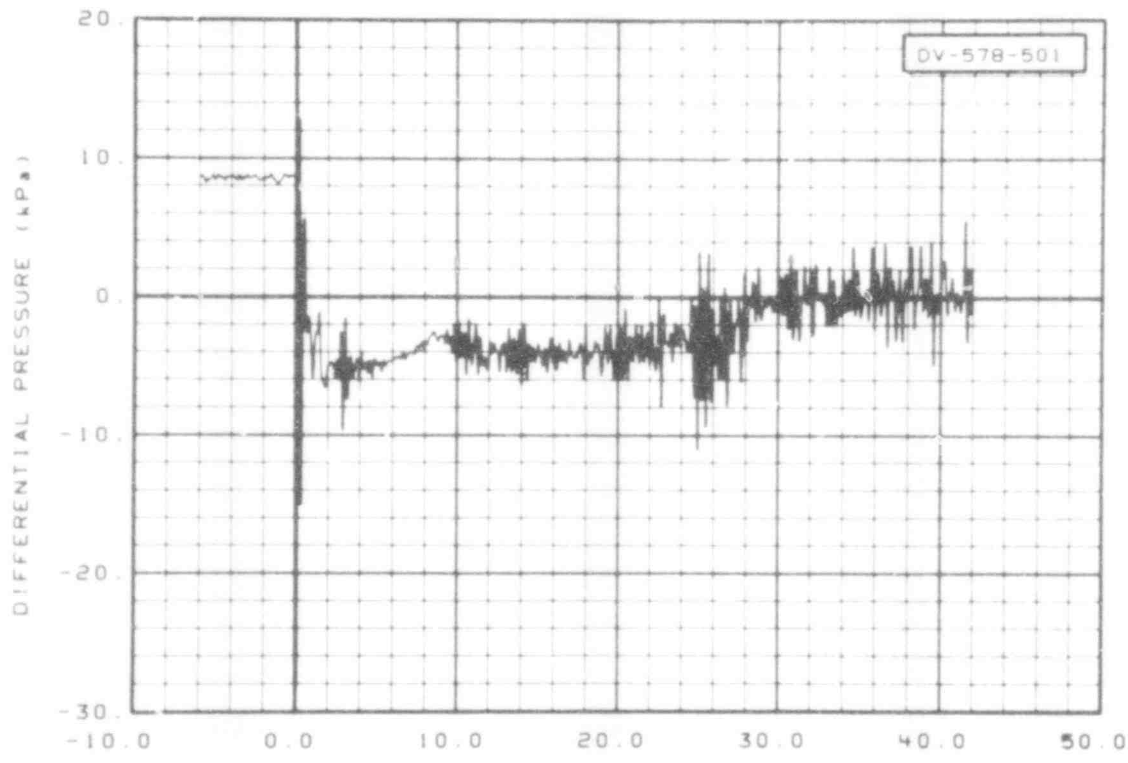

Fig. 172 Differential pressure in vessel (DV-578-501), from -6 to 42 s.

507 178

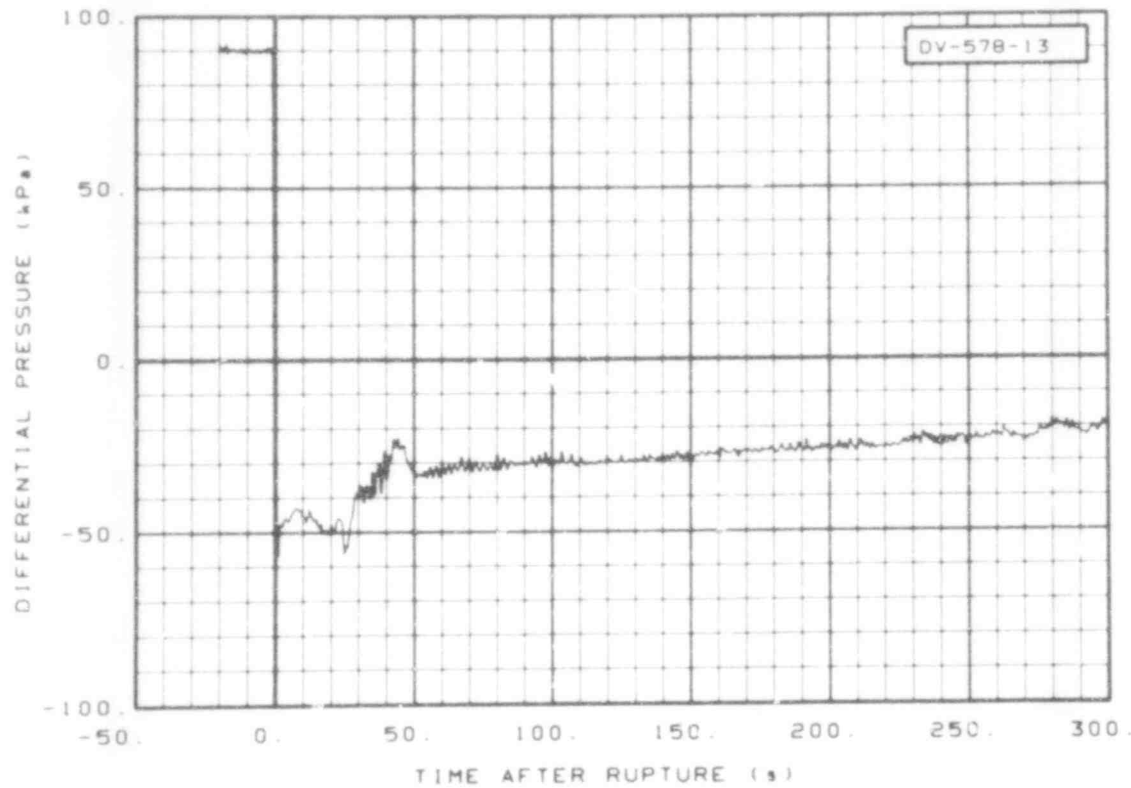

Fig. 173 Differential pressure in vessel (DV-578-13), from -20 to 300 s.

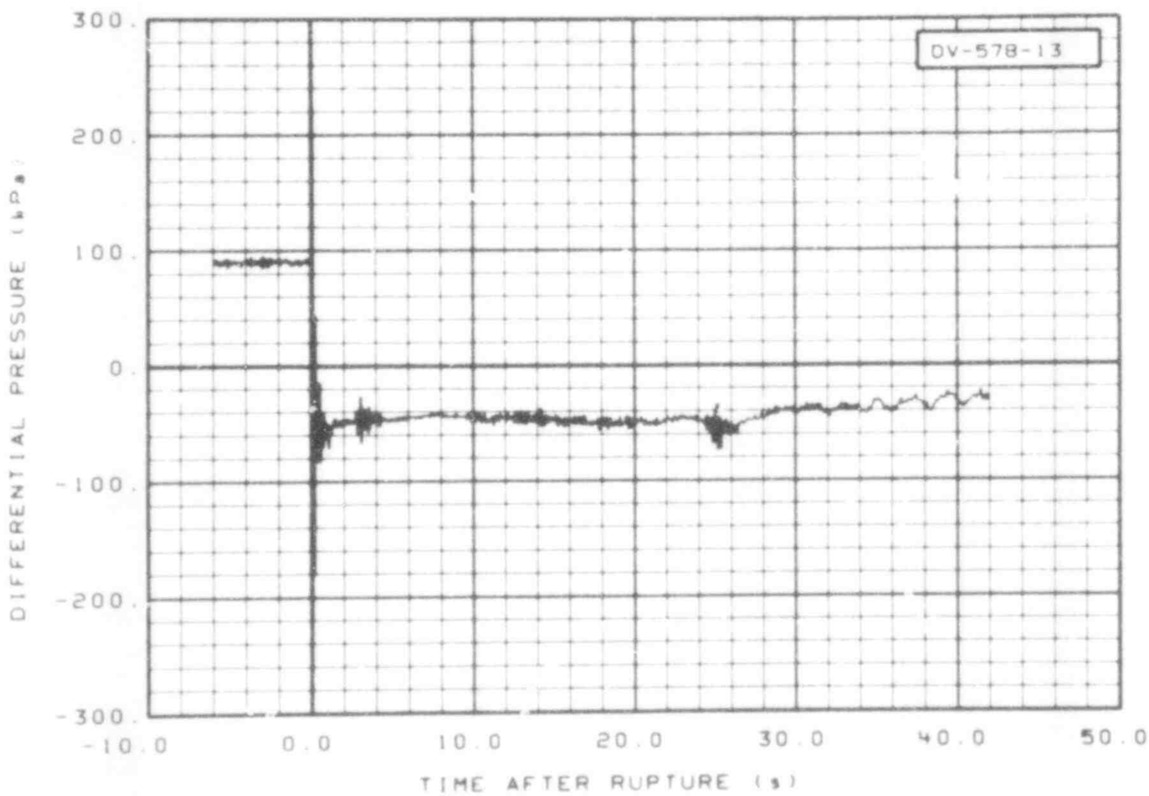

Fig. 174 Differential pressure in vessel (DV-578-13), from -6 to 42 s.

507 179

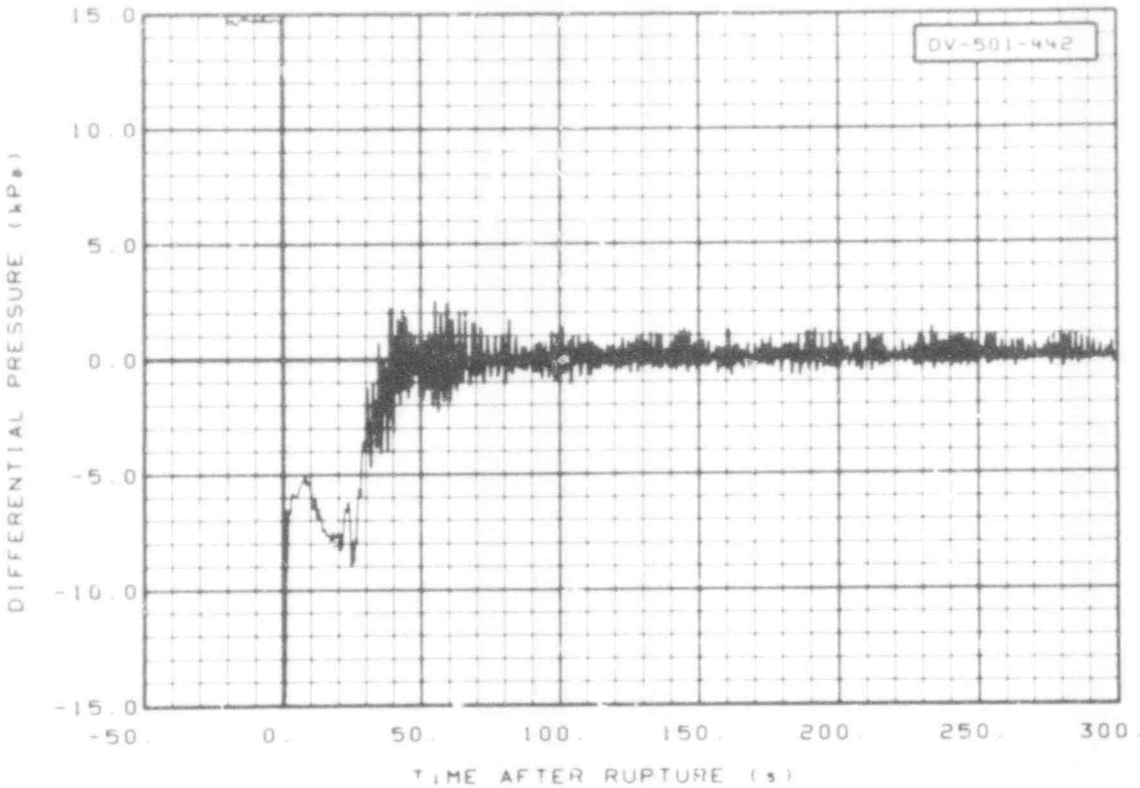

Fig. 175 Differential pressure in vessel (DV-501-442), from -20 to 300 s.

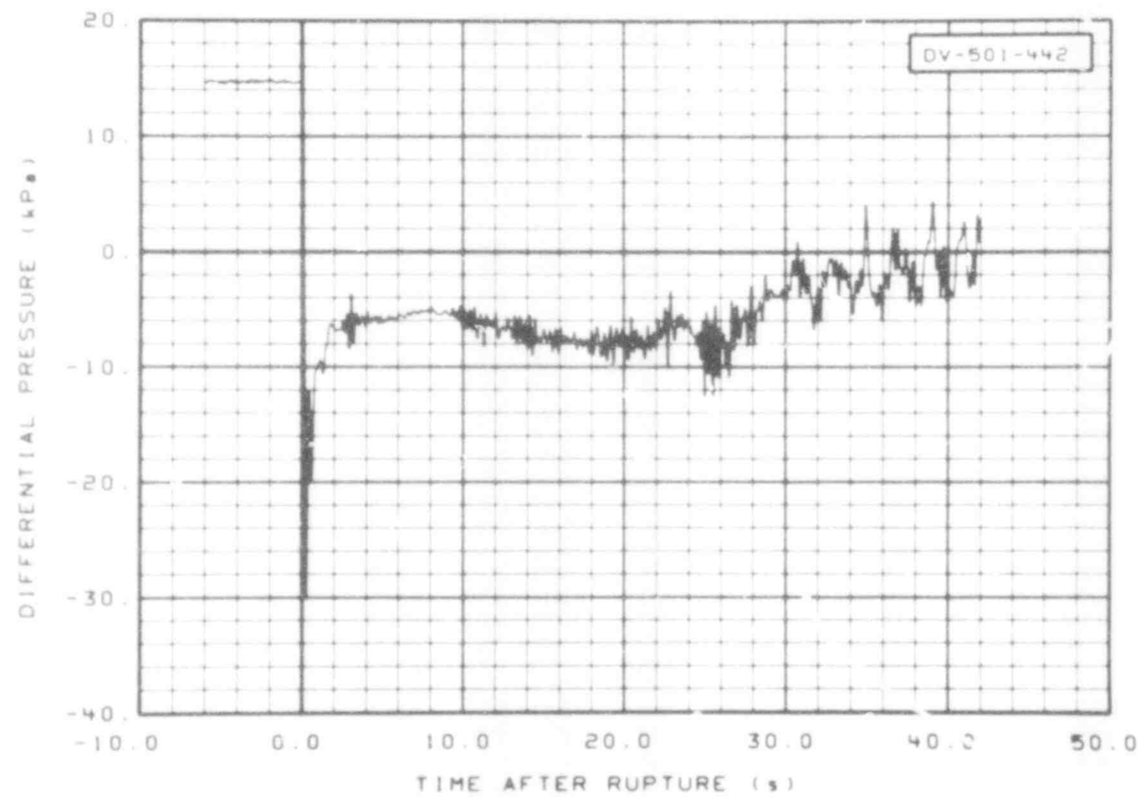

Fig. 176 Differential pressure in vessel (DV-501-442), from -6 to 42 s.

507 180

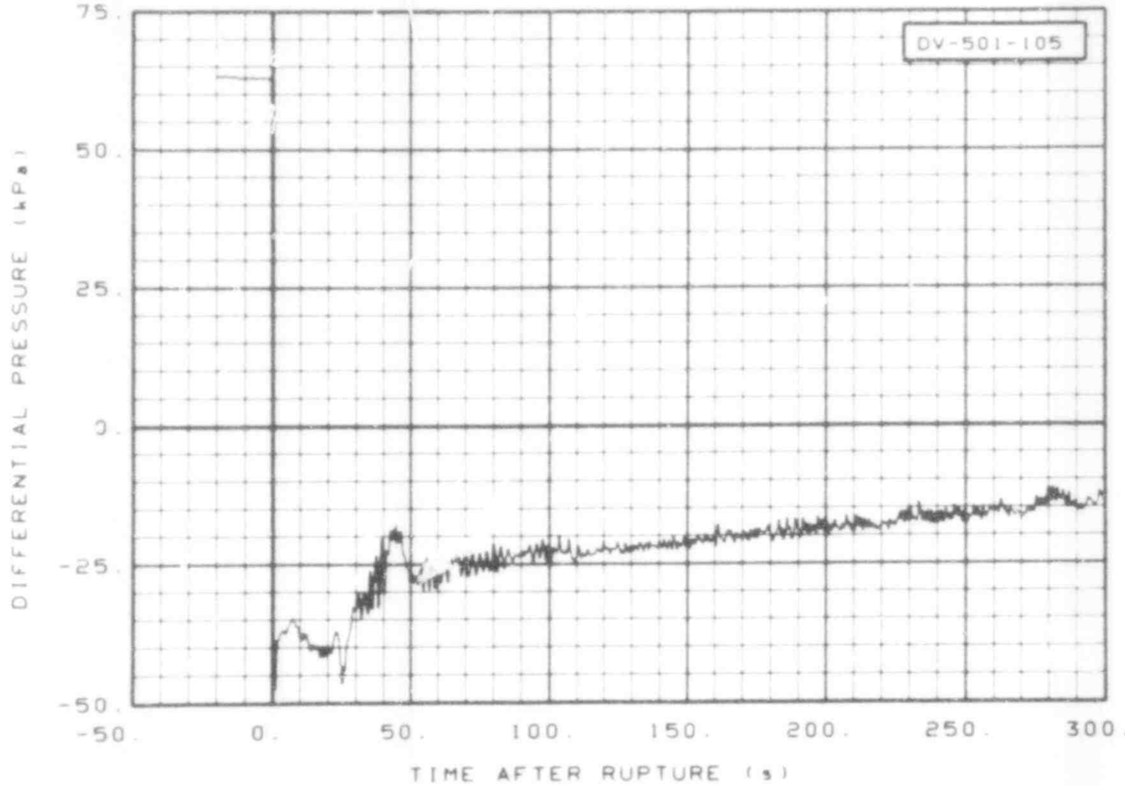

Fig. 177 Di.ferential pressure in vessel (DV-501-105), from -20 to 300 s.

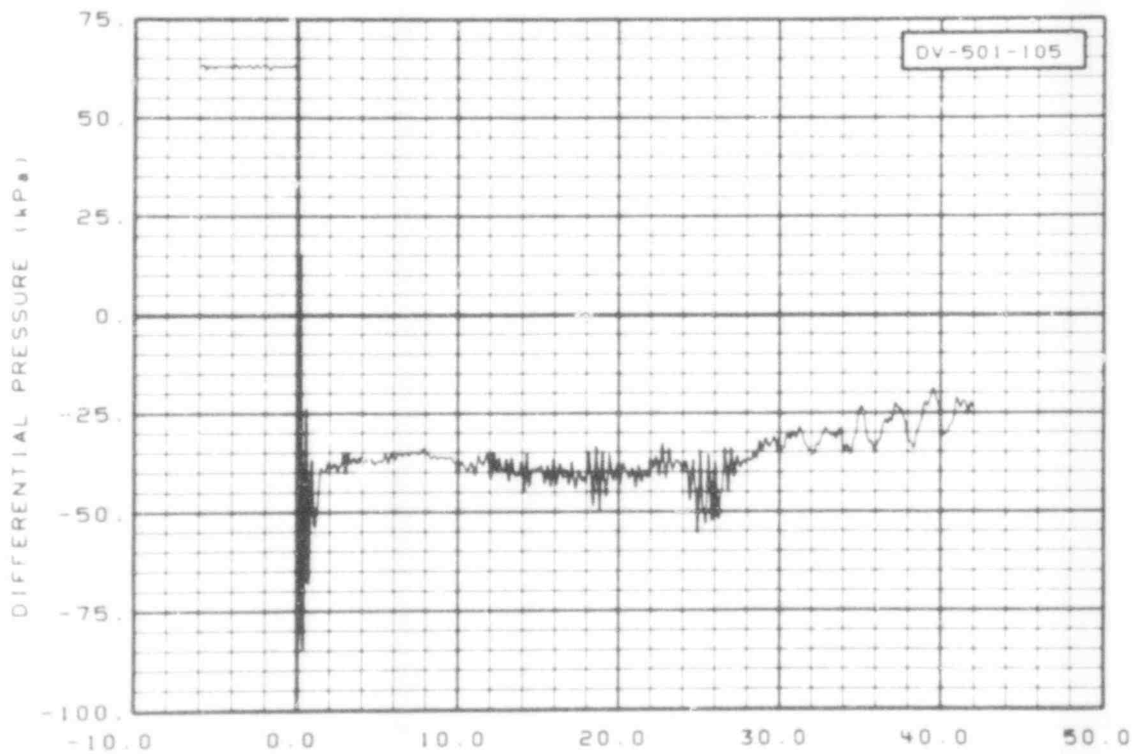

Fig. 178 Differential pressure in vessel (DV-501-105), from -6 to 42 s.

507 181

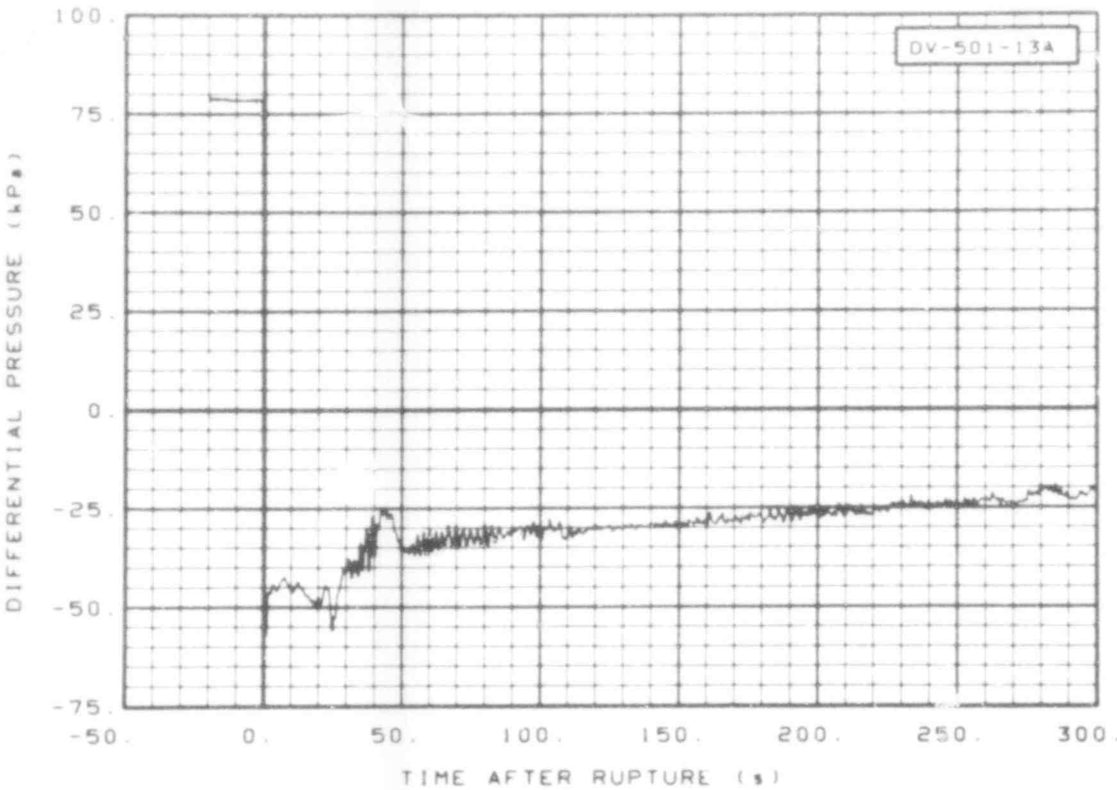

Fig. 179 Differential pressure in vessel (DV-501-13A) from -20 to 300 s.

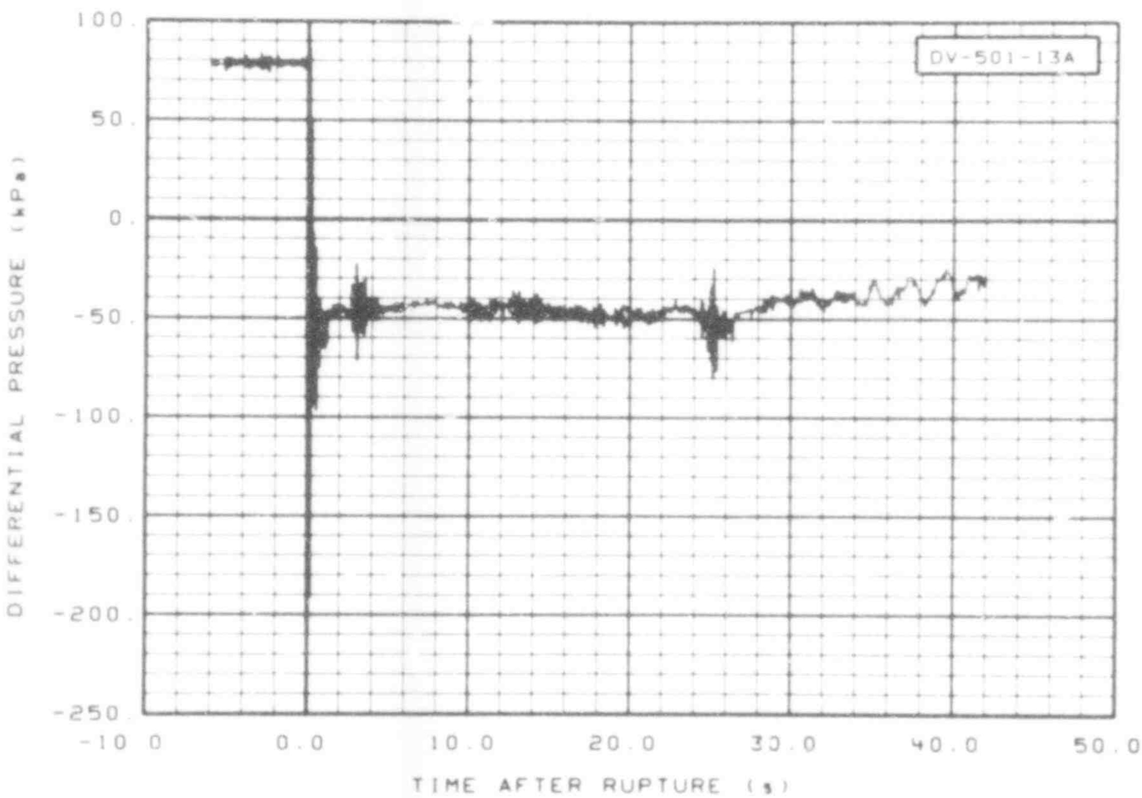

Fig. 180 Differential pressure in vessel (DV-501-13A), from -6 to 42 s.

507 182

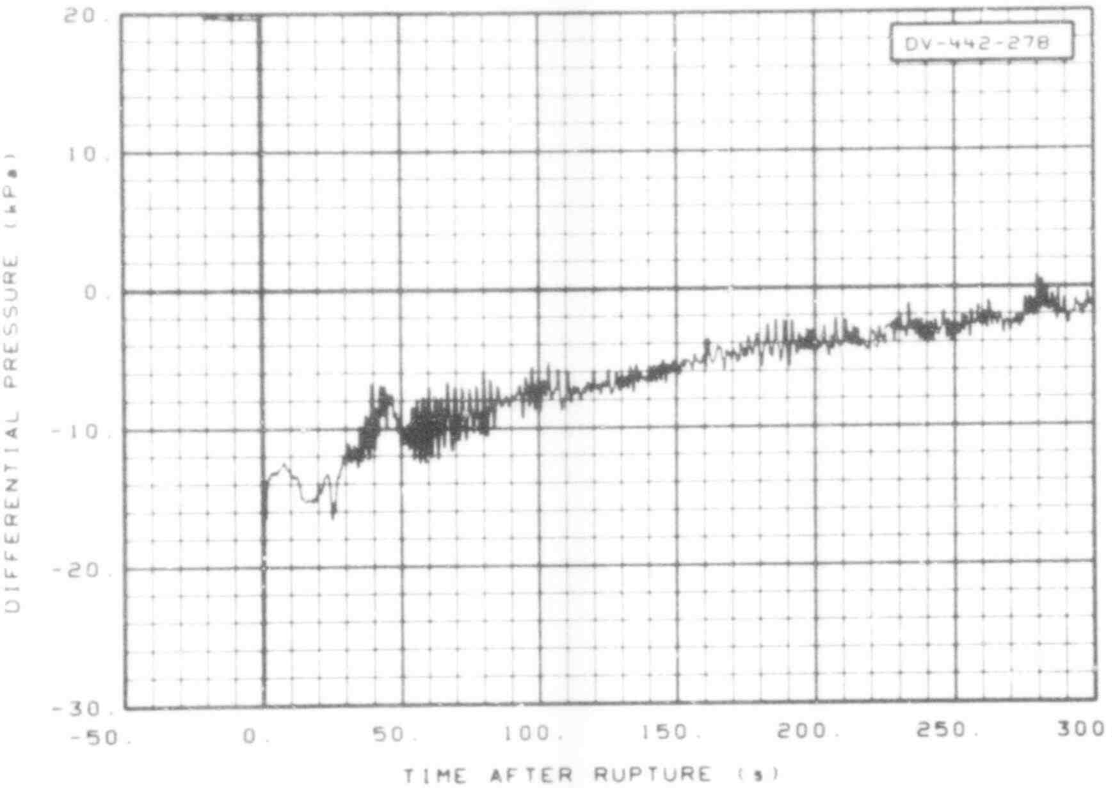

Fig. 181 Differential pressure in vessel (DV-442-278), from -20 to 300 s.

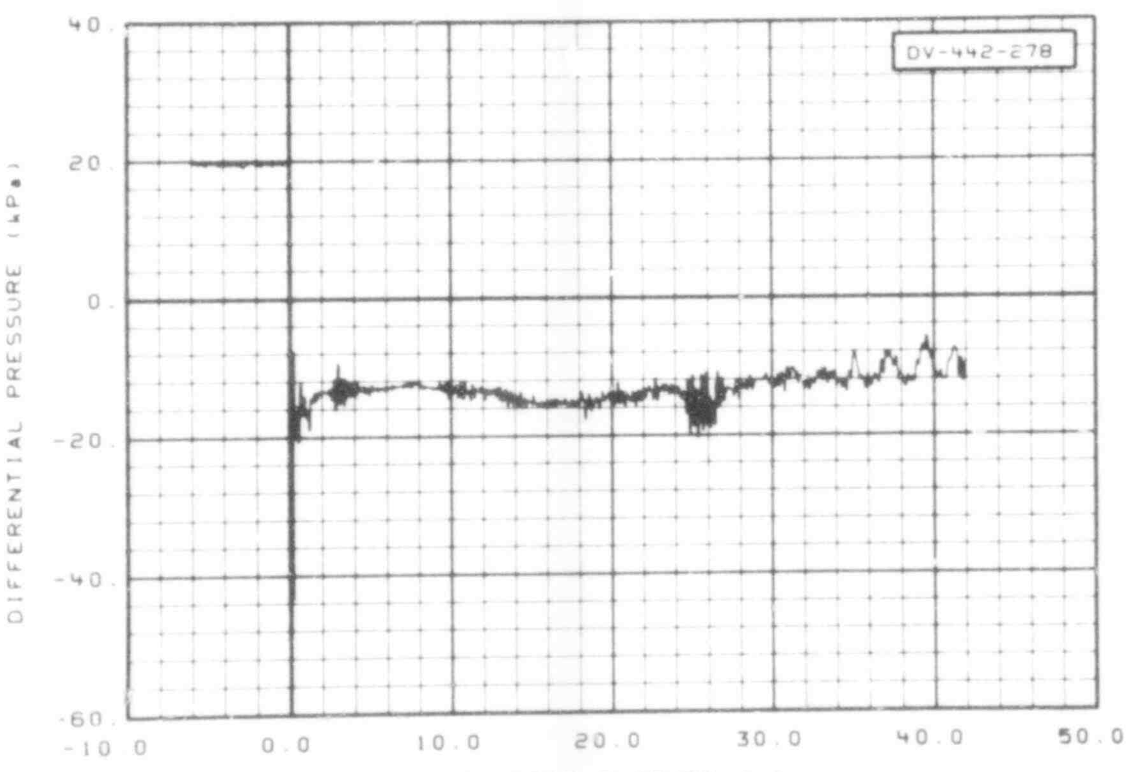

Fig. 182 Differential pressure in vessel (DV-442-278), from -6 to 42 s.

507 183

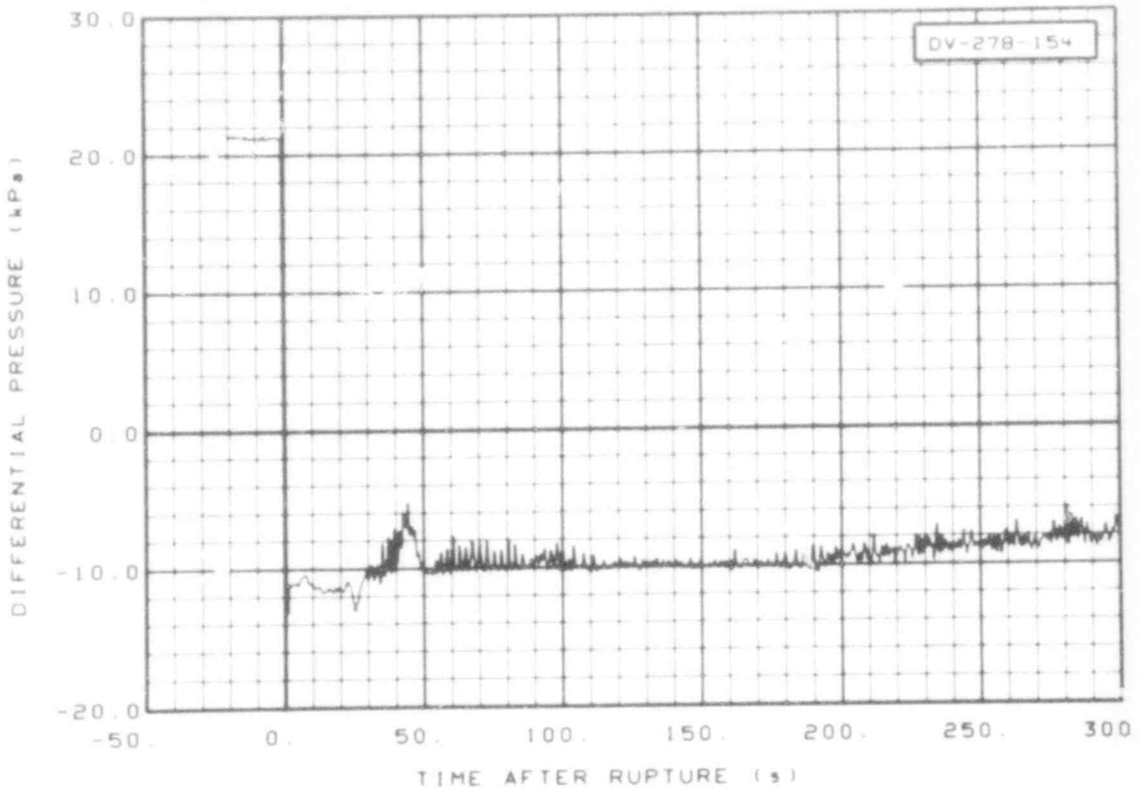

Fig. 183 Differential pressure in vessel (DV-278-154), from -20 to 300 s.

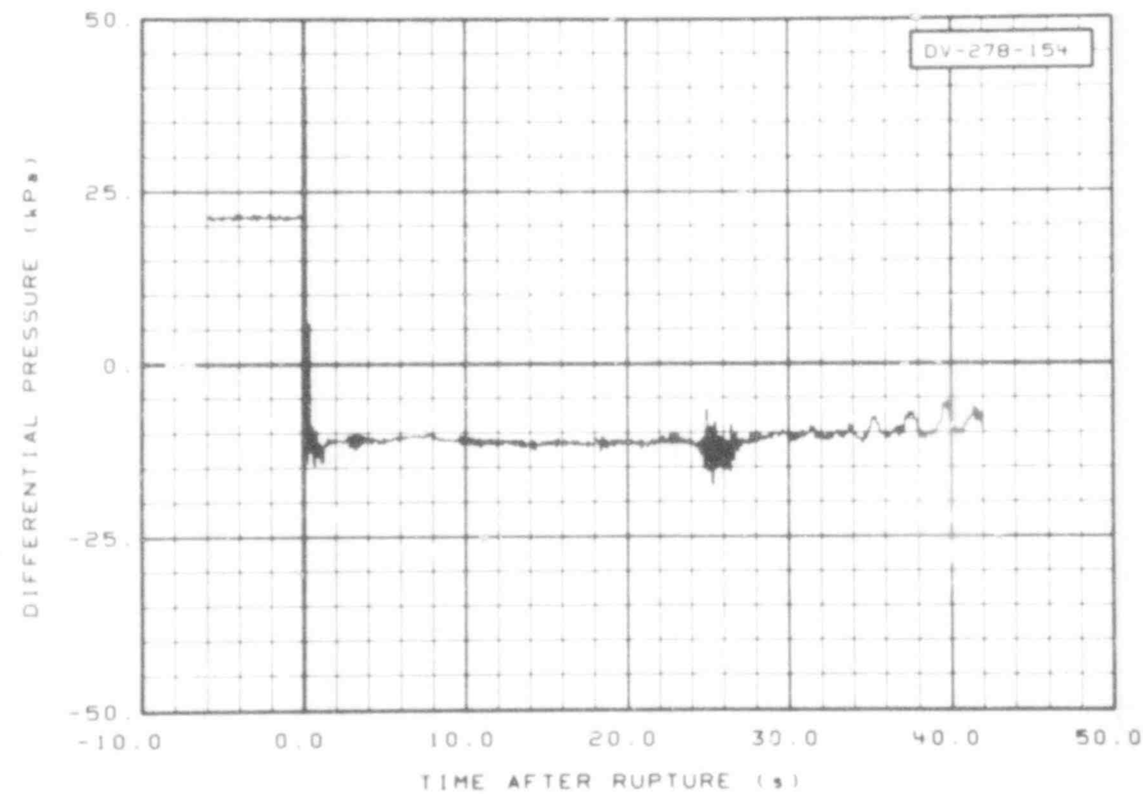

Fig. 184 Differential pressure in vessel (DV-278-154), from -6 to 42 s.

507 184

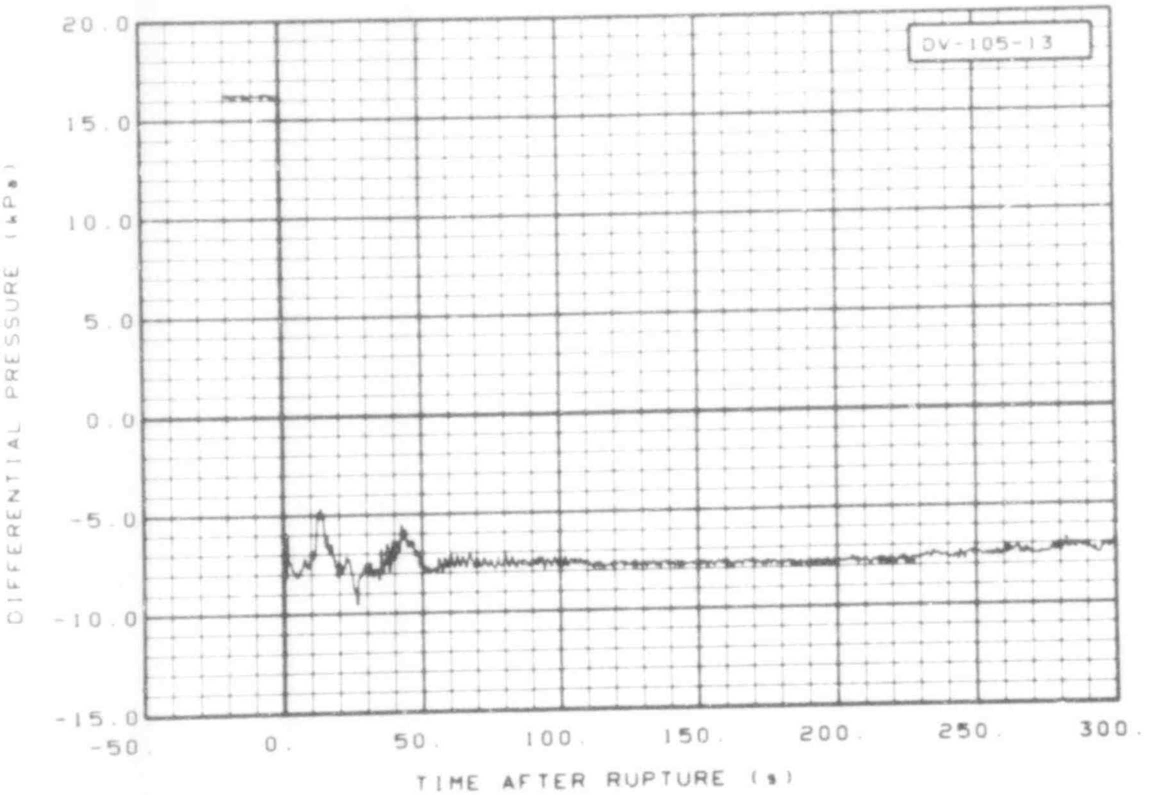

Fig. 185 Differential pressure in vessel (DV-105-13), from -20 to 300 s.

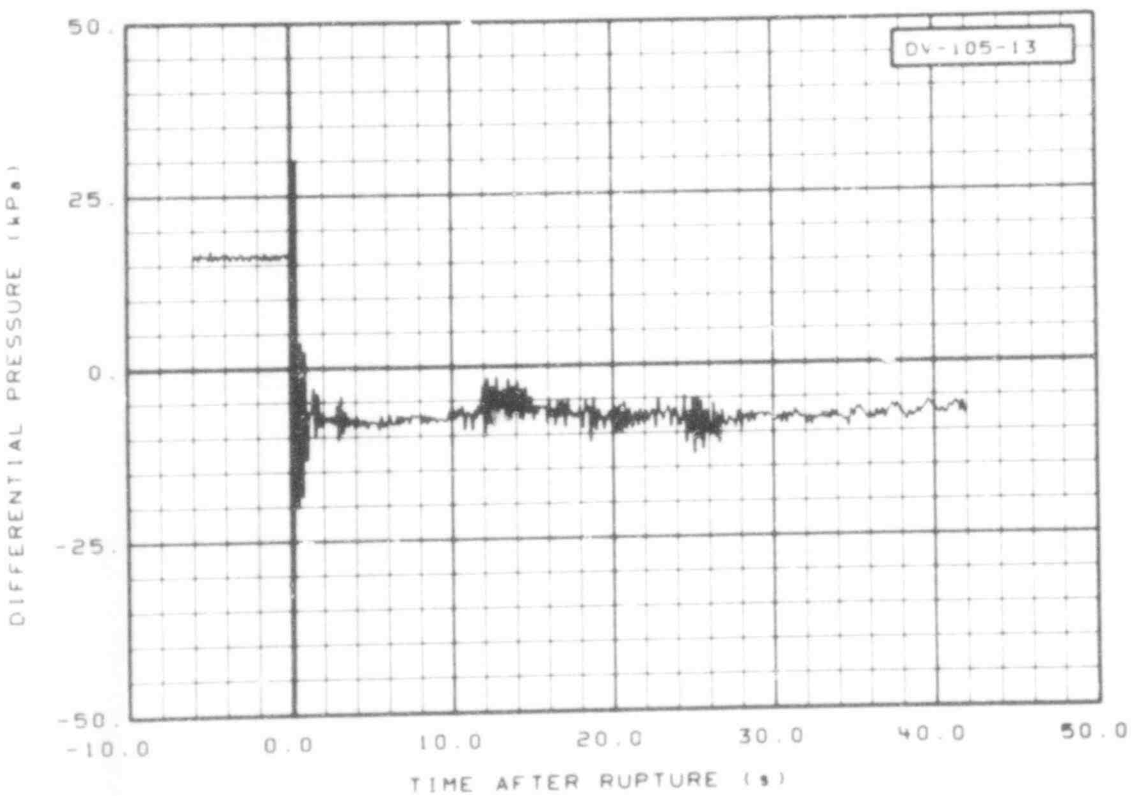

Fig. 186 Differential pressure in vessel (DV-105-13), from -6 to 42 s.

507 185

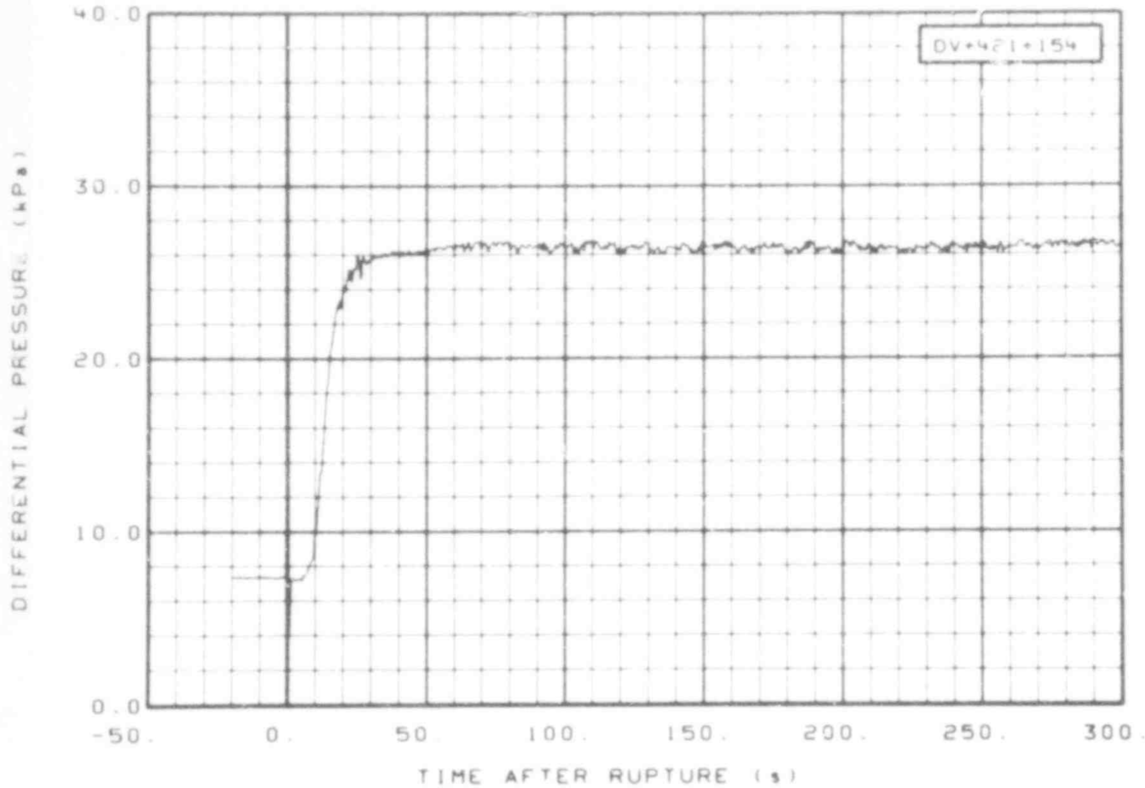

Fig. 187 Differential pressure in vessel (DV + 421 + 154), from -20 to 300 s.

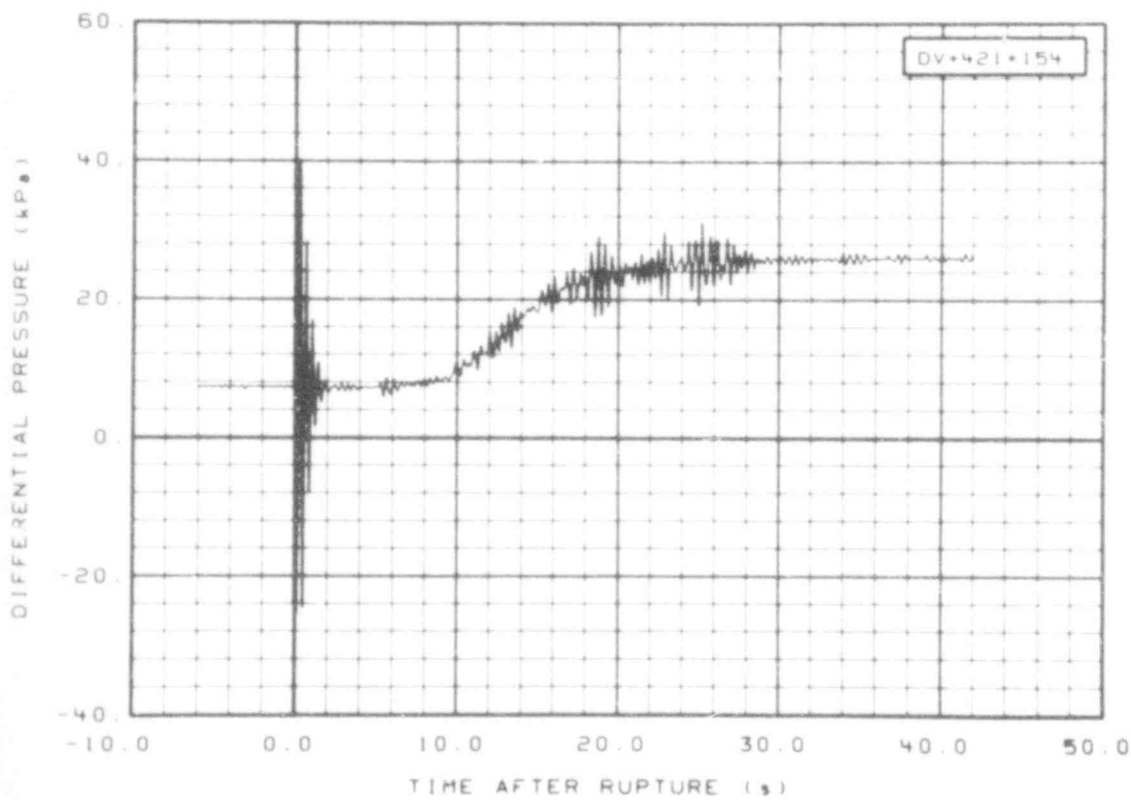

Fig. 188 Differential pressure in vessel (DV + 421 + 154), from -6 to 42 s.

507 186

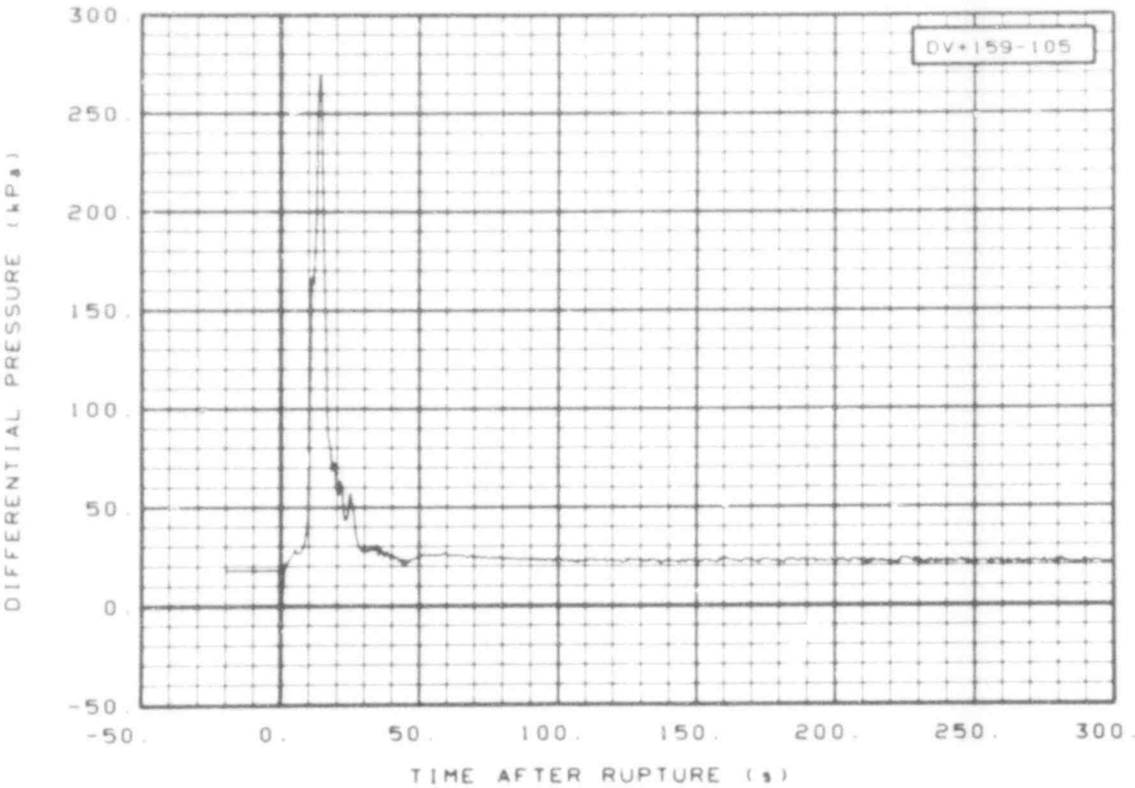

Fig. 189 Differential pressure in vessel (DV + 159-105), from -20 to 360 s.

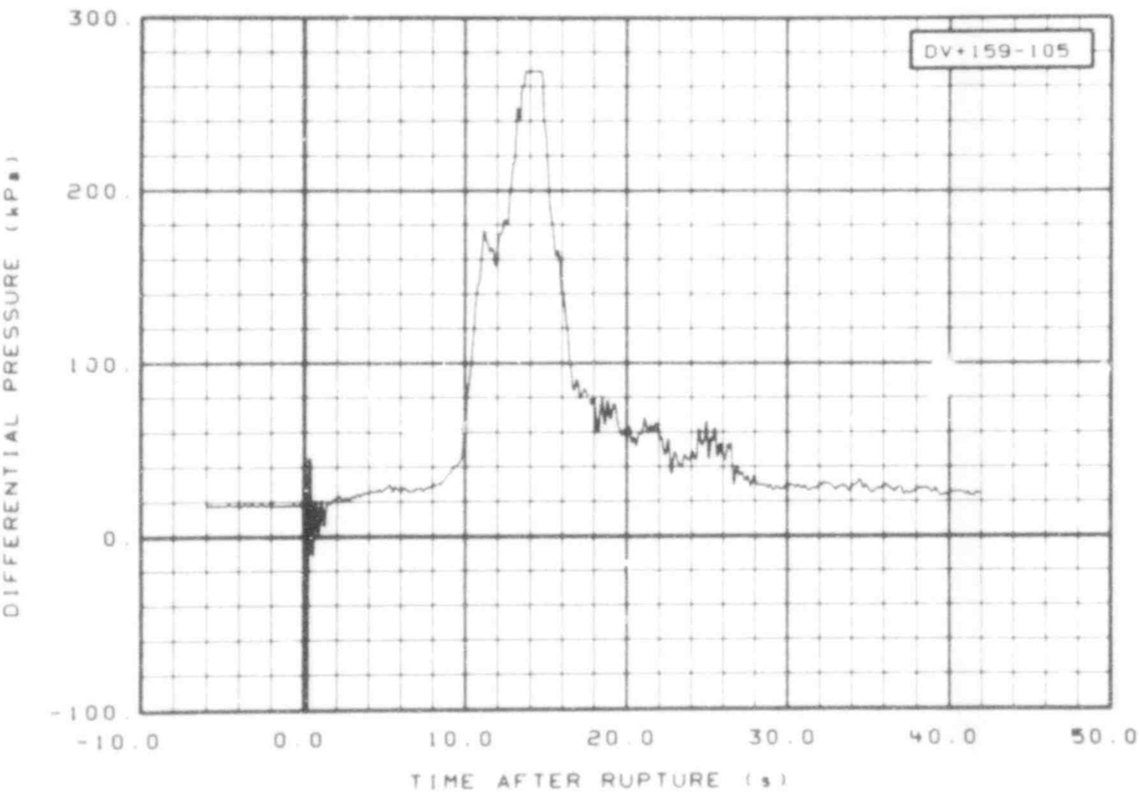

Fig. 190 Differential pressure in vessel (DV + 159-105), from -6 to 42 s.

507 187

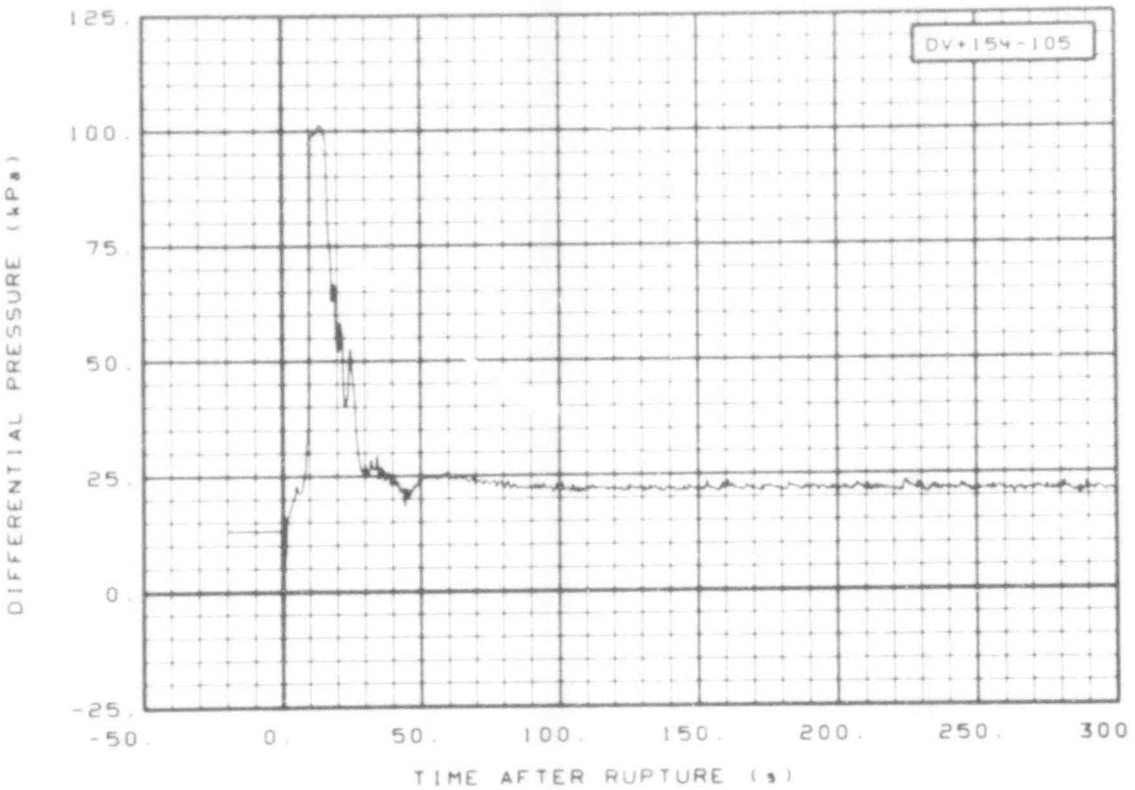

Fig. 191 Differential pressure in vessel (DV + 154-105), from -20 to 300 s.

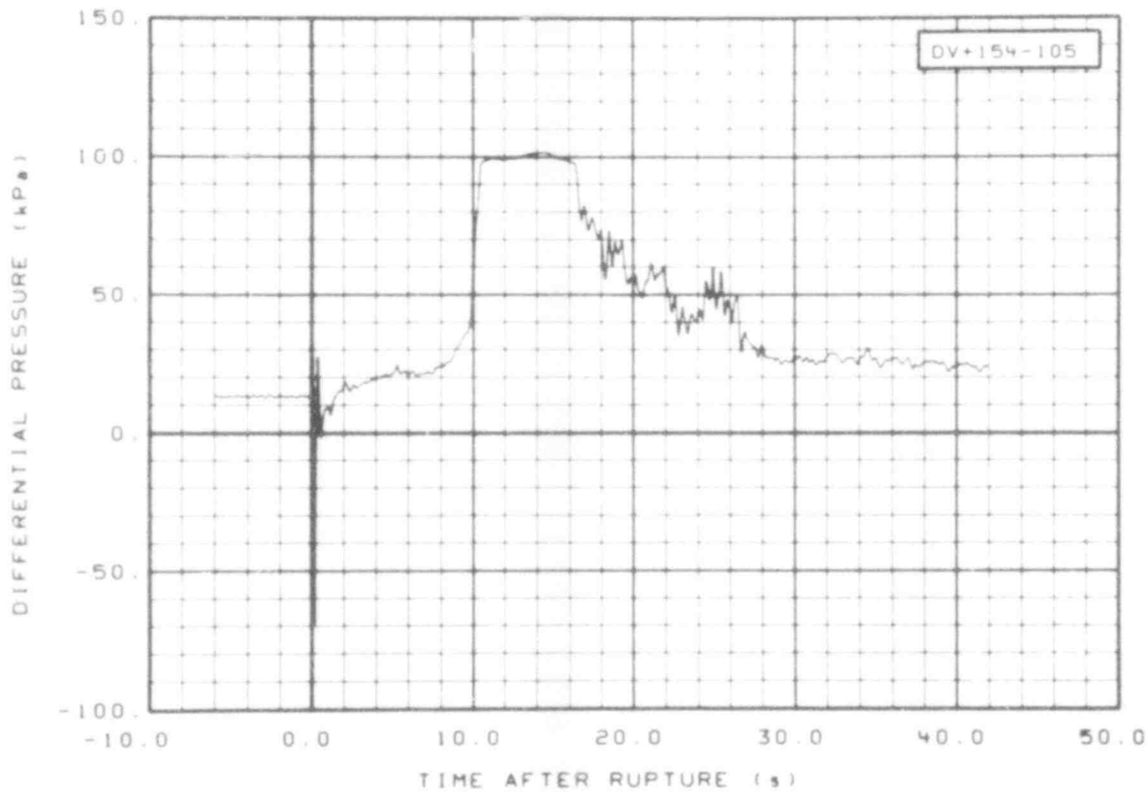

Fig. 192 Differential pressure in vessel (DV + 154-105), from -6 to 42 s.

507 188

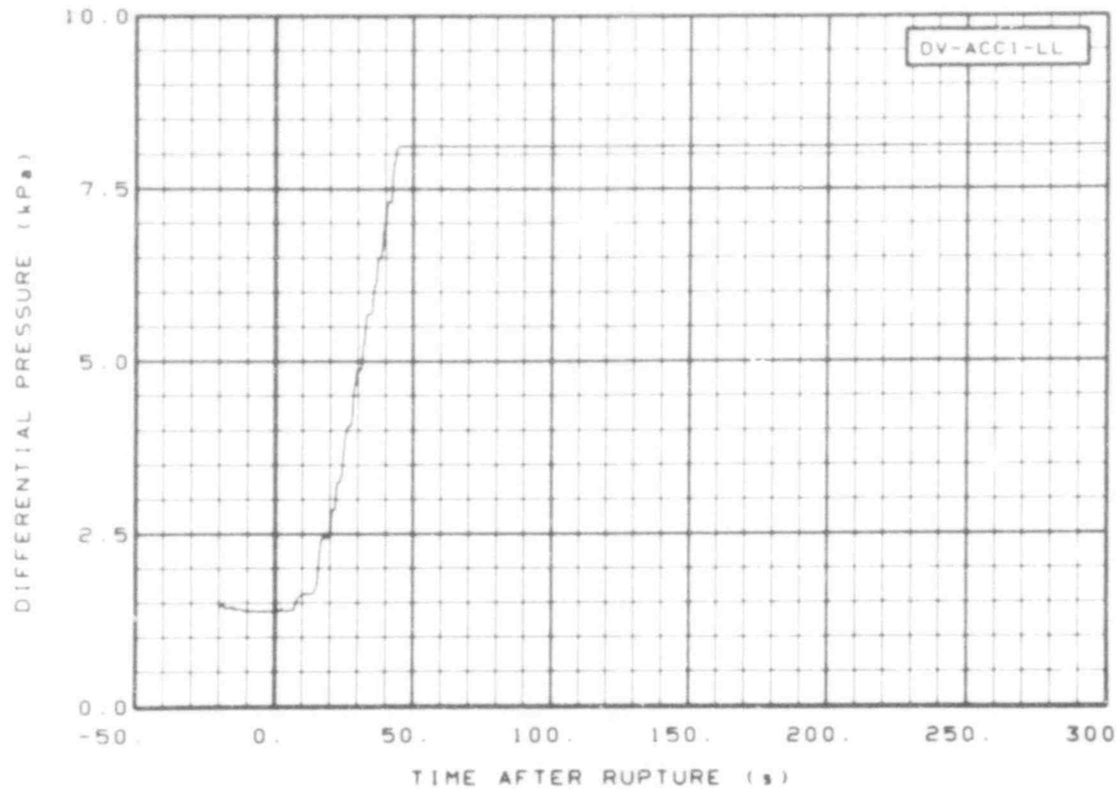

Fig. 193 Differential pressure in vessel ECC accumulator (DV-ACC1-LL), from -20 to 300 s.

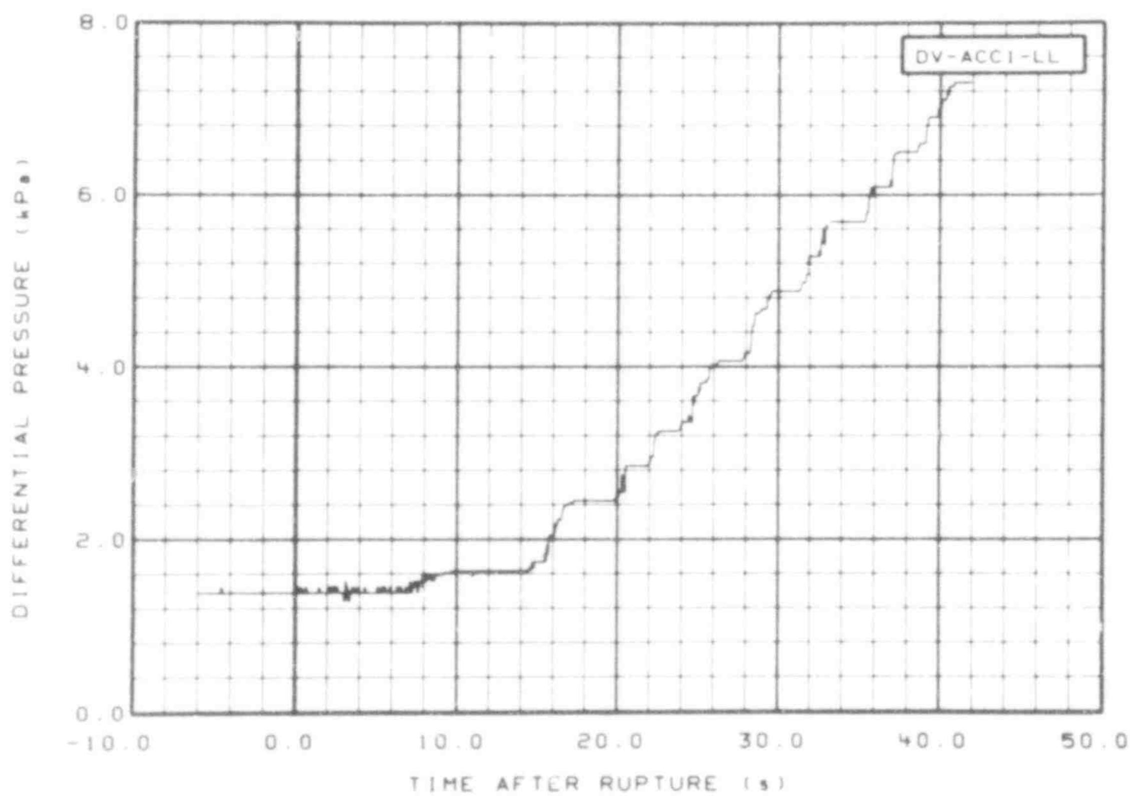

Fig. 194 Differential pressure in vessel ECC accumulator (DV-ACC1-LL), from -6 to 42 s.

507 189

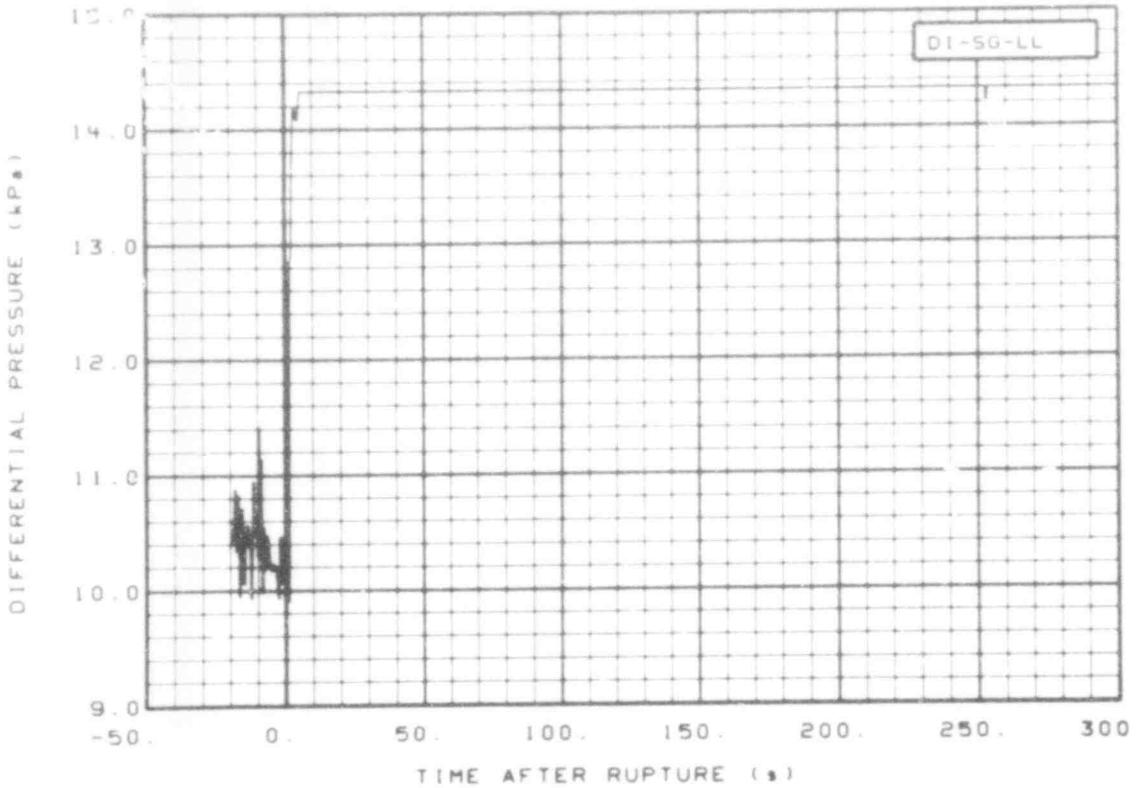

Fig. 195 Differential pressure in intact loop steam generator, secondary side liquid level (DI-SG-LL), from -20 to 300 s.

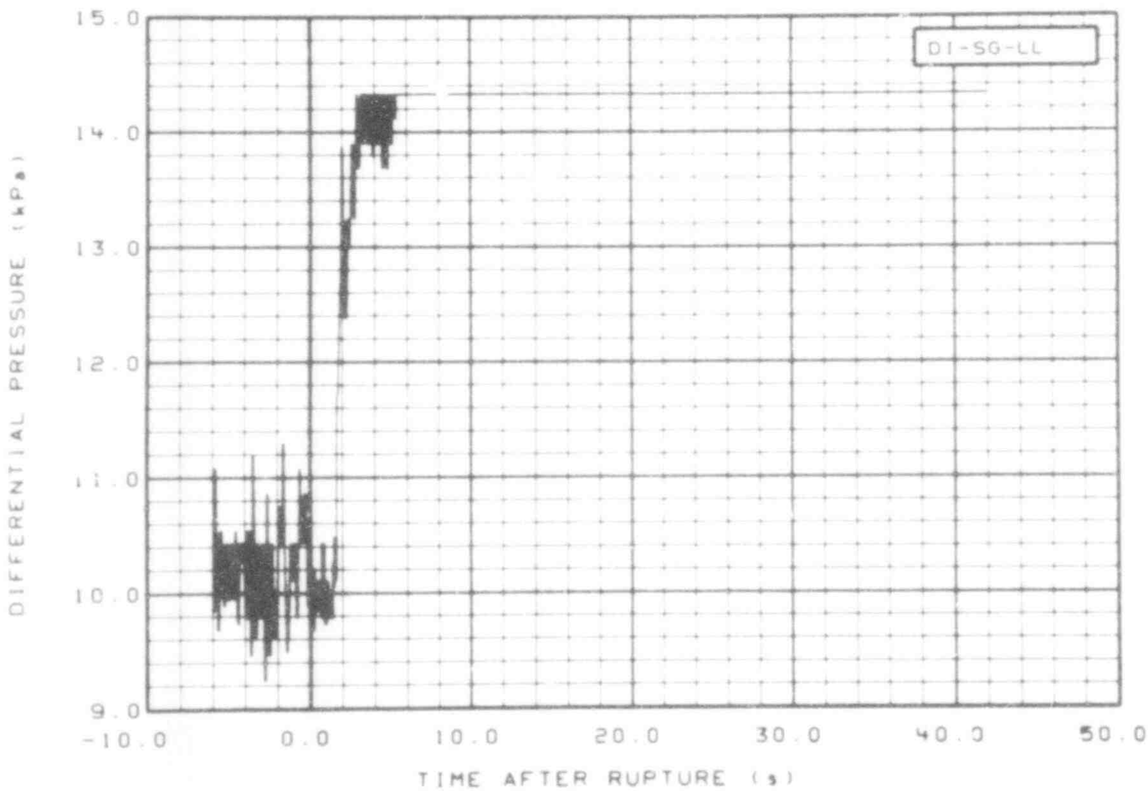

Fig. 196 Differential pressure in intact loop steam generator, secondary side liquid level (DI-SG-LL), from -6 to 42 s.

507 190

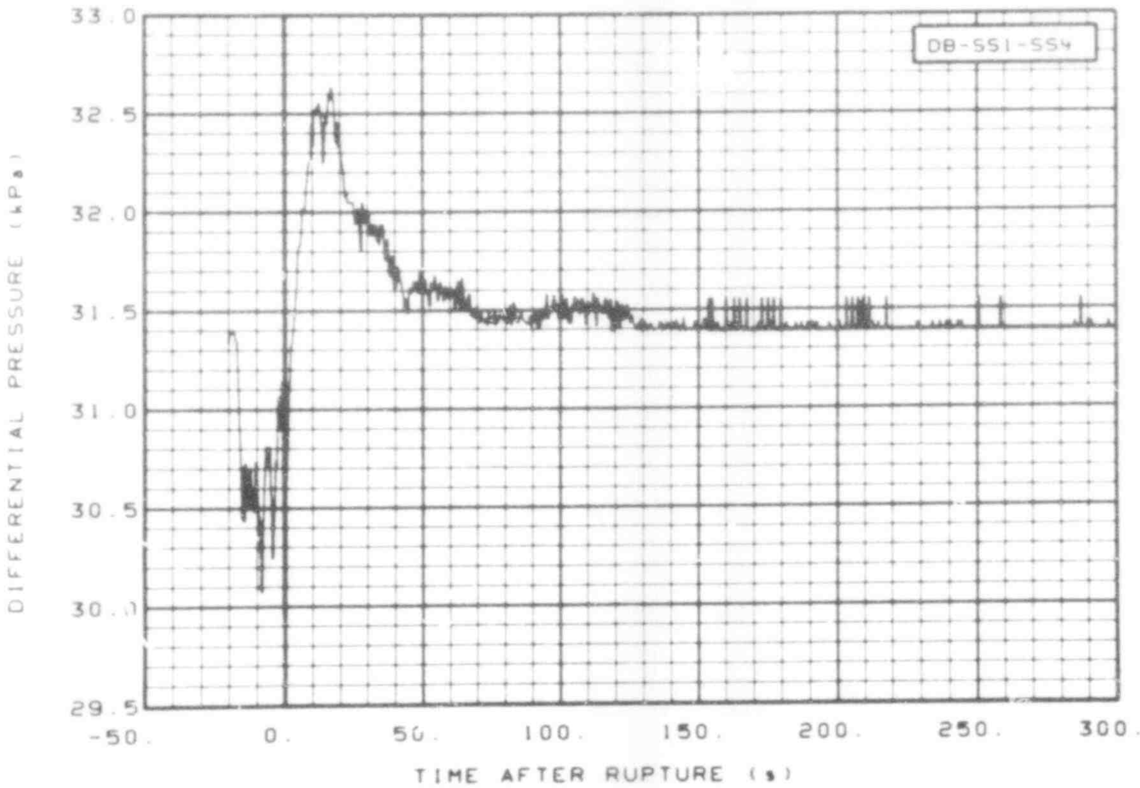

Fig. 197 Differential pressure in broken loop steam generator, secondary liquid level (DB-SS1-SS4), from -20 to 300 s.

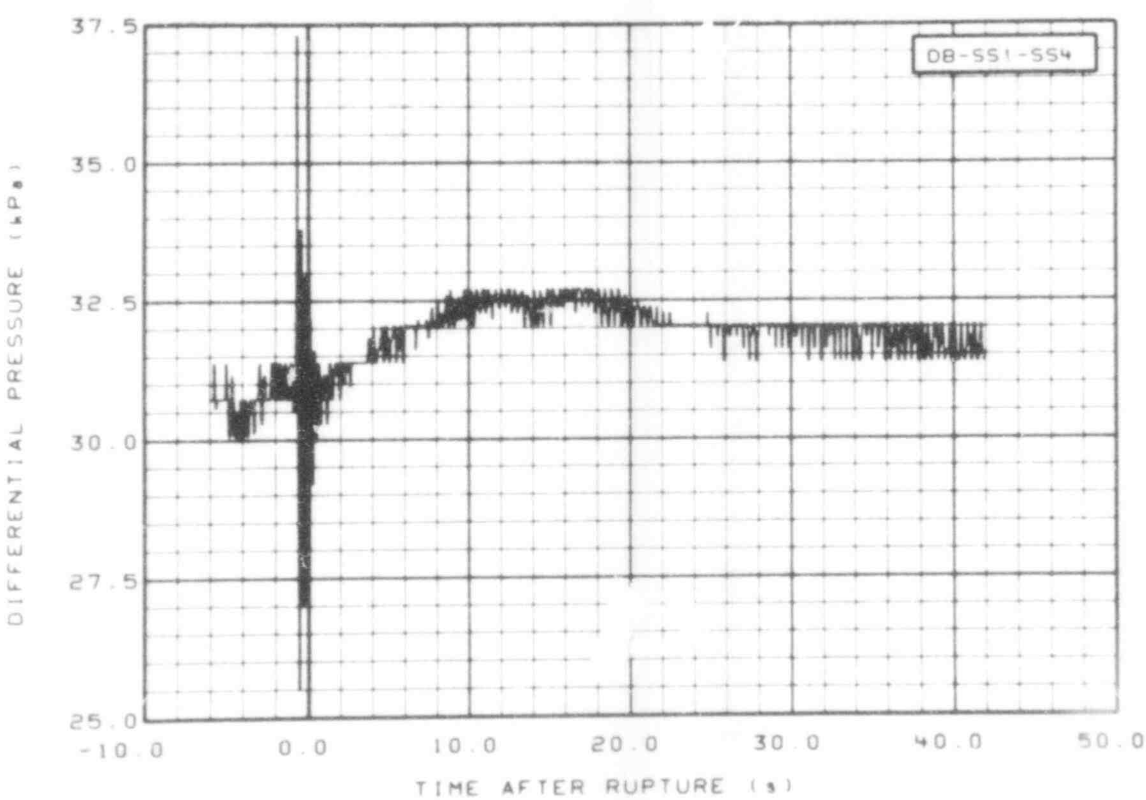

Fig. 198 Differential pressure in broken loop steam generator, secondary liquid level (DB-SS1-SS4), from -6 to 42 s.

507 191

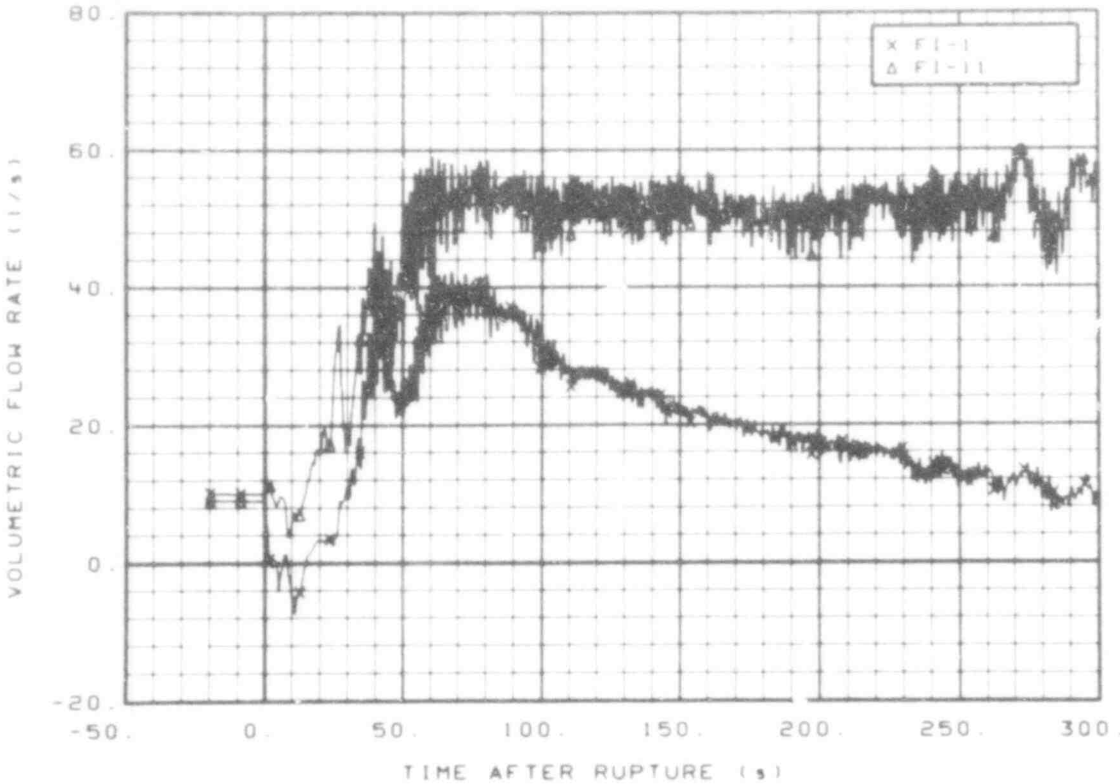

Fig. 199 Volumetric flow in intact loop (FI-1 and FI-11), from -20 to 300 s.

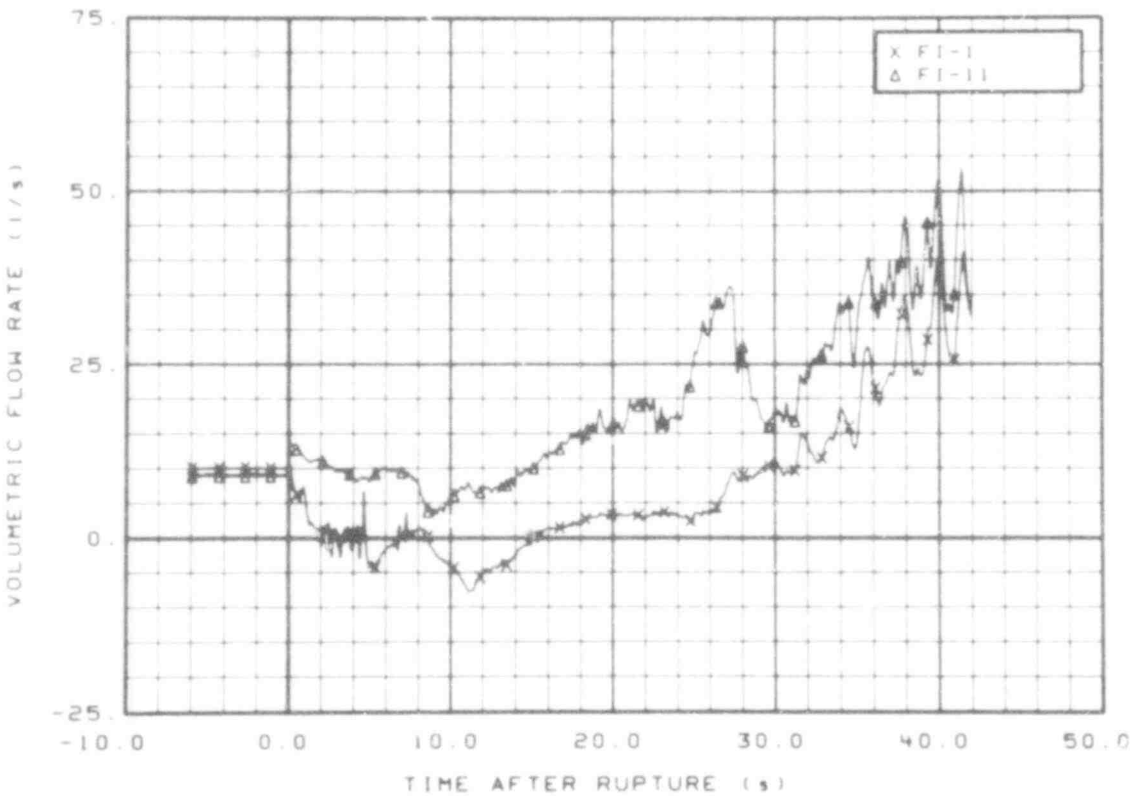

Fig. 200 Volumetric flow in intact loop (FI-1 and FI-11), from -6 to 42 s.

507 192

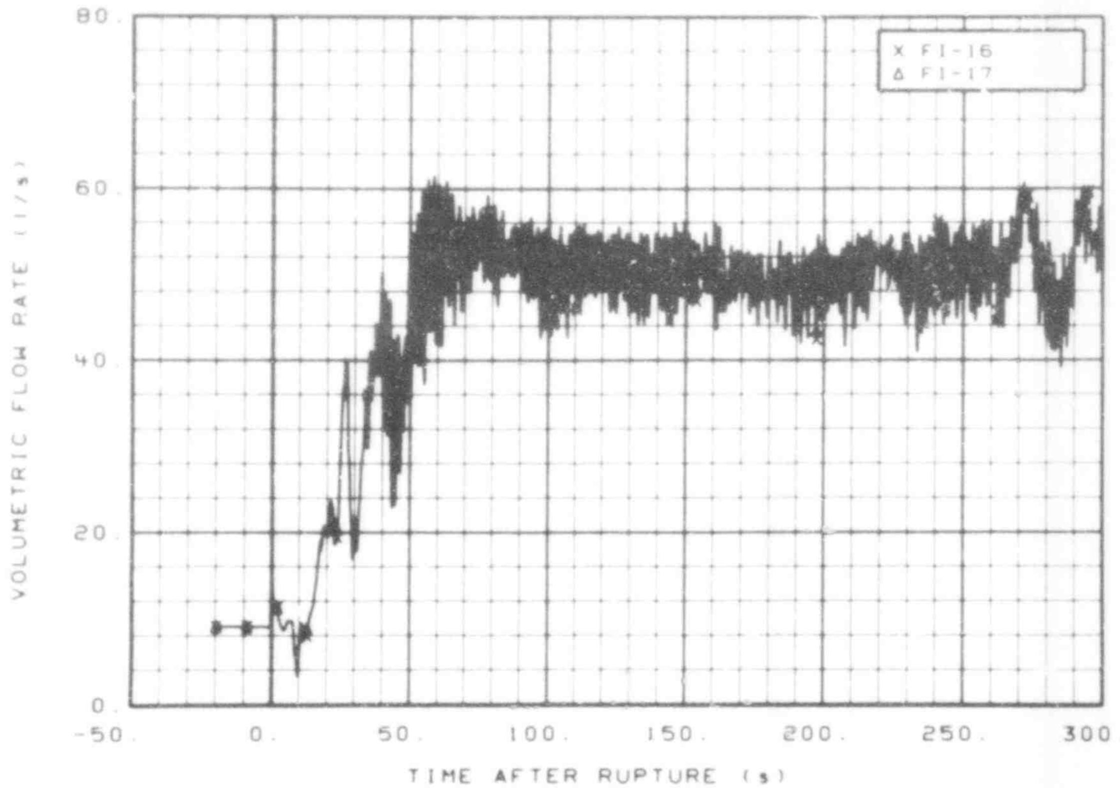

Fig. 201 Volumetric flow in intact loop (FI-16 and FI-17), from -20 to 300 s.

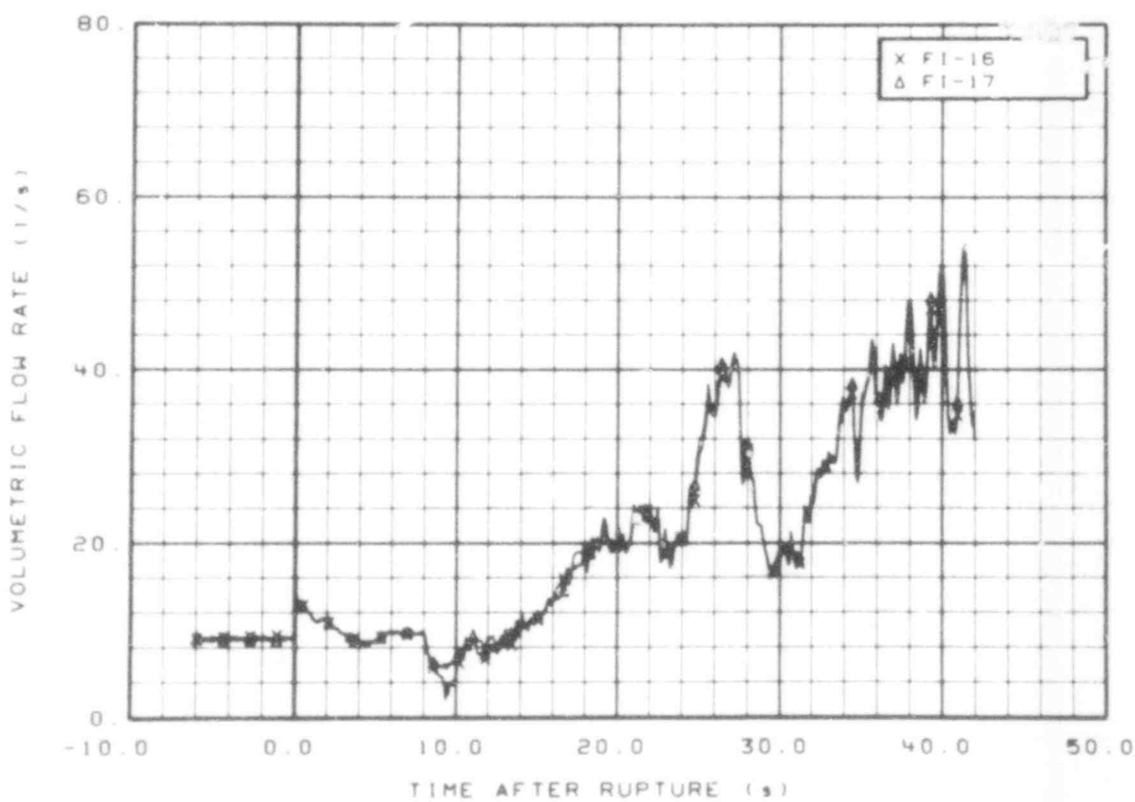

Fig. 202 Volumetric flow in intact loop (FI-16 and FI-17), from -6 to 42 s.

507 193

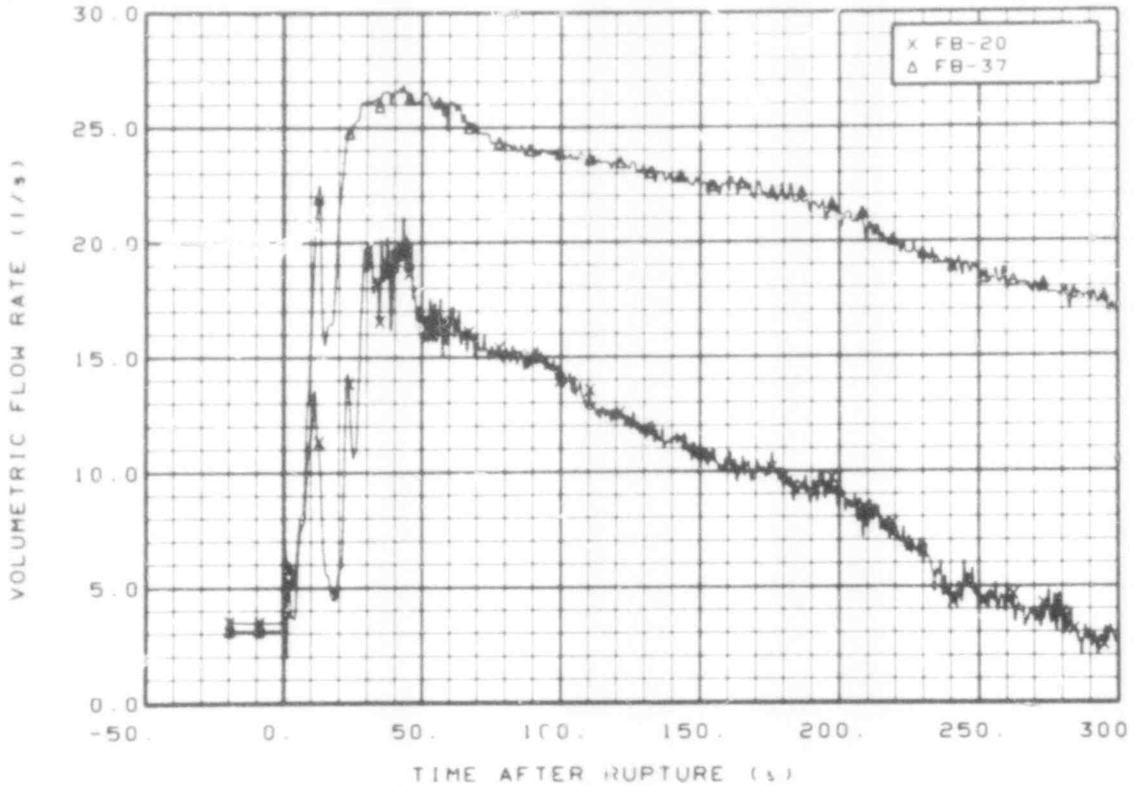

Fig. 203 Volumetric flow in broken loop (FB-20 and FB-37), from -20 to 300 s.

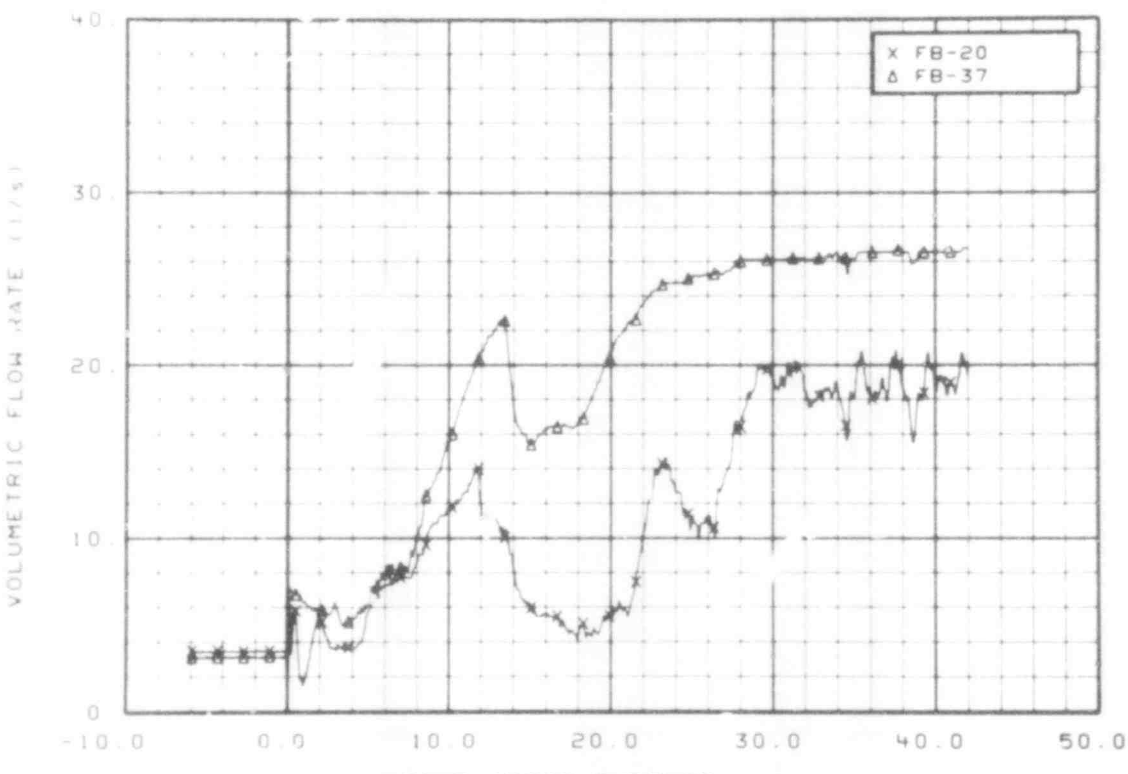

Fig. 204 Volumetric flow in broken loop (FB-20 and FB-37), from -6 to 42 s.

507 194

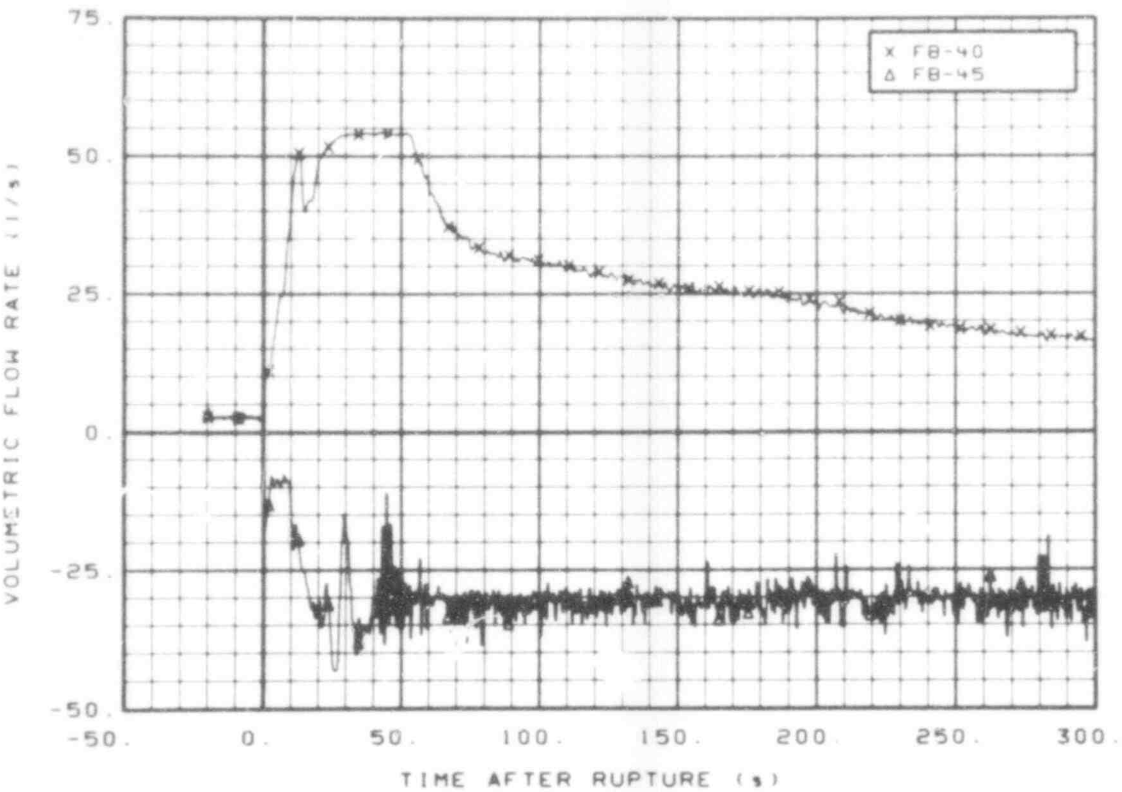

Fig. 205 Volumetric flow in broken loop (FB-40 and FB-45), from -20 to 300 s.

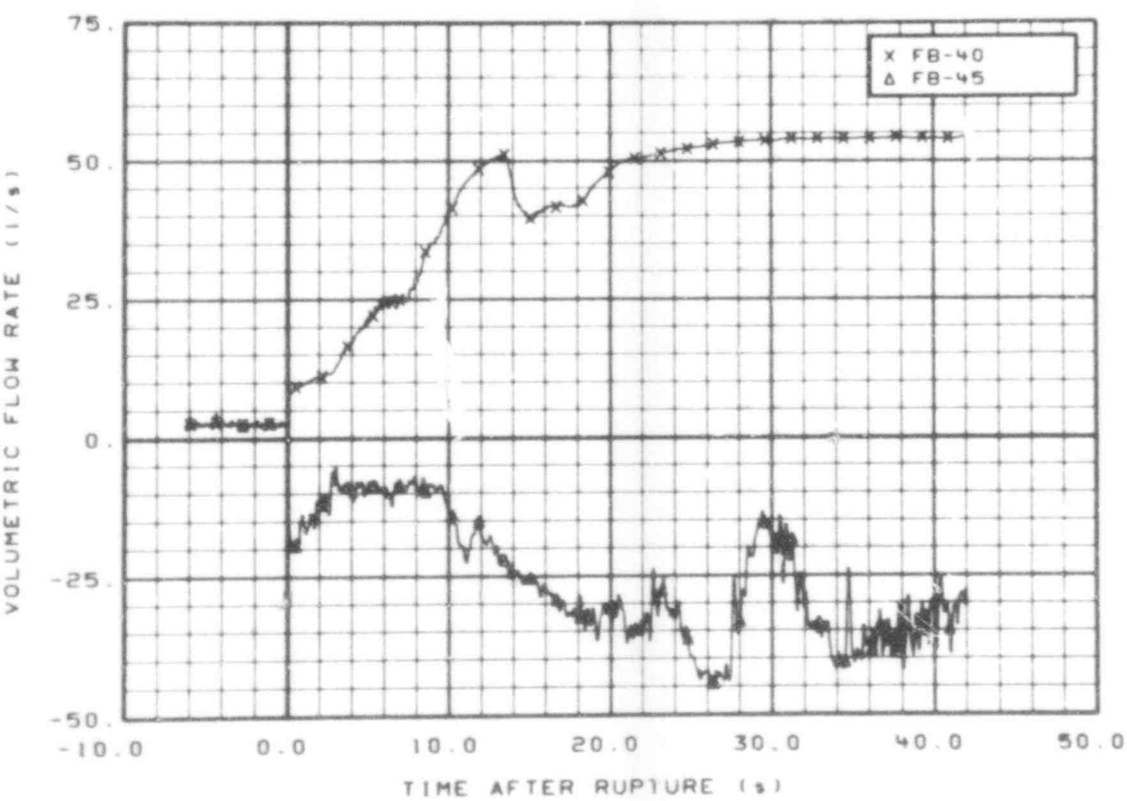

Fig. 206 Volumetric flow in broken loop (FB-40 and FB-45), from -6 to 42 s.

507 195

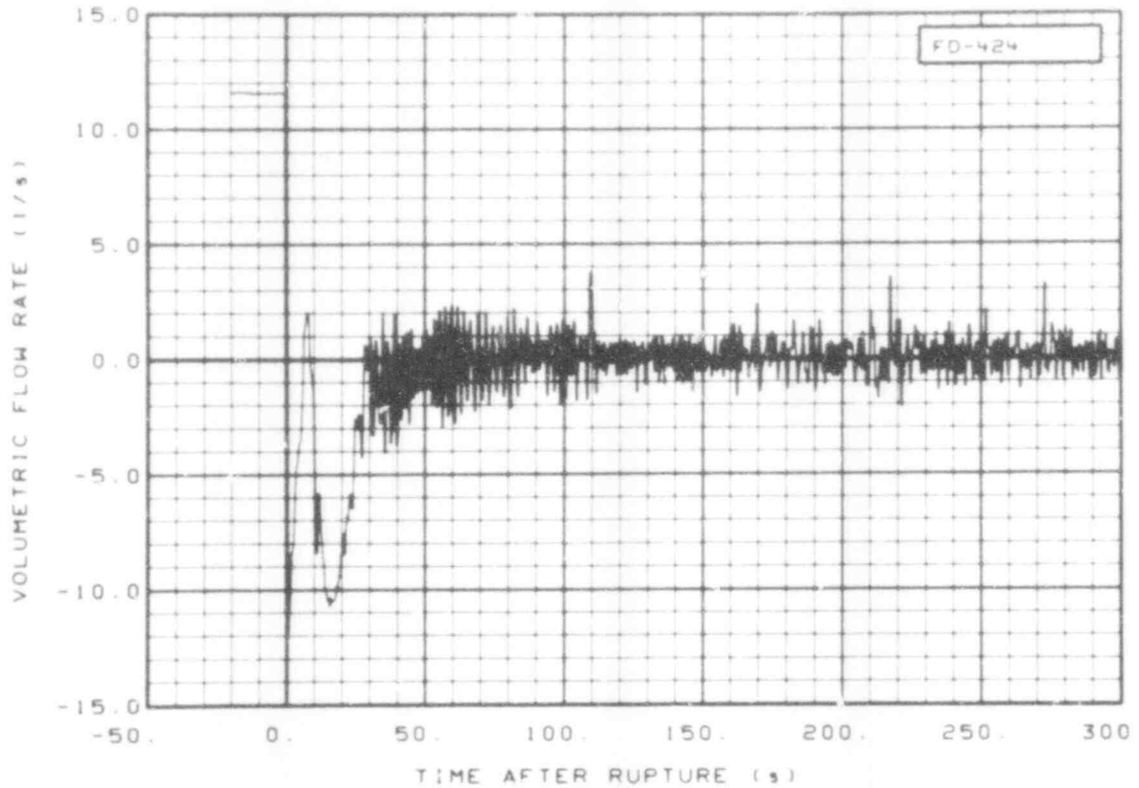

Fig. 207 Volumetric flow in downcomer (FD-424), from -20 to 300 s.

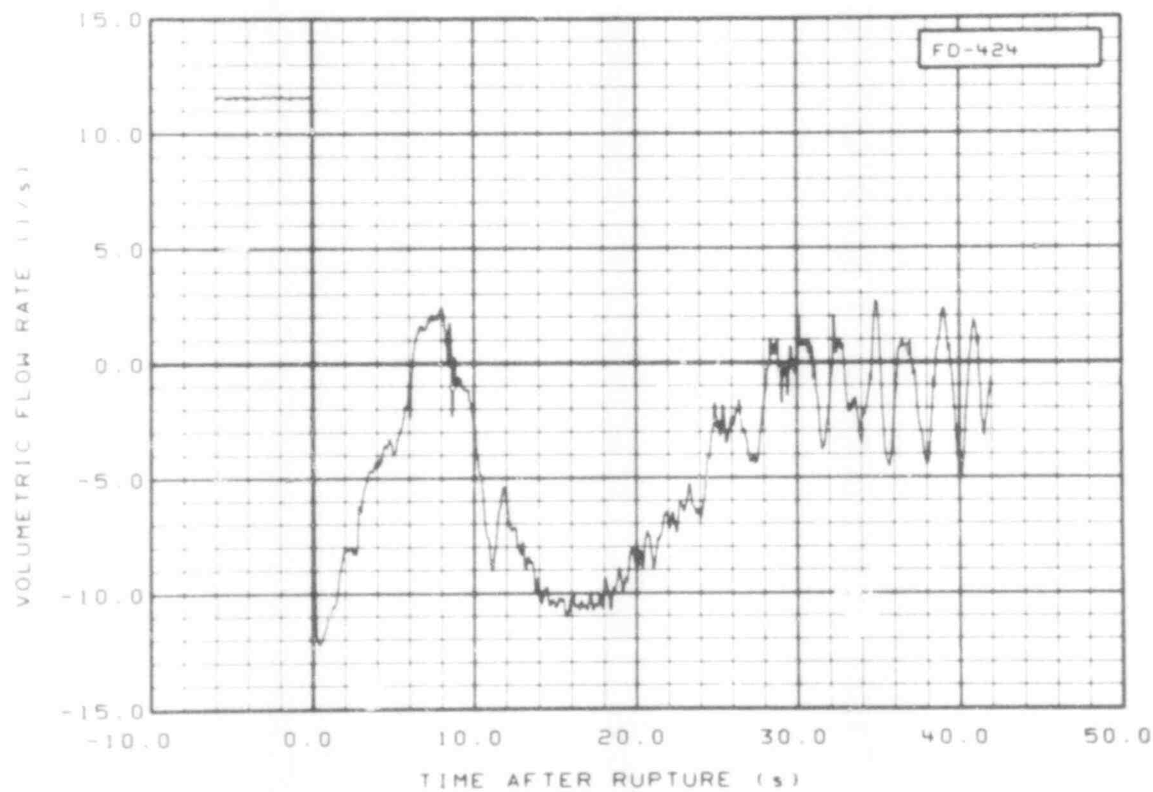

Fig. 208 Volumetric flow in downcomer (FD-424), from -6 to 42 s.

507 196

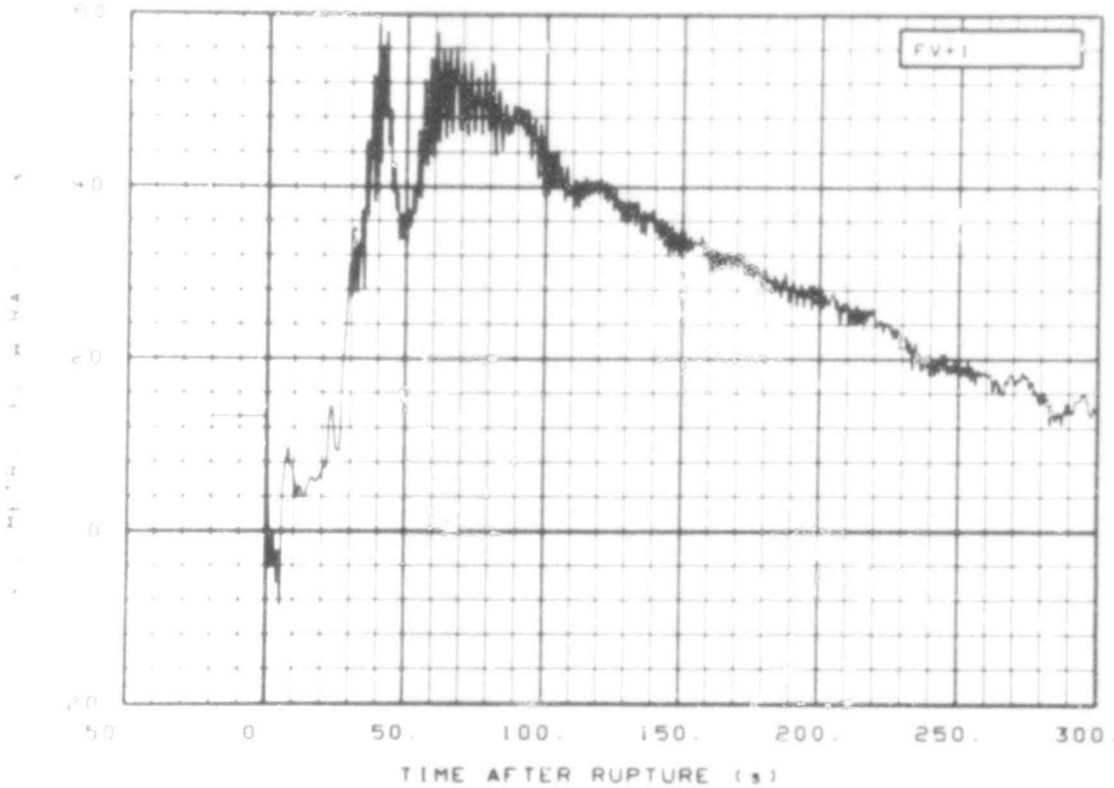

Fig. 209 Volumetric flow in vessel upper plenum (FV + 1), from -20 to 300 s.

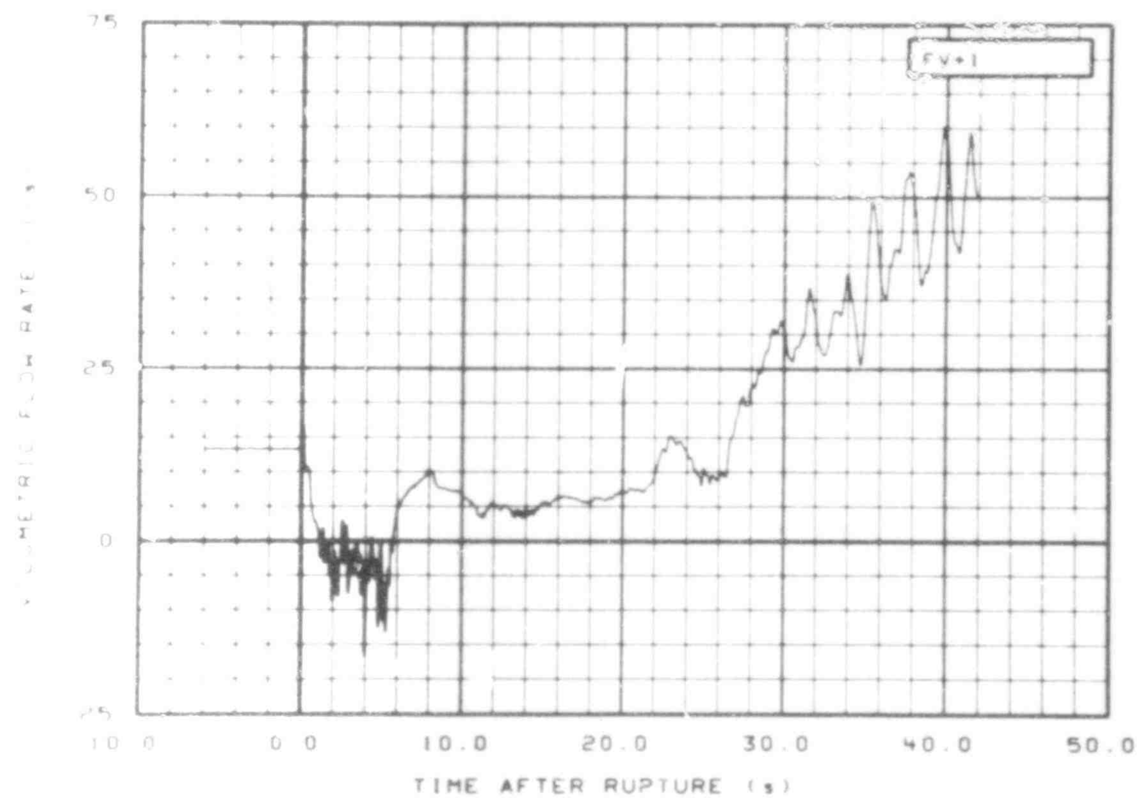

Fig. 210 Volumetric flow in vessel upper plenum (FV + 1), from -6 to 42 s.

507 197

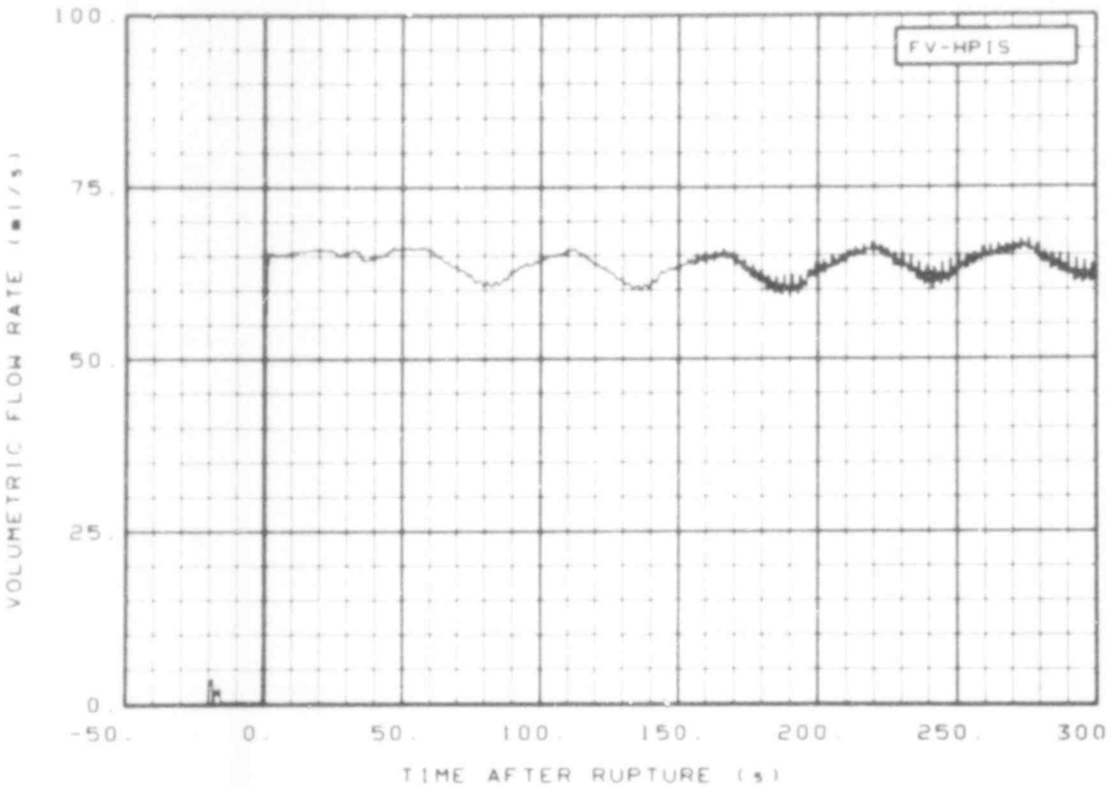

Fig. 211 Volumetric flow in vessel, high pressure injection system (FV-HPIS), from -20 to 300 s.

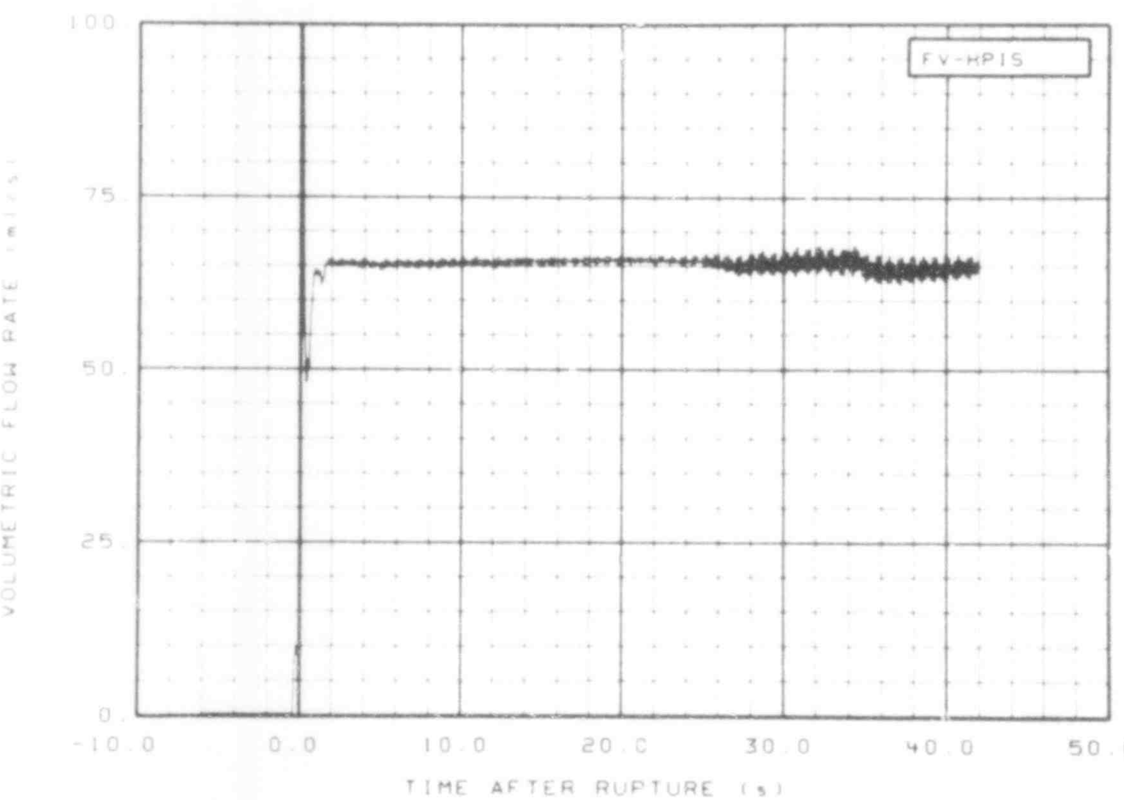

Fig. 212 Volumetric flow in vessel, high pressure injection system (FV-HPIS), from -6 to 42 s.

507 198

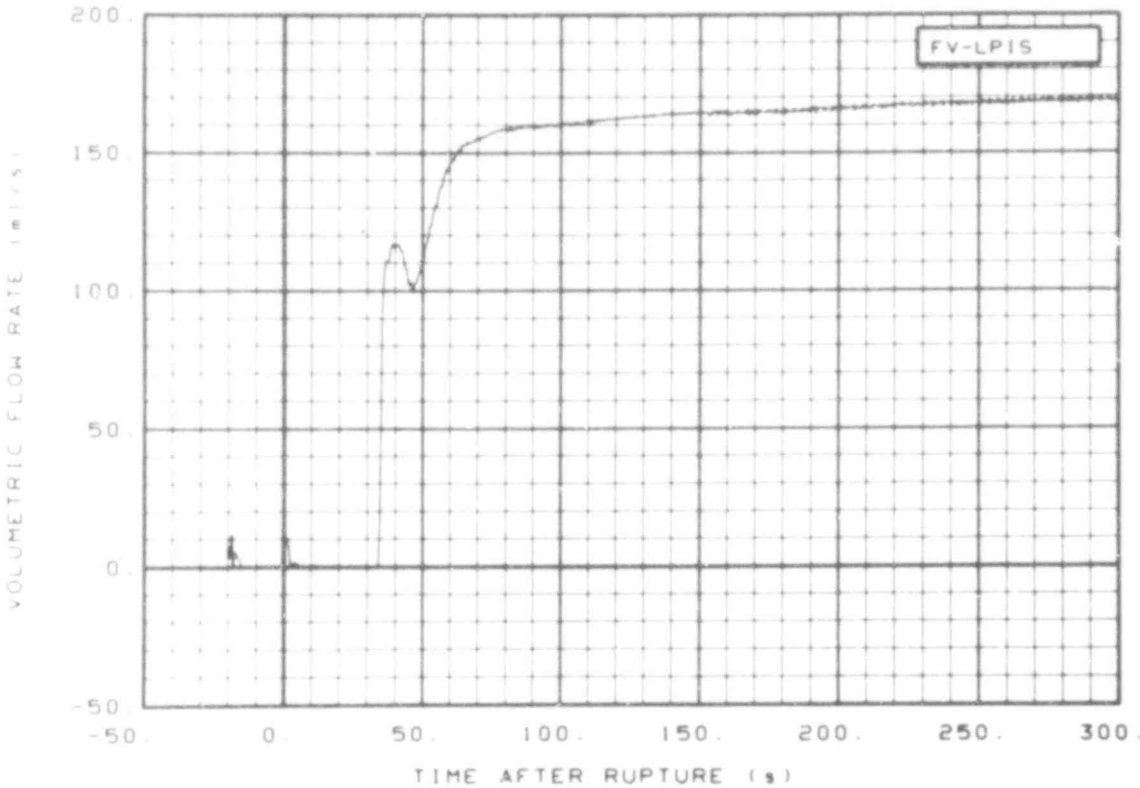

Fig. 213 Volumetric flow in vessel, low pressure injection system (FV-LPIS), from -20 to 300 s.

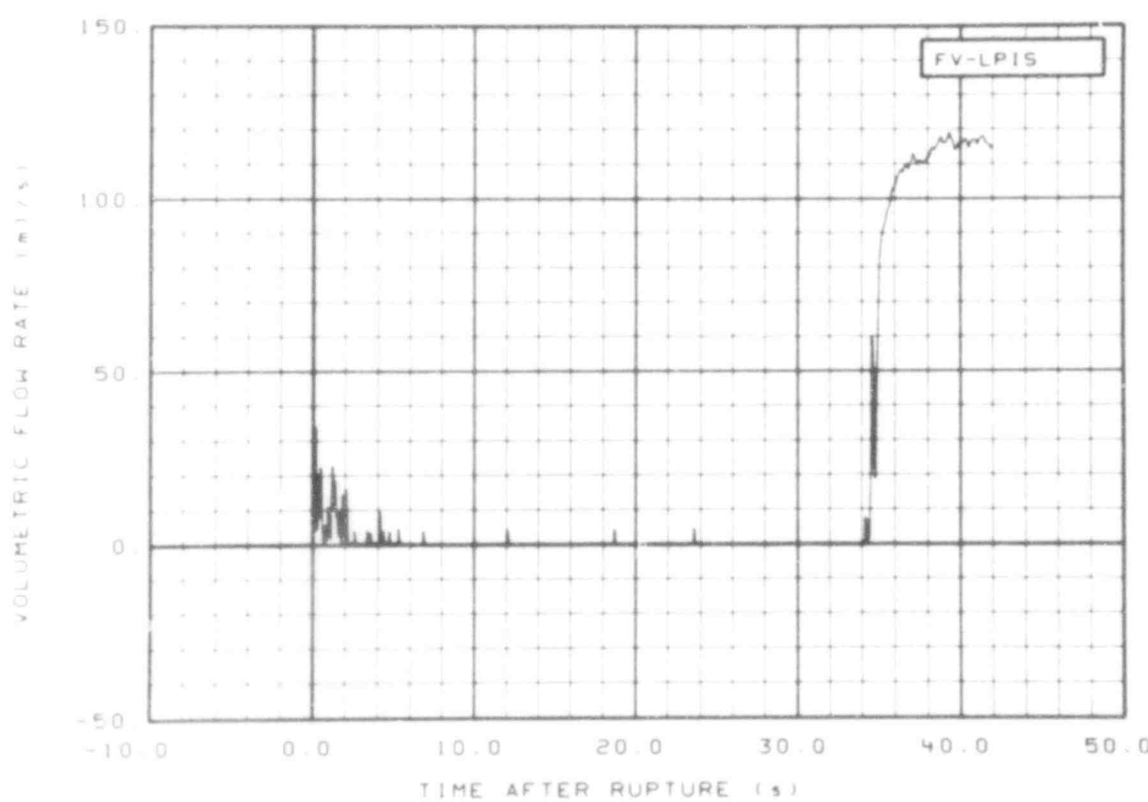

Fig. 214 Volumetric flow in vessel, low pressure injection system (FV-LPIS), from -6 to 42 s.

507 199

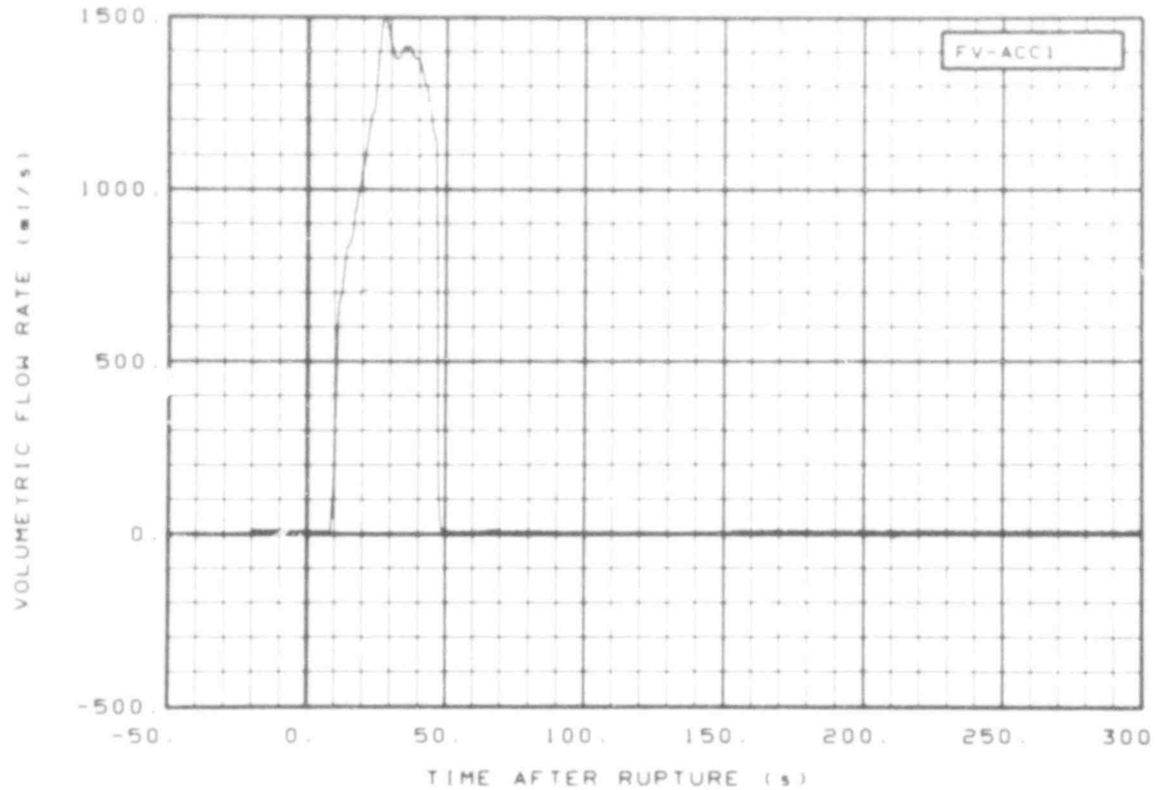

Fig. 215 Volumetric flow in vessel, ECC accumulator (FV-ACC1), from -20 to 300 s.

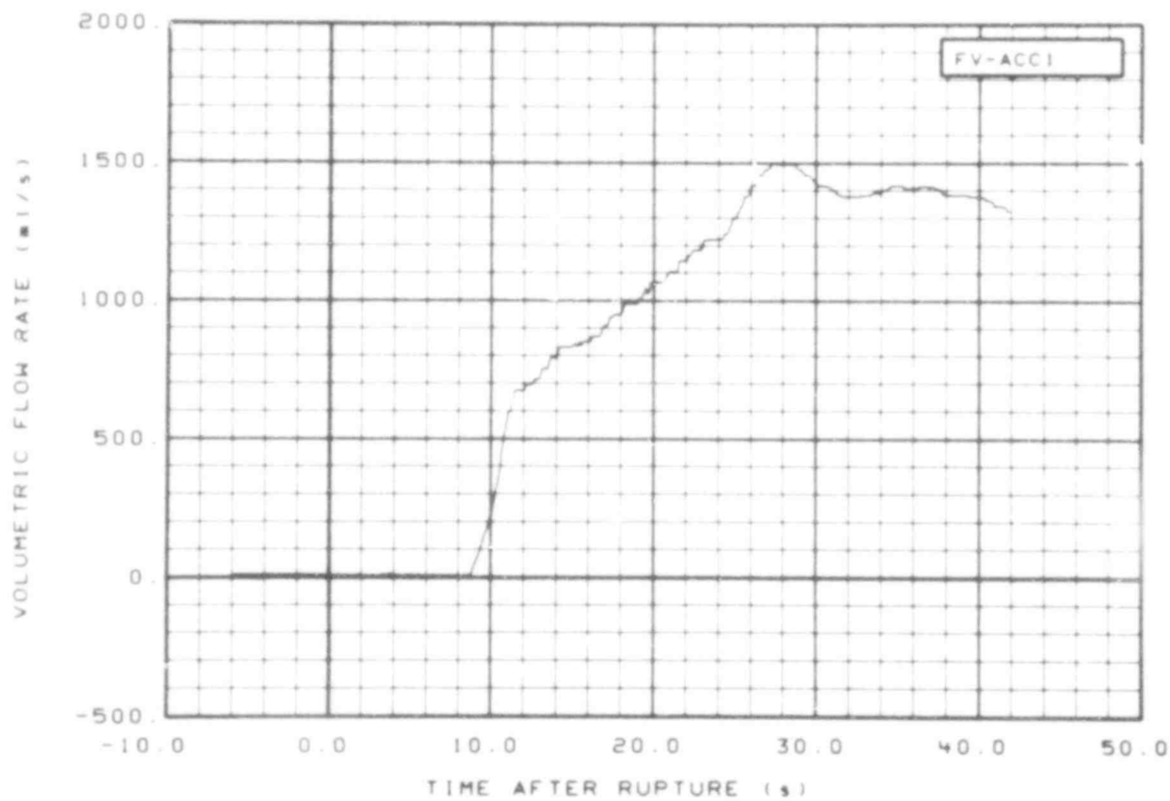

Fig. 216 Volumetric flow in vessel, ECC accumulator (FV-ACC1), from -6 to 42 s.

507 200

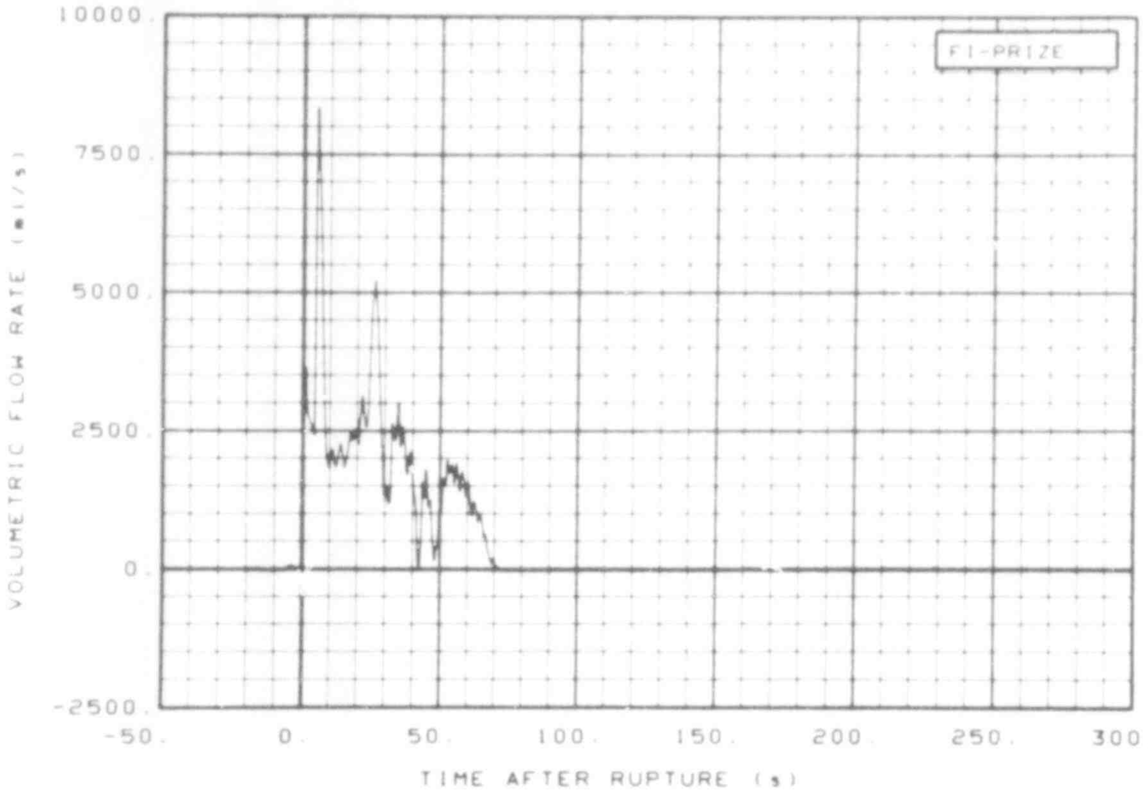

Fig. 217 Volumetric flow in intact loop, pressurizer surge line (FI-PRIZE), from -20 to 300 s.

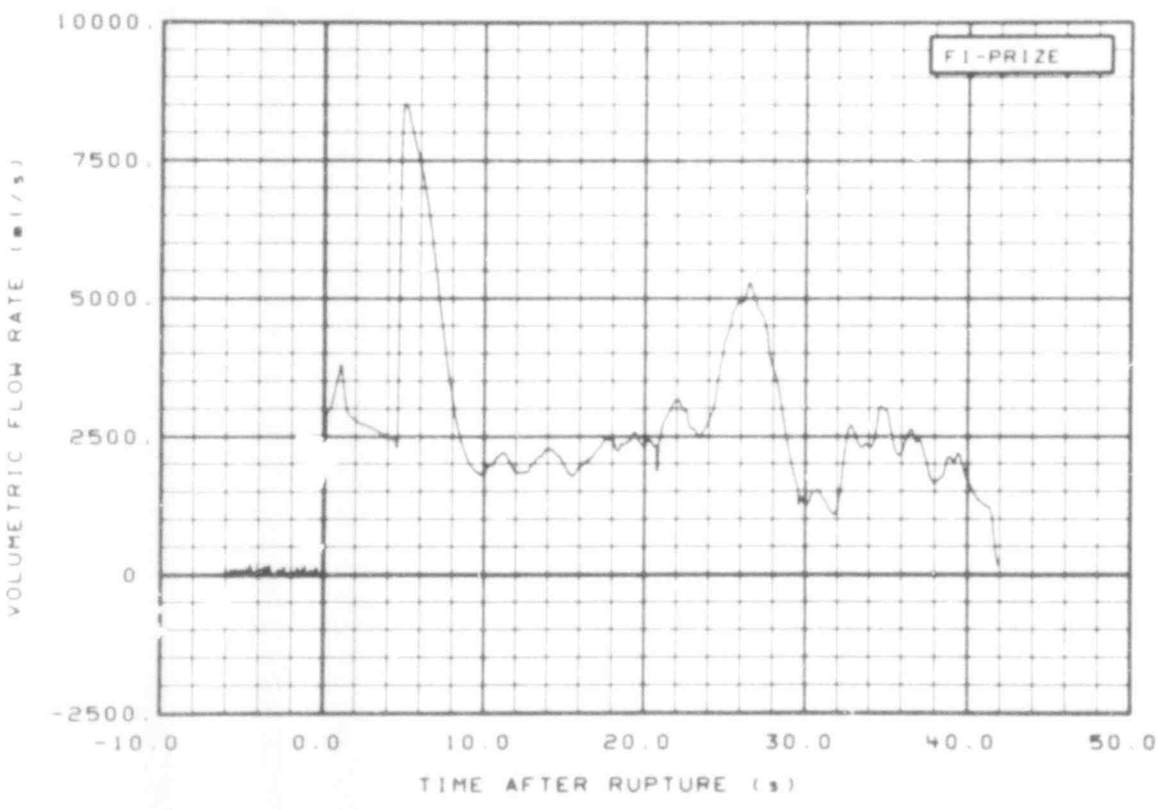

Fig. 218 Volumetric flow in intact loop, pressurizer surge line (FI-PRIZE), from -6 to 42 s.

507 201

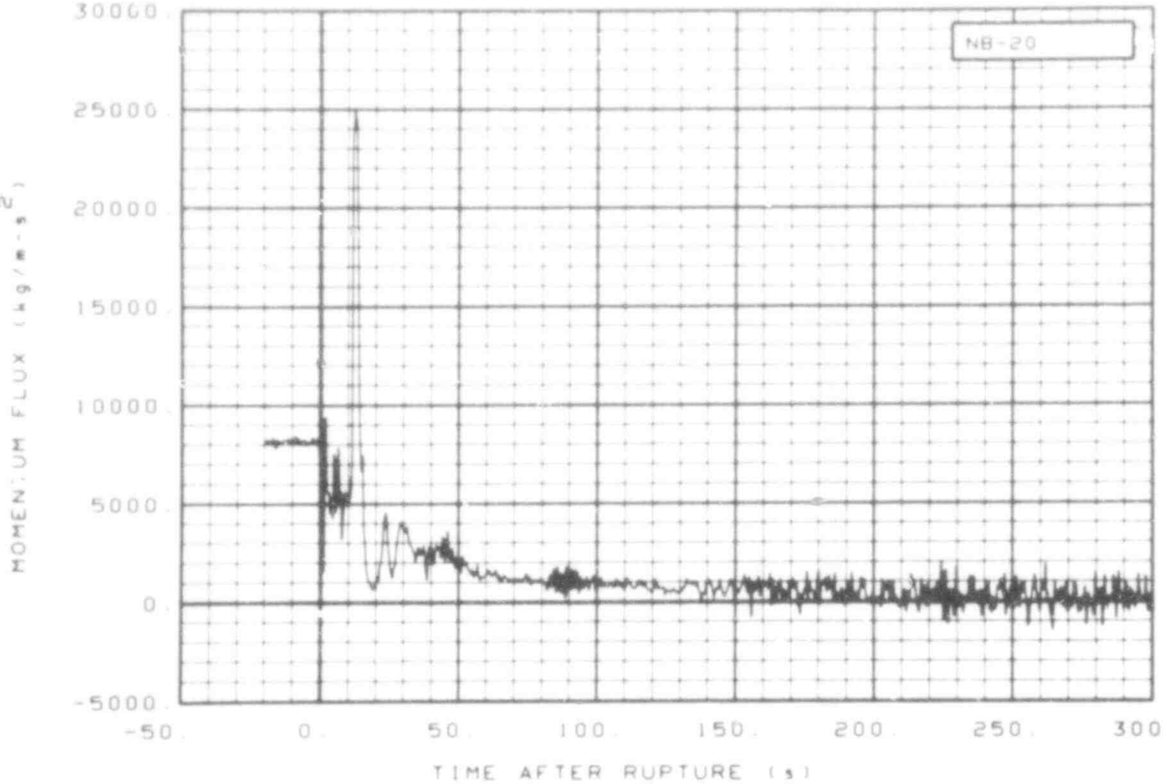

Fig. 219 Momentum flux in broken loop (NB-20), from -20 to 300 s.

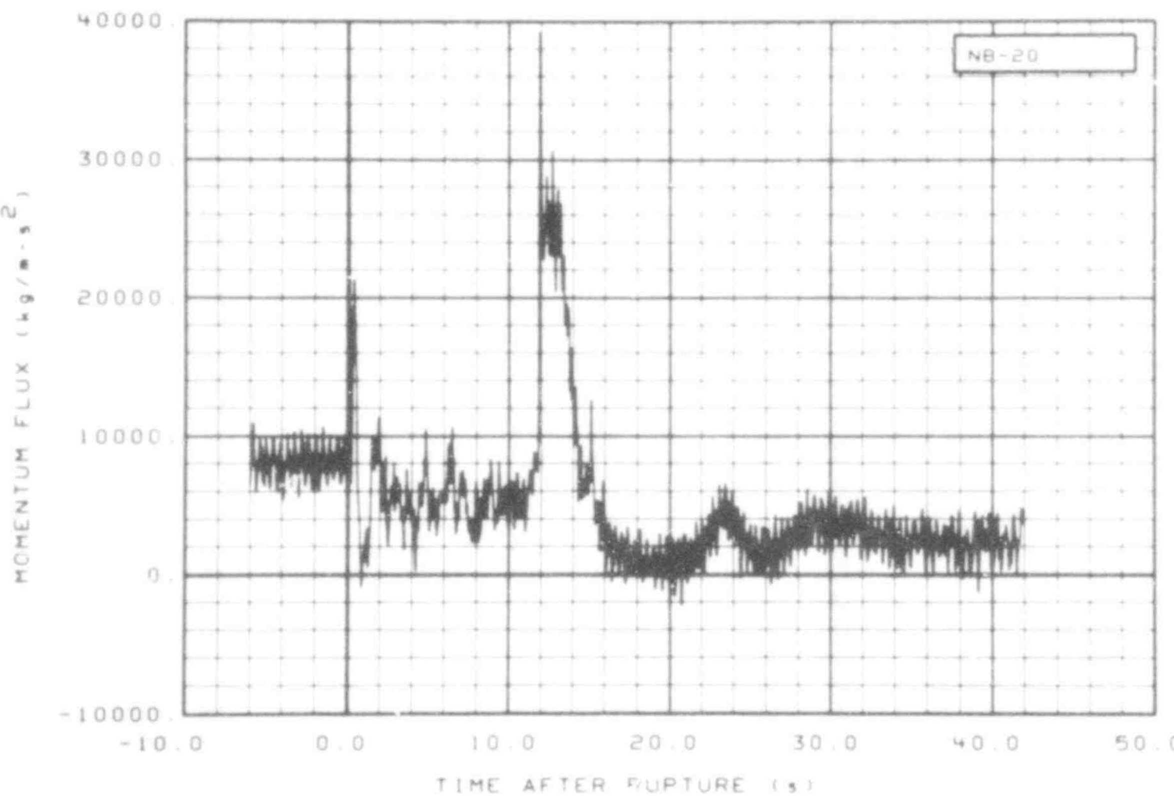

Fig. 220 Momentum flux in broken loop (NB-20), from -6 to 42 s.

507 202

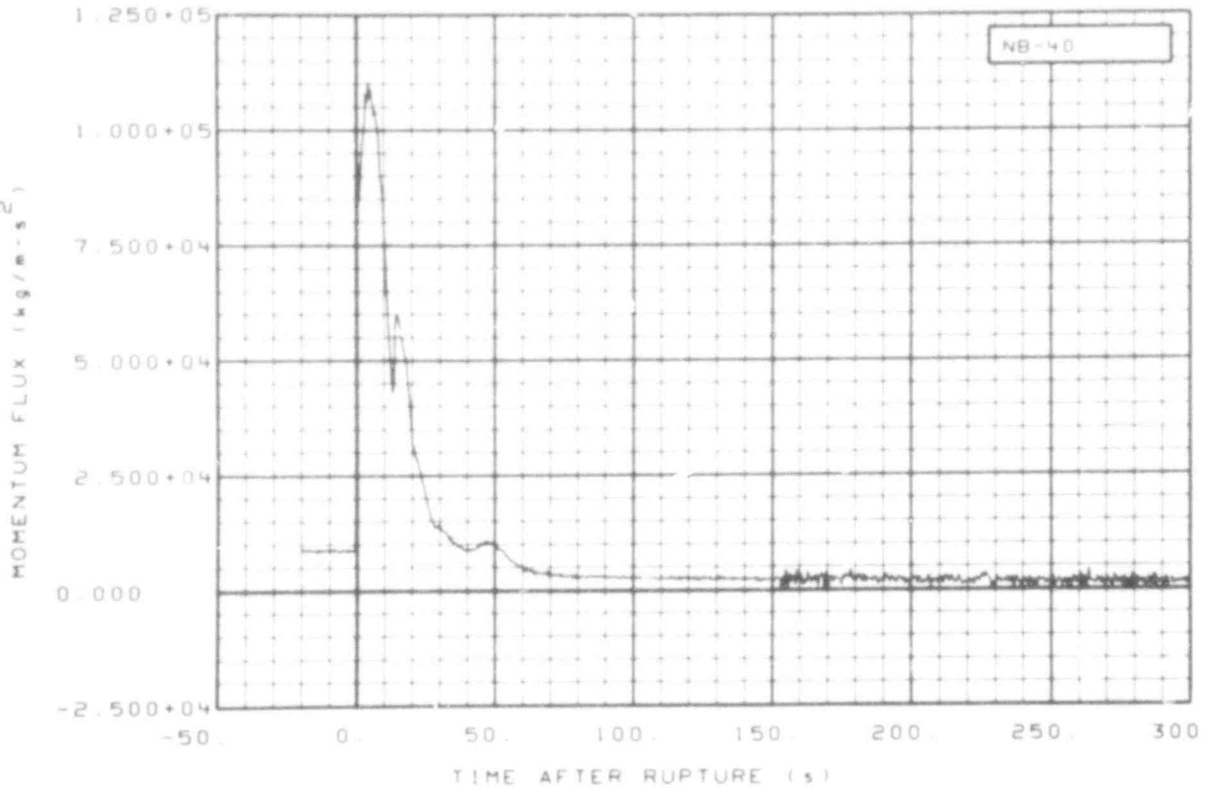

Fig. 221 Momentum flux in broken loop (NB-40), from -20 to 300 s.

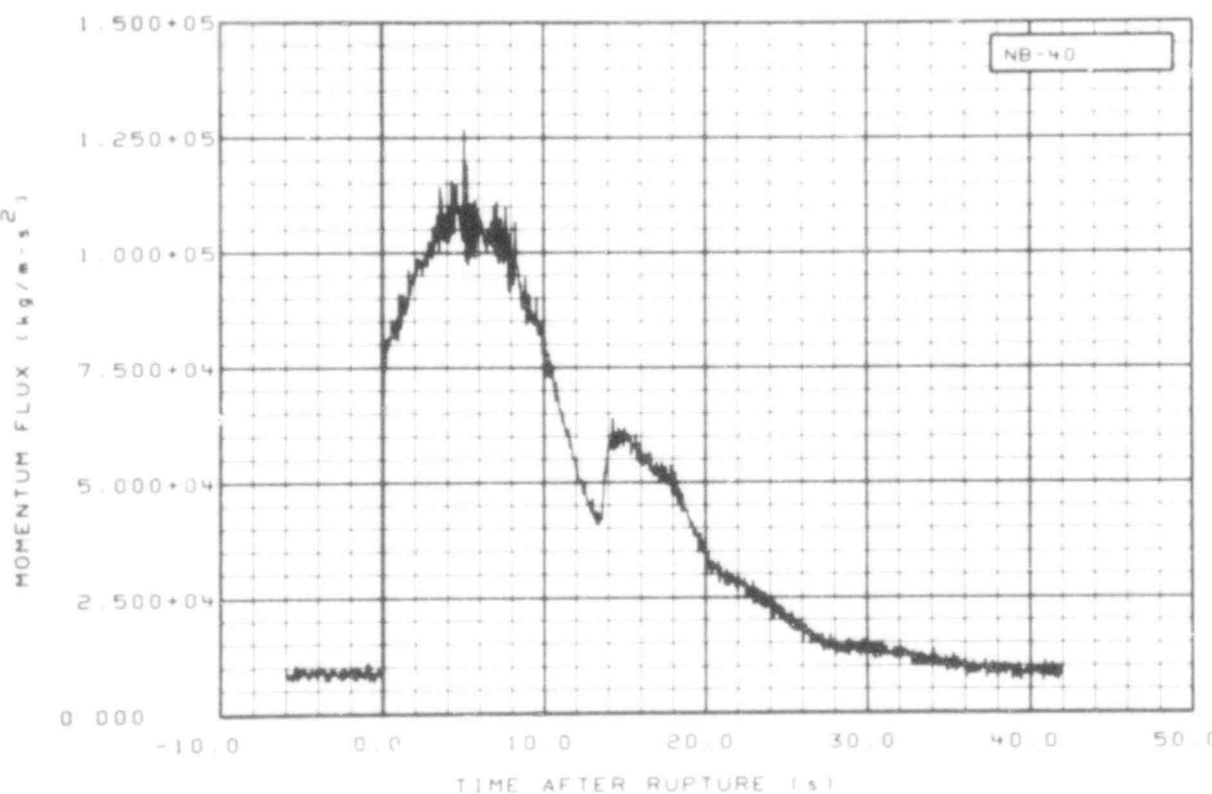

Fig. 222 Momentum flux in broken loop (NB-40), from -6 to 42 s.

507 203

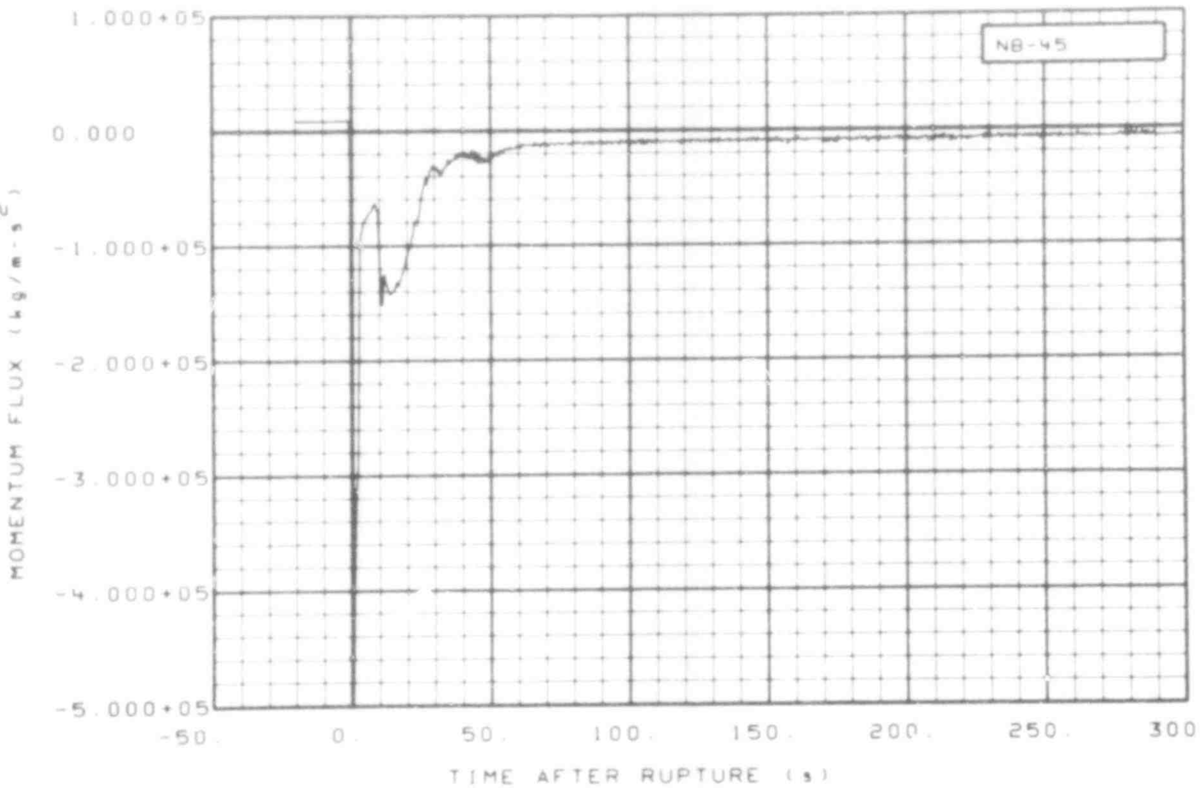

Fig. 223 Momentum flux in broken loop (NB-45), from -20 to 300 s.

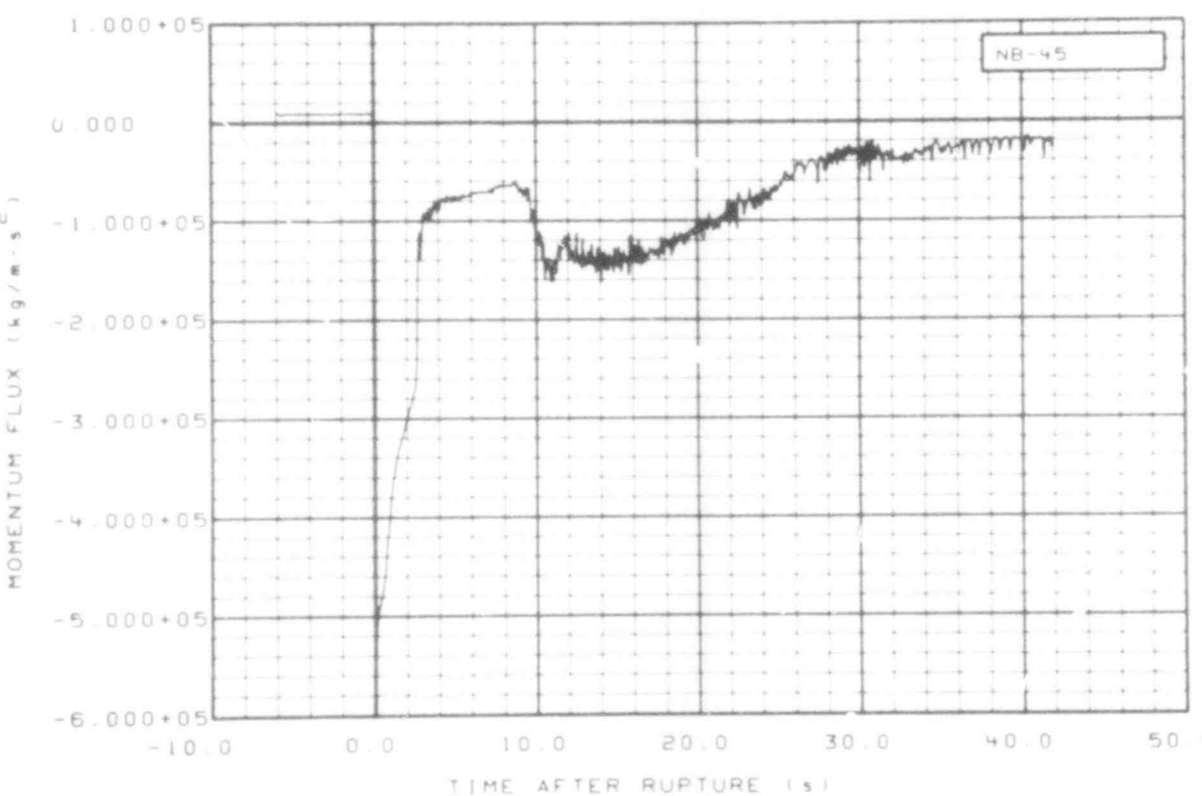

Fig. 224 Momentum flux in broken loop (NB-45), from -6 to 42 s.

507 204

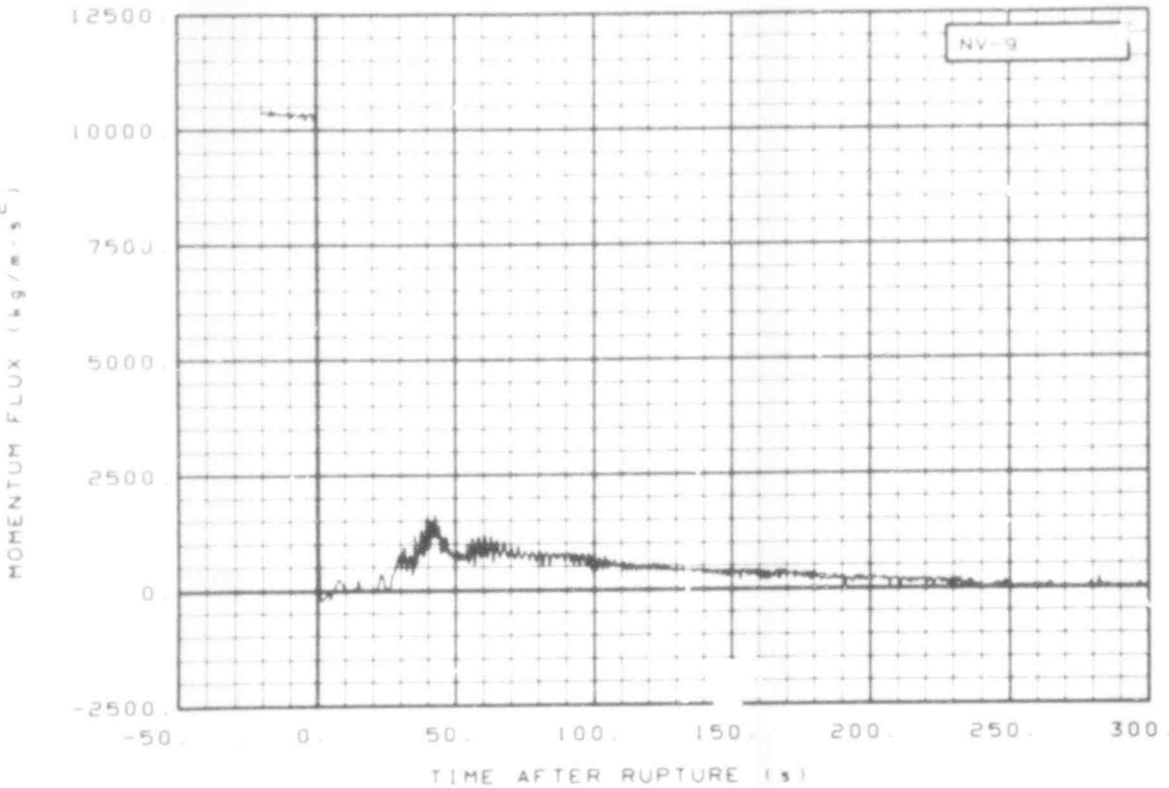

Fig. 225 Momentum flux in core outlet (NV-9), from -20 to 300 s.

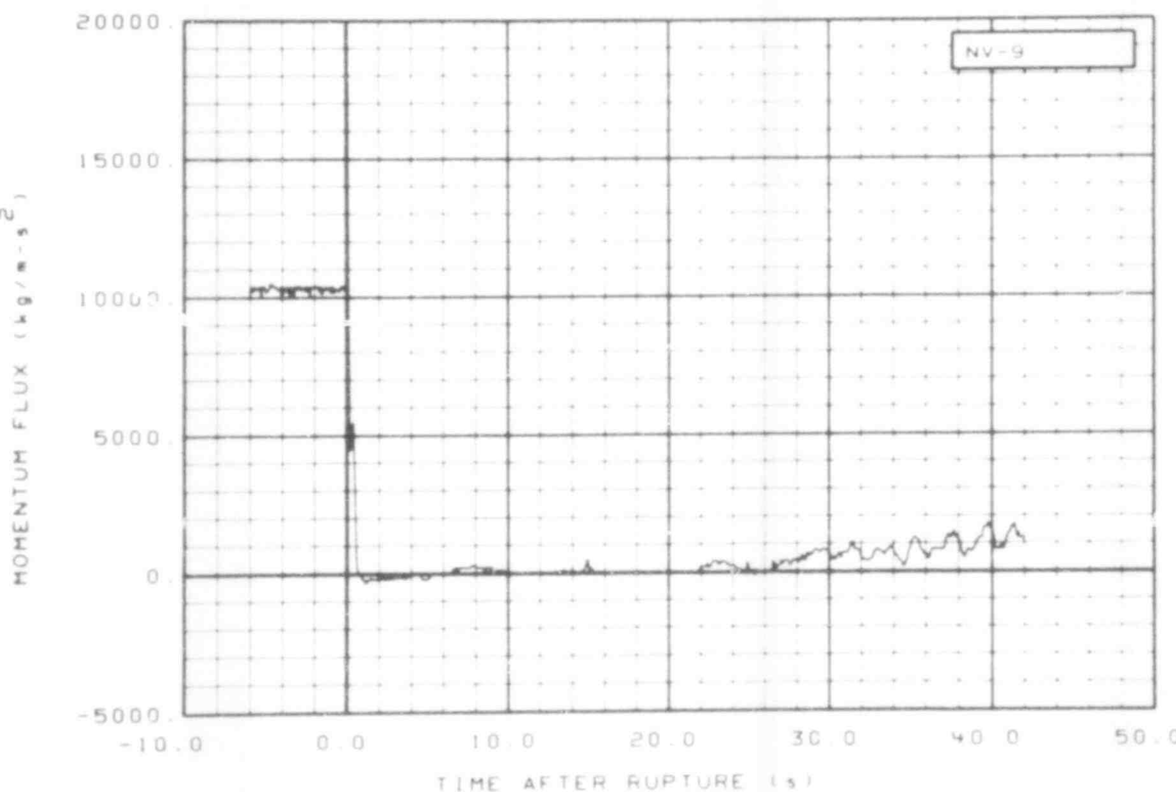

Fig. 226 Momentum flux in core outlet (NV-9), from -6 to 42 s.

507 205

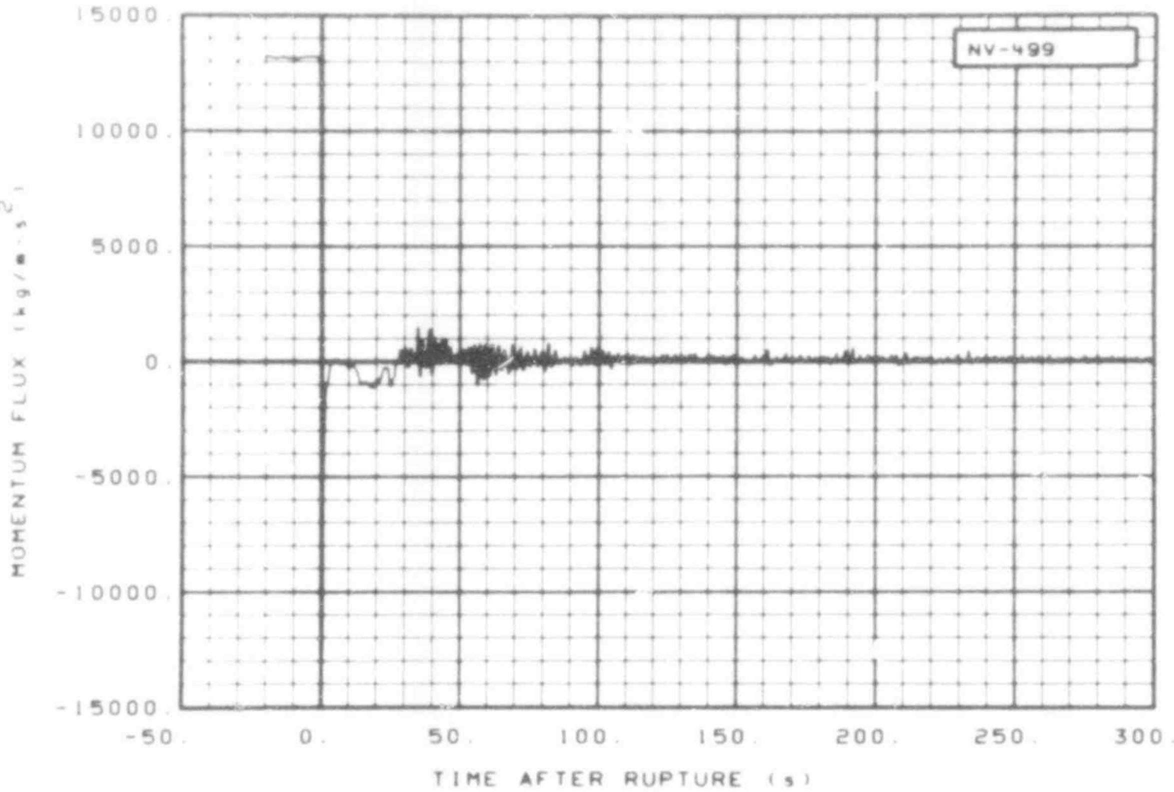

Fig. 227 Momentum flux in core inlet (NV-499), from -20 to 300 s.

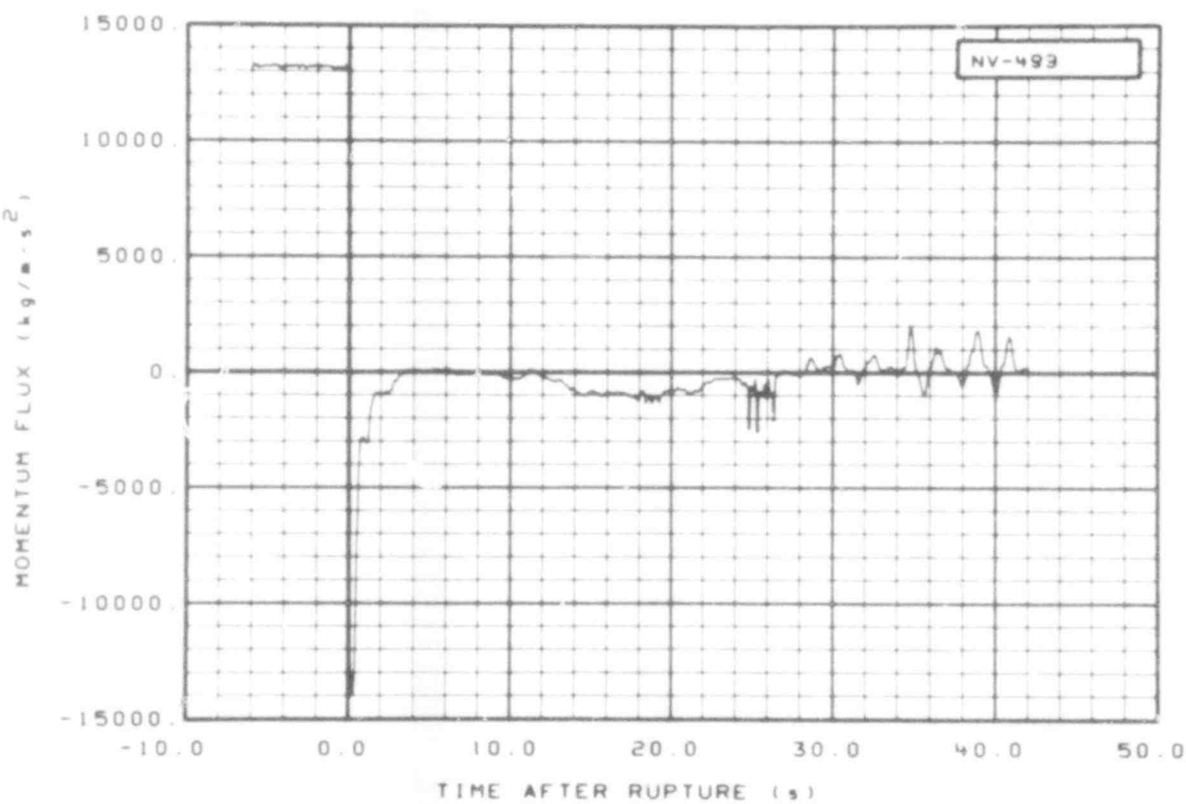

Fig. 228 Momentum flux in core inlet (NV-499), from -6 to 42 s.

507 206

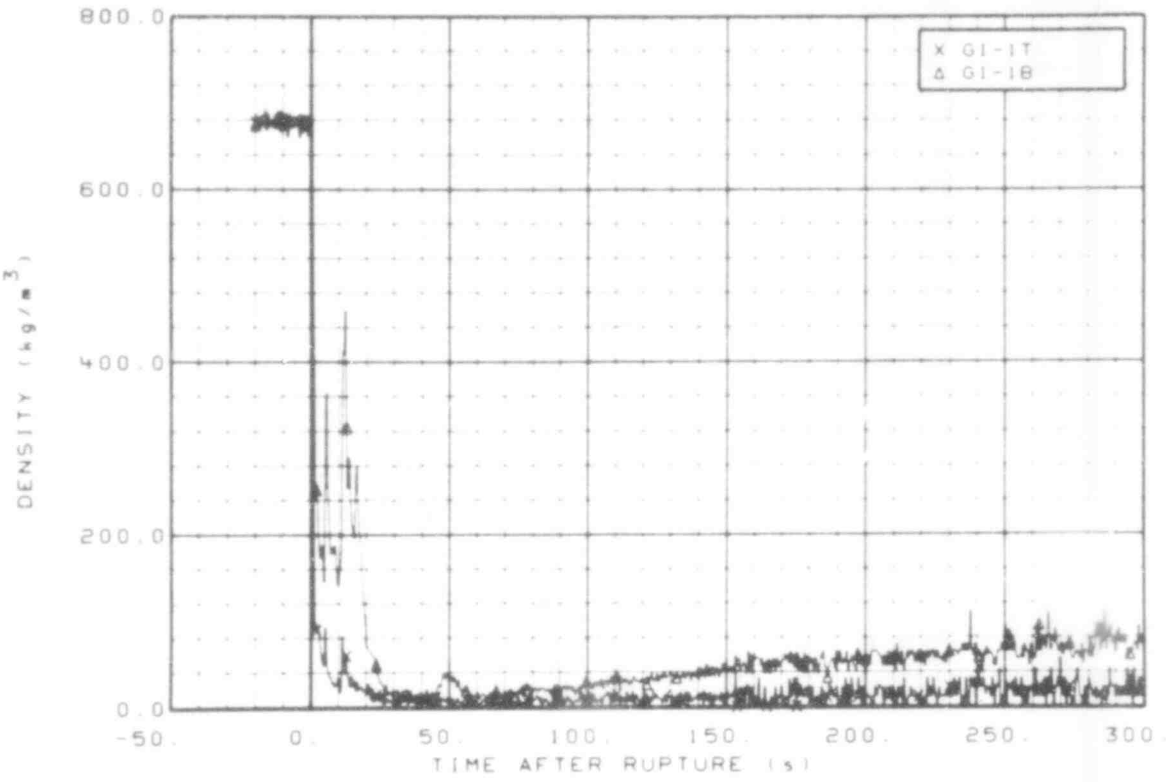

Fig. 229 Density in intact loop (GI-1T and GI-1B), from -20 to 300 s.

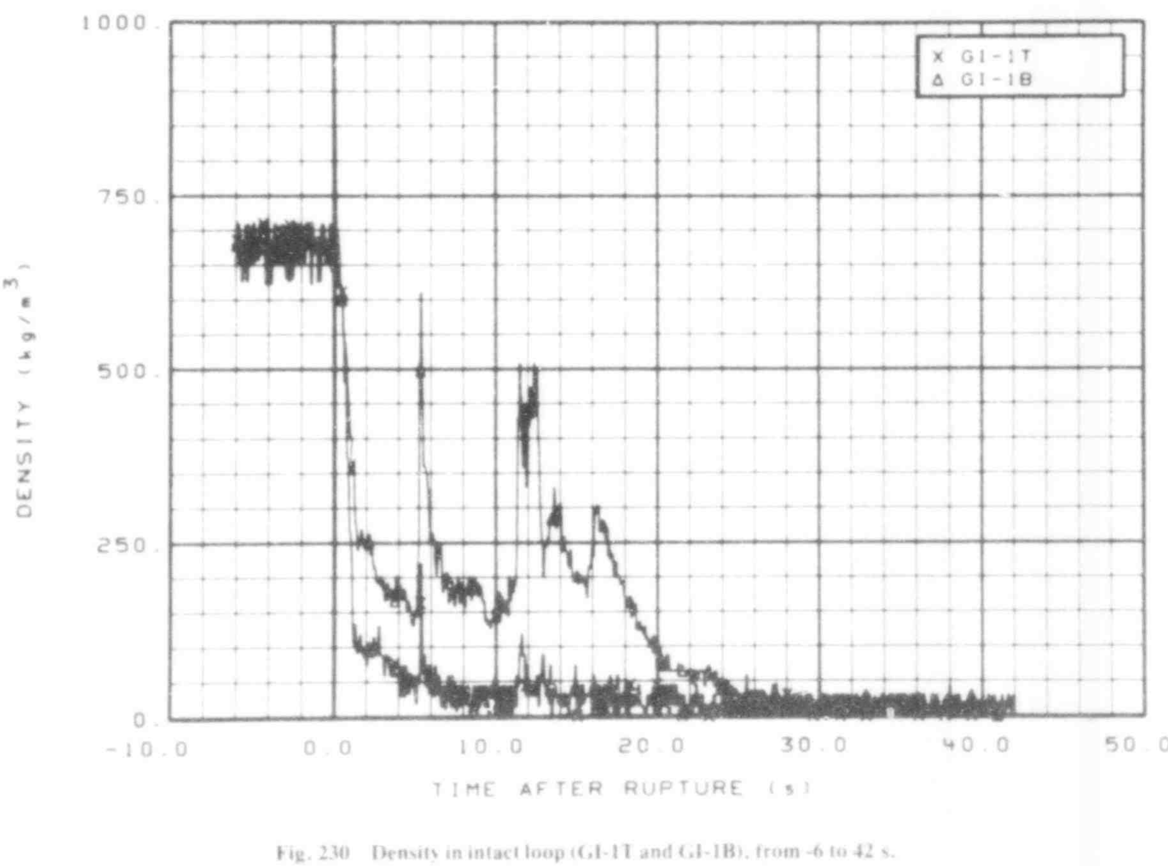

Fig. 230 Density in intact loop (GI-1T and GI-1B), from -6 to 42 s.

507 207

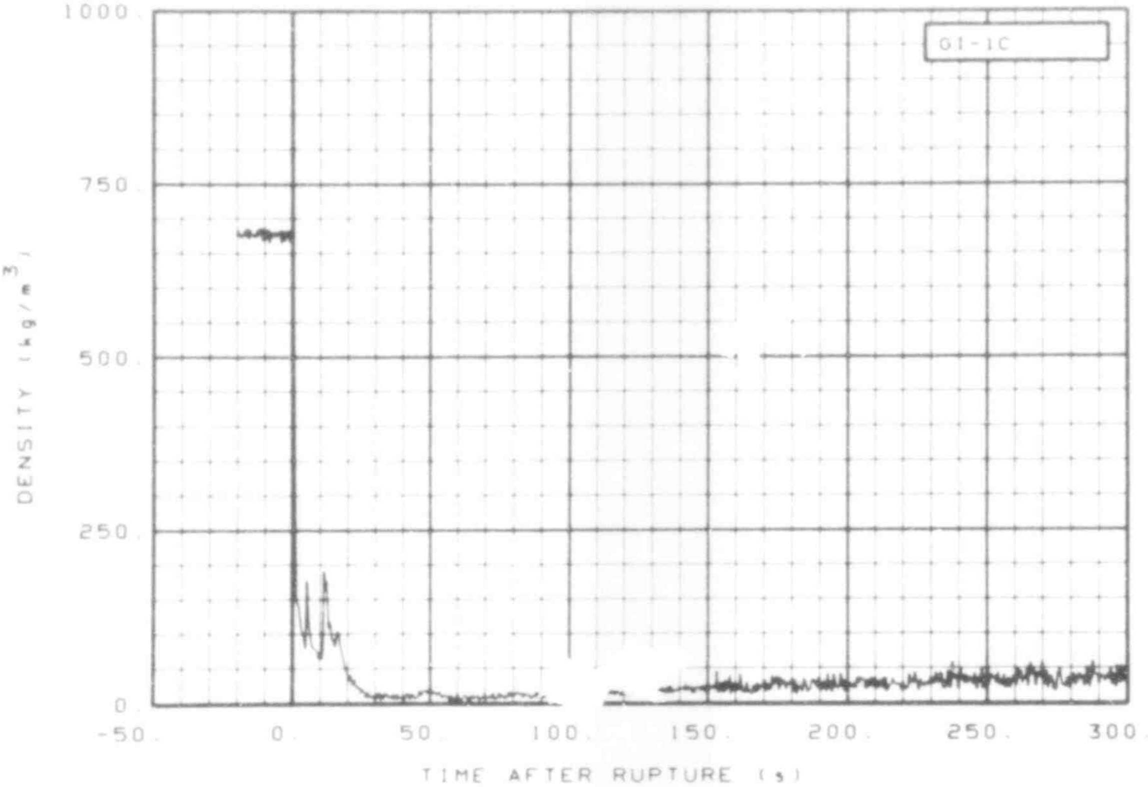

Fig. 231 Density in intact loop (GI-1C), from -20 to 300 s.

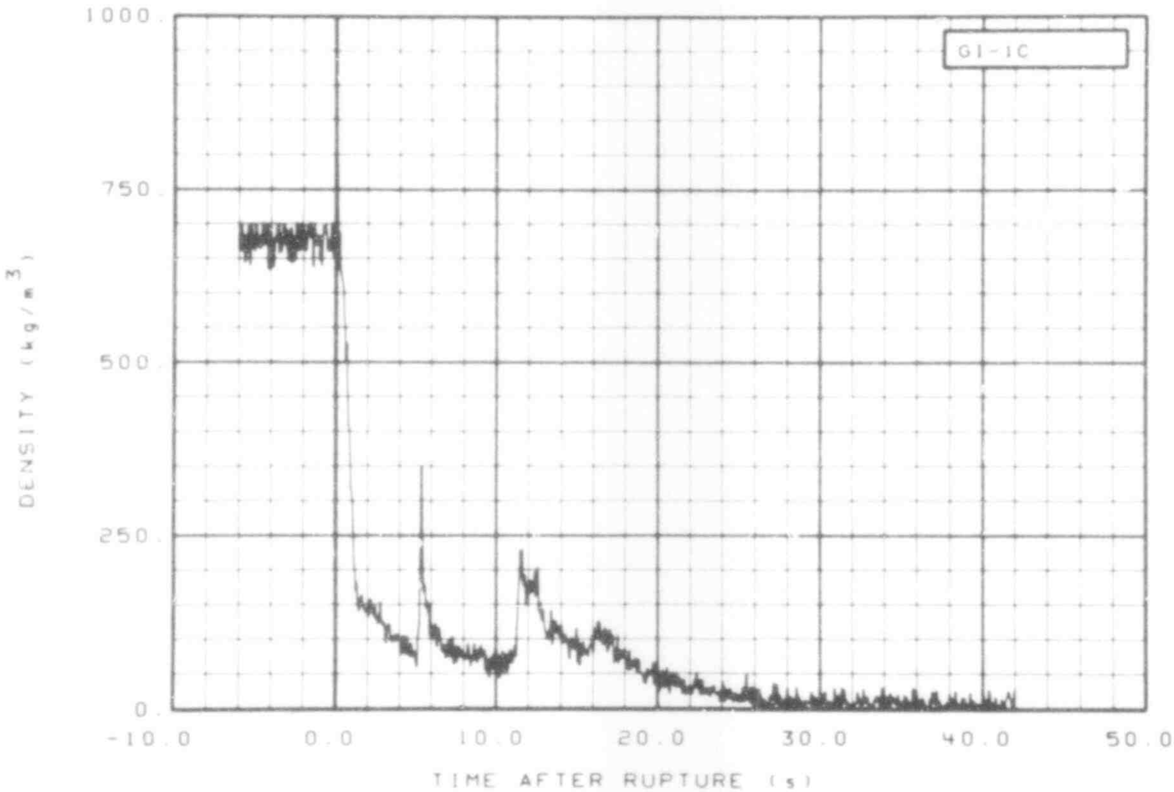

Fig. 232 Density in intact loop (GI-1C), from -6 to 42 s.

507 208

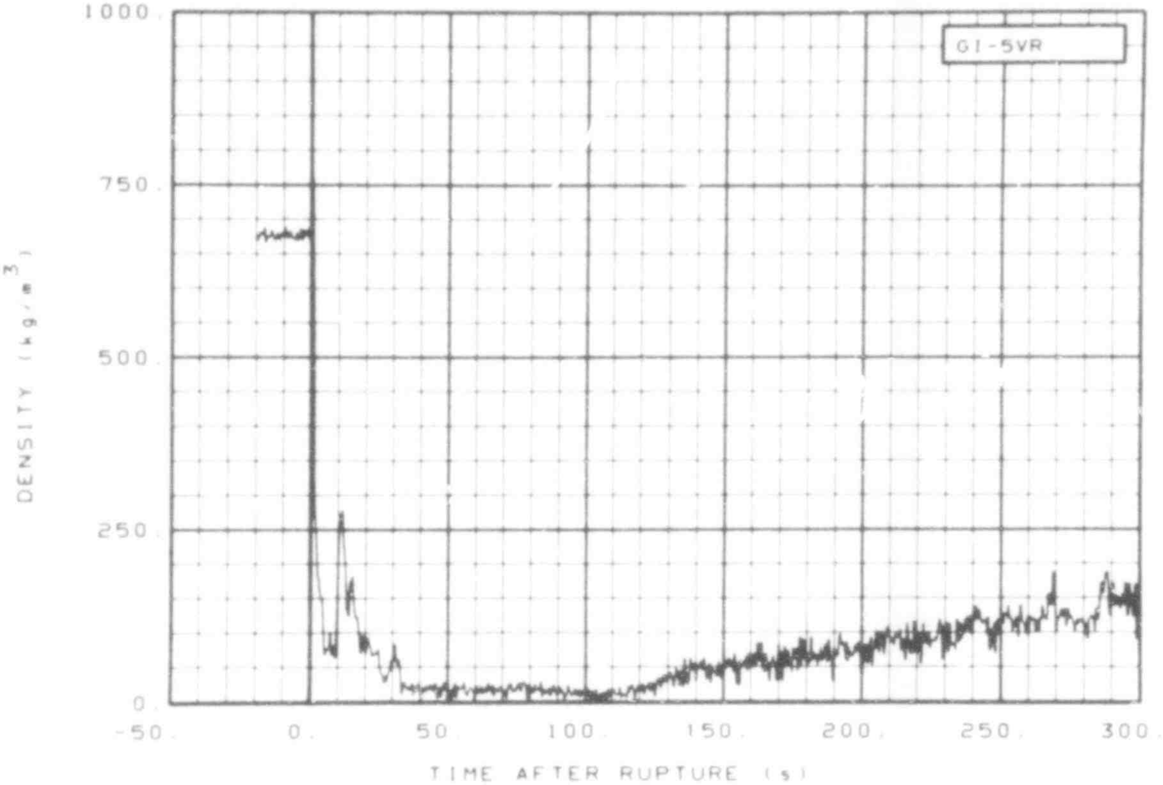

Fig. 233 Density in intact loop (GI-5VR), from -20 to 300 s.

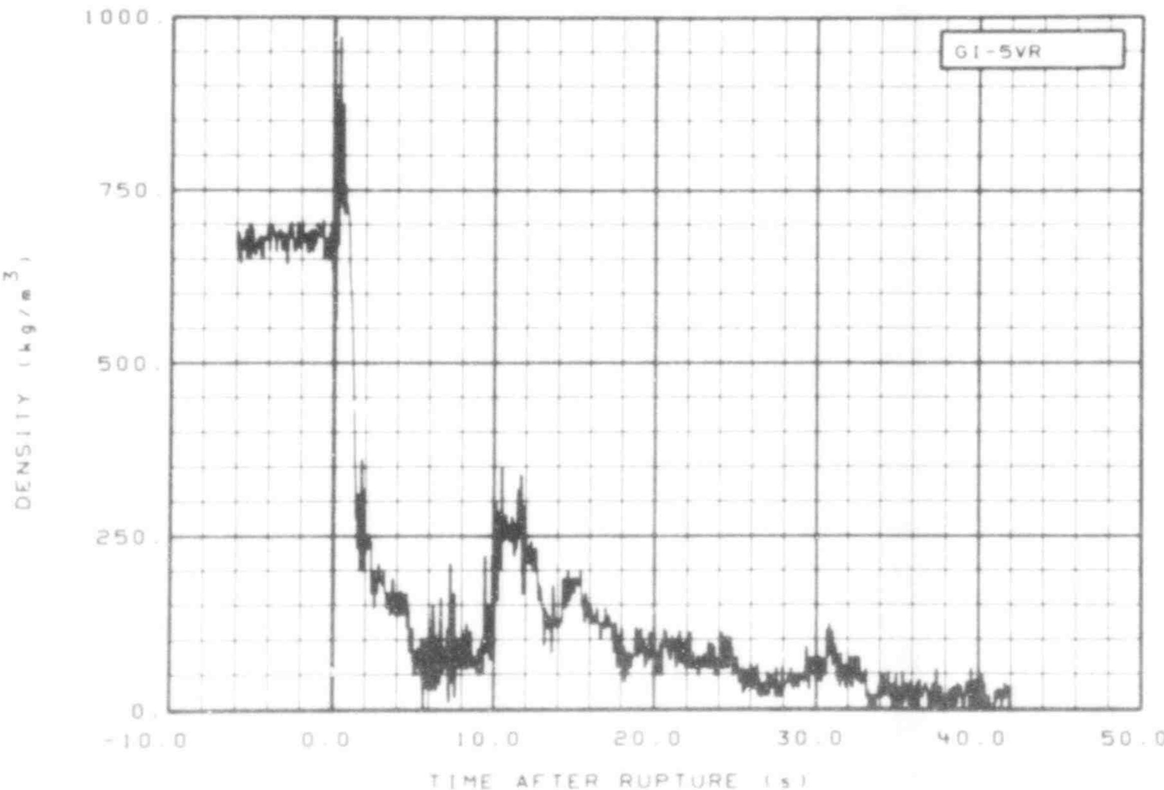

Fig. 234 Density in intact loop (GI-5VR), from -6 to 42 s.

507 209

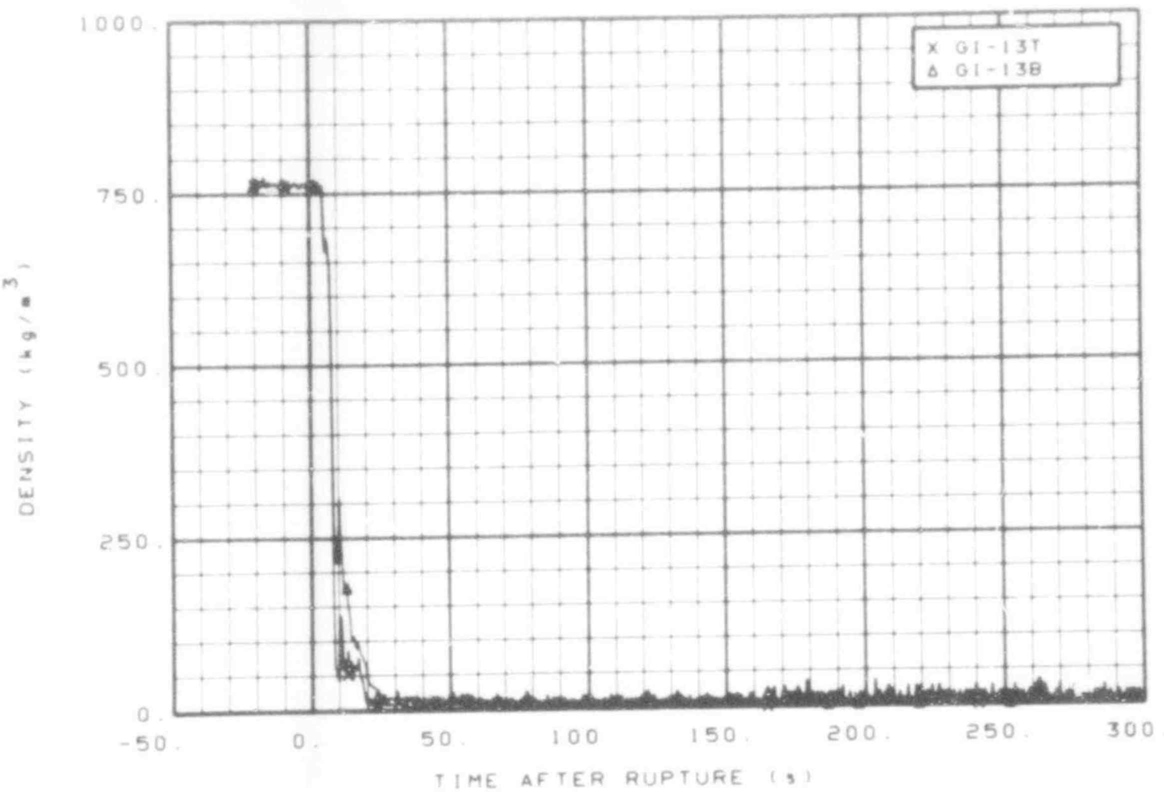

Fig. 235 Density in intact loop (GI-13T and GI-13B), from -20 to 300 s.

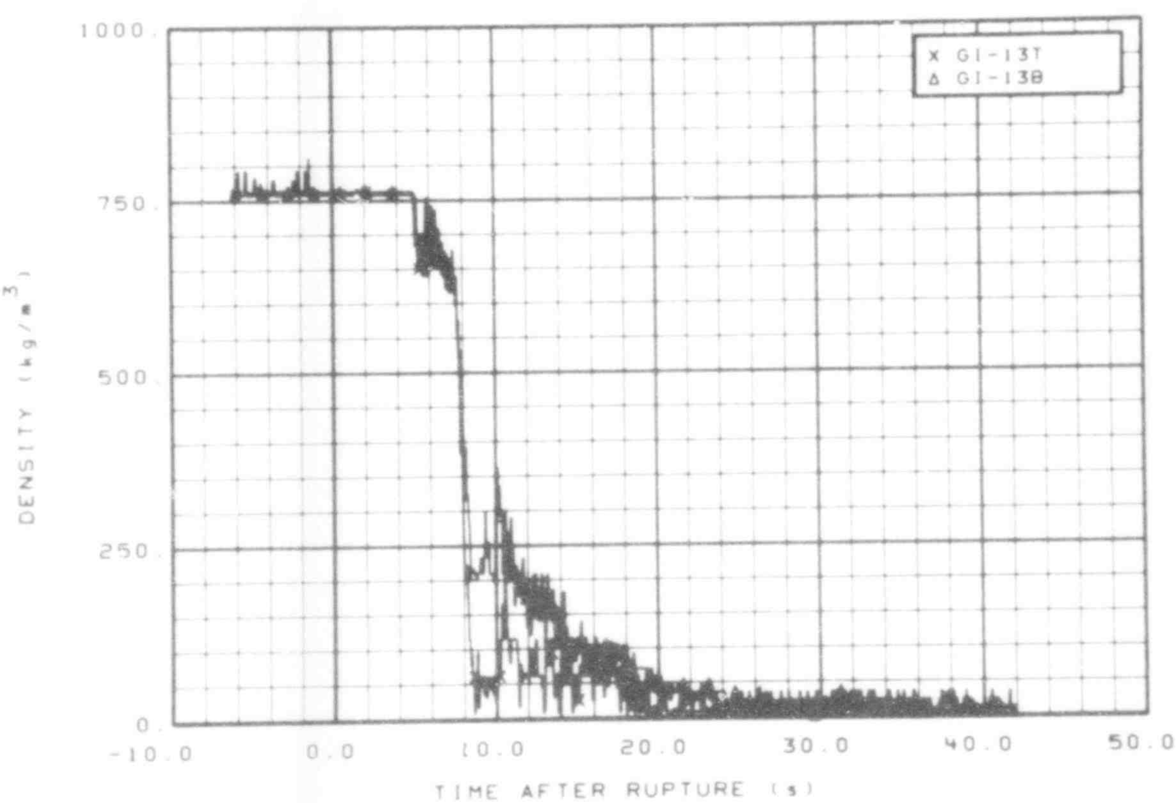

Fig. 236 Density in intact loop (GI-13T and GI-13B), from -6 to 42 s.

507 210

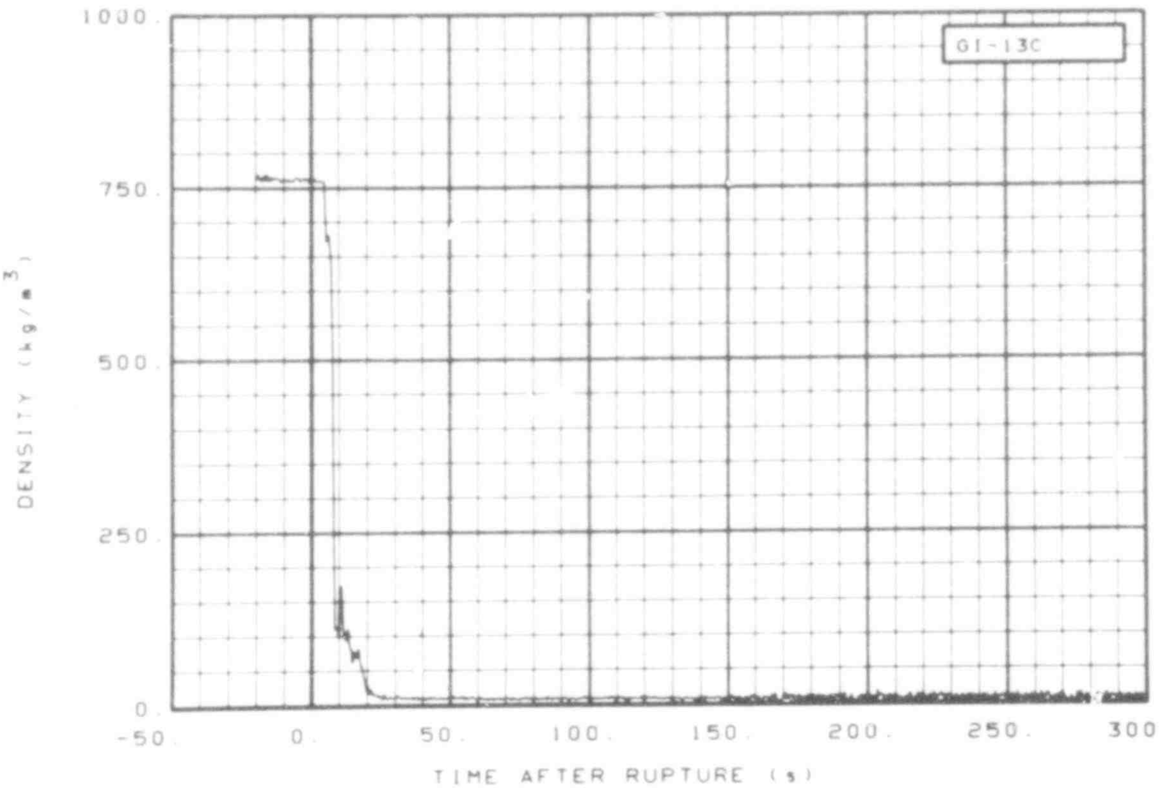

Fig. 237 Density in intact loop (GI-13C), from -20 to 300 s.

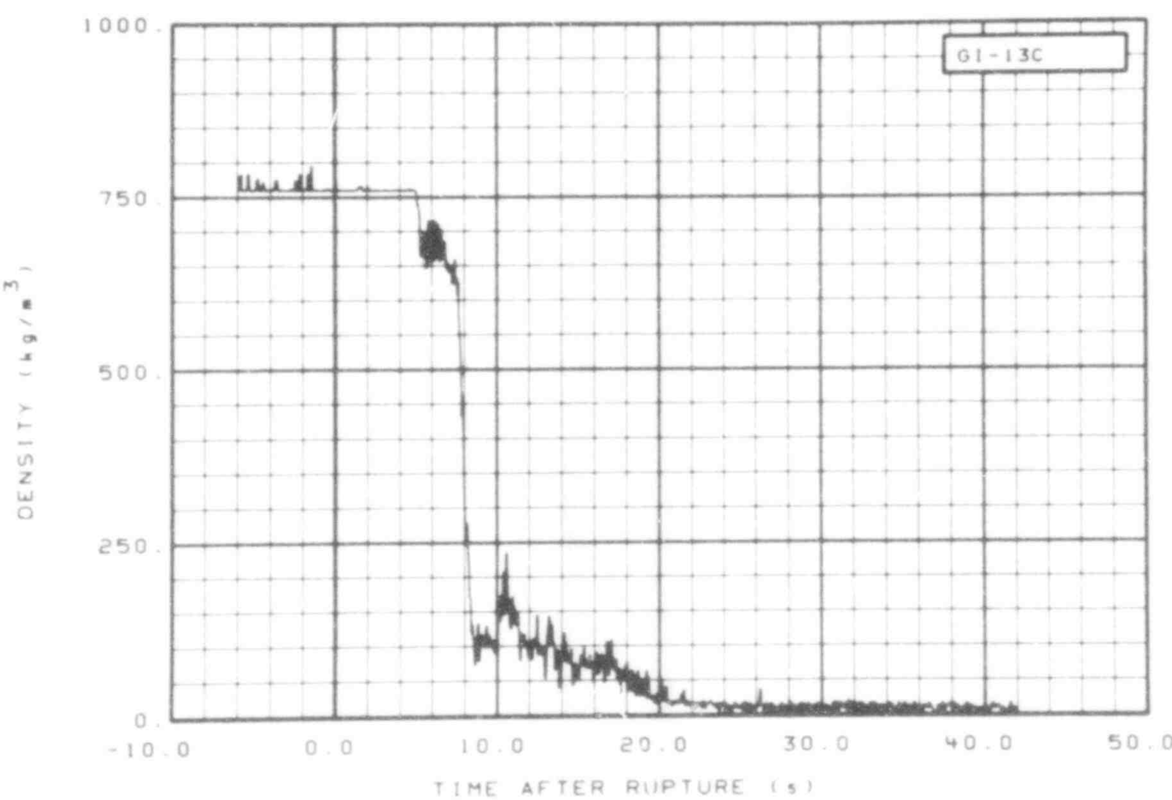

Fig. 238 Density in intact loop (GI-13C), from -6 to 42 s.

507 211

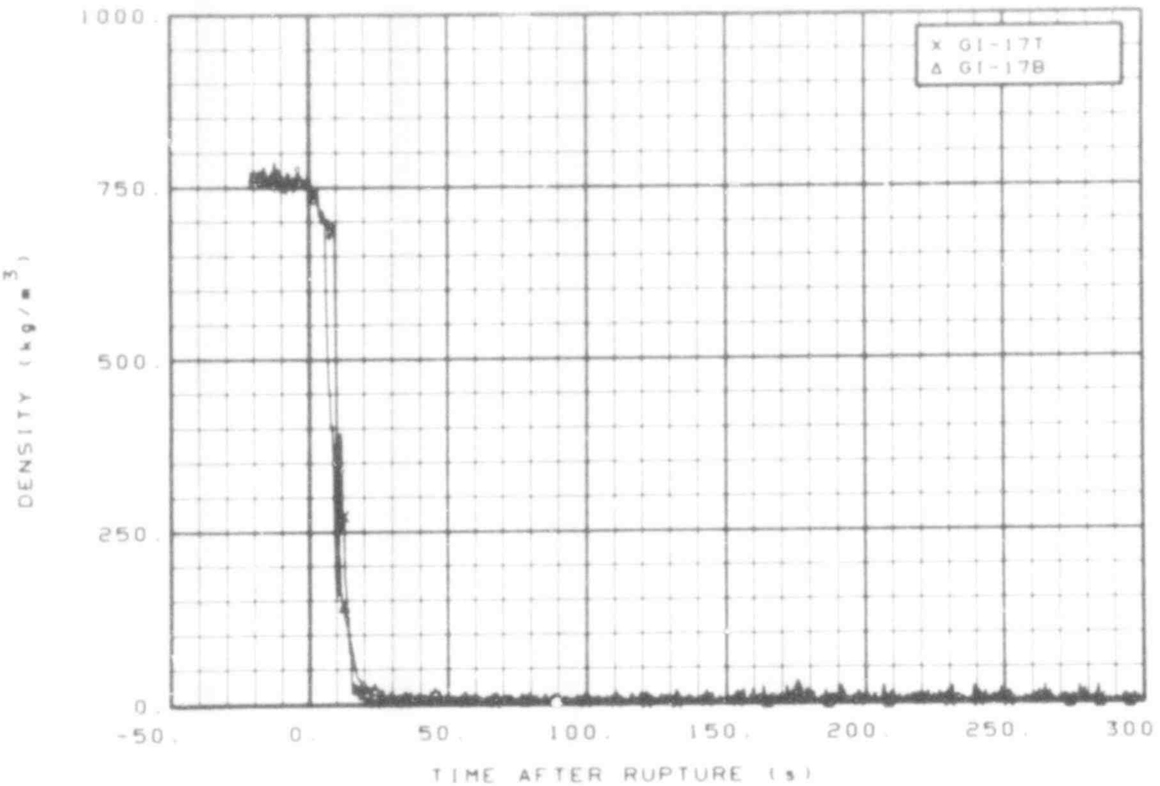

Fig. 239 Density in intact loop (GI-17T and GI-17B), from -20 to 300 s.

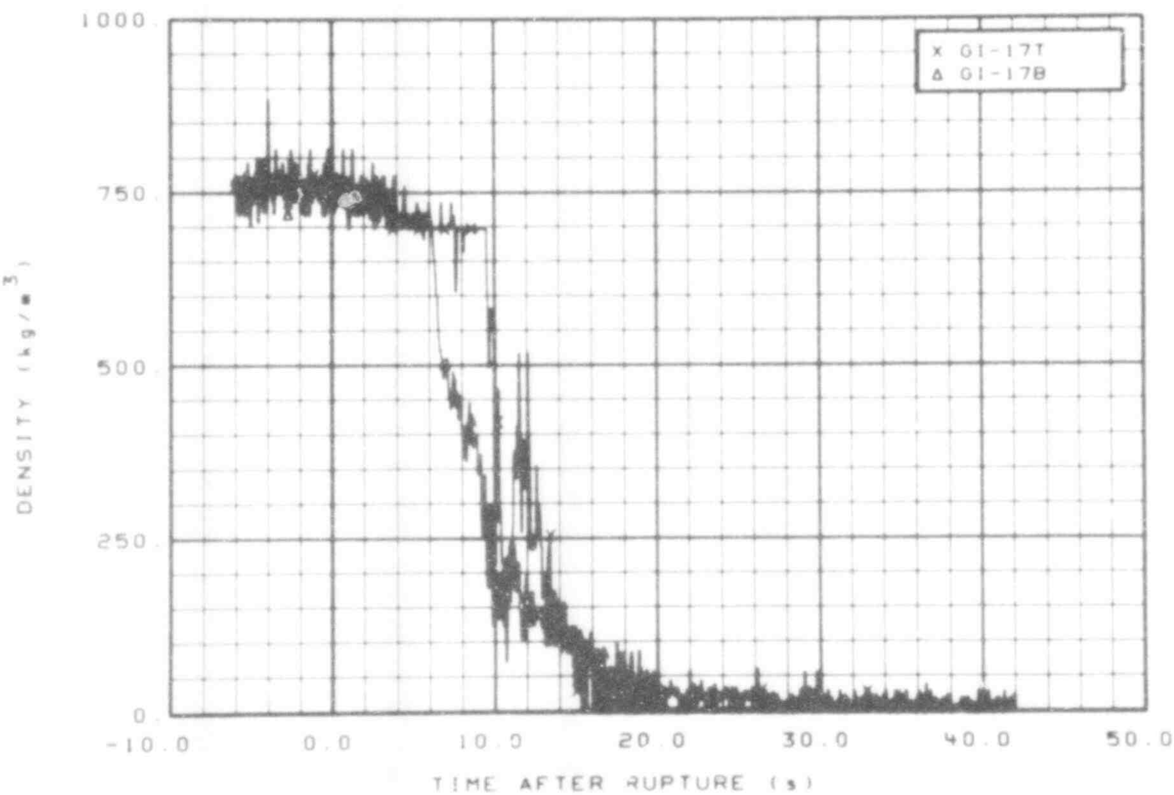

Fig. 240 Density in intact loop (GI-17T and GI-17B), from -6 to 42 s.

507 212

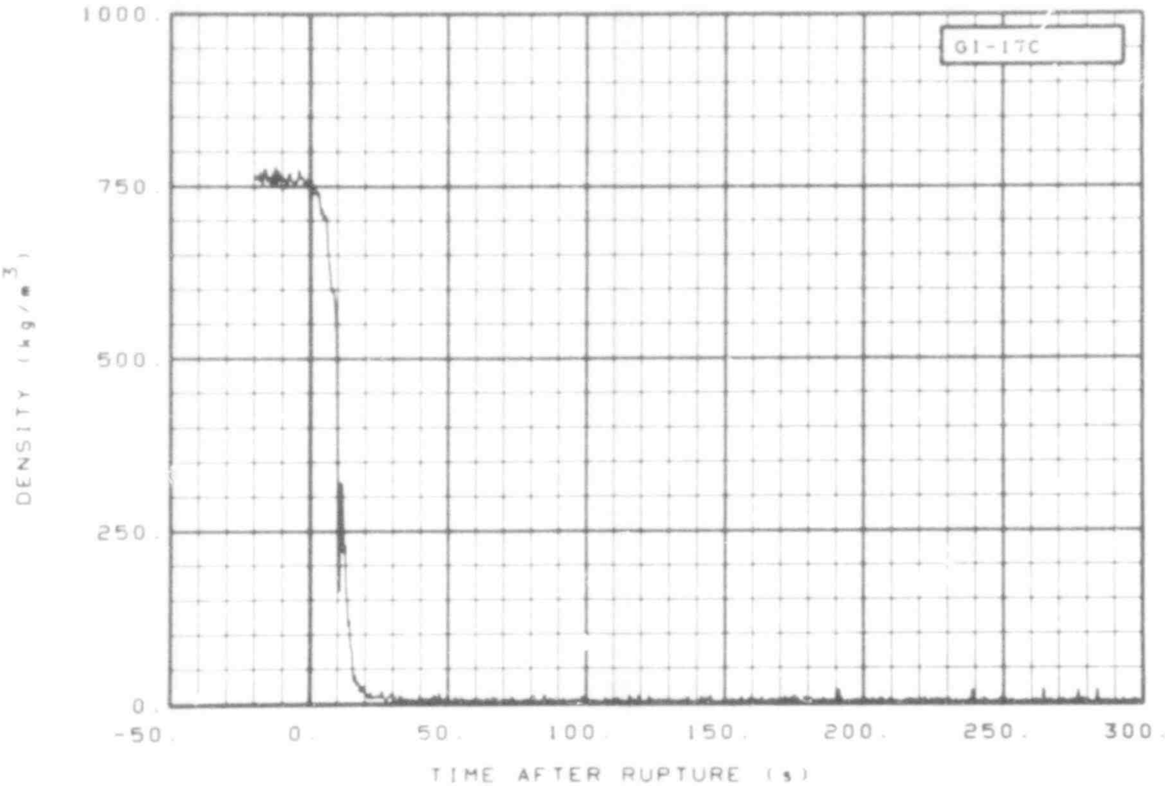

Fig. 241 Density in intact loop (GI-17C), from -20 to 300 s.

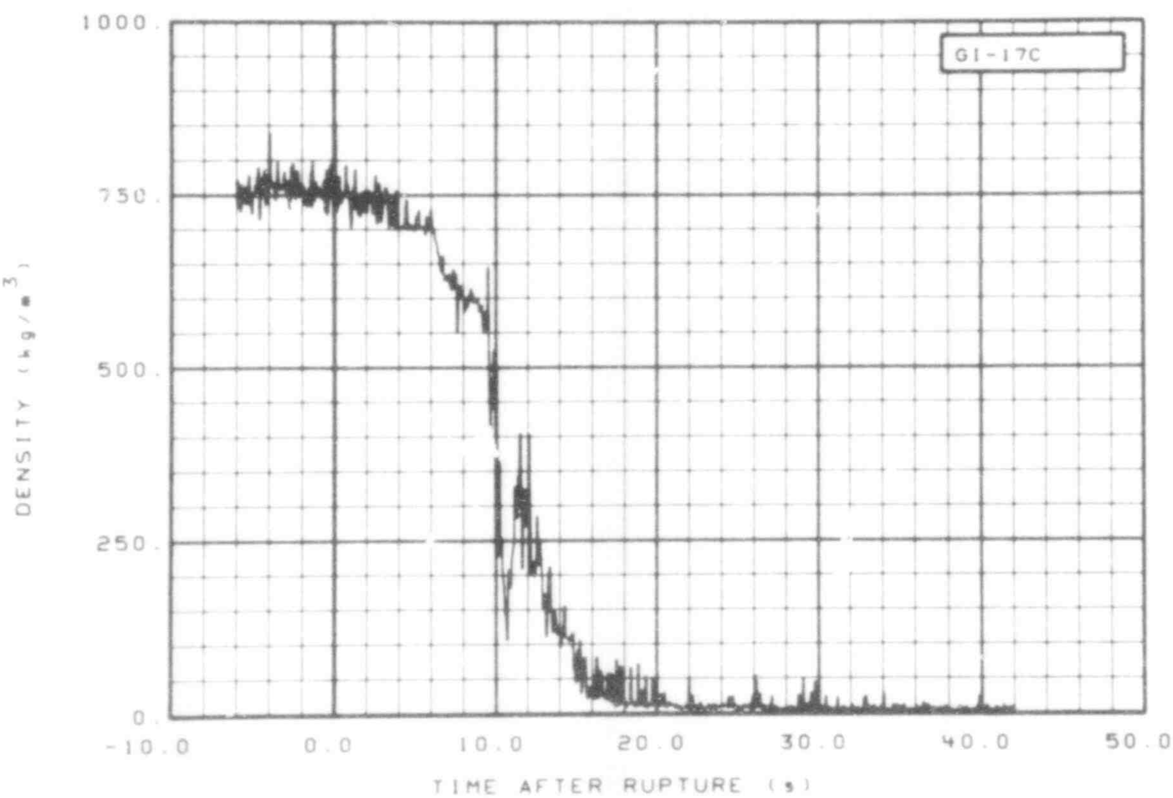

Fig. 242 Density in intact loop (GI-17C), from -6 to 42 s.

507 213

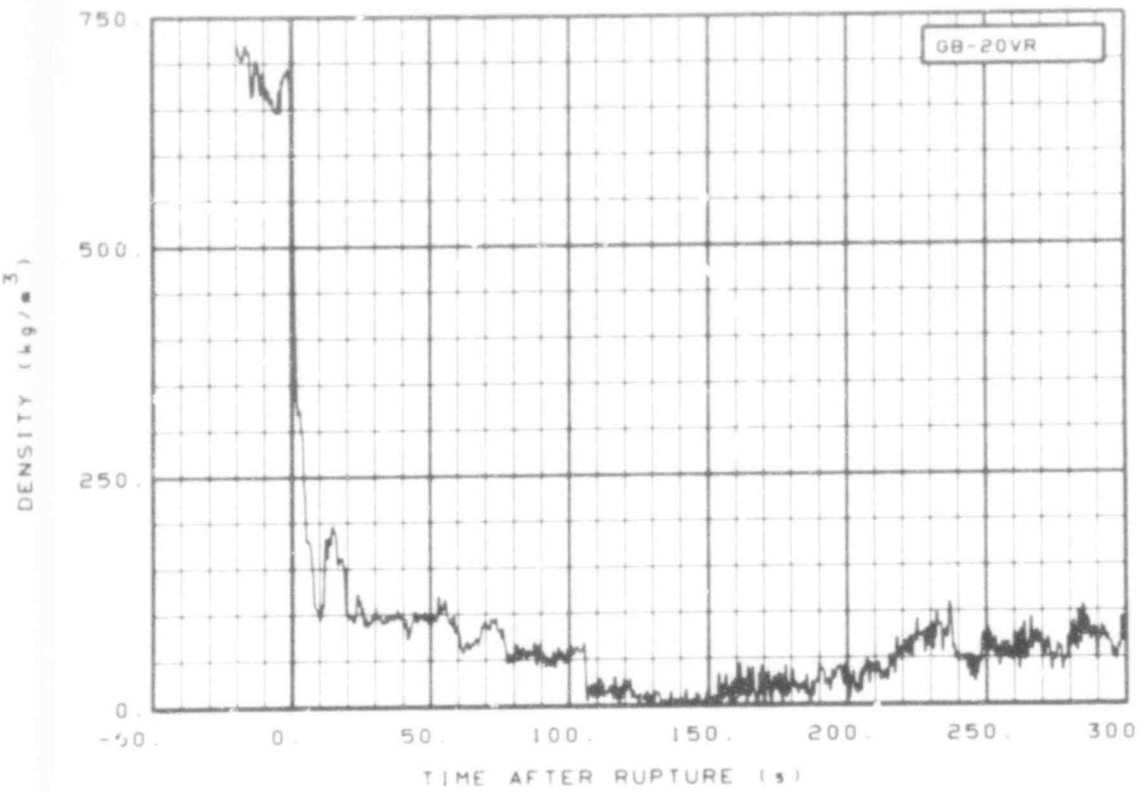

Fig. 243 Density in broken loop (GB-20VR), from -20 to 300 s.

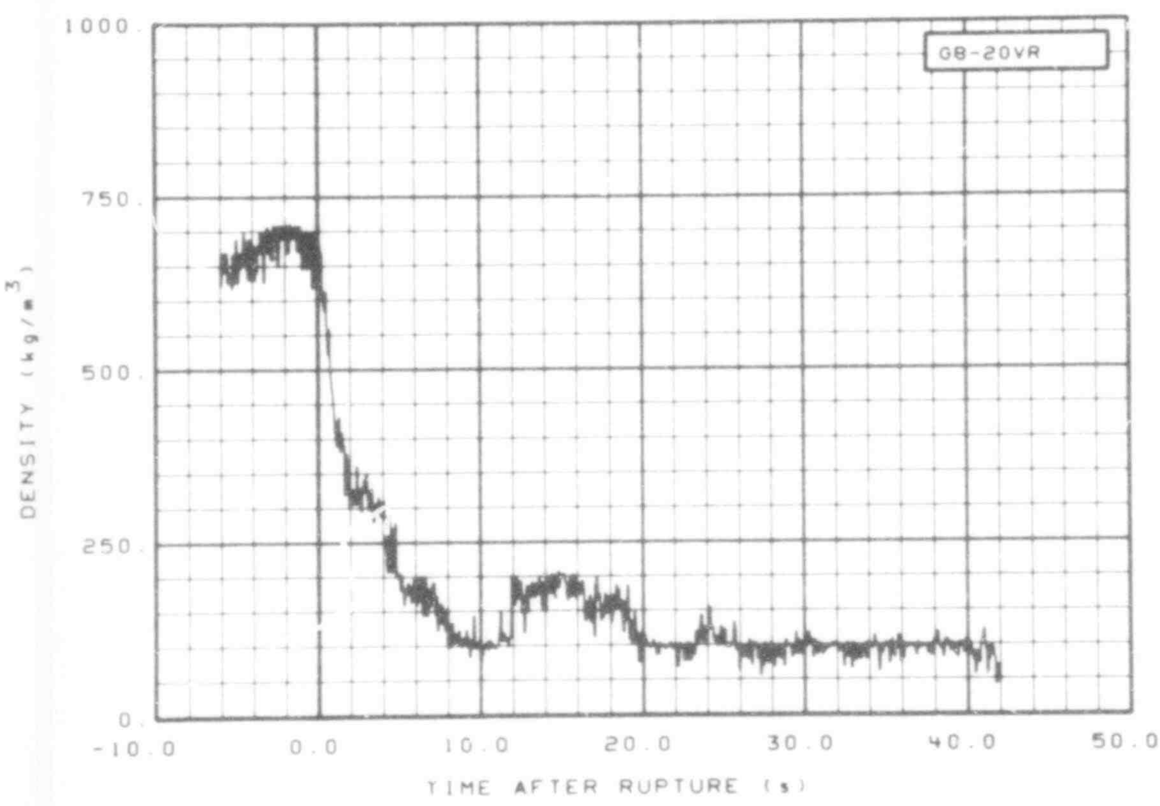

Fig. 244 Density in broken loop (GB-20VR), from -6 to 42 s.

507 214

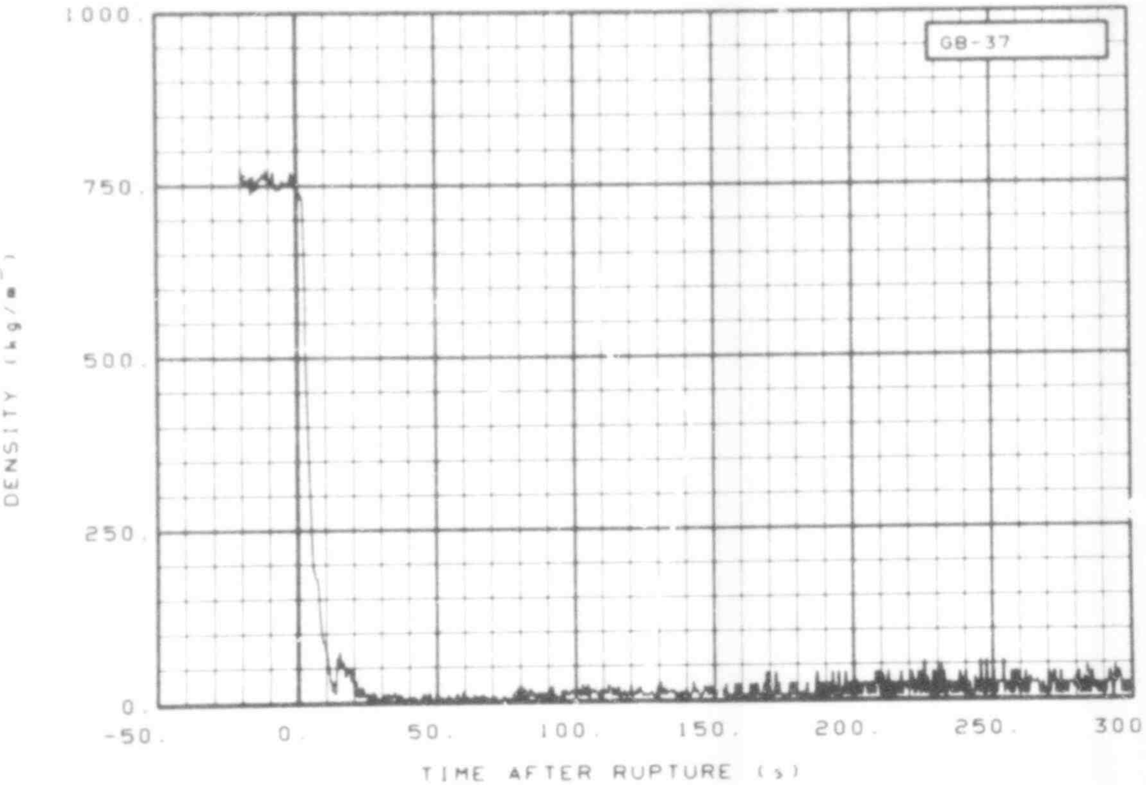

Fig. 245 Density in broken loop (GB-37), from -20 to 300 s.

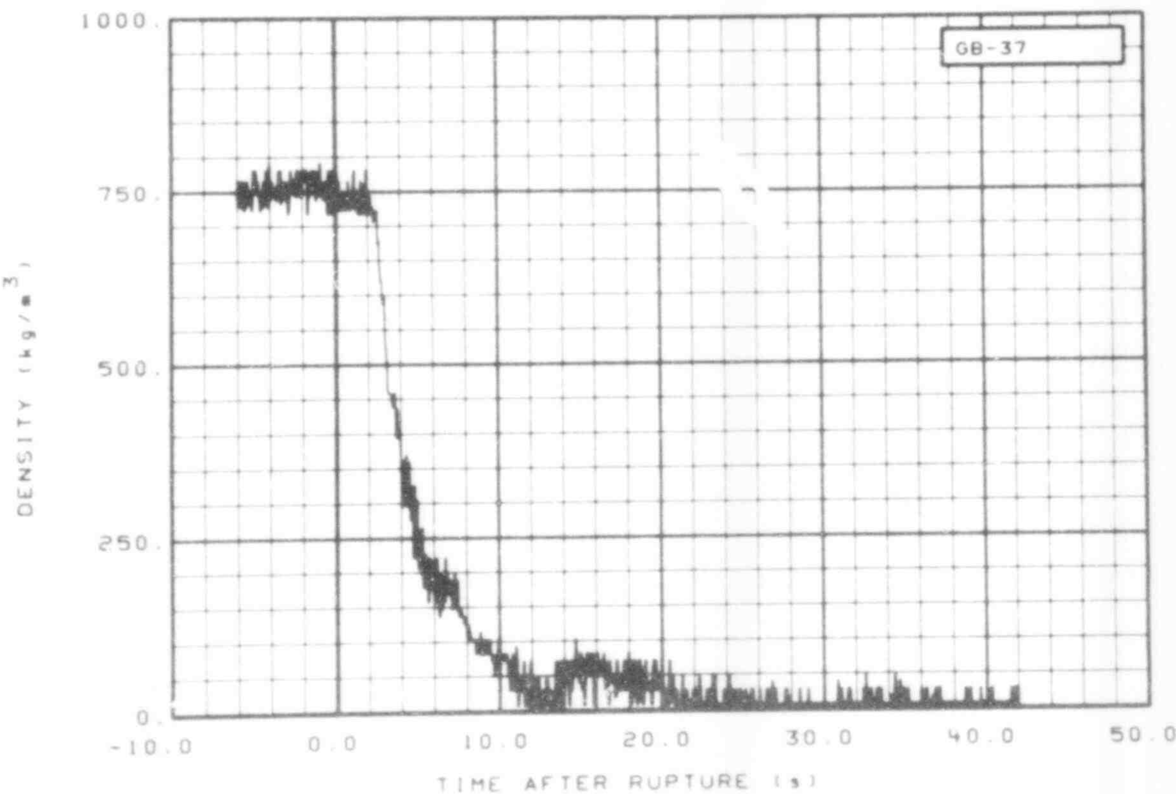

Fig. 246 Density in broken loop (GB-37), from -6 to 42 s.

507 215

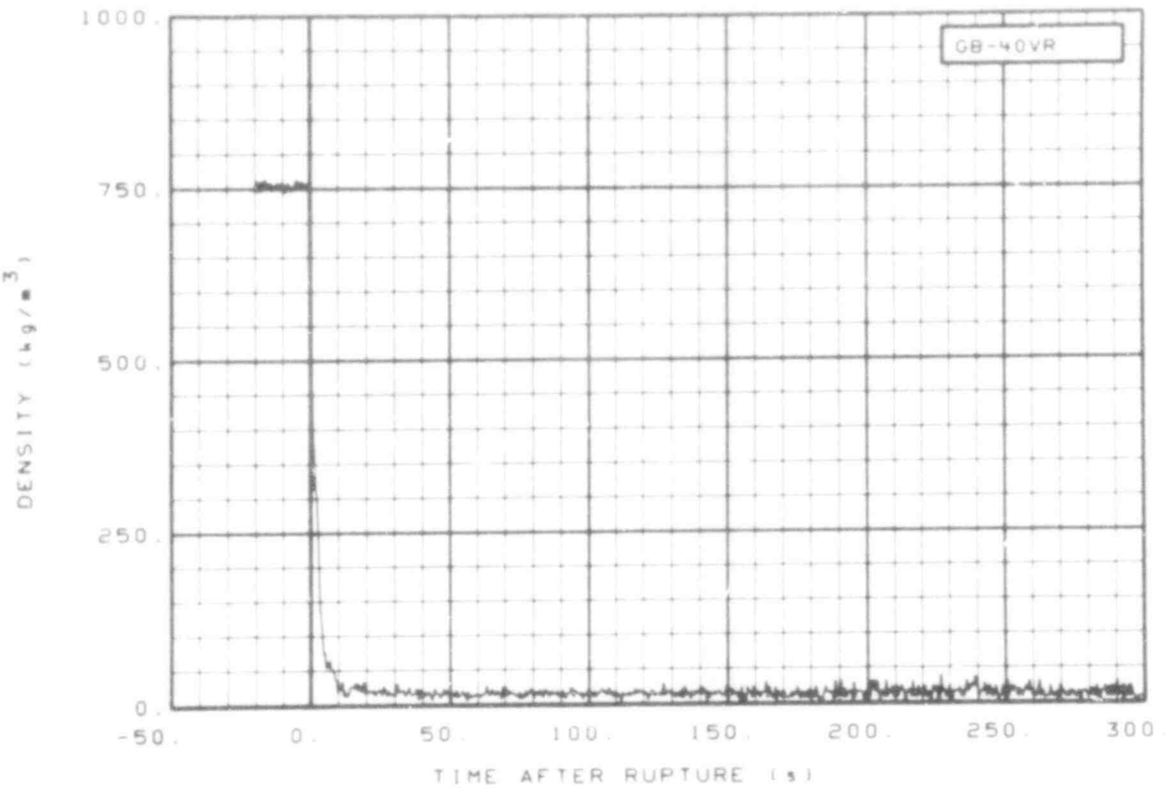

Fig. 247 Density in broken loop (GB-40VR), from -20 to 300 s.

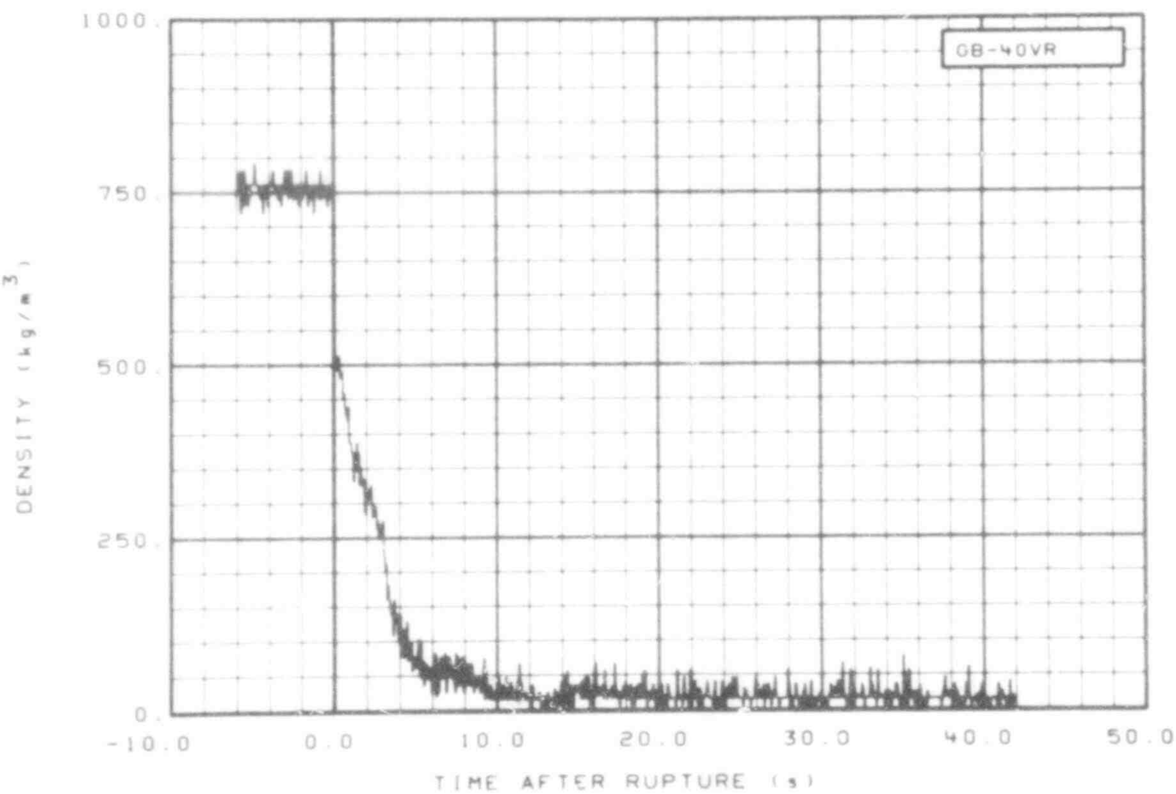

Fig. 248 Density in broken loop (GB-40VR), from -6 to 42 s.

507 216

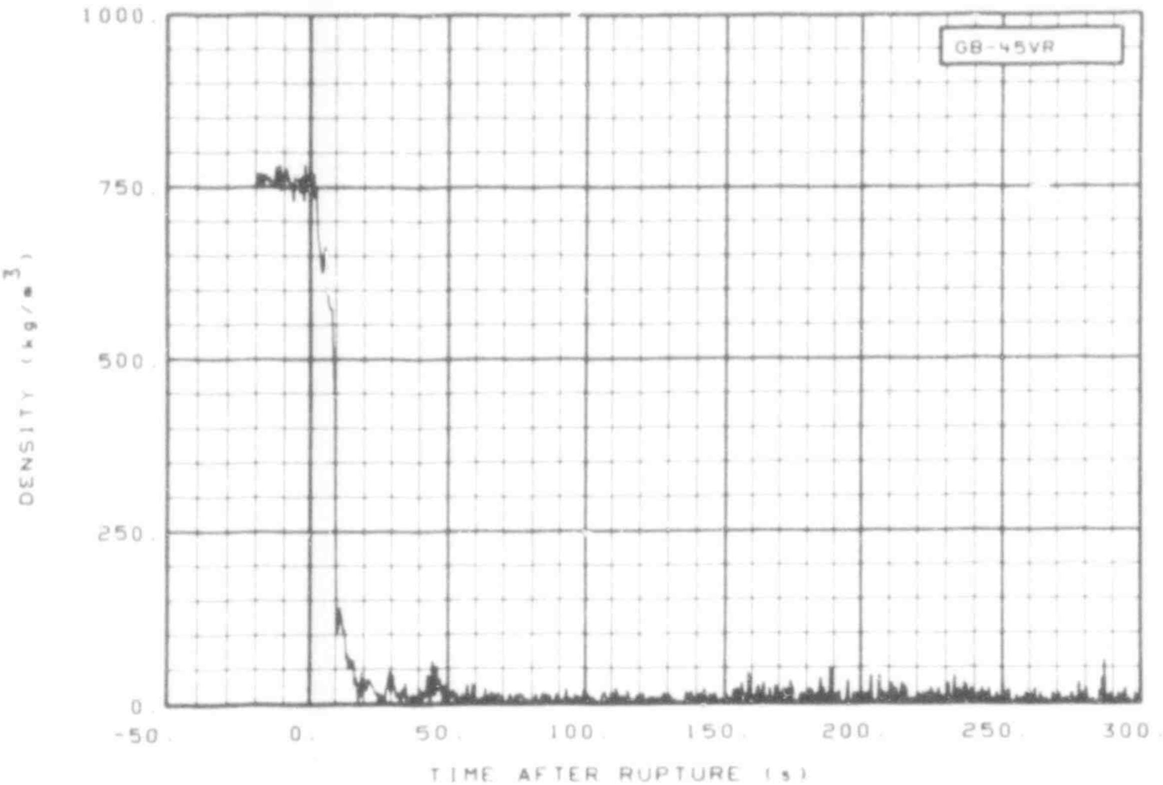

Fig. 249 Density in broken loop (GB-45VR), from -20 to 300 s.

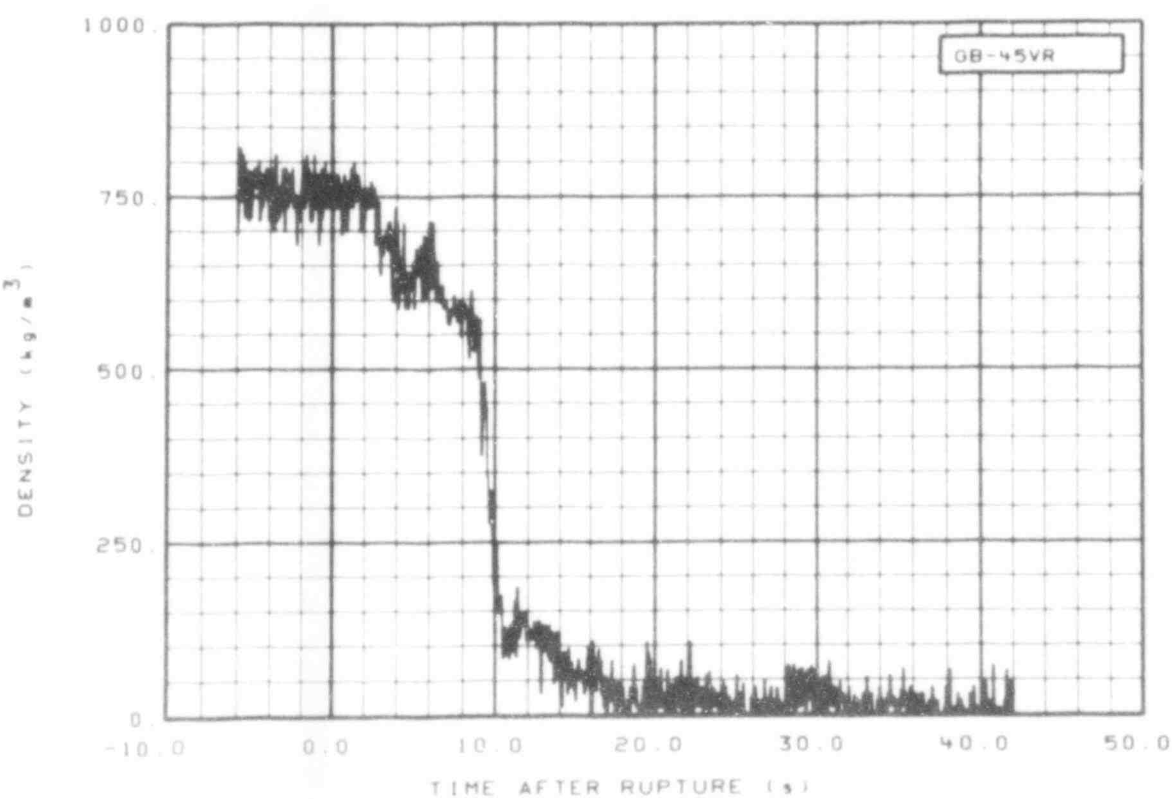

Fig. 250 Density in broken loop (GB-45VR), from -6 to 42 s.

507 217

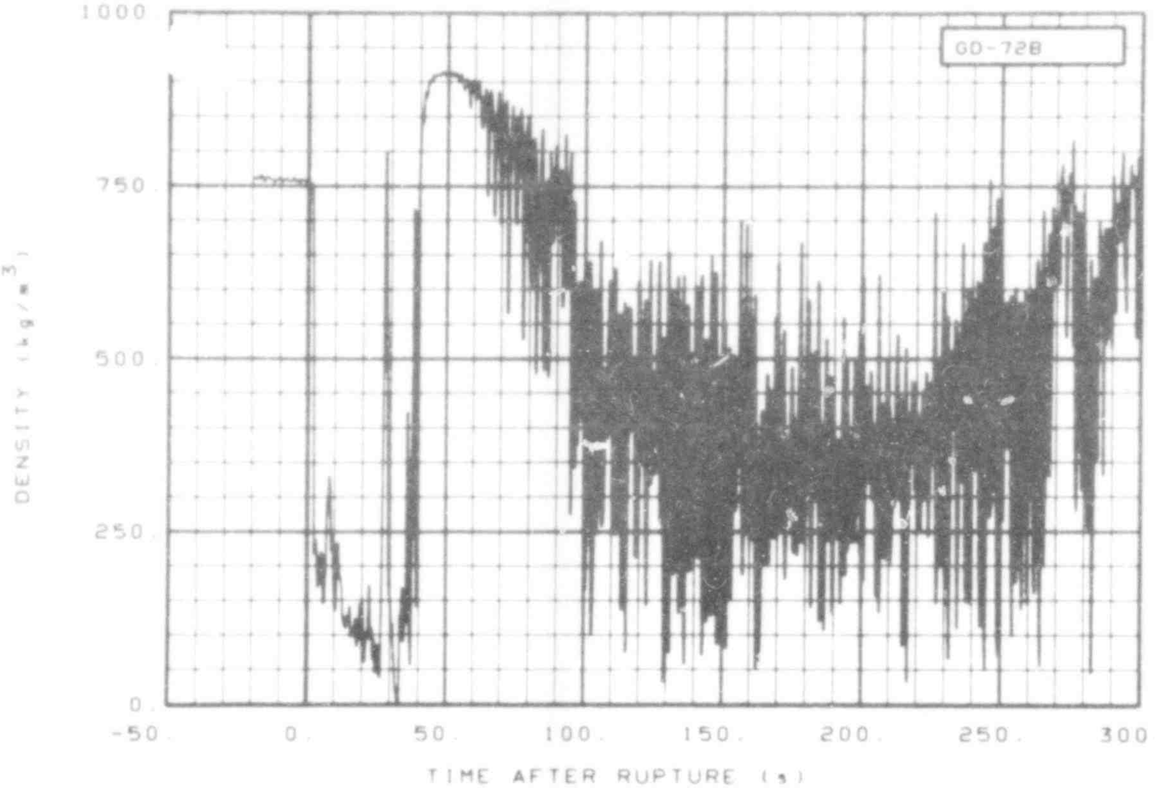

Fig. 251 Density in downcomer (GD-72B), from -20 to 300 s.

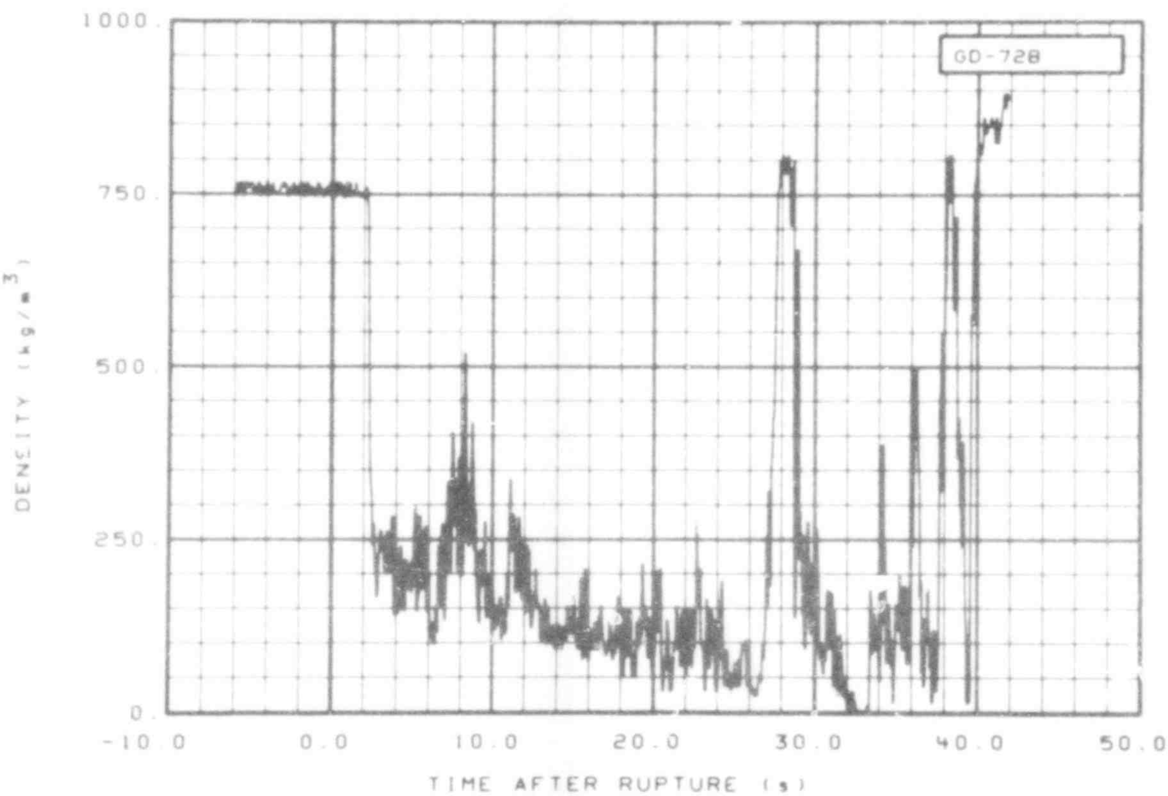

Fig. 252 Density in downcomer (GD-72B), from -6 to 42 s.

507 218

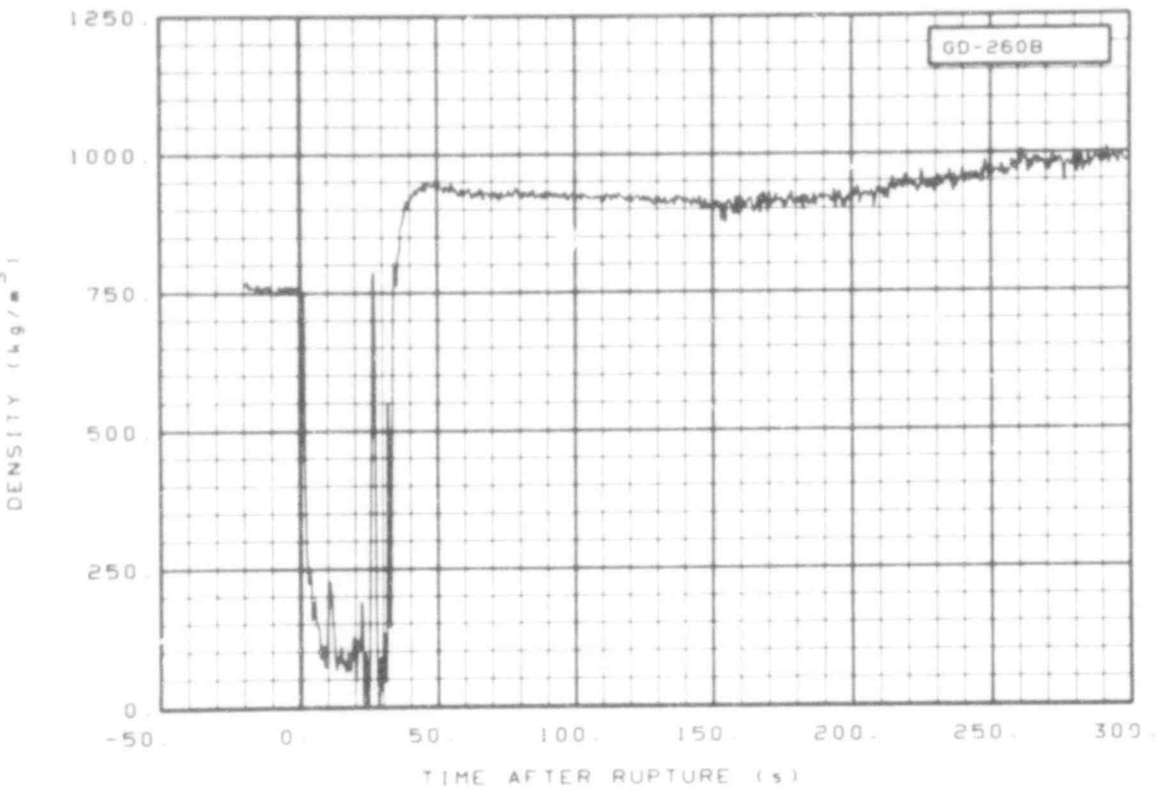

Fig. 253 Density in downcomer (GD-260B), from -20 to 300 s.

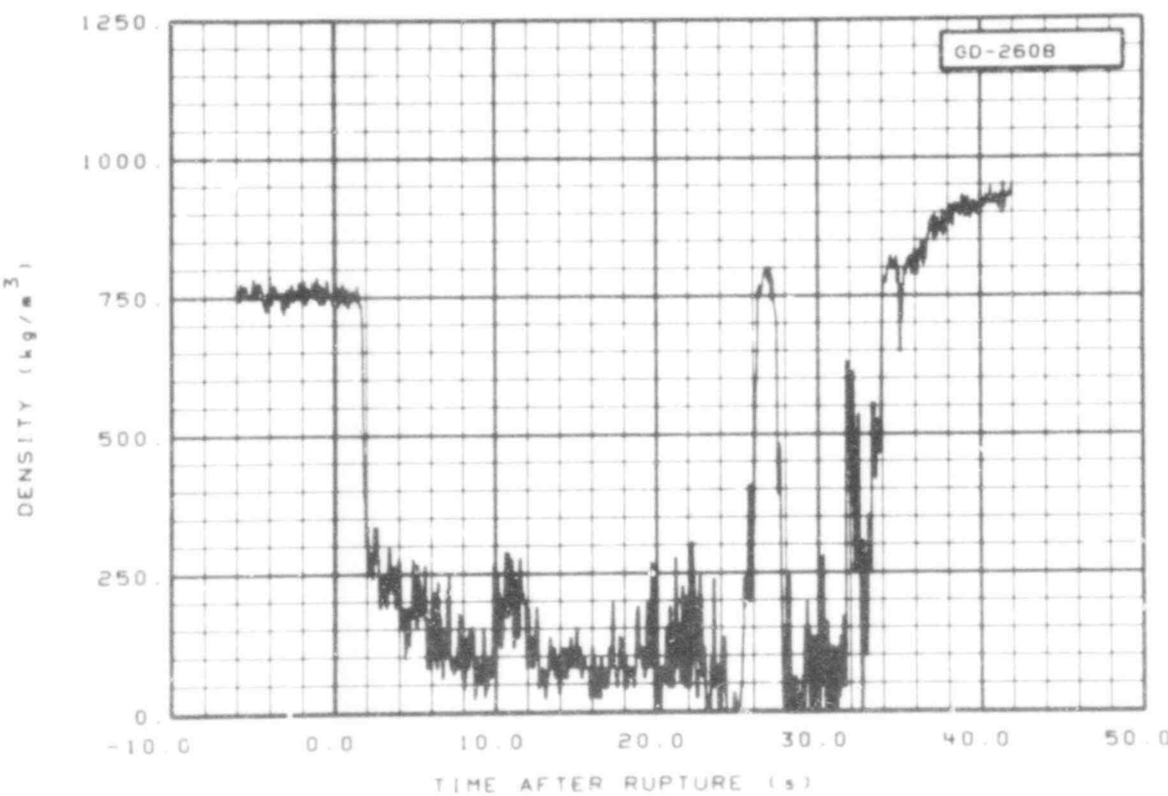

Fig. 254 Density in downcomer (GD-260B), from -6 to 42 s.

507 219

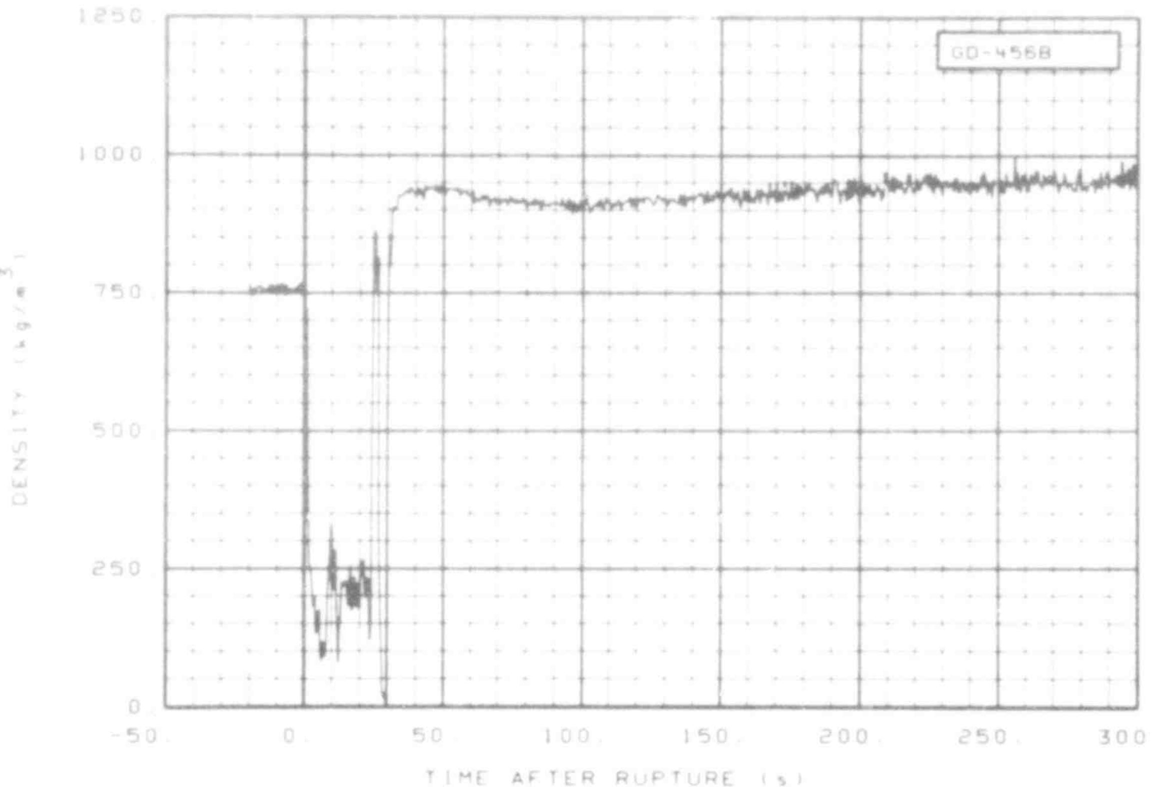

Fig. 255 Density in downcomer (GD-456B), from -20 to 300 s.

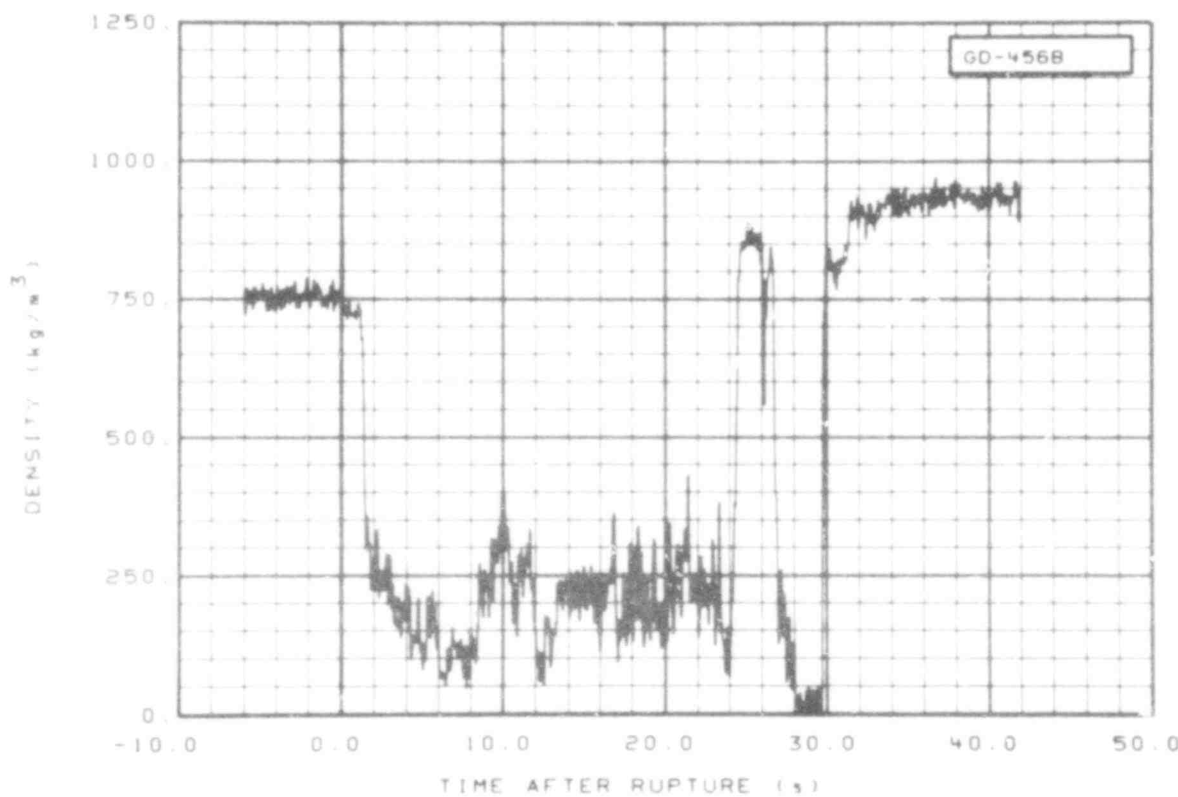

Fig. 256 Density in downcomer (GD-456B), from -6 to 42 s.

507 220

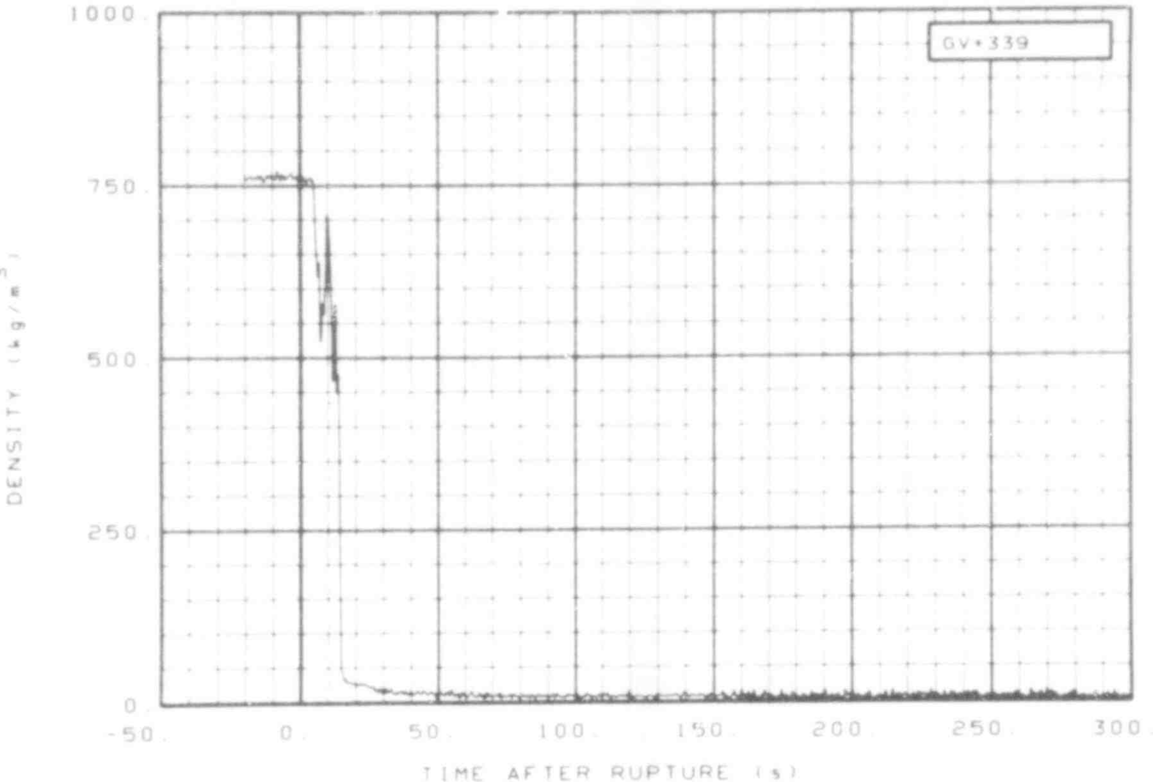

Fig. 257 Density in vessel (GV + 339), from -20 to 300 s.

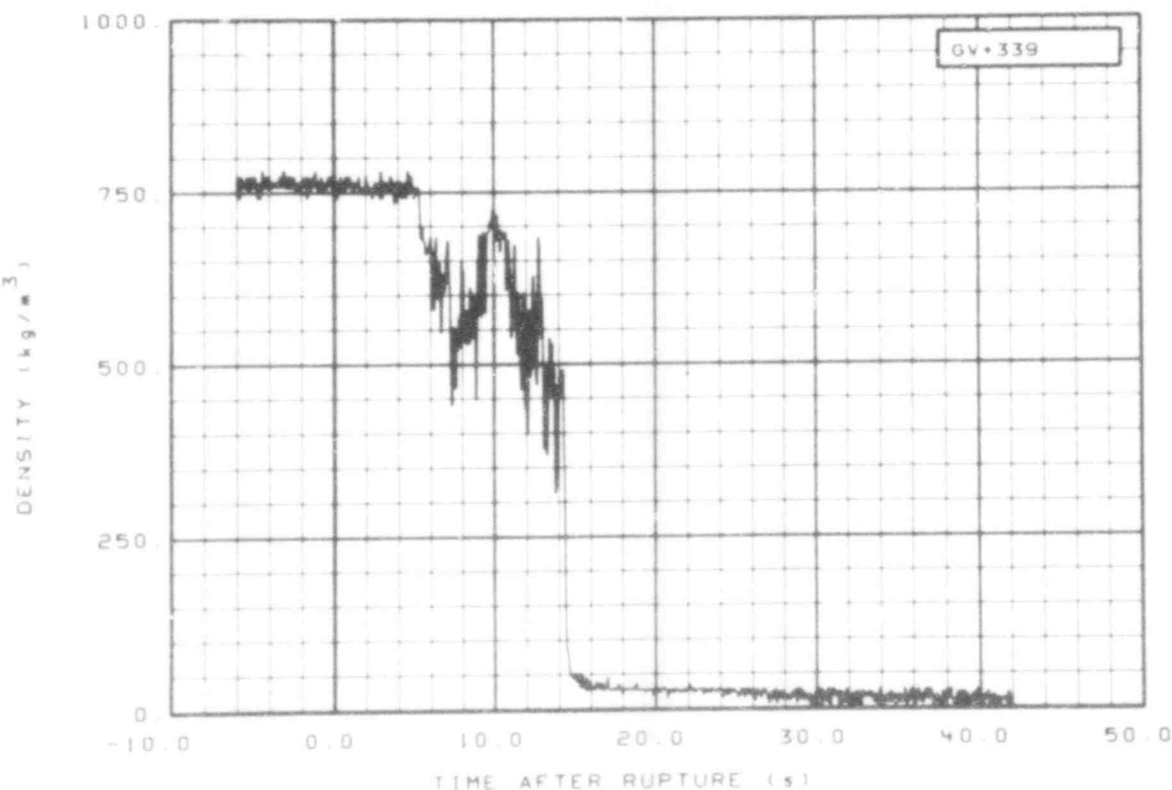

Fig. 258 Density in vessel (GV + 339), from -6 to 42 s.

507 221

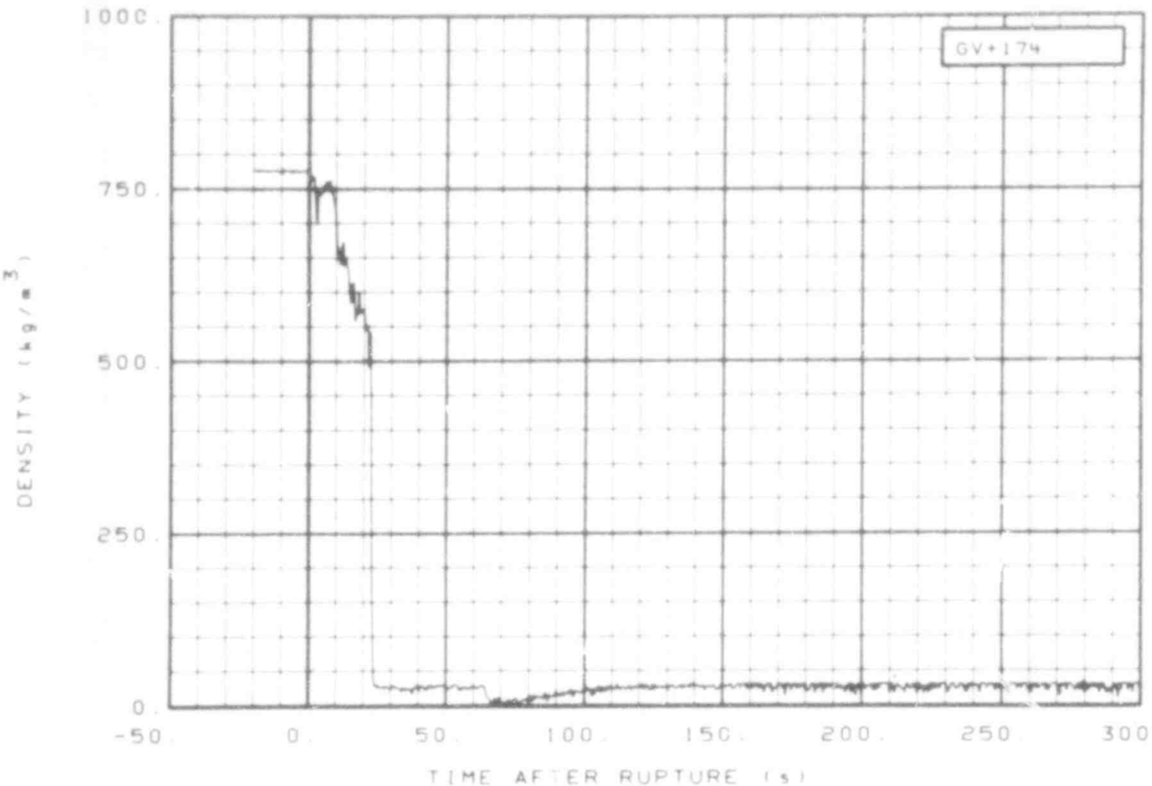

Fig. 259 Density in vessel (GV + 174), from -20 to 300 s.

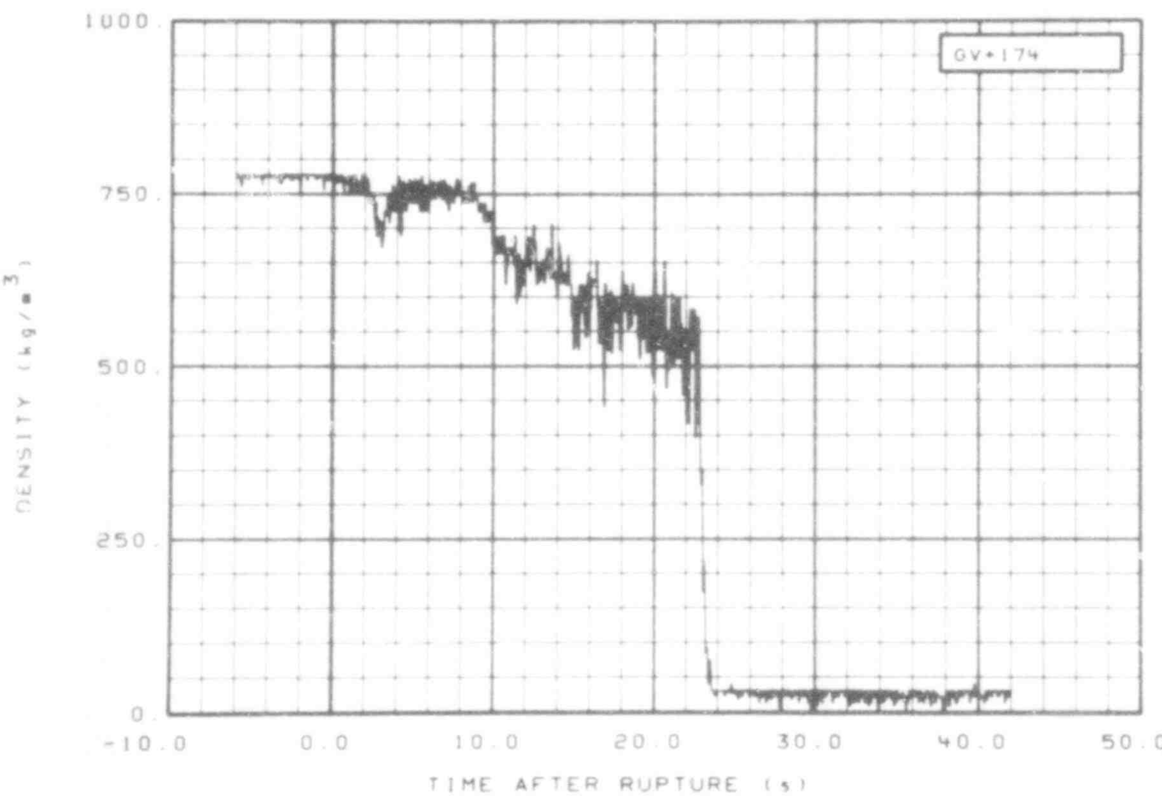

Fig. 260 Density in vessel (GV + 174), from -6 to 42 s.

507 222

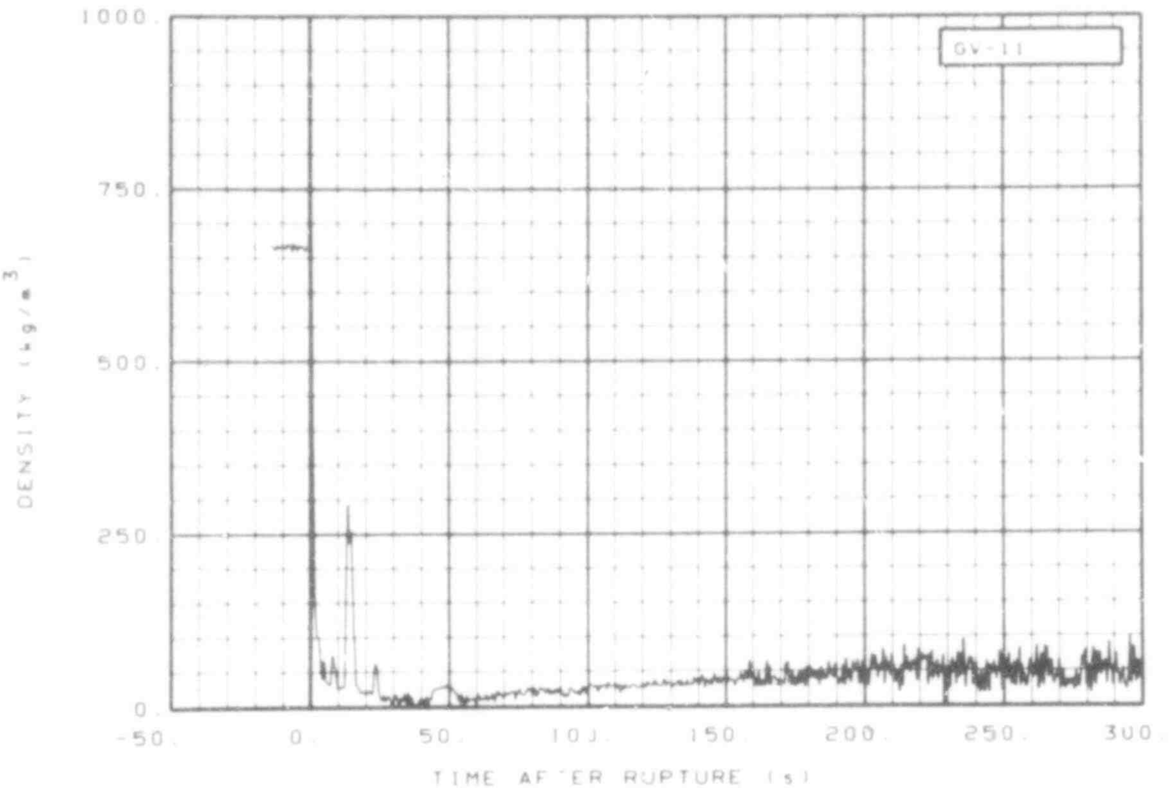

Fig. 261 Density in vessel (GV-11), from -20 to 300 s.

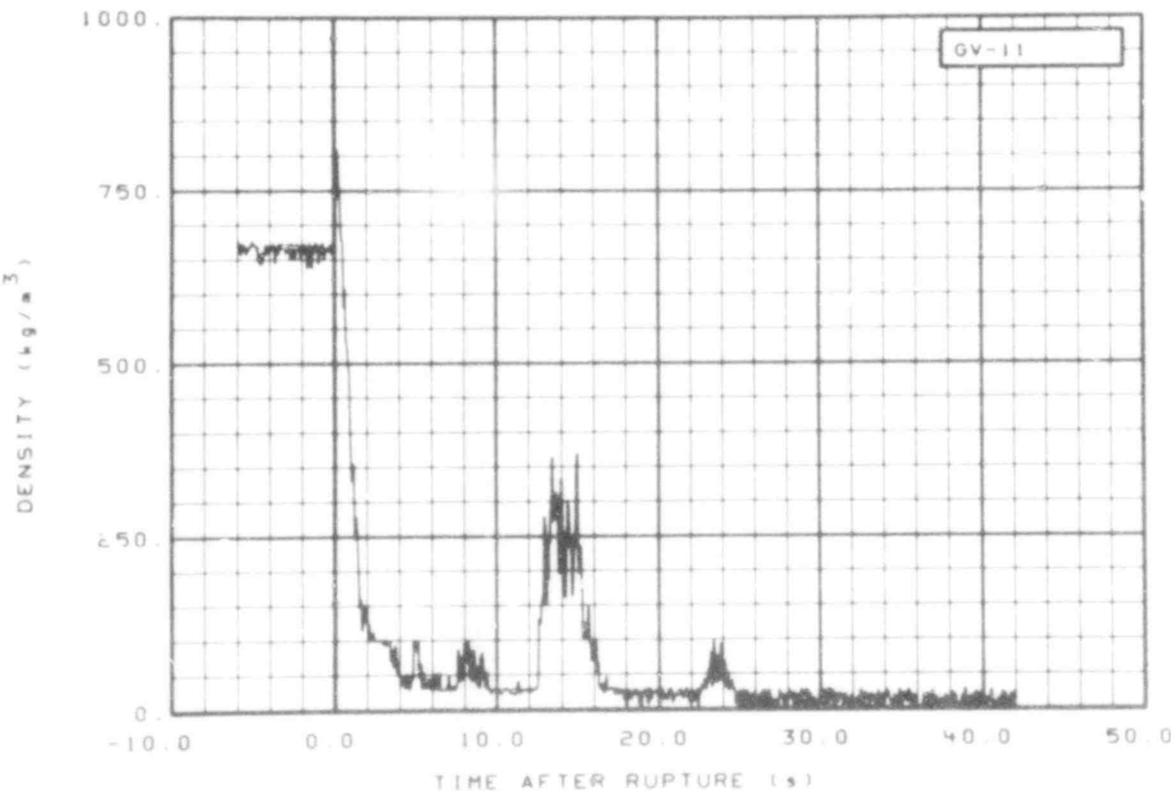

Fig. 262 Density in vessel (GV-11), from -6 to 42 s.

507 223

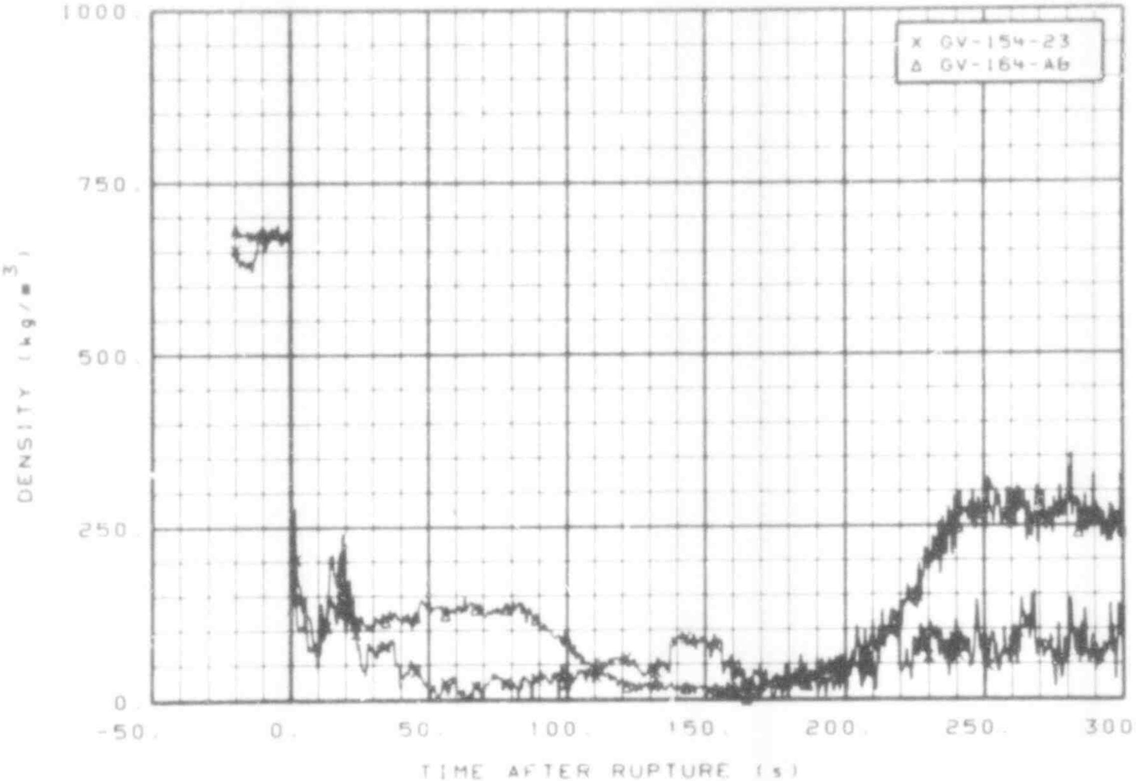

Fig. 263 Density in vessel (GV-154-23 and GV-164-AB), from -20 to 300 s.

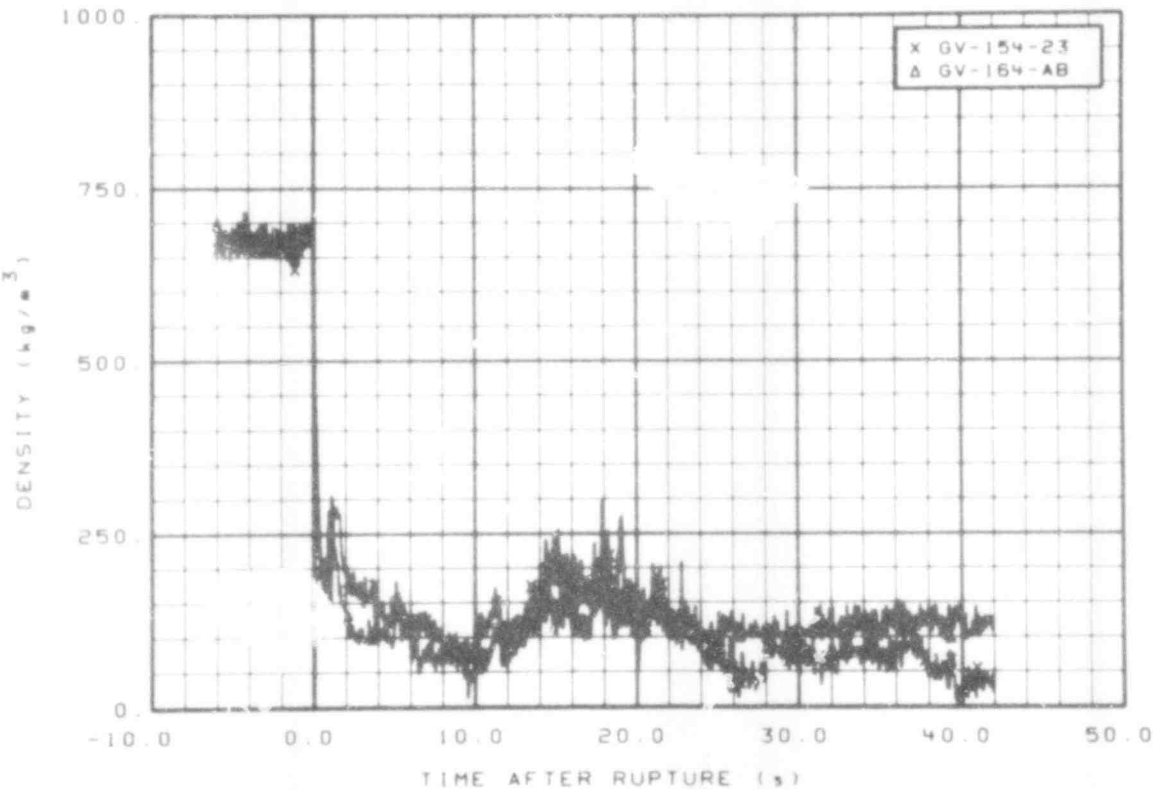

Fig. 264 Density in vessel (GV-154-23 and GV-164-AB), from -6 to 42 s.

507 224

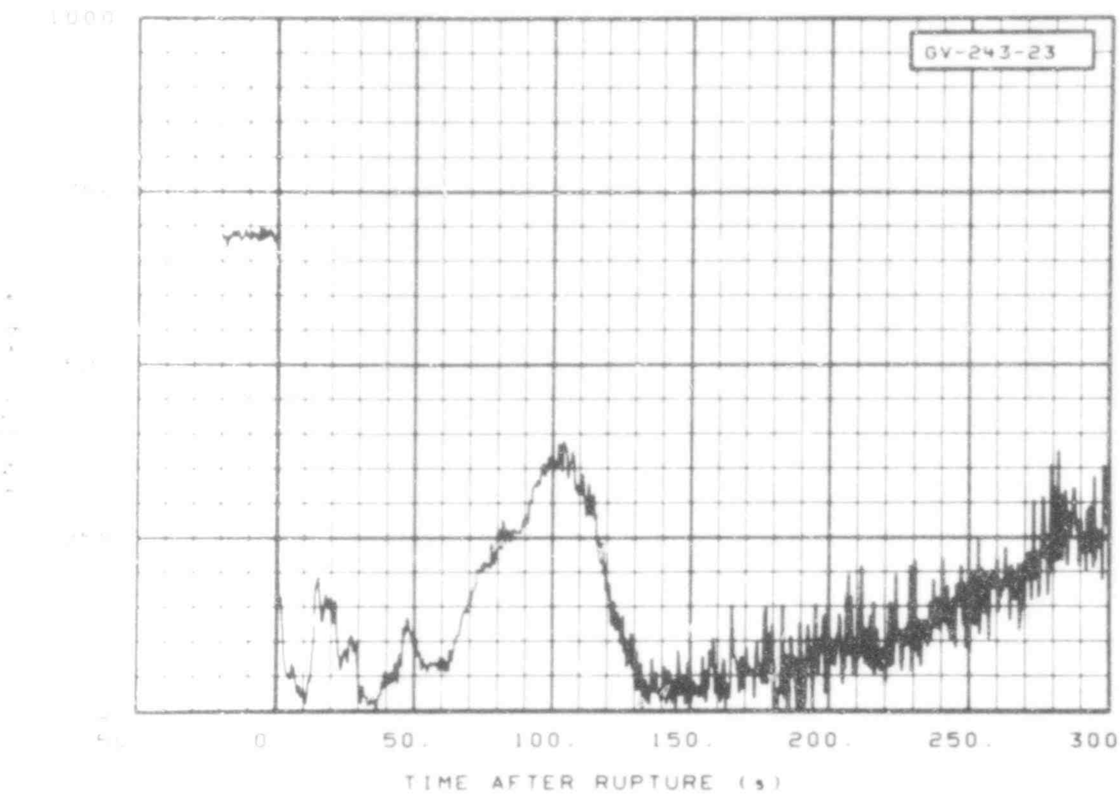

Fig. 265 Density in vessel (GV-243-23), from -20 to 300 s.

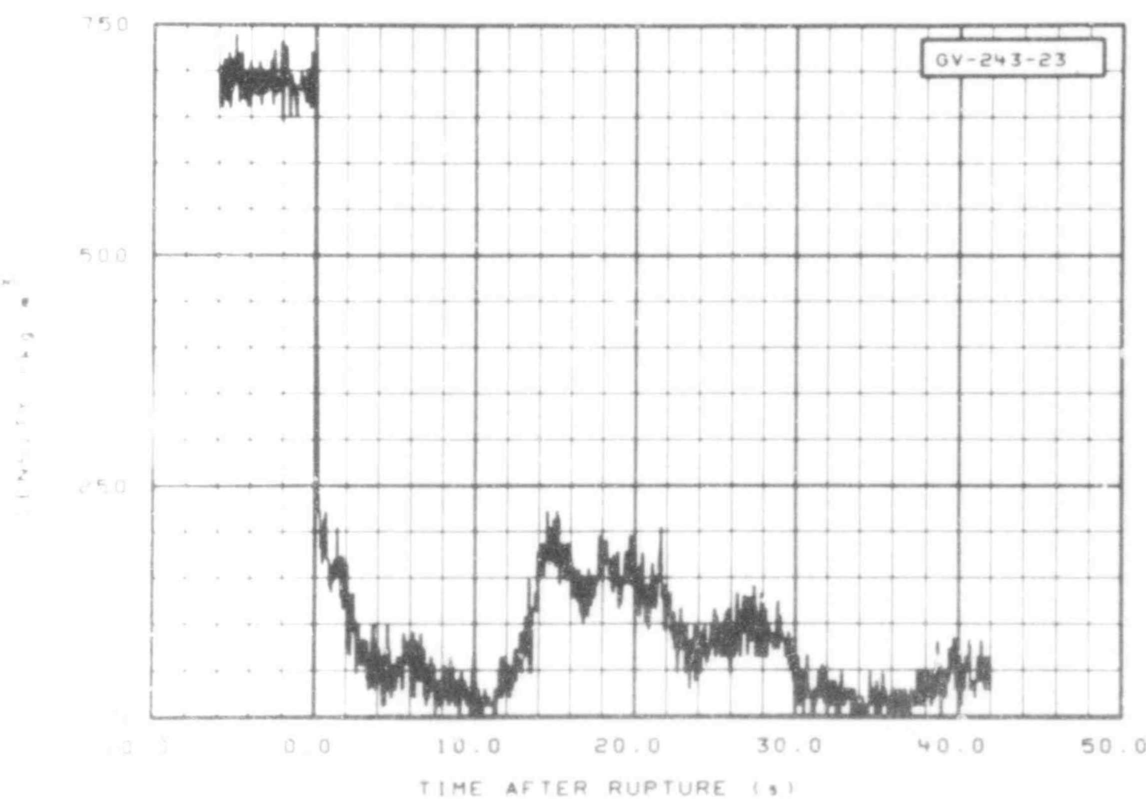

Fig. 266 Density in vessel (GV-243-23), from -6 to 42 s.

507 225

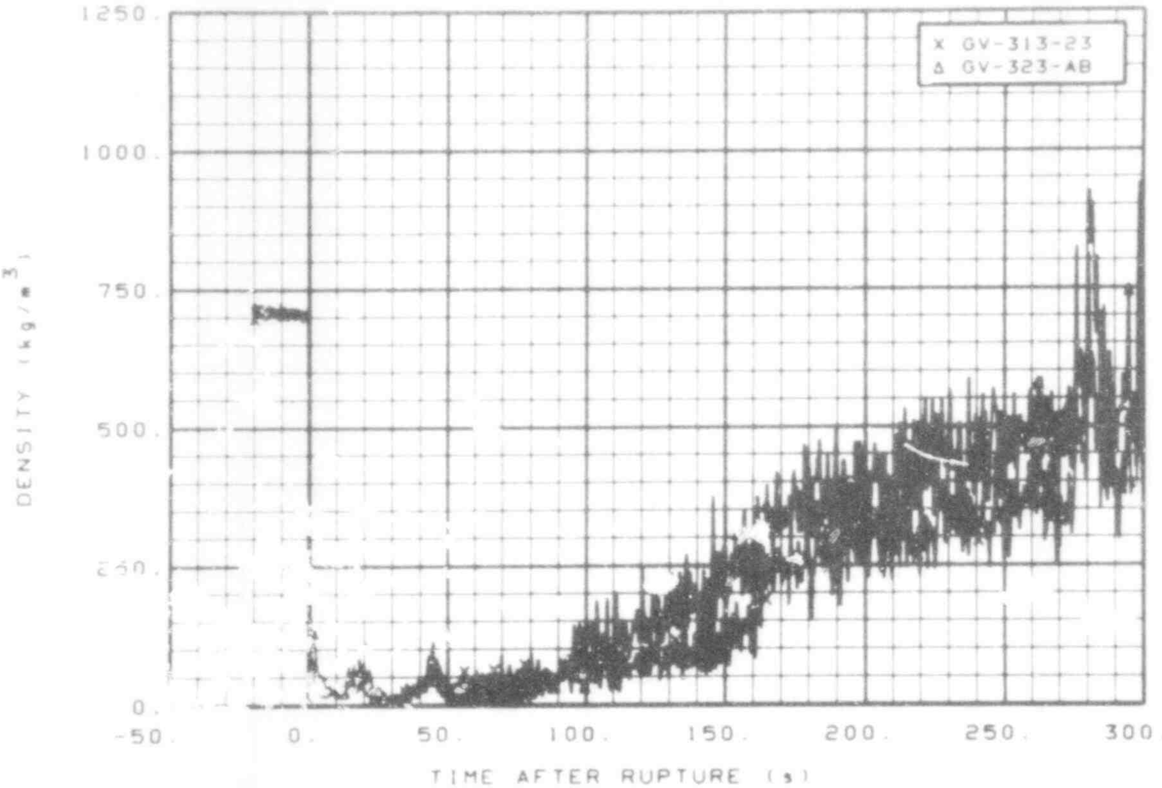

Fig. 267 Density in vessel (GV-313-23 and GV-323-AB), from -20 to 300 s.

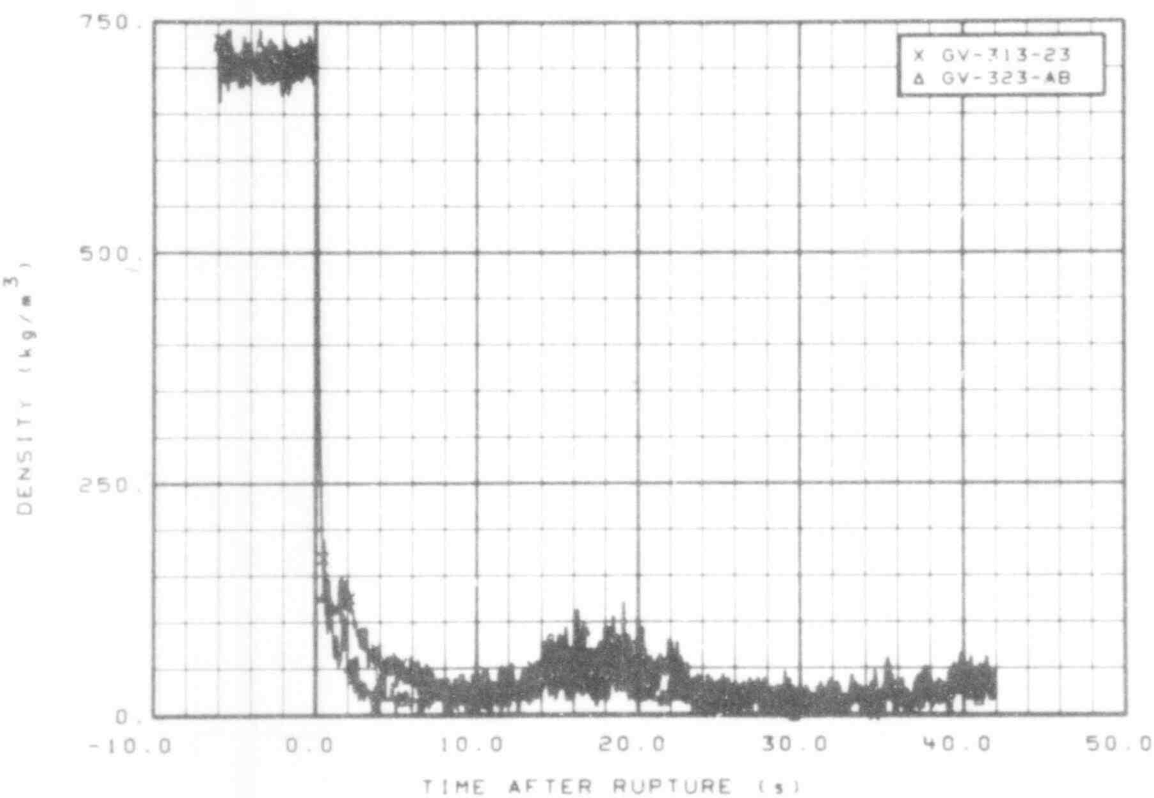

Fig. 268 Density in vessel (GV-313-23 and GV-323-AB), from -6 to 42 s.

507 226

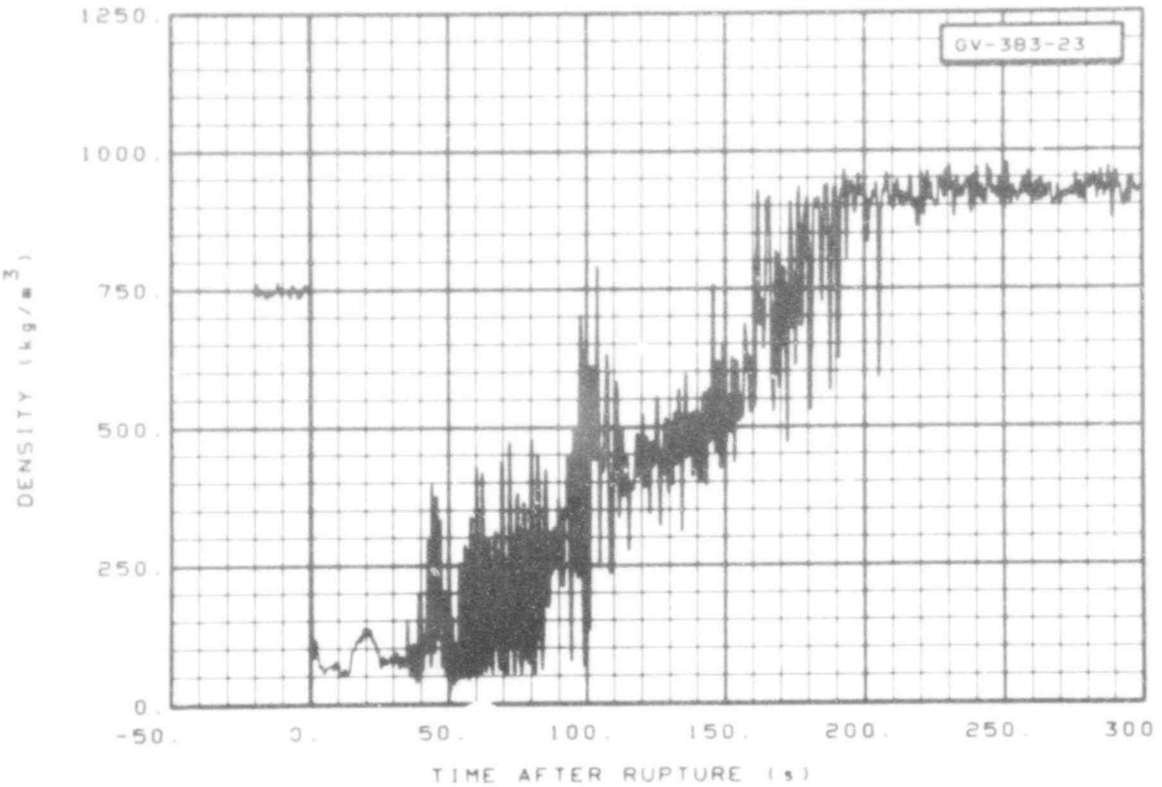

Fig. 269 Density in vessel (GV-383-23), from -20 to 300 s.

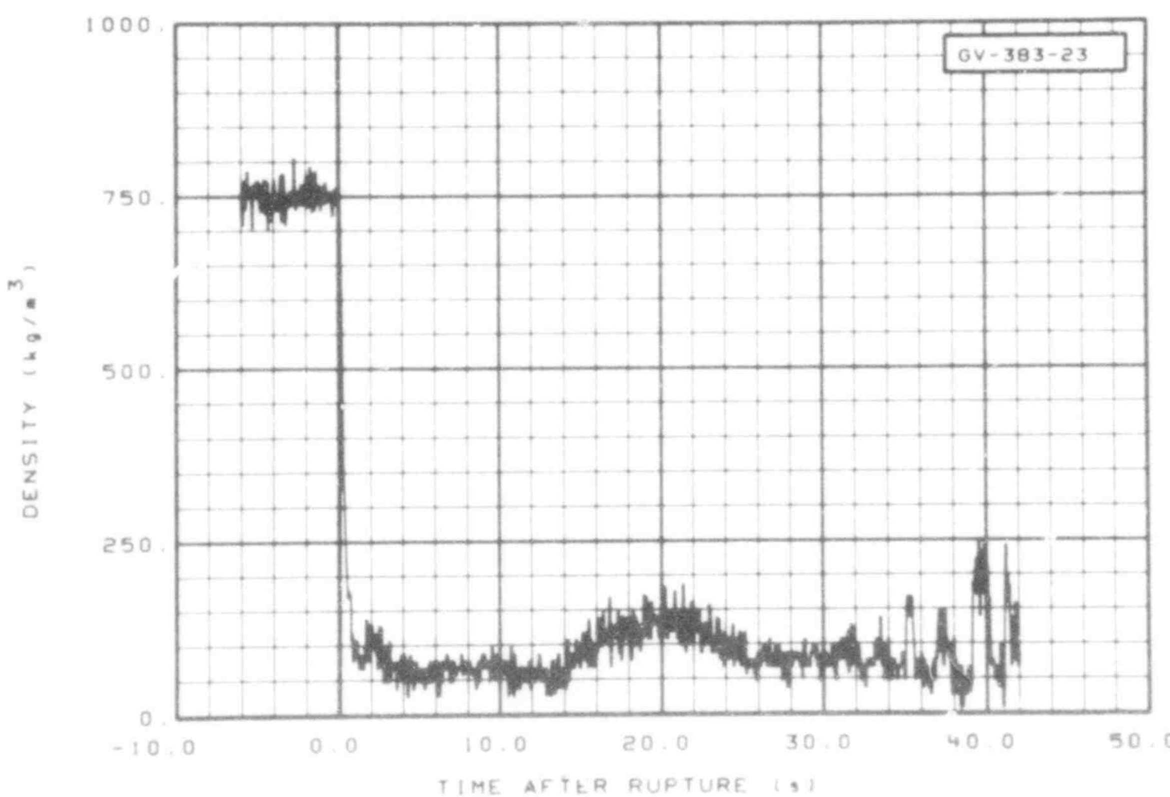

Fig. 270 Density in vessel (GV-383-23), from -6 to 42 s.

507 227

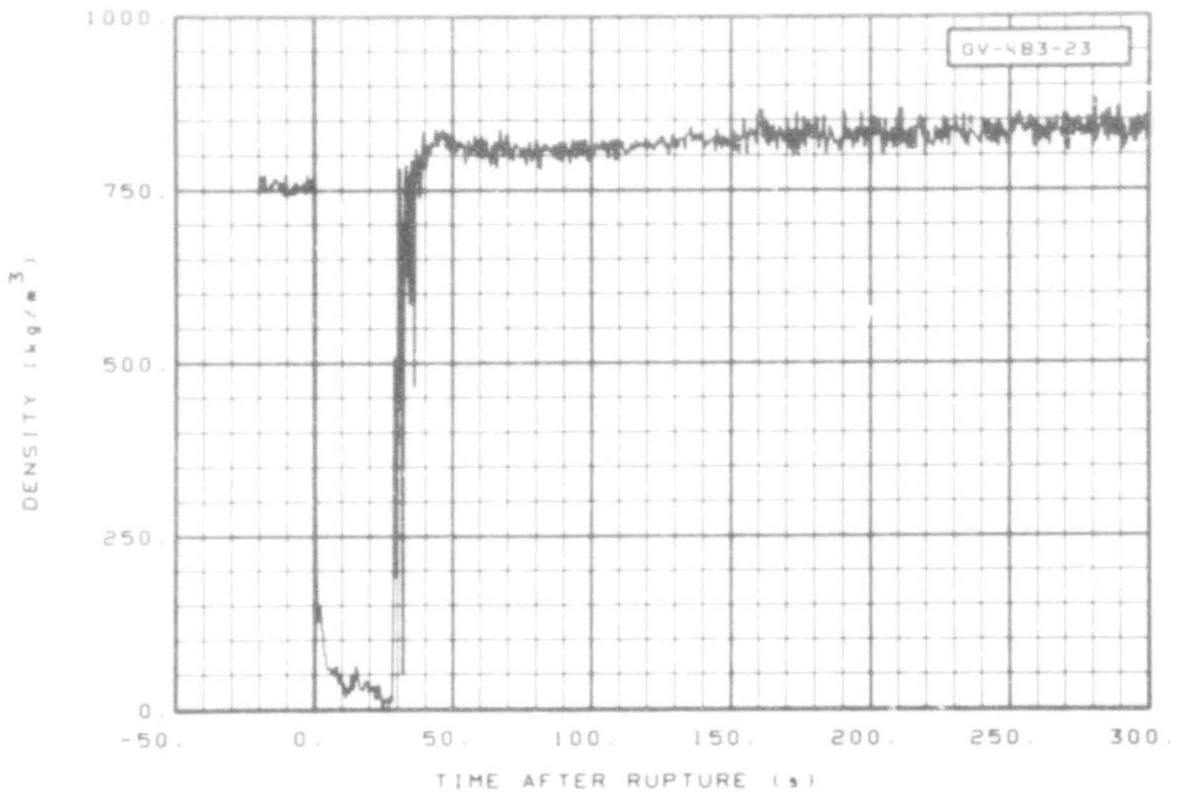

Fig. 271 Density in vessel (GV-483-23), from -20 to 300 s.

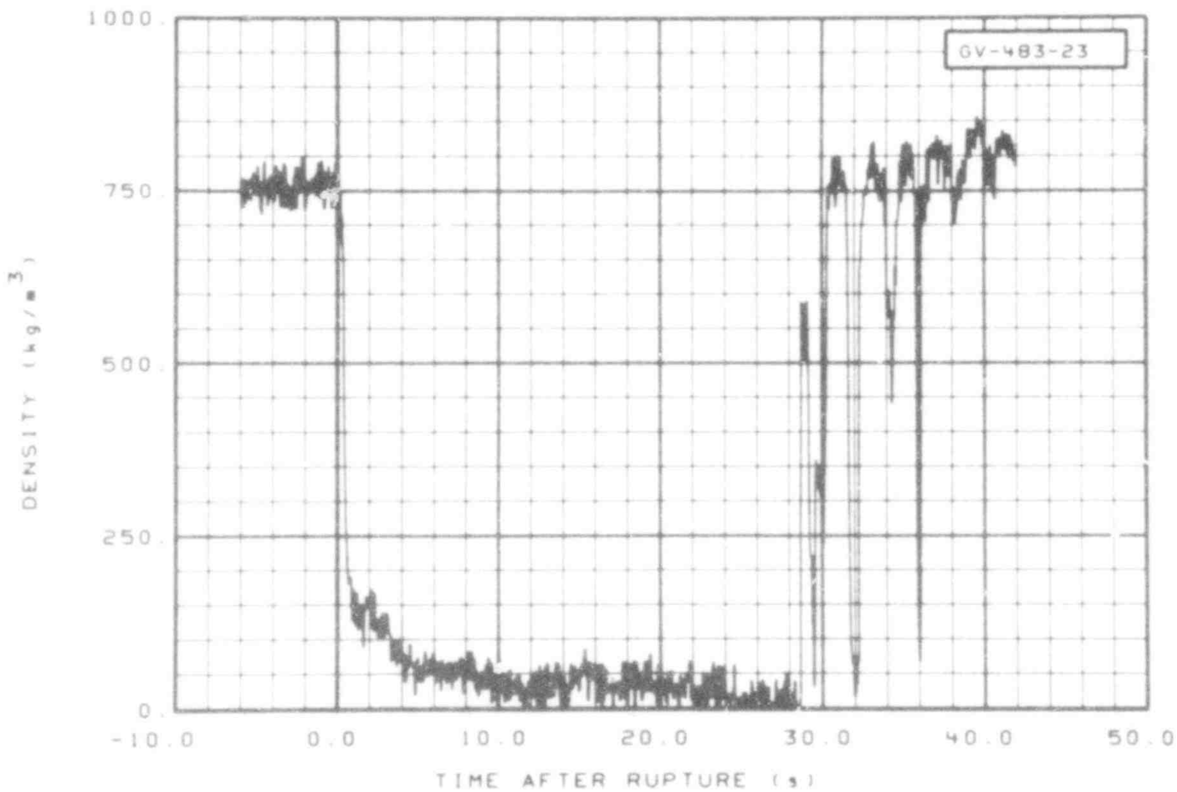

Fig. 272 Density in vessel (GV-483-23), from -6 to 42 s.

507 228

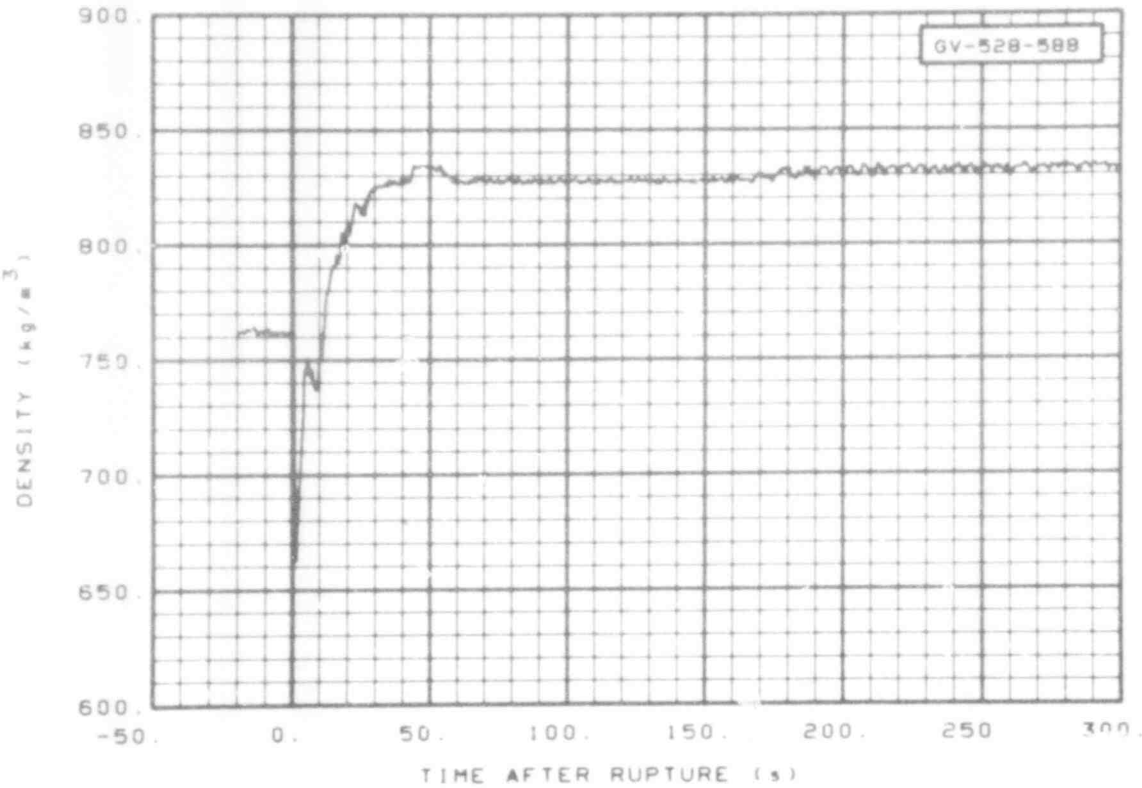

Fig. 273 Density in vessel (GV-528-588), from -20 to 300 s.

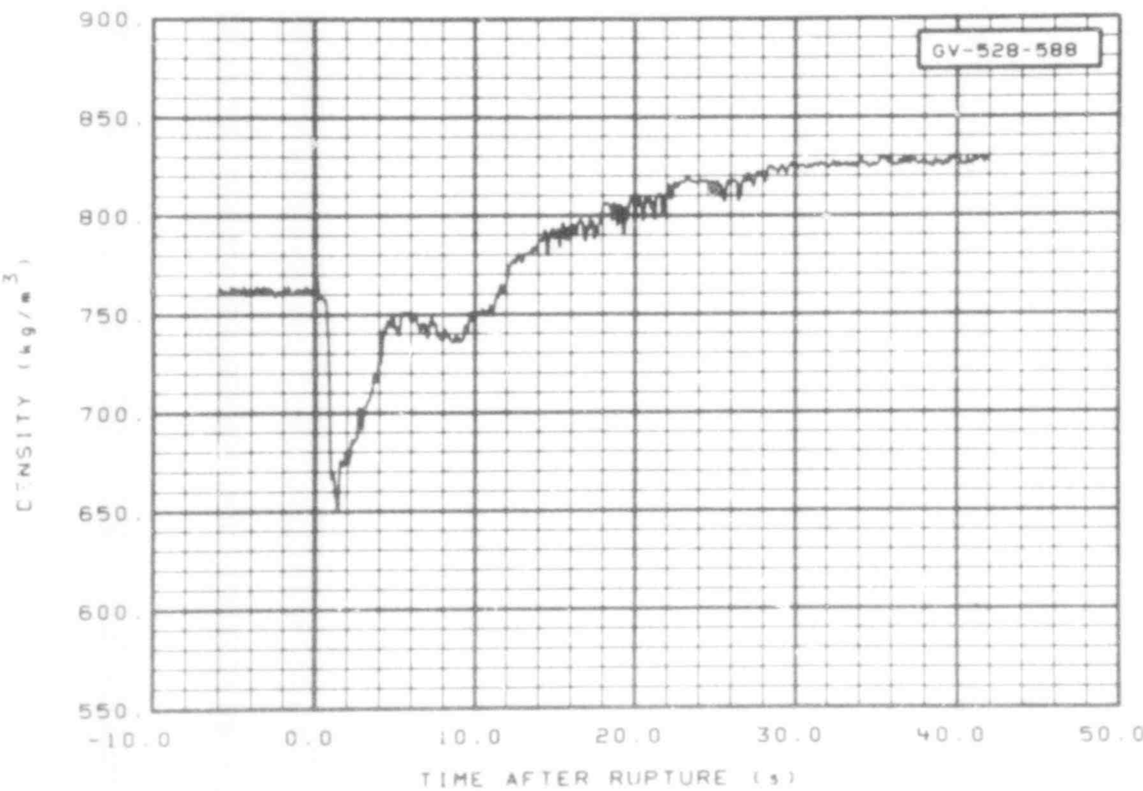

Fig. 274 Density in vessel (GV-528-588), from -6 to 42 s.

507 229

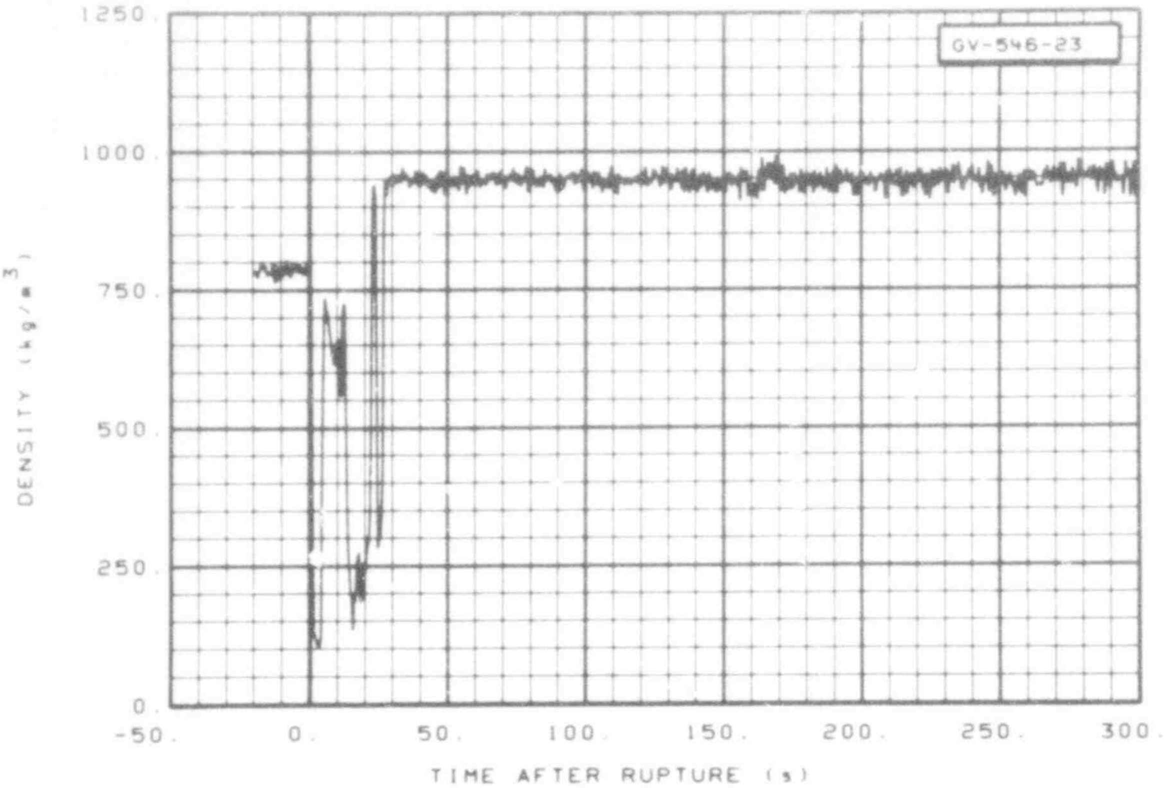

Fig. 275 Density in vessel (GV-546-23), from -20 to 300 s.

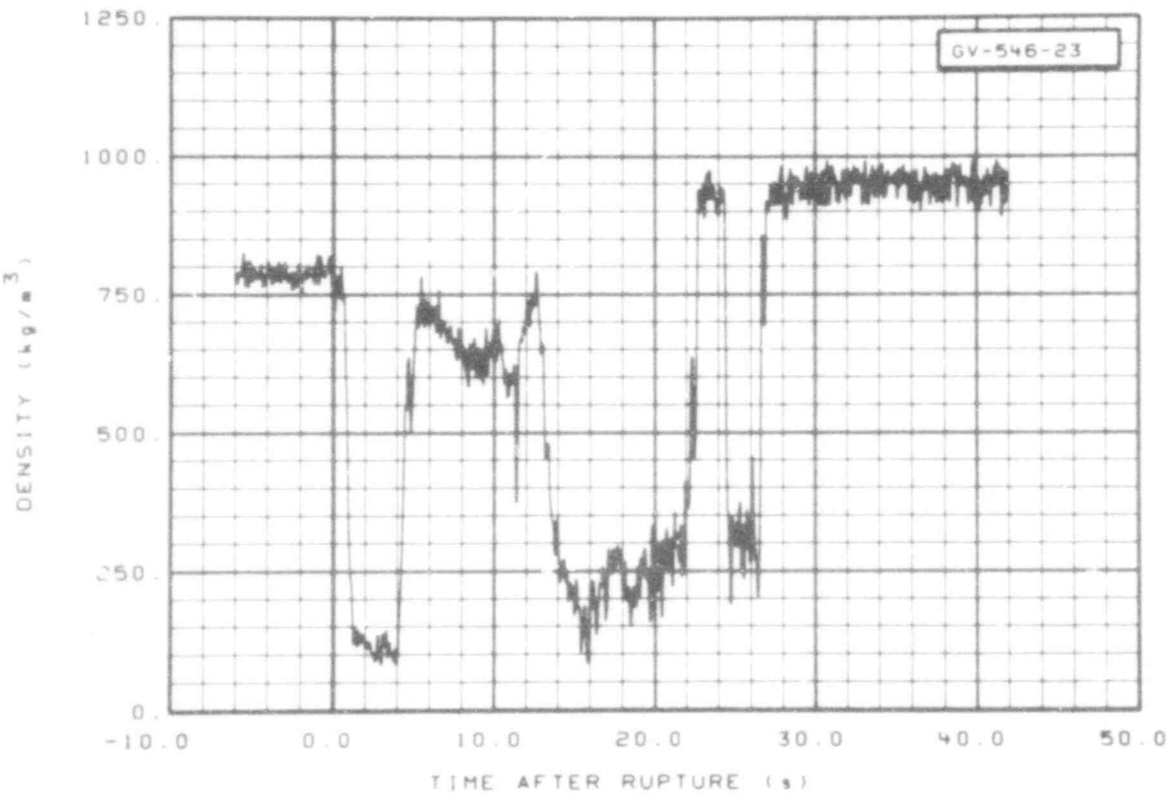

Fig. 276 Density in vessel (GV-546-23), from -6 to 42 s.

507 230

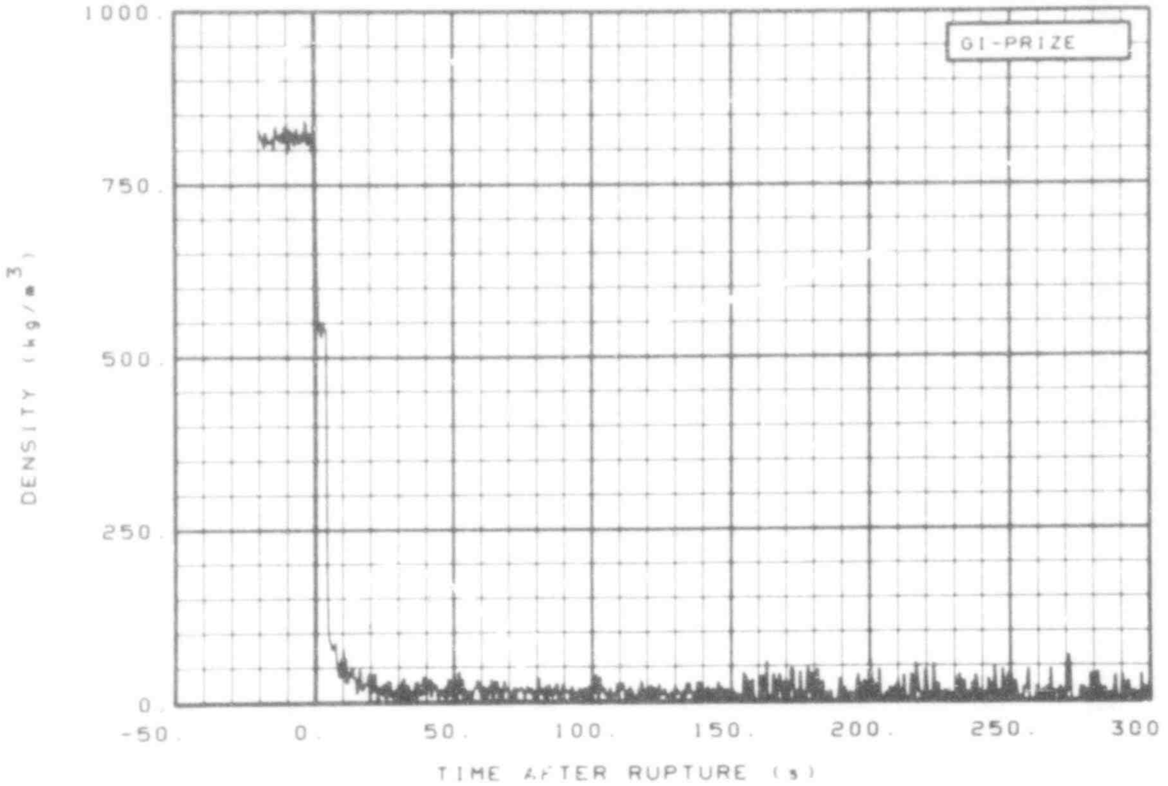

Fig. 277 Density in intact loop pressurizer (GI-PRIZE), from -20 to 300 s.

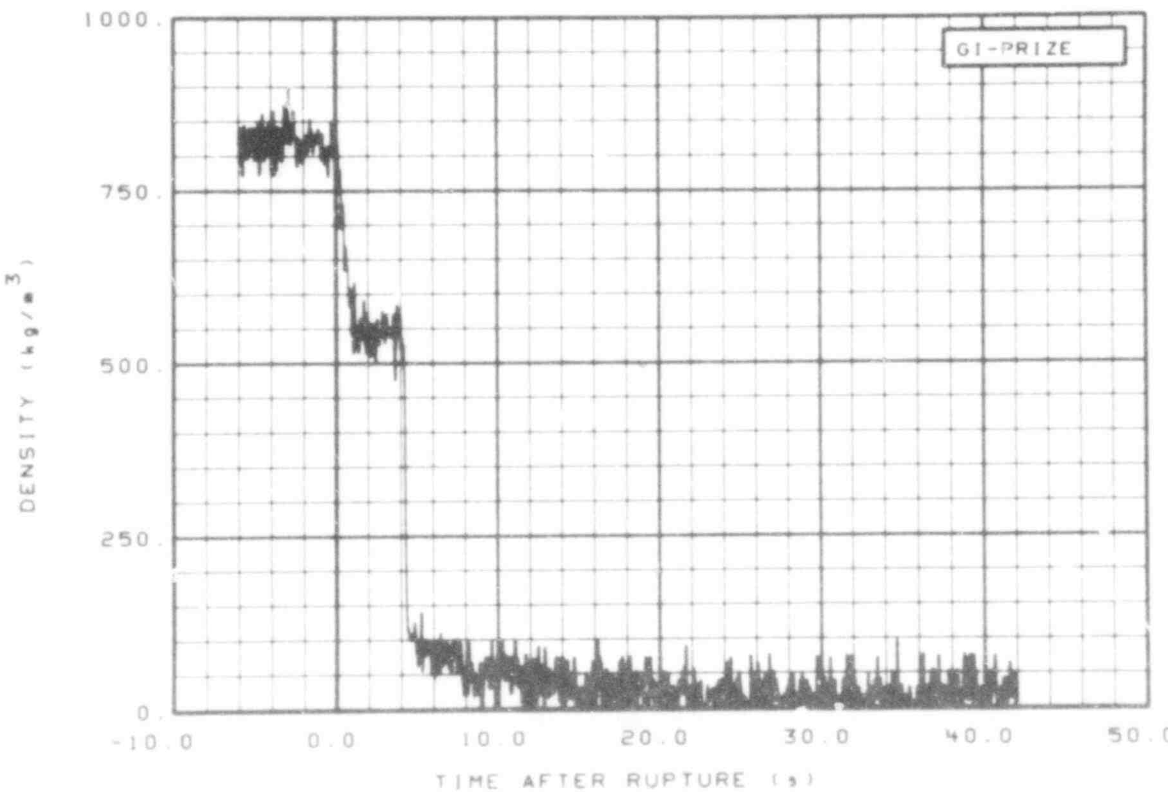

Fig. 278 Density in intact loop pressurizer (GI-PRIZE), from -6 to 42 s.

507 231

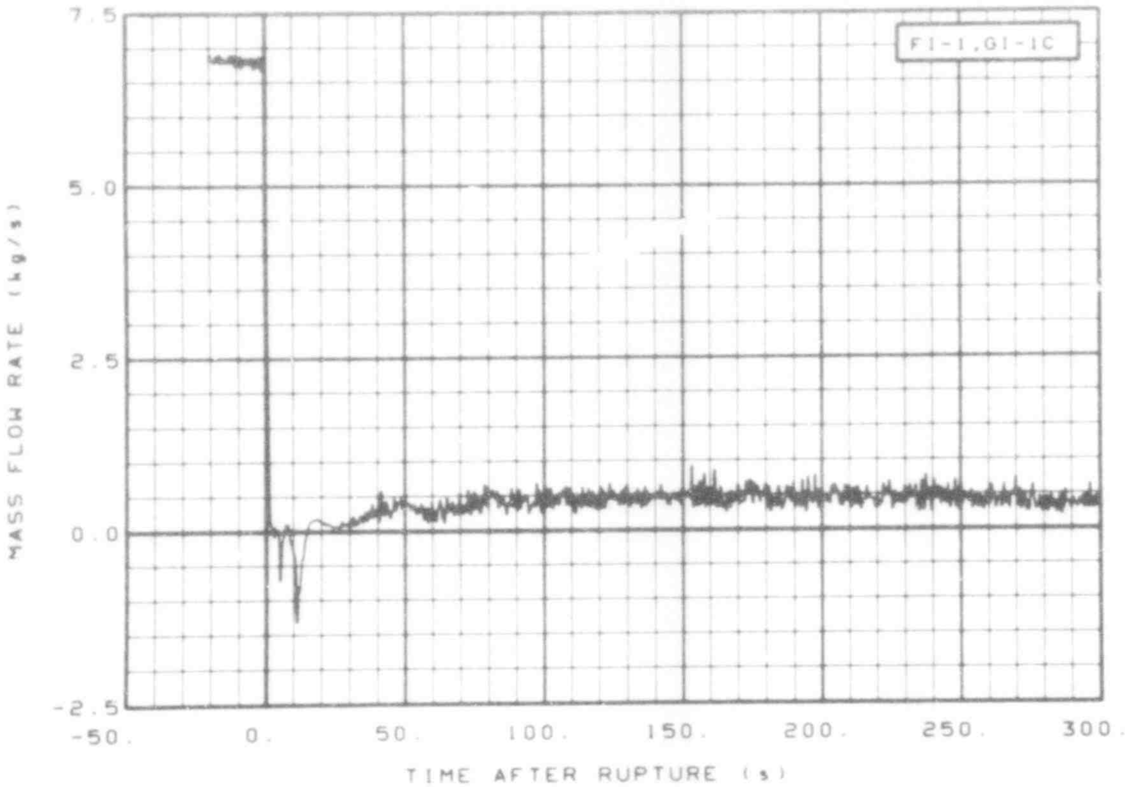

Fig. 279 Mass flow in intact loop (FI-1 and GI-1C), from -20 to 300 s.

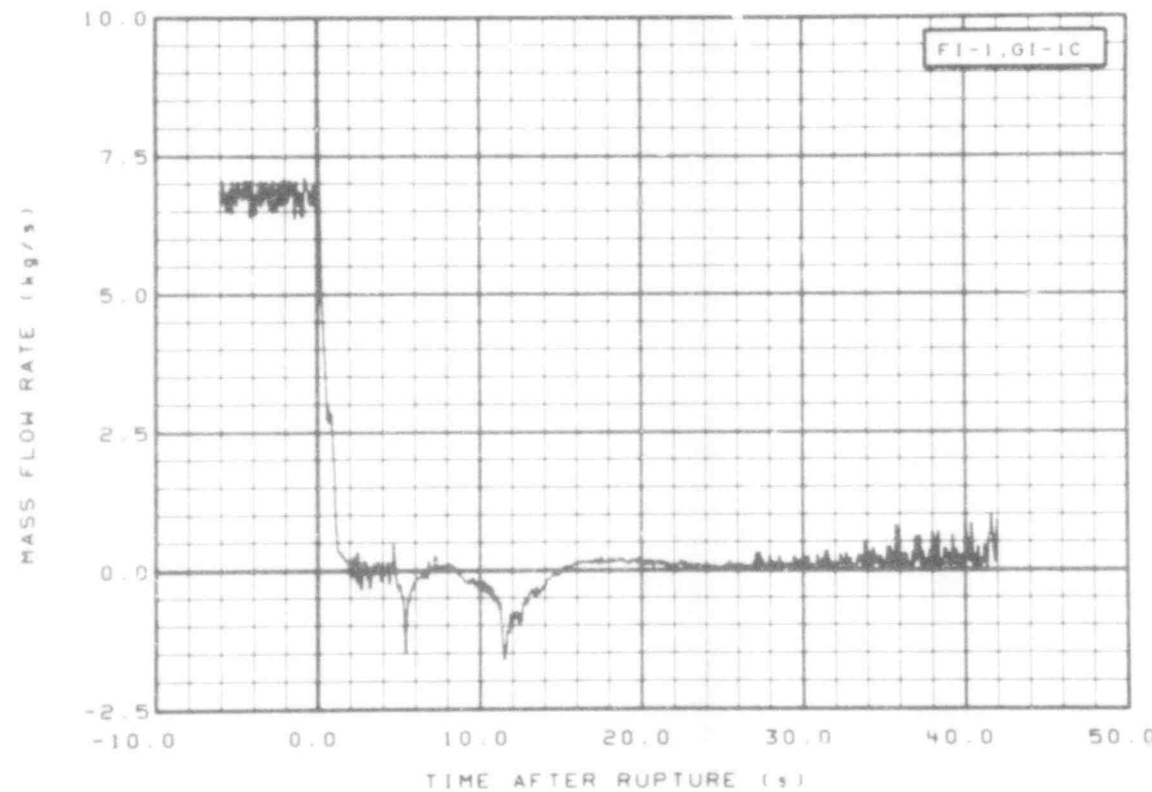

Fig. 280 Mass flow in intact loop (FI-1 and GI-1C), from -6 to 42 s.

507 232

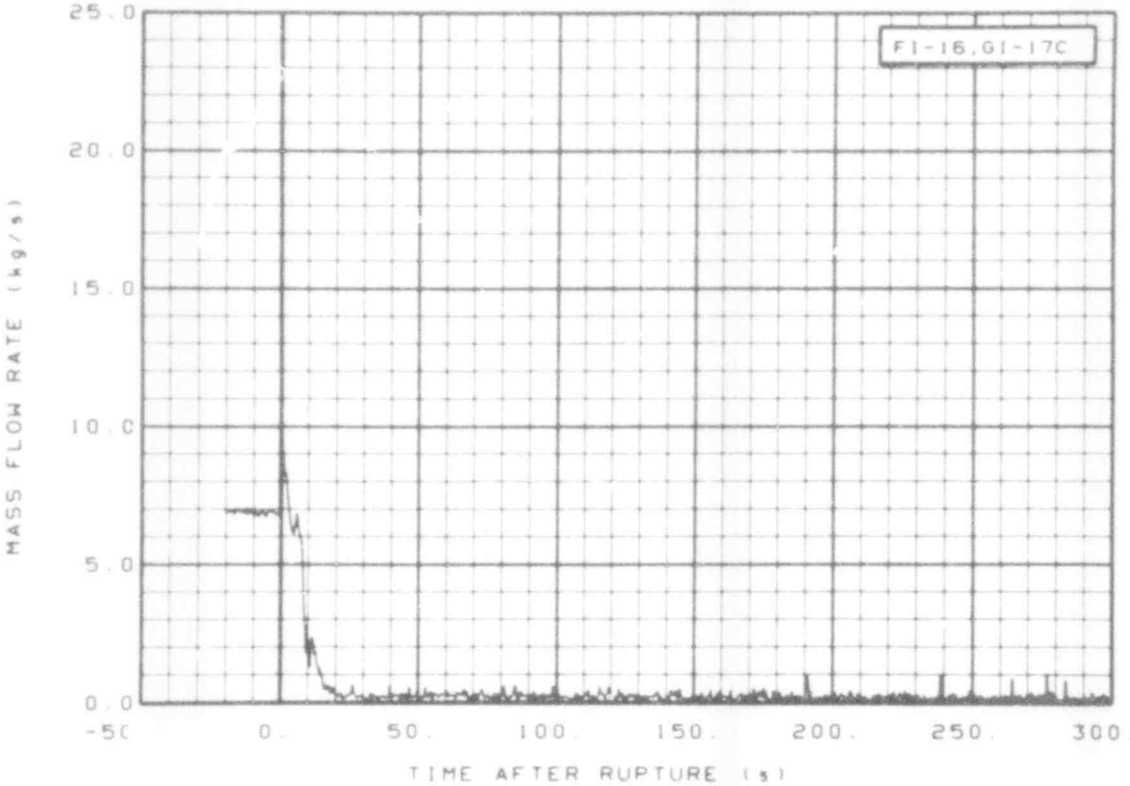

Fig. 281 Mass flow in intact loop (FI-16 and GI-17C), from -20 to 300 s.

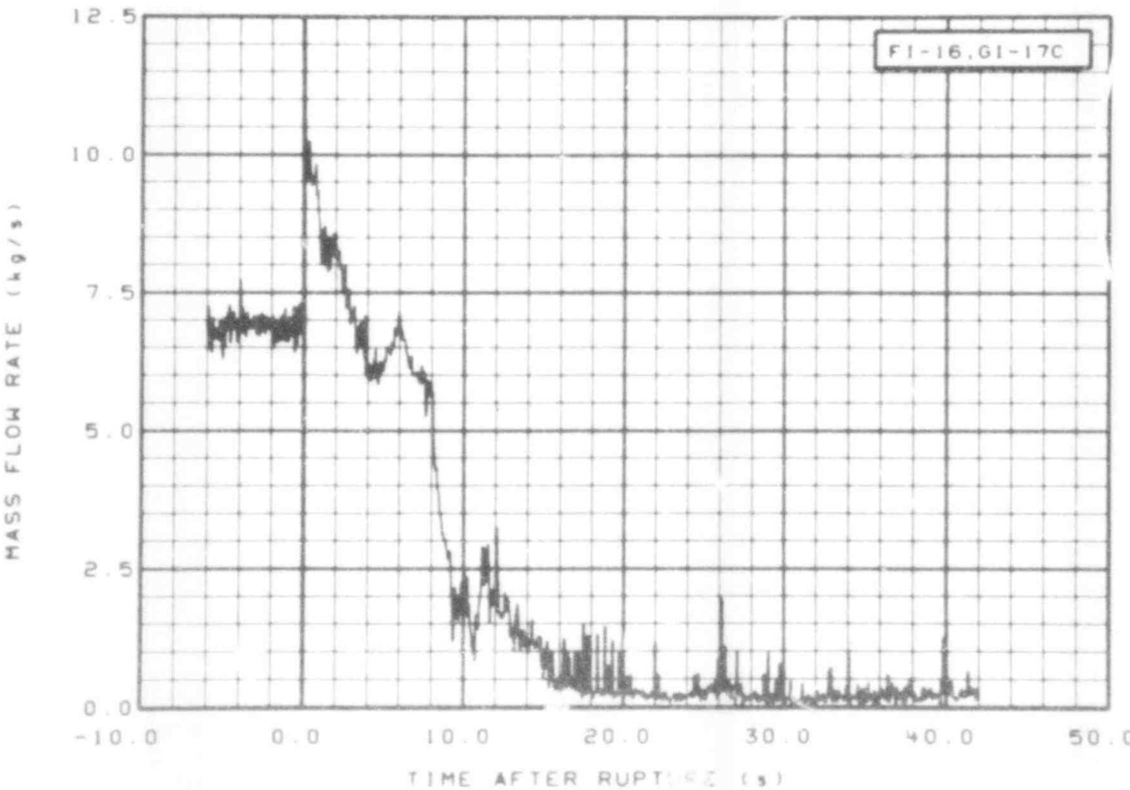

Fig. 282 Mass flow in intact loop (FI-16 and GI-17C), from -6 to 42 s.

507 233

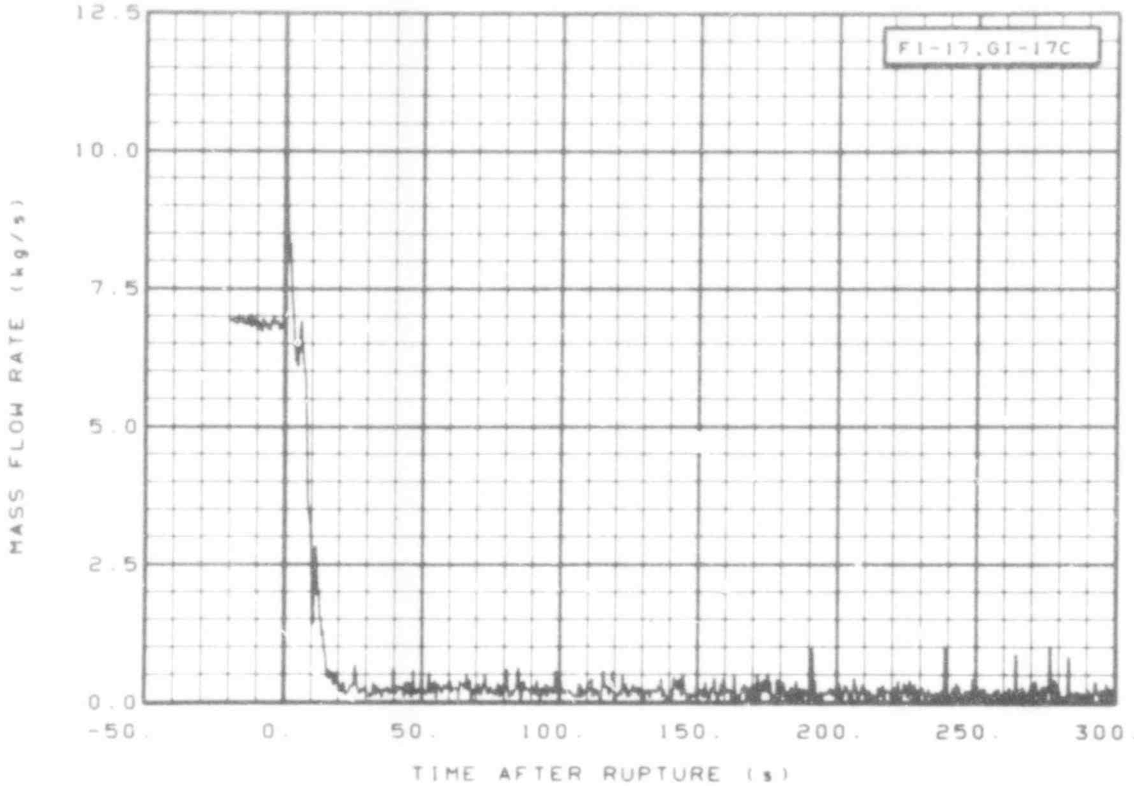

Fig. 283 Mass flow in intact loop (FI-17 and GI-17C), from -20 to 300 s.

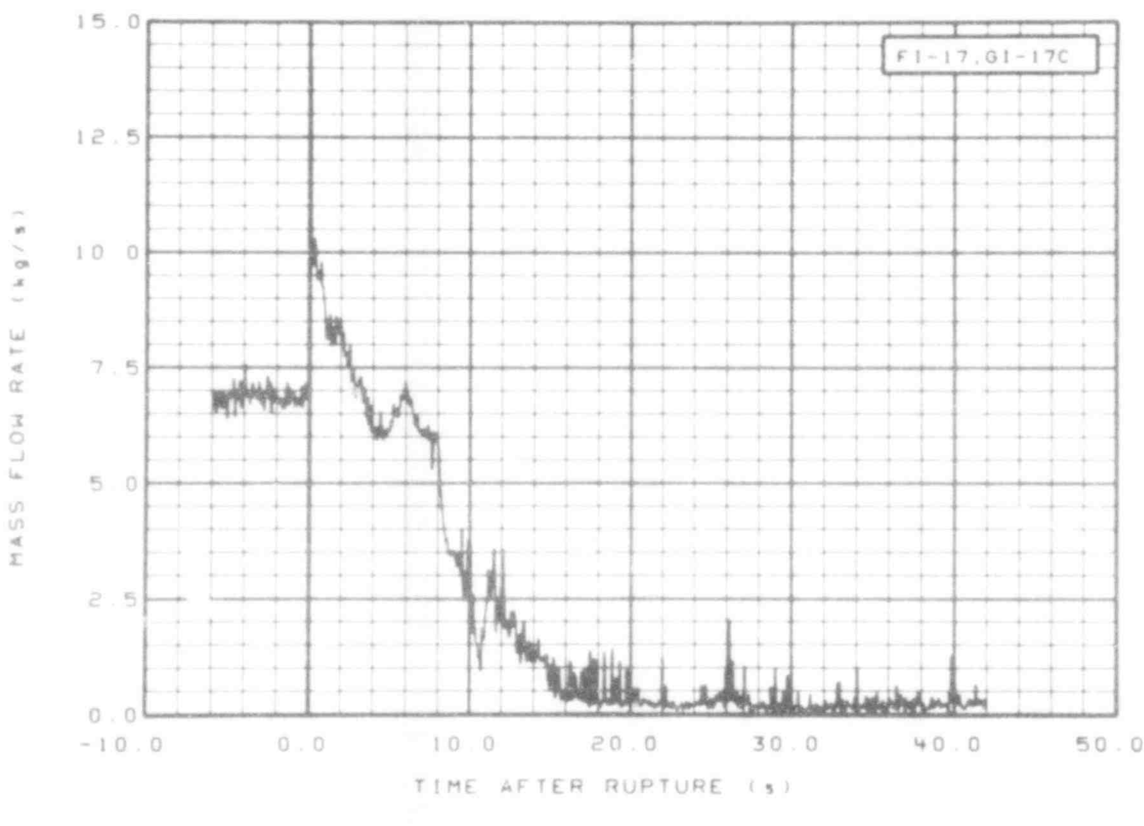

Fig. 284 Mass flow in intact loop (FI-17 and GI-17C), from -6 to 42 s.

507 234

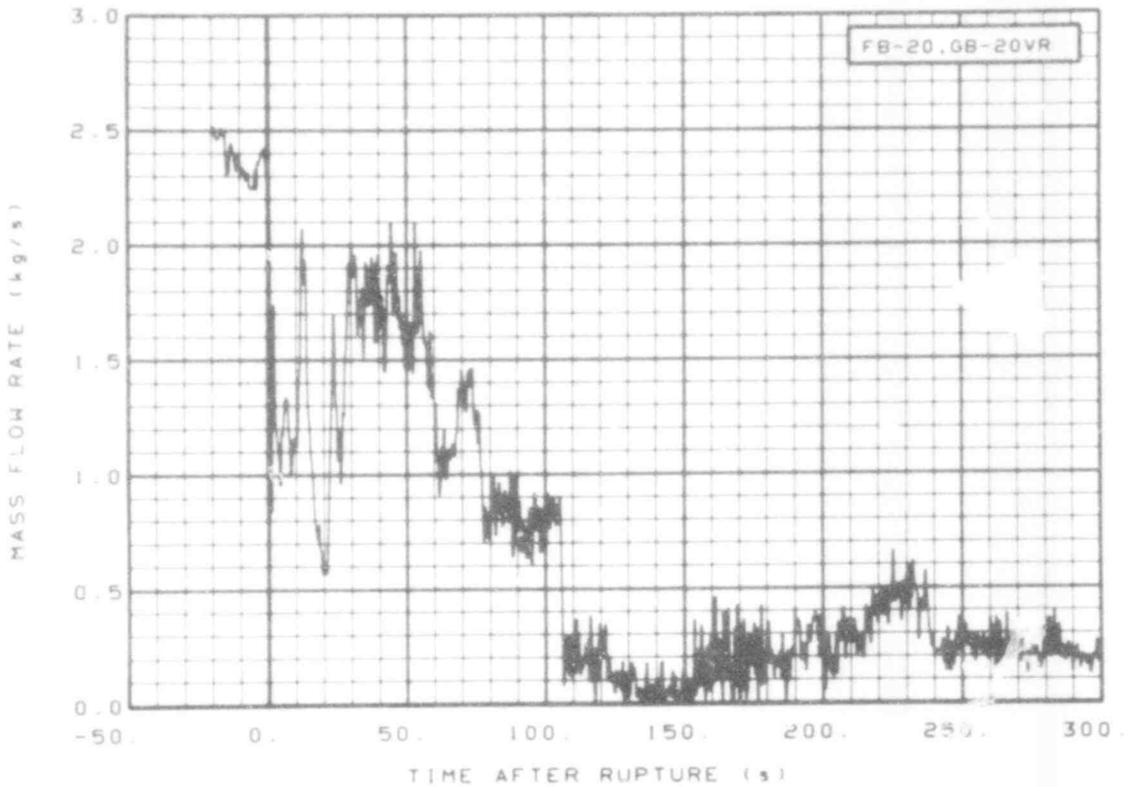

Fig. 285 Mass flow in broken loop (FB-20 and GB-20VR), from -20 to 300 s.

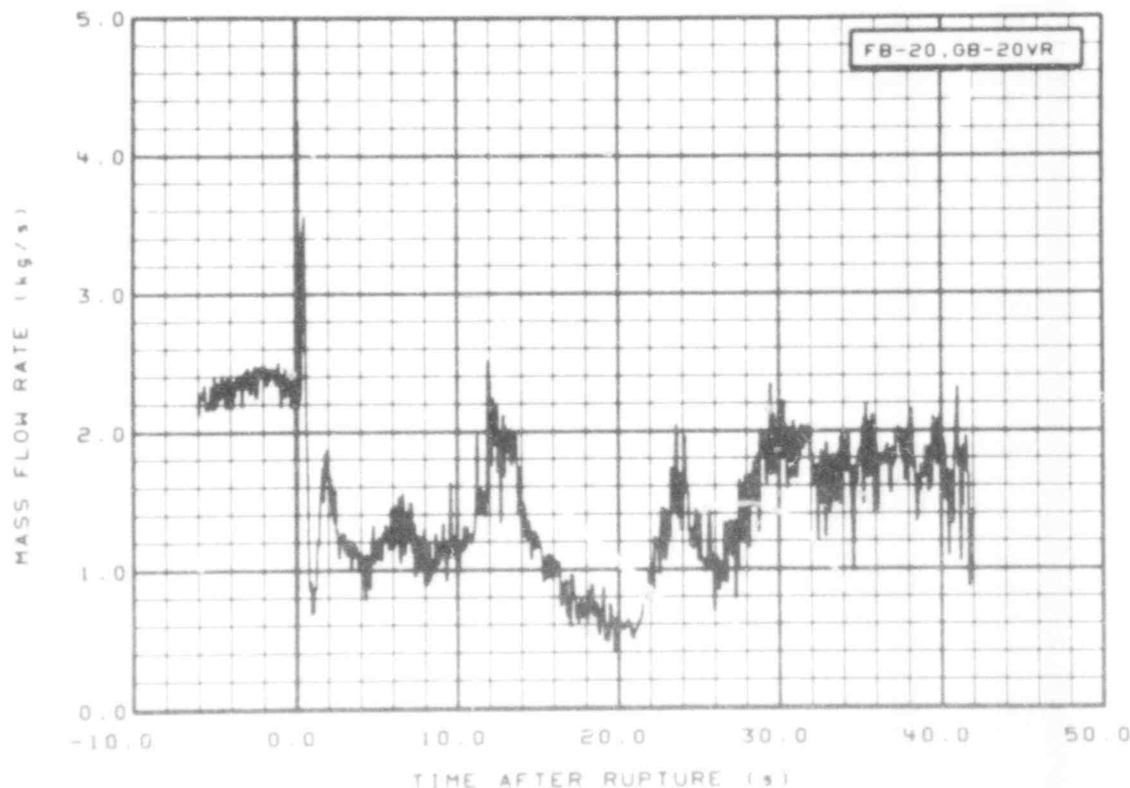

Fig. 286 Mass flow in broken loop (FB-20 and GB-20VR), from -6 to 42 s.

507 235

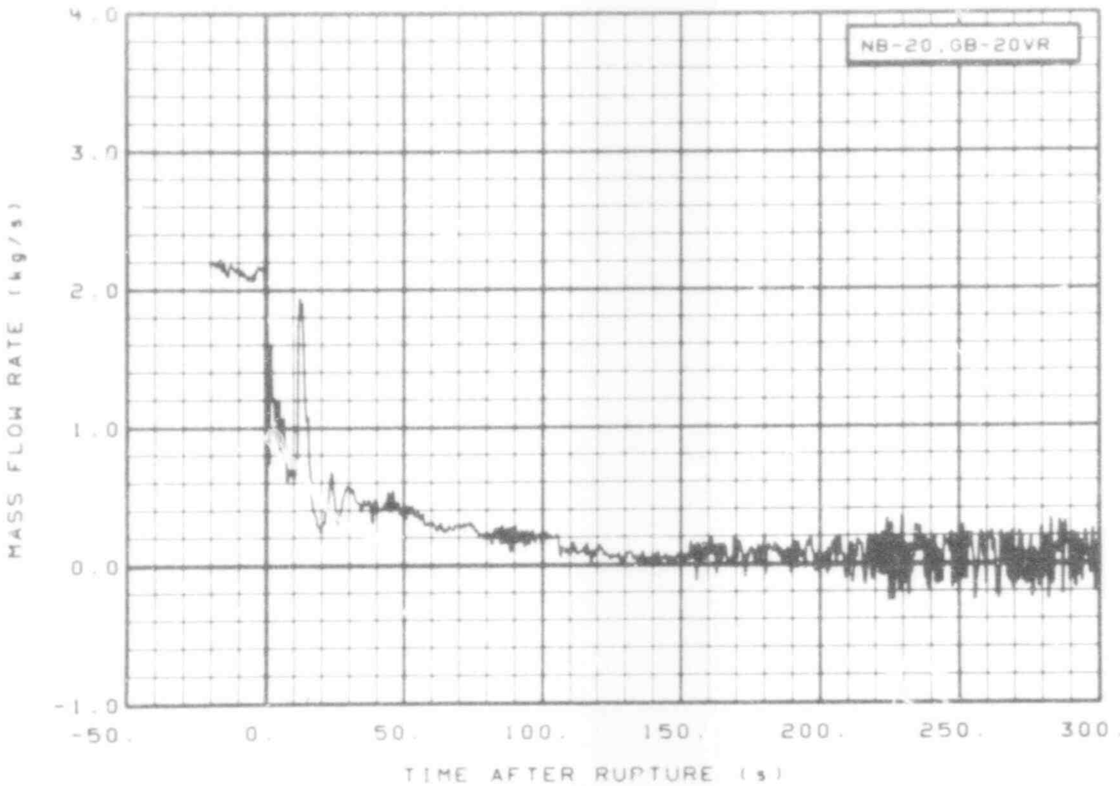

Fig. 287 Mass flow in broken loop (NB-20 and GB-20VR), from -20 to 300 s.

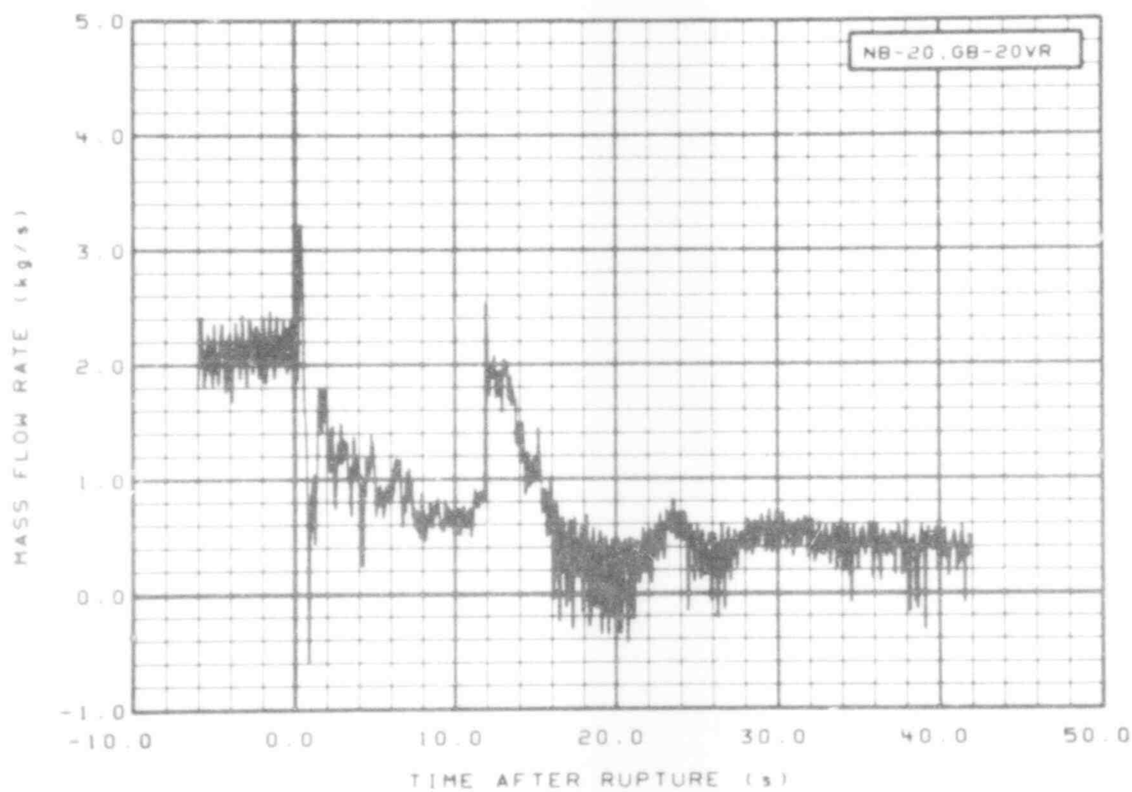

Fig. 288 Mass flow in broken loop (NB-20 and GB-20VR), from -6 to 42 s.

507 236

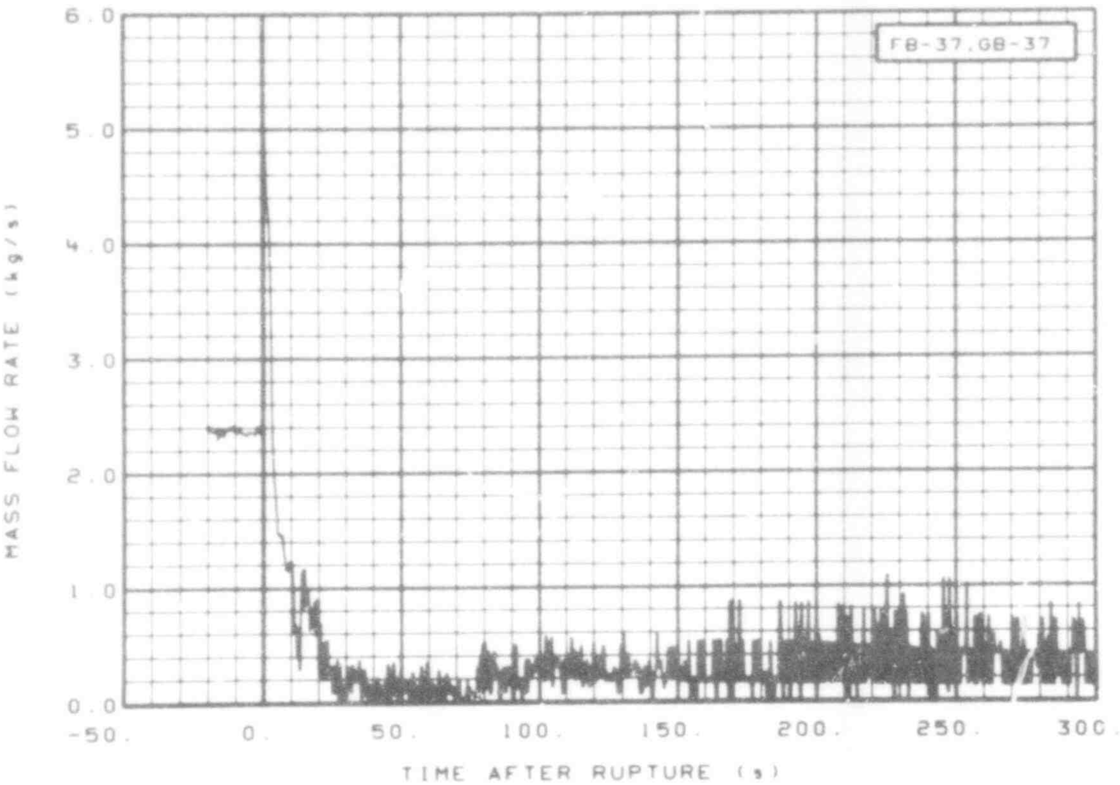

Fig. 289 Mass flow in broken loop (FB-37 and GB-37), from -20 to 300 s.

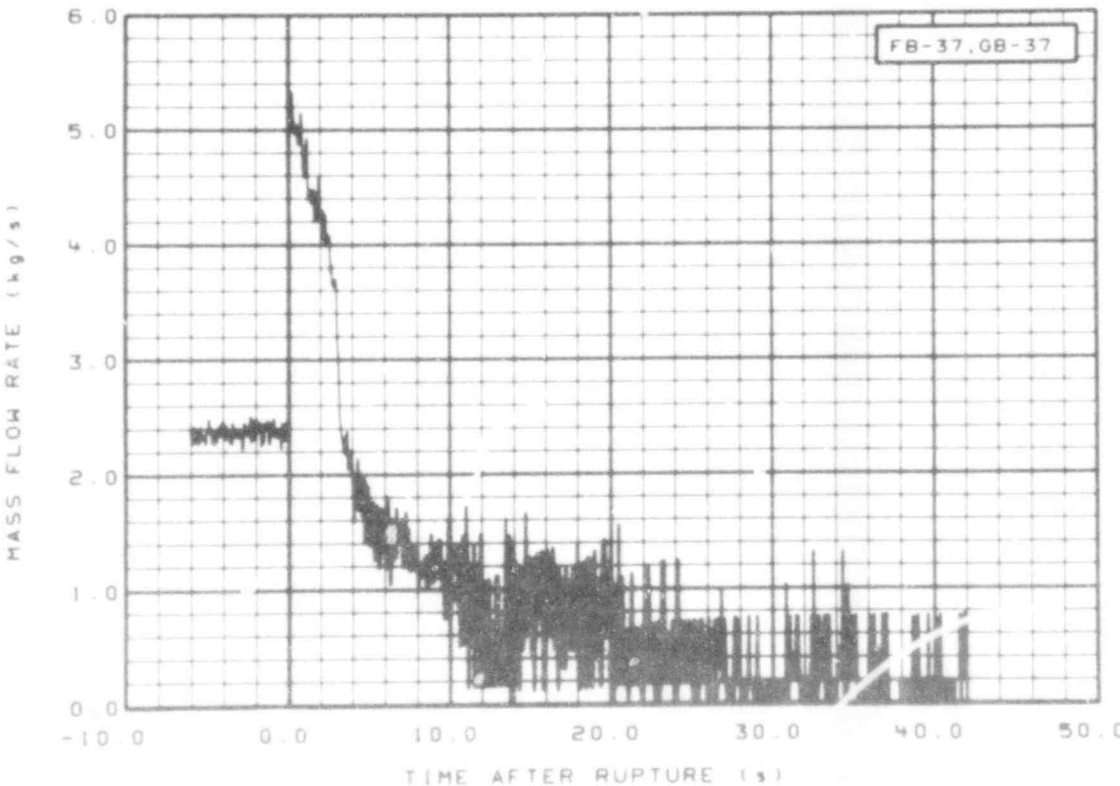

Fig. 290 Mass flow in broken loop (FB-37 and GB-37), from -6 to 42 s.

507 237

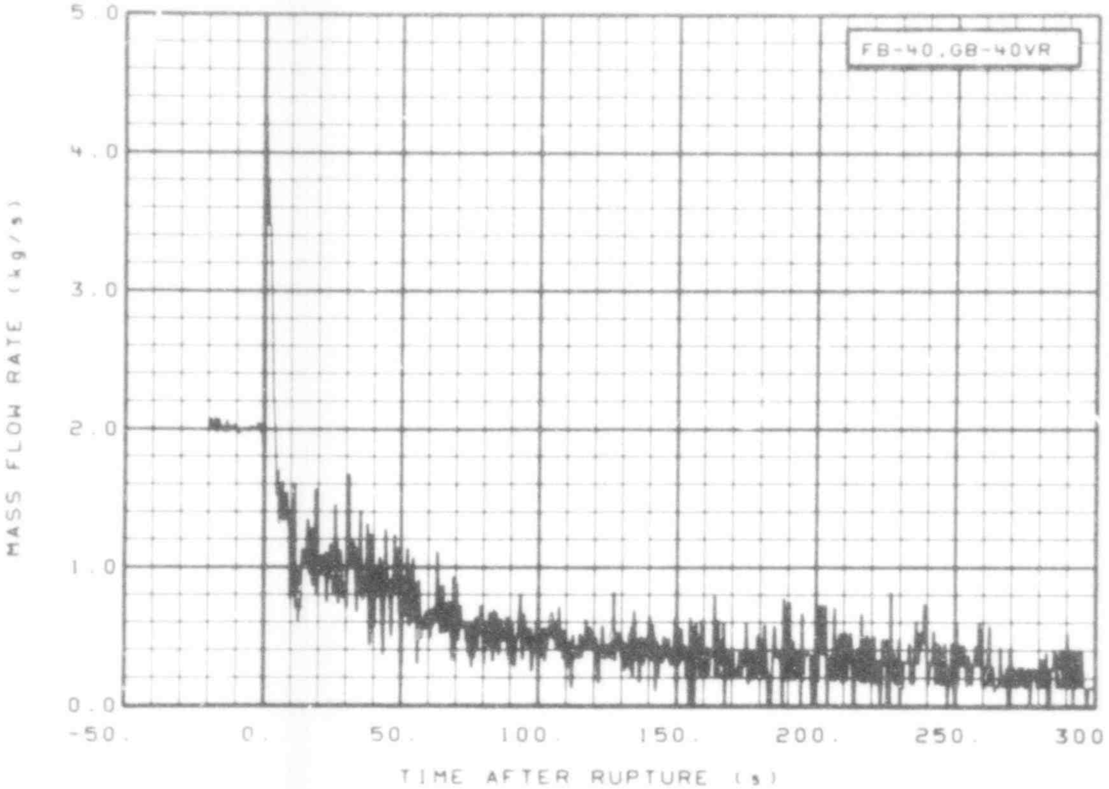

Fig. 291 Mass flow in broken loop (FB-40 and GB-40VR), from -20 to 300 s.

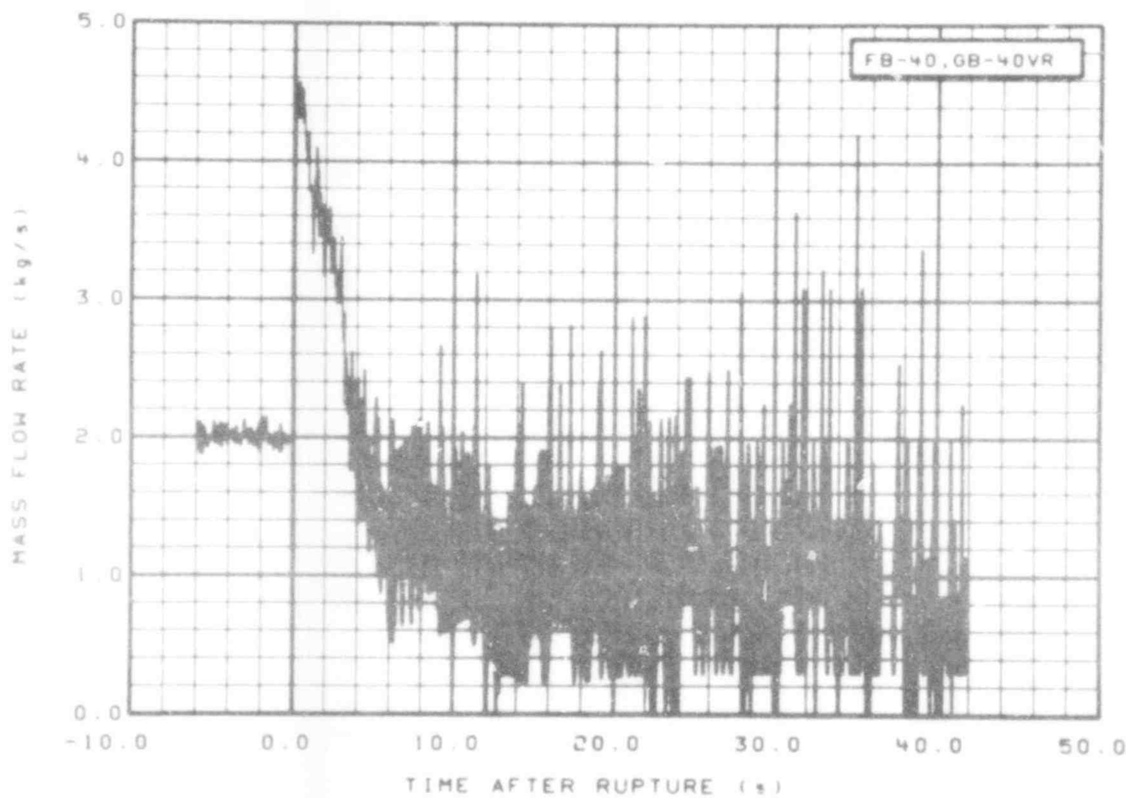

Fig. 292 Mass flow in broken loop (FB-40 and GB-40VR), from -6 to 42 s.

507 238

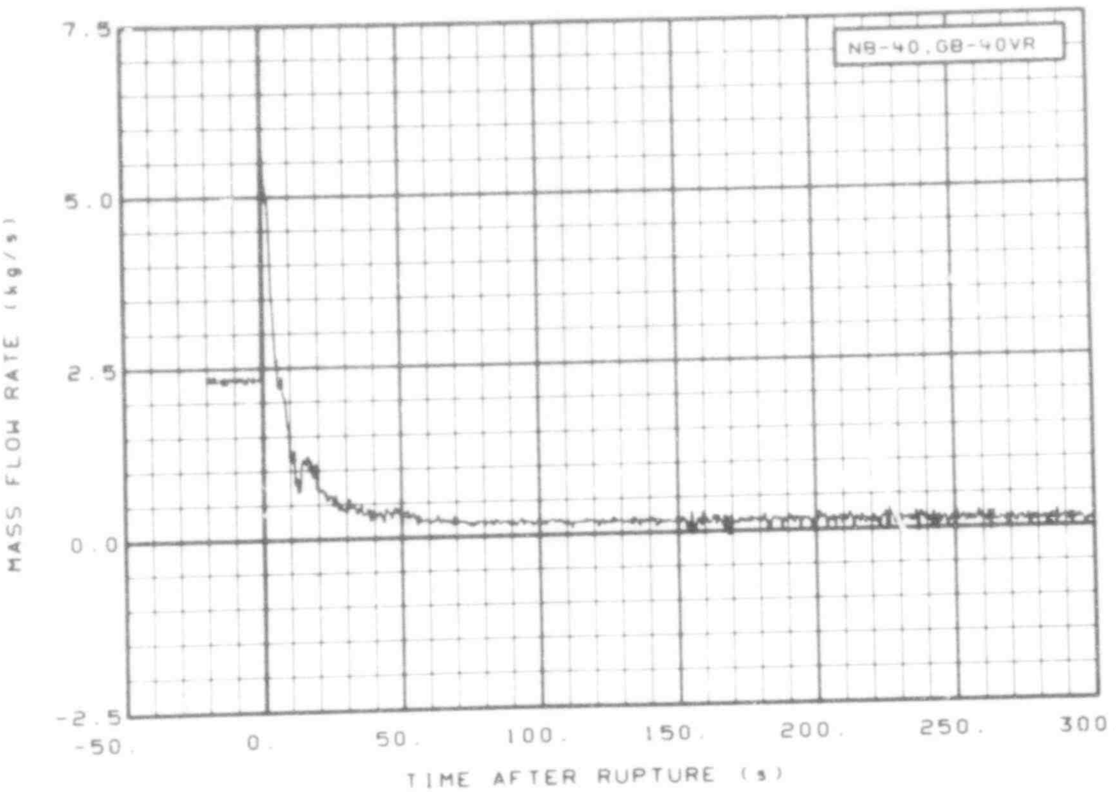

Fig. 293 Mass flow in broken loop (NB-40 and GB-40VR), from -20 to 300 s.

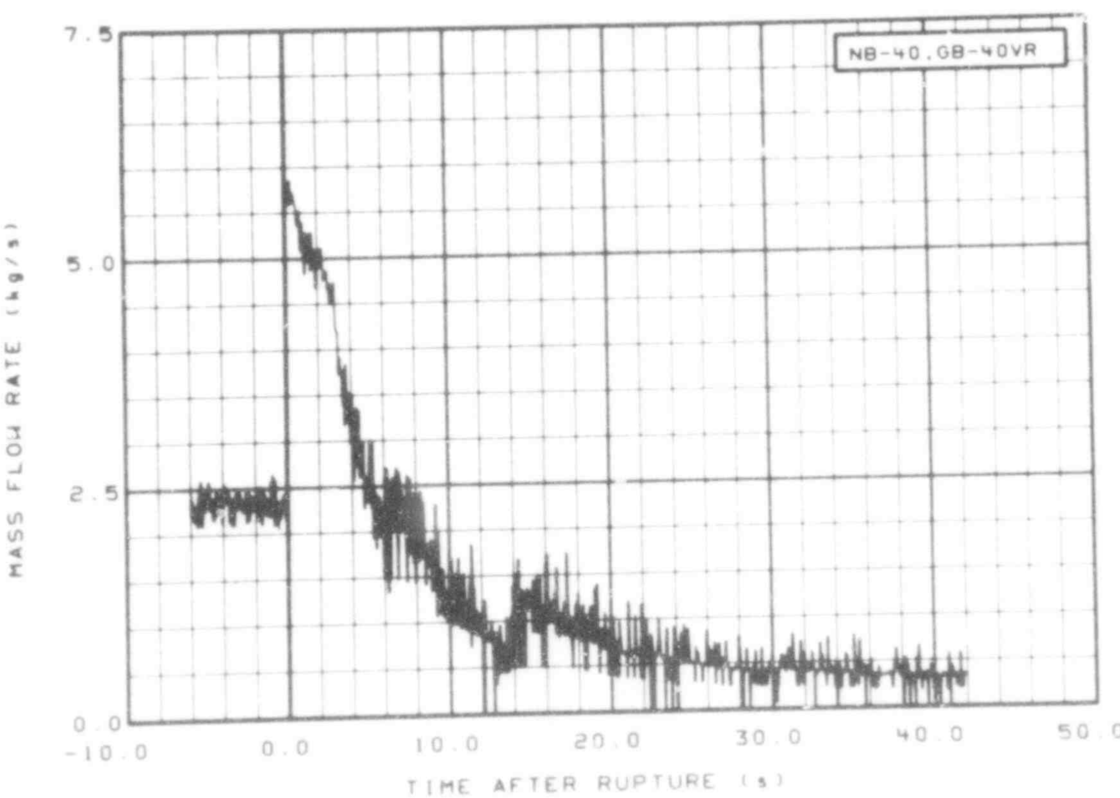

Fig. 294 Mass flow in broken loop (NB-40 and GB-40VR), from -6 to 42 s.

507 239

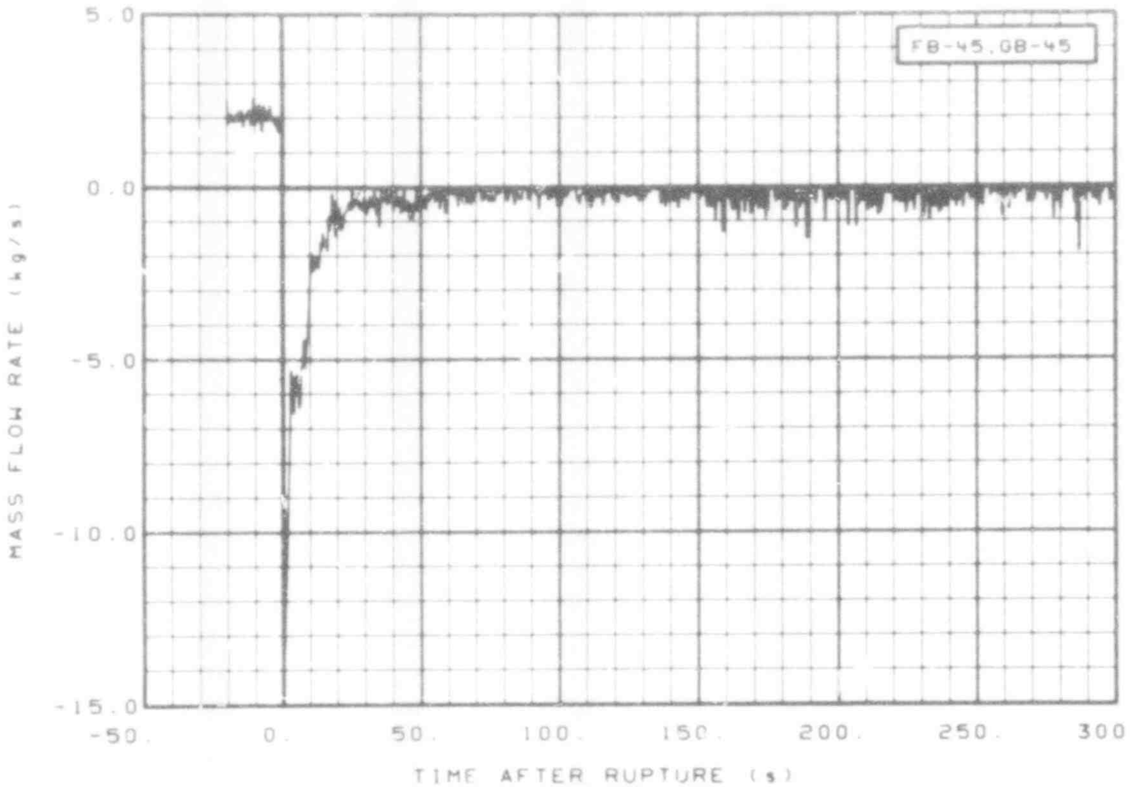

Fig. 295 Mass flow in broken loop (FB-45 and GB-45), from -20 to 300 s.

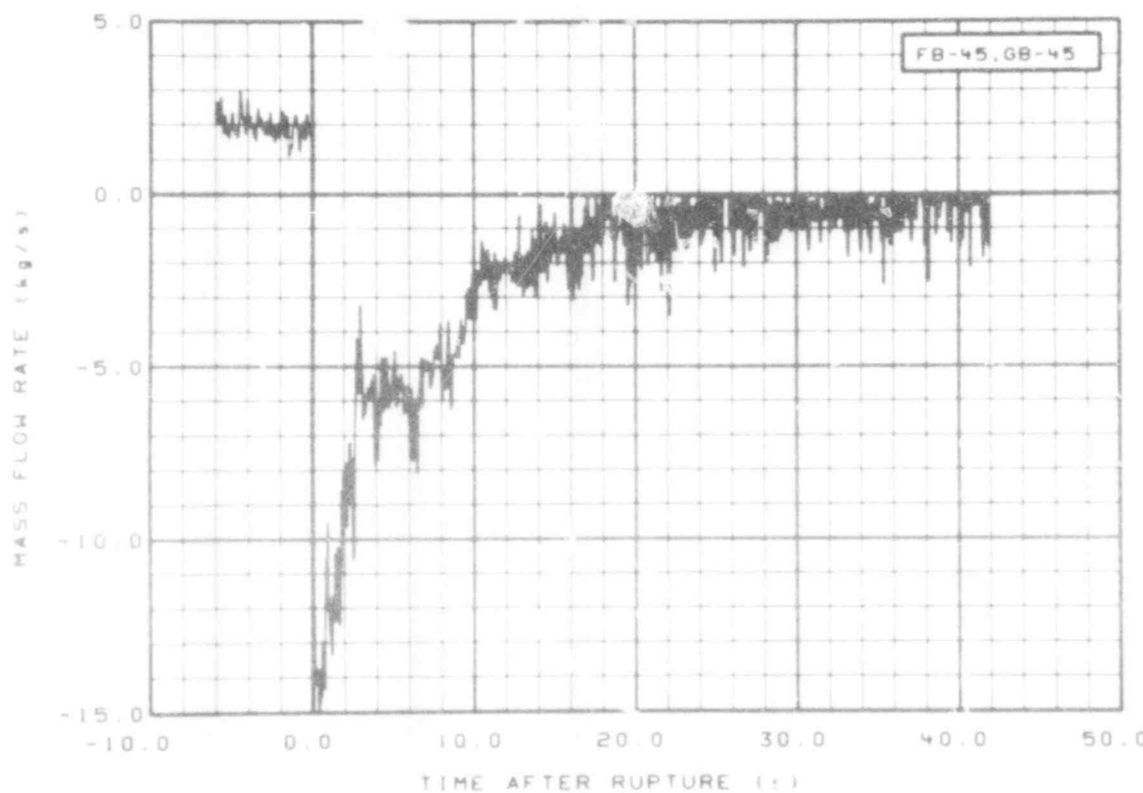

Fig. 296 Mass flow in broken loop (FB 45 and GB-45), from -6 to 42 s.

507 240

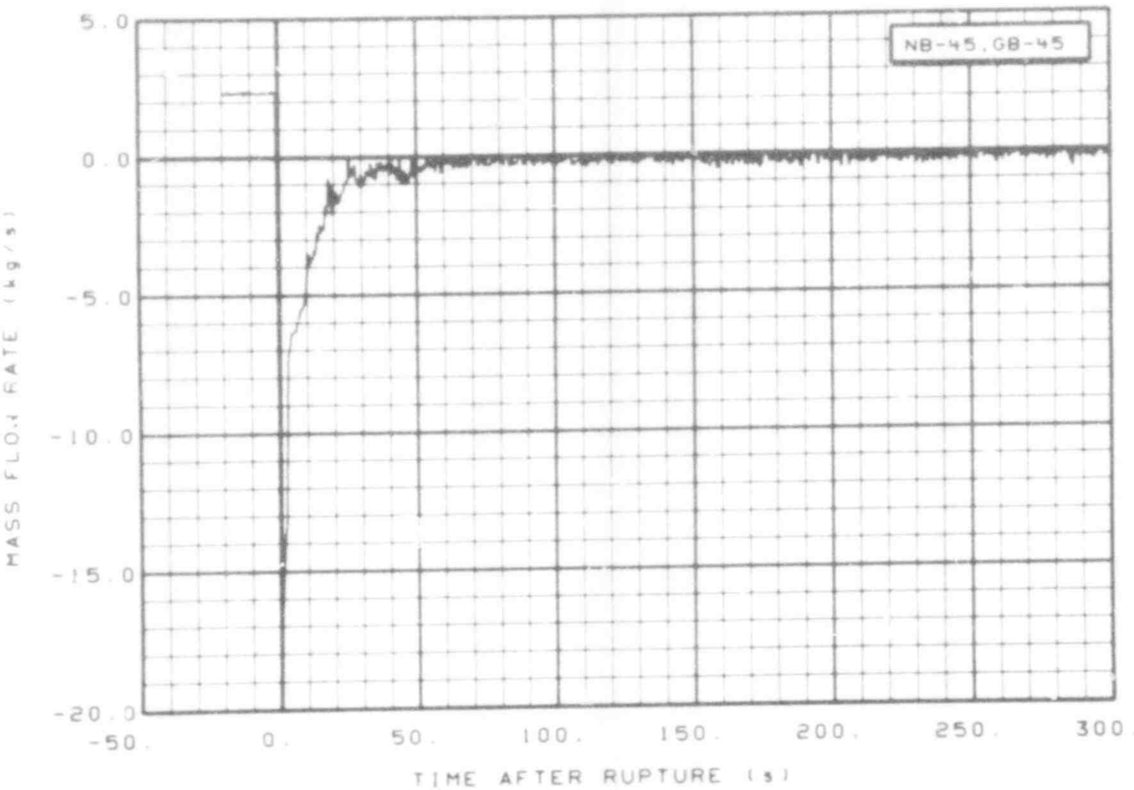

Fig. 297 Mass flow in broken loop (NB-45 and GB-45), from -20 to 300 s.

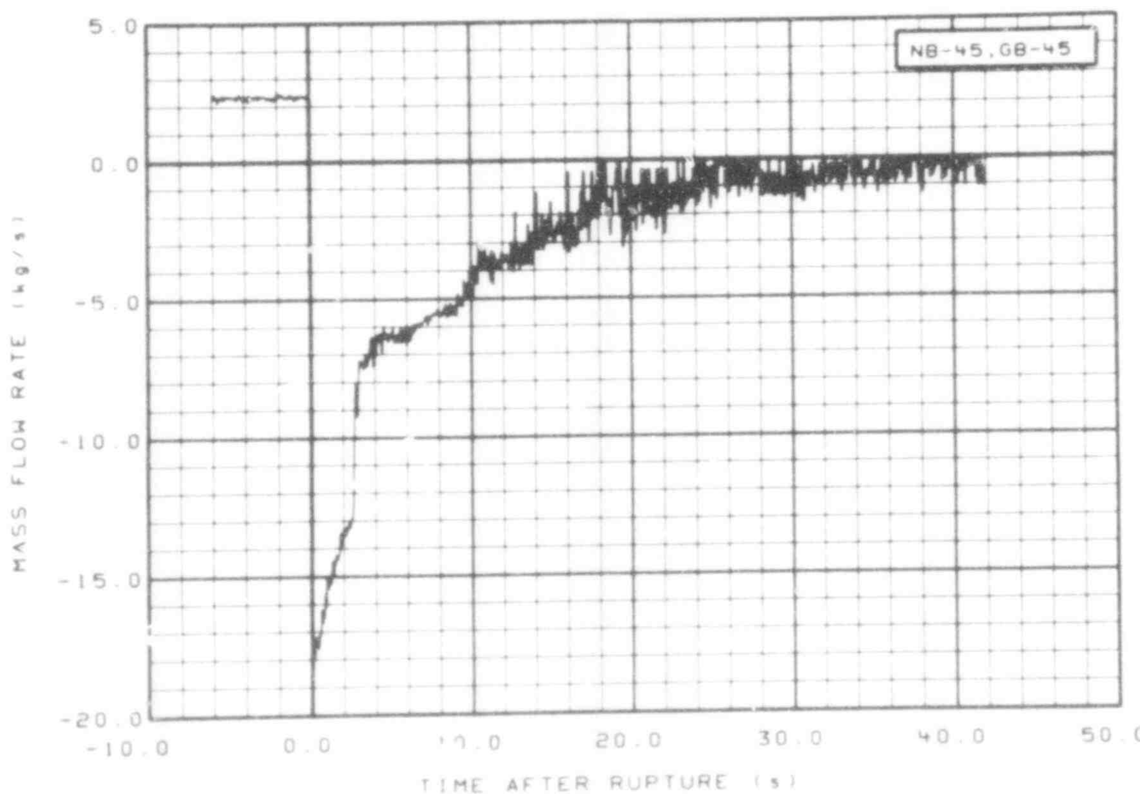

Fig. 298 Mass flow in broken loop (NB-45 and GB-45), from -6 to 42 s.

507 241

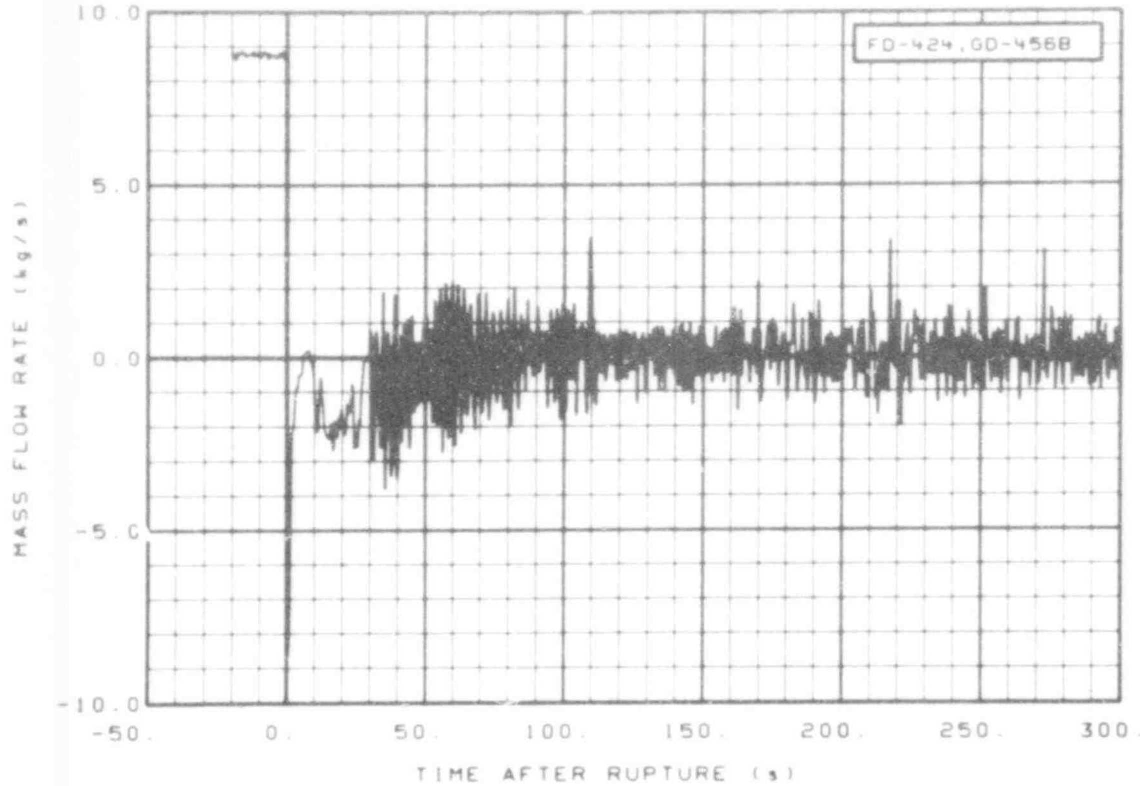

Fig. 299 Mass flow in downcomer (FD-424 and GD-456B), from -20 to 300 s.

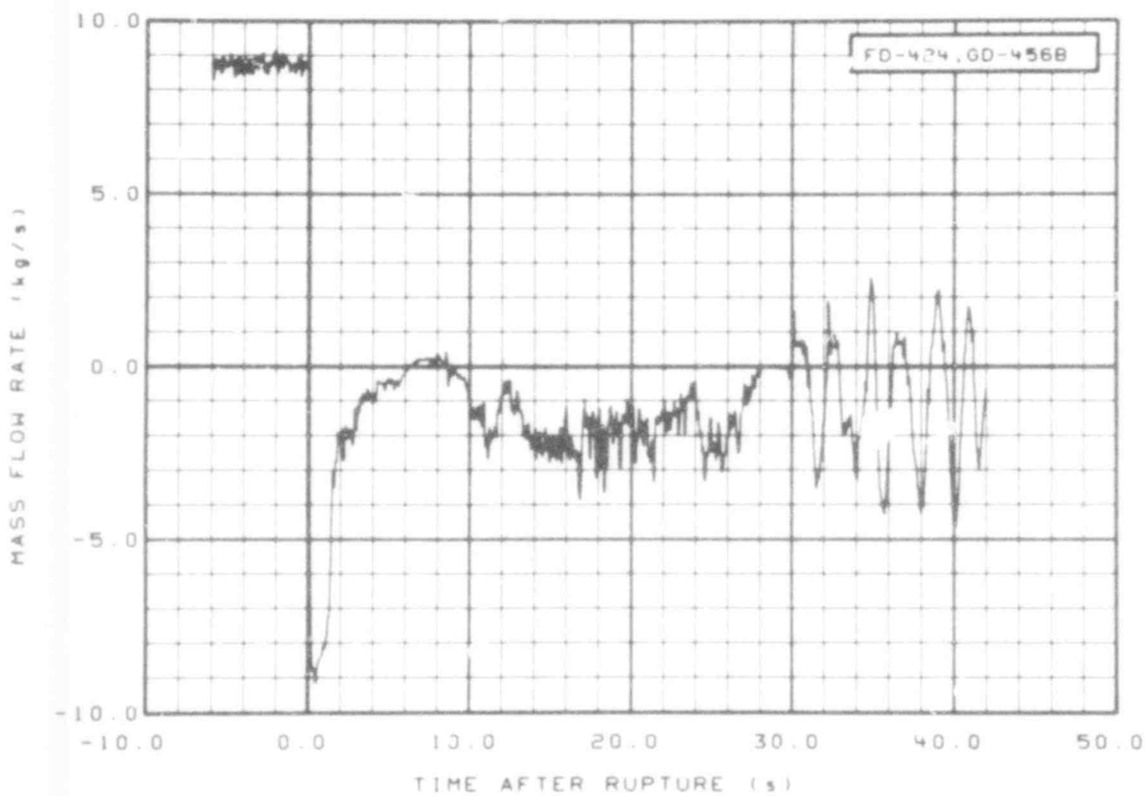

Fig. 300 Mass flow in downcomer (FD-424 and GD-456B), from -6 to 42 s.

507 242

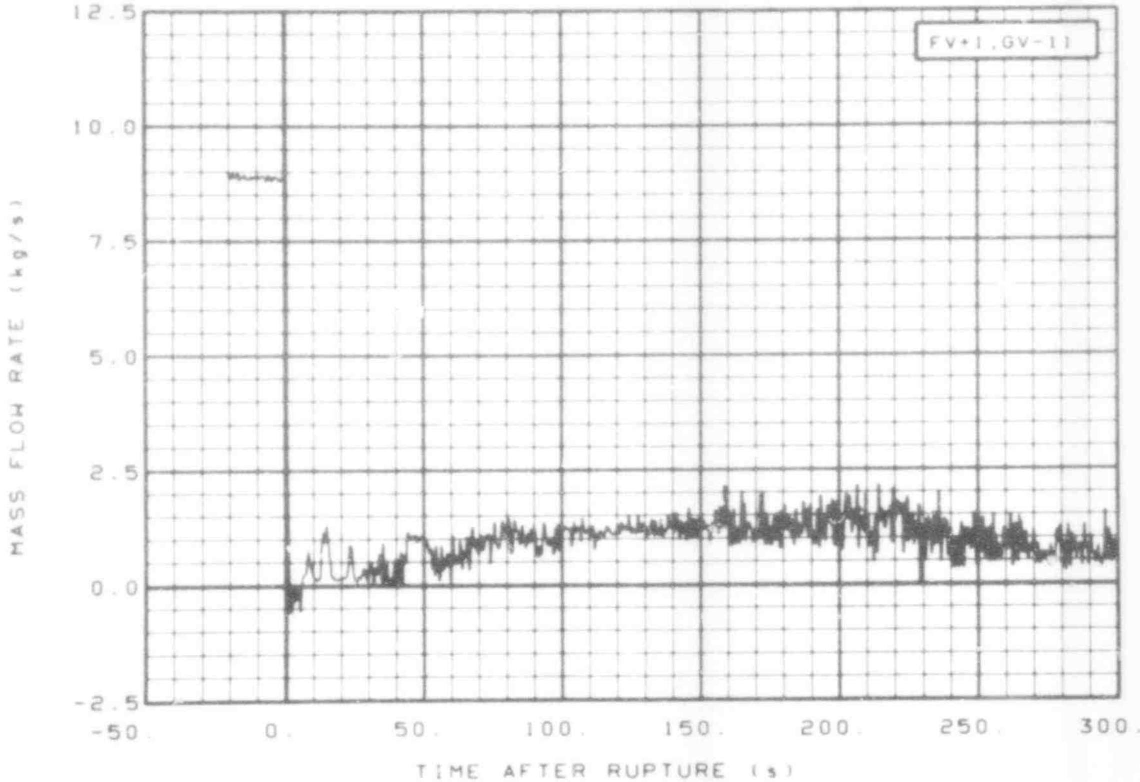

Fig. 301 Mass flow in vessel (FV + 1 and GV-11), from -20 to 300 s.

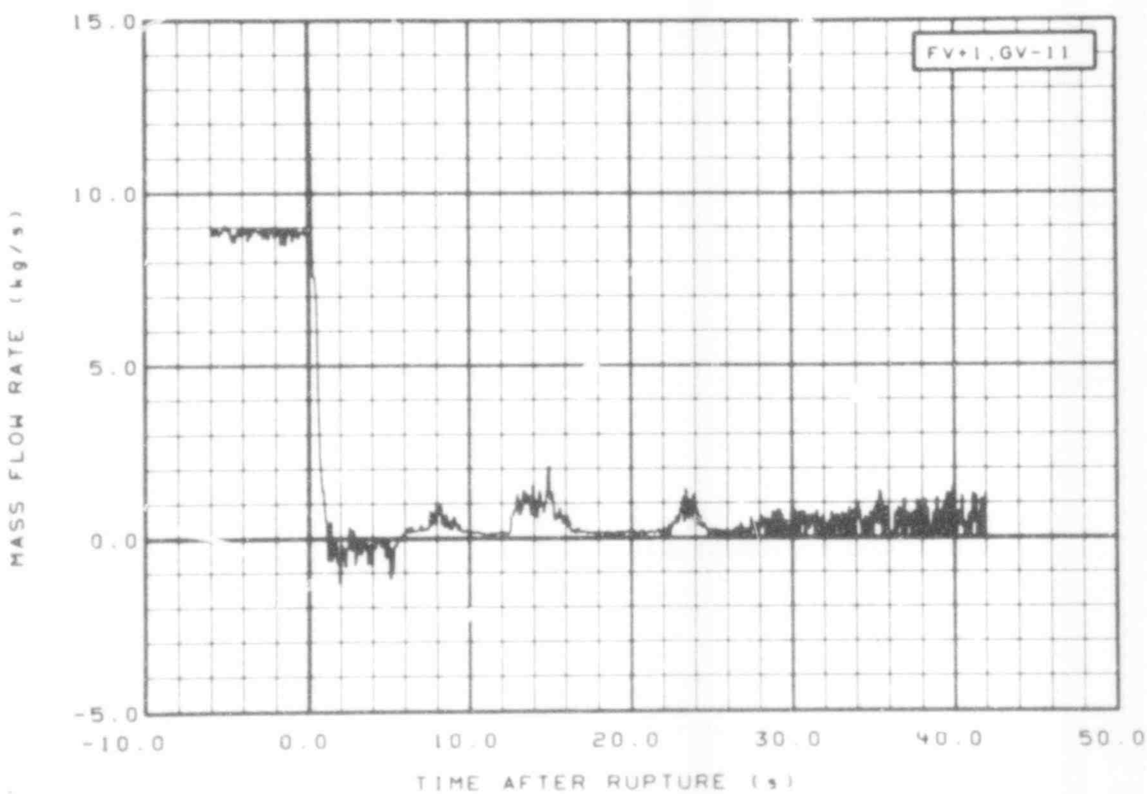

Fig. 302 Mass flow in vessel (FV + 1 and GV-11), from -6 to 42 s.

507 243

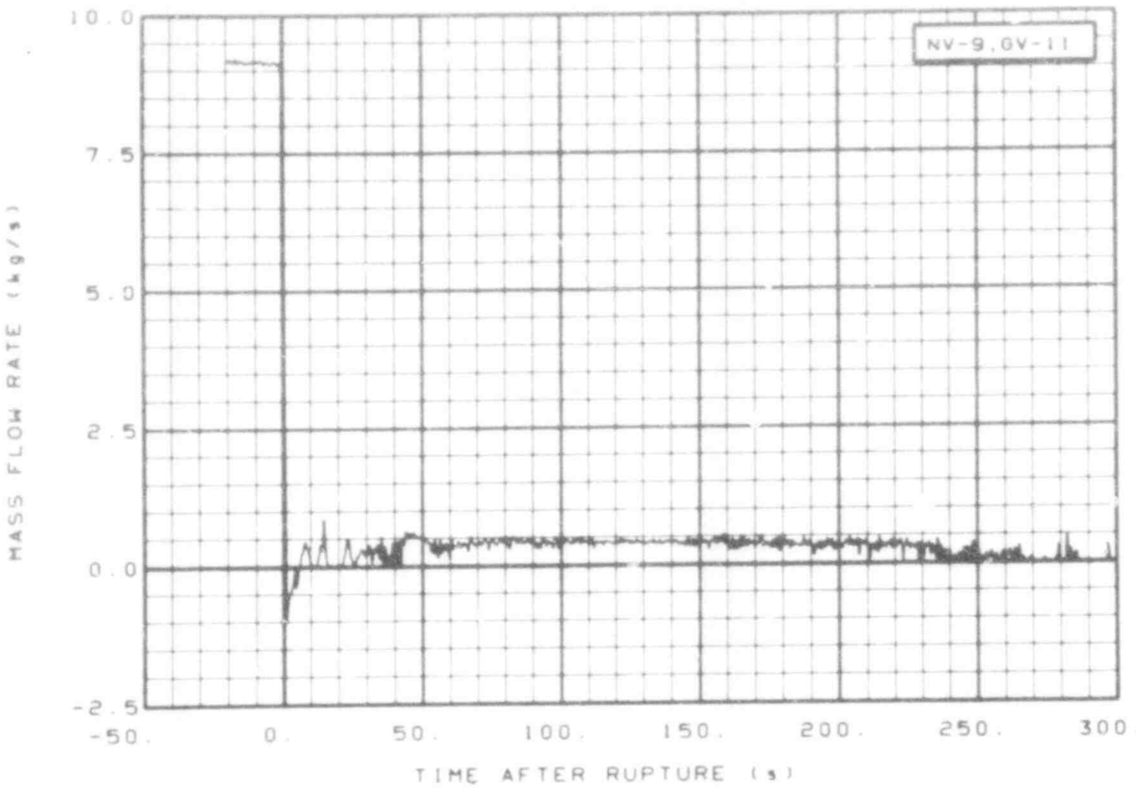

Fig. 303 Mass flow in vessel (NV-9 and GV-11), from -20 to 300 s.

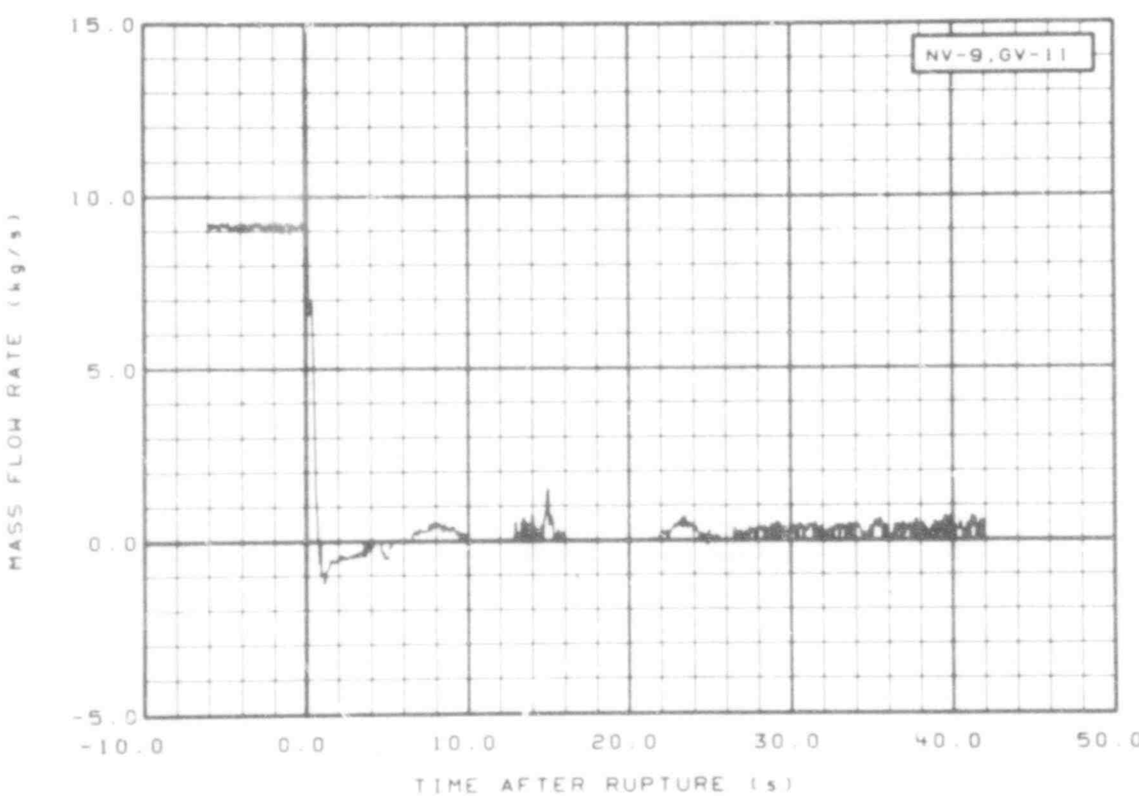

Fig. 304 Mass flow in vessel (NV " ınd GV-11), from -6 to 42 s.

507 244

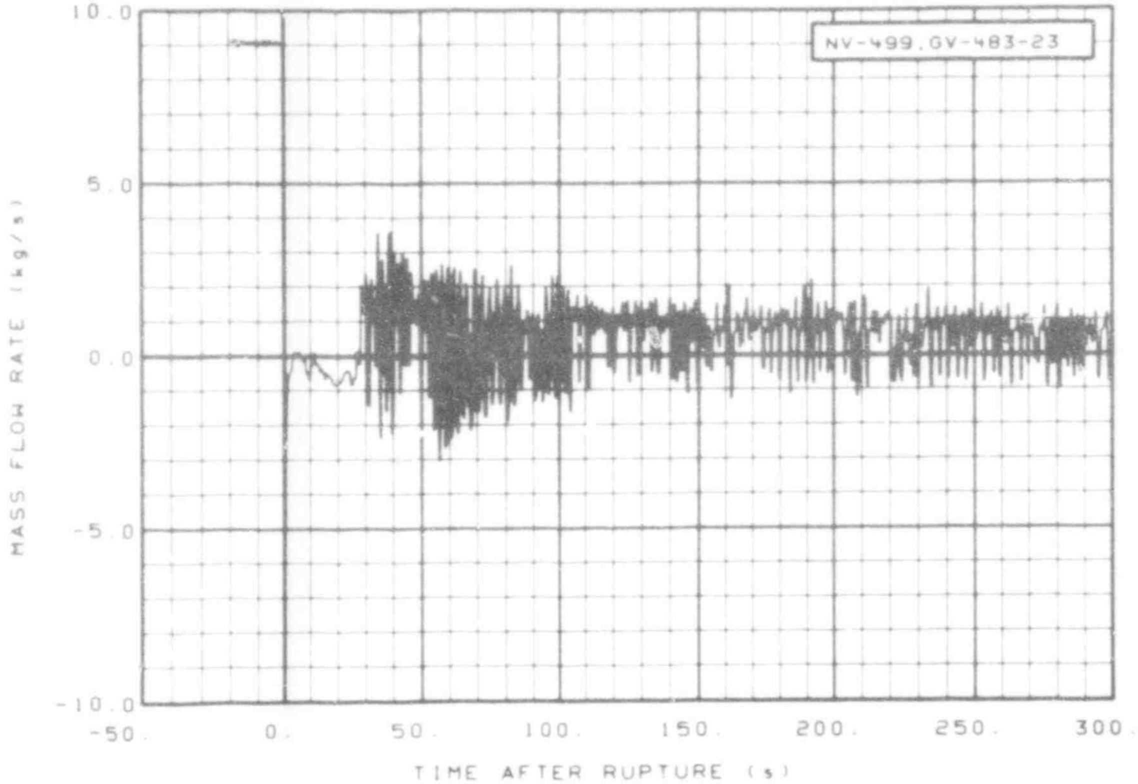

Fig. 305 Mass flow in vessel (NV-499 and GV-483-23), from -20 to 300 s.

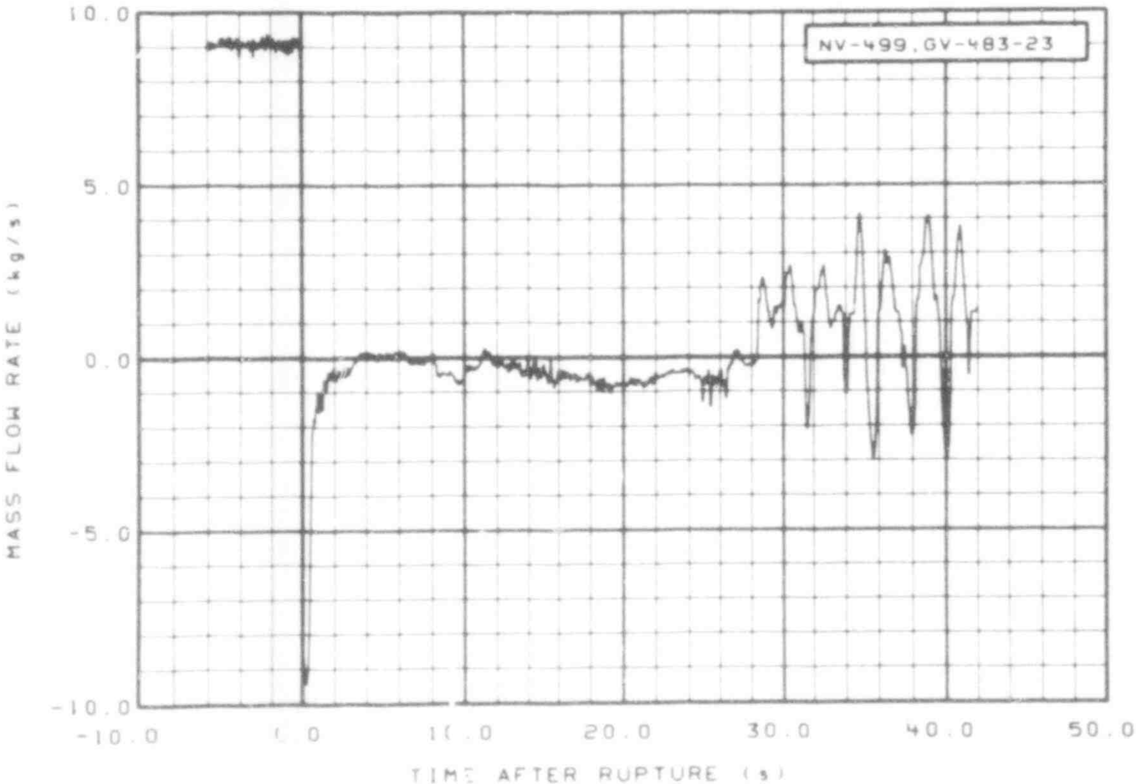

Fig. 306 Mass flow in vessel (NV-499 and GV-483-23), from -6 to 42 s.

507 245

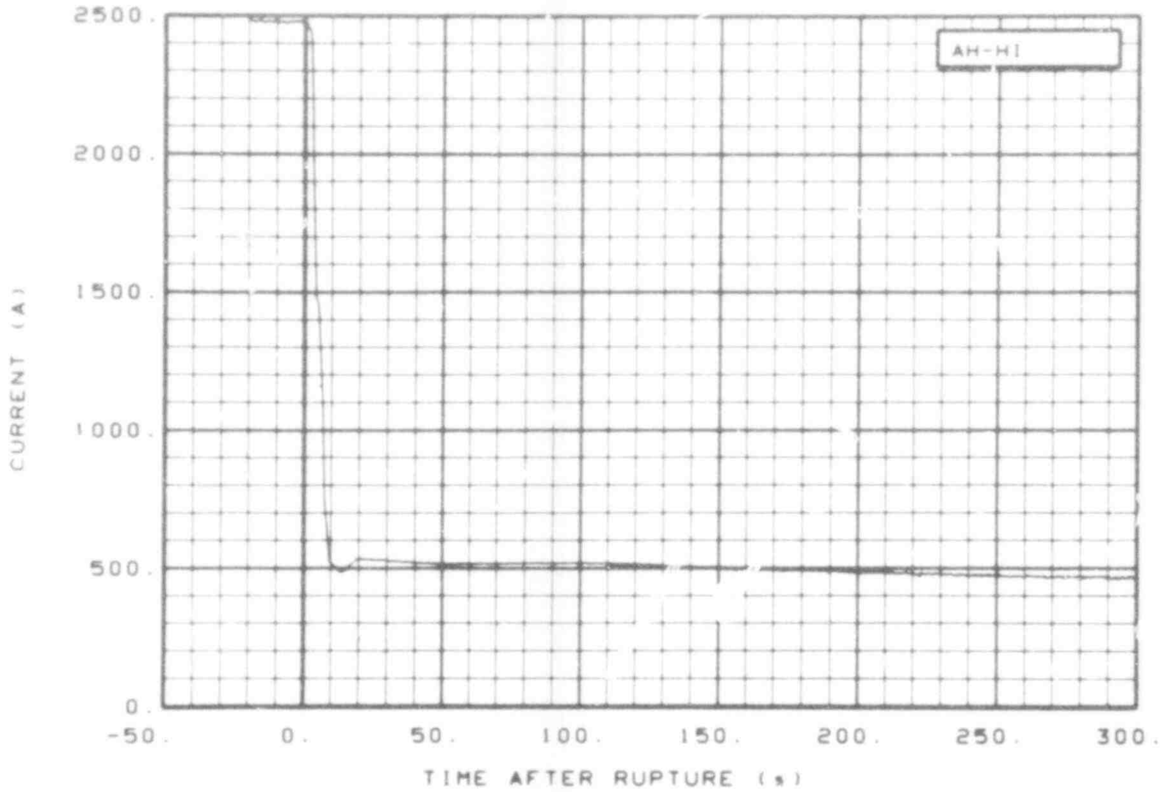

Fig. 307 Core heater high power bus amperage (AH-HI), from -20 to 300 s.

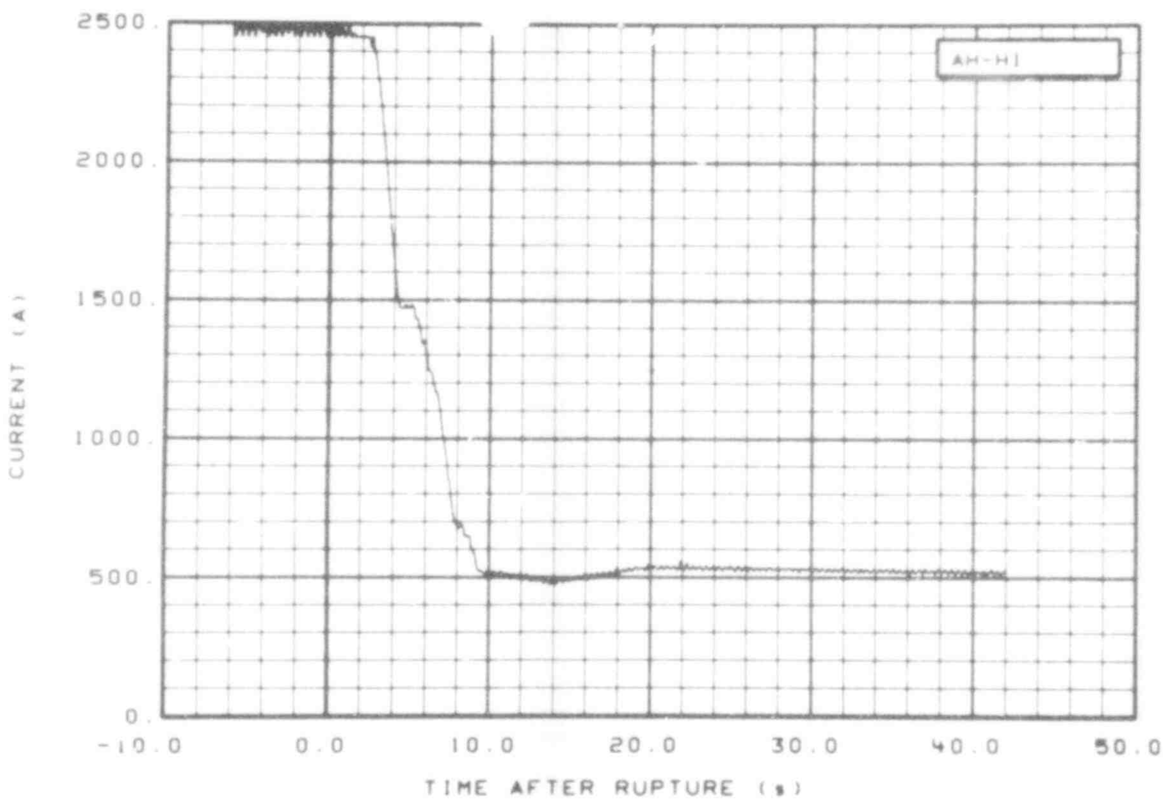

Fig. 308 Core heater high power bus amperage (AH-HI), from -6 to 42 s.

507 246

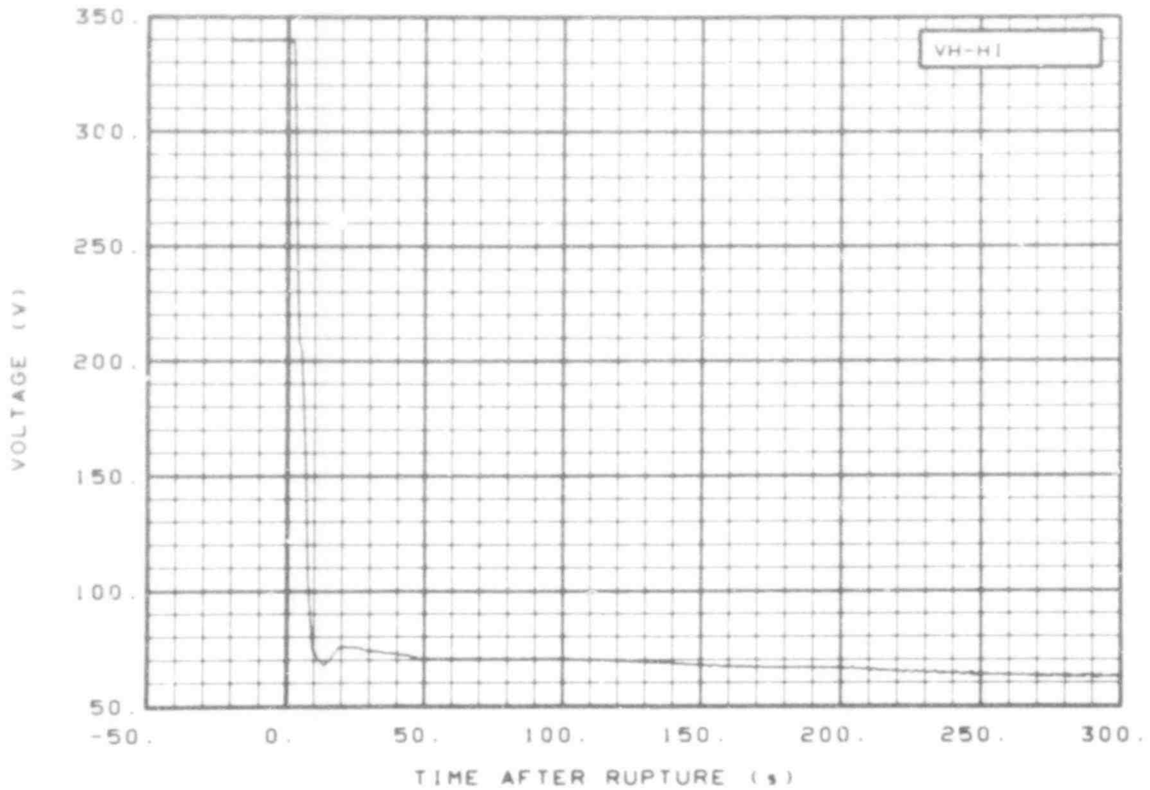

Fig. 309 Core heater high power bus voltage (VH-HI), from -20 to 300 s.

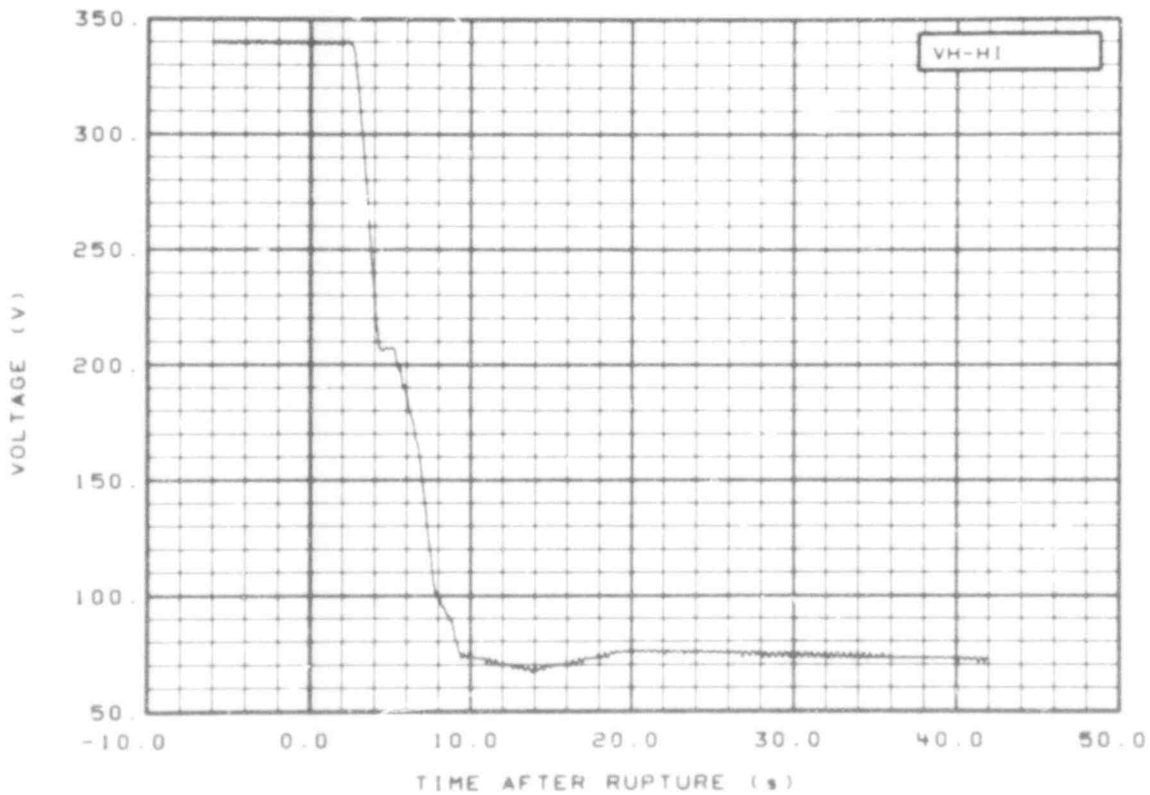

Fig. 310 Core heater high power bus voltage (VH-HI), from -6 to 42 s.

507 247

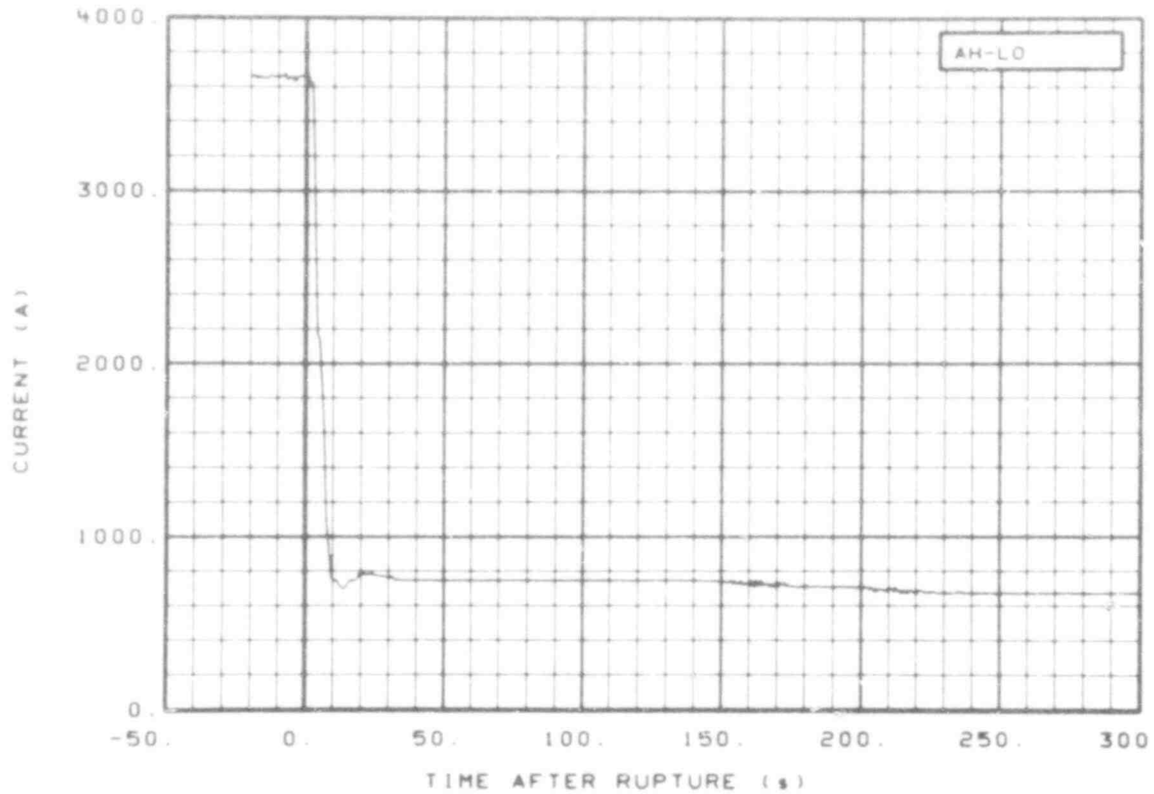

Fig. 311 Core heater low power bus amperage (AH-LO), from -20 to 300 s.

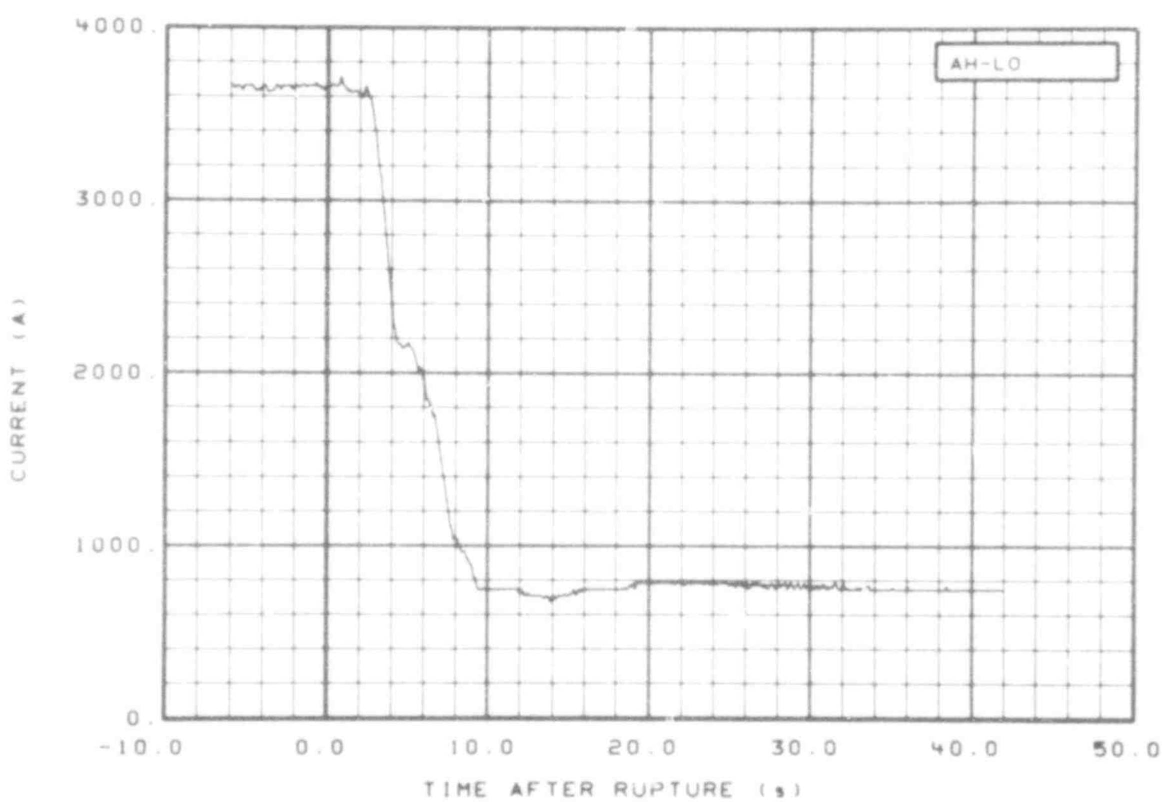

Fig. 312 Core heater low power bus amperage (AH-LO), from -6 to 42 s.

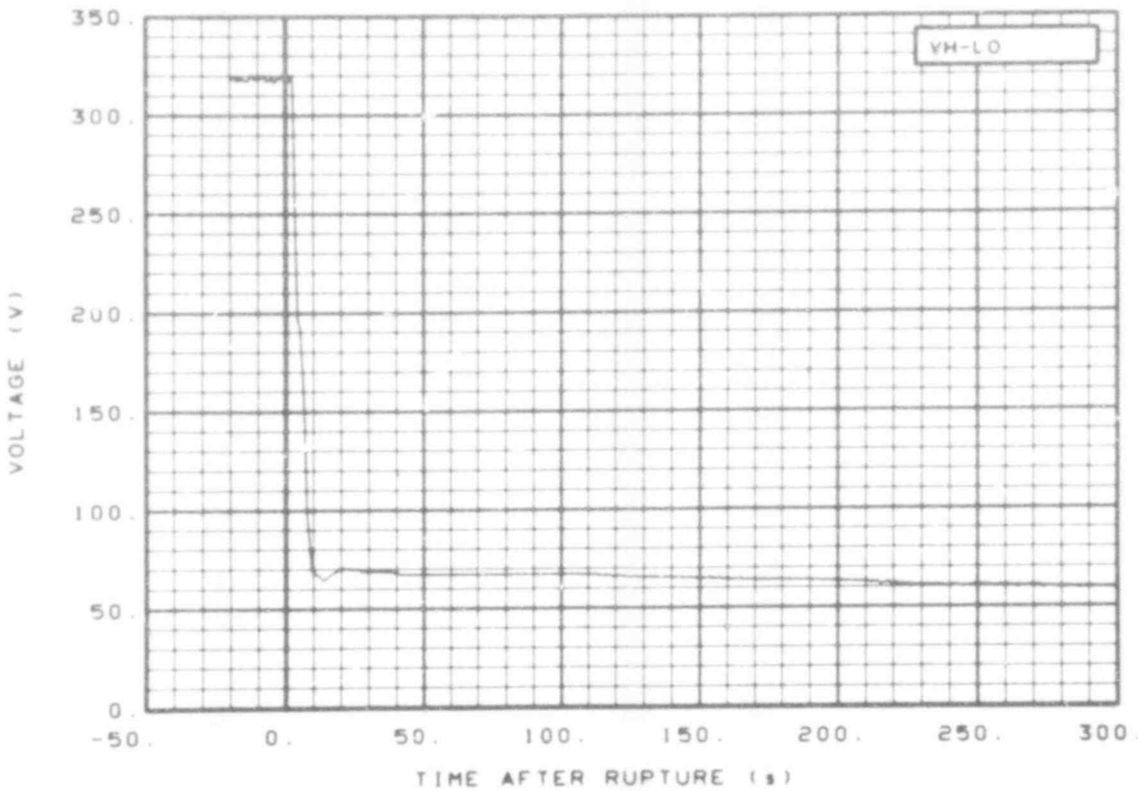

Fig. 313 Core heater low power bus voltage (VH-LO), from -20 to 300 s.

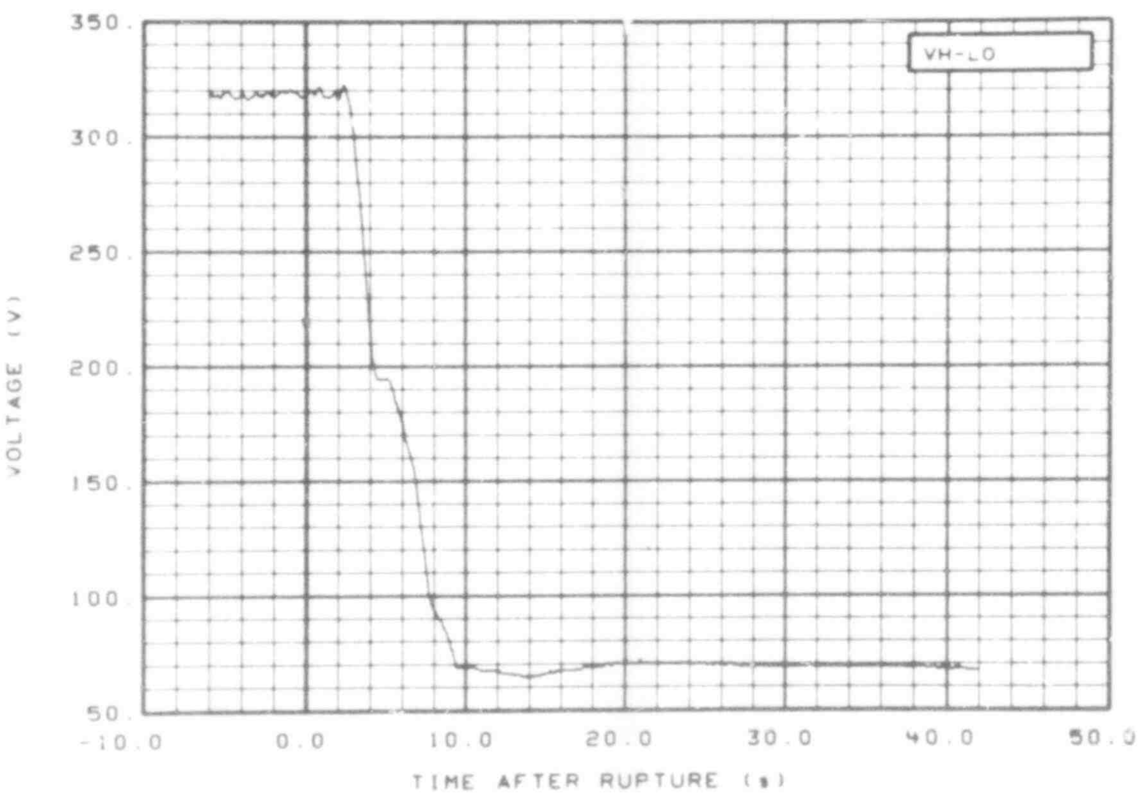

Fig. 314 Core heater low power bus voltage (VH-LO), from -6 to 42 s.

507 249

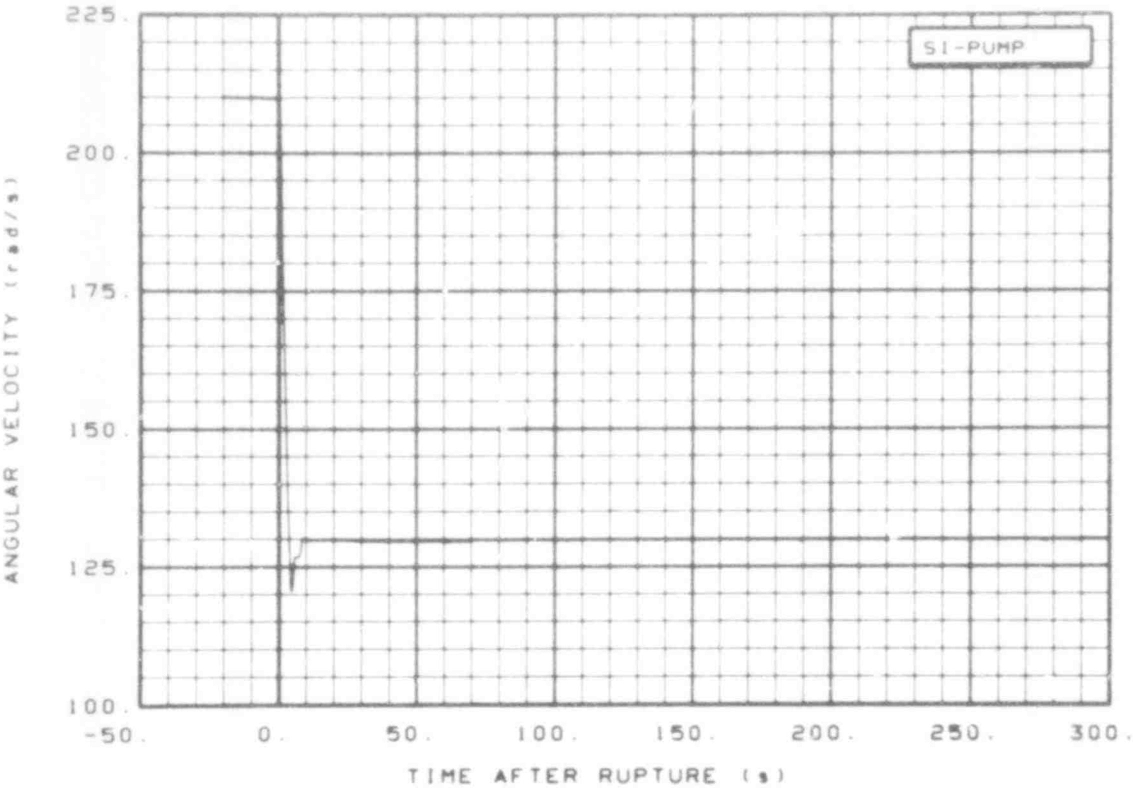

Fig. 315 Intact loop pump speed (SI-PUMP), from -20 to 300 s.

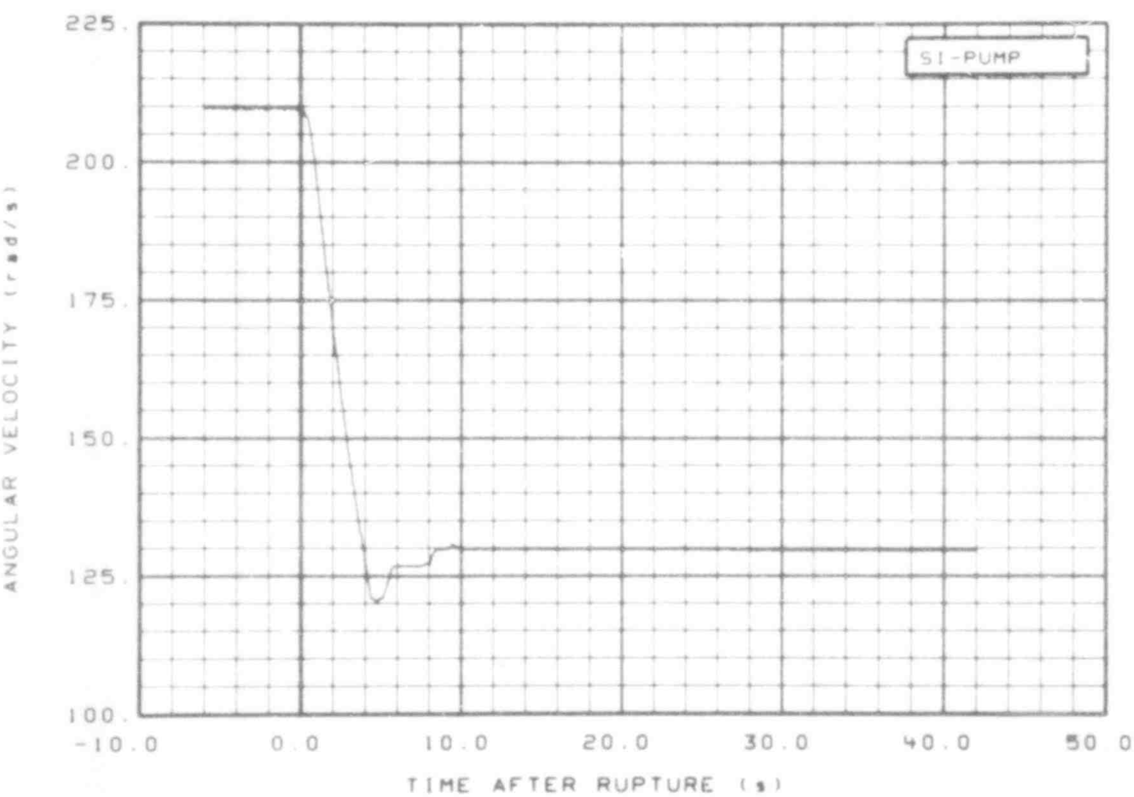

Fig. 316 Intact loop pump speed (SI-PUMP), from -6 to 42 s.

507 250

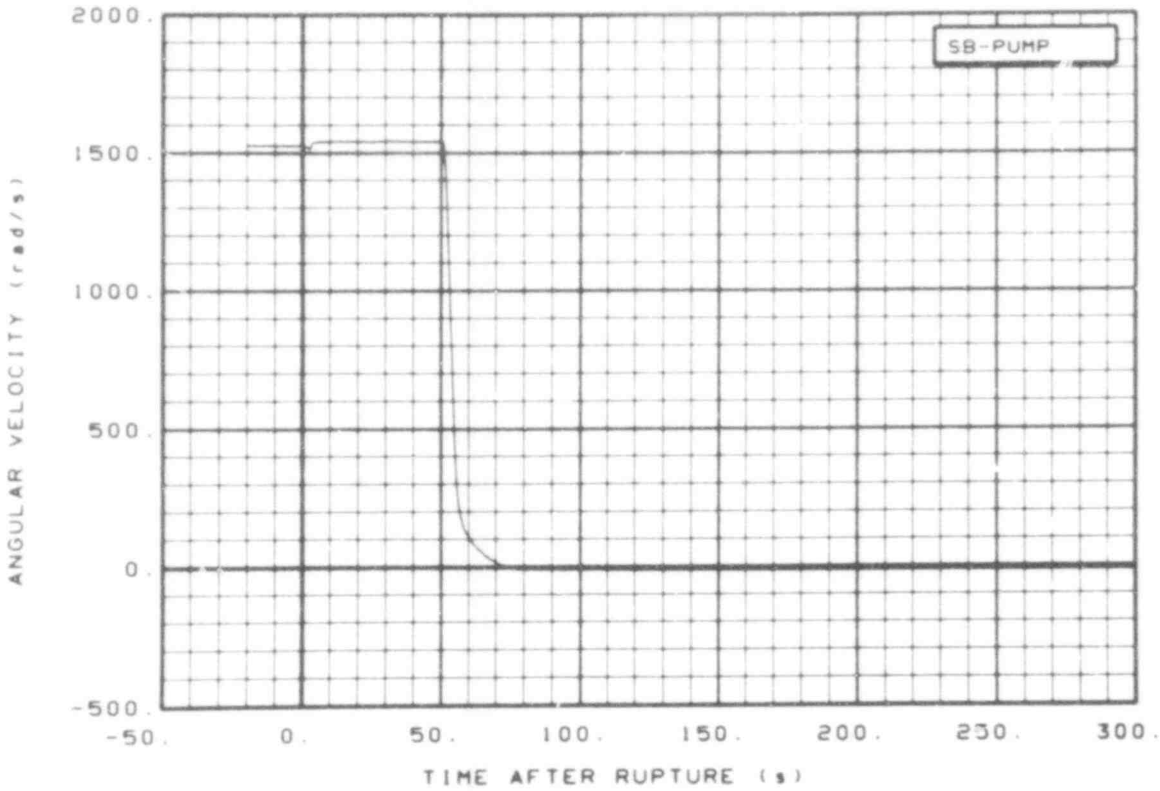

Fig. 317 Broken loop pump speed (SB-PUMP), from -20 to 300 s.

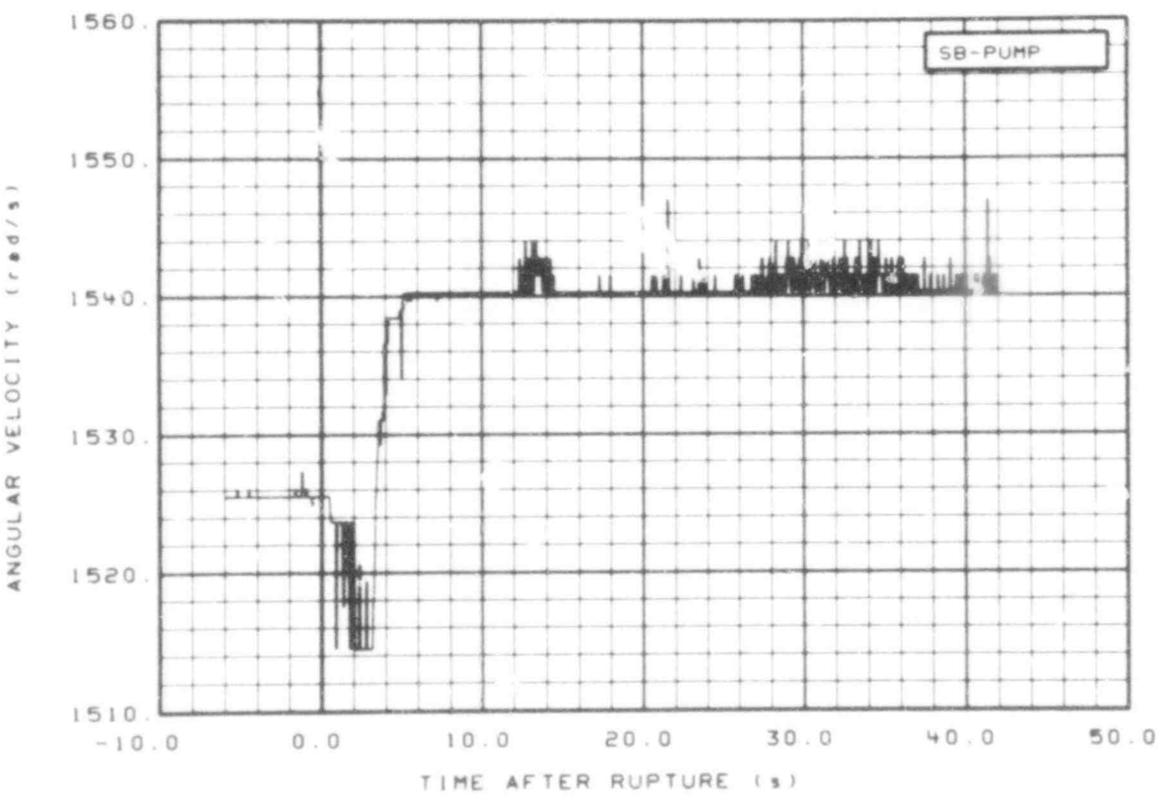

Fig. 318 Broken loop pump speed (SB-PUMP), from -6 to 42 s.

507 251

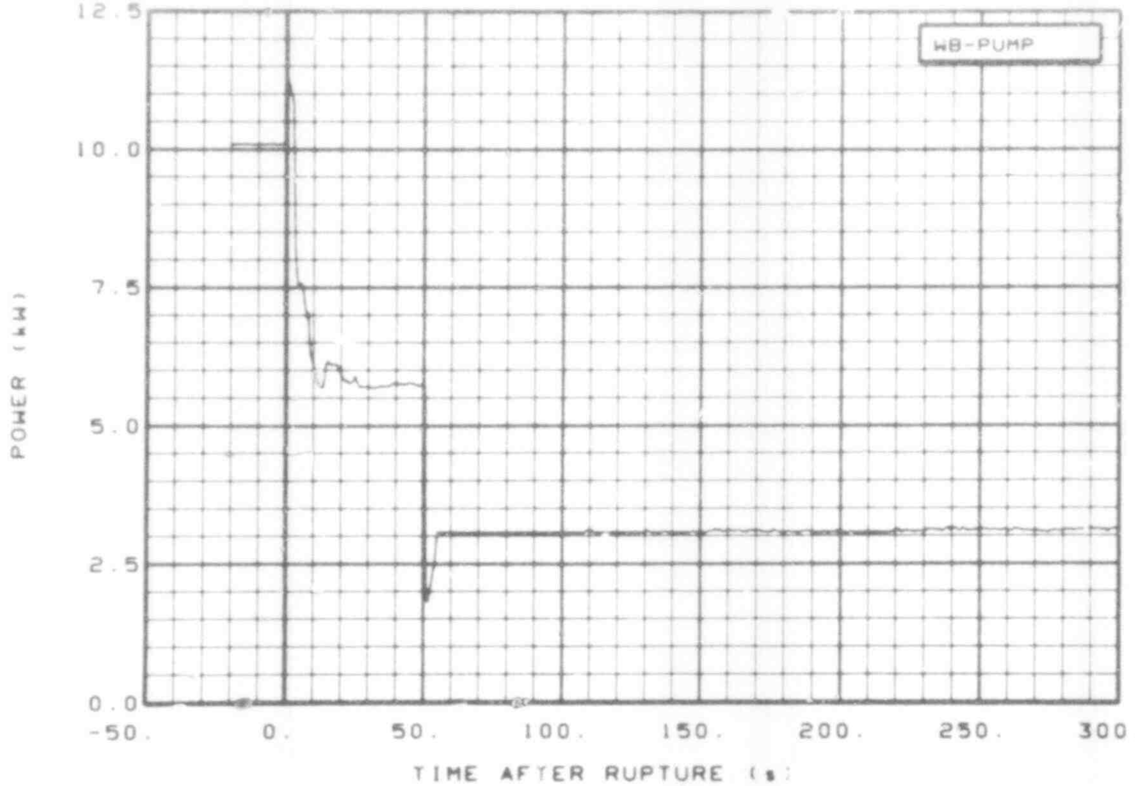

Fig. 319 Broken loop pump power (WB-PUMP), from -20 to 300 s.

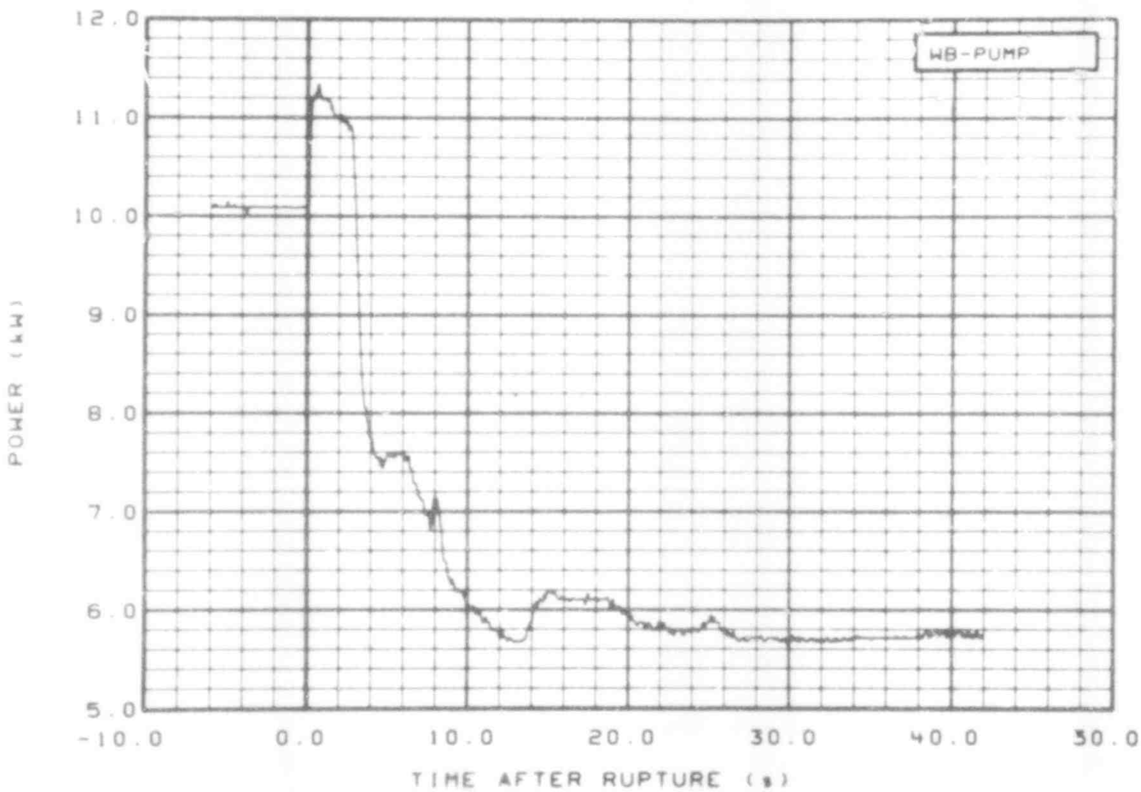

Fig. 320 Broken loop pump power (WB-PUMP), from -6 to 42 s.

507 252

IV. REFERENCES

L. J. Ball et al., *Semiscale Program Description*, TREE-NUREG-1210 (May 1978).

M. L. Patton, *Semiscale Mod-3 Test Program and System Description*, NUREG/CR-0239, TREE-NUREG-1212 (July 1978).

APPENDIX A

DATA ACQUISITION SYSTEM CAPABILITIES

APPENDIX A

DATA ACQUISITION SYSTEM CAPABILITIES

The Semiscale Mod-3 system provides for the acquisition, processing, and presentation of test data. The test data system comprises detectors, signal conditioners, signal processors, and recording and display equipment. The data obtained are principally recorded on an on-line digital system. Selected data channels are also recorded on an analog system.

The on-line digital system is called the digital data acquisition and processing system (DDAPS). The DDAPS has dual and single speed capabilities with identical storage and data output limitations. The dual speed mode is used to extend the recording time when obtaining high frequency data.

From each of up to 240 data channels, the test data system stores 20 blocks of data. Each block of data contains 920 words (each word is the abscissa and ordinate of a data point) of digital information. These 920 words represent a fixed storage display.

The maximum measured throughput rate for the system is 24 000 words per second. This throughput rate can be reduced in increments of 100 words per second. The throughput rate, the number of data channels recorded, and the fixed display of 920 points per block determine the time base for displaying the data.

After the data have been stored, data reduction can be made for presentation and analysis purposes. Because of hardware limitations and aesthetic considerations of data presentation, only certain time bases are used when the data are reduced. For data displayed from -20 to 300 s, the recorded data are made to occupy a 320-s span yielding a time base of 16 s.

Generally, 920 points from a given data channel are displayed in the nominal time base of 16 s. Integral (1 to 20) multiples of 16 s may be used as variations on the nominal time base. Because the output is fixed at 920 points, data compression is accomplished by averaging adjacent data points to give the desired compression.

APPENDIX B

POSTTEST ADJUSTMENTS TO DATA FROM SEMISCALE MOD-3 TEST S-07-9

507 256

APPENDIX B

POSTTEST ADJUSTMENTS TO DATA FROM SEMISCALE MOD-3 TEST S-07-9

Many of the transducers used in the Semiscale Mod-3 system exhibit significant sensitivity to one or more spurious inputs. Strain gage bridge circuits used in pressure transducers, differential pressure transducers, and drag discs are sensitive to changes in ambient temperature. Differential pressure cells are also sensitive to changes in system pressure. Photomultiplier tubes used as gamma ray detectors in the density transducers are sensitive to temperature changes, as well as to random variations in the locations of the radiation sources. Core power measurements depend on a calibrated resistor, whose resistance changes in value as a function of time and power level as it heats up.

Although the uncertainties introduced into the data by spurious secondary inputs generally do not exceed the specified uncertainty ranges of the transducers, significant improvement in measurement accuracy can be achieved if the secondary sensitivity can be identified and removed. Since the exact values of the spurious inputs to which different transducers might be sensitive cannot often be easily predicted and are sometimes inconvenient to measure, secondary effects have been accounted for by correcting the data after the test rather than by using elaborate real time programs in the data acquisition system computer. The methods and results of the posttest data correction analysis for Test S-07-9 are presented in the following paragraphs and tables.

1. DIFFERENTIAL PRESSURE MEASUREMENTS

Pressure sensitivity in the differential pressure cells in the main system loop is determined from the pretest system pressure check. Digital data are recorded for all measurements at ambient temperature, with no system flow, at pressures of ambient, 5575, 8964, 10 817, 12 517, and 15 751 kPa. The output of the differential pressure cells is plotted against system pressure, with the resulting plots used to describe the pressure response of the transducers.

Corrections to differential pressure data were made using the following equation:

$$F'(t) = F(t) + P_1 \, P(t) \tag{B-1}$$

where

$F'(t)$ = corrected data, kPa

$F(t)$ = raw data, kPa

P_1 = pressure sensitivity, kPa/MPa

$P(t)$ = pressure data from indicated transducer used for pressure correction sensitivity, MPa.

Values of the constants are given in Table B-I.

507 257

TABLE B-I

CONSTANTS FOR DIFFERENTIAL PRESSURE MEASUREMENT CORRECTION
(TEST S-07-9)

Detector Identification	P_1	P(t)
DI-13V-1A	-0.024	PV-13
DI-1A-6		
DI-6-7	-0.053	PI-16
DI-SGI-SGO	0.027	PI-16
DI-7-13	-0.027	PI-16
DI-13-15	1.567	PI-16
DI-15-17A		
DI-17A-DIA		
DB-13V-20B	0.100	PV-13
DB-20B-21	0.090	PV-13
DB-21-27A	-1.067	PV-13
DB-SGI-SGO	2.000	PV-13
DB-27A-37A	-0.053	PV-13
DB-37A-40B	-0.290	PV-13
DB-37A-40L	-0.066	PV-13
DB-40B-43A		
DB-40B-45A	0.018	PB-45A
DB-45A-43		
DB-45A-DIA	0.467	PB-45A
DD-DIA-13V	-0.400	PI-16
DD-DIA-170	-0.057	PI-16
DD-DIA-578	-0.011	PI-16
DD-170-435	-0.055	PI-16
DD-435-578	-0.033	PI-16
DV+421+154	0.020	PV-13
DV+159-105	-0.305	PV-13
DV+154-105	0.027	PV-13
DV-578-501	-0.021	PV-13
DV-578-13A	-1.933	PV-13

507 258

TABLE B-I (continued)

Detector Identification	P_1	P(t)
DV-501-442	-0.027	PI-16
DV-501-105	0.057	PV-13
DV-501-13A	-0.100	PI-16
DV-442-278	-0.013	PI-16
DV-278-154	-0.033	PI-16
DV-105-13A		
DI-SG-LL		
DB-SS1-SS4		
DV-ACC1-LL		

2. DENSITY MEASUREMENTS

Density calculations are based on the voltage output of the photomultiplier tubes in the gamma-attenuation densitometer assemblies. The equation used for converting voltage to density is as follows:

$$\rho = C_o + C_1 F(t) \quad \text{(B-2)}$$

where

ρ = the density, kg/m^3

C_o = offset, kg/m^3

C_1 = conversion factor, $(kg/m^3)/v$

F(t) = transducer output, v.

Constants C_o and C_1 are adjusted to match the final data to density values calculated from measured pressure and temperature values at the preblowdown and post drain conditions, effectively giving the data an in-place calibration. These calculations are made in the Mod-3 system prior to initial data release and are not considered posttest adjustments.

Some density measurements are obtained using a two-beam gamma densitometer which operates on the same basic principle of gamma attentuation as does the single-beam gamma densitometer. Each beam originates from the same gamma source and is allowed to pass through separate portions of the piping cross-sectional flow area to obtain an average density measurement in that particular region. The geometrical relationship of the gamma beam path through the piping and geometrically related variables used for processing of data from a two-beam gamma densitometer are shown in Figure B-1. The average density measured by each individual gamma beam is obtained using the same equation as is used for the single-beam gamma densitometers.

507 259

In the Semiscale Mod-3 system, two-beam gamma densitometers provide information which allows the calculation of a better average density than that obtained from a single beam in a horizontal pipe. A mathematical model is used for processing the two-beam data to obtain the improved average density information. The processing method used is based on a froth-water model coupled with information from the two individual gamma beams and related beam path and piping cross-sectional geometry. The resulting information is recorded and reported under the density measurement identification ending with a "C", for example, GI-17C.

The use of the froth-water model for obtaining average density from a two-beam gamma densitometer in a horizontal pipe is based on observations indicating that flow regimes in the Semiscale Mod-3 system can be modeled by a layer of water on the bottom of the pipe with a degree of froth on the surface. For homogeneous flow conditions such as all froth or all liquid the model remains valid. At any point in time slug flow is also modeled. The froth-water model does not model annular or inverted annular flows very well. However, these flows are not expected to exist for significant portions of a Semiscale Mod-3 system blowdown in horizontal piping. Density gradients from the top to the bottom of the pipe may exist showing no distinct location change from water to froth. This flow is neither totally homogeneous nor stratified, but the froth-water model does provide an adequate approximation of the average density characteristic of this flow pattern.

The average density obtained by using the gamma beam geometry shown in Figure B-1 and by applying the froth-water model is given by

$$\bar{\rho} = \alpha_f \, \rho_1 + (1 - \alpha_f) \, \rho_w \ \text{kg/m}^3 \qquad \text{(B-3)}$$

where

$\bar{\rho}$ = average cross-sectional density

ρ_1 = average density measured by the upper beam (measures the froth density)

ρ_w = density of liquid water (at local system conditions)

α_f = $1 + (1/2\pi)(\sin\beta - \beta)$ = volumetric fraction containing froth.

The angle which β represents is shown in Figure B-1. Values for β are obtained as follows:

$$\beta = 2 \cos^{-1} (1 - 2h) \qquad \text{(B-4)}$$

where

h = $\frac{H}{D} = \cos^2\theta \left(\frac{\rho_2 - \rho_1}{\rho_w - \rho_1}\right)$

where

H = $l_w \cos\theta$ (l_w and θ are defined in Figure B-1)

D = piping inside diameter

ρ_2 = the average density measured by the lower gamma beam.

507 260

Average density is not calculated using the two-beam froth-water model when the angle is not favorable due to system hardware restrictions in positioning the source. The froth-water model requires separate density sampling in both the upper and lower portions of the piping cross section.

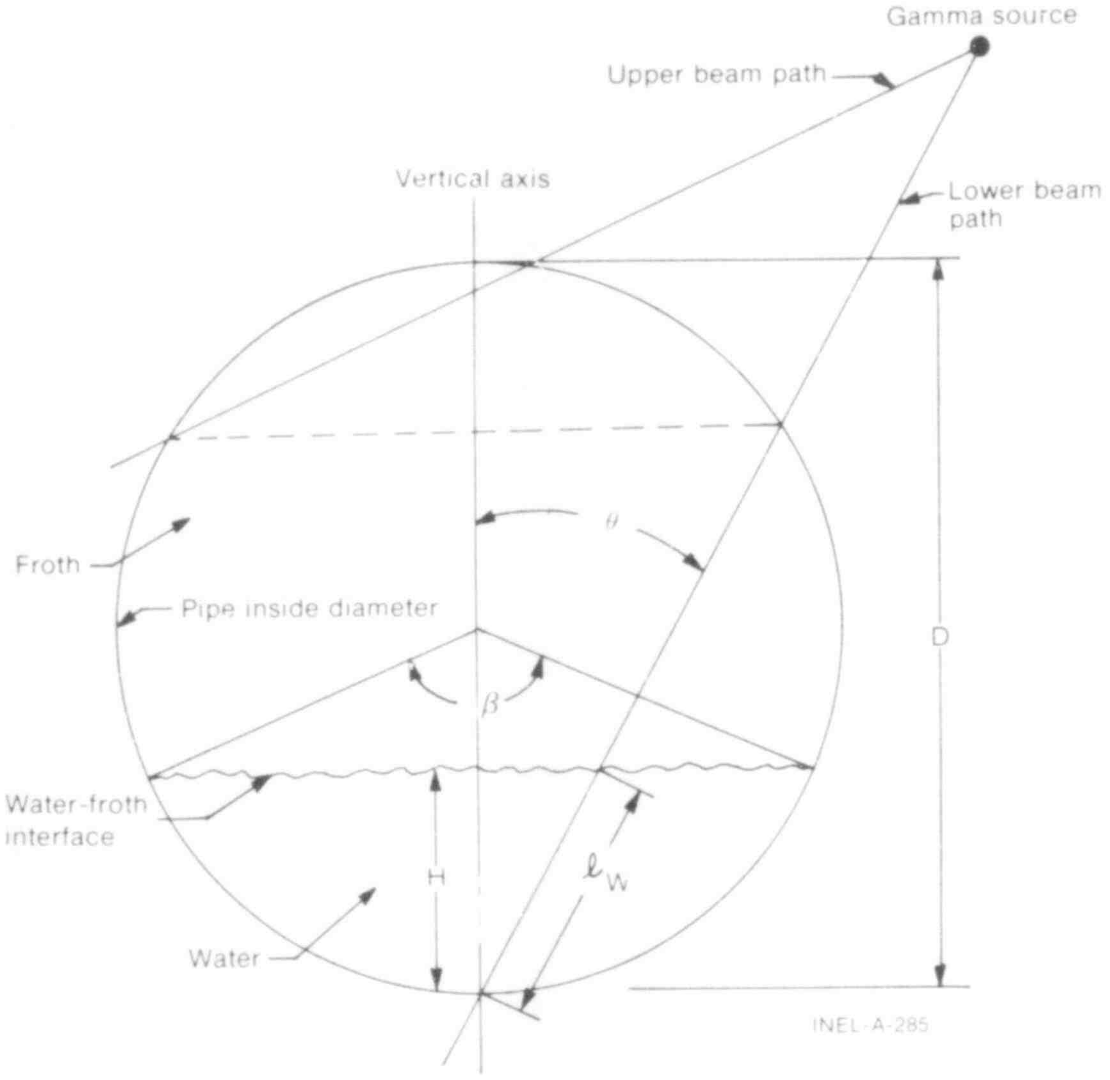

Fig. B-1 Geometry used for processing of density data obtained from two-beam gamma densitometers.

507 261

APPENDIX C

SELECTED DATA WITH ESTIMATED TOTAL UNCERTAINTY BANDS FROM SEMISCALE MOD-3 TEST S-07-9

507 262

APPENDIX C

SELECTED DATA WITH ESTIMATED TOTAL UNCERTAINTY BANDS FROM SEMISCALE MOD-3 TEST S-07-9

Analysis has been performed on selected data from Test S-07-9 to provide a guide to the uncertainty associated with data measurements in the Semiscale Mod-3 system. The end result of the analysis is presented as uncertainty bands about the measured data which represent a 95% confidence level.

The uncertainty bands are obtained by combining uncertainties obtained from analysis of the data itself (random uncertainty) and engineering analysis of the measurement system (engineering uncertainty). The procedure by which uncertainty bands were established for the data presented in this appendix is described in the following paragraphs.

The data trace under analysis was empirically fitted with a linear difference equation, which was subject to a white noise input at each sampling time point. The objective of the empirical fitting procedure was to characterize the white noise, which was taken to represent the random uncertainty. The procedures for fitting the difference equation are discussed in depth in Reference C-1. A data trace was often segmented and different equations were fitted to each segment with statistical correlations between successive observations accounted for by the fitting procedure. The white noise input was assumed to arise from a normally distributed population. The standard deviation of the white noise, as found during the fitting procedures, was taken as an estimate of the random uncertainty standard deviation and is shown in Table C-I in appropriate engineering units. The traces of the uncertainty band analysis are shown in Figures C-1 through C-40.

Other uncertainties in the data exist because of such factors as variability in installation procedures and techniques, calibration uncertainties, variability in materials, and temperature and pressure sensitivities. These uncertainties and the procedures for estimating them are discussed in Reference C-2. They are referred to as engineering uncertainties and the estimates are largely subjective. Because of the continuing effort to improve the accuracy of the measured data, such as through the use of better transducers, better signal conditioning and processing equipment, and better calibration and installation techniques, the engineering uncertainties for data from most of the transducer systems have changed from those published in Reference C-2. Table C-II provides a summary of engineering uncertainty values obtained from current analysis techniques as applied to the data presented herein.

In addition to the normal hardware and installation related sources of engineering uncertainty, a significant measurement uncertainty results when the current transducer systems are subjected to separated two-phase flow regimes during the course of the blowdown transient. Accordingly, for those data affected (fluid density, volumetric flow, and mass flow), which are presented in this appendix, a more extensive assessment was conducted of additional engineering uncertainty due to flow regime effects. Table C-III identifies the data analyzed and the period in the blowdown process for which flow regime uncertainties were included as a part of the total engineering uncertainty. The time of occurrence of separated two-phase flow and the resulting effect on the uncertainty of the data were evaluated by considering, on an individual basis, each detector output with reference to indications by other auxiliary measurements.

The gamma densitometer density measurement data are affected by two-phase separated flow regimes. The resulting transducer output is a measurement of the average attenuation of the gamma beam through the measured medium. The beam attenuation, in turn, is interpreted through physical relationship to be a measure of the average density along the beam path. When stratified type flow was considered present, the gamma beam attenuation was considered to be a result of a liquid layer and steam at system conditions.

507 263

With this assumption and the system geometry, a void fraction was calculated and a new "effective" average density was calculated. The difference between the average density based on the assumption of homogeneous conditions and the average density for stratified conditions was considered to be the uncertainty.

The flow regime uncertainties of the turbine flowmeter were estimated by calculating a void fraction and the cross-sectional liquid and steam flow area for stratified flow. This calculation was accomplished using methods similar to those used to calculate the average density for stratified flows. A simple model was used to equate the forces on the turbine with the assumption of a known void fraction, stratified flow, known component densities, and slip ratio greater than unity. This process provided phase velocities. With the phase densities, velocities, and void fraction, a volumetric flow rate could be calculated. The difference between this value and the measured value was considered to be the uncertainty.

The overall standard deviation of a data point is taken as the root of the sum of the random uncertainty variance and the total engineering uncertainty variance; that is,

$$\sigma_o = \sqrt{\sigma_R^2 + \sigma_E^2} \qquad \text{(C-1)}$$

where

σ_o = overall standard deviation of a data point

σ_R^2 = random uncertainty variance

σ_E^2 = engineering uncertainty variance.

The uncertainty bands for the data are computed about the value given by the fitted difference equation y_i at time point i; that is,

$$\text{uncertainty band} = y_i \pm 1.96\,\sigma_o\ . \qquad \text{(C-2)}$$

With due regard to the fact that σ_E has been estimated subjectively, the uncertainty band may be interpreted as an approximate 95% confidence interval within which any true value of the measured variable is consistent with the data.

On certain occasions, the symmetrical uncertainty band given by Equation (C-2) is not appropriate. On those occasions, asymmetrical uncertainty bands were computed; that is, with the width being greater on one side of y_i than on the other.

Finally, the original data trace, along with its uncertainty band from Equation (C-2), was input to a computer plot package. The resulting plot contained the actual data trace surrounded by an uncertainty band derived both from random uncertainty and engineering uncertainty considerations. The indicated uncertainty bands after thermocouple dryout occurred for the fluid temperature measurements should be ignored. Uncertainty bands for these segments of the data were not obtained and bands only appear because of limitations in the plotting package.

TABLE C-I

RANDOM UNCERTAINTY STANDARD DEVIATION
(TEST S-07-9)

Measurement	Random Uncertainty Standard Deviation σ_R	Period of Application (s)	Figure
TFI-1	0.004	-20 to -0.4	C-1
	1.51[illegible]	-0.4 to 5	
	1.935	5 to 48	
	0.408	48 to 300	
TFB-20	0.141	-20 to -0.4	C-2
	1.935	-0.4 to 4	
	1.541	4 to 69	
	3.168	69 to 300	
TFD-294	0.004	-20 to -0.4	C-3
	2.807	-0.4 to 27	
	6.208	27 to 55	
	1.405	55 to 113	
	0.610	113 to 180	
	1.386	180 to 300	
TFV-578A	0.0	-20 to 0.04	C-4
	3.296	0.04 to 5	
	0.964	5 to 300	
TIFV+79D	0.994	-20 to 0.9	C-5
	1.374	0.9 to 8	
	0.394	8 to 84	
	0.558	84 to 153	
	0.186	153 to 238	
	0.146	238 to 300	
TFG-5AB-45	0.0	-20 to -0.4	C-6
	22.793	-0.4 to 5	
	17.778	5 to 11	
	[illegible].001	11 to 17	
	7.713	17 to 21	
	28.077	21 to 26	
	23.364	26 to 35	
	27.941	35 to 41	
	1.502	41 to 300	
TMI-1T16	0.079	-20 to 2	C-7
	0.345	2 to 300	

507 265

TABLE C-I (continued)

Measurement	Random Uncertainty Standard Deviation σ_R	Period of Application (s)	Figure
TMB-20B16	0.041	-20 to 0.04	C-8
	0.652	0.04 to 5	
	0.724	5 to 48	
	0.852	48 to 55	
	0.249	55 to 101	
	1.078	101 to 107	
	0.366	107 to 300	
TMD-364	0.280	-20 to 300	C-9
TMV+79D	0.168	-20 to 0.9	C-10
	0.618	0.9 to 8	
	0.282	8 to 32	
	0.086	32 to 253	
	0.214	253 to 300	
TH-C2-8	0.070	-20 to -0.4	C-11
	2.791	-0.4 to 6	
	0.885	6 to 28	
	15.681	28 to 33	
	3.597	33 to 55	
	1.509	55 to 90	
	0.786	90 to 300	
TH-C2-180	1.075	-20 to -0.4	C-12
	8.174	-0.4 to 5	
	4.648	5 to 174	
	2.011	174 to 300	
PI-16	0.006	-20 to -0.4	C-13
	1.006	-0.4 to 5	
	0.021	5 to 300	
PB-45A	0.002	-20 to -0.4	C-14
	1.104	-0.4 to 5	
	0.026	5 to 300	
PV-ACC1	0.0003	-20 to 6	C-15
	0.013	6 to 13	
	0.006	13 to 46	
	0.003	46 to 300	
PB-SD	0.008	-20 to 180	C-16
	0.005	180 to 220	
	0.020	220 to 300	

507 266

TABLE C-I (continued)

Measurement	Random Uncertainty Standard Deviation σ_R	Period of Application (s)	Figure
DI-6-7	0.544	-20 to -0.8	C-17
	23.294	-0.8 to 4	
	3.437	4 to 36	
	3.910	36 to 80	
	1.668	80 to 300	
DI-7-13	0.136	-20 to -0.8	C-18
	1.159	-0.8 to 4	
	2.360	4 to 12	
	4.325	12 to 19	
	0.389	19 to 70	
	0.099	70 to 300	
DB-57A-40L	1.652	-20 to -0.8	C-19
	222.84	-0.8 to 5	
	0.002	5 to 32	
	6.436	32 to 36	
	9.119	36 to 47	
	3.232	47 to 300	
DD-DIA-578	0.189	-20 to -0.8	C-20
	18.657	-0.8 to 5	
	3.474	5 to 34	
	8.490	34 to 90	
	2.558	90 to 300	
DV-501-105	0.108	-20 to -0.8	C-21
	22.765	-0.8 to 5	
	1.874	5 to 53	
	0.942	53 to 300	
DI-SG-LL	0.312	-20 to -0.4	C-22
	0.655	-0.4 to 4	
	0.112	4 to 300	
FI-1	0.024	-20 to -0.4	C-23
	1.064	-0.4 to 5	
	1.528	5 to 36	
	3.407	36 to 50	
	1.317	50 to 220	
	0.934	220 to 300	
FI-17	0.034	-20 to -0.4	C-24
	1.082	-0.4 to 5	
	1.770	5 to 34	
	4.924	34 to 56	
	2.874	56 to 268	
	3.109	268 to 300	

TABLE C-I (continued)

Measurement	Random Uncertainty Standard Deviation σ_R	Period of Application (s)	Figure
FB-45	0.457	-20 to -0.4	C-25
	4.546	-0.4 to 4	
	1.006	4 to 10	
	1.886	10 to 14	
	2.563	14 to 38	
	3.776	38 to 53	
	2.578	53 to 300	
FD-424	0.020	-20 to -0.4	C-26
	4.547	-0.4 to 5	
	0.905	5 to 28	
	0.982	28 to 110	
	0.740	110 to 300	
FV+1	0.019	-20 to -0.4	C-27
	2.541	-0.4 to 5	
	2.003	5 to 29	
	4.035	29 to 50	
	1.188	50 to 300	
FV-LPIS	1.756	-20 to -0.8	C-28
	3.083	-0.8 to 9	
	0.254	9 to 34	
	10.036	34 to 39	
	2.112	39 to 46	
	0.558	46 to 300	
GI-1T	7.408	-20 to 0.04	C-29
	61.927	0.04 to 5	
	7.029	5 to 161	
	11.290	161 to 300	
GI-1B	2.713	-20 to -0.4	C-30
	35.415	-0.4 to 5	
	57.173	5 to 20	
	7.265	20 to 235	
	14.595	235 to 300	
GI-1C	4.832	-20 to -0.04	C-31
	55.050	-0.04 to 5	
	23.382	5 to 25	
	3.606	25 to 151	
	9.112	151 to 300	
GI-17T	12.831	-20 to 9	C-32
	75.417	9 to 16	
	8.614	16 to 300	

507 268

TABLE C-I (continued)

Measurement	Random Uncertainty Standard Deviation σ_R	Period of Application (s)	Figure
GI-17B	4.152	-20 to 0.5	C-33
	31.449	0.5 to 11	
	6.440	11 to 156	
	5.925	156 to 300	
GI-17C	7.457	-20 to 0.5	C-34
	13.535	0.5 to 9	
	51.434	9 to 17	
	4.257	17 to 300	
GB-45VR	11.651	-20 to 3	C-35
	19.221	3 to 8	
	33.902	8 to 18	
	9.382	18 to 155	
	14.014	155 to 300	
GV-11	2.686	-20 to -0.4	C-36
	66.754	-0.4 to 4	
	14.172	4 to 12	
	36.746	12 to 20	
	7.881	20 to 30	
	5.015	30 to 160	
	21.030	160 to 300	
FI-1, GI-1C	0.053	-20 to -0.4	C-37
	0.579	-0.4 to 5	
	0.167	5 to 26	
	0.111	26 to 300	
FI-17, GI-17C	0.060	-20 to -0.8	C-38
	0.828	-0.8 to 6	
	0.461	6 to 12	
	0.166	12 to 300	
FB-45, GB-45VR	0.216	-20 to -0.4	C-39
	3.408	-0.4 to 4	
	0.557	4 to 22	
	0.209	22 to 151	
	0.294	151 to 300	
FV+1, GV-11	0.040	-20 to -0.4	C-40
	1.316	-0.4 to 5	
	0.235	5 to 50	
	0.199	50 to 151	
	0.324	151 to 300	

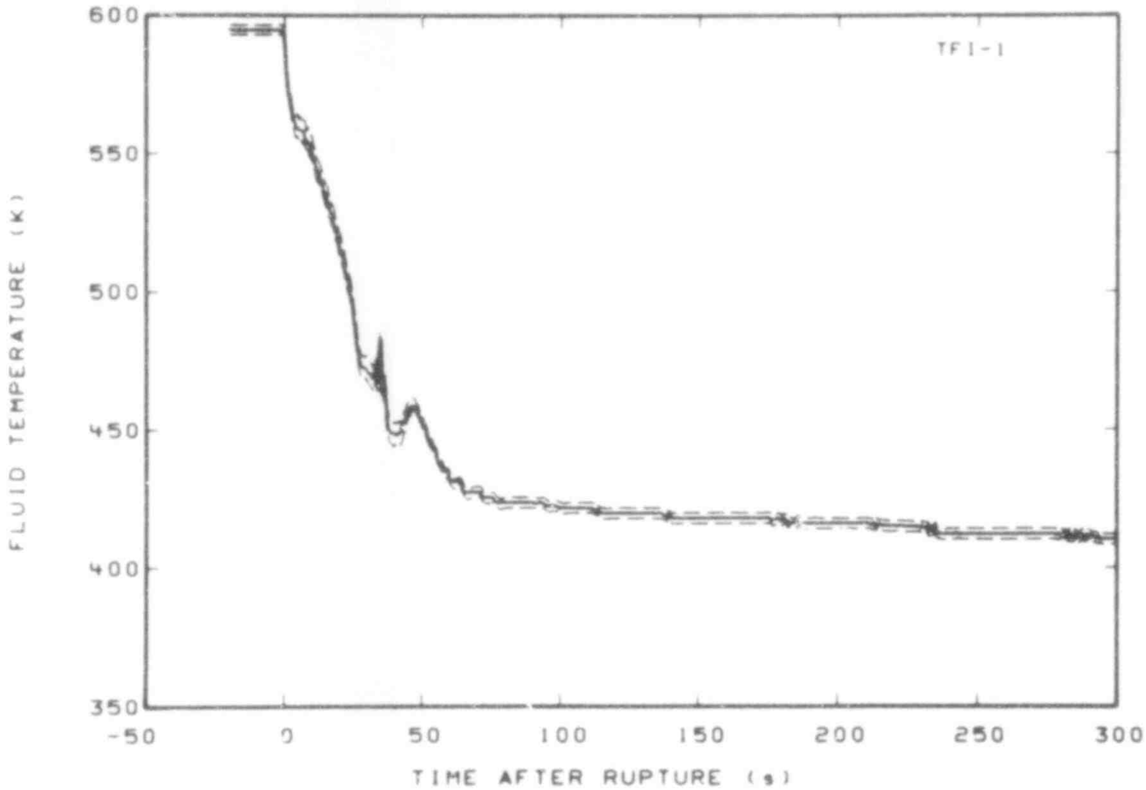

Fig. C-1 Fluid temperature in intact loop hot leg (TFI-1).

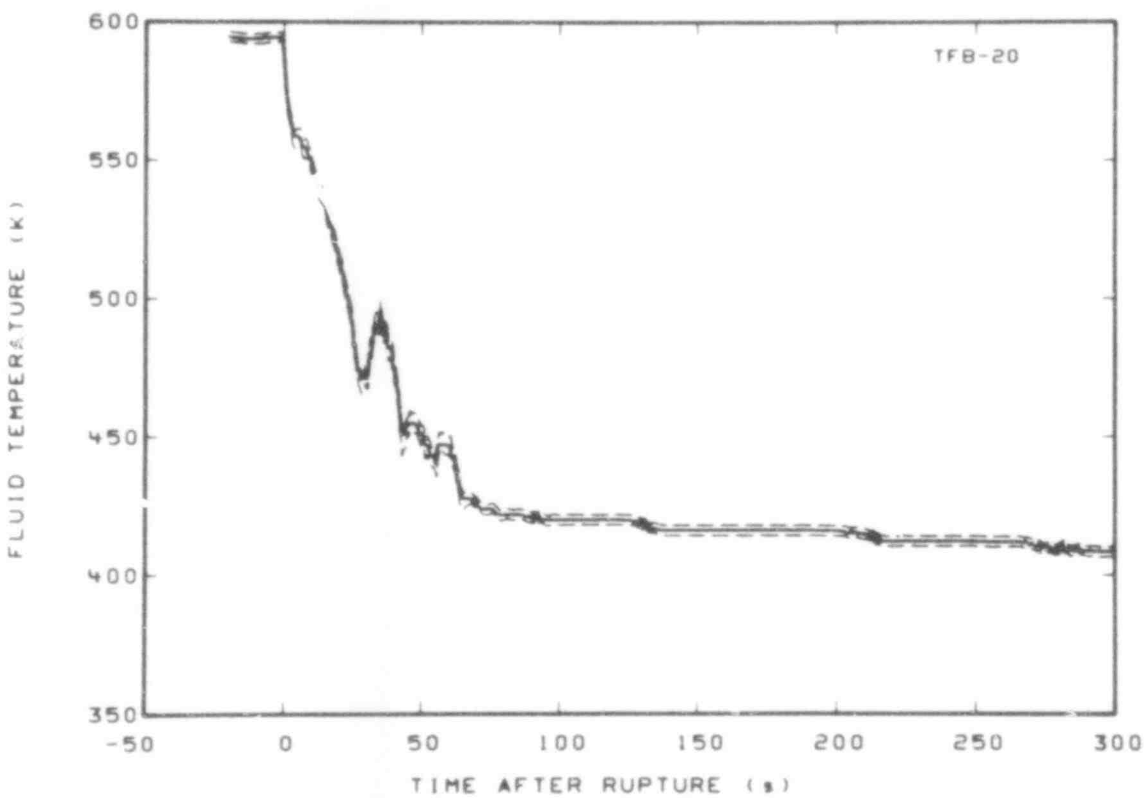

Fig. C-2 Fluid temperature in broken loop (TFB-20).

507 270

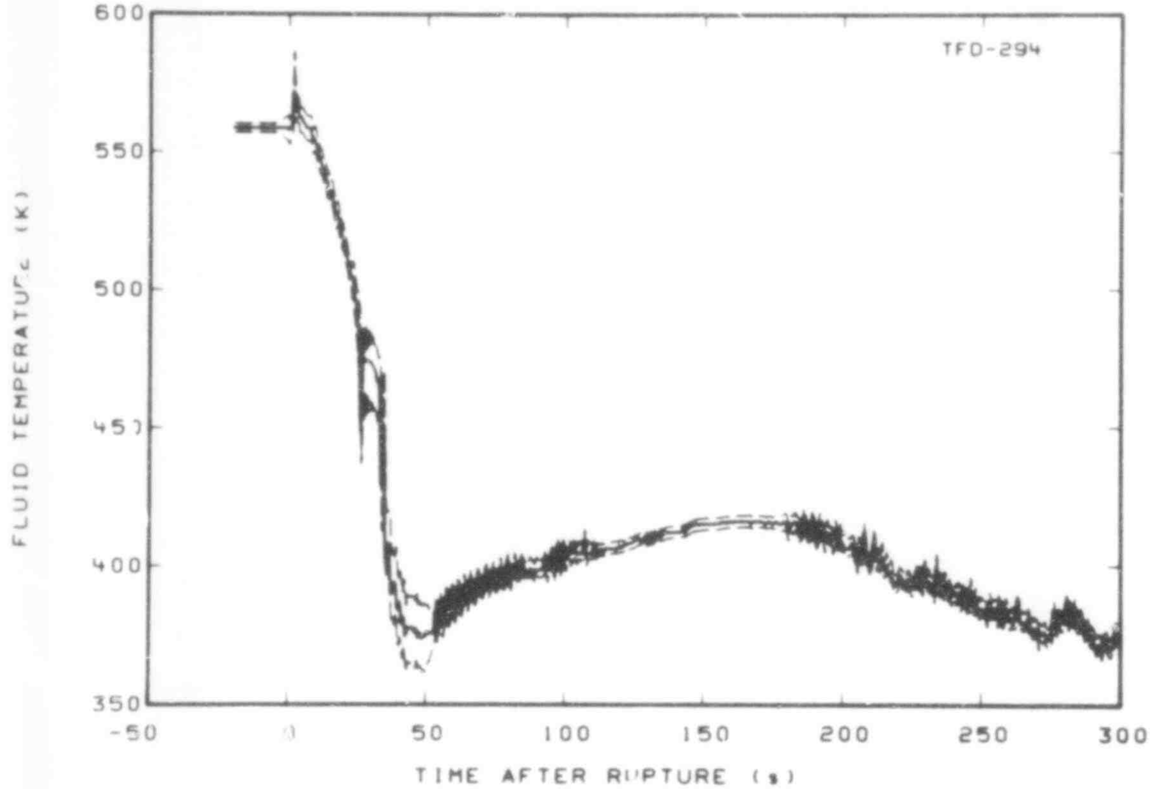

Fig. C-3 Fluid temperature in downcomer (TFD-294).

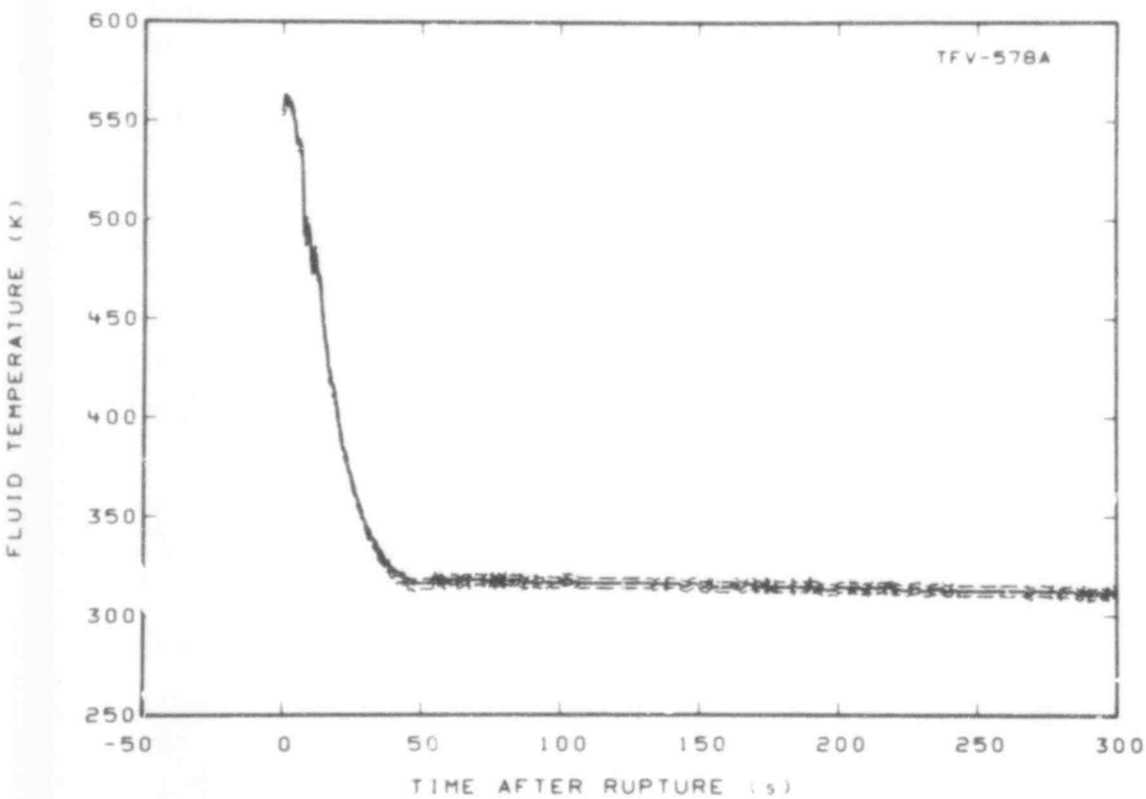

Fig. C-4 Fluid temperature in vessel (TFV-578A).

507 271

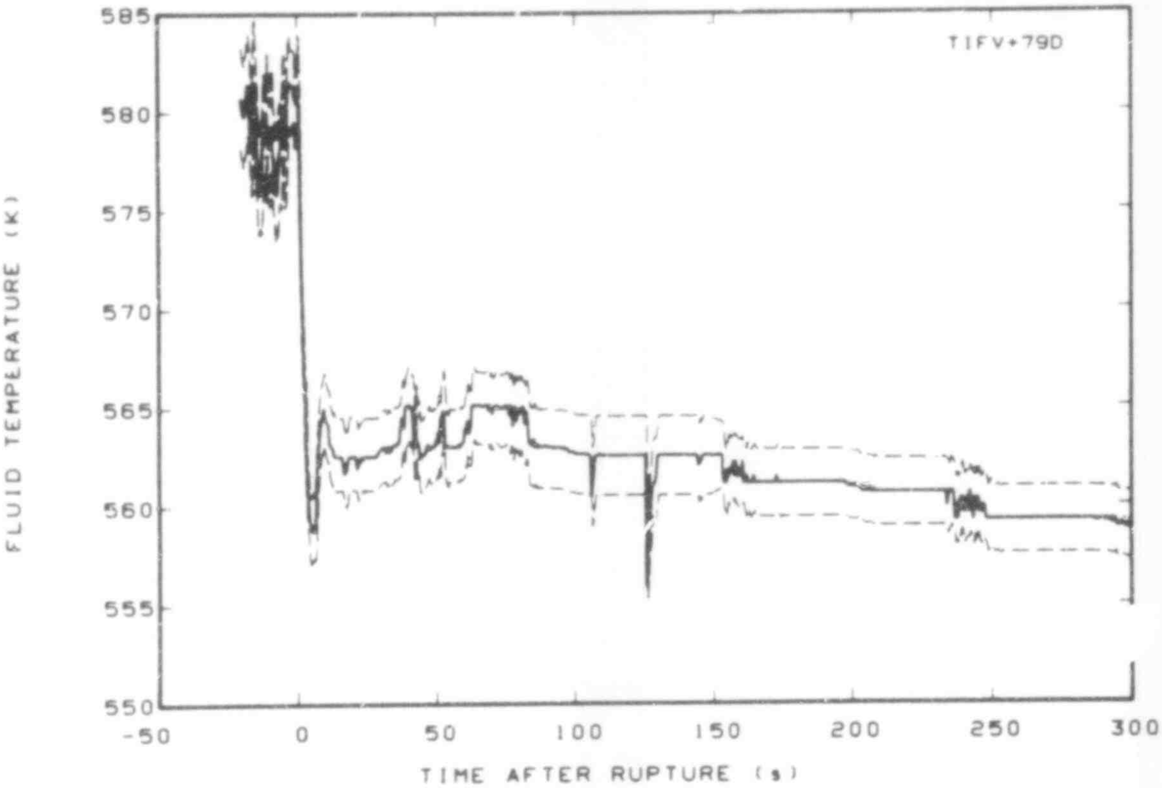

Fig. C-5 Fluid temperature in vessel (TIFV + 79D).

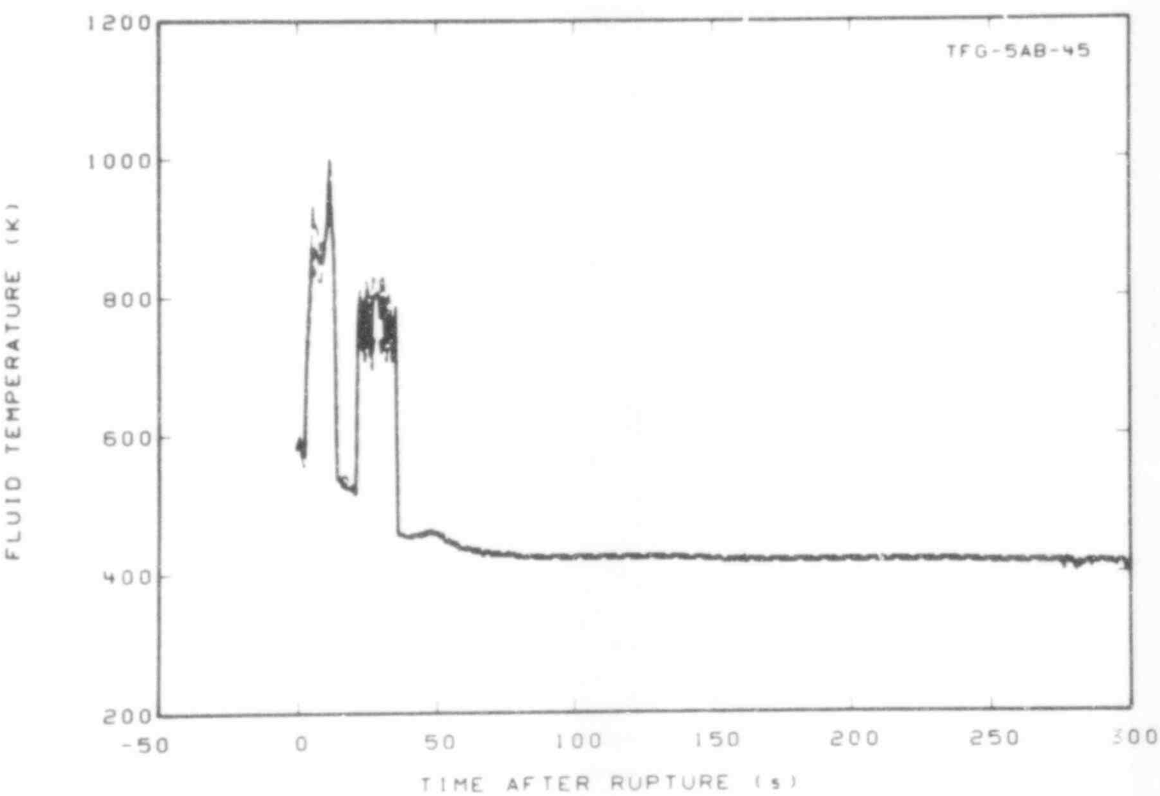

Fig. C-6 Fluid temperature in core, Grid Spacer 5 (TFG-5AB-45).

507 272

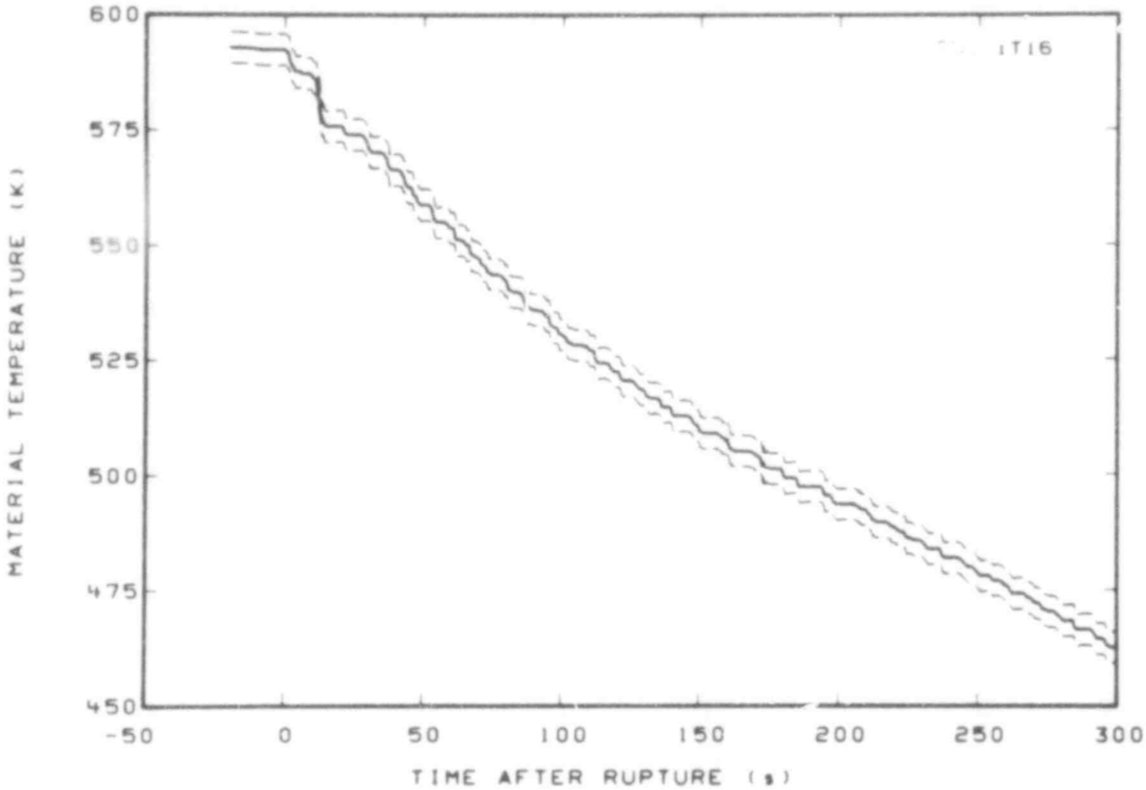

Fig. C-7 Material temperature in intact loop hot leg (TMI-1T16).

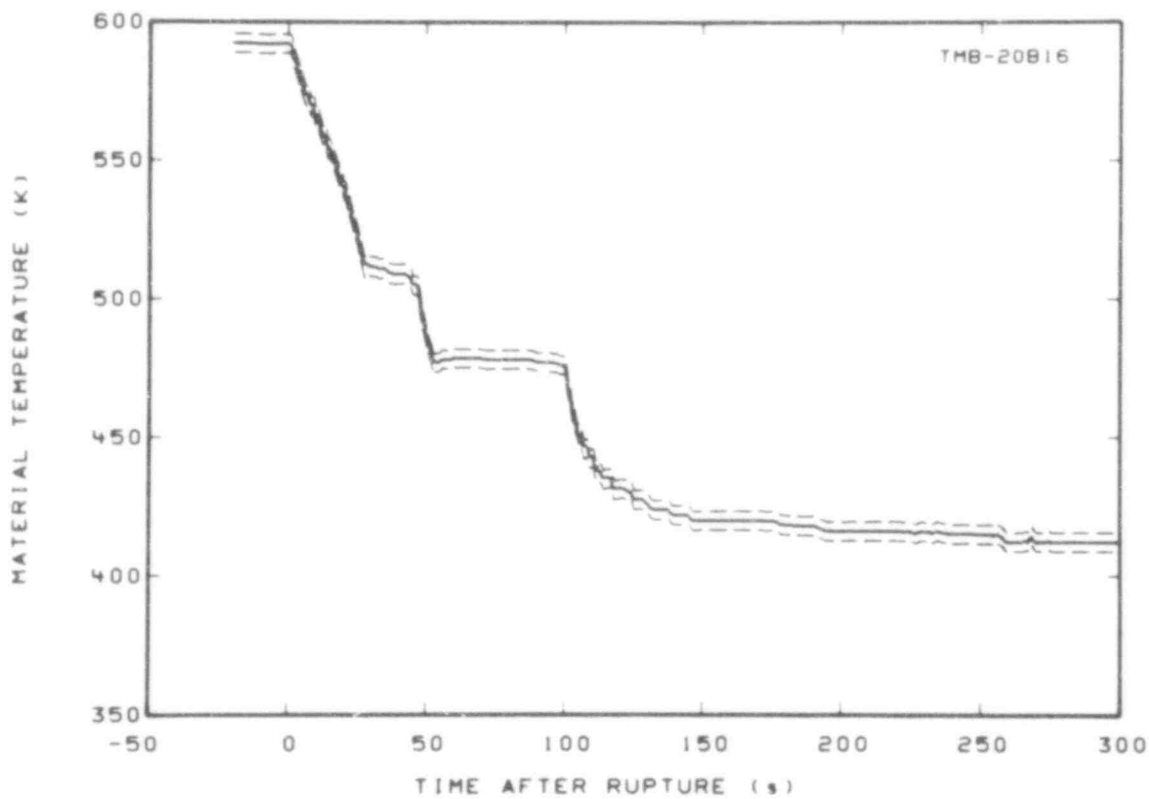

Fig. C-8 Material temperature in broken loop hot leg (TMB-20B16).

507 273

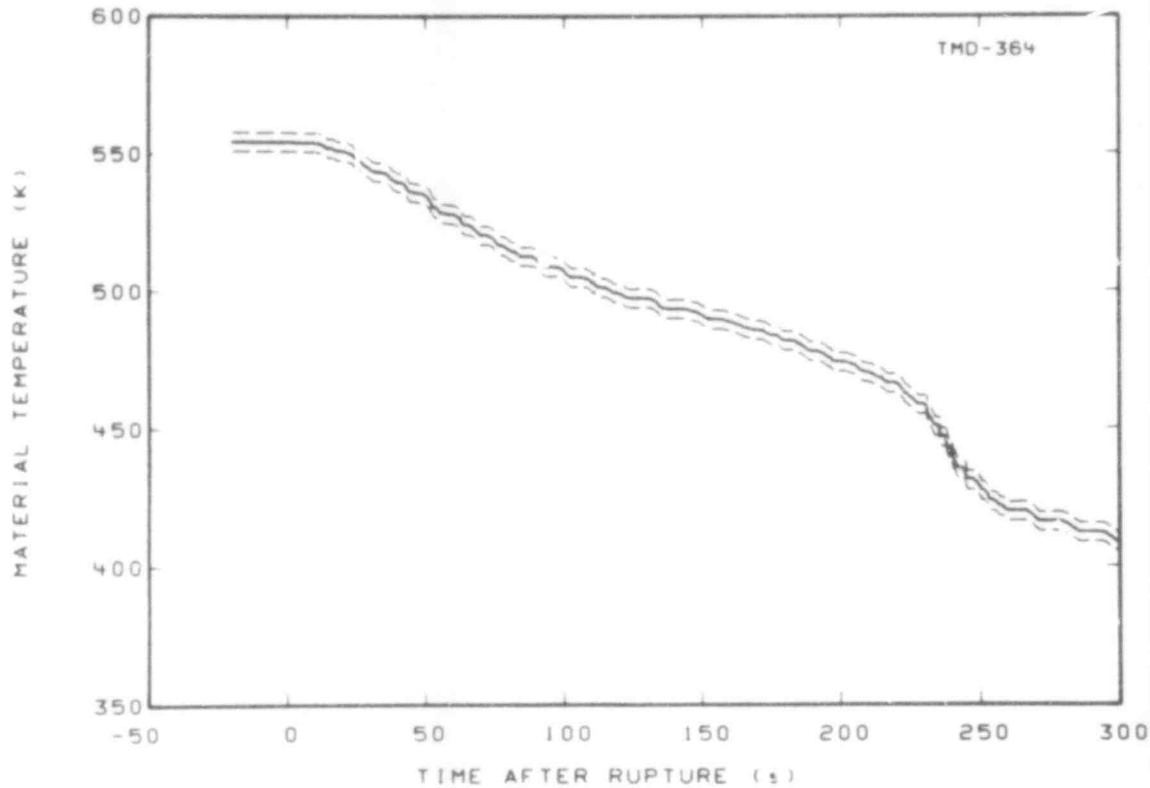

Fig. C-9 Material temperature in downcomer (TMD-364).

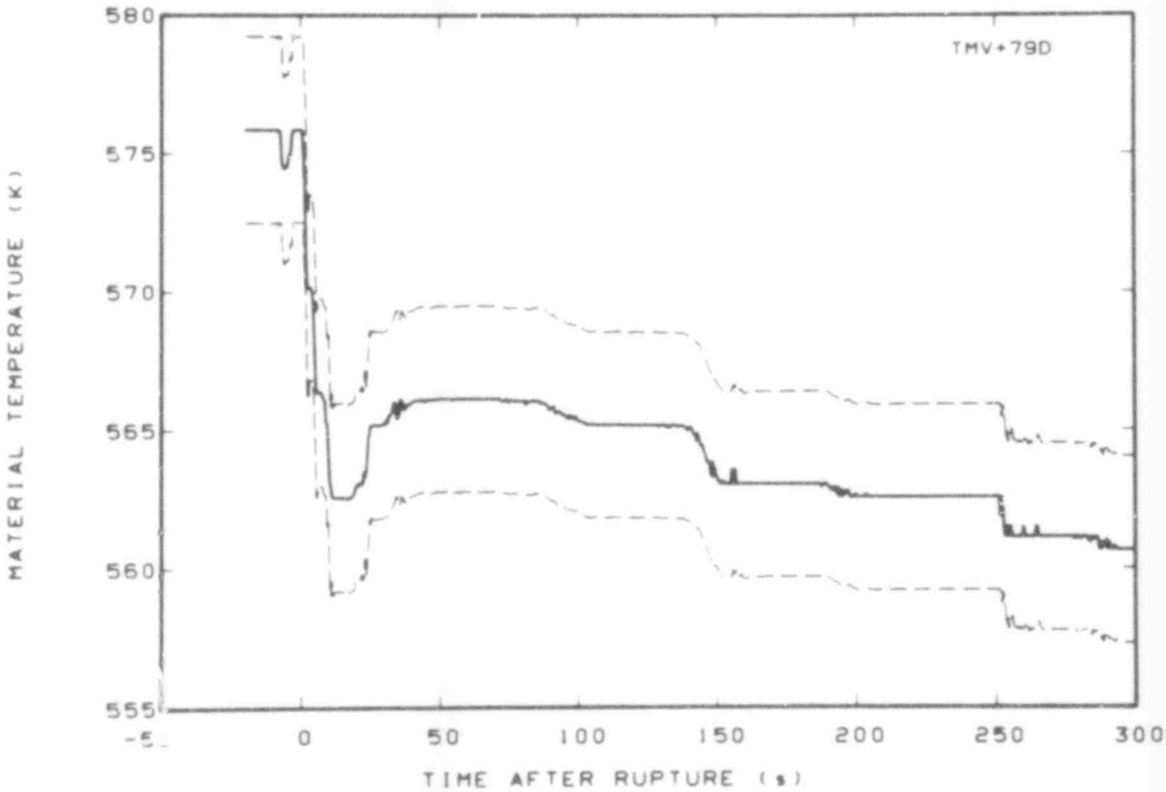

Fig. C-10 Material temperature in vessel (TMV + 79D).

507 274

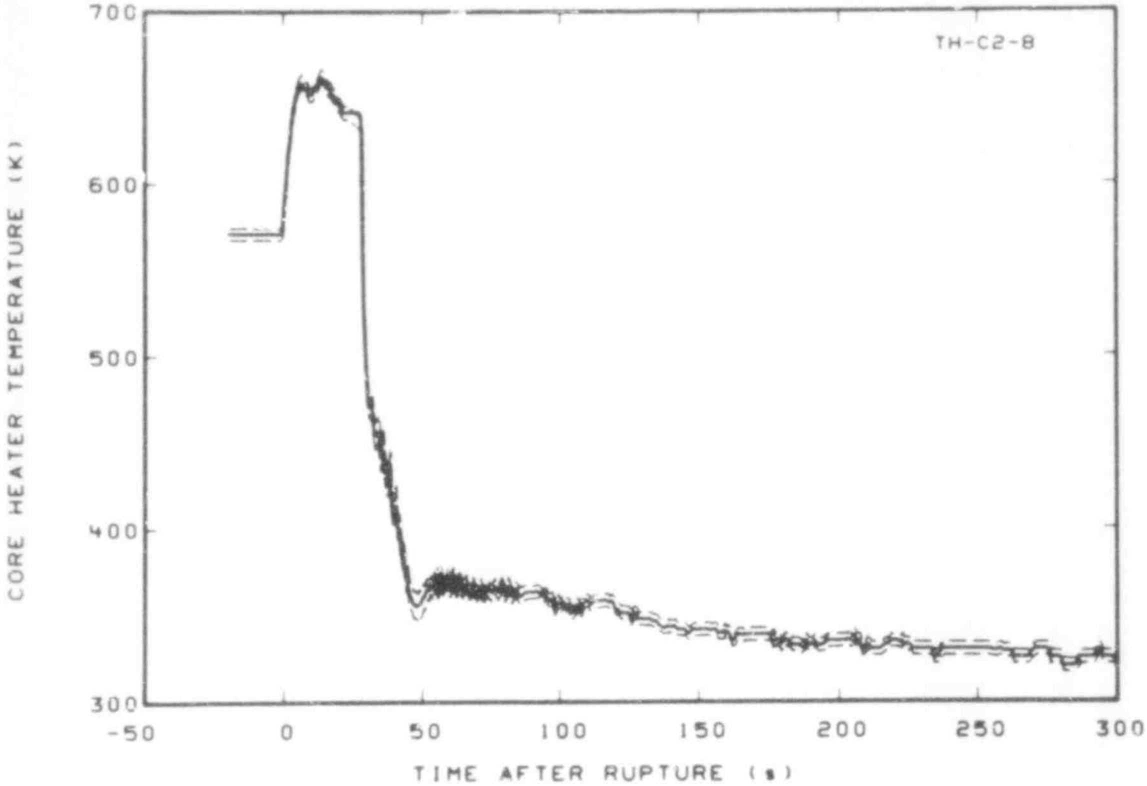

Fig. C-11 Core heater temperature, Rod C-2 (TH-C2-8).

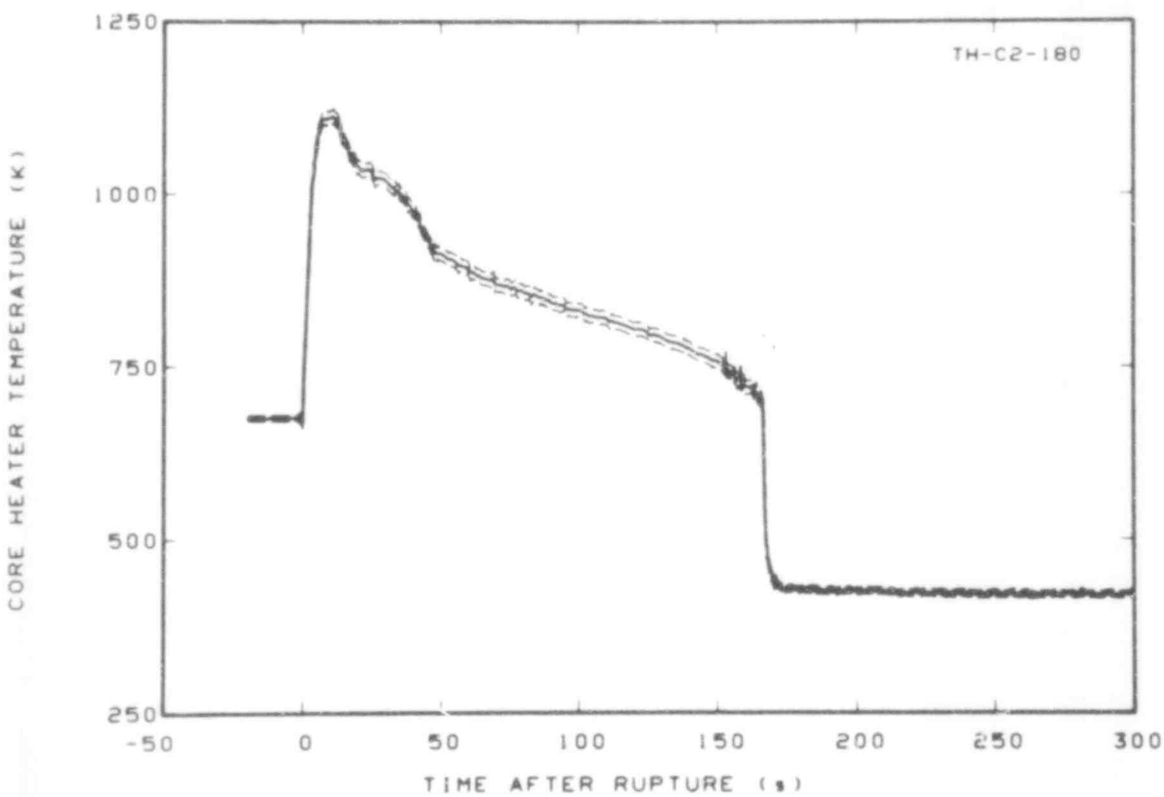

Fig. C-12 Core heater temperature, Rod C-2 (TH-C2-180).

507 275

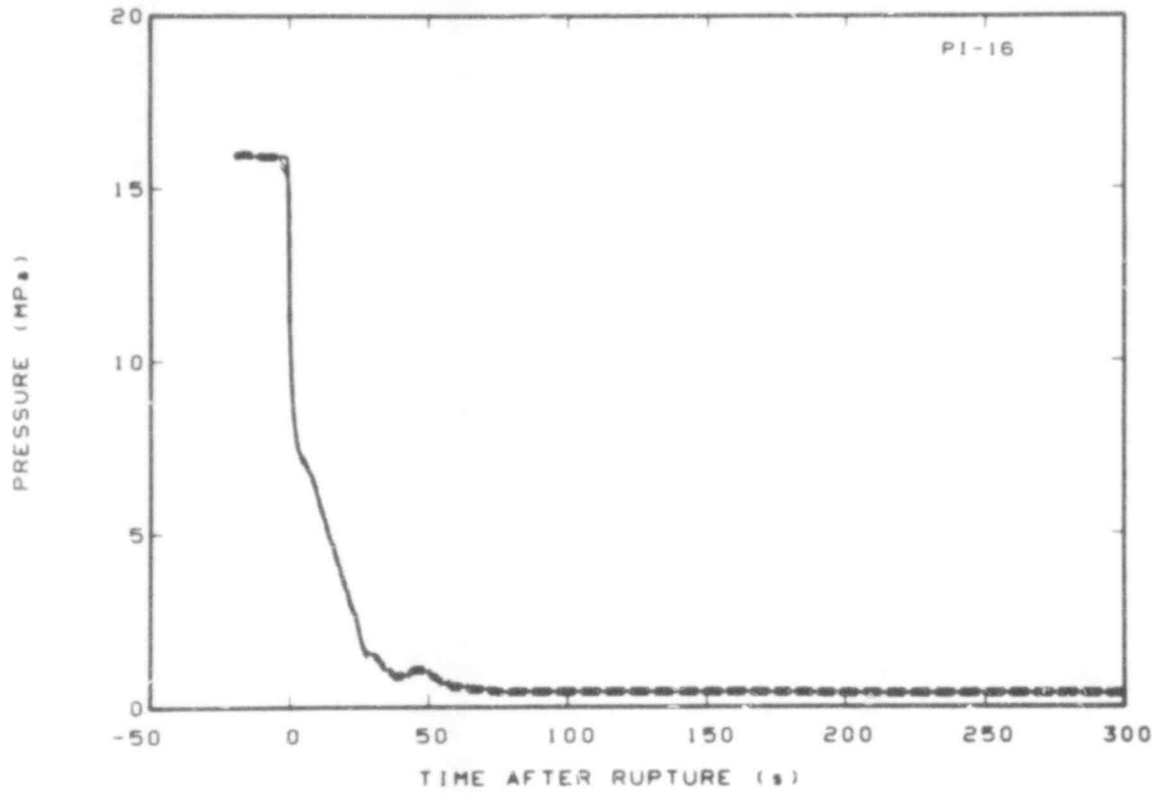

Fig. C-13 Pressure in intact loop cold leg (PI-16).

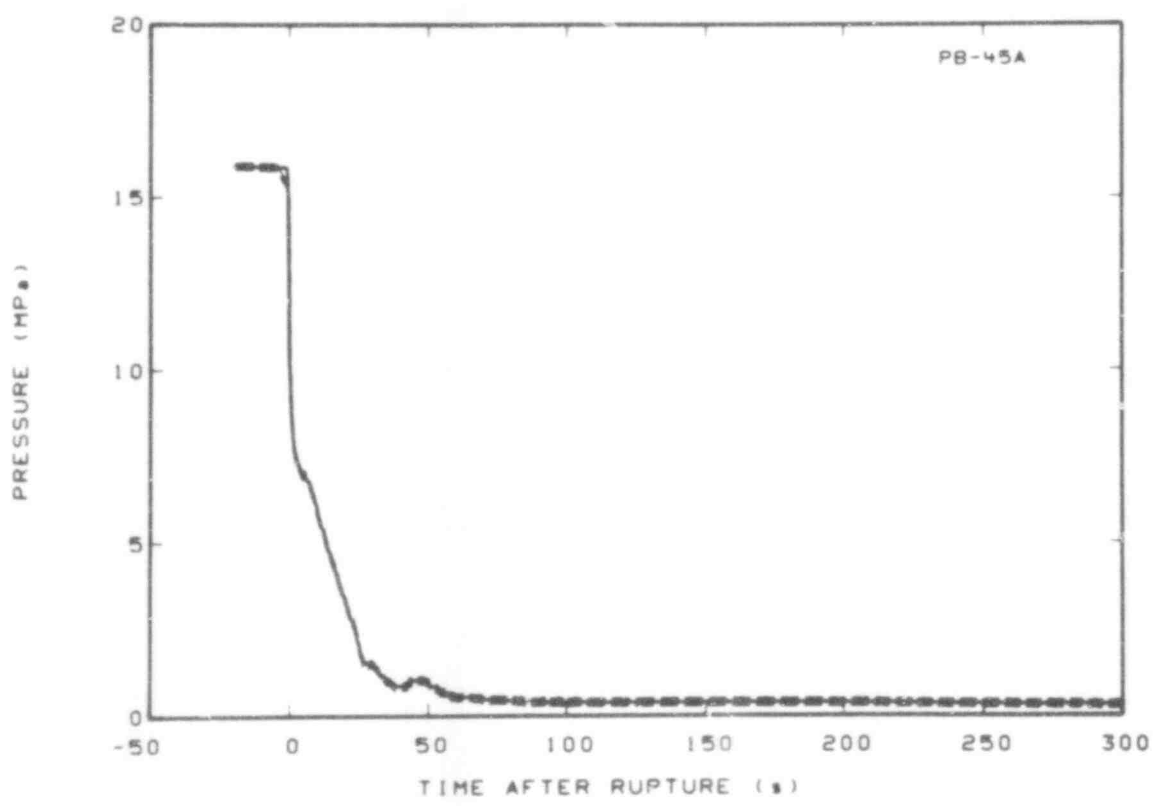

Fig. C-14 Pressure in broken loop cold leg (PB-45A).

507 276

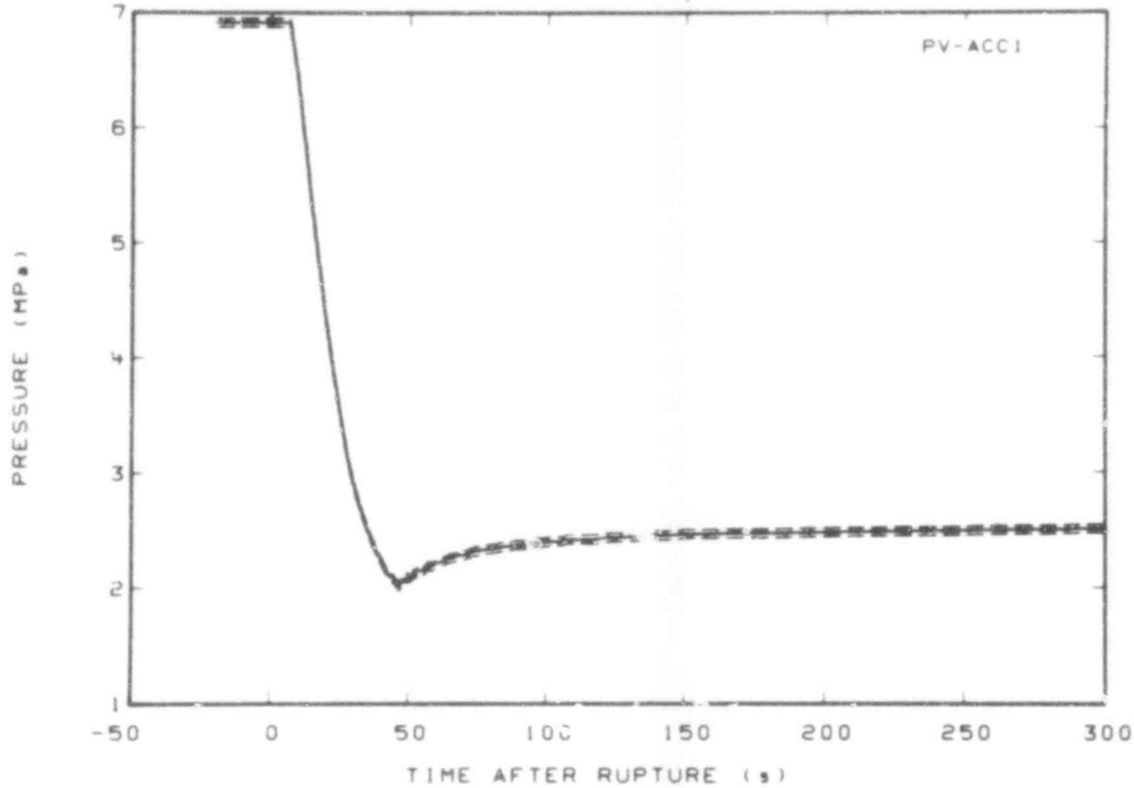

Fig. C-15 Pressure in vessel accumulator (PV-ACC1).

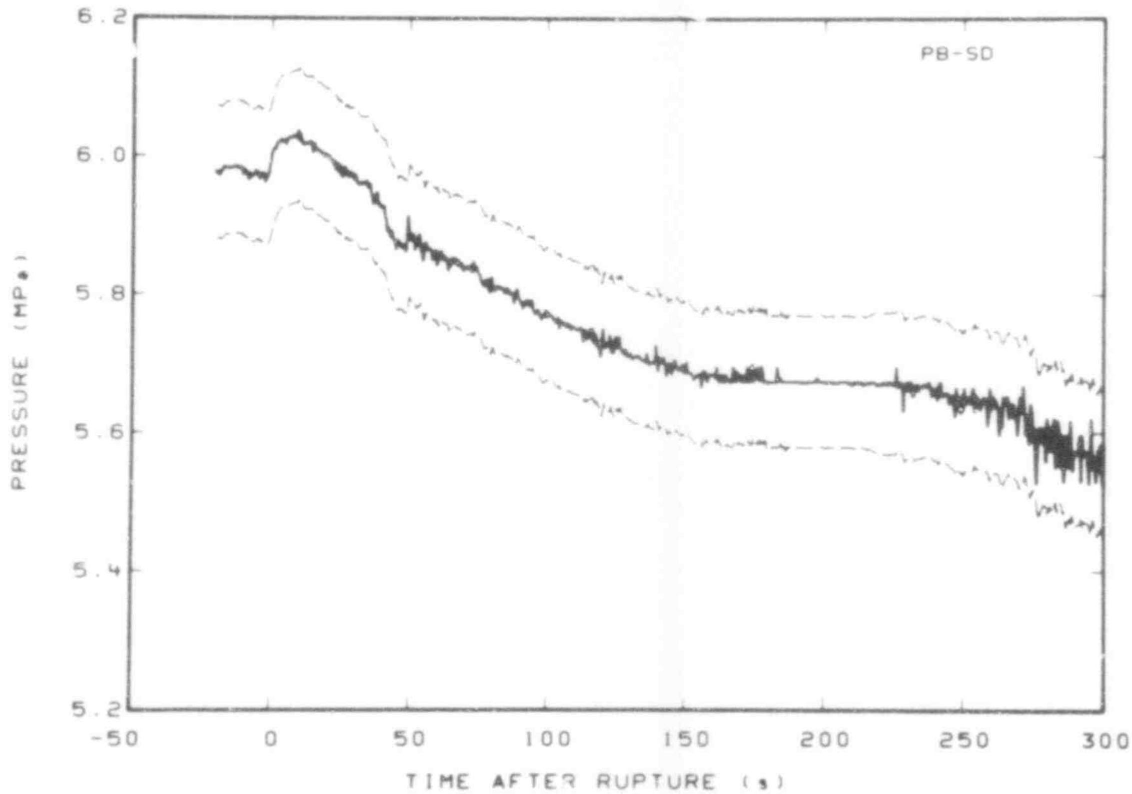

Fig. C-16 Pressure in broken loop steam generator, secondary side steam dome (PB-SD).

507 277

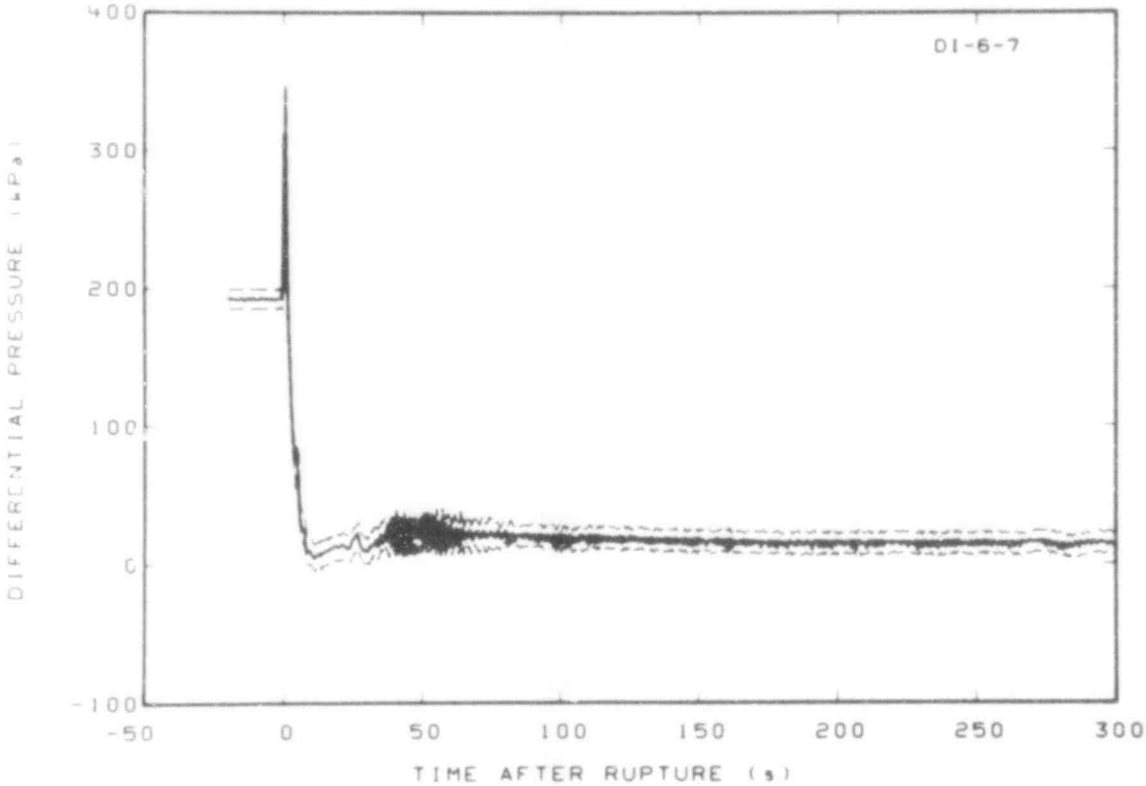

Fig. C-17 Differential pressure in intact loop (DI-6-7).

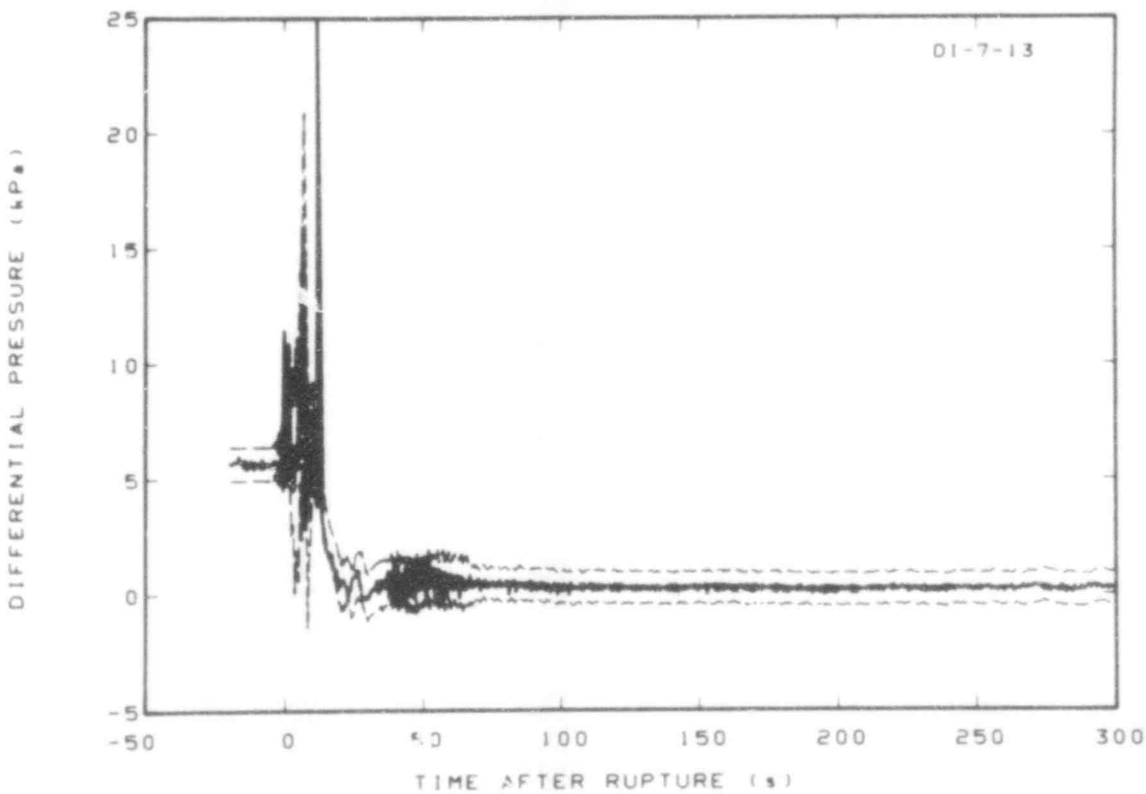

Fig. C-18 Differential pressure in intact loop (DI-7-13).

507 278

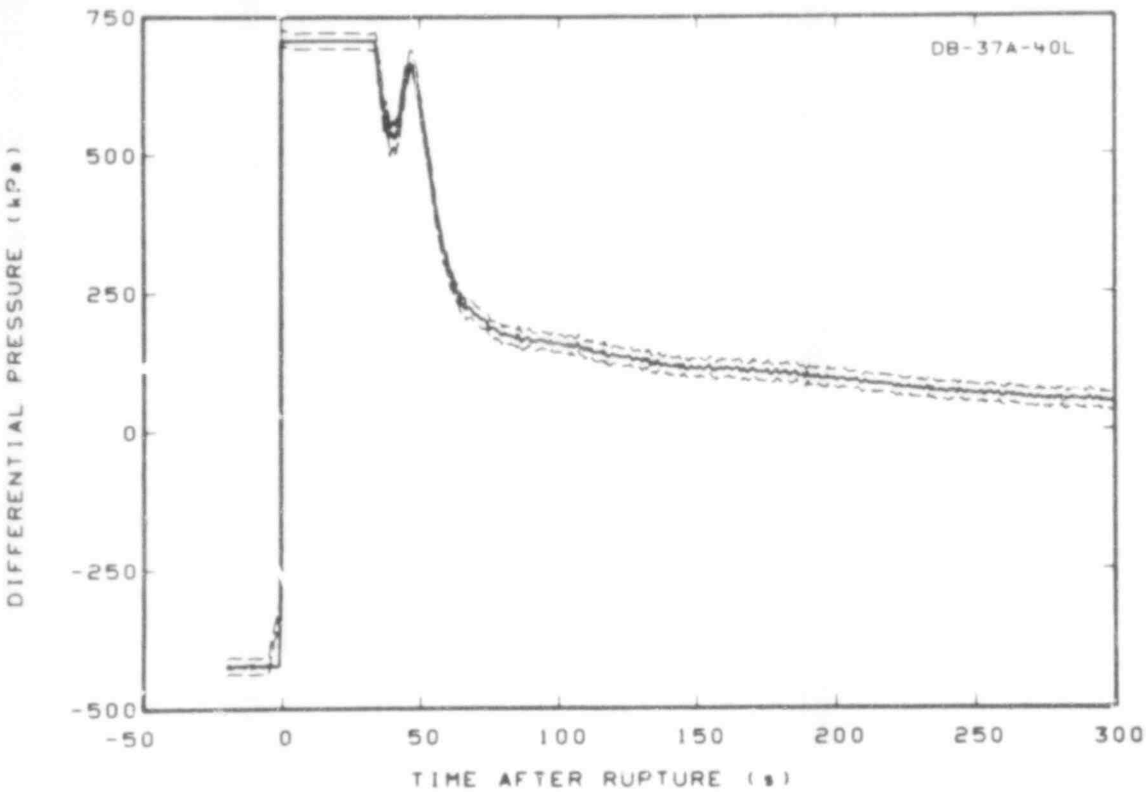

Fig. C-19 Differential pressure in broken loop (DB-37A-40L).

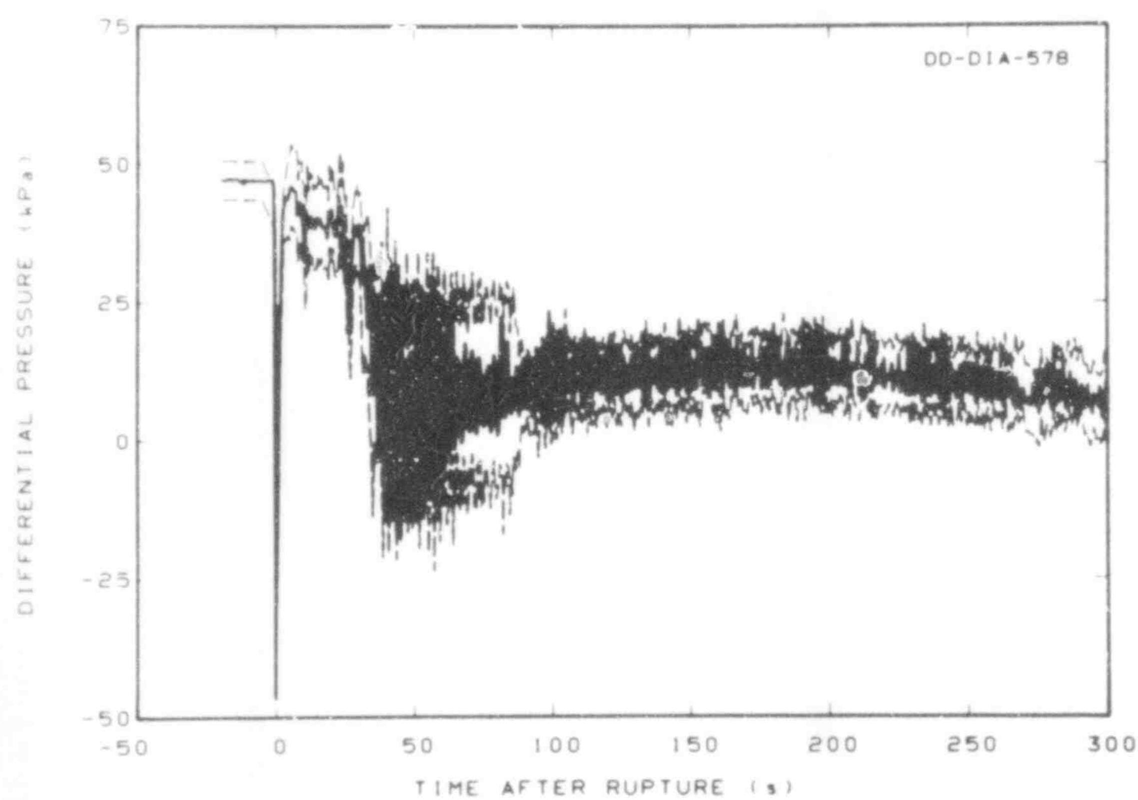

Fig. C-20 Differential pressure in downcomer (DD-DIA-578).

507 279

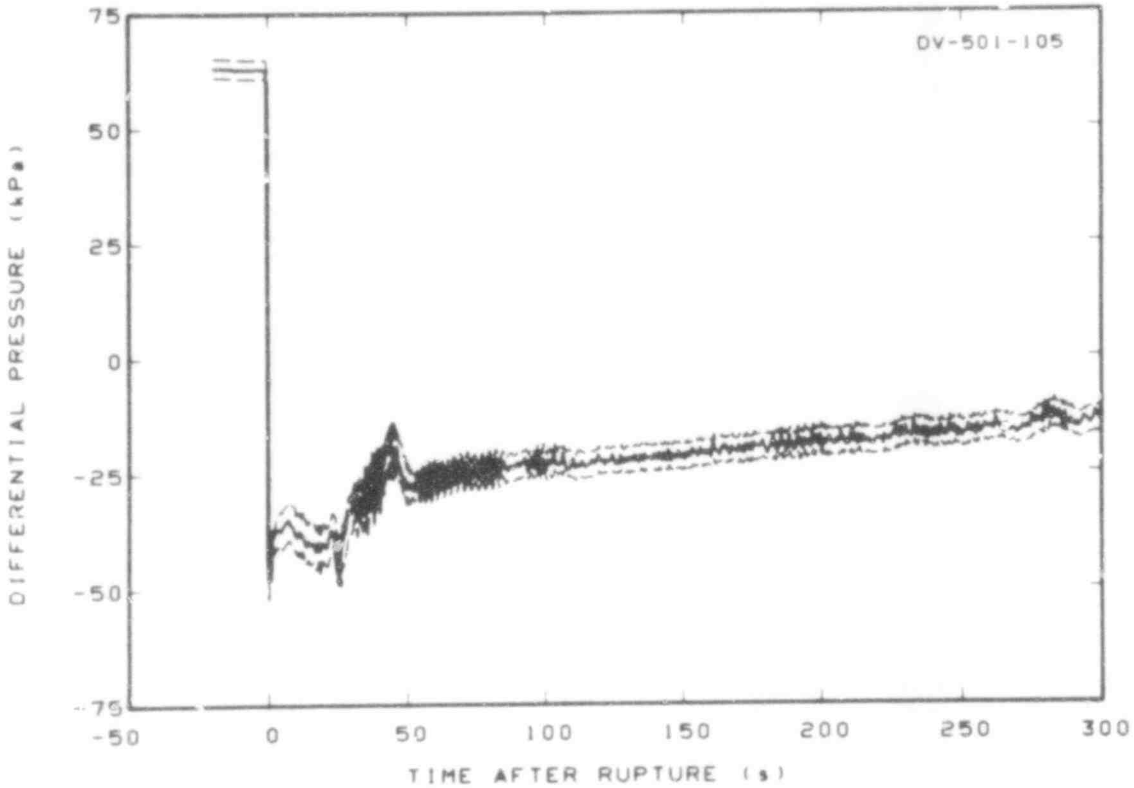

Fig. C-21 Differential pressure in vessel (DV-501-105).

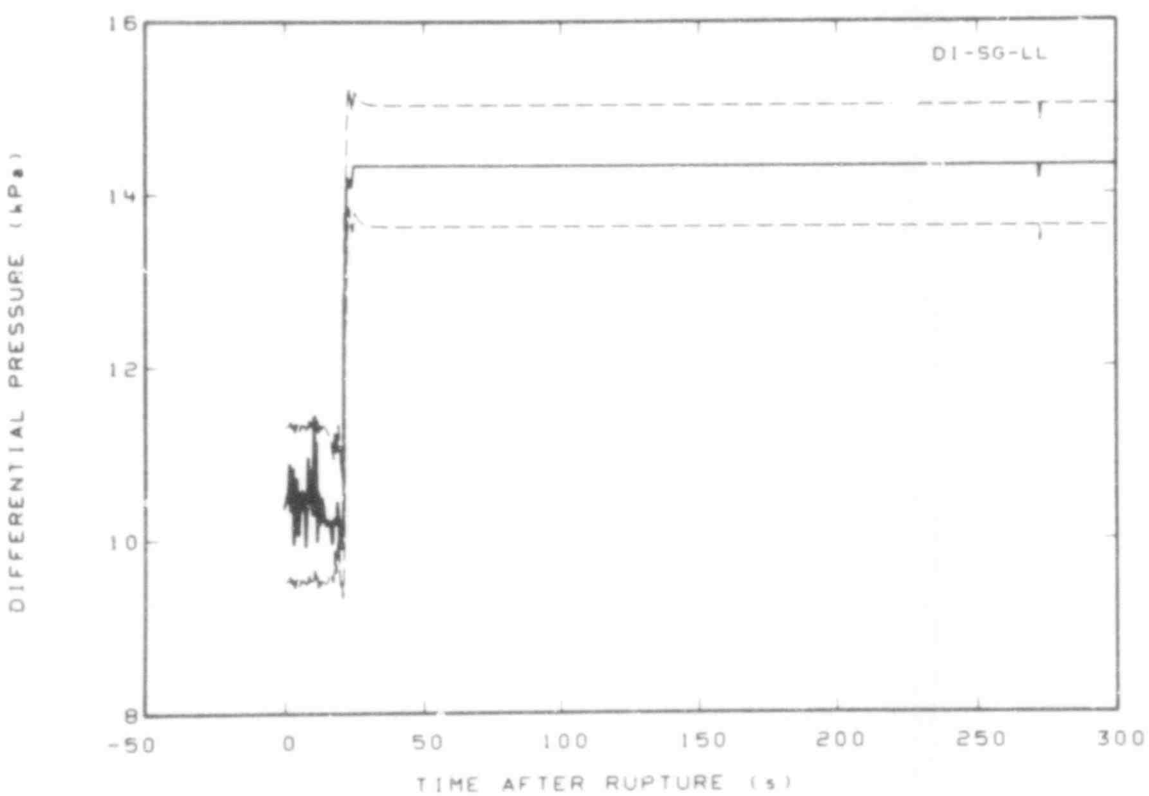

Fig. C-22 Differential pressure in intact loop steam generator, secondary side liquid level (DI-SG-LL).

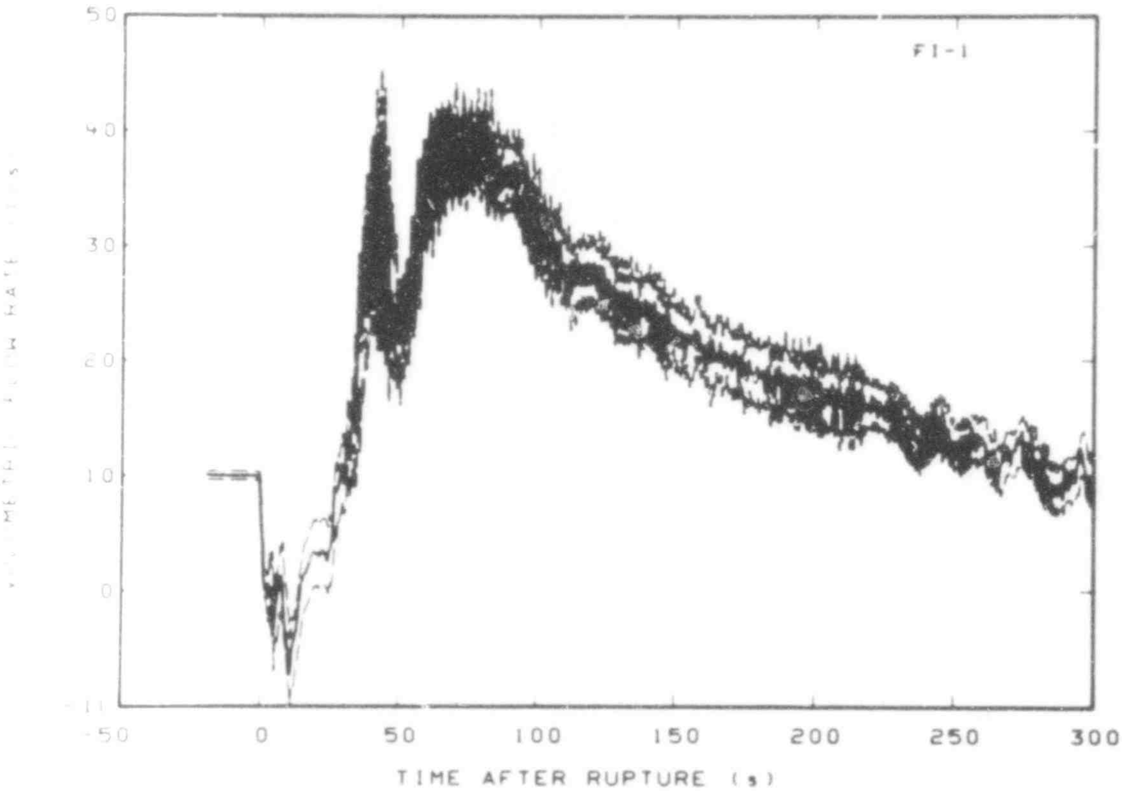

Fig. C-23 Volumetric flow in intact loop (FI-1).

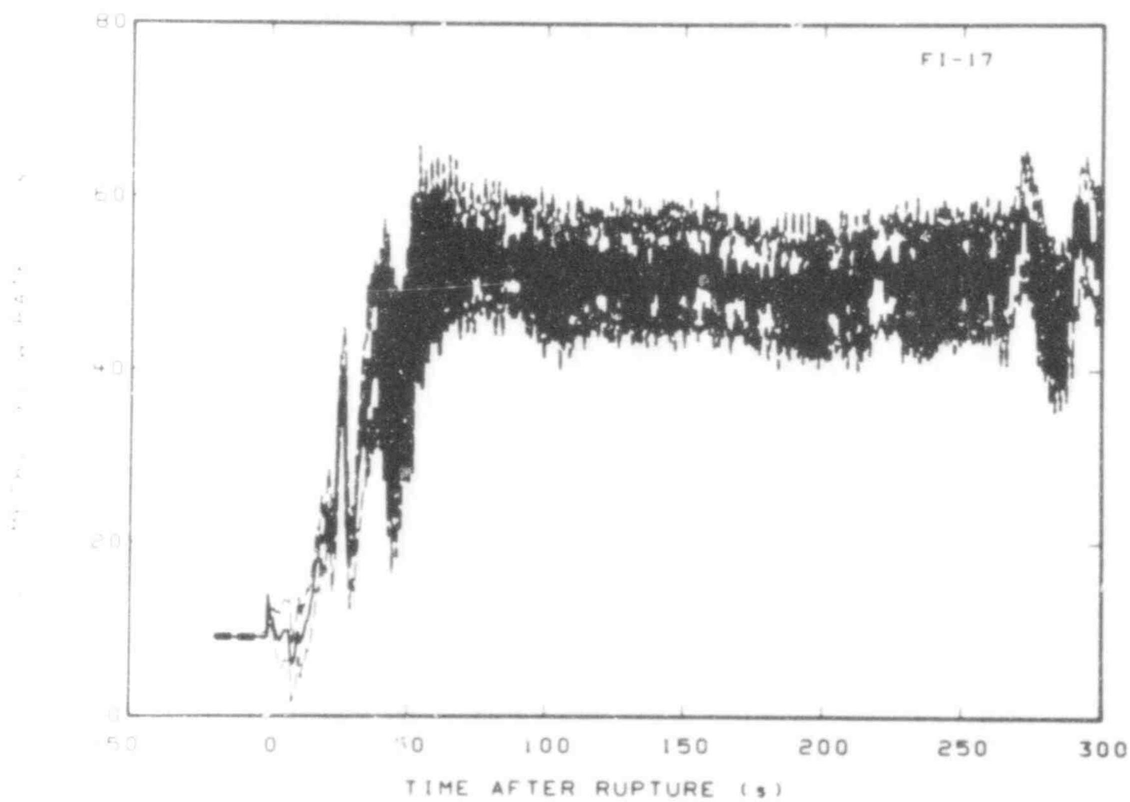

Fig. C-24 Volumetric flow in intact loop (FI-17).

507 281

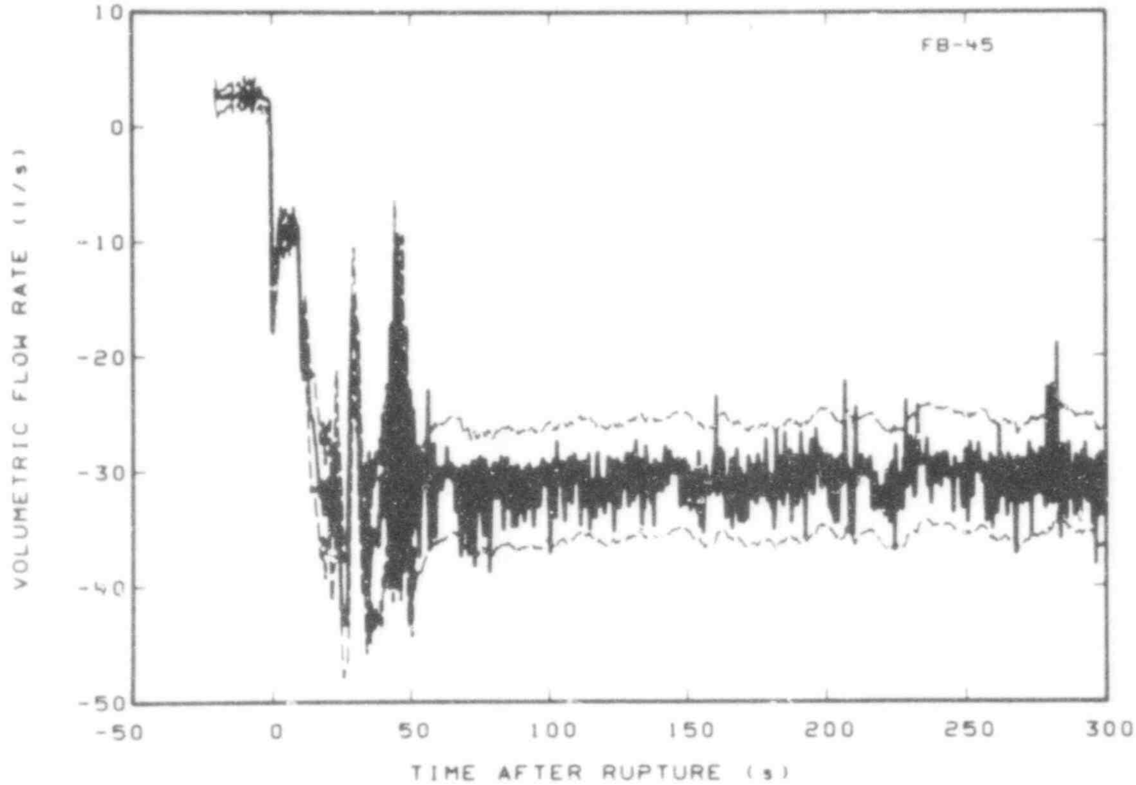

Fig. C-25 Volumetric flow in broken loop (FB-45).

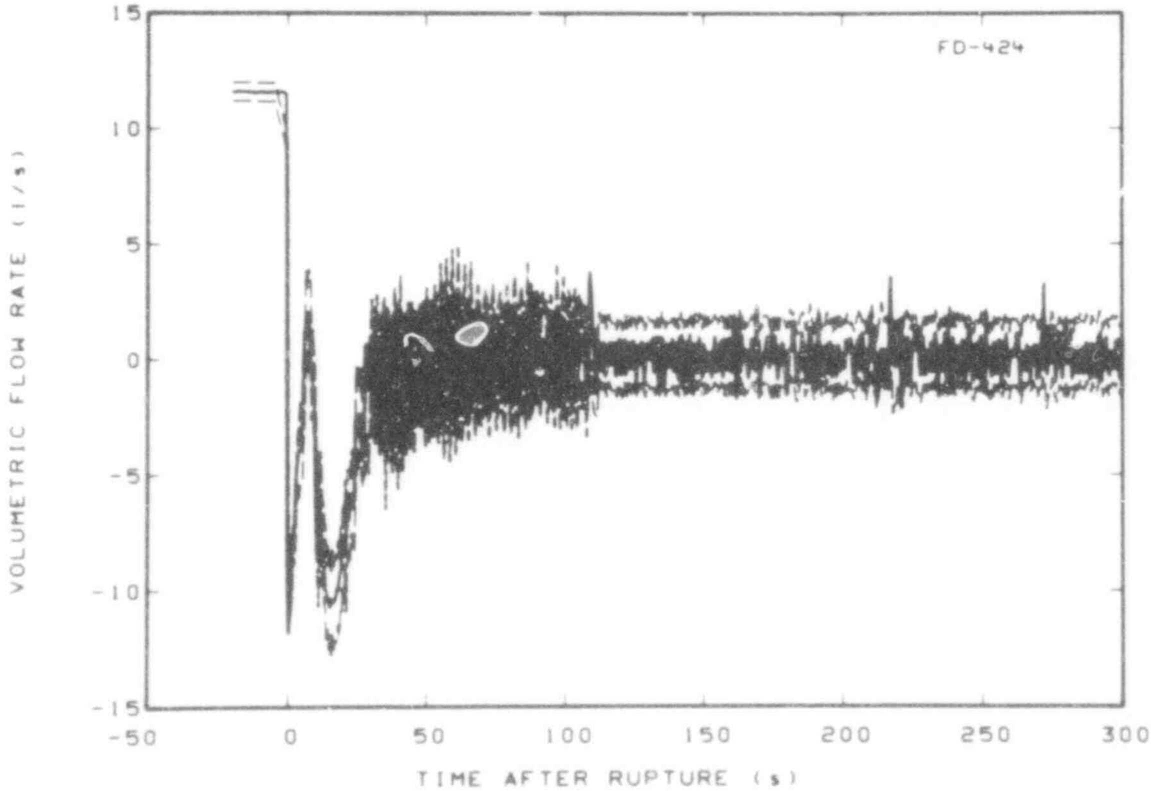

Fig. C-26 Volumetric flow in downcomer (FD-424).

507 282

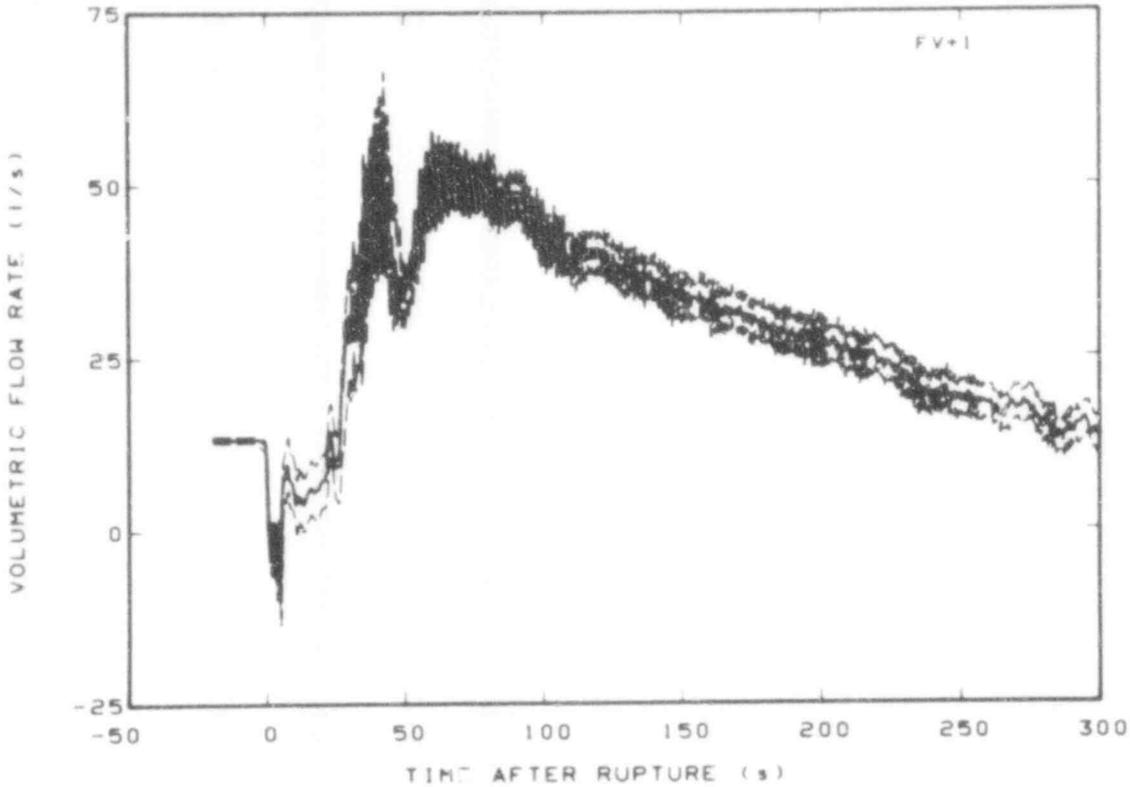

Fig. C-27 Volumetric flow in vessel upper plenum (FV + 1).

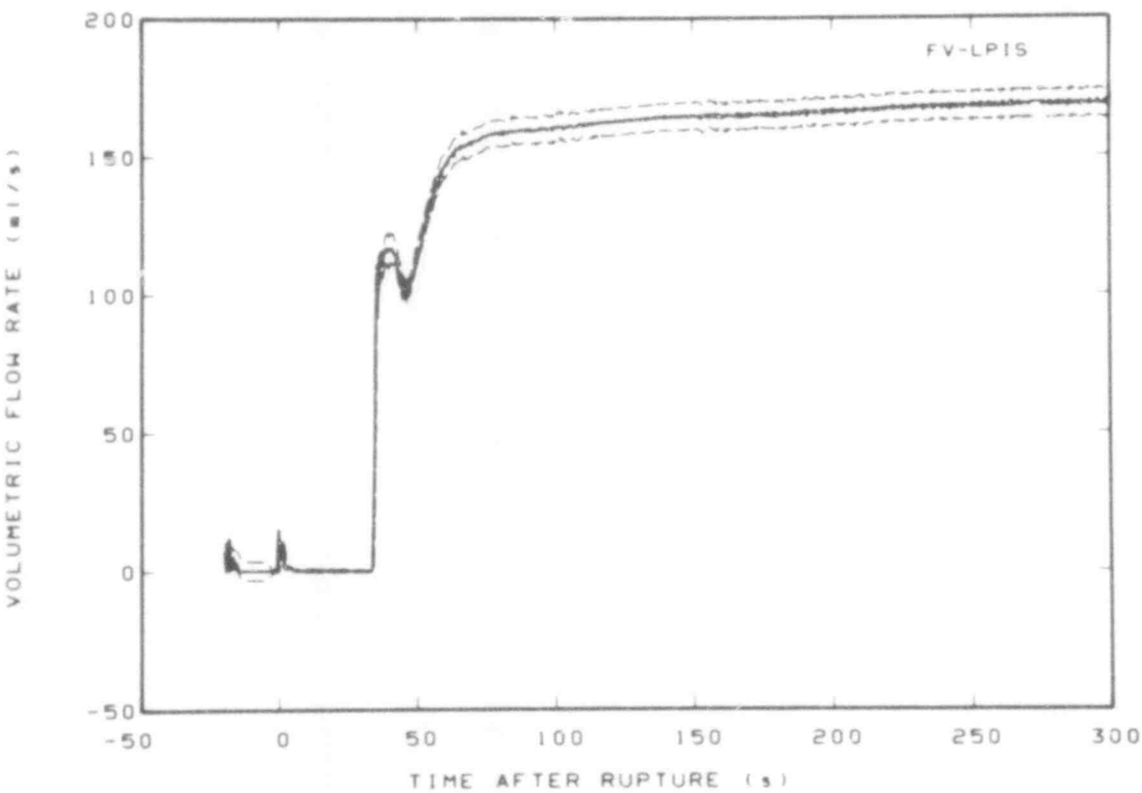

Fig. C-28 Volumetric flow in vessel lower plenum, low pressure injection system (FV-LPIS).

507 283

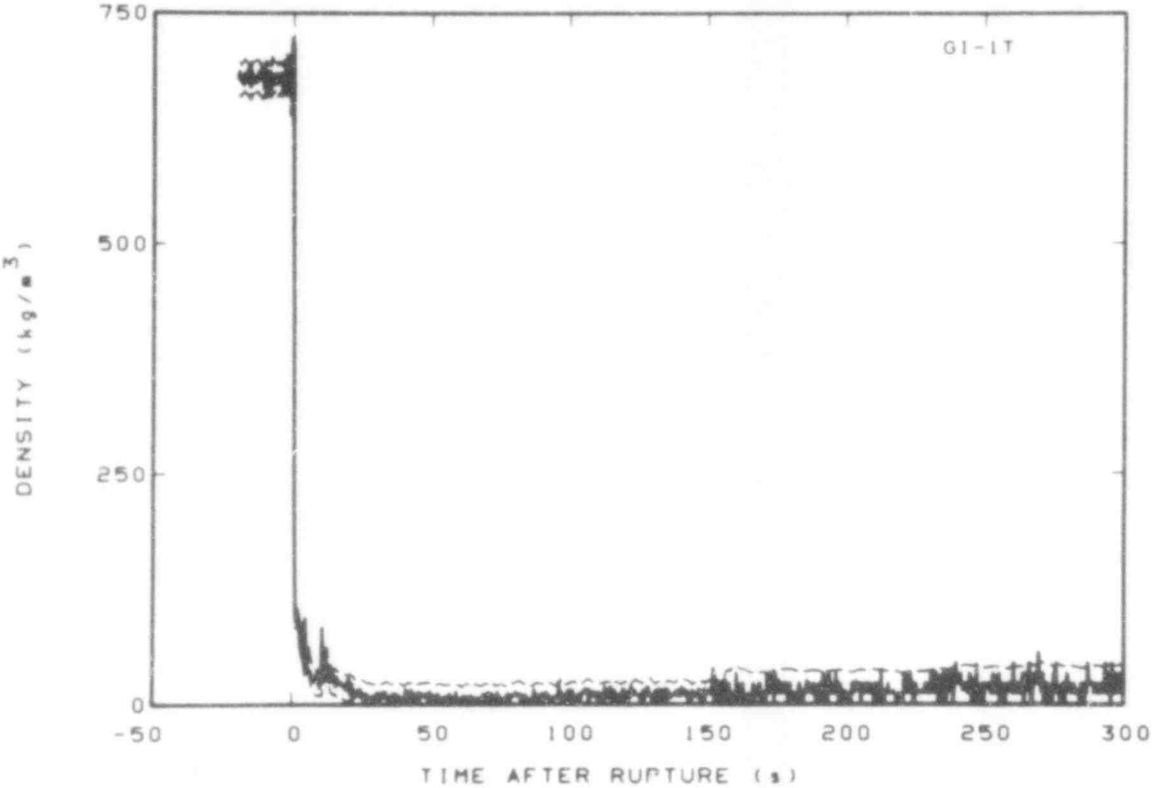

Fig. C-29 Density in intact loop (GI-1T).

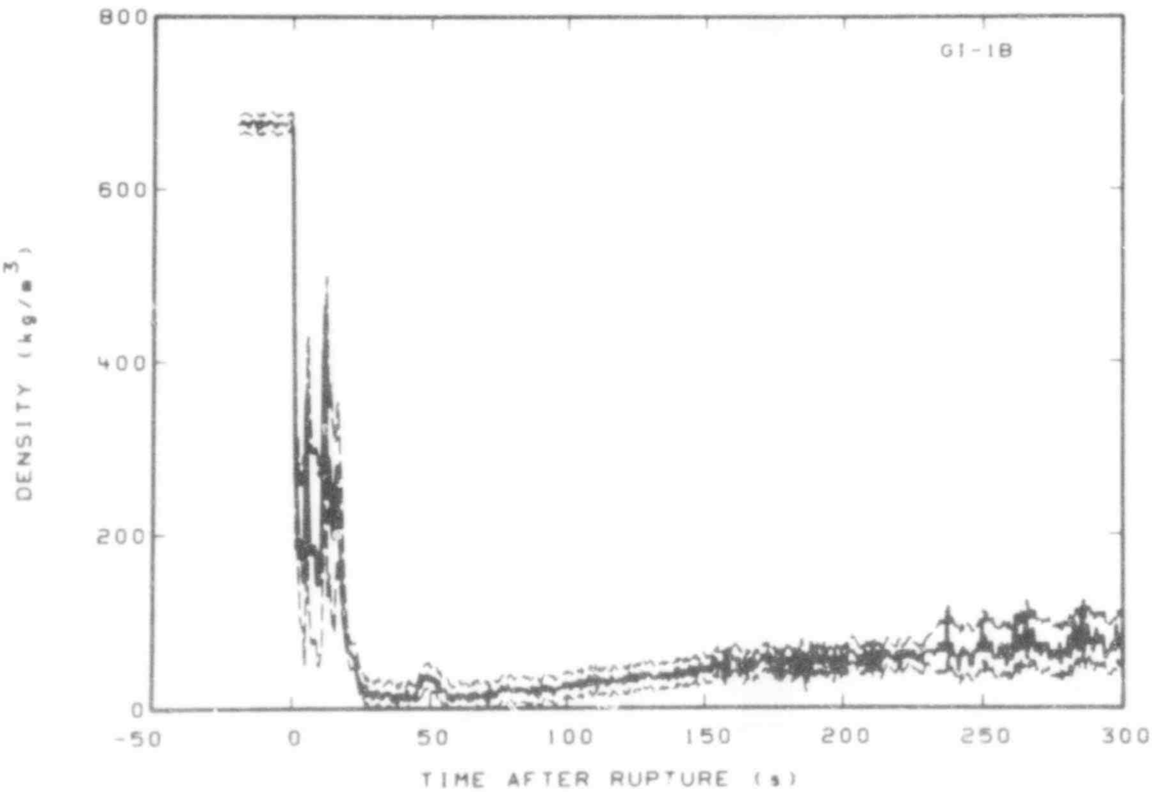

Fig. C-30 Density in intact loop (GI-1B).

507 284

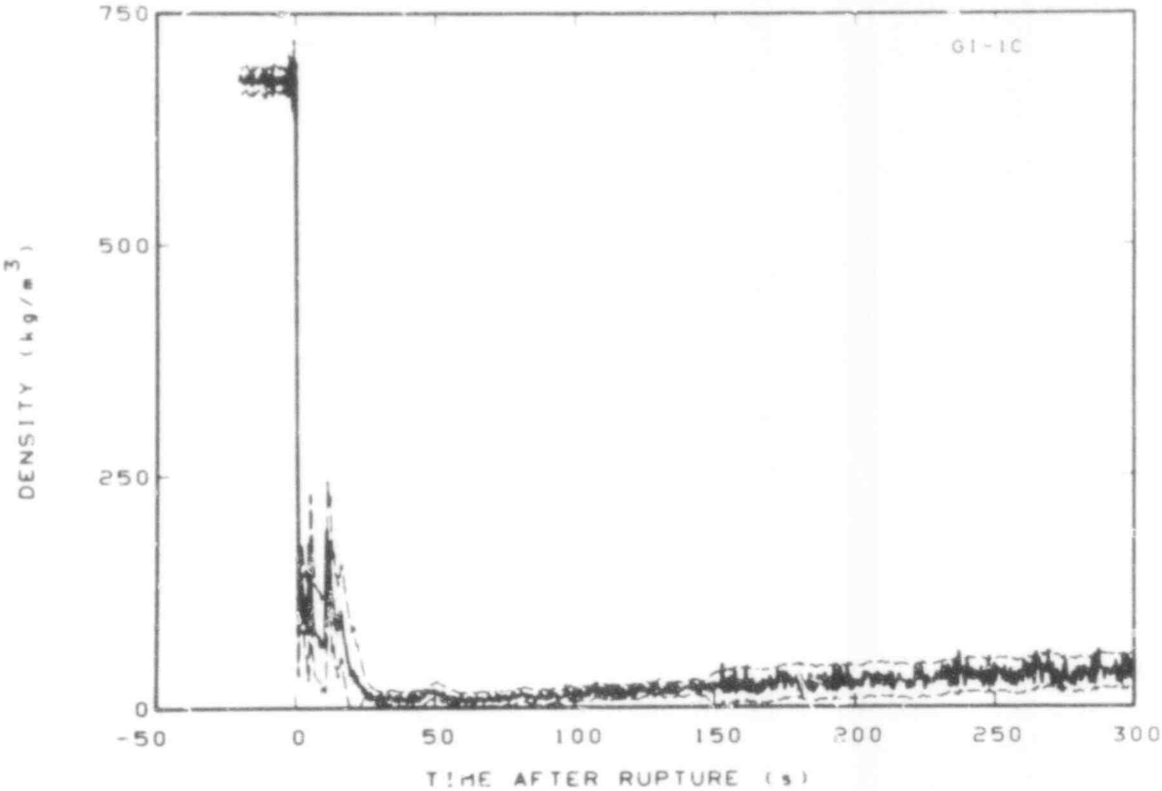

Fig. C-31 Density in intact loop (GI-1C).

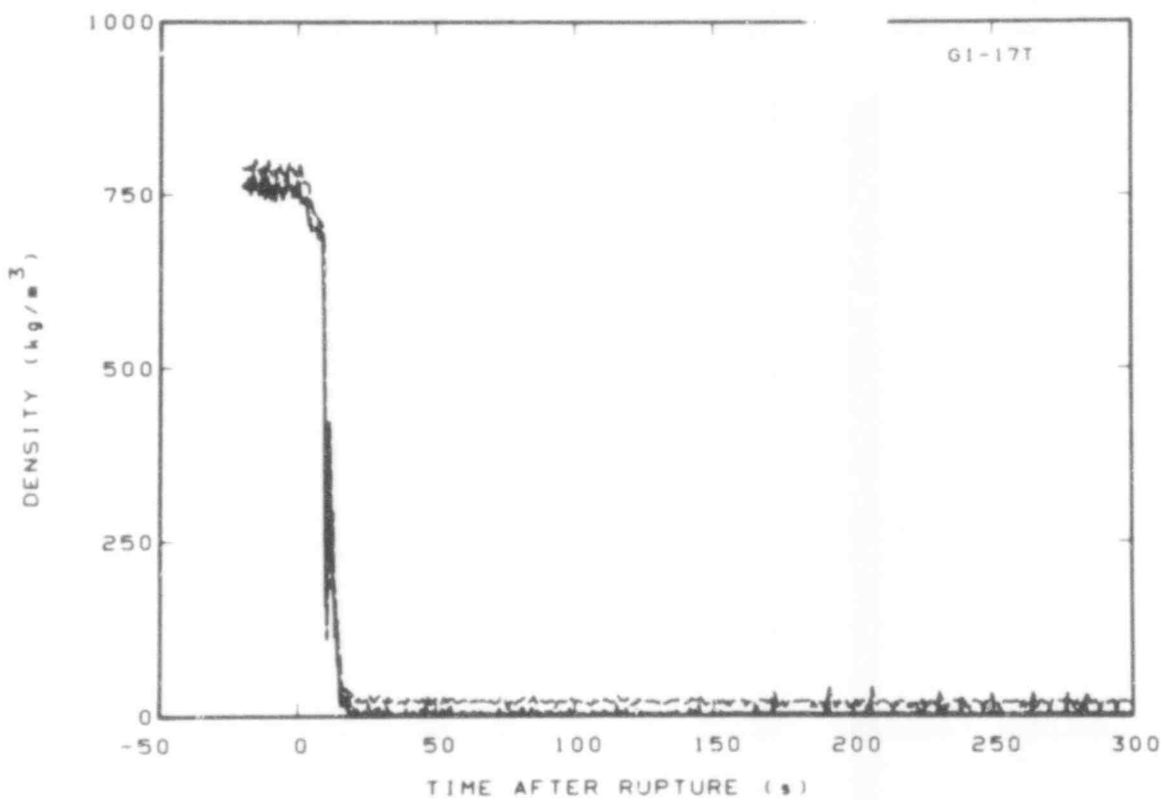

Fig. C-32 Density in intact loop (GI-17T).

507 285

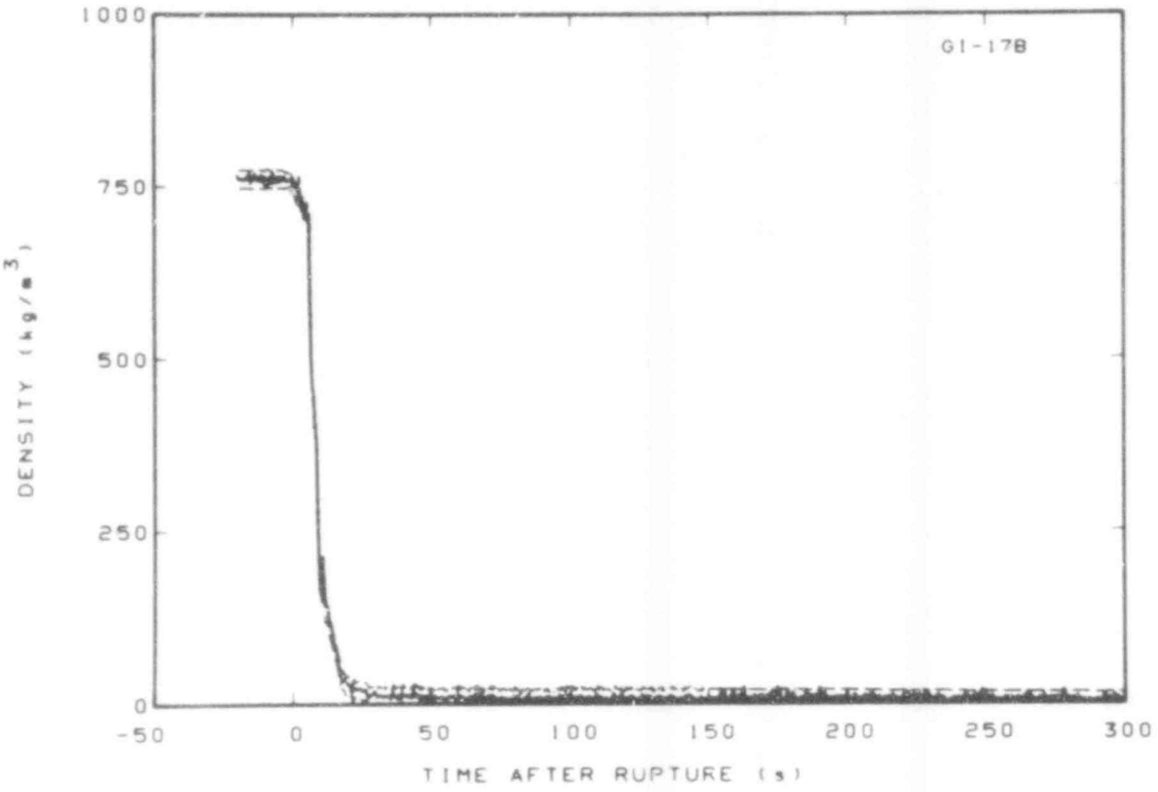

Fig. C-33 Density in intact loop (GI-17B).

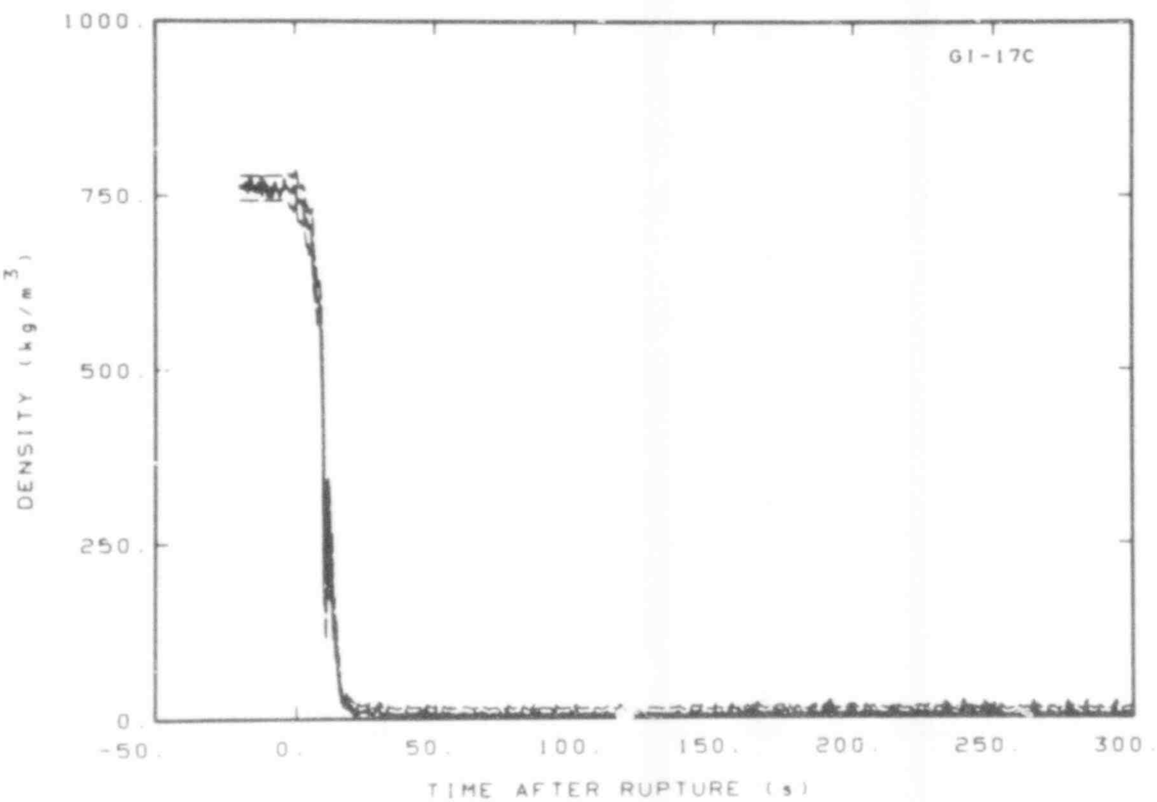

Fig. C-34 Density in intact loop (GI-17C).

507 286

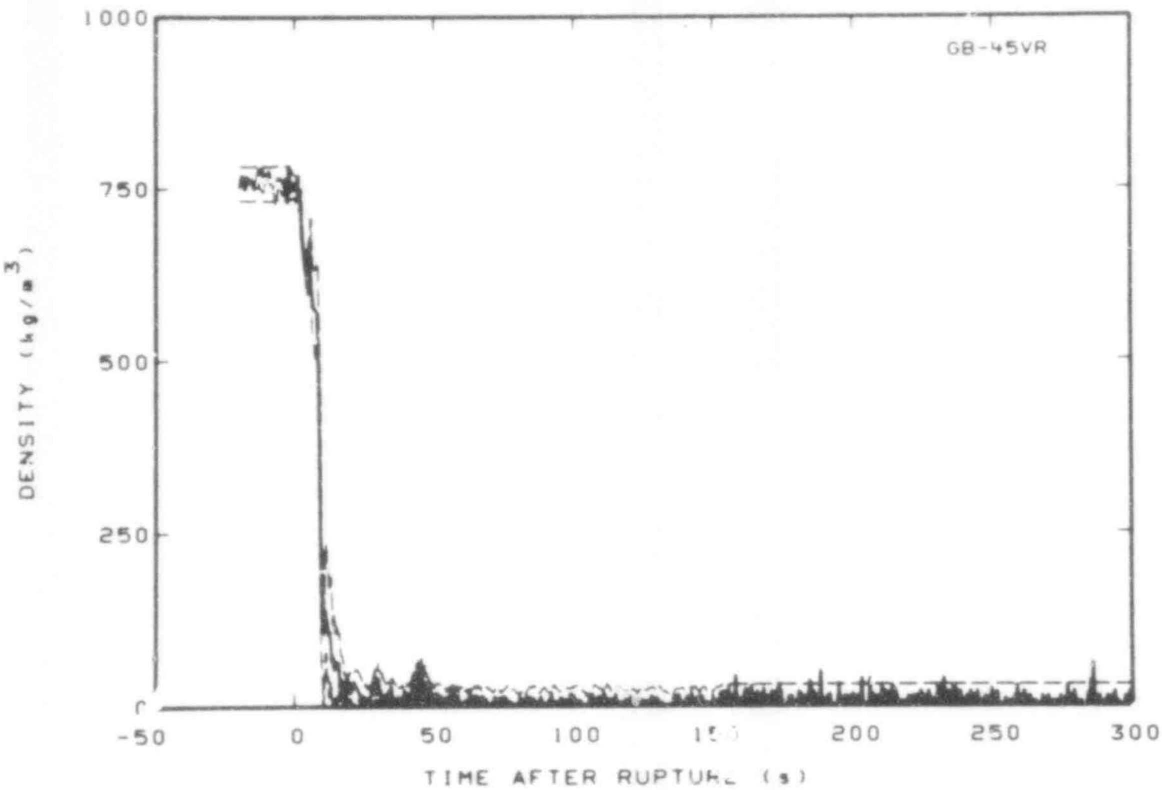

Fig. C-35 Density in broken loop (GB-45VR).

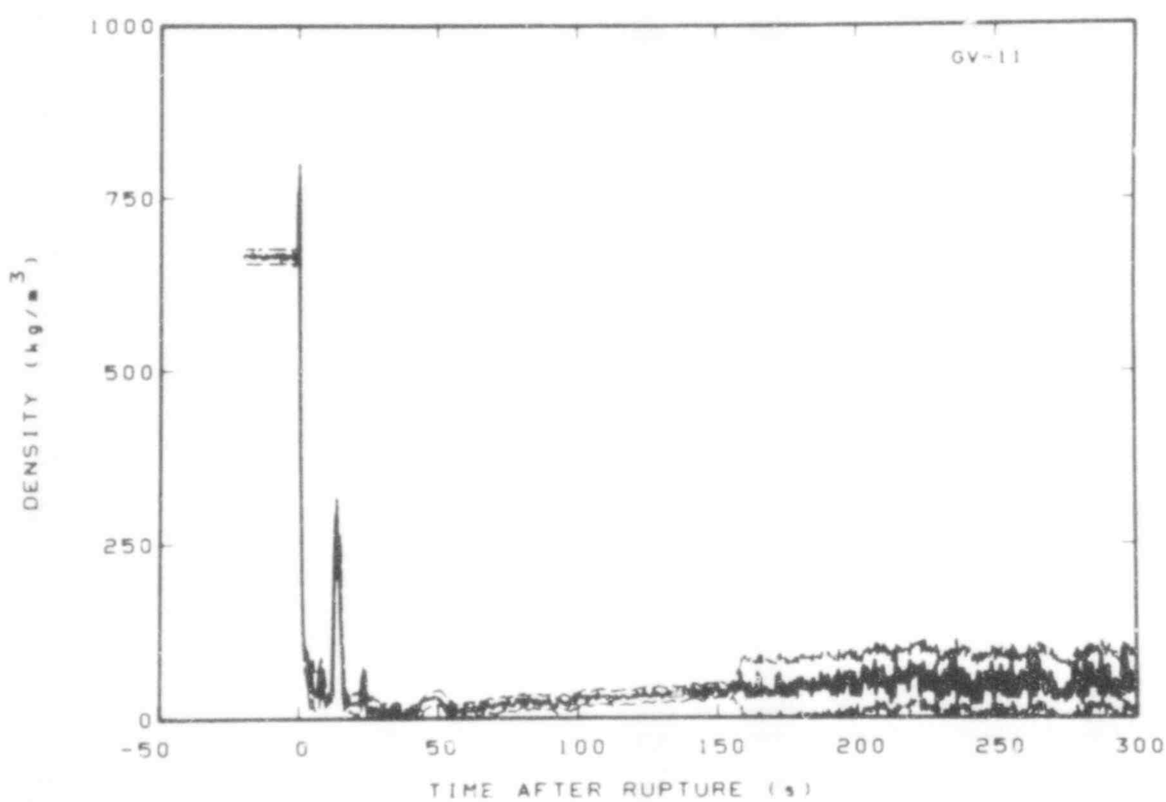

Fig. C-36 Density in vessel (GV-11).

507 287

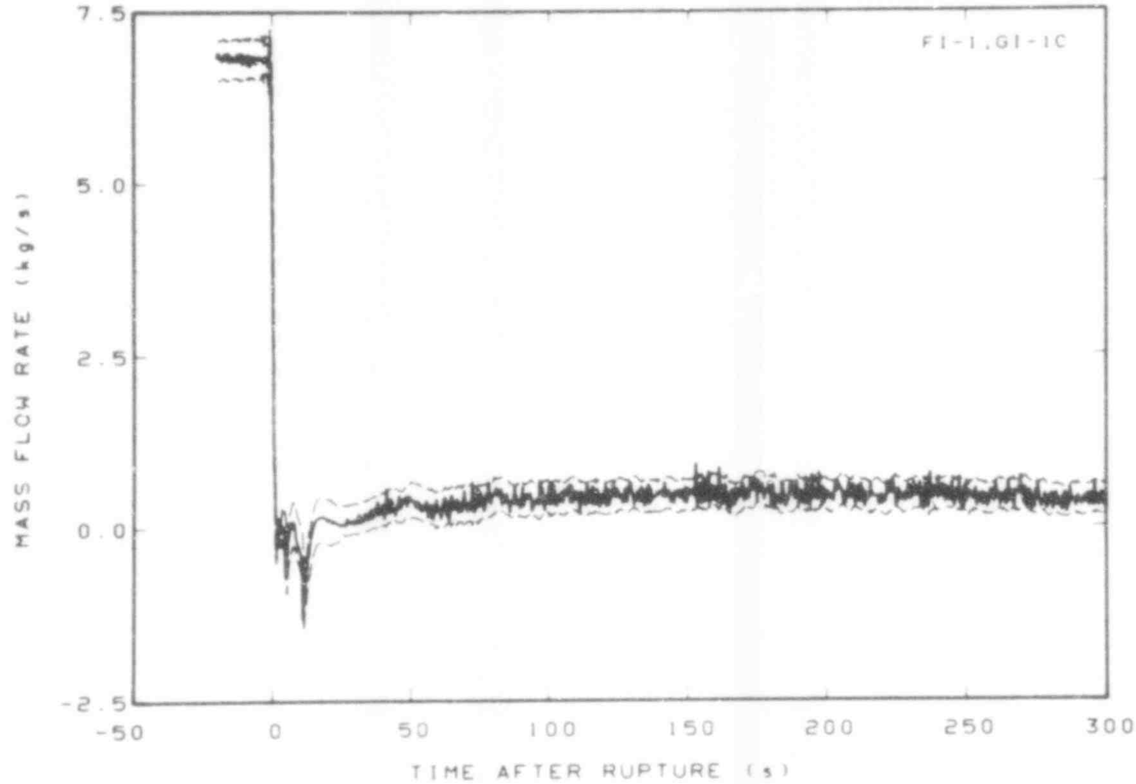

Fig. C-37 Mass flow in intact loop (FI-1 and GI-1C).

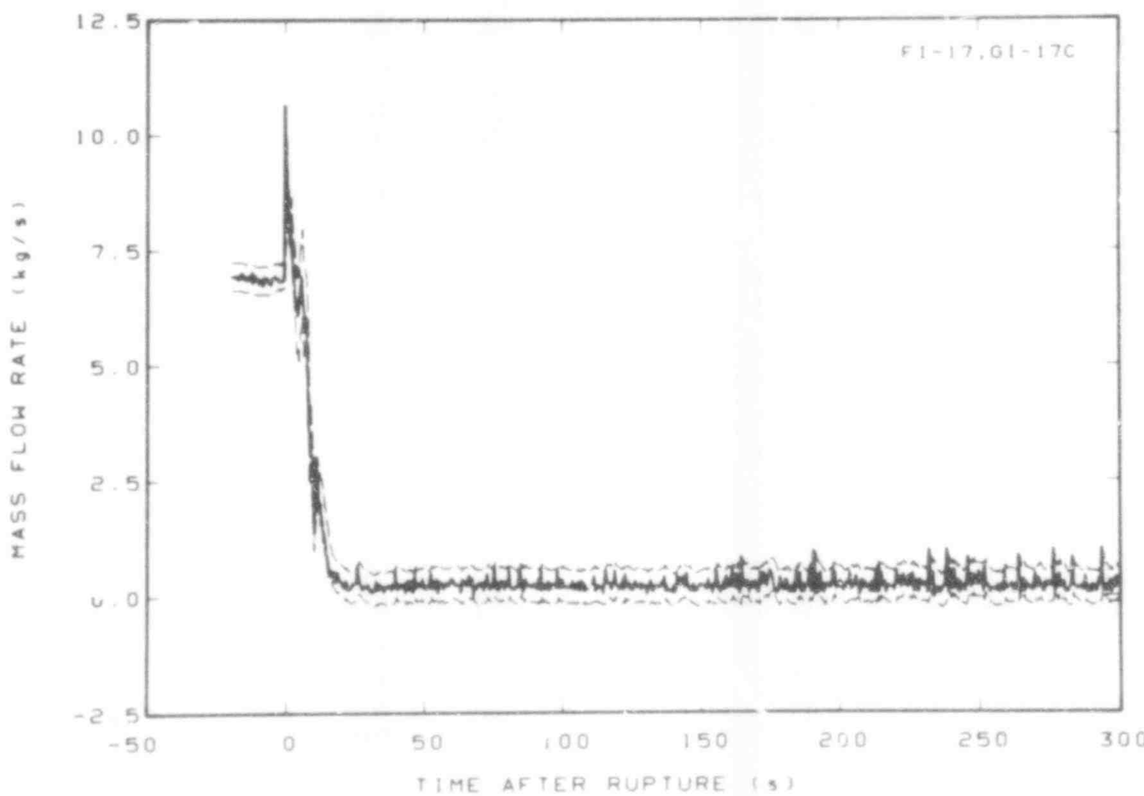

Fig. C-38 Mass flow in intact loop (FI-17 and GI-17C).

507 288

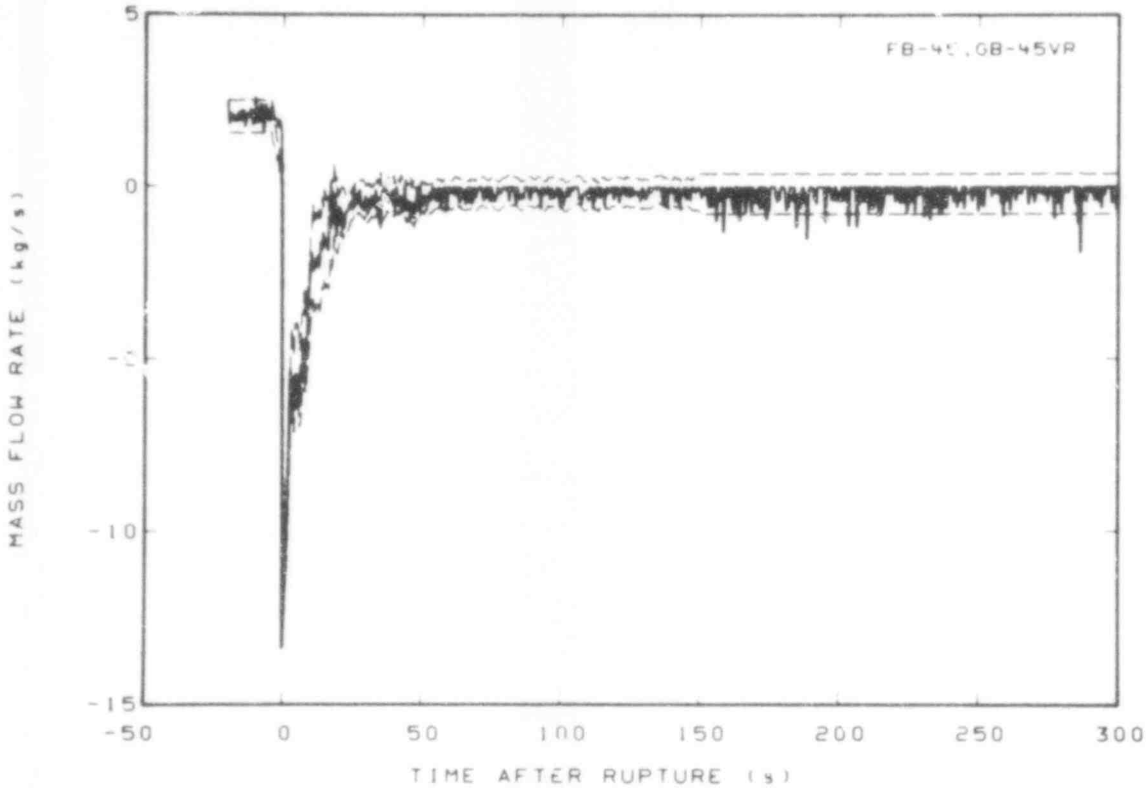

Fig. C-39 Mass flow in broken loop (FB-45 and GB-45VR).

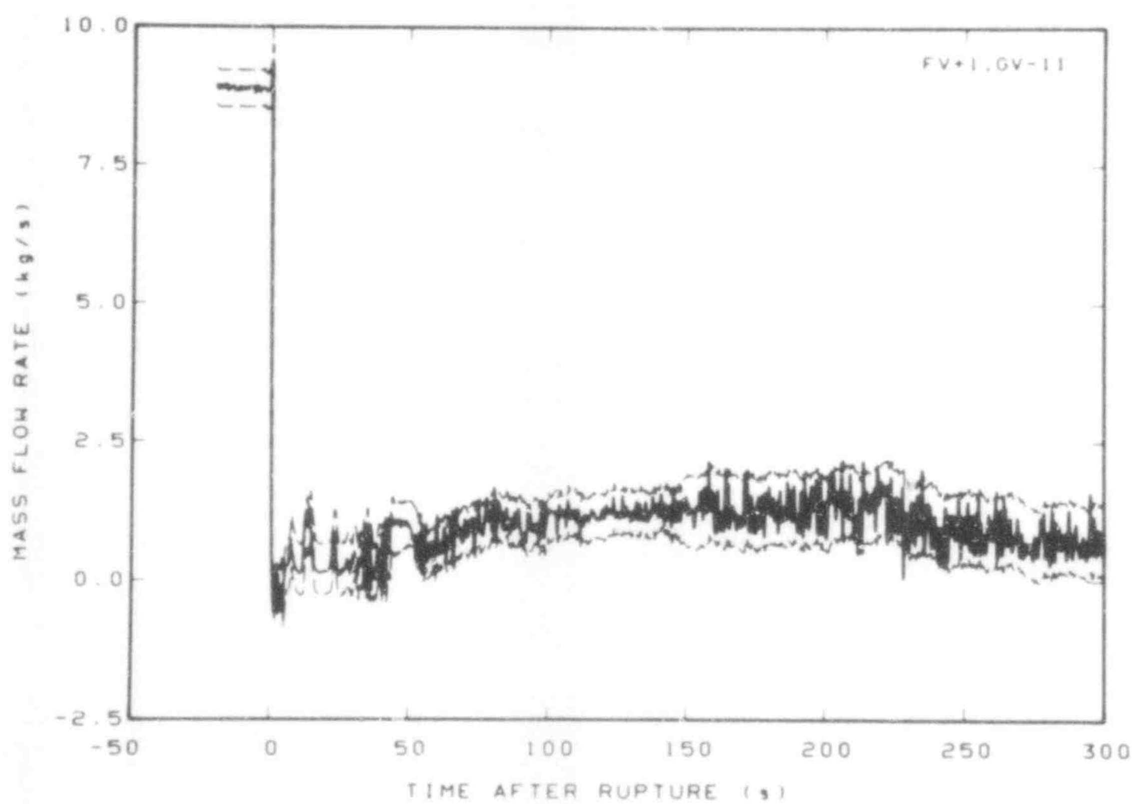

Fig. C-40 Mass flow in vessel (FV + 1 and GV-11).

507 287

TABLE C-II

GENERAL MEASUREMENT ENGINEERING UNCERTAINTY SOURCES AND UNCERTAINTY VALUES
(TEST S-07-9)

Measurement Category	Uncertainty Sources	Uncertainty Value	Expected Uncertainty Values
Fluid Temperature	Changes in homogeneity of the thermocouple wire due to cold working	±1.11 K	±1.66 K, R ≤ 550 K[a]
	Data interpretation from standard reference tables	±1.11 K, to 550 K ±0.0021 R, R > 550 K	$\pm[1.42 + (0.0021\ R)^2]^{1/2}$, R > 550 K[a]
	General data acquisition processing	±0.42 K	where R = transducer reading (K)
	Thermal aging of the thermocouples	±0.28 K	
Material Temperature	Changes in homogeneity of the thermocouple wire due to cold working	±1.11 K	
	Thermocouple radial position	±2.78 K	±3.33 K, R ≤ 550 K
	Data interpretation from standard reference tables	±1.11 K, to 550 K ±0.0021 R, R > 550 K	$\pm[9.75 + (0.0021\ R)^2]^{1/2}$, R > 550 K

507 290

TABLE C-II (continued)

Measurement Category	Uncertainty Sources	Uncertainty Value	Expected Uncertairty Values
Material Temperature (continued)	General data acquisition and processing	±0.42 K	where R = transducer reading (K)
	Thermal aging of the thermocouples	±0.28 K	
Pressure	Entrance effects	±0.3% of transducer full scale	±0.44% of transducer full scale
	Calibration	±0.26% of transducer full scale	
	Temperature sensitivity	±0.13% of transducer full scale	
	General data acquisition and processing	±0.15% of system full scale	
Differential Pressure	Installation	±0.3% of transducer full scale	

TABLE C-II (continued)

Measurement Category	Uncertainty Sources	Uncertainty Value	Expected Uncertainty Values
Differential Pressure (continued)	Calibration Transducer ranges ±4.96 through ±199.26 kPa	$\pm[(0.05) + (0.5\ R/FS)]^{2\ 1/2}\%$ of transducer full scale	
	Transducer ranges ±3.44.74, ±689.47, ±3447 kPa	$\pm[(0.03) + (0.5\ R/FS)^2]^{1/2}\%$ of full scale	
	Transducer ranges ±6894, ±10 342 kPa	$\pm[(0.02) + (0.5\ R/FS)^2]^{1/2}\%$ of full scale	±2% of transducer full scale[b] where R = transducer reading (kPa) FS = transducer range full scale (kPa)
	Temperature sensitivity	±0.5% of transducer full scale	
	General data acquisition and processing	±0.15% of system full scale	
	Air entrapment	±0.069 kPa	
Density	Calibration	±1.0% of reading (kg/m^3)	
	Detector system Uncertainty	±2.1 kg/m^3	c
	General data acquisition and processing	±0.15% of system full scale (kg/m^3)	

507 292

TABLE C-II (continued)

Measurement Category	Uncertainty Sources	Uncertainty Value	Expected Uncertainty Values
Density (continued)	Flow regime	Gr[c] where Gr = flow regime uncertainty (kg/m^3)	
Volumetric Flow (turbine flow-meter)	Calibration instrument reading	±0.25% of transducer full scale	c
	Calibration standards	$\pm 19.56 \times 10^{-2}$ l/s	
	Velocity profile	±2.9% of reading	
	Frequency-to-voltage conversion	±0.25% of transducer full scale	
	General data acquisition and processing	±0.15% of system full scale	
	Dead bands	±5% of transducer full scale	
	Flow regimes	c	

TABLE C-II (continued)

Measurement Category	Uncertainty Sources	Uncertainty Value	Expected Uncertainty Values
Mass Flow Rate (from volumetric flow and density data)	Combined results from individual uncertainty sources for volumetric flow and density data[d]	c	c

a. This value is no longer valid after thermocouple dryout occurs.

b. Value is based on observed system performance. It is more conservative than that obtained from the statistical summation of the identified engineering uncertainties.

c. Uncertainty value is time and flow regime dependent.

d. The general method for combining volumetric flow with density data to obtain mass flow rate and the resulting uncertainties in the data are explained in Reference C-2.

TABLE C-III

TIME PERIODS WHEN FLOW REGIME UNCERTAINTIES WERE APPLIED
(TEST S-07-9)

Detector Identification	Time During Which Flow Regime Uncertainties Were Applied (s)	Figure
FI-1	1 to 26	C-23
	50 to 75	
FI-17	5 to 18	C-24
FB-45	10 to 48	C-25
GI-1C	1 to 26	C-31
	50 to 75	
GI-17C	5 to 18	C-34
GB-45VR	10 to 48	C-35
FI-1, GI-1C	1 to 26	C-37
	50 to 75	
FI-17, GI-17C	5 to 18	C-38
FB-45, GB-45VR	10 to 48	C-39

REFERENCES

C-1. G. E. P. Box and B. M. Jenkins, *Time Series Analysis — Forecasting and Control*, San Francisco: Holden-Day, 1970.

C-2. E. M. Feldman and S. A. Naff, *Error Analysis for 1-1/2-Loop Semiscale System Isothermal Test Data*, ANCR-1188 (May 1975).

507 295

DISTRIBUTION RECORD FOR NUREG/CR-0815
(TREE-1229)

Internal Distribution

1 - R. J. Beers, ID

2 - P. E. Litteneker, ID

3-5 - INEL Technical Library

6-10 - Authors

11-41 - Special Internal

External Distribution

42-50 - Special External

51-52 - Saul Levine, Director
Office of Nuclear Regulatory Research, NRC
Washington, D.C. 20555

53-341 - Distribution under R2, Water Reactor Safety Research - Systems Engineering

507 2?6